Secondary metabolites from benthic organisms: ecological and chemical aspects

Michela NAPPO

UNIVERSITAT DE BARCELONA

Facultat de Farmàcia

Departament de Productes Naturals, Biologia Vegetal i Edafologia

Secondary metabolites from benthic organisms: ecological and chemical aspects

MICHELA NAPPO

2010

Universitat de Barcelona

Facultat de Farmàcia

Departament de Productes Naturals, Biologia Vegetal i Edafologia

Programa de Doctorat: Medicaments, Alimentació i Salut

Bienni: 2004-2006

Secondary metabolites from benthic organisms: ecological and chemical aspects

Memòria presentada per Michela Nappo per optar al títol de Doctor en Farmàcia per la Universitat de Barcelona

Els directors

Prof. **Jaume Bastida**

Facultat de Farmàcia
Universitat de Barcelona

Prof. **Conxita Avila**

Facultat de Biologia
Universitat de Barcelona

La doctoranda

Michela Nappo

Facultat de Farmàcia
Universitat de Barcelona

MICHELA NAPPO

2010

Ai miei genitori . . .

Acknowledgments

En marzo de 2005 cogí mi maleta, todos mis sueños y mis esperanzas, y salí de mi país con rumbo Barcelona. No hablaba ni una palabra de castellano, ni conocía a nadie. Estaba asustada, pero al mismo tiempo tenía muchas ganas de aprender y conocer a gente nueva. Y así fue... A lo largo de mi camino muchísimas fueron las personas que me ayudaron para que pudiera realizar lo que entonces me parecía pura cienciaficción, y a estas personas quiero y debo agradecer desde lo más profundo de mi corazón porque gracias a ellas este trabajo ha podido ver la luz. En primer lugar, quiero agradecer a mis directores de tesis, la prof. Conxita Avila y el prof. Jaume Bastida. Gracias Conxita, por haber siempre creído y confiado en mí, incluso cuando yo tampoco lo hacía, y por darme la posibilidad de cursar mis estudios de doctorado en España. Gracias Jaume, por tu gran paciencia con mis series venezolanas "a pesar de que fuera italiana" y, además, rara como todos los italianos. Y gracias por hacerme escuchar las canciones de Celentano y Bocelli para que no echara de menos a mi tierra. Gracias al prof. Carles Codina por sus consejos, por corregir siempre mis faltas de inglés y por su amabilidad. Y gracias al dr. Strahil Berkov, mi maestro de GC-MS, porque, además de sus preciosas lecciones químicas,

con sus sonrientes “es lo que hay” me enseñó a no desesperar cuando algo salía mal. Todà rabbà to dr. Amir Sagi and his group (BGU): dr. Eli Aflalo, dr. Rivka Manor, dr. Simy Weil, and dr. Tomer Ventura. Thanks for your help and, above all, for resolving important problems within the PHARMAPOX Project. And also for your kindness, the wonderful hospitality during the workshop in Israel and the best *hummus* ever eaten in my life. My suitcase still smells of it… Alla dott.ssa Simona Zupo dell’Istituto Tumori di Genova (Italia) e alle sue collaboratrici, Carlotta Massucco e Valentina Di Maria, per aver effettuato i saggi delle diatomee sulle linee tumorali. Al dott. Valerio Zupo e alla dott.ssa Patrizia Messina della Stazione Zoologica di Napoli “A. Dohrn”, per aver coltivato le diatomee e realizzato i saggi su *H. inermis*, ma non solo. A Valerio per il progetto, con tutti i suoi pro e contro, ed a Patty per l’immensa pazienza nel rispondere alle mie domande. Ed alla dott.ssa Raffaella Raniello per la sua collaborazione nella fase iniziale del PHARMAPOX. Thanks to prof. Vassilios Roussis, prof. Costas Vagias and dr. Fay Ioannou, for their precious help during my PhD stay in Athens. E grazie di cuore a tutti i ricercatori dell’ICB-CNR di Pozzuoli, dott.ssa Marianna Carbone, Franco Castelluccio, dott. Ernesto Mollo, dott.ssa Letizia Ciavatta, dott. Emiliano Manzo, dott. Guido Villani, dott. Guido Cimino. E, soprattutto, alla dott.ssa Margherita Gavagnin per l’affetto ed il sapere trasmessomi, ed a Guido V. per le meravigliose foto. Grazie ai dott. Angelo Fontana, Giuliana D’Ippolito ed Adele Cutignano (ICB) per i suggerimenti sulle diatomee. Ed a tutti quelli che incontrai lavorando lì, dra. Pilar López, dr. Veaceslav Kulcitki, dra. Maya

Mitova, dott.ssa Sara Tucci, dott. Simone Di Micco, dott.ssa Teresa Docimo, Stella García, Yan Li, Javi Pascual, e Dolores. Grazie al dott. Vincenzo Di Marzo (ICB) ed al suo gruppo per aver saggiato i composti della *Sinularia* sulle cellule tumorali, ed alla dott.ssa Domenech Merck per aver realizzato i saggi di attività antimicrobica. Ai compagni di laboratorio dell'ICB, Markus, Olga, Giovanna, Miriam, Antonella, Vincenzo, e Nadia. A Raffaele Turco, per avermi fornito buona parte del materiale bibliografico e per la grande disponibilità durante il servizio civile; ed a Manuela, per le ore trascorse a riordinare le riviste dell'ICB. Ad Aniello Lopez, a quelli dell'amministrazione ed a tutti i tecnici del Servizio NMR dell'ICB. E grazie alla dott.ssa Adrianna Ianora della Stazione Zoologica "A. Dohrn" di Napoli per avermi inviato i suoi articoli e fornito spunti fondamentali nella ricerca sulle diatomee. Gracias al prof. Manuel Ballesteros de la Facultat de Biologia de la Universitat de Barcelona por haberme proporcionado las fotos de *Aplysia*. Y a todos los compañeros del laboratorio de Productes Naturals de la Facultat de Farmàcia de la UB, dra. Eva Castells, dr. Edison Sorio, dra. Laura Torras, Jean Andrade, por su amistad y palabras bonitas, y a Natalia, Beatrice y Alina. Al prof. Paco Viladomat y su "no sé si m'explico". A Modes y Mari, y a Gloria de la oficina de recerca de la Facultat de Farmàcia por solucionar los problemas económicos de los pobres becarios. Y a la dra. Asún Marín de los Serveis Científico-tècnics de la UB, por realizar los análisis GC-MS. Y a todas las personas que conocí en el CEAB y en Blanes, y que volvieron tan divertida mi temporada en la Costa Brava. Un agradecimiento particular es para

Sergi Taboada, porque no sólo fue un compañero de trabajo, sino también un amigo verdadero y siempre presente. Nunca te agradeceré lo bastante todo lo que hiciste por mí, desde la manta que me diste cuando llegué a Blanes hasta todas las aventuras del Chocopox... Y gracias a Yvonne, mi amiga doctora Grzymbowski, por haberme ofrecido tu casa cuando tampoco nos conocíamos y haber sido mi hermana mayor cuando no tenía a mi familia cerca. Gracias a Laura Núñez-Pons, mi cariñosa, maja y ruidosa compañera de despacho, por alegrar todos mis días, incluso los más grises. Y por aguantar, durmiendo, las llamadas de Pasqualina. Y gracias a Jenny Vázquez por su ayuda en el lab y su amistad, y a Blanca Figuerola por su aporte a la bibliografía. Gracias a Maika García por su cariño, y por haberme demostrado que es fuerte no quien siempre gana, sino quien consigue levantarse tras las caidas. A su Jordi. Y a su primo Oscar, por alojarnos en su casa en Madrid y ser tan majo en guiarnos por la ciudad. Gracias a la dra. Jara Vassallo por los desayunos en el café Acciò, donde aprendí la diferencia entre un cortado corto de café y un café con leche. Nunca olvidaré todas las cervezas y fiestas en la playa, el desembarco en Normandía con operación *Noctiluca*, el corto de Maçanet y el Vodka absolut con los ceabinos y blandengues: dra. Ana Riesgo, gracias por sus fotos y sus fiestas pijas, dra. Anna Hervas, Adriana Villamor, Francis López, Dani y Anabel Crespo, Domingo Ramírez, Vanesa, Torio Fernández, Carmen C. y David, Ester Batista, David Soto, Romero Roig, Charlotte Noyer, Virginia Jiménez y Jorge, Virginia García, Begoña Ezcurra, Begoña Martínez, JC y Arianna, Carmen Gutiérrez, Silvia, João Gil, Gilberto Cardoso,

Oriol Sacristán, Johan cuñao, dr. Eduard Ariza y su treumalito, Guillermo Mendoza, Marc Terrades y sus algas, Raffaele Bernardello, Simone Farina, Miquel, Xavi Torras, Javi Sánchez, Dani Garrido, y a Biagio Laudicina. Al dr. Rafa Sardá y a las niñas, Laura y Júlia. Agradezco también a toda la administración del CEAB, el gerente, Roser, Marta, Concha, y a Carmela, Susanna Pla, Ángel el manita, Valentín, Andrés y los demás vigilantes. Y a Ramón, por todas las veces que solucionaste mis problemas informáticos. A las compañeras del equipo de remo Treumal, porque a pesar de que nunca ganamos en las regatas, me divertí un montón con vosotras. Y porque descubrí que yo también tengo abdominales, aunque bien escondidos. Y a Anna Ponce, mi linda compañera de piso en Molins de Rei, gracias por tu amistad, por todas las rutas modernistas y por cuidarme y escucharme siempre. Y a su Oscar. Y a Nori, Joan y a todas las personas que conocí en Molins de Rei. Gracias a María Cuadrado, no sólo por haberme revelado los secretos de la salsa y de los bailes caribeños, y por las excursiones por toda Catalunya, sino también por ser mi amiga. A todas las personas sin nombre que cruzaron mi camino y me regalaron una sonrisa. A los chicos que encontré durante el curso BIOMA en Banyuls-sur-Mer, y a los profes del Observatoire Océanologique Laboratoire Arago, Université Pierre et Marie Curie, CNRs (Francia). And, in particular, thanks to dr. Christos Arvinitidis of the Hellenic Center for Marine Research (Crete, Greece) for his precious advice. If I am writing the acknowledgments of my thesis is because I followed it. Ai miei compagni della III E del liceo classico “A. Diaz”, ed alle mie amiche di sempre

Rossella, Raffaella, Loredana e Claudia. A tutti coloro che ho incontrato lungo il cammino verso Santiago de Compostela, e grazie soprattutto ad Aldo, Maria Cristina, Michael, Pierrot, Massimo e Ramón, per tutti i bei momenti che abbiamo vissuto insieme. Ai ragazzi dell'Associazione Vivila, in particolare a Giuseppe e Flaviano. Ed ai miei nuovi amici Rino, Luigi, Martina, Salvatore, Felicia, Mara, Alfredino, Antonia, Montuoro, Sbarbino, Giovanni, Annamaria, Laura, Antonio, Valeria, Nicola, Sara, Helen, Gaetano, Francesca, Massimo, Simona, Maria, Ersilia, Lucio, Gianni ed architetti tutti.

Ed infine, a tutta la mia famiglia. Non ringrazierò mai abbastanza i miei genitori per gli innumerevoli sacrifici e l'immenso affetto dimostratomi. Anche quando i doveri e lo studio mi hanno allontanato da voi. E soprattutto a te papà, grazie per esserci sempre accanto facendoci apprezzare, anche adesso, la preziosità di ogni tuo sguardo e di ogni tuo sorriso. Alle mie sorelle, Teresa e Valentina, per tutte le mie mancanze, per avermi appoggiato sempre, consigliato ed anche rimproverato. A Francesco e Giuseppe, ed al mio adorato nipotino Salvatore. Ai miei nonni, zii e cugini tutti. A zio Luciano ed ai miei cari che non sono più qui. Alla famiglia Iovino, per avermi accolta come una di voi. Ed al dott. Luigi Iovino per le correzioni d'inglese.

Ed a te Alfredo, per aver preso quel treno delle 7.44… per aver sempre creduto in me ed avermi sostenuto nei momenti più difficili.

Grazie.

Michela

Index

I. Abbreviations and Symbols

AA	arachidonic acid
Ac_2O	acetic anhydride
AcOH	acetic acid
AG	androgenic gland
AMDIS	Automated Mass Spectral Deconvolution and Identification System
Apaf1	Apoptotic protease activating factor 1
Asp	aspartate
ATP	adenosine triphosphate
B.C.	before Christ
BGU	Ben-Gurion University
br	broad
BSTFA	*N,O*-bis-(trimethylsilyl) trifluoroacetamide
$CaCl_2$	calcium chloride
CDA	Chiral Derivatizing Agent
CEAB	Centre d'Estudis Avançats de Blanes
CET-TPP	carbethoxyethylidene-triphenylphosphorane
CFU	colony forming unit
$C_9H_{11}NO$	4-dimethylamino benzaldehyde
$CHCl_3$	chloroform
CH_2Cl_2 (DCM)	dichloromethane
cHx	cyclohexane
CI	Chemical Ionization
CNR	Consiglio Nazionale delle Ricerche
CoA	coenzyme A
conc.	concentrate
COSY	COrrelation SpectroscopY
CSIC	Consejo Superior de Investigaciones Científicas
cyt *c*	cytochrome *c*
d	doublet
δ	chemical shift (ppm)
Δ	difference (or position of the double bonds)
dd	double doublet
ddd	double double doublet
dddd	double double double doublet
DEPT	Distorsionless Enhancement by Polarization Transfer
DMAP	dimethylaminopyridine
DMAPP	dimethylallyl PP
DMSO	dimethylsulphoxide
DNA	deoxyribonucleic acid
dt	double triplet
DW	dry weight
EE	diethyl ether extract
e.g.	*exempli gratiā* (Latin for "for example")
EIMS	Electron Impact Mass Spectrometry
EMEA	European Medicines Evaluation Agency
EnzSH	enzyme with SH groups
EPA	eicosapentaenoic acid

ESI-HRMS	Electron Spray High Resolution Mass Spectrometry
ESIMS	Electron Spray Mass Spectrometry
et al.	*et alii* (Latin for "and others")
etc.	*et cetera* (Latin for "and more")
EtOAc	ethylacetate
EtOH	ethanol
EU	European Union
FAB-HRMS	Fast Atom Bombardment-High Resolution Mass Spectrometry
FADD	Fas Associated protein with Death Domain
FAME	fatty acid methyl ester
FDA	Food and Drug Administration
Fig.	figure
F/tot	female/total individuals
GC-MS	Gas Chromatography-Mass Spectrometry
GPP	geranyl PP
GGPP	geranylgeranyl PP
h	hour
HCl	chlorhydric acid
HMG	hydroxymethylglutaryl
H_2SeO_3	metasilicic acid
H_2SO_4	sulphuric acid
HIV	Human Immunodeficiency Virus
HMBC	Heteronuclear Multiple Bond Coherence
HPL	hydroperoxide lyase
HPLC	High Performance Liquid Chromatography
HRMS	High Resolution Mass Spectrometry
HSQC	Heteronuclear Single Quantum Coherence
IC_{50}	half maximal Inhibitory Concentration
ICB	Istituto di Chimica Biomolecolare
ind.	individual
INRC	Istituto Nazionale Ricerca sul Cancro
IPP	isopentenyl PP
IR	infrared
J	coupling constant
KOH	potassium hydroxide
LOX	lipoxygenase
m	multiplet
$M^{+\cdot}$	molecular ion
MeOH	methanol
min	minute
MOA	methoxyamine
MTPACl	α-methoxy-α-trifluoromethyl-phenylacetic acid chloride
MUFA	monounsaturated fatty acid
mult.	multiplicity
MW	molecular weight
n	number
NaCl	sodium chloride
Na_2CO_3	sodium carbonate
NADPH	nicotinammide adenine dinucleotide
NaOH	sodium hydroxide
Na_2SiO_3	sodium silicate
Na_2SO_4	sodium sulphate
N.D.	not determined
n-Hx	normal hexane
NF	nuclear factor
NMR	Nuclear Magnetic Resonance
n.O.e	Nuclear Overhauser Effect
NOESY	Nuclear Overhauser Effect Spectroscopy
n.s.	not significant

PCIMS	Positive Chemical Ionization Mass Spectrometry
PE	light petroleum
PP	pyrophosphate
PPP	pharnesyl PP
ppm	parts per million
PS	phosphatidylserine
PUA	polyunsaturated aldehyde
PUFA	polyunsaturated fatty acid
Pyr	pyridine
q	quartet
RBL	rat basophilic leukaemia
R_f	retention factor
RI	Kovats index
R_t	retention time
R_v	retention volume
rpm	revolutions per minute
rt	room temperature
s	singlet
SCUBA	Self Contained Underwater Breathing Apparatus
SD	standard deviation
SDS	sodium dodecylsulphate
sec	second
SEM	Scanning Electron Microscopy
SFA	saturated fatty acid
sp.	species
SPE	Solid Phase Extraction
SPSS	Sigma-plot software
SZN	Stazione Zoologica di Napoli
t	triplet
TIC	total ion current
TLC	Thin Layer Chromatography
TMS	tetramethylsilane
TMSi	trimethylsilane
TNF	tumor necrosis factor
TNFR1	TNF receptor 1
tr	traces
TRADD	TNF Receptor-Associated Death Domain
TUNEL	Terminal deoxyUridine triphosphate (dUTP) Nick End Labelling
UB	Universitat de Barcelona
UV	ultraviolet
VLC	Vacuum Liquid Chromatography
vs.	*versus*
v/v	volume/volume ratio

II. Presentation of the report and Objectives

The present Thesis deals with the importance of marine natural products and their impact in modern drug discovery. Organisms belonging to different phyla (Algae, Mollusca and Cnidaria) and from diverse geographical regions have been studied, highlighting the problems which characterize this kind of research and the enormous pharmacological potentialities of metabolites of marine origin.

The work has been carried out in the following Institutes:

- Centre d'Estudis Avançats de Blanes (CEAB), Consejo Superior de Investigaciones Científicas (CSIC), Girona, Catalunya, Espanya;
- Universitat de Barcelona, Facultat de Farmàcia, Departament de Productes Naturals, Biologia Vegetal i Edafologia, Barcelona, Catalunya, Espanya;
- University of Athens "Panepistimiopolis Zografou", School of Pharmacy, Department of Pharmacognosy and Chemistry of Natural Products, Athens, Greece;
- Istituto di Chimica Biomolecolare (ICB), Consiglio Nazionale delle Ricerche (CNR), Pozzuoli, Napoli, Italia.

The study regarding *Cocconeis* diatoms has been performed in the frame of the European Project "PHARMAPOX: Chemistry, Pharmacology and Bioactivity of a novel apoptotic compound - a sex regulator in decapod crustaceans with promising environmental and medical applications (FP6-2003-NEST-A/STREP 4800)", granted by the EU through both the CEAB-CSIC and the Universitat de Barcelona, and it was realized in both places.

The study on *Aplysia fasciata* molluscs has been done in the University of Athens with the support of the Greek General Secretariat for Research and Technology and the Spanish Ministry of Education and Science, in the framework of a Joint Research and Technology Program between Greece and Spain (2005-2007; HG-2005-0027).

The study on the Chinese soft coral *Sinularia* sp. has been carried out in the ICB (CNR) in the frame of an Italian-Chinese Action.

The report consists in 10 chapters. In the first one a general introduction to marine natural products is reported highlighting, in particular, the increasing interest of the current research towards this branch of Organic Chemistry, and considering the tremendous impact of certain marine compounds in the pharmacological therapy. The role of secondary metabolites within the marine ecosystems has been treated as well, with particular attention to the chemical weapons produced by benthic organisms. Due to the complexity of the item and the multiplicity of the targets of the PHARMAPOX Project, the argument itself has been divided into four chapters. In chapter 2 the elucidation of the project, its background and targets, along with the

mechanisms of apoptosis and possible applications of the apoptotic factor(s) in medicine and aquaculture have been exposed. Chapter 3 has dealt with the attempts to improve the diatom biomass production. This has represented a crucial step within the project, since inadequate quantities of biological material have been a limiting factor for a satisfying achievement of the prefixed targets. The problems encountered in this part of the investigation and the reasons which justified the shift of the diatom species (from *Cocconeis neothumensis* to *C. scutellum*) have been explained as well. In chapter 4 the chemical analyses realized on *C. scutellum* diatoms, in particular the determination of their metabolic pattern by GC-MS and the search for aldehyde compounds, have been described. Finally, chapter 5 has dealt with the biological activities of the diatom extracts and their fractions. In particular, *in vivo* tests on *Hippolyte inermis* shrimps, both *in vitro* and *in vivo* assays on crustaceans of commercial interest, and *in vitro* experiments on human cancer cell lines have been carried out. In chapter 6, the chemical study on the anaspidean mollusc *Aplysia fasciata* has been reported along with the structural elucidation of the new isolated compounds. In chapter 7, the chemical investigation on the Chinese soft coral *Sinularia* sp. has been shown, along with the structural characterization of the new compounds and the performed biological assays (feeding deterrence, cytotoxicity, and antimicrobial activity experiments). For each studied organism, the scheme has been articulated in a general introduction about the species and the sampling geographical area, a section regarding the extraction and isolation, the

chemical investigation, the obtained results and the discussion. The experimental section has been reported in chapter 8. Final conclusions of all the studies realized within the doctorate program have been exposed in chapter 9. A summary in Spanish language has been included as well in chapter 10, in which the items, the main results, the discussion and the concluding remarks have been reported. In the last part of the memory the bibliographic references have been reported.

Focusing on natural products from the sea, the main objective of this PhD Thesis has been to underline the interest in marine compounds as central players in the future research strategies of the pharmaceutical development. The study, in addition, has led to the publication of four scientific articles, published in international journals indexed in the Science Citation Index, as well as two more manuscripts which are in preparation.

- Ioannou, E.; Nappo, M.; Avila, C.; Vagias, C.; Roussis, V. (2009). Metabolites from the sea hare *Aplysia fasciata*. Journal of Natural Products 72: 1716-1719.

- Nappo, M.; Berkov, S.; Codina, C.; Avila, C.; Messina, P.; Zupo, V.; Bastida, J. (2009). Metabolite profiling of the benthic diatom *Cocconeis scutellum* by GC-MS. Journal of Applied Phycology 21: 295-306.

- Raniello, R.; Iannicelli, M.M.; Nappo, M.; Avila, C.; Zupo, V. (2007). Production of *Cocconeis neothumensis* (Bacillariophyceae) biomass in batch cultures and bioreactors for biotechnological applications: light and nutrient requirements. Journal of Applied Phycology 19: 383-391.

- Zupo, V.; Messina, P.; Buttino, I.; Sagi, A.; Avila, C.; Nappo, M.; Bastida, J.; Codina, C.; Zupo, S. (2007). Do benthic and planktonic diatoms produce equivalent effects in crustaceans? Marine and Freshwater Behaviour and Physiology 40(3): 169-181.

The main questions which this PhD Thesis has tried to answer are:

1) Which compound of *C. scutellum* diatoms affects the sex reversal in *H. inermis*?
2) Do these compounds uniquely act on *H. inermis*' male gonad or also on other tissues and other organisms? In particular, can these compounds affect the sex also in crustaceans of commercial interest? If so, is it possible to use the diatoms to manipulate the crustaceans' sex? And, in addition, can *Cocconeis* diatoms act on human tissues?
3) Considering the proapoptotic effect of *C. scutellum* diatoms, can they be exploited as a source of anticancer compounds?
4) Can *A. fasciata* and *Sinularia* sp. afford new interesting compounds? Are their metabolites provided with biological activities?

5) Can we conclude that the considered marine organisms are a good source of potential new drugs?

These objectives have been pursued by extracting the biological material (*C. scutellum*, *A. fasciata* and *Sinularia* sp.) with different organic solvents, separating the obtained extracts and purifying the interesting compounds with several chromatographic methods. The structural elucidation has been carried out by means of spectrometric and spectroscopic techniques (GC-MS, mono- and bidimensional NMR) and the biological activities have been evaluated by means of *in vitro* and *in vivo* bioassays.

1. Introduction to Marine Natural Products

1.1. Chemistry of Natural Products

Natural products have wined an overwhelming success in our society, becoming one of the main branches of Organic Chemistry. Many substances of natural origin, mainly derived from the vegetal kingdom, have contributed to help humanity in reducing pain and curing pathologies. Chemistry of Natural Products was born, in fact, as an investigation of the plants and, subsequently, it has embraced the animal kingdom as well. Documents as Ebers Papyrus (1550 B.C.) and Edwin Smith Papyrus (1600 B.C.) are a testimony of the traditional habits of using medicinal plants for treating several diseases. *Cannabis sativa*, *Papaver somniferum*, *Aloe* sp., *Mentha piperita* are just some examples of the plants used in Egyptian medicine (Bryan 1931). The employment of plants and animals as therapeutic instruments, originally entrusted to which-doctors, was standardized during the eighteenth century becoming, thus, a real science. Hippocrates extracted the predecessor of aspirin from willow tree bark (*Salix* genus) in the fifth century B.C., although it was probably used even before in Egypt and Babylonia in the treatment of fever, pain and childbirth

(Keifer 1997). Synthetic salicylates started to be produced on a large scale in the nineteenth century, and in 1897 it was discovered at Bayer that the acetyl derivative of salicylic acid (Fig. 1.1) was able to reduce its acidity, bad taste and stomach irritation (Shapiro 2003).

Fig. 1.1. From the natural source to the commercial product. On the left, the willow tree (*Salix* sp.), whose bark was used for extracting the salicylic acid. On the right, aspirin and its chemical structure.

Both the rich structural diversity and complexity of natural products have prompted synthetic chemists to produce them in the laboratory (Clardy & Walsh 2004), and still nowadays most of the drugs used in therapeutics derive from natural sources, plants, animals and bacteria. These compounds have revolutionized medicine, doubled the average life span and, simultaneously, improved human life quality. Natural products display an important role in drug discovery and development process (Cragg *et al.* 1997), demonstrated by the presence of natural substances in many anticancer and antiinfective drugs, not only as remedies themselves but also as

"source of inspiration" for new drugs (Newman & Cragg 2007). With only 5-15 % of the approximately 250,000 species of higher plants systematically investigated, and the potential of the marine environment barely tapped, nature represents a rich font of novel bioactive compounds (Cragg & Newman 2005). For example, during the time frame 1981-2006 of the 174 new chemical entities discovered (Table 1.1), 41 were of biological type (isolated from natural sources or obtained by biotechnologies), 12 were natural products, 38 derived from natural sources but subjected to semisynthetic modifications, 54 totally synthetic products (often obtained by conversion of an existing agent), 10 synthetic and natural product mimics, 5 obtained by total synthesis but provided with a natural pharmacophore, 7 obtained by total synthesis, provided with a natural pharmacophore and also natural product mimics, and 7 vaccines (Newman & Cragg 2007). It has been estimated that 200,000 natural compounds are currently known and many of them exhibit particular biological activities in the producer organism. It has been hypothesized that when the same natural compound is produced by unrelated species, it must have an important biological function, *e.g.* addressing a specific target, because fortuitous production of a particular compound by totally unrelated species is extremely improbable (Tulp & Bohlin 2005).

		Origin of drug							
Indication	**Total**	**B**	**N**	**ND**	**S**	**S/NM**	**S***	**S*/NM**	**V**
analgesic	16		1		11	2	2		
anesthetic	5				5				
anti-Alzheimer's	4		1			3			
anti-Parkinsonism	12			2	1	5		4	
antiallergic	16		1	3	12				
antianginal	5				5				
antiarrhythmic	16		1		13			2	
antiarthritic	15	5		1	3	6			
antiasthmatic	14	1		3	2	6		2	
antibacterial	109		10	64	23			1	11
anticancer	100	17	9	25	18	12	11	6	2
anticoagulant	17	4		12			1		
antidepressant	22				7	13		2	
antidiabetic	32	18	1	4	4	4	1		
antiemetic	10				1	1		8	
antiepileptic	11			2	6		2	1	
antifungal	29	1		3	22	3			
antiglaucoma	13			4		5	1	3	
antihistamine	12				12				
antihyperprolactinemia	4			4					
antihypertensive	77			2	27	14	2	32	
antiinflammatory	51	1		13	37				
antimigraine	10				2	1		7	
antiobesity	4			1		3			
antiparasitic	14		2	5	4		2		1
antipsoriatic	7	2		3			1	1	
antipsychotic	7				3	2		2	
antithrombotic	28	13	1	5	2	5		2	
antiulcer	32	1	1	12	18				
antiviral	78	12		2	7	1	20	11	25
anxiolytic	10				8	2			
benign prostatic hypertrophy	4		1	1	1	1			
bronchodilator	8			2				6	
calcium metabolism	17			8	8	1			
cardiotonic	13			3	2	3		5	
chelator & antidote	5				4	1			
contraception	7			7					
diuretic	5				4	1			
gastroprokinetic	4				1	2		1	
hematopoiesis	6	6							
hemophilia	11	11							
hormone	22	12		10					
hormone replacement therapy	8			8					
hypnotic	12				12				
hypocholesterolemic	11		3	1	2			5	
hypolipidemic	8		1		7				
immunomodulator	4	2	1	1					
immunostimulant	10	4	3	2	1				
immunosuppressant	12	4	5	3					
male sexual dysfunction	4							4	
multiple sclerosis	4	3					1		
muscle relaxant	10			4	2	1	3		
neuroleptic	9				1	6		2	
nootropic	8			3	5				
osteoporosis	4	2		1	1				
platelet aggregation inhibitor	4			3		1			
respiratory distress syndrome	6	3	1		1	1			
urinary incontinence	4				2	2			
vasodilator	5			3	2				
vulnerary	5	2		2	1				
grand total	1010	124	43	232	310	108	47	107	39

Table 1.1. New chemical entities and medical indications during 1981-2006. B: biological (usually a large peptide/protein isolated from an organism/cell line or produced by biotechnologies); N: natural product; ND: derived from a natural product and modified by semisynthesis; S: totally synthetic drug; S*: totally synthetic, but with a pharmacophore from a natural product; V: vaccine. Subcategory NM: natural product mimic (from Newman & Cragg 2007).

1.2. Secondary metabolism

Nature has invented an incredible universe of molecules, with an amazing diversity of skeletons and biological/pharmacological properties. Natural products are basically represented by secondary metabolites. Contrastingly to primary metabolic pathways, in which ubiquitous compounds are synthesized, degraded and transformed, secondary metabolism concerns products with a much more limited distribution in nature. Secondary metabolites, usually present in small amounts in living beings, are characteristic of specific organisms or groups of organisms and are an expression of the individuality of the species. They are not necessarily produced under all conditions and, in most of cases, the function and the advantages that these compounds provide to the producer are unknown yet, although some of them are undoubtedly synthesized for easily appreciated reasons. These metabolites, in fact, can be synthesized during starvation (*e.g.* carbapenem antibiotics produced by *Pseudomonas* bacteria), development (*e.g.* antibiotics made by *Streptomycetes* during cellular differentiation), signalling (quorum-sensing molecules biosynthesized at particular culture densities of microbes) (Walsh 2003) or as antipredation weapons. In any case, it is logical to assume that all of them do play some vital paper for the well-being of the producer organism. The area of secondary metabolism supplies, furthermore, most of the pharmacologically active natural products (Dewick 2001). Secondary metabolism has evolved in response to needs and challenges of the

surroundings and, consequently, nature has been continuously elaborating its own version of combinatorial chemistry for over three billion years (Verdine 1996). During that time, producers of secondary metabolites evolved according to their neighboring environment: if the metabolites were useful to the organism, the biosynthetic genes were retained and further genetic modifications improved the evolutionary process. Thus, natural products have been selected by nature for specific biological interactions, as well as to bind proteins and have drug-like properties. Combinatorial chemistry practiced by nature is much more sophisticated than that in the laboratory, yielding exotic structures rich in stereochemistry, concatenated rings and reactive functional groups (Verdine 1996). In particular, the comparison between natural products and synthetic drugs has highlighted the advantages provided by the former. First, most natural products typically have more stereogenic centres and architectural complexity than synthetic molecules fashioned by medicinal chemists. Second, natural products contain relatively more carbon, hydrogen and oxygen atoms, and less nitrogen and other elements than synthetic medicinal agents. Third, many useful natural products have molecular masses in excess of 500 Da and high polarities (Clardy & Walsh 2004). Nevertheless, the part of the molecule responsible for interacting with the biological target is usually limited to a very small cluster of atoms. On the other hand, one of the basic problems in this field is that natural sources usually provide scarce quantities of compounds and obtaining a renewable supply of active metabolites from biological sources can be

problematic. However, the increasing efficiency of Synthetic Organic Chemistry has reduced the barrier posed by limited natural furnish, even for products with very complex structures, enabling to obtain larger amounts of compounds to be subjected to clinical trials. Sometimes the isolated compound shows *in vitro* but not *in vivo* pharmacological activity, due to the way of administration of the product or its metabolization in the organism. Herein, structure/activity relation studies are requested to modify the lead compound in order to improve its pharmacokinetic and pharmacodynamic profiles and, consequently, introduce it in the pharmaceutical field.

1.3. Why marine natural products?

Contrastingly to plants, marine organisms do not have a long and significant history of use in the popular medicine, exception given by some molluscs producing a purple secretion used by the ancient Phoenicians to dye clothes, and seaweeds employed to fertilize the soil (Cragg & Newman 2005). Nevertheless, during the last three decades the trend/interest of many scientists, in particular chemists and pharmacologists, has moved over sea organisms and compounds of marine origin. Why marine natural products? The answer has to be searched not only in the extraordinary richness of chemical structures due to the high marine biodiversity (Faulkner 2000; Pietra 2002), but also in the large array of biological and

pharmacological activities exhibited by marine compounds (Jacobs *et al.* 1993; Wallace 1997; Cragg & Newman 2005). The sea is the original source of life on Earth and many organisms communicate one another by signalling systems represented by primordial chemical messengers. From an evolutionary point of view, humans are connected to marine organisms, leading to conclude that it is not surprising that many molecules from the marine environment have profound effects on human tissues and cells (Wallace 1997). The marine environment is a very rich reservoir of compounds which have revealed to be good candidates for the development of new drugs. Since marine biodiversity regarding phyla is much higher than terrestrial, "the oceans represent the better place to start to develop a natural Pharmacy" (Kijjoa & Sawangwong 2004). In fact, among 34 fundamental phyla of life, 17 occur on land whereas 32 occur in the sea, with some overlaps (Kijjoa & Sawangwong 2004). In addition, the chemical investigation of marine fauna and flora has been encouraged upon the great development of the technologies required for studying the underwater environment.

Oceans cover about the 70% of the planet surface and correspond to the 90% of the biosphere. Only in 2008, 1065 new compounds were found in marine sources, an increase of about 11% with respect to the number recorded in 2007 (Blunt *et al.* 2010). In particular, studies on sea habitats have been prompted due to the perspective of potential technological applications of marine natural products in many fields, from healthcare to food additives (Bongiorni & Pietra 1996). Approximately, every habitat

from Antarctica (Amsler *et al.* 2001; Avila *et al.* 2008) to coral reefs (Hay 1997) has been studied. Of the isolated marine natural products, 25% are from algae, 33% from sponges, 18% from cnidarians (sea whips, sea fans and soft corals), and 24% from representatives of other invertebrate phyla such as tunicates, opisthobranch molluscs, echinoderms (starfishes, sea cucumbers, *etc.*) and bryozoans. An over-simplified analysis of these data reveals that the search for "drugs from the sea" progresses at the rate of a 10% increase in new compounds per year, and researchers are concentrating their efforts on slow-moving or sessile invertebrate phyla characterized by soft bodies, and lack of spines and shell (Faulkner 1995a). Most of the 14,500 molecules of marine source listed in MarinLit database (http://www.chem.canterbury.ac.nz/research/marinlit.shtml) derive from benthic organisms, *i.e.* those living close or related to the sea bottom. Despite either their scarce mobility or fixing to the bottom, and lack of mechanical and physical protection, the survival of some benthic organisms has been guaranteed by the acquisition of alternative protective strategies, in particular the production of chemical weapons. In fact, in the sea, during millions of years, innumerable life forms evolved, developing an enormous variety of defensive systems of exclusive sophistication to survive in an extremely competitive environment. In agreement with the "adaptationist theory", the secondary metabolites have to furnish some benefits to the producer in order to justify the metabolic expenses (in terms of structural complexity or high concentrations) invested into their synthesis. Other

evidences of the defensive function of secondary metabolites include the strong correlation between the absence of obvious mechanisms of physical protection in an organism and the presence of unusual compounds in its tissues. Indeed, the richest sources of secondary metabolites are those organisms showing soft textures, sessile habits and scarce protection, in contrast to the mobile and armored fauna (crustaceans, echinoderms, snails) usually lacking chemical arms (Pawlik 1993). This is clear in Fig. 1.2, showing marine organisms with anticancer activity.

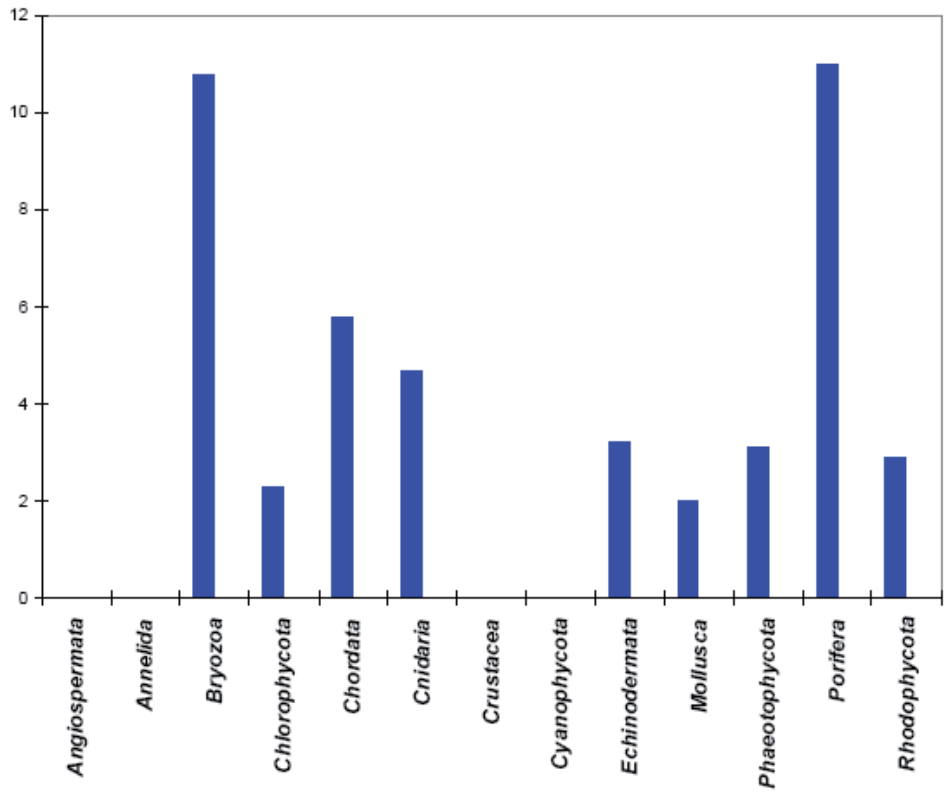

Fig. 1.2. Marine phyla with anticancer activity (adapted from Garson 1994).

In fact, Bryozoa and Porifera have demonstrated to be the richest phyla in anticancer compounds, followed by Chordata and Cnidaria (Garson 1994).

A completely different hypothesis is that secondary metabolites have no ecological function (Haslam 1986), but they would represent a "biochemical garbage", due to accumulation of collateral products of synthetic pathways, enzymatic activities on unsuitable substrata or waste/detoxification products.

In agreement with the adaptationist version, marine secondary metabolites can play different functions. The most common role is the predator deterrence, but other suggested functions include also antifouling activity, overgrowth inhibition or UV radiation shielding (Paul 1992; Pawlik 1993). Benthic organisms are subject to an intense competition for space and food and, thus, the production of allelopathic metabolites is a mechanism that ensures the survival of species with slow development (Jackson & Buss 1975) or avoids the colonization of planktonic larvae, preserving the established species (Goodbody 1961). It is known that the primary metabolic composition of marine organisms does not differ from that of terrestrial ones, suggesting a unity in the primary metabolic pathways in all the living species. The situation of the secondary metabolism is, instead, completely different. In fact, the biosynthetic pathways of terpenes, acetogenins, aromatic compounds and alkaloids are unusually different in marine species compared with terrestrial organisms. Halogens, which are abundant in sea water, take part in the biosynthesis of terpenes, brominated acetogenins and phenolic compounds (Fenical 1982). In

addition, the sea is an important source of unusual nucleosides (Bhakuni & Rawat 2005a) and new peptides provided with significant biomedical value (Bhakuni & Rawat 2005b). Along with the biological properties, these compounds exhibit important pharmacological activities. Trabectedin (ET-743, Yondelis™, Fig. 1.3), originally isolated from the tunicate *Ecteinascidia turbinata* and obtained by synthesis at present, has been approved from the EMEA for advanced pre-treated sarcoma, and it is in phase III clinical development in ovary cancer and in phase II in breast, prostate and pediatric tumors (Jimeno 2007).

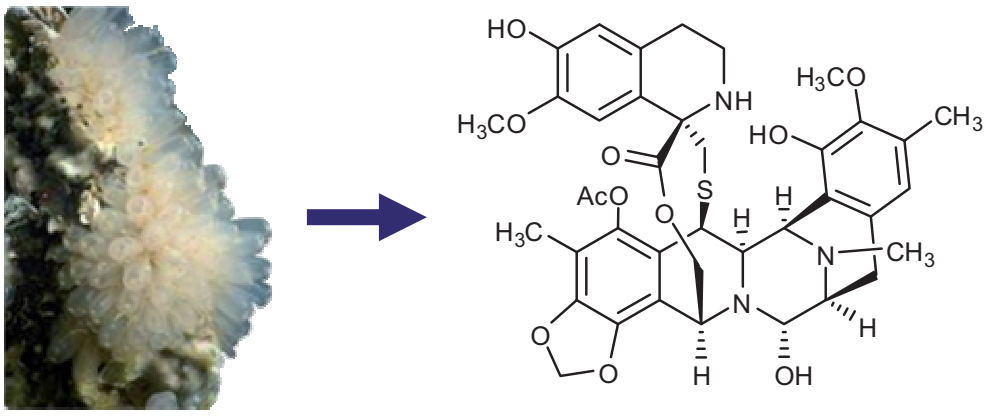

Fig. 1.3. *Ecteinascidia turbinata* (from htpp://www.yondelis.com) and trabectedin.

1.4. Different approaches in the study of marine natural products

In the study of marine natural products, as well as terrestrial ones, the starting point in order to detect biologically active compounds is to distinguish potentially useful

molecules among the huge number of metabolites without any applicative importance. Traditionally, the approaches in the study of marine natural products were divided into two general strategies (Fig. 1.4).

Approach 1 is based on an indiscriminate procedure of isolation and characterization of the secondary metabolites, followed by an evaluation of the pharmacological activities of all the purified compounds. The main disadvantages of this approach are the enormous number of tests required to obtain a wide amount of inquiries about the activity of the examined substances, and the work to isolate all the compounds.

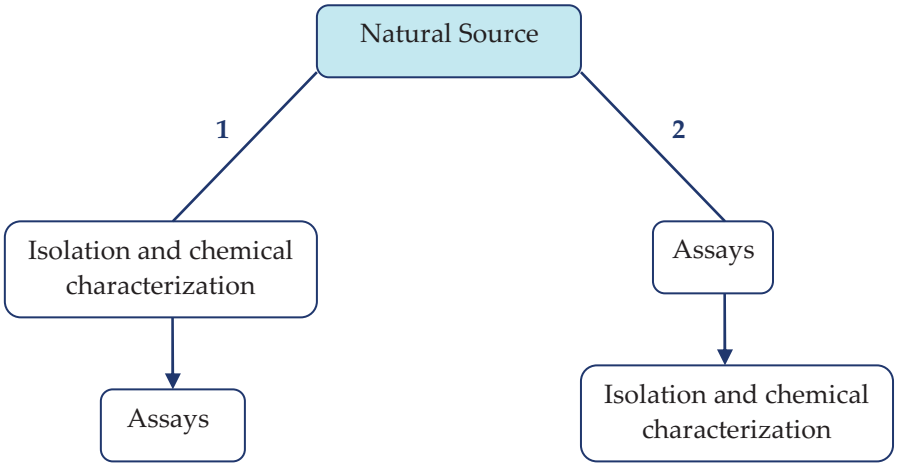

Fig. 1.4. The two traditional approaches used in the study of the natural products. Approach 1: pharmacological assays on purified products. Approach 2: bioassay-guided fractionation of extracts.

Approach 2 is represented by the bioassay-guided fractionation: pharmacological assays on crude extracts or their fractions are previously performed to select only

those ones provided with a specific activity. The active fractions are subjected to further purifications and bioassays in order to select smaller and smaller fractions until obtaining the pure active compound. The critical point of approach 2 is to screen extracts on animals, even if crude extracts are generally tested by *in vitro* assays, while purified compounds are assayed by *in vivo* tests. Antimicrobial and enzymatic inhibition tests are simple and fast-to-realize for a preliminary check. In this approach the principal risk is to ignore fractions that are not positive in the performed assay, but that could have other interesting activities. Both approaches 1 and 2 are expensive in terms of human and economic resources and thus, more recently, they have joined another method, approach 3 (Fig. 1.5).

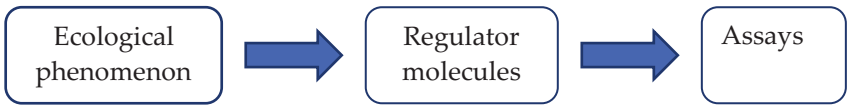

Fig. 1.5. The ecological approach.

This last method consists in selecting biologically active molecules studying, from a chemical point of view, the ecological relations within their environment. It can be called "ecological approach" and it is the basis of Chemical Ecology, defined as the chemical investigation of the inter- and intraspecific relations among organisms sharing the same habitat. Although this subject mainly aims at studying the

mechanisms of the fundamental biological processes (individuation of the food, defence against predators, communication phenomena, reproductive cycles), it can also be used to select compounds with interesting applications. Thus, from the observation of biological effects, it is possible to find regulator molecules with a wider activity range than the same ecological function. In the ecological approach, the expensive requirement of preliminary tests is substituted by "in field" observations and, from this perspective, the studied organisms become natural "probes" rich in biologically interesting compounds. The ecological approach has represented the thread of this PhD Thesis, whose background has been the observation of some biological effects occurring in the nature. The influence of *Cocconeis* benthic diatoms on the sex reversal of *Hippolyte inermis* shrimp has been the focal point of the PHARMAPOX Project. This effect, due to the production of apoptotic compound(s), led us to search for this/these molecule(s), investigate its/their structure(s) and test it/them on other organisms in order to evaluate possible applications (*e.g.* in medicine and aquaculture). The soft texture along with the lack of mechanical and physical protection of both the anaspidean mollusc *Aplysia fasciata* and the soft coral *Sinularia* sp. suggested the involvement of chemical weapons in the defensive mechanisms of the animals. Therefore, we considered not only organisms belonging to diverse phyla (diatoms, opisthobranch molluscs and cnidarians), but also from different geographical areas as well as Mediterranean (Italy and Spain) and

China Sea. The biological and taxonomic features of each considered species will be exposed next.

1.5. Diatoms

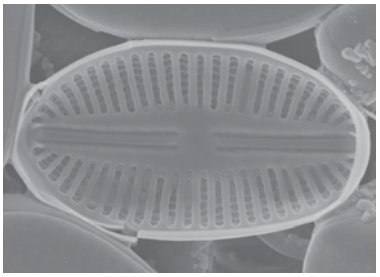

Fig. 1.6. *Diploneis* sp.

Diatoms are eukaryotic unicellular and brown-coloured phycophytes (algae), characterized by a siliceous cell wall (Lebeau & Robert 2003a). The classification is still unsettled, and they may be treated as a division (or phylum), kingdom, or something in-between. Accordingly, groups like the diatoms may be ranked anywhere from class (usually called Diatomophyceae) to division (usually called Bacillariophyta), with corresponding changes in the ranks of their subgroups. Diatoms are traditionally divided into two orders: centric diatoms (Centrales), which are radially symmetric, and pennate diatoms (Pennales), which are bilaterally symmetric. A more recent classification (Round & Crawford 1990) divides the diatoms into two classes: 1) centric diatoms (Coscinodiscophyceae), 2) pennate diatoms of which a) without a *raphe* (Fragilariophyceae) and b) with a *raphe* (Bacillariophyceae). The class Bacillariophyceae is comprehensive of two subclasses, Centricae and Pennatae, and five orders. Centricae are dish-shaped central shell diatoms, include almost exclusively planktonic (*i.e.* living in the water column)

species and are divided into three orders: Discoideae, Solenioidae and Biddulphioideae. The subclass Pennatae is mainly represented by benthic species and embraces the orders Araphideae and Raphidiodeae (Table 1.2).

Phylum	**Algae**	
Class	**Bacillariophyceae**	
Subclass	**Centricae**	**Pennatae**
Order		**Araphideae**
		Raphidiodeae

Table 1.2. Taxonomic placement of diatoms of the subclass Pennatae.

There are estimated to be about 10^5 diatom species (Dixit *et al*. 1992; Lenoci & Camp 2008), widely distributed in most aquatic habitats such as seas, fresh and brackish waters. Some of them live also in wet soil and musk. Their length range can be between 2 μm and 1.5 mm, in some cases even reaching 4 mm. The cell wall made of silica (hydrated silicon dioxide) is called frustule and it is composed by two box-like joined parts: the *epitheca* (the upper half and larger size) and the *hypotheca* (the downer and smaller part). Every part is provided with a covering layer (*valva*) and an annular belt (*pleura*). In many Pennatae, the *valva* is characterized by three enlargements directed inside, one in the middle (central button), and two in the edges (terminal buttons). The buttons are joined by means of a line, the *raphe*, which connects the protoplasm with the surrounding water. Diatoms are characterized by

an uncoloured cytoplasma and yellow, brown-yellowish, green, brown-greenish chromatophores. The most common pigments are represented by chlorophyll, carotenoids and xanthophylls. Planktonic species are arranged to float. *Raphe*-provided benthic species, helped by the plasmatic current coming out of the pores of the *raphe*, are able to skim slowly. The first identification of diatoms, especially for planktonic species, is performed by microscopy or through fixing. A preliminary acid treatment is required in order to highlight the structure and, thus, obtain the identification of the diatom. The study of the cellular content is carried out by special dyes, whereas diatoms are conserved in 5% alcohol. Planktonic and benthic species, epizoic or epiphyte, are found on every kind of substratum, generally until 200 m depth. Planktonic species are collected by thin fishing-nets, while nanoplankton is sampled with bottles, or by centrifuging or sedimenting water samples. Benthic species, instead, are collected along with the bottom (sediment, stones, aqueous plants and annexed animals) by hand, or by means of a toothed dredger or a rake. The reproduction is vegetative, through transversal division in which the *hypotheca* is *de novo* reconstructed at every cycle. The cell size gradually becomes smaller and smaller after every reproductive cycle, but this reduction is equilibrated by a swelling process in which auxospores (in both sexual or asexual ways) are generated. The maximum development usually occurs in spring, but a second maximum growth has been observed in ending autumn as well (Round & Crawford 1990; Hasle & Syvertsen 1997).

1.6. Opisthobranch molluscs

Fig. 1.7. The nudibranch mollusc *Peltodoris atromaculata.*

Opisthobranchs (Mollusca, Gastropoda) are almost exclusively benthic invertebrates characterized by partial or complete loss of the shell. This subclass, comprehensive of approximately 3,000 species, is split into nine orders: Cephalaspidea, Anaspidea, Notaspidea, Sacoglossa, Nudibranchia, Acochlidea, Rhodopemorpha, Thecosomata and Gymnosomata (Rudman & Willan 1998), of which the most abundant ones are the first five groups. Opisthobranchs play a crucial role within the benthos, occupying different ecological niches and establishing trophic relationships with organisms belonging to many different phyla, such as Poriphera, Cnidaria, Bryozoa, Tunicates and others. The systematic classification of opisthobranchs is reported in Table 1.3.

In shelled gastropods, the mechanical defence offered by the shell is the main protective strategy. From the evolutionary point of view, the loss of the external envelope represents an economical advantage in terms of saving the costs of both production and transport but, at the same time, it has required the development of alternative defensive strategies in order to survive to the predation risk. It is

noteworthy that, besides the lack of mechanical protection, most opisthobranchs are usually slow-moving, thus unable to efficiently escape in case of danger.

Phylum	**Mollusca**				
Class	**Gastropoda**				
Subclasses	**Prosobranchia**	**Pulmonata**	**Opisthobranchia**		
Orders			**Cephalaspidea**	**Anaspidea**	**Notaspidea**
			Sacoglossa	**Nudibranchia**	**Acochlidea**
			Rhodopemorpha	**Thecosomata**	**Gymnosomata**

Table 1.3. Systematic placement of opisthobranchs (as reported by Rudman & Willan 1998).

The alternative protective strategies which opisthobranchs have acquired during the evolution are grouped into three main categories: behavioural, morphological and chemical (Todd 1981; Faulkner & Ghiselin 1983; Perrone 1989). Some species are active at night when predators asleep or cannot see them, or live hidden under rocks (cryptic behaviour). A few opisthobranchs exhibit an indistinguishable coloration (homochromy), shape (homomorphy) or texture from the surrounding environment. In some species the mantle (*i.e.* the external skin) is characterized by the presence of calcareous *spicula*, while other molluscs can accumulate in their dorsal appendixes nematocysts derived from dietary cnidarians (Thompson 1976; Edmunds 2009). Through deimatic display, molluscs exhibit bright colour patterns which are usually hidden, but can be quickly exposed as a mean of startling and frightening off

potential predators. This behaviour is present in *Hexabranchus sanguineus*, commonly known as "Spanish dancer" for its wiggly representations to surprise the predators, which shows brilliant red and white colour pattern on the dorsal side just when it is disturbed and begins to swim (Edlinger 1982). After aggression, some molluscs detach from themselves particularly exposed parts of the body (autotomy) in order to distract the predators and run away when "mutilated". But, undoubtedly, among the protective strategies which guarantee the adaptive success, the production of chemical weapons is the most interesting and noteworthy (Thompson 1960; Avila 1995). Opisthobranchs avoid the predation by producing repellent or toxic compounds, often coupled to warning (aposemantic) colorations (Ros 1976; Avila 1995), so that grazers associate bright colorations to bad taste. According to the "pre-adaptation theory" (Faulkner & Ghiselin 1983; Cimino & Ghiselin 1998, 1999), the development of chemicals has probably preceded the elimination of the shell. The bioactive molecules often derive from the diet: opisthobranchs can acquire from their preys toxic compounds which are generally stored in vesicles or in the digestive gland, then transferred into the mantle and/or into dorsal *cerata* (the most predator-exposed parts), or they can be secreted through the mucous in response to an aggression. Some species are able to biotransform the dietary metabolites in order to convert them into less noxious (for the animal itself) or repellent (*vs.* the predator) compounds (Avila 1995, 2006). Other opisthobranchs can perform a completely *de novo* biosynthesis from simple precursors (Cimino & Ghiselin 1999; Cimino *et al.*

2001). Among the nine orders belonging to the subclass Opisthobranchia, Anaspidea Fischer 1883, also known as Aplysiomorpha, is one of the most studied. The term "Anaspidea" derives from Greek and it means "no-shell" or "shell-less". In fact, these molluscs possess an external clear thin leaf-like layer instead of the shell (Carefoot 1987). The order Anaspidea consists of two superfamilies, Akeroidea and Aplysioidea, both containing one family, Akeridae and Aplysiidae, respectively (Willan 1998). Akeroidea are primitive opisthobranchs characterized by an external, lightly calcified layer, and they have not been studied so far from the chemical point of view. Molluscs of the family Aplysiidae, known as "sea hares" because of their rabbit-like appearance, contain 9 genera: *Aplysia, Bursatella, Dolabella, Dolabrifera, Notarchus, Petalifera, Phyllaplysia, Stylocheilus* and *Syphonota*. They range in size from species growing less than 2 cm to larger species which can reach over 70 cm length. The shell, when present, is reduced to a thinly calcified internal plate (Rudman 2004). All anaspideans are provided, in the mantle cavity, with two glands: the opaline gland on the lower part of the mantle, secreting a colorless smelly mucous fluid, and the purple gland on the upper part, which produces a red or purple ink derived from pigments of dietary algae, mainly Rhodophyta (Cimino *et al.* 2001). It is noteworthy that a progressive reduction of the shell has been observed from Akeridae to Aplysiidae molluscs. The always-internal shell of the Aplysiidae ranges from thick and whorled in the genus *Dolabella*, to thin and plate-like in the genera *Aplysia* and *Syphonota*, to a calcareous wedge in *Dolabrifera*, *Petalifera* and *Phyllaplysia*, and finally

to the completely absence after metamorphosis in *Stylocheilus*, *Bursatella* and *Notarchus* (Rudman & Willan 1998).

1.7. Soft corals

Soft corals are marine benthic organisms usually attached to reefs or seabeds, and belonging to the phylum Cnidaria, a group that includes anemones, jellyfishes, hydroids, sea-pens, true corals and other coral groups. The taxonomic placement of soft corals is reported in Table 1.4. Cnidarians are characterized by having just two germ layers (ecto- and endoderm), stinging-cells, and principal radial symmetry. Another salient characteristic is that they have a single sac-like body cavity (the gastrovascular cavity) provided with one opening that serves as both mouth and anus. They have simple nervous nets and simple anatomy. The phylum Cnidaria is separated into three classes depending on the principal form they take as life stages: Scyphozoa, Hydrozoa and Anthozoa. Scyphozoa, the jellyfishes, are mainly bell-shaped free-living medusae; Hydrozoa are hydroids and hydromedusae; Anthozoa are attached polypoids and consist in sea anemones, corals, sea pens, *etc*. Anthozoans are further subdivided into two subclasses: Hexacorallia and Octocorallia, differing

Fig. 1.8. The gorgonian *Lophogorgia sarmentosa*.

in the morphological structure of their tentacles, among other characteristics. Hexacorallia have tentacles and mesenteries (*i.e.* internal body divisions) in multiples of six, and are divided into six orders: Zoanthidea, Actinaria, Scleractinia, Corallimorpharia, Ceriantharia, and Antipatharia. On the other hand, Octocorallia, characterized by colonial polypoids with eight-numbered mesenteries and hollow bird's feather-like tentacles, consist in six orders: Stolonifera, Telestacea, Alcyonacea, Coenothecalia, Gorgonacea, and Pennatulacea (Brusca & Brusca 2005). In both Octocorallia and Hexacorallia groups, some species are characterized by soft, fleshy and fragile tissues without physical defence capability neither the possibility to escape freely and quickly from their potential predators. On the contrary, others do have very hard skeletons which provide physical protection. Although provided with fragile texture, some soft corals defend themselves by producing antipredatory, antimicrobial, allelopathy and antifouling agents, which could represent lead compounds in drug development (Changyun *et al.* 2008).

Phylum	**Cnidaria**				
Classes	**Scyphozoa**	**Hydrozoa**	**Anthozoa**		
Subclasses			**Hexacorallia**	**Octocorallia**	
Orders			**Stolonifera**	**Telestacea**	**Alcyonacea**
			Coenothecalia	**Gorgonacea**	**Pennatulacea**

Table 1.4. Taxonomic placement of soft corals (Alcyonacea).

2. The PHARMAPOX Project: background and targets

2.1. Introduction

The European Project PHARMAPOX "Chemistry, Pharmacology and Bioactivity of a novel apoptotic compound - a sex regulator in decapod crustaceans with promising environmental and medical applications" has aimed at isolating and identifying from benthic diatoms of the *Cocconeis* genus the apoptotic factor(s) responsible for affecting the sex reversal in *Hippolyte inermis* decapods. The project was carried out by an international multidisciplinary team with experience in specific items, such as marine biology, chemistry, pharmacology and human pathology. Several countries (Spain, Italy and Israel) took part in the investigation (Fig. 2.1), in which they were represented by:

- Departament de Productes Naturals, Biologia Vegetal i Edafologia, Facultat de Farmàcia, Universitat de Barcelona (UB), Barcelona, Catalunya, Espanya;
- Centre d'Estudis Avançats de Blanes (CEAB), Consejo Superior de Investigaciones Científicas (CSIC), Girona, Catalunya, Espanya;

- Laboratorio di Ecologia del Benthos, Stazione Zoologica "A. Dohrn" (SZN), Ischia, Italia;
- Diagnostica Malattie Linfoproliferative, Istituto Nazionale per la Ricerca sul Cancro (INRC), Genova, Italia;
- Department of Life Sciences and the National Institute for Biotechnology in the Negev, Ben-Gurion University (BGU), Beer Sheva, Israel.

Fig. 2.1. The Institutes participating in the project. From the left, above: the Universitat de Barcelona, the Centre d'Estudis Avançats de Blanes and the Stazione Zoologica "A. Dohrn". From the left, below: the Istituto Nazionale per la Ricerca sul Cancro and the Ben-Gurion University.

The research work was performed in sequence by the different Institutes, each one involved in certain tasks within the project. The chemical study (diatom extraction, isolation, structural elucidation and repartition of extracts and fractions to the partners), main and crucial phase for all the other steps of the investigation, was realized in both UB and CEAB. *Cocconeis* diatoms and *Hippolyte inermis* decapods

were cultivated in SZN, where the biological assays on *H. inermis* postlarvae were carried out as well. Antiproliferative tests on cancer cell lines were done in INRC in order to evaluate whether diatoms induced apoptosis not only in *H. inermis*, but also in human tissues. Researchers of BGU, on the other hand, evaluated the effects of the diatom extracts and their fractions on prawns and crayfishes, in the perspective of possible applications in aquaculture. The high-risk/high-gain project has represented with its far-sightedness, thus, a pioneer attempt to share knowledge, pool potentialities of different disciplines and focalize them on a common purpose.

2.2. Background

The idea of the PHARMAPOX Project was born in 2004 as a result of previous studies (Zupo 2000, 2001) dealing with the influence of *Cocconeis* benthic diatoms on the sex reversal of *Hippolyte inermis* shrimps.

Fig. 2.2. *Hippolyte inermis.*

H. inermis Leach 1815 (Fig. 2.2) is a decapod crustacean living in shallow waters of the Mediterranean Sea and along the Atlantic coasts of Spain (Zariquey 1968) where it forms stable populations in seagrass meadows, such as *Posidonia oceanica* (Gambi *et al.* 1992) and *Cymodocea nodosa* (Guillén 1990). The order Decapoda (Fig. 2.3) is the largest natural group within the Malacostraca and it

is divided into two suborders: the swimming decapods, or Natantia, and the walking decapods, or Reptantia. *H. inermis*, belonging to Natantia, is a protandric shrimp (*i.e.* individuals experience a male stage before switching to females) and the sex reversal was demonstrated by histological (Reverberi 1950) and castration studies (Veillet *et al.* 1963). Contrastingly to other crustaceans, *H. inermis* is physiologically characterized by the absence in adult males of both female gonad buds and ovotestis, *i.e.* contemporaneous presence of both male and female gonads (Zupo & Messina 2007), as demonstrated also by other authors (Cobos *et al.* 2005).

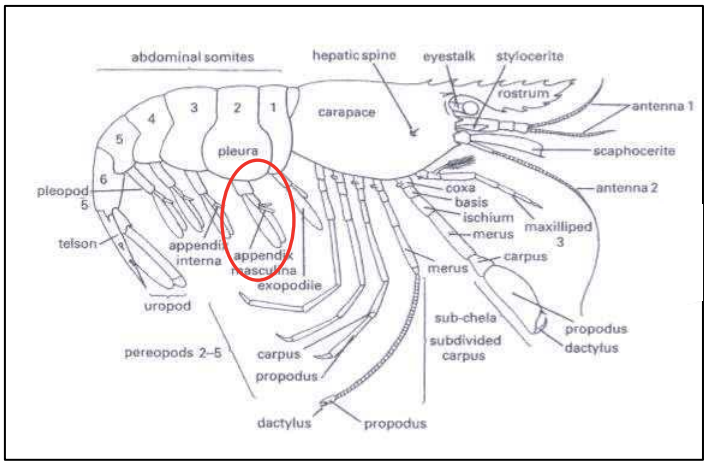

Fig. 2.3. Anatomical representation of decapods. The *appendix masculina* is enclosed in the red oval.

The new female gland is not produced from starting buds (Charniaux-Cotton 1960), but from undifferentiated cells after the complete disruption of the androgenic gland (Zupo & Messina 2007). The life cycle of *H. inermis* is characterized by two yearly

reproductive periods synchronized with the seasonal growth of *P. oceanica*: autumn and spring (Buia *et al.* 1992). Autumn-born individuals are originally males and switch to females (alpha females) about a year after hatching (Zupo 1994). The sex differentiation occurs in 5-7 mm long postlarvae (Veillet *et al.* 1963), while the sex reversal is observed in 10-13 mm individuals corresponding to 7-12 month old shrimps (Zupo 1994). But not all the decapods exhibit the same feature. In fact, spring new populations are characterized by the presence of both male and female individuals (beta females). Beta females, directly derived by differentiation of postlarvae, are smaller and grow up faster than alpha females, those originated by sex reversal of the male shrimps. Laboratory experiments showed that the different seasonal behaviour was due to the influence of the diet on the sex differentiation of the crustaceans (Zupo 2001). Indeed, upon observation of *H. inermis*' gut contents by means of the optical microscopy, a close correlation was hypothesized between the life cycle of the decapod and the abundance of algal food in the environment. Among the total amounts of consumed items, macroalgae and diatoms of *Cocconeis* genus (common organisms in the leaf stratum of seagrasses), were the most representative preys. It has been shown that in *P. oceanica* beds the diatom community represents the main food for herbivores such as molluscs and crustaceans (Mazzella & Russo 1989; Scipione & Mazzella 1992), and *Cocconeis* is the most frequent and abundant genus throughout the seasons and all along the depth range of the seagrass distribution (Mazzella *et al.* 1994). *Cocconeis* diatoms, following a parallel trend to the

P. oceanica growth pattern, are nearly absent in autumn and very abundant in spring, period of higher occurrence of beta females (Zupo 2001). Laboratory experiments confirmed the field-based evidence (Zupo 2000) and, in addition, highlighted that individuals born from the same female develop as males or females depending on the absence or presence, respectively, of diatoms in their diet (De Stefano *et al.* 2000). It has been demonstrated by molecular and ultrastructural analyses that the influence of *Cocconeis* diatoms on the shrimp sex reversal was due to specific and selective apoptosis of *H. inermis*' androgenic gland (AG) (Zupo & Messina 2007). The destruction of AG during the postlarval stage, before the sex differentiation, determines the development of female sexual characters and, thus, females not derived by sex reversal of male individuals. *Cocconeis* diatoms, therefore, seem to anticipate the process of sex change that, in their absence, naturally occurs about a year after hatching. The diatom-induced apoptosis has demonstrated to be an adaptive strategy for maintaining a constant sex ratio and guaranteeing a sufficient number of females for the autumn mating period (Zupo 2001). The genus *Cocconeis* includes scarcely mobile single-cell species, strongly adherent to the substratum by the production of mucilaginous compounds which allow the firm adherence of the cells. Benthic diatom communities, and predominantly Pennatae, are still less studied because they are difficult to sample and quantify compared with planktonic diatoms, whose ecology and biology are, on the contrary, widely reported in the literature. Even less data have been collected so far on *Cocconeis* biology: the low growth rates

and strong adhesion to the substratum make the isolation and the manipulation of these cultures not easy to perform. In addition, *Cocconeis* diatoms grow on monolayer cultures, and this requires a lot of space for their cultivation in the laboratory.

2.3. Diatom toxicity

Diatoms are responsible for more than 50% of marine primary production (Nelson *et al.* 1995) and constitute a rich diet for many herbivores (Newell & Newell 1963; Raymont 1983) both in the marine benthos and in the water column, due to their high concentration of lipids (Sicko-Goad & Andresen 1991). Although traditionally they are supposed to represent a key point in the global carbon cycle, the function of diatoms as good food or poor food for copepod reproduction has been subsequently questioned upon the observation of harmful effects of some diatoms on their predators (Ianora *et al.* 1996). The evolutionary success of these microalgae, in fact, has been attributed not only to efficient resource acquisition strategies, but also to allelochemical production that favours their selection over competitors (Andrianasolo *et al.* 2008). Diatom secondary metabolites can function not only as sexual pheromones (Pohnert & Boland 2002) and allelogens (Legrand *et al.* 2003), but also as feeding deterrents (Shaw *et al.* 1995) and toxins (Landsberg 2002). An example can be the domoic acid (Fig. 2.4), a neuroexcitatory amino acid produced by the marine diatom *Nitzschia pungens* forma *multiseries* and responsible for shellfish

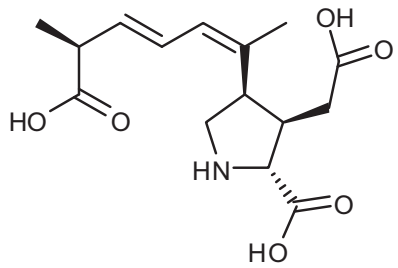

Fig. 2.4. Domoic acid.

poisoning (Douglas *et al.* 1992). Defensive mechanisms have been exhaustively studied for planktonic diatoms which, unable to escape fast from their predators, defend themselves by releasing a diverse array of chemicals into their surroundings. It has been demonstrated that some diatom species produce noxious compounds towards their grazers' offspring (Fontana *et al.* 2007) rather than to the predators themselves. This mechanism, which consists in compromising future generations of copepods, contrasts with most of known prey-predator interactions in the sea, which are usually based on direct repellence or poisoning, rather than reproductive failure as well as abort, birth defects and high mortality (Ianora *et al.* 2004). A class of compounds involved in this kind of chemical protection was identified as polyunsaturated aldehydes (PUAs), belonging to the oxylipin family and among the most studied molecules able to inhibit copepod reproduction (Miralto *et al.* 1999). By definition, oxylipins are oxygenase-mediated oxygenated derivatives of polyunsaturated fatty acids (PUFAs) produced by many organisms, including plants (Weber 2002) and algae (Ponhert & Boland 2002), in which they play a crucial paper in ecophysiological processes (Blée 2002; Howe & Schilmiller 2002). The aldehydes 2-*trans*-4-*cis*-7-*cis*-decatrienal, 2-*trans*-4-*trans*-7-*cis*-decatrienal and 2-*trans*-4-*trans*-decadienal were isolated from the planktonic diatom *Thalassiosira rotula*,

along with 2-*trans*-4-*cis*-octadienal, 2-*trans*-4-*cis*-7-*cis*-octatrienal and 2-*trans*-4-*cis*-heptadienal produced by both *T. rotula* and *Skeletonema costatum* (Fig. 2.5).

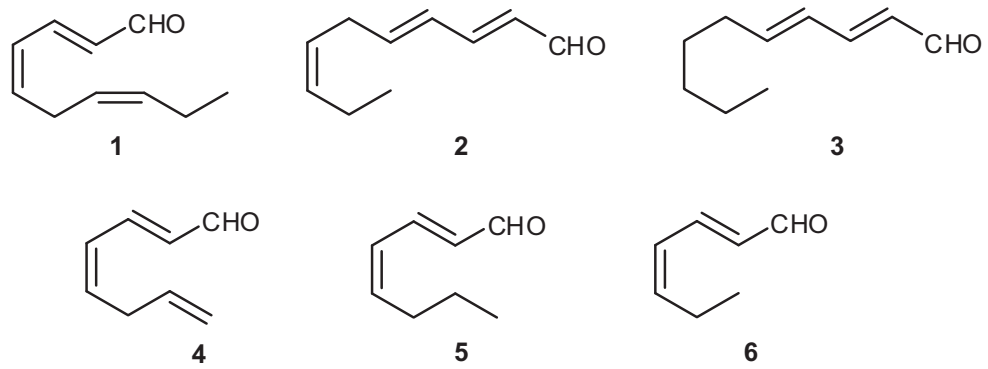

1 2-*trans*-4-*cis*-7-*cis*-decatrienal
2 2-*trans*-4-*trans*-7-*cis*-decatrienal
3 2-*trans*-4-*trans*-decadienal
4 2-*trans*-4-*cis*-7-*cis*-octatrienal
5 2-*trans*-4-*cis*-octadienal
6 2-*trans*-4-*cis*-heptadienal

Fig. 2.5. PUAs from *Skeletonema costatum* and *Thalassiosira rotula.*

These molecules had a negative impact on copepod populations by either drastically reducing fecundity and/or reducing hatching success and larval recruitment. Despite their simple chemical structure, PUAs showed to inhibit also cleavage of sea urchin, polychaete and ascidian embryos, and replication of human tumour cell lines (Caldwell *et al.* 2002; Romano *et al.* 2003; Tosti *et al.* 2003). The aldehyde-induced effects were proportional to both time of exposure and diatom concentration (Laabir *et al.* 1995; Turner *et al.* 2001). In addition, aldehydes showed to be detrimental only on embryos and targeted gametes, but not on adult individuals, indicating a greater

vulnerability of the first ones (Miralto *et al.* 1999). When ingested, *S. costatum* and similar planktonic diatoms induce abortive effects on egg development in copepods like *Calanus helgolandicus*, reducing the egg's viability. The embryos which do manage to hatch are morphologically abnormal, their body tissues are positively marked for apoptosis and they die soon after hatching (Fontana *et al.* 2007). PUAs are not produced by all diatoms and there are differences among species and even strains. Furthermore, different diatom species can produce aldehyde compounds which differ in toxicity and biological activity: those with α,β-unsaturation and longer chain are more noxious towards copepods than other aldehydes (Adolph *et al.* 2003; Romano *et al.* 2003). Biosynthetic studies have demonstrated that the production of aldehydes results from mechanical damage: aldehydes are not detected in extracts of intact diatoms (Ponhert 2000). In fact, in a continuous moving fluid, such as marine water, a mechanism based on leakage of aldehydes would be inappropriate since most of the molecules would be washed away before an effective concentration level could be achieved. On the contrary, production of these molecules only after cell lysis would increase the local concentration, and toxic compounds would be released directly into the body of the grazers (Fontana *et al.* 2007). After wounding, the release of eicosanoic fatty acids by a phospholipase A2 triggers an enzymatic cascade involving a lipoxygenase (LOX) and a hydroperoxide lyase (HPL) (Ponhert 2002). In particular, decadienal has been proposed to derive from arachidonic acid, while heptadienal and decatrienal originate from

eicosapentaenoic acid (EPA). C_{16} unsaturated fatty acids, in particular 6,9,12-hexadecatrienoic and 6,9,12,15-hexadecatetraenoic acids (two major lipid components of diatom glycolipids), have shown to be the precursors of octadienal and octatrienal (Fig. 2.6).

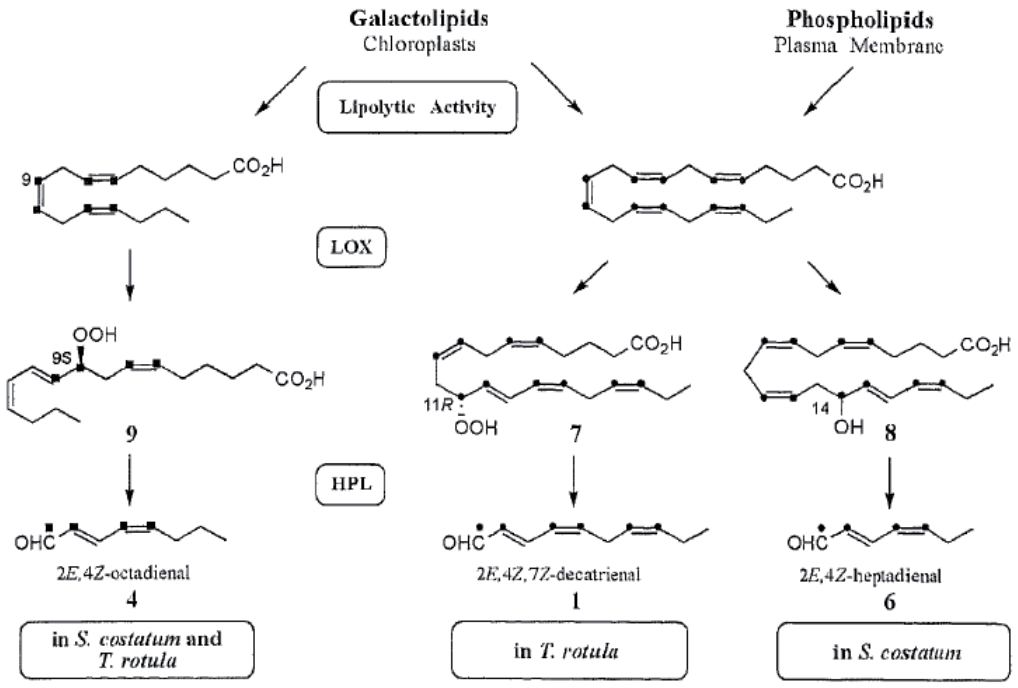

Fig. 2.6. Biosynthesis of PUAs in *T. rotula* and *S. costatum* (■ = deuterium, • = tritium, adapted from Fontana *et al.* 2007).

However, synthesis of PUAs in marine diatoms is only a minor part of a broader biochemical scenario that has been recently emerging. In fact, diatoms produce a plethora of other fatty acid derivatives as well as hydroxy- and ketoacids, which could be involved in the reproductive failure in copepods (Fontana *et al.* 2007). More

recently, apoptosis-inducing galactolipids have been isolated from the diatom *Phaeodactylum tricornutum* (Andrianasolo *et al.* 2008). Monogalactosyldiacylglycerols are chloroplast membrane lipids in higher plants and algae which are involved in the light-initiated reactions of photosynthesis. They are also provided with antiviral (Bergsson *et al.* 2001), antimitotic (Williams *et al.* 2007), tumor suppressor (Morimoto *et al.* 1995), antistress (Gupta *et al.* 2007) and antiinflammatory properties (Larsen *et al.* 2003).

2.4. Apoptosis and drug discovery

2.4.1. Apoptosis: main features

An elucidation about the apoptosis phenomenon will be useful to comprehend the significance and the mechanism of action of the diatom compounds implicated in the induction of such a process. Apoptosis is a regulated process of cell-suicide that is modulated either genetically in response to specific stimuli (such as cytokines, TNF α or the Fas ligand) or after various forms of cell injury or stress (Michaelson 1991; Gerschenson & Rotello 1992). The term, derived from the Greek apo-TOE-sis, refers to the similitude between the cell elimination in tissues and the autumn leaf fall from the trees. The programmed cell death process is responsible for eliminating superfluous/redundant precursors or mature cells, *e.g.* self-reacting lymphocytes during the development of the immunitary system (Spinedi & Piacentini 1999),

remodelling tissues, *e.g.* the formation of fingers and toes in the fetus during the embryo ontogenesis, and removing those cells which would be functionally unhelpful in adult individuals. Furthermore, apoptosis contributes to the reaction of the organism to the surroundings: unnecessary cells may kill themselves to allow the growth and the differentiation of cells that are better geared to deal with the changing environment demands (Hannun 1997). The morphological changes occurring during apoptosis (Fig. 2.7) include:

- cell shrinkage,
- membrane blebbing,
- nuclear chromatin condensation,
- internucleosomal DNA fragmentation,
- packaging of the cell into apoptotic bodies, subsequently engulfed by phagocytes, preventing the release of intracellular components (Buttke & Sandstrom 1994; Cory 1995; Thompson 1995) which could provoke inflammatory phenomena.

Apoptosis differs from necrosis, which is induced by deregulation of normal cellular activities under extreme stress conditions, and is characterized by extensive cytoplasm vacuolization, mitochondrial swelling, endoplasmatic reticulum dilatation and plasma membrane rupture, without formation of vesicles. Thus, contrastingly to apoptosis, in the necrotic process cellular contents are liberated into the intracellular

space damaging neighboring cells and evoking inflammatory responses (Leist & Jaattela 2001).

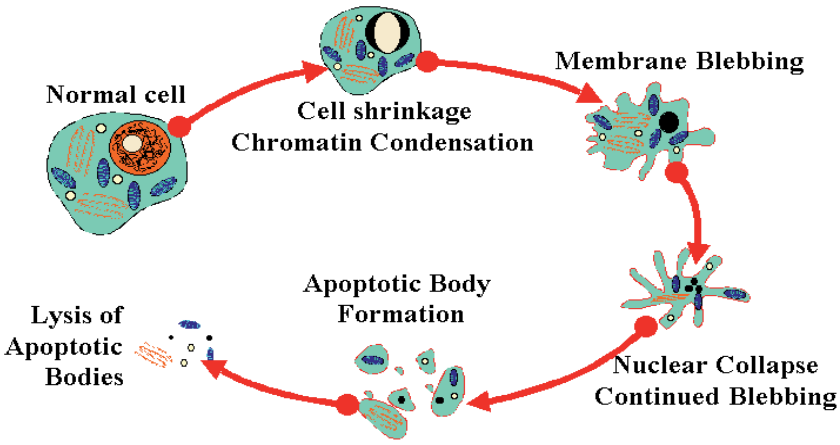

Fig. 2.7. Morphological changes occurring during programmed cell death (from www.microbiologybytes.com).

Apoptosis is the end point of a chain of events (Fig. 2.8) resulting from the selective proteolytic cleavage of several intracellular polypeptides (Earnshaw *et al.* 1999). Most of these cleavages result from the action of a unique family of cysteine-dependent proteases, called caspases. The various members of this protease family differ in primary structure and substrate specificity, but share some common features:

- each caspase cleaves on the carboxyl side of aspartate (Asp) residues;
- each active caspase is a tetramer consisting of two identical large subunits and two identical small subunits;

- each caspase is synthesized as a zymogen that contains an *N*-terminal prodomain, a large subunit and a small subunit;
- the proteolytic cleavage to liberate each caspase involves sequential cleavages at two or more Asp residues, resulting in the separation of both the large and small subunits from one another and from the prodomain.

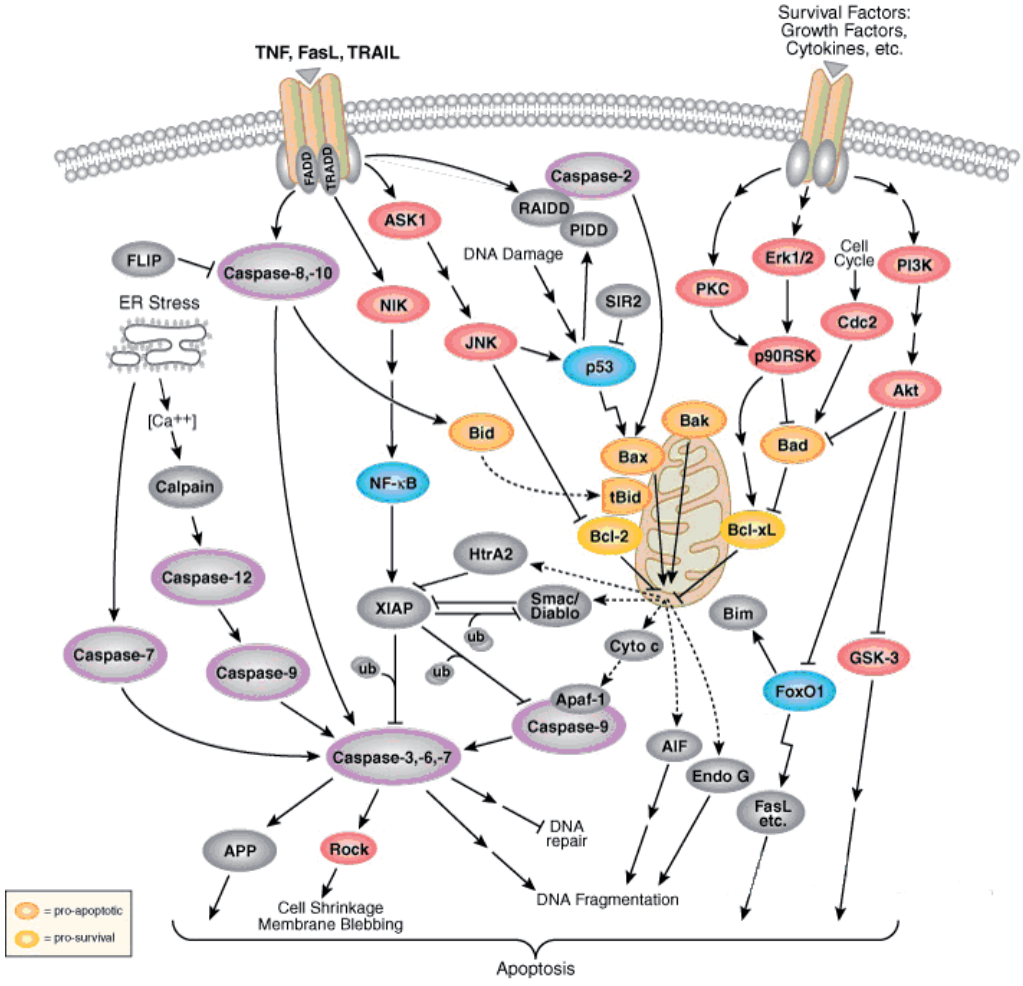

Fig. 2.8. Cascade of events resulting in apoptosis (from www.cellsignal.com).

Of the eleven or twelve known human caspases (depending on certain hereditary polymorphisms), six of them (caspases 3, 6, 7, 8, 9 and 10) are definitely involved in apoptosis in various model systems (Reed *et al.* 2004). One current classification scheme divides the apoptotic caspases into two classes, effector (or "downstream") caspases, which are responsible for most of the cleavages that disassemble the cell, and initiator (or "upstream") caspases, which transduce various signals initiating the proteolytic cascade. Caspases 3, 6 and 7 are the major effector caspases, while caspases 8 and 9 are the major initiator caspases identified to date. Upon activation, caspases 8 and 9 acquire the ability to cleave and activate effector caspases (Kaufmann & Earnshaw 2000).

Two different signaling pathways responsible for triggering apoptosis have been elucidated so far in great detail: the intrinsic, mitochondria-mediated pathway, and the extrinsic, receptor mediated-pathway (Fig. 2.9). The intrinsic pathway centers on mitochondria as initiators of cell death. Multiple signals, including DNA damage, cytokines, microtubule disruption, growth-factor deprivation *inter alia*, converge on mitochondria, causing the release of cytochrome *c* (cyt *c*) and other apoptogenic proteins into the cytosol. In the cytosol cyt *c* binds the caspase-activating protein Apaf1 (apoptotic protease-activating factor 1), inducing its oligomerization into a heptameric complex which binds procaspase 9, forming a multiprotein structure known as "apoptosome" (Salvesen & Renatus 2002).

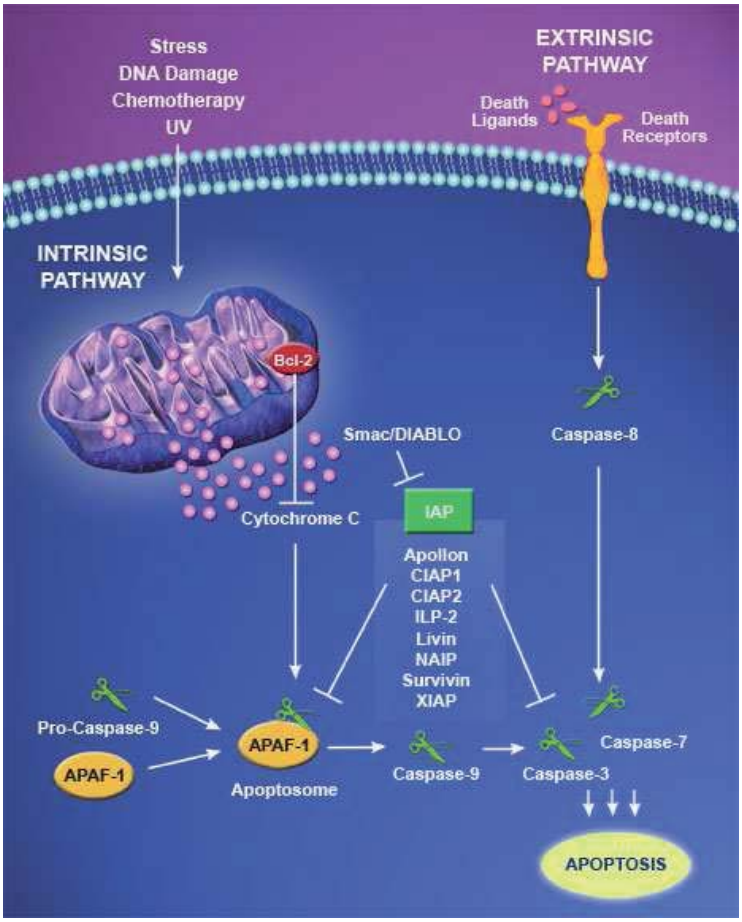

Fig. 2.9. The intrinsic and extrinsic pathways of apoptosis (from www.imgenex.com).

The activation of apoptosome-associated cell death protease caspase 9 initiates a proteolytic cascade, where activated caspase 9 cleaves and activates downstream effector proteases, such as procaspase 3 (Reed & Pellecchia 2005) and go on, until apoptosis is triggered. In contrast, the extrinsic pathway relies on the activation of the "death receptors" by specific molecules (Ashkenazi & Dixit 1998). These receptors belong to the TNF receptor family. Upon binding, TNF α trimerizes its

receptor TNFR1 resulting in the subsequent recruitment of the signal transducing molecules TRADD (TNF receptor-associated death domain). TRADD recruits a TNF receptor-associated factor leading to activation of nuclear factor κB (NF-κB) which suppresses TNF α-induced apoptosis (Takeuchi *et al.* 1996). On the other hand, TRADD can recruit FADD (Fas with death domain) which provokes the activation of caspase 8. Activated caspase 8 initiates a protease cascade that cleaves cellular targets and results in apoptotic cell death (Ashkenazi & Dixit 1998). Both intrinsic and extrinsic pathways, mediated by caspases 9 and 8 respectively, induce the stepwise activation of effector caspases, such as caspase 3, which cleaves specific proteins and leads to the biochemical and morphological changes of the cell death. In addition, there are multiple connections between both the apoptosis-activating pathways (Roy & Nicholson 2000).

In 1980s two main endogenous regulators of apoptosis were identified. It was demonstrated that p53 protein is a cell death inductor, especially in response to DNA damaging events, whereas Bcl-2 functions as antiapoptotic protein (Hannun 1997). Thus, a delicate balance between proapoptotic and antiapoptotic regulators of apoptosis ensures the survival of long-lived cells and the proper turnover of short-lived cells in a variety of tissues, including the bone marrow, thymus and peripheral lymphoid tissues (Reed & Pellecchia 2005).

2.4.2. Pharmacological applications: new goals in cancer therapy

In the last decade the basic research has produced remarkable advances in understanding cancer biology and genetics. Among the most important progresses, there is the comprehension that apoptosis and the genes that control it have a profound effect on the malignant phenotype. Programmed cell death, in fact, plays a crucial paper in the development and homeostasis of multicellular organisms (Vaux & Korsmeyer 1999) and its deregulation can contribute to the occurrence of several diseases. Excessive apoptosis of certain neurons determines the pathogenesis of neurodegenerative conditions, both acute insults and chronic degenerations, while imbalances in the delicate dance of proapoptotic and antiapoptotic proteins, with a prevalence of antiapoptotic factors, promote neoplasia (Reed & Pellecchia 2005). Cancer is the largest cause of death in both men and women, claiming over 6 million lives each year in the world. It has been demonstrated that some oncogenic mutations disrupt apoptosis leading to tumor initiation, progression or metastasis (Lowe & Lin 2000). The killing of tumors through specific induction of apoptosis in malignant cells, avoiding drug-resistance and side effects, has now been recognized as a novel strategy in cancer therapy. Herein cell suicide is an important cellular mechanism for preventing oncogenesis (Evan & Littlewood 1998) because growth-deregulating mutations can induce neoplasia only when apoptosis has been suppressed, which could be due to an overexpression of apoptosis inhibitors or

inactivation of p53 gene (Hannun 1997). Some antitumoral agents employed in the conventional chemotherapy have revealed to promote apoptosis in cancer cells rather than in normal ones. Drugs like etoposide, dexamethasone, vincristine, cisplatinum, *etc*. represent only an exiguous part of the plethora of treatments provided with apoptotic activity (Kaufmann 1989; Huschtscha *et al.* 1996) (Table 2.1).

Class	**Drug**
Antimetabolites	cytarabine, fludarabine, 5-fluoro-2'-deoxyuridine, gemcitabine, hydroxyurea, methotrexate
DNA fragmenting agents	bleomycin
DNA cross-linking agents	chlorambucil, cisplatin, cyclophosphamide, nitrogen mustards
Intercalating agents	adriamycin (doxorubin), mitoxantrone
Protein synthesis inhibitors	L-asparaginase, cycloheximide, puromycin, diphtheria toxin
Topoisomerase I poisons	camptothecin, topotecan
Topoisomerase II poisons	etoposide, teniposide
Microtubule-directed agents	colcemid, colchicine, paclitaxel, vincristine
Kinase inhibitors	Flavopiridol, staurosporine, STI571 (CPG 57148B), UCN-01 (7-hydroxystaurosporine)
Miscellaneous investigational agents	PS-341, phenylbutyrate, ET-18-OCH3
Farnesyl transferase inhibitors	L-739749, L-744832
Hormones	glucocorticoids, fenretinide
Hormone antagonists	tamoxifen, finasteride, LHRH antagonists
Biologicals	tumor necrosis factor α, TRAIL, αnti-CD20, endostatin

Table 2.1. Anticancer treatments inducing apoptosis (adapted from Kaufmann & Earnshaw 2000).

In addition, since the same mutations that suppress apoptosis during tumour development also reduce treatment sensitivity, apoptosis furnishes a conceptual framework to link cancer genetics with cancer therapy. In fact, the loss of p53 can contribute not only to aggressive tumour behaviour, but also to therapeutic resistance (Vogelstein *et al.* 2000; El-Deiry 2003). Herein, a wide part of the current research is devoted to find new apoptotic agents, mainly from natural sources. The knowledge and the advances in the technology obtained in recent years have contributed to increase the interest towards the sea as potential source of new anticancer candidates.

In comparison with the terrestrial organisms, the sea is a surprisingly rich font of cytotoxic products (Fig. 2.10), some of which have been approved in clinical trials and have been introduced into therapeutic protocols. Very often, marine organisms able to defend themselves by their predators producing chemical weapons, are good candidates to have success in finding antitumoral compounds suggesting, therefore, a close correlation between the antineoplastic activity of marine secondary metabolites and their ecological role within the environment. It is noteworthy that many sponges, tunicates, molluscs, *etc.*, soft texture-provided or slow-moving organisms, are among the main producers of new drugs. An example can be afforded by the marine metabolites mycalamide A and pateamine (Fig. 2.11), isolated from the sponge *Mycale* sp., which besides of antiviral, antifungal and cytotoxic properties, exhibit proapoptotic activity (Hood *et al.* 2001).

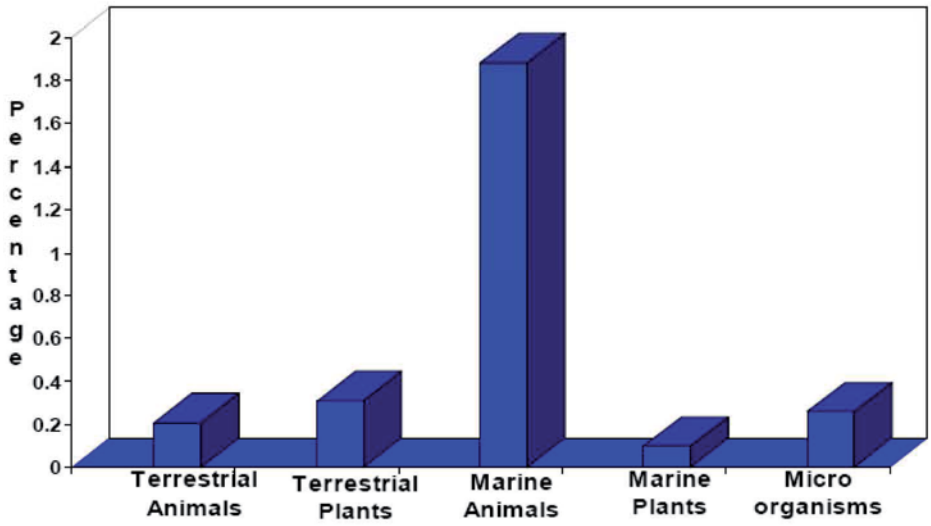

Fig. 2.10. Percentage of organisms showing cytotoxic activity (adapted from Garson 1994).

Also marine microrganisms, with their greatest biodiversity, have revealed to be a good source of novel cytotoxic compounds with sustainable supply (Kelecom 2002; Isnansetyo & Kamei 2003; Lin *et al.* 2005).

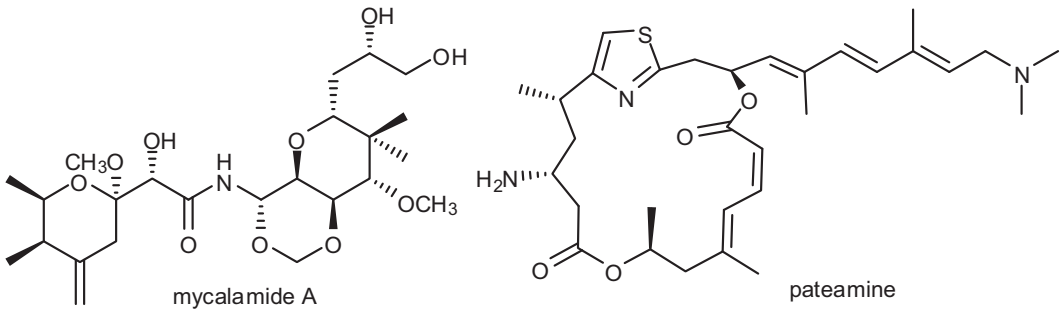

Fig. 2.11. The structures of mycalamide A and pateamine, two marine inducing-apoptosis metabolites isolated from the sponge *Mycale* sp.

2.5. Applications in aquaculture

Another objective of the PHARMAPOX Project was to establish whether *C. scutellum* diatoms were able to induce apoptosis also in the androgenic gland of other species, as well as commercially important crustaceans, in particular crawfishes and prawns. In many crustaceans, as well as in the crawfish *Cherax quadricarinatus* and the freshwater prawn *Macrobrachium rosenbergii* (Fig. 2.12), males and females differ in terms of growth rates, behaviour patterns and alimentary needs (Aflalo *et al.* 2006). Most of them, in fact, exhibit bimodal development models in which males grow faster and/or are larger than females or *vice versa* (Hartnoll 1982). It is known that prawns and crayfishes of all-male populations reach market size at a faster rate, a factor that prolongs the fresh product marketing period (Sagi *et al.* 1986). Thus, it is obvious that cultures of monosex populations represent an economically advantageous strategy in aquaculture, especially in countries in which crustaceans constitute an important source of incomes (Sagi & Aflalo 2005). It is widely demonstrated that the sexual differentiation in crustaceans, based on their genetically determined predisposition, is mediated by the AG, which plays a pivotal

Fig. 2.12. Males (on the left) and females (on the right) of *Macrobrachium rosenbergii*.

role in the regulation of male differentiation and in the inhibition of female differentiation (Sagi & Cohen 1990; Sagi *et al.* 1997; Okamura & Hara 2004). In male crustaceans, the endocrine and gametogenic functions are clearly separated into two distinct organs: the AG and the testis, respectively (Ginsburger-Vogel & Charniaux-Cotton 1982; Charniaux-Cotton & Payen 1988). The AG is the sole source of the hormone responsible for sex differentiation (*i.e.* the commitment of the embryo towards the male or female pathway) and bilateral ablation of this gland provokes blockage of the differentiation of secondary male characteristics and decrease of spermatogenesis (Charniaux-Cotton 1954). Thus, sex differentiation can be manipulated through the surgical removal of the AG, without damaging the gonads. Males which have been andrectomized during the early developmental phase and which are unable to secrete the androgenic hormone, present a high degree of feminization, including initiation of oogenesis and development of oviducts and female gonopores, while ablation in late stages determines either partial or no feminization at all (Nagamine *et al.* 1980). In *M. rosenbergii* juvenile the surgical removal of the AG at an early growth stage results in a complete sex reversal, leading to the appearance of functional females capable of mating and producing progeny (Sagi *et al.* 1997). The common large-scale procedure applied so far to obtain all-male populations consists in microsurgical AG ablation and mass production of "neo-females" to produce all-male progeny. The occurred sex reversal is checked by removing the second left pleopod, which is that one bearing the male sex character,

the *appendix masculina*. After AG ablation in juvenile prawns and development of the secondary female sexual characters, neo-females (genetically males) are crossed in multiple steps with normal males, producing all-male offsprings (Aflalo *et al.* 2006, Fig. 2.13). This protocol is rather laborious, expensive in terms of time and money, and requires skilful workers.

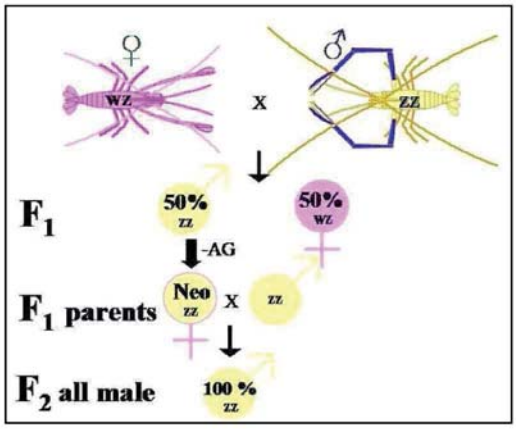

Fig. 2.13. Traditional procedure for obtaining all male populations of crustaceans. The surgical ablation of the androgenic gland (AG) leads to the occurrence of neo-females (genetically males) which are crossed with normal males. The new offspring is composed by all male individuals.

The advantage of the production of all-male populations by removing the AG has gone suggesting the need to establish novel technologies for sex reversal. In particular, it is going to drive attempts to find chemical methods for AG ablation, in particular by administrating specific apoptotic agents, which would avoid long progeny testing. Administrating apoptotic compounds at an early developmental step (chemical ablation), or silencing genes related to specific sex differentiation stages, could lead to sex reversal and, thus, yield all-male populations (Sagi & Aflalo

2005). In the frame of the PHARMAPOX Project, diatom extracts and their fractions were tested on crustaceans of commercial interest in order to evaluate a possible effect of *Cocconeis* diatoms on their AG. Applications of diatoms in aquaculture could represent a faster and elegant method to manipulate the sex in crustaceans and yield all-male populations, resulting in an increase of their production and sales.

3. Increasing the diatom biomass production

3.1. Introduction

One of the main problems to solve during the first phase of the investigation was represented by the small quantities of biological material, limiting factor for all the participant Institutes and the following steps of the work. Inadequate amounts of material did not allow purifying consistent quantities of compounds for both spectroscopic analysis and biological assays. The optimization of the cultivation methods and the consequent increase of the yields of diatom production were required, thus, as a first goal in the study. Since previous laboratory experiments had indicated *Cocconeis neothumensis* Kramer (Fig. 3.1) as one of the most active diatoms to induce apoptosis in *Hippolyte inermis*' androgenic gland among all the tested species (Zupo & Messina, unpublished data), producing 55.1% ± 7.5% females/total individuals (F/tot), the efforts for increasing the production were mainly focused on this species

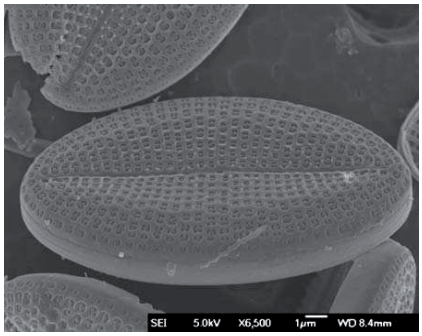

Fig. 3.1. *Cocconeis neothumensis.*

(Fig. 3.2). Parameters such as light intensity and nutrient concentration, along with two different systems of cultivation, traditional Petri dishes and bioreactor with continuous medium flow, were considered in our experiments in order to evaluate their influence on the diatom growth rate and maximum produced biomass.

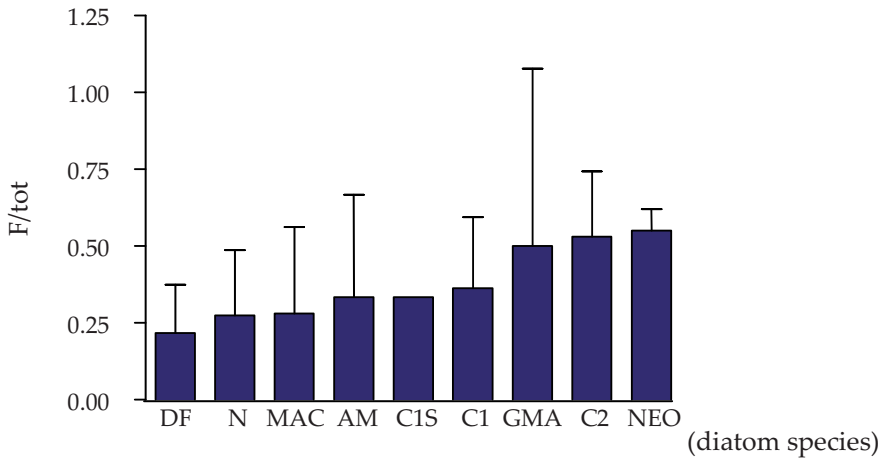

Fig. 3.2. Previous *in vivo* bioassays demonstrating that *C. neothumensis* produced the highest F/tot in *H. inermis* shrimps. DF = dried basic food (control); N = *Navicula* sp.; MAC = macroalgae; AM = *Amphora* sp.; C1S = freeze-dried *C. scutellum scutellum*; C1 = fresh *C. scutellum scutellum*; GMA = green microalgae; C2 = *C. scutellum parva;* NEO = *C. neothumensis* (Zupo & Messina, unpublished data).

Light is certainly one of the most important parameters affecting the growth rate of photoautotrophic organisms along with the concentration of silicates and selenium in the medium (Harrison *et al.* 1988; Round & Crawford 1990). In the experiment, the growth performances of *C. neothumensis* were estimated at various light intensities, in presence of selenium and at different silicate concentrations, along with the interactions between the two micronutrients. Benthic diatoms are commonly

cultivated in batch culture conditions (*i.e.* Petri dishes). The first bioreactor was developed in order to promote the growth of a benthic diatom, *Nitzschia* sp. used as food source (Fukami *et al.* 1997). Besides a reduced operational time and smaller overall dimensions, the main advantage of cultivations in bioreactors is the continuous renewal of the growth medium on the cell surface, which reduces the depletion of nutrients in comparison with batch conditions. The diethyl ether extracts (dry weight) of *C. neothumensis*, obtained per unit of substrate area, were used to compare the efficacy of both cultivations in batch conditions and bioreactor. Finally the effects of both different irradiances and changes in silicate and selenium availability on diatom growth were described.

3.2. Influence of different light intensities and micronutrient concentrations on the diatom growth rate

In order to determine the influence of different light intensities on *C. neothumensis* growth, three irradiances were tested (60, 100 and 140 µmol photons m^{-2} sec^{-1}), which are the most frequent intensities recorded in April, when the sex reversal of *H. inermis* occurs (Lorenti, unpublished data from the monitoring program of the Laboratorio di Ecologia del Benthos). A previous comparison of growth curves obtained at 17°C with those derived at a higher temperature (20°C), showed a significant decline in the length of the pre-exponential phase and, subsequently, a noteworthy reduction of the time requested to reach the maximal cell production.

Thus, 17°C was established as the optimal temperature for cultivating the benthic diatom. Five replicates were incubated for each established irradiance, in f/2 medium, at 17°C and at a 18:6 h photoperiod.

In parallel, the effect of different micronutrient concentrations on the development of the cultures was tested growing groups of five replicates of *C. neothumensis* in the following conditions:

- traditional f/2 medium without a selenium source and with 0.11 mM Na_2SiO_3;
- f/2 medium with a double concentration of silicates (0.22 mM Na_2SiO_3);
- f/2 medium plus a source of selenium at the concentration reported in the literature as the most favourable for the growth of several diatoms (10^{-8} M H_2SeO_3, Harrison *et al.* 1988);
- f/2 medium enriched both in silicates and selenium (0.22 mM Na_2SiO_3 and 10^{-8} M H_2SeO_3).

In this phase of the experiment, all the treatments were incubated at 140 µmol photons m^{-2} sec^{-1}, at 17°C and at a 18:6 h photoperiod. Cells were counted during the 17 days of incubation. Some diatoms were not able to survive for a long time, due to the damage provoked by scraping them from the bottom of the Petri dish. For this reason, the cell concentration of the cell suspension was not determined before its incubation. On the contrary, the cell density (number of cells mm^{-2}) was directly calculated for each replicate two days after the addition of the *inoculum* by counting the living cells adherent to the substratum per surface unit with a light microscope.

The cell density at the beginning of the experiments (*i.e.* two days after the inoculation) was *ca.* 3 cells mm^{-2} and this value represented the starting point for building the growth curves. Cell counts were subsequently realized every two days until reaching the stationary phase. For each replicate, the main parameters of the growth curve, *i.e.* the exponential growth rate (day^{-1}) and the cell density at saturation (cell mm^{-2}), were modelled and described with the four parameter logistic functions for asymptotic growth (Ratkowsky 1990), by means of Sigma-plot software (SPSS). In particular, the growth rate was derived for the region showing a straight-line relationship between variables in a semilog plot of cell density *vs.* time. The following equation was utilized:

$$(\ln C_2 - \ln C_1) x (t_2 - t_1)^{-1}$$

where C_2 and C_1 were the cell density at the experimental time t_2 and t_1, respectively (Wood *et al.* 2005). Light microscopic observations suggested that *C. neothumensis* formed a single layer of cells on the cup bottom; thus, the method we used did not cause significant errors in cell density estimations. In fact, the comparison of diatom dry weighs obtained after 17 days of incubation confirmed the proportions existing among the cell densities at saturation as derived for the different treatments by microscope counts.

3.3. Methods of cultivation

Besides the influence of different light intensities and micronutrient concentrations on the diatom growth rate, two diverse methods of cultivation were compared in terms of yielded biomass: traditional Petri dishes and bioreactor. Cultivation by Petri dishes (Fig. 3.3) is a quite laborious method. The fact that *Cocconeis* diatoms grow on monolayers requires a large available cultivation area. In addition, once attached to the bottom, diatoms have to be scraped off with a blade. In our experiment, diatoms cultures in Petri dishes were incubated in a thermostatic chamber at 17°C, 100 µmol photons m^{-2} sec^{-1}, at a 18:6 h photoperiod, according to the conditions which were used in previous experiments (Zupo 2001). The small-scale bioreactor (Fig. 3.4) was composed by a plexiglas pipe (26 cm length, 4.7 cm diameter), filled with 2 mm diameter glass beads forming several concentric layers used as substratum for algal growth. The glass beads allowed increasing the cultivation area, affording 7,157 cm^2 of substrate surface available for diatom development, equivalent to a surface of *ca.* 50 Petri dishes of 14 cm diameter, employed for batch cultures. All non-autoclavable components were sterilized by UV radiation.

Fig. 3.3. Diatom cultures in Petri dishes.

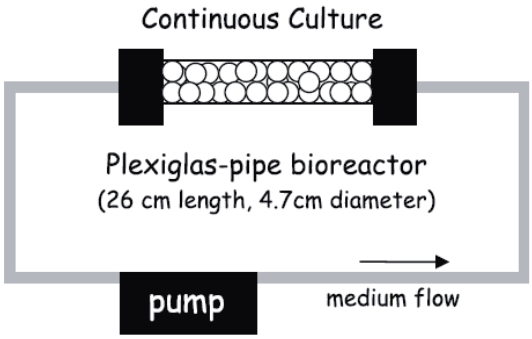

Fig. 3.4. Scheme of the continuous medium flow culture system.

A centrifugal pump provided a continuous f/2 medium flow of 7 l h^{-1} cm^{-2}, corresponding to *ca.* 540 turnovers per hour. The f/2 medium flowing inside the bioreactor was completely replaced every two days in order to limit the nutrient depletion during the cultivation period. A cell suspension, obtained from three *Cocconeis* cultures grown in Petri dishes, was inoculated into the system through the beaker in which the pump was immersed. At the beginning of the incubation, light intensity on the most superficial bead layer was 170 µmol photons m^{-2} sec^{-1}. When the culture reached the saturation point, probably as a result of substrate exhaustion rather than light limitation, the glass beads with *Cocconeis* diatoms still adherent on their surface, were washed with distilled water in order to eliminate salts and, afterwards, were frozen and freeze-dried until extraction.

3.4. Results

3.4.1. Effects of different light intensities on diatom growth

The growth curves at 60, 100 and 140 µmol photons m^{-2} sec^{-1} are shown in Fig. 3.5. Culture saturation was reached within 17 days of incubation at all the tested

irradiances. No significant differences were detected for the maximum cell density (*ca.* 2,000 cells mm^{-2} at all light intensities), while the exponential growth rate was significantly different ($p \leq 0.05$) among the three irradiances. The highest growth rate value was found at 60 µmol photons m^{-2} sec^{-1} (0.91 ± 0.04 day^{-1}), followed by 100 µmol photons m^{-2} sec^{-1} (0.73 ± 0.08 day^{-1}) and 140 µmol photons m^{-2} sec^{-1} (0.53 ± 0.02 day^{-1}).

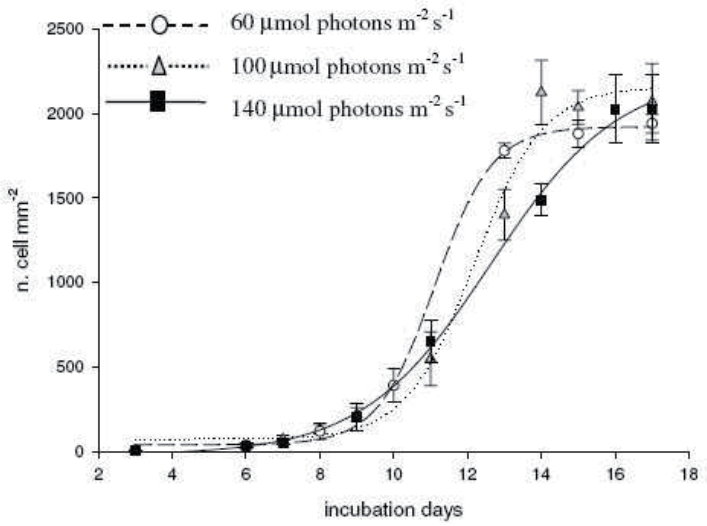

Fig. 3.5. Growth curves derived at three different irradiances (60, 100 and 140 µmol photons m^{-2} sec^{-1}).

3.4.2. Effects of different nutrient concentrations on diatom growth

The growth curves at 140 µmol photons m^{-2} sec^{-1} and at different micronutrient concentrations are shown in Fig. 3.6. The highest exponential growth rates were observed in f/2 medium plus selenium (1.03 ± 0.13 day^{-1}) and in the medium containing the double concentration of silicates (0.85 ± 0.11 day^{-1}) without significant

differences between the two treatments. These experimental conditions also provided the highest cell density at saturation (*ca.* 2,700 cells mm^{-2}). The lowest maximum cell densities at saturation (*ca.* 2,000 cells mm^{-2}) and exponential growth rates (*ca.* 0.53 day^{-1}) were measured in the f/2 medium with 0.11 mM Na_2SiO_3, and in the medium containing both the selenium source and the double concentration of silicates, without statistically significant differences between these two treatments.

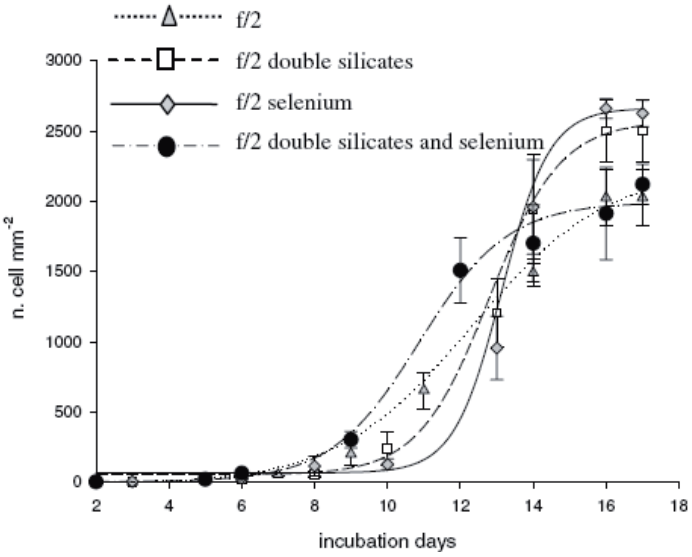

Fig. 3.6. Growth curves for *C. neothumensis* cultures incubated in f/2 medium with different Na_2SiO_3 and H_2SeO_3 concentrations at 140 µmol photons m^{-2} sec^{-1}.

3.4.3. Comparison between cultures in Petri dishes and bioreactor

The comparison of the two cultivation systems (Petri dishes and bioreactor) was carried out in terms of dry weight (DW) of diethyl ether extract. The yields of both culture systems expressed as mg of diethyl ether extract are shown in Table 3.1.

Culture system	Total substrate surface (cm^2)	Freeze-dried diatoms (mg)	Diethyl ether extract (mg-DW)
Batch culture (50 Petri dishes)	7,157	200	17 ± 3
Bioreactor system (one bioreactor)	7,157	N.D.	24 ± 5

Table 3.1. Quantitative comparison between the two culture systems in terms of mg-DW diethyl ether extract. N.D. not determined due to the use of the glass beads.

The diatom cultures in 14 cm diameter Petri dishes reached the saturation after 17 days of incubation, with an average yield of 4 mg-DW diatom powder per dish. Thus, 50 Petri dishes, corresponding to 7,157 cm^2 of substratum surface, provided *ca.* 200 mg-DW of diatom powder, with an average yield of 17.3 mg of diethyl ether extract (derived from three independent extractions). In the prototype, diatoms extensively covered the glass beads and reached the saturation after 17 days of incubation, when the bioreactor took a dark golden colour. The absorption factor of light through the bioreactor increased from 0.20 at the beginning of the incubation to 0.63 at culture saturation as a consequence of diatom growth on the outer bead layers. The increasing absorption factor determined the decrease of light intensity at the middle of the bioreactor from 100 µmol photons m^{-2} sec^{-1} to a final value of 40 µmol photons m^{-2} sec^{-1}. At saturation *ca.* 24.0 mg-DW of diethyl ether extract were afforded by the bioreactor, a significant higher yield (t-test; $n = 3$; $p \leq 0.05$) than from the same substrate area in batch cultures by Petri dishes. The different tested culture systems are shown in Fig. 3.7. Finally, a TLC comparison of the diethyl ether extracts

derived from the two culture systems showed the absence of significant differences between their metabolic patterns.

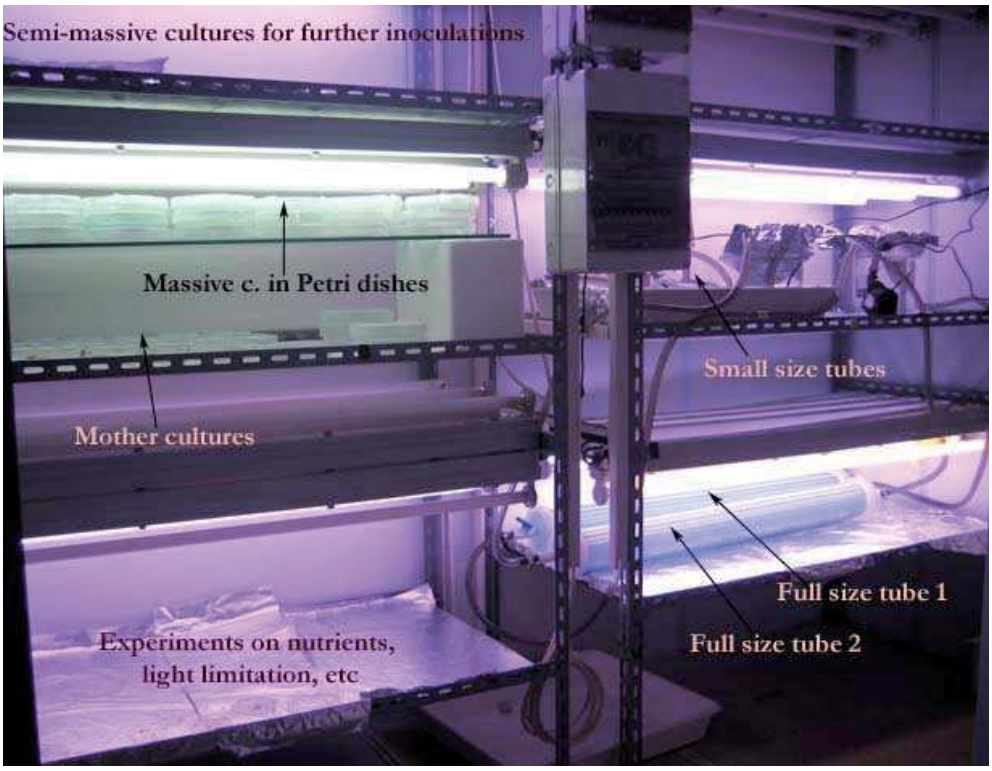

Fig. 3.7. The different systems of diatom cultivation. On the left, traditional Petri dishes (both mother cultures in 2.5 cm diameter Petri dishes and massive cultures in 14 cm diameter Petri dishes) and, on the right, the small prototype bioreactor and the large tube.

3.5. Discussion

These experiments demonstrated the advantage of the bioreactor system, in terms of operational time and overall dimensions in comparison with the traditional Petri dishes, for *C. neothumensis* cultivation. Moreover, the bioreactor furnished a

continuous medium flow, reducing the progressive depletion of nutrients at the cell surface which is characteristic in batch cultures. If nutrient availability was not the main limiting factor for cell growth inside the bioreactor, diatom development was affected by irradiance variability. In their habitat characterized by shaded areas on *Posidonia oceanica* leaves, epiphytes live at low light regimes. Nevertheless, the preferential environment for *Cocconeis* diatoms is represented by the apex of the most external leaf side (Mazzella *et al.* 1994), where the light attenuation is due to both seagrass canopy and epiphyte competition, and where the higher hydrodynamism favours the most strongly adherent species, *e.g. Cocconeis*. The experiments showed that *C. neothumensis* exhibited a faster growth at low light intensity, although with a good acclimation capacity in the range from 60 to 140 µmol photons m^{-2} sec^{-1}. A lower growth rate at the highest irradiances could be the result of photoinhibition, with a consequent reduction of cell growth and division rates. On the other hand, changes in light intensities did not affect the maximum cell density, clearly related to other factors, as well as nutrients. The good growth performances obtained in the range of 60-140 µmol photons m^{-2} sec^{-1} allowed the successful utilization of the bioreactor system. A characteristic of this culture system is the increasing self-shading due to the light absorption by the external layers. The irradiance in the middle of the bioreactor declined at 40 µmol photons m^{-2} sec^{-1} only at culture saturation but, according to our experiments, this light intensity was not critical for *C. neothumensis*. The continuous re-circulation of the medium and its replacement

every two days reduced the nutrient depletion on the cell surface, depletion that was typical for batch cultures. In addition to both reduced operational time and overall dimensions in comparison with the traditional cultures, the bioreactor was more advantageous also comparing the yields expressed by the DW of the diethyl ether extracts. Another parameter to be considered for improving the diatom biomass production was the medium composition. Contrastingly to macronutrients, which are selected and dosed in the most common culture media to satisfy the general requirement of a wide range of photoautotrophic organisms, the availability of micronutrients is more susceptible to optimization in relation to the particular physiological conditions and specific cultured organism (Keller & Selvin 1987). The presence of selenium in the medium improved both the exponential growth rate and the maximum cell density, probably due to its antioxidant function (Harrison *et al.* 1988). In particular, Price & Harrison (1988) demonstrated the existence of a selenoenzyme glutathione peroxidase in *Thalassiosira pseudonana* Hasle & Heindal, in which the presence of selenium also affected the diatom size, its ultrastructure and morphology (Doucette *et al.* 1987). Silicates are critical nutrients for diatoms both as components of the cell wall (the *frustula*) and as metabolic regulators (Round & Crawford 1990). Protein, DNA, chlorophyll and carotenoid synthesis are inhibited in absence of silicates, while photosynthesis and glycolysis are reduced (Werner 1978), and lipid synthesis is enhanced or altered (Taguchi *et al.* 1987; Roessler 1988). Furthermore, the activity of isocitrate dehydrogenase may be indirectly or directly

regulated by silicates (Werner 1978), while silicon would regulate gene expression (Okita & Volcani 1980) and two of the four DNA polymerases identified in the diatom *Cylindrotheca fusiformis* Reimann & Lewin are synthesized only in presence of silicates (Okita & Volcani 1978). These several roles of silicates in diatom physiology justified the reported positive effects of the increased silicate concentration on *C. neothumensis* cultures, in terms of both exponential growth rate and cell density at saturation. In the medium enriched with selenium and a doubled silicate concentration, in turn, no increase in both the exponential growth rate and cell density at saturation was evidenced. On the contrary, in this case no significant differences were observed between this treatment and the normal f/2 medium. Thus, the simultaneous increase of silicate concentration and presence of selenium led to a loss of the positive effects observed with the single nutrients, suggesting a possible antagonism in selenium and silicate uptake or negative interactions between the two micronutrients. It was demonstrated that selenium accumulation in *Skeletonema costatum* was inversely dependent on the environment silicate concentration and this suggested that the same transport pathway worked in the diatom for both the anionic metals with a consequent competition in silicate and selenium uptake (Wang & Dei 2001). Thus, a higher SiO_3^{2-} amount in the medium was hypothesized to reduce SeO_3^{2-} uptake by *C. neothumensis* cells and *vice versa*. In addition, a negative interaction between selenium and silicates inside the cell was another possible explanation of these results, although limited data have been reported so far in the

literature about the metabolic interference between selenium and silicates (Müller *et al.* 2005). In conclusion, the increase of silicate concentration or the addition of selenium to the culture medium could be considered as possible alternative strategies for improving *C. neothumensis* biomass production in bioreactors, which showed to afford higher yields and less laborious work than the classical cultivation of benthic diatoms in Petri dishes.

3.6. Problems and delays

3.6.1. Towards the scaled up production

Once demonstrated the better performances of the "small" prototype with respect to the traditional Petri dishes in maximising the diatom production and shortening the time for reaching sufficient biomass, we tried to improve the bioreactor system in order to obtain a scaled up biomass production. With this purpose, a new production system was devised, consisting of two identical plexiglas tubes (150 cm length, 9 cm diameter each one) filled with 2 mm glass beads. When diatoms reached the stationary phase, the optical microscope observation revealed the presence of chitinolytic bacteria (*i.e.* cyanobacteria corroding the shrimp's exoskeleton, Fig. 3.8)

Fig. 3.8. Presence of chitinolytic bacteria inside the large full-size tube.

instead of diatoms. Cyanobacteria-infected larvae grew slowly and, when they reached the end of the experiment, they were smaller than normal individuals, often immature. During the incubation, a continuous increase of the pH was recorded in the medium, reaching a peak of 9.4. A CO_2 diffuser was added in order to stabilize the pH at 8.4, but when the pipes were opened, chitinolytic bacteria were found again, suggesting the occurrence of contamination during the inoculation into the pipes. Despite all the attempts of sanitization (sterilization of all the autoclavable components, washing with hydrogen peroxide of all non-autoclavable components, in particular plastic tubes, rubber tubing, pumps, *etc*., and filtration of the seawater), the new bioreactor continued not to afford diatoms. Afterwards, it was hypothesized that these results were due to the higher water flow rate in the large bioreactor with respect to the conditions applied in the prototype. Because a high flow rate could negatively affect the diatom growth, it was reduced to 30 l h^{-1} cm^{-2}, and the several phases of the production were monitored introducing microscope slides in the collector beaker. The procedure was repeated changing some variables (*e.g.* light irradiance, because a high light in a f/2 medium could favour different organisms from diatoms), and the system was stopped earlier in order to avoid the diffusion of cyanobacteria but, nevertheless, no sign of diatoms was detected. In addition, since the higher speed of the water pump of the large bioreactor could produce breakage of the inoculated diatoms due to the impact with the rotor, a different inoculation system was devised. It consisted in aspirating the diatoms by a sterile syringe whose

needle was directly inserted into the rubber tubing connecting the culture tubes with the medium tank, and it enabled the diatoms to be transferred directly on the beads, without passing through the pump. But also with these measures, results continued to be negative. Another production system based on a wave generator (Fig. 3.9) was experimented as well and the preliminary results seemed to be encouraging in terms of diatom yields. It consisted in a large container positioned under the light, containing a devise able to spry water and produce waves. The container was connected to a large bowl, positioned below, in a dark area, terminating with a sedimentation device connected with a tube for sampling. All the structure was autoclaved whereas the plastic non-autoclavable parts were sanitized using hydrogen peroxide. Diatoms were inoculated into the large glass container by a pump. After some days, diatoms started to grow on the bottom. Some of them were detached by the generated waves and, through the water flow, reached the sedimentation device. After 2 weeks, diatoms could be collected on the bottom of the dark device. Collected diatoms were rinsed with distilled water, freeze-dried and weighed, prior to be bioassayed. The wave reactor produced a total of 219 mg of acetone extract, corresponding to about 700 mg of dried diatoms in about 1 month of

Fig. 3.9. The wave generator system.

activity. But, despite the yields, the obtained extracts demonstrated negligible activity and the system was interrupted. In order to avoid stopping the production and not accumulate further delays, it was decided to return to the traditional diatom cultivation by Petri dishes, a more laborious but safer method (with less variables) than the bioreactor. In the meantime, the performances of sealed (by synthetic film, Parafilm®) and not sealed Petri dishes were evaluated. It was observed, in fact, that sealed Petri dishes produced less amounts of diatoms than open Petri dishes, probably due to a higher availability of atmospheric CO_2 in the latter ones, as reported in Table 3.2. As demonstrated, open Petri dishes afforded 26 x 10^6 diatoms/dish, corresponding to 672 mg of diatoms, whereas sealed Petri dishes yielded 16 x 10^6 diatoms/dish corresponding to 450 mg of diatoms. Paired t test, applied on 69 couples of data, afforded significant differences between open and closed Petri dishes: the former produced 33% more than the latter ($p < 0.0001$).

Petri dishes	**Number of Petri dishes**	**Dry weight (mg of diatoms)**
Open	100	672
Sealed	101	450

Table 3.2. Yields of both open and sealed Petri dishes.

3.6.2. Change of the diatom species

The first part of the project was exclusively centred on *C. neothumensis*, since it was reported to be the most active diatom to induce apoptosis in *H. inermis*' AG in studies realized prior to the PHARMAPOX Project. Although the conditions of the production and the biological effect of the diatom had been previously studied (Zupo 2001), many factors had to be re-examined and changed in the frame of the project due to the peculiar experimental conditions forced by the protocols. One of the main aspects which has not been clarified yet is the loss of activity of *C. neothumensis* demonstrated by *in vivo* bioassays on *H. inermis* shrimps. These experiments, realized incorporating diatom extracts into the shrimp food with the purpose of identifying the most active extract in triggering apoptosis in the shrimp's AG, showed a high percentage of male individuals. It meant that the diatoms had a scarce effect on the shrimp sex reversal. The loss of activity was suggested to be probably due to stress of the larvae or employment of a different diatom strain, but no one of these hypothesis could be demonstrated. Consequently, upon comparing *C. neothumensis* extracts with other diatom species (*C. posidonia*, *C. dirupta*, *etc.*), *C. scutellum* was chosen as the best candidate significantly affecting the F/tot ratio of *H. inermis*. Thus, since the new lines of *C. neothumensis* were not anymore adequate to our purpose and *C. scutellum* continued to have an effect comparable with that observed in the previous studies (Fig. 3.2), it was established to use *C. scutellum* for the following steps. *C. scutellum*

was cultivated in Petri dishes, according to the results of the studies for improving the diatom production. The change of diatom species produced remarkable delays in all the phases of the project, especially in the chemical studies.

3.6.3. Mortality and stress in *Hippolyte inermis* shrimps

Other important factors which limited the performance of *in vivo* bioassays on *H. inermis* and biassed the results of many experiments, were the high mortality (close to 100%) and the stress of larvae and postlarvae. The stress, acting on larvae and postlarvae, negatively influenced the male/female ratio. In order to by-pass these serious limitations, several foods were tested. The best experimental conditions for the maximum performances during the larval rearing were represented by 4 nauplii of *Artemia salina* enriched in Algamac per ml of culture medium, and 4 individuals of *Brachionus plicatilis* per ml of culture medium. On the other hand, the best diet for postlarval growth consisted of: Tetra AZ shrimp food (33% weight), pure *Spirulina* (33% weight) and enriched lyophilized *Artemia* (33% weight). This diet was sufficient to maximize the larval and postlarval growth and minimize both mortality and stress, producing largest percentages of males in the controls, without influencing the tests. The presence of so high larval and postlarval mortality and stress was never experienced before the start of the project, and it was probably due to the peculiar conditions imposed by the procedures.

4. Chemical composition of the benthic diatom *Cocconeis scutellum*

4.1. GC-MS: features and applications

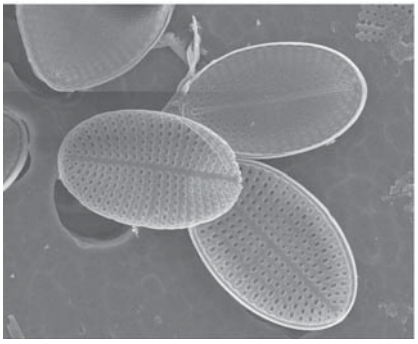

Fig. 4.1. *Cocconeis scutellum.*

The determination of the metabolic pattern of *Cocconeis scutellum* Ehrenberg, 1838 (Fig. 4.1) has been a crucial step of the investigation, because it has allowed hypothesizing the nature of the compounds responsible for the apoptotic effects on *Hippolyte inermis*' androgenic gland. The chemical study of *C. scutellum* was performed by gas chromatography in combination with mass spectrometry (GC-MS), one of the most powerful tools in the modern analysis to separate and identify complex mixtures of compounds. GC-MS is a technique which provides high separation, rapid automatic identification of known compounds, acquisition of structural information about unknown compounds, analysis of isomers and identification of co-eluting molecules. In turn, it is limited to volatile, thermostable and less than 1,000 Da compounds. The apparatus consists in a

gas-chromatograph, which volatizes and separates the sample, and a mass spectrometer, which allows determining the molecular weight (MW) of each isolated compound. Depending on the ionization source, the compounds can undergo fragmentation in the mass spectrometer, which affords further structural information. The fragmentation is particularly evident in EIMS, *i.e*. MS in electron impact mode, in which the ionization is provoked by a high energy electron beam. In CIMS, *i.e.* with chemical ionization source, the electron beam is substituted by a gas, usually methane, and the fragmentation is lower than in EIMS so that it is easier to detect the molecular ion and, thus, the molecular weight of the compound. In ESIMS, *i.e.* with electron spray source, the sample is dissolved in a polar (protic) solvent in order to favour acid-base reactions and generate ions. After vaporization by means of an atomic gun, ions are accelerated by an electric field and directed to the analyzer. In FAB mode, *i.e.* with fast atom bombardment source, ionization and volatilization of the sample (dissolved in a polar solvent) occur contemporaneously by means of a beam of heavy atoms, such as xenon. In addition, high resolution mass spectrometry (HRMS), affording the exact MW of the compounds (due to the exact isotopic masses), enables to determine their molecular formula.

Many plant metabolites are usually analyzed by GC-MS: alkaloids, hydrocarbons, fatty acids, fatty alcohols, sterols, terpenes, organic acids, amino acids, sugars, alcohols, glycerides. Polar compounds cannot be detected by GC, but derivatization enables to transform them into more apolar and volatile molecules. Fatty acids (FAs),

in fact, are usually identified after conversion into their methyl esters (FAMEs). The protection of the polar groups permits to increase the peak height and resolution, which is very important for the identification of minor components. Many compounds, *e.g.* alcohols, instead, have to be transformed into their trimethylsilyl (TMSi) derivatives in order to mask their hydroxy groups. In addition, lipids and glycerides in particular have to be hydrolyzed in order to convert them into lower molecular weight compounds (Christie 2003).

In our investigation GC-MS was chosen as preliminary technique of analysis in order to have a general idea of the molecular classes of metabolites contained in the diatoms, in parallel to the bio-guided fractionation.

4.1.1. Fragmentation

In MS in EI mode, the electron-transferred energy triggers molecular fragmentation. When a compound undergoes fragmentation, some bond cleavages are preferred rather than others, depending on the structural characteristics of the fragmenting ion. Among all the possible fragmentations, the favourite ones are generally those provoking the most stable fragments, *i.e.* the most branched radicals and/or the most substituted carbocations. The several classes of compounds are characterized by certain fragmentation profiles and some peaks are particularly diagnostic for a specific molecular class. Here we report the usual MS profile of some groups of

compounds which were detected in *C. scutellum*, in particular saturated and unsaturated fatty acids, glycerides and sterols.

In mass spectra of saturated fatty acids (SFAs, Fig. 4.2), the presence of peaks at *m*/*z* 43, 57, 60, 73, 129, $[M - 43]^+$ (loss of a propyl), $[M - 29]^+$ (loss of an ethyl) is common. The peak of the molecular ion of a linear chain monocarboxylic acid is weak, but usually distinguishable. The most characteristic peak (sometimes the base peak) is at *m*/*z* 60, deriving from McLafferty rearrangement (involving the O atom of the carboxy group and the H at γ position with respect to CO). The fragmentation profile is similar to that of an alkylic chain because it is characterized by groups of peaks differing one another in 14 mass units, corresponding to CH_2. The most abundant fragments correspond to C_3 and C_4 units (*m*/*z* at 43 and 57, respectively). In long chain fatty acids the spectrum is composed by two series of peaks deriving from all C-C bond cleavages with retention of the electric charge on the oxygenated fragment or the alkylic portion.

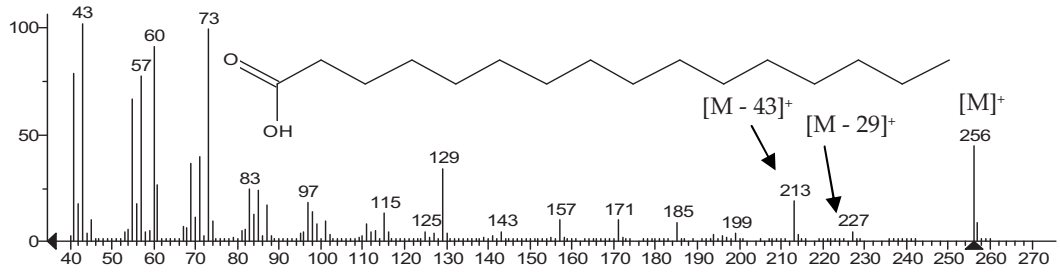

Fig. 4.2. Mass spectrum of *n*-hexadecanoic acid, a saturated fatty acid.

In the mass spectrum of monounsaturated fatty acids (MUFAs, Fig. 4.3), the fragments containing the double bond show peaks of two H units less than the corresponding SFAs (*m*/*z* at 41, 55, 69, 83, *etc*.). The loss of water from the molecular ion, $[M - 18]^+$, is also noteworthy. In simple alkenes the migration of the double bond makes difficult to determine its position.

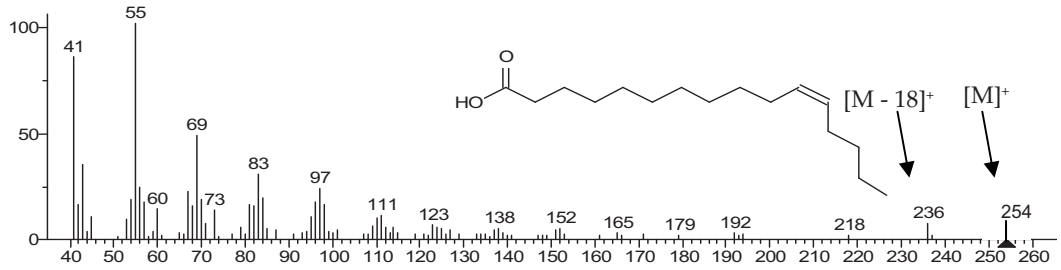

Fig. 4.3. Mass spectrum of (*Z*)11-hexadecenoic acid, a monounsaturated fatty acid.

Saturated fatty acid methyl esters (Fig. 4.4) show peaks at *m*/*z* 43, 55, 74, 87, 129, 143, $[M - 31]^+$ (representing loss of the methoxy group) and $[M - 43]^+$ (loss of a C_3 unit *via* a complex rearrangement).

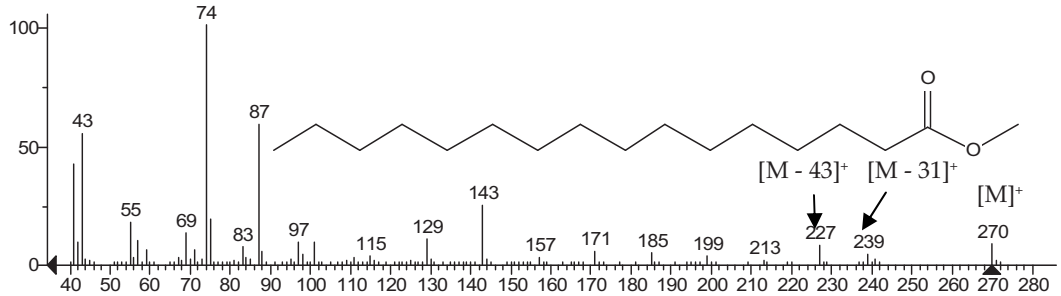

Fig. 4.4. Mass spectrum of hexadecanoic acid, methyl ester.

The molecular ion of a FAME is generally clearly visible, and ions caused by loss of methanol and McLafferty rearrangement are abundant. The peak at *m/z* 74, due to McLafferty rearrangement (Fig. 4.5), is diagnostic for methyl esters without α-ramifications and it represents the base peak for linear chain C_6-C_{26} methyl esters.

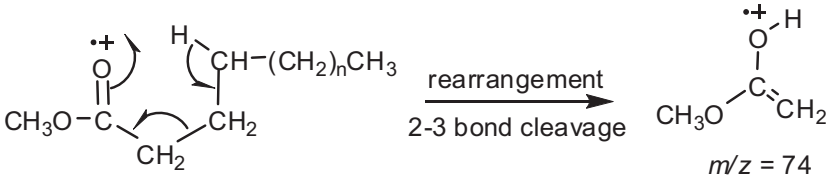

Fig. 4.5. McLafferty rearrangement in methyl esters.

The MS profile of monounsaturated FAMEs is characterized by the presence of peaks at *m/z* 41, 55, 69, 74, 83, $[M - 32]^+$, $[M - 74]^+$. The peak $[M - 116]^+$ is noteworthy, along with homologous ions, due to loss of a fragment containing the carboxy group derived from the C-5/C-6 cleavage with addition of a rearranged hydrogen atom. Thus, in contrast to the spectra of saturated fatty acid methyl esters, hydrocarbon ions with general formula $[C_nH_{2n-1}]^+$ dominate the spectrum with *m/z* 55 as base peak usually. Furthermore, there is no feature that permits the location of the double bond, because this can migrate to any position when the alkyl chain is ionized in the mass spectrometer. Thus, all the *cis*- and *trans*-isomers have virtually identical spectra between them (Fig. 4.6).

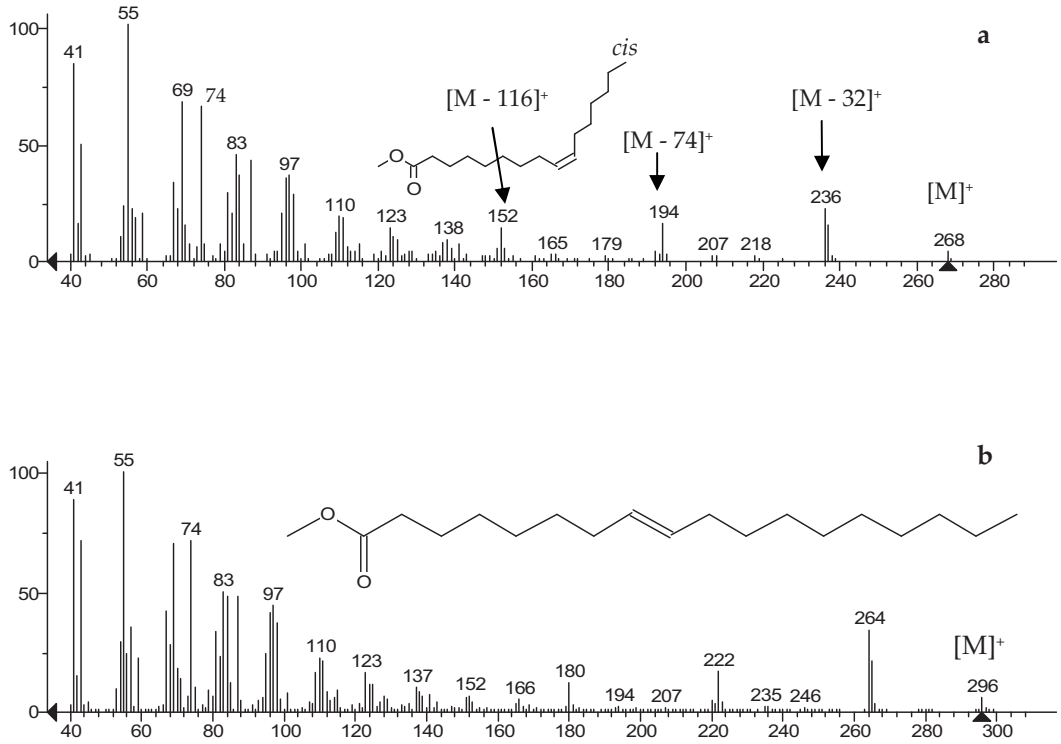

Fig. 4.6. Mass spectra of *cis* and *trans* monounsaturated FAMEs, the 9-*cis*-hexadecenoic acid, methyl ester (a) and the 8-*trans*-octadecenoic acid, methyl ester (b). The two spectra show the same peaks and the same losses.

Double bonds can be indicated by two different ways: counting from the carboxy group (C-1) or the terminal CH_3, opposite to the carboxy group. In this latter manner, the double bond is indicated with ω or n preceded by a number corresponding to its position with respect to the terminal methyl. In PUFAs, it is possible to localize the ω double bond by means of particularly significant peaks: *m*/*z* at 108 for ω-3 double bonds, *m*/*z* at 122 for ω-4, *m*/*z* at 150 for ω-6, and *m*/*z* at 192 for the ω-9 family.

Dienes (Fig. 4.7) are characterized by peaks at *m*/*z* 41, 55, 67, 81, 95, 109, $[M - 31]^+$ (loss of the methoxy group), and $[M - 74]^+$.

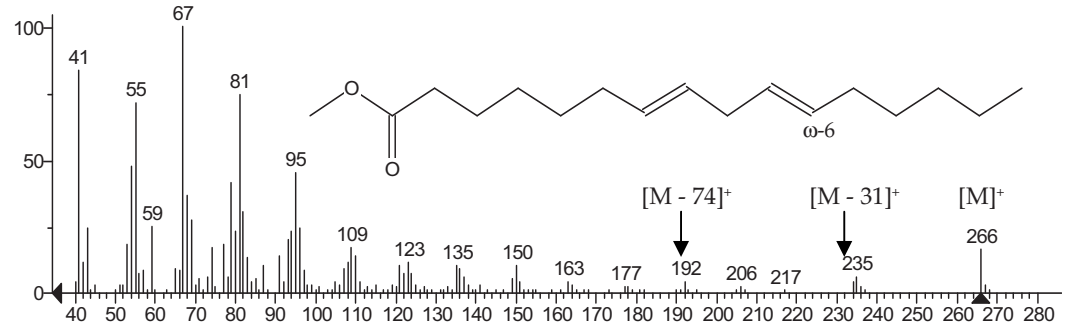

Fig. 4.7. Mass spectrum of 7,10-hexadecadienoic acid, methyl ester. The peak at *m*/*z* 150 is diagnostic for ω-6 fatty acids.

In trienes (Fig. 4.8), peaks at *m*/*z* 41, 55, 67, 79, 95, 108, $[M - 31]^+$ are present. Here, in the lowest molecular weight region, hydrocarbon ions of general formula $[C_nH_{2n-5}]^+$ tend to dominate the spectrum with the ion at *m*/*z* 79 as base peak**.**

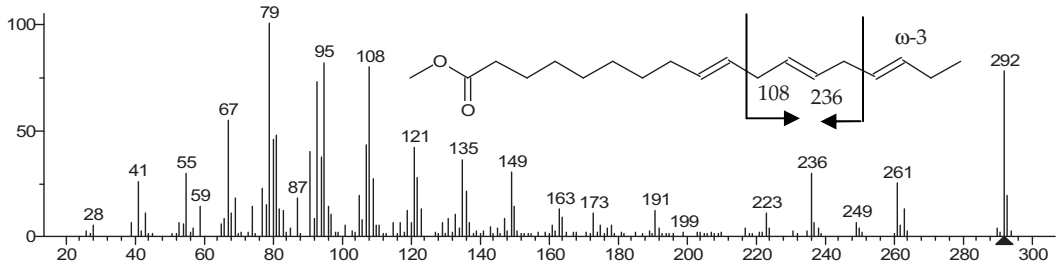

Fig. 4.8. Mass spectrum of 9,12,15-octadecatrienoic acid, methyl ester. The presence of the base peak at *m*/*z* 79 is particularly noteworthy. The peak at *m*/*z* 108 is indicative for ω-3 fatty acids.

Characteristic fragments in tetraenes are at *m*/*z* 41, 55, 67, 79, 95, 105 (Fig. 4.9).

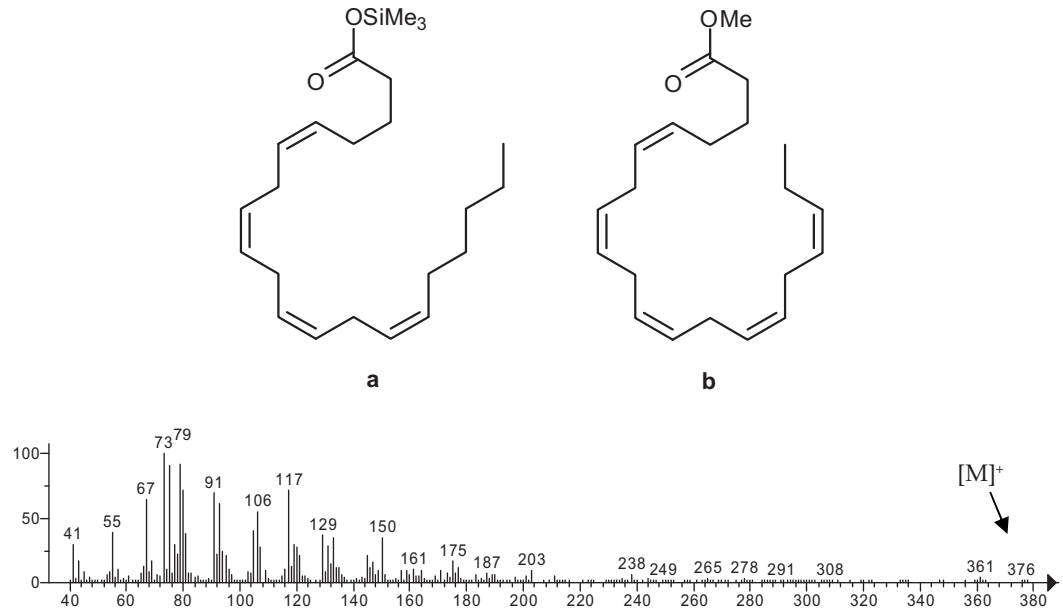

Fig. 4.9. Mass spectrum of **a**: 5,8,11,14-eicosatetraenoic acid (arachidonic acid), TMSi ester (all *Z*).

In pentaenes the molecular ion is just discernable with some amplification of the spectrum, but it is very difficult to individuate the "diagnostic" ω ion at *m*/*z* 108 for ω-3 double bonds (Fig. 4.10).

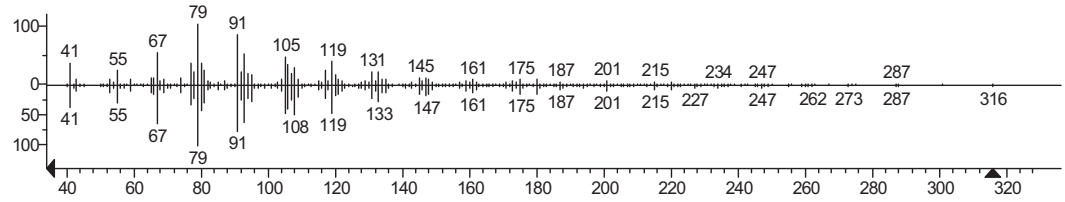

Fig. 4.10. Mass spectrum of **b**: 5,8,11,14,17-eicosapentaenoic acid (EPA), methyl ester (all *Z*).

The molecular ion in fatty alcohols is quite small (Fig. 4.11). Derivatization or CI source may be requested in order to make discernible the molecular ion and, thus, the molecular weight. The cleavage of the C-C bond at α with respect to the oxygen atom is of general occurrence. A distinct peak can be found at *m/z* $[M - 18]^+$ due to the loss of water. The fragmentation of long chain alcohols is dominated by the hydrocarbon pattern.

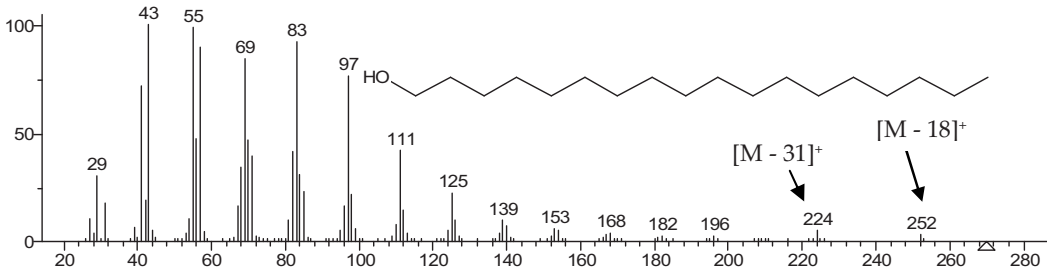

Fig. 4.11. Mass spectrum of 1-octadecanol.

Mass spectra of glycerol as TMSi derivative (Fig. 4.12), and tocopherol (Fig. 4.13) are also reported.

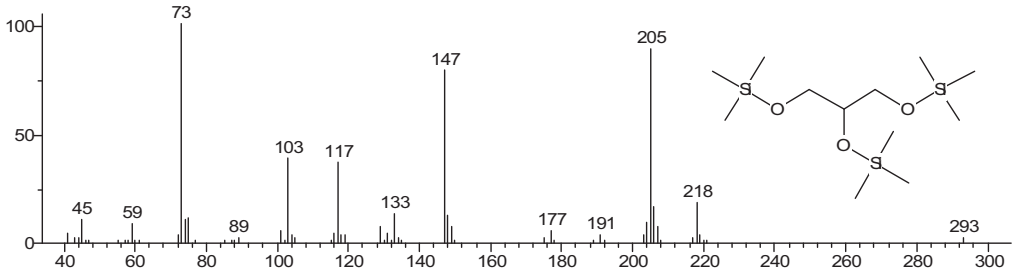

Fig. 4.12. Mass spectrum of glycerol as TMSi derivative.

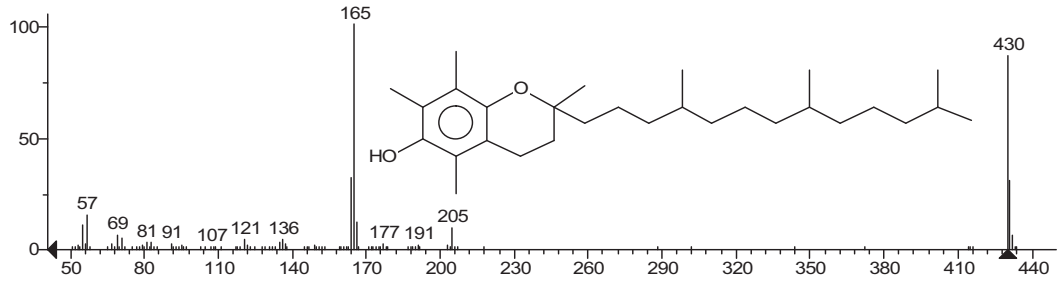

Fig. 4.13. Mass spectrum of tocopherol (vitamin E).

Sterols have intensive molecular ions and fragments depending on both the length and structure of the side chain. Mass spectra of some sterols found in *C. scutellum* (brassicasterol, ostreasterol and 24-methylcholesterol) are shown in Fig. 4.14-4.16.

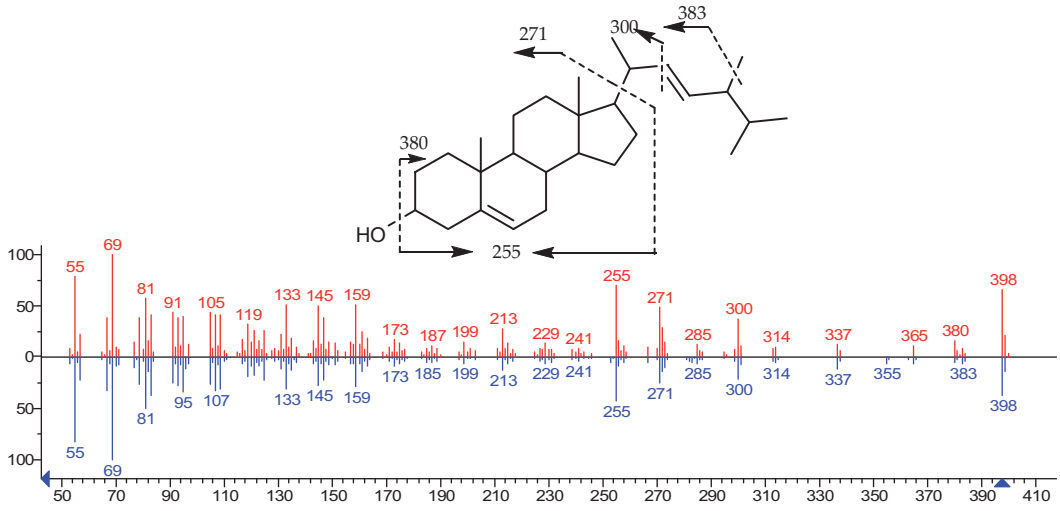

Fig. 4.14. Brassicasterol (red) in comparison with the mass spectrum of a standard compound from NIST 98 library (blue).

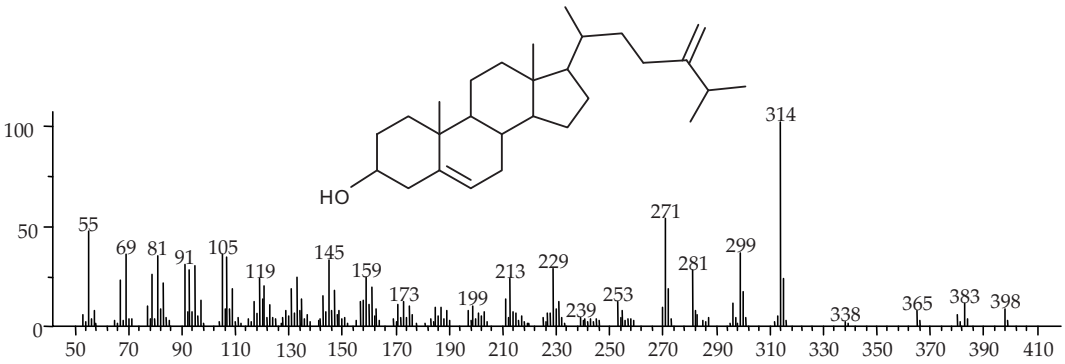

Fig. 4.15. Mass spectrum of 24-methylencholesterol (ostreasterol).

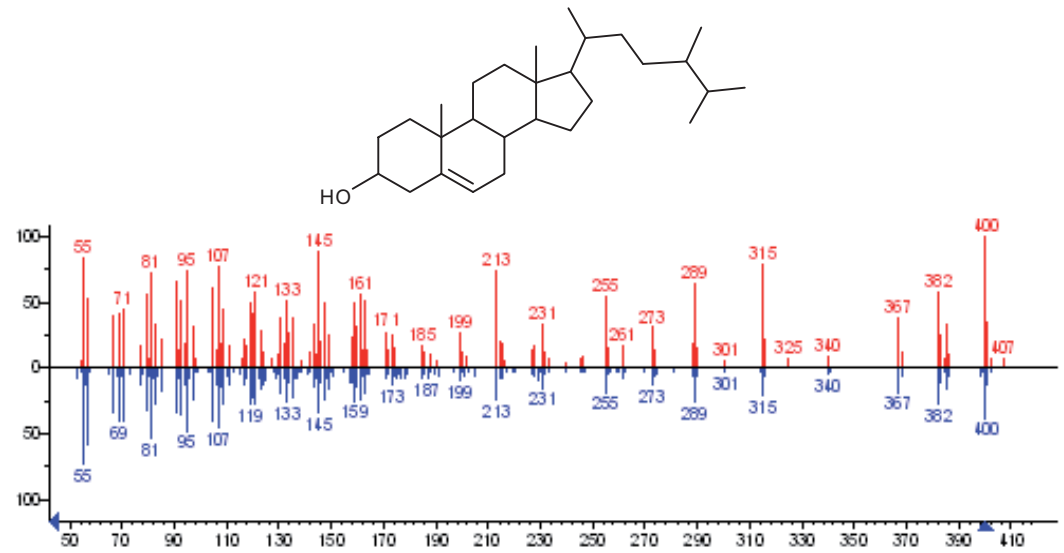

Fig. 4.16. Mass spectra of 24-methylcholesterol (red) in comparison with the standard extracted from NIST 98 library (in blue).

4.1.2. GC parameters

The identification of the metabolic composition of *C. scutellum* was performed on the basis of the mass spectra of the diatom extracts in comparison with the instrument

database. In the analysis of the data some parameters were considered, such as the retention time (R_t) and, mainly, the retention index *RI* (or Kovats retention index).

R_t is the time recorded between the sample injection and the emergence of the maximum peak of the analyzed compound. It is indicative for each kind of compounds but it is not reproducible, because it depends on the instrumental variables, the laboratory conditions, *etc*.

RI allows quantifying the relative elution times of compounds in GC. It is a number obtained by interpolation (usually logarithmic), expressing the retention of a compound in terms of R_v (retention volume) or R_t compared with two standards, one eluting before, and another one eluting after the peak of the sample component. The standards are represented by *n*-alkanes and *RI* is given by the equation:

$$RI = 100\left[\frac{\log X_i - \log X_z}{\log X_{(z+1)} - \log X_z} + z\right]$$

where X refers to the adjusted retention volume or time for the sample compound (i), z is the *n*-alkane standard eluting before the sample, and $z + 1$ represents the *n*-alkane standard eluting after the sample. *RI* expresses, thus, the number of carbon atoms (multiplied by 100) of a hypothetical *n*-alkane which would have an adjusted R_v (or R_t) identical to that of the peak of interest when analyzed under identical conditions.

4.2. Isolation and purification

4.2.1. Biological material

Cocconeis scutellum diatoms were collected in spring along Ischia coasts, Italy (Fig. 4.17) and cultivated in the Stazione Zoologica "A. Dohrn" (Ischia) within the period March 2005-January 2008. The collected biomass was freeze-dried and transferred to the CEAB-UB, where it was stored at -20°C until extraction.

Fig. 4.17. Site of collection, Ischia, Italy.

4.2.2. Extraction

A sample of freeze-dried *C. scutellum* (*ca.* 2.2 g) was reconstituted with distilled water and extracted with acetone, an organic solvent that allows the extraction of large polarity range compounds. The acetone is water-mixable, not very reactive neither very expensive and promotes an exhaustive extraction of the biological material. The

extraction was improved by ultrasound sonication in order to increase the cell membrane disruption and the release of compounds from them. The afforded suspension was filtered on a paper filter, the organic solvent was evaporated under reduced pressure and, afterwards, the residue was further diluted in distilled water. In order to differentiate more apolar from less apolar compounds, the aqueous phase was partitioned first between water and diethyl ether and, subsequently, between water and *n*-butanol. The water/diethyl ether extraction enables a good repartition of polar and apolar components and, in addition, the diethyl ether is able to separate itself very efficiently from the water. On the other hand, the *n*-butanol is more polar than diethyl ether and allows extracting compounds like alkaloids, small peptides, *etc*. Both the diethyl ether and the butanol extracts were subjected to preliminary TLC screening using different eluant systems, and the silica plates were developed with several reagent solutions in order to evaluate the presence of specific functional groups. In particular, cerium sulphate is a general reactive for organic compounds; Erhlich's reagent allows detecting heterocyclic compounds, mainly furano derivatives; both diphenylboric acid and diazo solutions are able to detect phenolic compounds; ninhydrine is specific for amino acids; Dragendorff's reactive is useful to recognize alkaloids. Among these reagents, only the cerium sulphate solution gave positive reaction with the crude extracts, indicating the absence of those functionalities the other reagents were specific for. As observed on the TLC plate, the metabolic pattern of the diethyl ether extract consisted mainly in glycerides (in the

upper part of the silica plate), fatty acids (characterized by the skimming half-moon shape, below the glycerides) and sterols (R_f 0.5 light petroleum/diethyl ether 1:1 v/v) (Fig. 4.18).

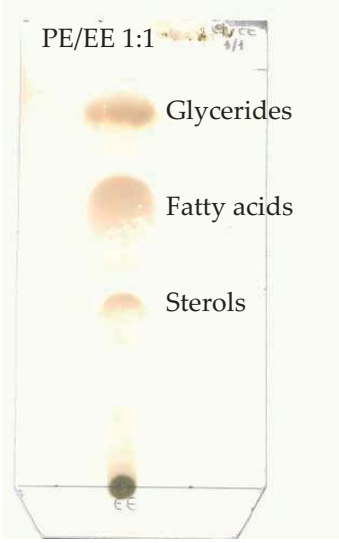

Fig. 4.18. A TLC plate of the diatom diethyl ether extract developed in light petroleum/diethyl ether 1:1 v/v. The common profile of glycerides, fatty acids and sterols is discernible on the chromatofolium. Glycerides are in the upper part of the plate. Fatty acids are below glycerides and have got a characteristic skimming shape, while sterols are usually in the middle of the plate (R_f 0.5 in light petroleum/diethyl ether 1:1 v/v).

Subsequently, both the diethyl ether and the butanol extracts were analyzed by GC-MS after adequate derivatization. The procedure of derivatization is shown in Fig. 4.19. The recorded spectra were evaluated by AMDIS software and compared with the data reported in literature for analogous compounds. The GC-MS analysis of both the extracts confirmed the occurrence of glycerides, fatty acids and sterols in the diethyl ether extract, and showed the presence of sugars, fatty acids, glycerides and isoprenoid compounds in the *n*-butanol fraction.

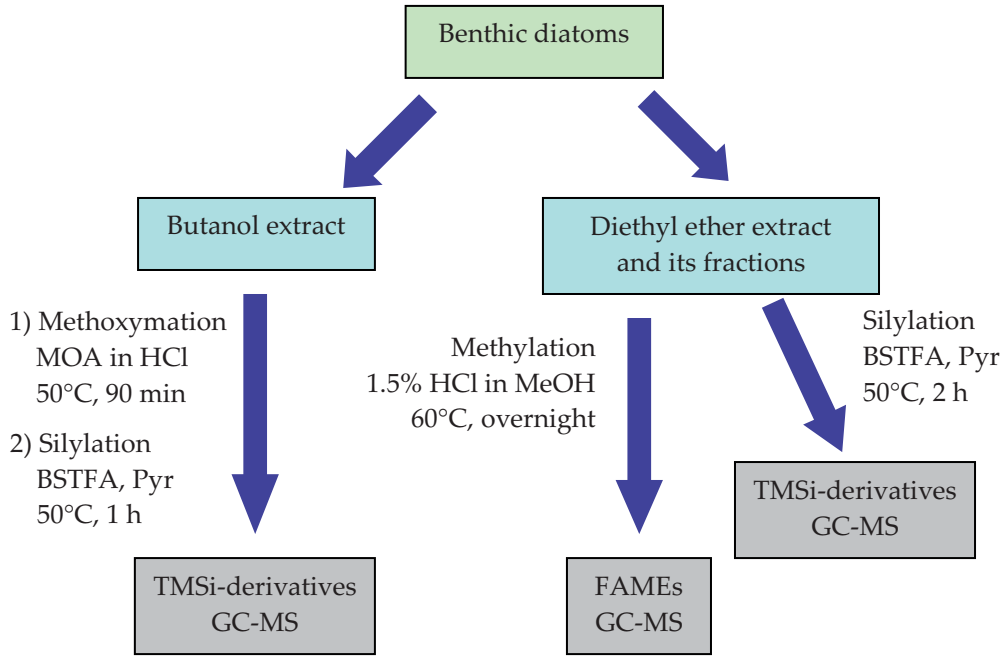

Fig. 4.19. Procedure of derivatization of the diatom extracts.

4.2.3. Fractionation

The diethyl ether extract was fractionated by size exclusion chromatography. The extract was loaded onto a pre-packed Sephadex LH-20 column and eluted with chloroform/methanol 1:1 v/v. The collected fractions were combined into three main portions, named **1**, **2** and **3**, respectively (Fig. 4.20), and analyzed by GC-MS after careful derivatization. Fraction **1** was mainly characterized by glycerides, whereas FAs were present in traces; fraction **2** contained glycerides and FAs and, finally, fraction **3** consisted of FAs and low amounts of sterols.

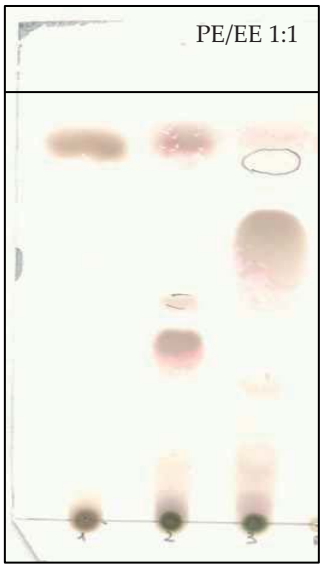

Fig. 4.20. TLC plate of the three fractions obtained by purification of the diatom diethyl ether extract. The plate was eluted with light petroleum/diethyl ether 1:1 v/v.

4.3. Search for aldehydes

Polyunsaturated aldehydes (PUAs), produced by planktonic diatoms, have been recognized as responsible for teratogenic effects and reduced fecundity in copepods. The harmful effects towards copepod populations exhibited by octa-2,4-dienal, octa-2,4,7-trienal, hepta-2,4-dienal produced by *Skeletonema costatum* and *Thalassiora rotula*, along with those of deca-2,4,7-trienal synthesized by *T. rotula*, have been widely reported in the literature (Miralto *et al.* 1999; d'Ippolito *et al.* 2002; Fontana *et al.* 2007). During the chemical investigation on *C. scutellum*, a possible role of aldehyde compounds in the diatom-induced apoptosis was hypothesized. In order to evaluate the presence of aldehydes in *C. scutellum* diatoms, we followed the protocol proposed for the extraction and determination of such compounds (d'Ippolito *et al.* 2002).

According to the literature, a sample of frozen *C. scutellum* diatoms (*ca.* 1 g) was defrosted, diluted in distilled water, sonicated at room temperature, left on the bench and, afterwards, extracted with acetone. The suspension was centrifuged and the supernatant was partitioned between acetone and chloroform. After separation, the chloroform phase was dehydrated with Na_2SO_4 and evaporated to dryness. Both the $CHCl_3$ extract and the reference compounds (heptadienal, octadienal and decadienal) were derivatized with (carbetoxyethylidene)-triphenylphosphorane (CET-TPP). The treatment with CET-TPP enables to transform, by Witting reaction, eventual unstable and cumbersome aldehydes into their ethyl esters (Fig. 4.21).

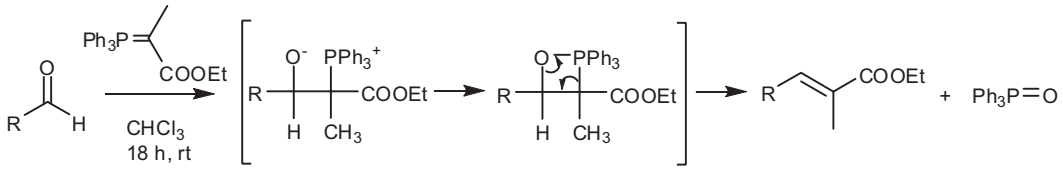

Fig. 4.21. Mechanism of action of Witting reaction.

These derivatives can be stored and, above all, are much more easily detectable by routine GC-MS than aldehydes themselves (d'Ippolito *et al.* 2002). Both the derivatized extract and the reference aldehyde derivatives were analyzed by GC-MS. The mass spectra of the CET-derivatized extract were compared with those of the CET-aldehyde derivatives and the NIST 2005 mass spectral library.

4.4. Results of the chemical study

The GC-MS analysis of both the diethyl ether and *n*-butanol extracts resulted in the detection of 124 metabolites, about 100 of which were identified. The chemical pattern of *C. scutellum* diatoms is reported in Tables 4.1 and 4.2 (pp. 103-107). The extraction procedure allowed partitioning the diatom compounds into an apolar fraction (diethyl ether extract, 12% of the total diatom biomass) and a polar fraction (*n*-butanol extract, 5% of the original sample). Representative chromatograms of both the diethyl ether and *n*-butanol extracts are shown in Fig. 4.22.

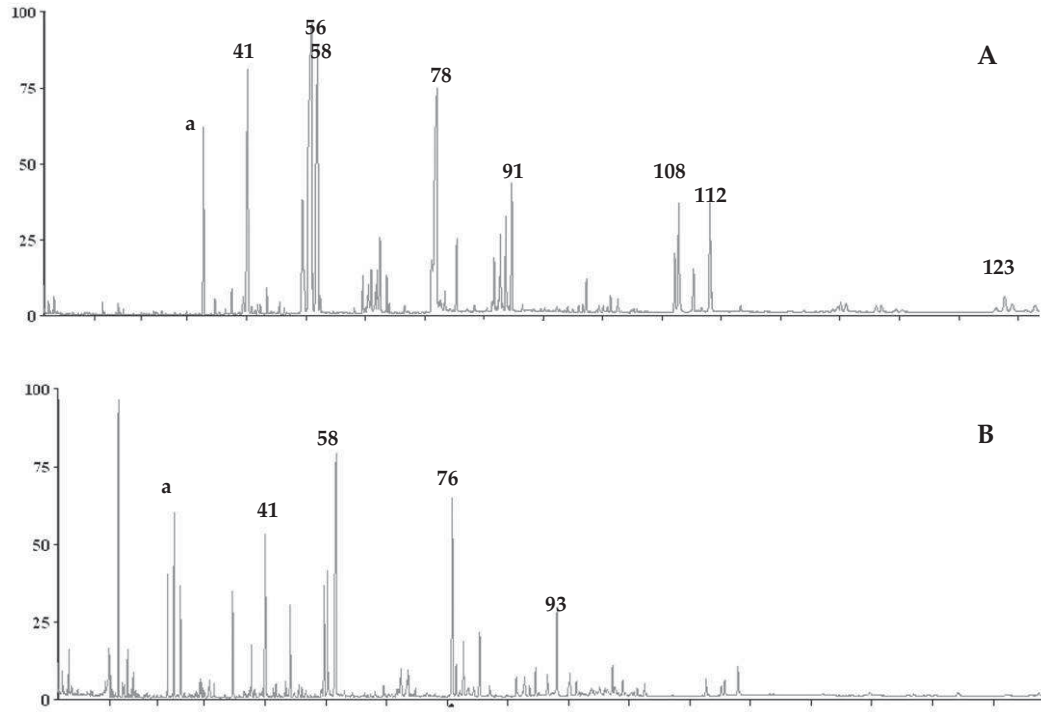

Fig. 4.22. GC-MS chromatograms of both the diethyl ether (A) and the *n*-butanol extracts (B) of *C. scutellum*. The numbers correspond to the compounds of Table 4.1 pp. 103-106 (a: diethyl ether stabilizer).

All the identified compounds and those still to be characterized (but comprising more than 0.2% of the total ion current, TIC) are included in the tables.

The chemical pattern of the diethyl ether extract consisted of FAs (75.8%), glycerides (10.8%), sterols (4.7%), isoprenoid compounds (3.6%) as well as alkanes, fatty alcohols and phosphates in minor amounts (Table 4.2 page 107, and Fig. 4.23).

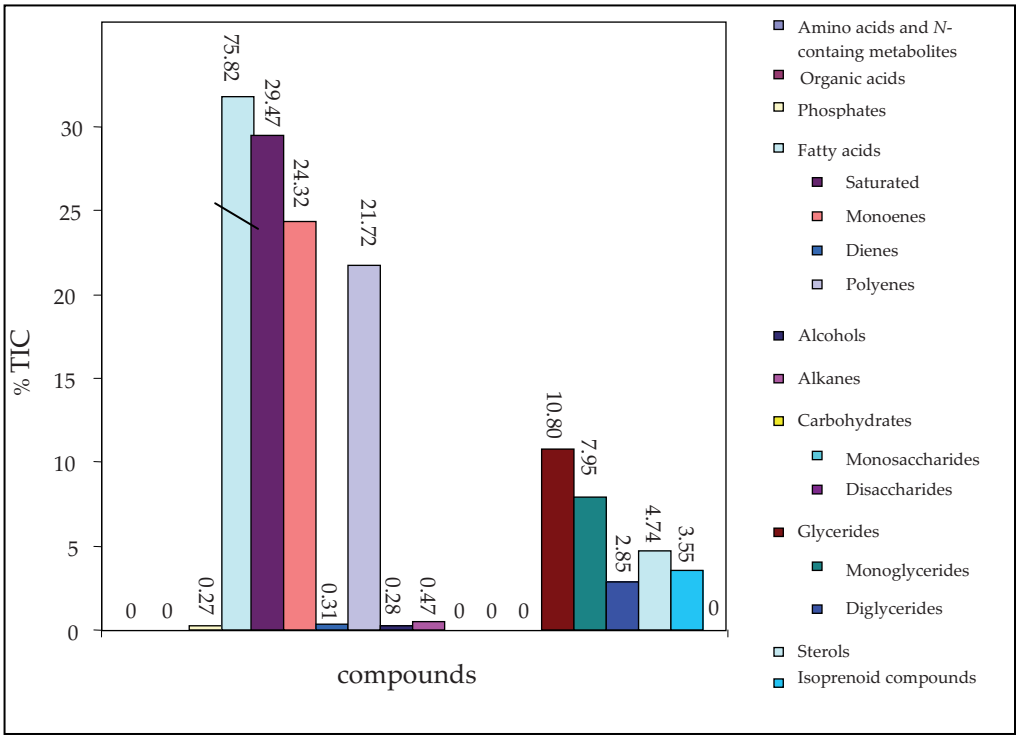

Fig. 4.23. Metabolic composition (% of TIC) of the diethyl ether extract determined by GC-MS.

It was characterized by FAs from C_{10} to C_{26}, dominated by C_{16} and C_{20} (expressed as percentage of total FAs): 16:0 (16.2%), $16{:}1\Delta^{9}$ (29.2%), $16{:}4\Delta^{6,9,12,15}$ (5.5%) and $20{:}5\Delta^{5,8,11,14,17}$ (16.4%). Relatively high levels of 14:0 (9.5%) and 15:0 (9.1%) FAs were

found as well. FA pattern was dominated by SFAs (38.9%), followed by MUFAs (32.1%) and PUFAs (28.6%). The glyceride pattern was dominated by monoglycerides with a mono/diglyceride ratio of 2.8:1. The glycerol-esterified FAs were 14:0, 16:0, 16:1, 18:0 and 18:1. The main esterified FAs (presented as % of total glycerides) in monoglycerides are 16:0 (53.3%) and 16:1 (39.0%). The diglycerides were esterified mainly with 14:0 and 16:1, or 16:0 (24.3%) and 16:1 and/or 16:0 (75.7%) FAs. Five sterols were detected in *C. scutellum*: 24-methylenecholesterol (ostreasterol, 51.9% of total sterols) was the main compound followed by sterol A (23.0%), brassicasterol (20.0%), cholesterol (3.4%) and campesterol (1.6%).

The profile of the *n*-butanol fraction (Fig. 4.24) was dominated by FAs (44.6%) followed by low molecular carbohydrates (24.5%), amino acids and other *N*-containing compounds (9.5%), alcohols (8.8%), glycerides (4.4%), organic acids (2.5%), isoprenoid compounds (1.2%) and phosphates (0.1%). GC-MS analysis resulted in the identification of several monosaccharides (96.5% of total carbohydrates) and one disaccharide (sucrose **94**, 3.5% of total carbohydrates). The most abundant low molecular carbohydrate was floridoside (2-*O*-glycerol-D-galactopyranoside **76**, 45.7% of all carbohydrates). Amino acids (ten identified compounds) comprised 18.1% of all detected *N*-containing compounds, while the nucleosides adenosine and uridine along with urea were 44.9%, 4.7%, and 24.6%, respectively. Alcohols were represented mainly by glycerol (8.6% of the polar fraction). Several organic acids, including the phenolic hydroxycinnamic acid,

monoglycerides, two isoprene compounds (tocopherol and phytol) and glycerol-3-phosphate were detected in trace amounts in the extract as well.

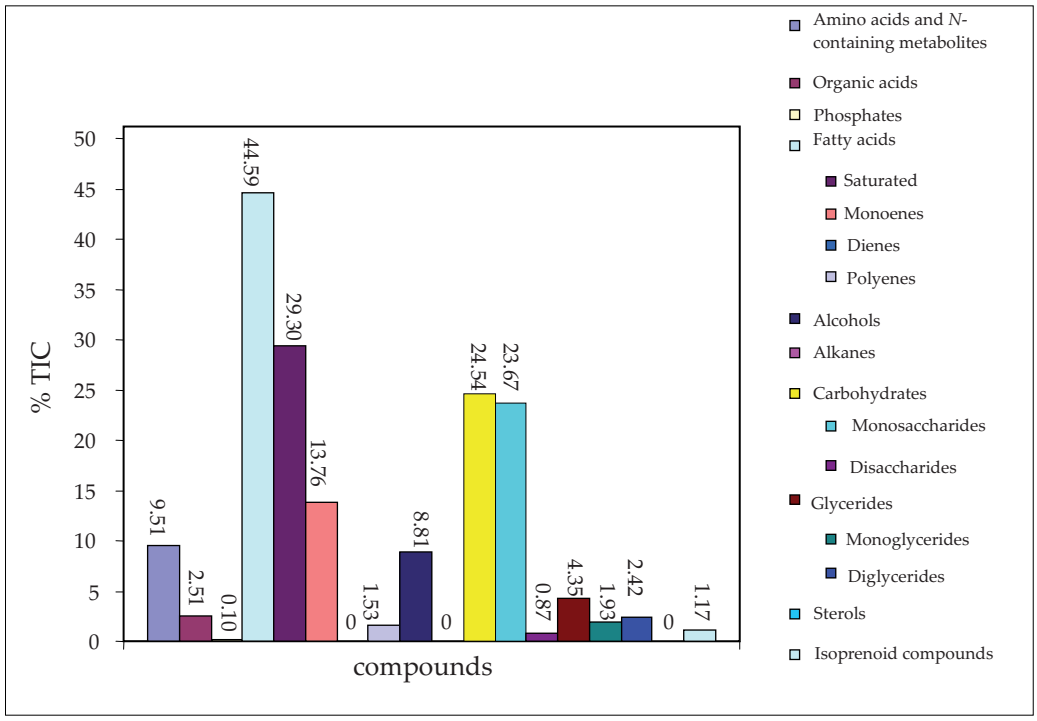

Fig. 4.24. Metabolic composition (% of TIC) of the butanol extract determined by GC-MS.

The metabolic composition of the three fractions in which the diethyl ether extract was separated is reported in Table 4.3 (page 108). Fraction **1** contained FAs (2.4% of TIC), isoprenoid compounds (3.7%) and glycerides (77.2%), of which 27.5% were monoglycerides and 49.7% diglycerides. Fraction **2** consisted of FAs (66.7% of TIC), of which 25.5% were saturated, 35.0% monounsaturated and 6.2% polyenes, as well as phytol (0.51%), sterols (3.1%) and monoglycerides (11.0%). Fraction **3** was represented by FAs (81.7% of TIC), of which 14.4% were saturated, 51.7%

monounsaturated and 15.6% polyunsaturated and, furthermore, by 24-methylcholesterol (2.31%). Many compounds found in the whole diethyl ether extract were not detected in the fractions, probably because they were retained in the column during the fractionation or too diluted to be recorded.

On the other hand, GC-MS analysis did not support the presence of aldehyde compounds in *C. scutellum*. The comparison of the mass spectra of the CET-derivatives of the reference compounds with those of the CET-derivatized diatom extract did not show common fragmentation profiles between the standards and the diatom extract.

4.5. Discussion

The chemical pattern of the diatom *C. scutellum* was determined by GC-MS in both EI and CI modes. The lipid chemistry of algae, and diatoms in particular, relies mainly on the analysis of FAs as FAMEs by GC-EIMS (Mansour *et al.* 2005). In the present work, FAs of both the diethyl ether and the *n*-butanol extracts were analyzed as FAMEs in parallel to their TMSi derivatives in order to obtain additional information using their specific MS fragmentation (α and ω ions) to determine the position of double bonds in PUFAs (Christie 2003; Mjos & Pettersen 2003). In EIMS of FAs, $[M]^+$ and $[M - 15]^+$ for the TMSi derivatives, and $[M]^+$ and $[M - 31]^+$ for the FAMEs, were easily distinguishable and this allowed, along with other characteristic ions, their

unambiguous identification. In other cases, such as long chain PUFAs, these ions were hardly detectable and GC-MS analysis in CI mode was used to display their MW. The $[M + 1]^+$ of FAs in CIMS spectra was the most abundant ion (base peak), while in EIMS spectra $[M]^+$ was decreasing at the increase of the number of carbons and double bonds. An example is given in Fig. 4.25, in which $16:4\Delta^{6,9,12,15}$ and $16:2\Delta^{9,12}$ co-eluted and their separation, MS deconvolution and identification in EIMS mode were problematic due to the similarity of their fragmentation pattern, low amount of $16:2\Delta^{9,12}$ and very low abundance of their $[M]^+$ and $[M - 15]^+$ ion fragments. However, GC-CIMS analysis provided unambiguous identification and separation by their base peak ($[M + 1]^+$ at *m*/*z* 321 for $16:4\Delta^{6,9,12,15}$ and at *m*/*z* 325 for $16:2\Delta^{9,12}$. Recently, such an approach was used for the analysis of FAs in samples of fish origin (Dayhuff & Wells 2005). The FA composition of *C. scutellum* was similar to that published for other diatoms (Rousch *et al.* 2003; Pistocchi *et al.* 2005). The presence of the odd chain 15:0 FAs is noteworthy, since this has been only rarely reported for diatoms (Parrish *et al.* 1991; Gordon *et al.* 2006), although it has been found in other organisms such as bacteria and thraustochytrids (mycoplancton) (Naganuma & Horikoshi 1994; Kamlangdee & Fan 2003).

The identification of mono- and diglycerides was based on comparison of their fragmentation pattern with reference compounds, and defining their $[M]^+$ (when detectable) and $[M - 15]^+$ ion fragments in EIMS mode.

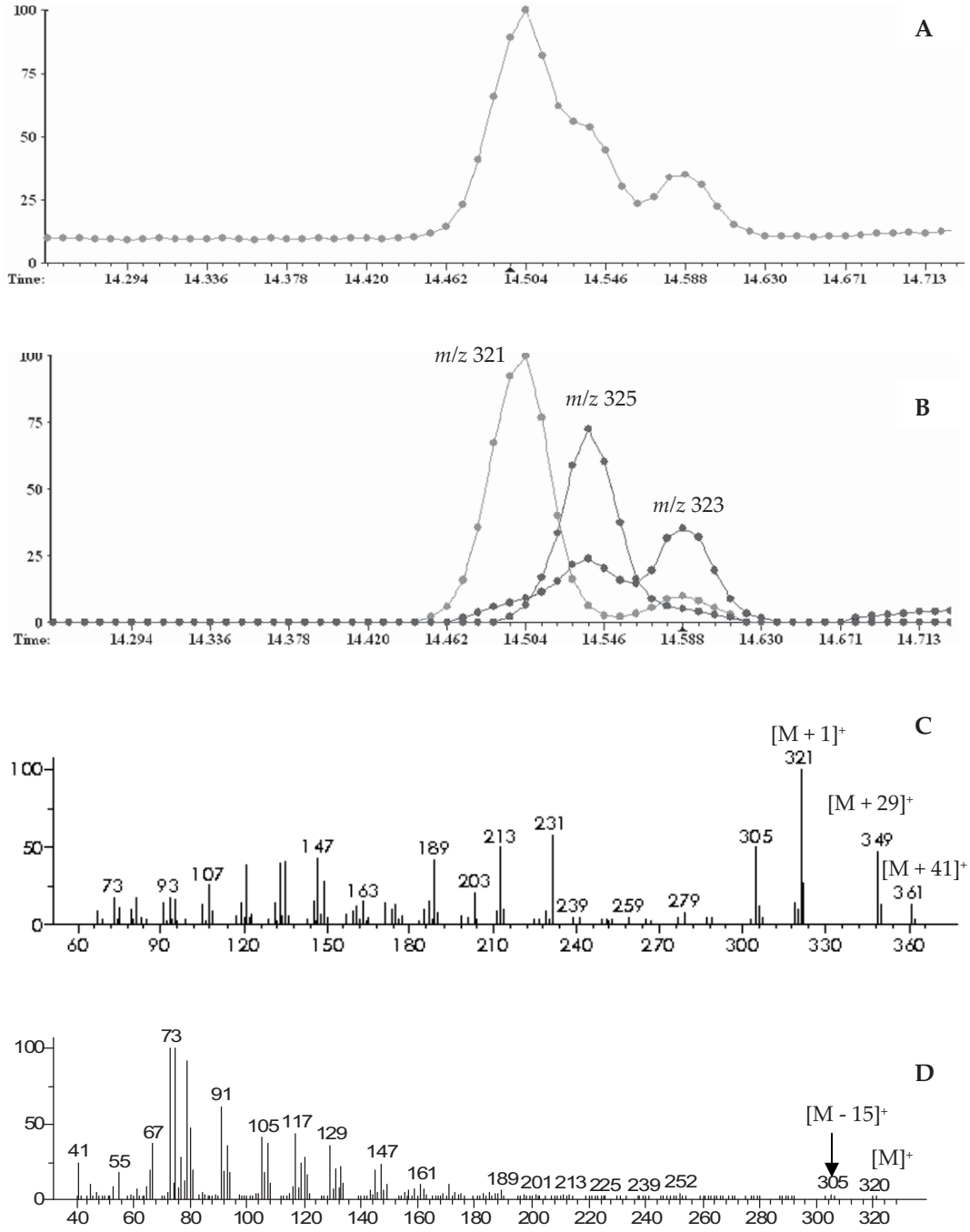

Fig. 4.25. GC-CIMS separation of 16:4$\Delta^{6,9,12,15}$ ([M + 1]$^+$ at *m/z* 321), 16:2$\Delta^{9,12}$ ([M + 1]$^+$ at *m/z* 325) and 16:3$\Delta^{6,9,12}$ ([M + 1]$^+$ at *m/z* 323). TIC chromatogram (A), selected ion chromatogram (B), GC-CIMS of 16:4$\Delta^{6,9,12,15}$ (C) and GC-EIMS of 16:4$\Delta^{6,9,12,15}$ (D).

The 1-monosubstituted glycerides showed an intense $[M - 103]^+$, often as base ion, and detectable $[M - 15]^+$ and $[M]^+$. The 2-monosubstituted glycerides showed a base peak ion at *m/z* 103 or 129 and characteristic losses $[M - 15]^+$, $[M - 90]^+$, $[M - 161]^+$ and $[M - acyl]^+$. In contrast to EIMS, the CIMS spectra of 1- or 2-monosubstituted glycerides displayed similar fragmentation pattern with relatively intense $[M + 1]^+$ ions, confirming their MW (Fig. 4.26). Diglycerides possessed relatively intense $[M - 15]^+$ ions and characteristic fragmentation depending on the position of substitution as indicated in Fig. 4.27. The presence of triglycerides was not confirmed by GC-MS since their boiling-point would be above the highest temperature used in the elution program. The structures of sterols were confirmed by comparing EIMS of both TMSi derivatives (in terms of *RI*) and non-derivatized compounds with those of reference compounds or literature data. Sterols determine the diatom value as food, which can affect predators' growth, as reported in oysters (Patterson *et al.* 1993). Unlike higher plants, algae and microalgae contain a large diversity of sterols (Boutry *et al.* 1979; Véron *et al.* 1998) whose profiles can be sometimes characteristic of a particular class, family, genus or even species and, thus, used for chemotaxonomic and phylogenetic purposes (Volkman 1986; Patterson 1992). 24-Methylenecholesterol (**112**) was the principal sterol as in other diatoms (Gladu *et al.* 1991; Pistocchi *et al.* 2005). It showed a $[M]^+$ at *m/z* 398, a base peak at *m/z* 314 (characteristic of the 24-methylene group) and an intense ion at *m/z* 271 (loss of the side chain) in agreement with literature data (Gladu *et al.* 1991; Souchet & Laplante 2007).

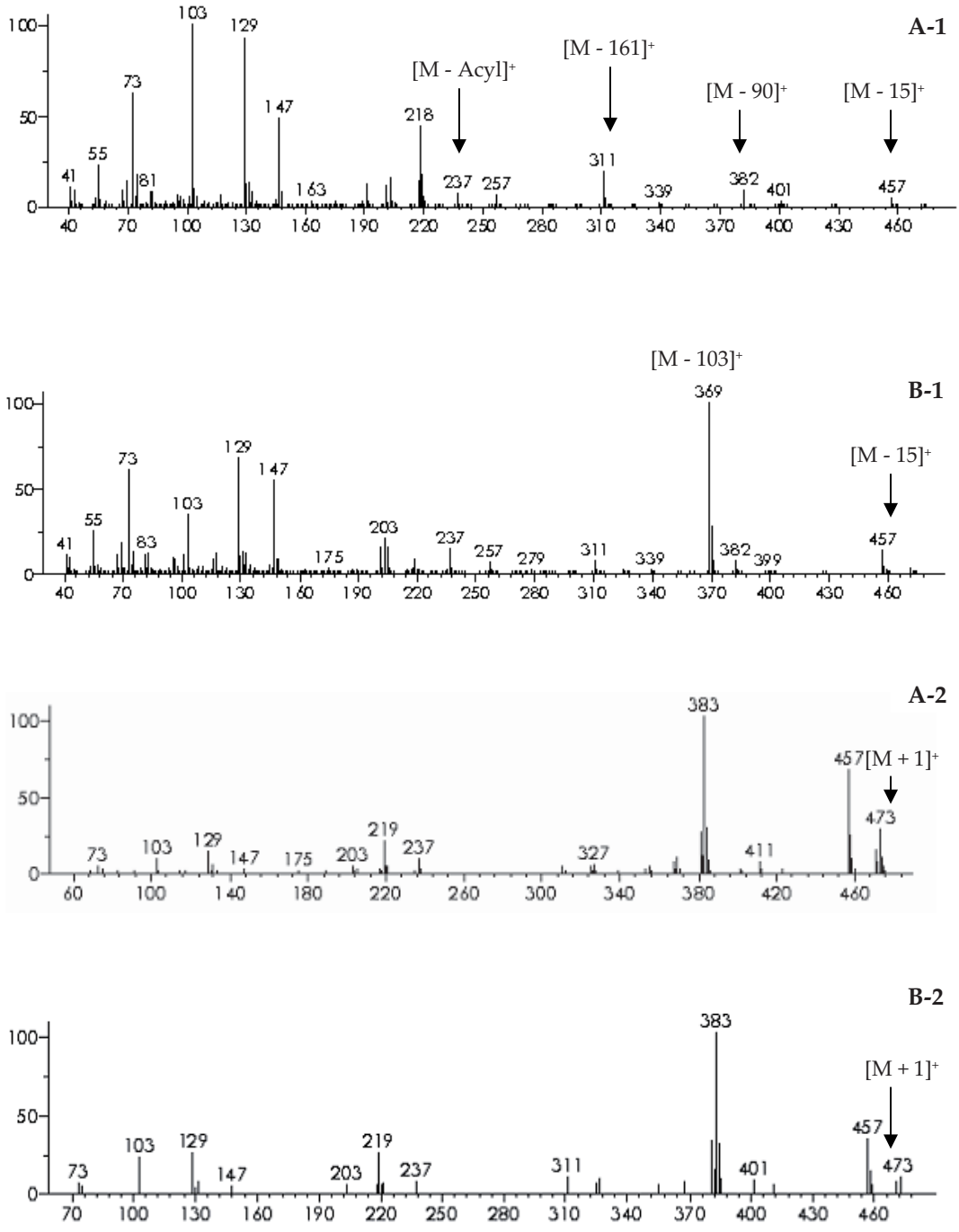

Fig 4.26. GC-EIMS (A) and GC-CIMS (B) of 1-monohexadecenoylglycerol (1) and 2-monohexadecenoylglycerol (2).

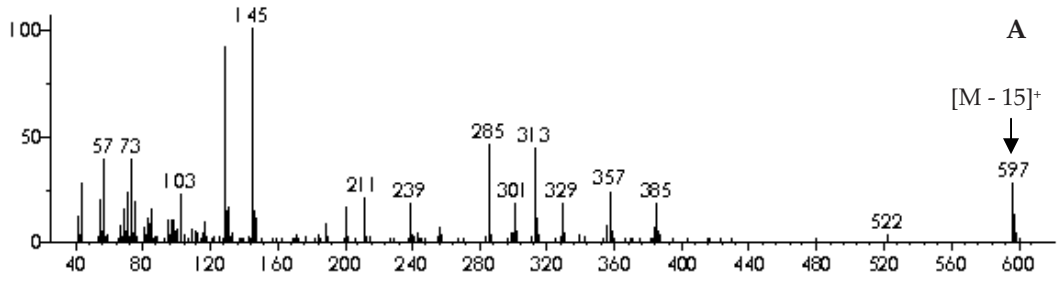

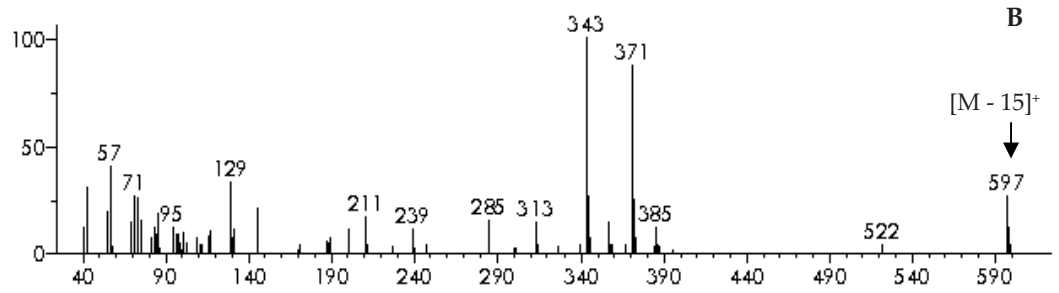

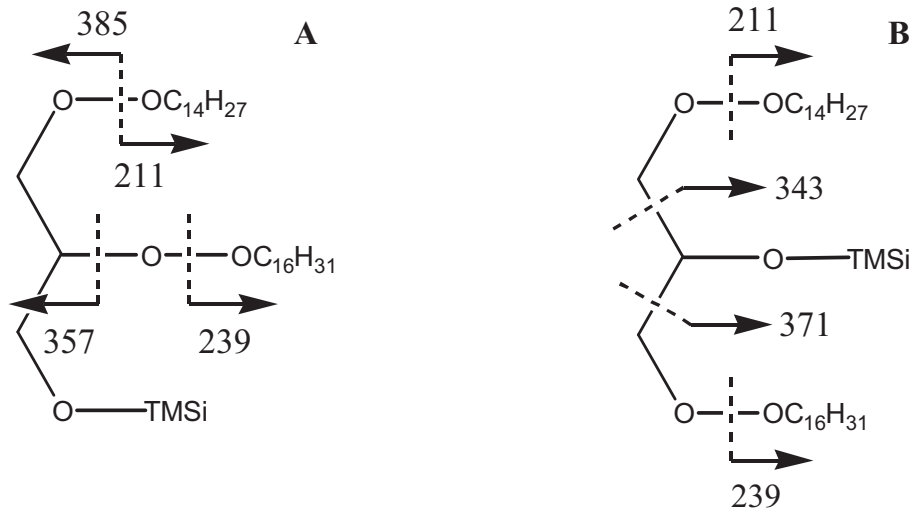

Fig. 4.27. MS of 1-*O*-tetradecanoyl-2-*O*-hexadecanoylglycerol (A) and 1-*O*-tetradecanoyl-3-*O*-hexadecanoylglycerol (B).

This compound was isolated from plant pollens, as that from *Pyrus malus* (Hügel 1962), and from the soft coral *Sinularia* sp. (Ahmed *et al.* 2006), and it is a common constituent not only of algae, but also of clams, silkworms and oysters. Sterol A (**103**) showed equal MS spectra in both FAME fraction and TMSi derivatized sample indicating absence of a hydroxy group, a molecular ion at *m*/*z* 380 (confirmed by CI), and an intense ion at *m*/*z* 255 which is characteristic of $\Delta^{5,22}$ sterols (Souchet & Laplante 2007). In addition, $[M - 18]^+$ ion fragment, characteristic of compounds with a hydroxy group (at C-3), was not detected. Its MS was similar to that of an ergost-3,5,22-trien structure.

Several isoprenoid compounds were detected in the diethyl ether extract, including a γ-lactone-4,8,12,16-tetramethylheptadecane-4-olide (**75**), previously found in marine sediments (Rontani & Volkman 2005), α- and β-tocopherols, found in many microalgae (Brown *et al.* 1999), phytol and squalene. Relatively low amounts (< 0.5% of total compounds) of phosphates (phosphoric acid, glycerol-2-phosphate and glycerol-3-phosphate), fatty alcohols (from C_{12} to C_{18}) as well as *n*-alkanes (from C_{16} to C_{30}) were identified in the studied diethyl ether fraction. Despite the characteristic fragmentation and *RI*, the *n*-alkanes showed detectable $[M]^+$ in EI mode.

The metabolites in the *n*-butanol extract (amino acids, *N*-containing compounds, organic acids and saccharides) were identified by matching their mass spectra and *RI* with the databases and the literature (Nagashima & Fukuda 1981; Medeiros & Simoneit 2007), as indicated in Table 4.1 (pp. 103-106). The FA composition was

dominated by SFAs and MUFAs, while PUFAs were considerably less abundant in the *n*-butanol extract compared with the diethyl ether extract (Table 4.2, page 107). Floridoside (**76**), found to be dominant monosaccharide also in other unicellular algae, showed under GC-MS conditions distinguishable $[M]^+$ at *m/z* 671, mass fragmentation pattern and *RI* identical to those reported in the literature (Nagashima & Fukuda 1981) and databases. Galactose, arabinose, glucose, talose and two unidentified carbohydrates were also found in the *n*-butanol fraction, as well as in other algae (Abdel-Fattah & Edrees 1977; Nagashima & Fukuda 1981). The high relative amount of *N*-containing compounds in the polar fraction (9.5%) was noteworthy.

The three fractions obtained by separation of the diethyl ether extract were examined by GC-MS and their patterns were compared with that recorded for the corresponding crude fraction. Among the three fractions, fraction **1** was the richest in glycerides. In fact, it contained more monoglycerides than fraction **2** (27.5% of TIC in fraction **1** *vs*. 11.0% in fraction **2**) in which, instead, diglycerides were completely absent. In addition, fraction **1** contained traces of FAs, very abundant in fraction **2** where they represented the 66.7% of TIC. Fraction **3** contained FAs, mainly 5,8,11,14,17-eicosapentaenoic acid (EPA, $20{:}5\Delta^{5,8,11,14,17}$, Fig. 4.28), which was 15.55% of TIC *vs*. 6.34% in fraction **2**. In aquaculture industries, EPA is important

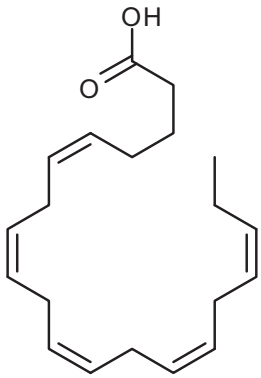

Fig. 4.28. EPA.

for the growth and development of fishes, crustaceans and bivalves (Borowitzka 1997). On the other hand, the intake of a sufficient amount of EPA is necessary for human health and nutrition (Ruxton *et al.* 2004). Some diatom species, such as *Nitzschia alba* and *N. laevis*, contain considerable amounts of EPA (Barclay *et al.* 1994; Lebeau & Robert 2003b; Chen *et al.* 2007) which are physiologically variable depending on environmental conditions.

The chemical analysis did not reveal the presence of short chain polyunsaturated aldehydes in the diatom extract. This result indicated that the considered aldehyde compounds (heptadienal, octadienal and decadienal) were not involved in the sex reversal of *H. inermis*, according to *in vivo* experiments on these crustaceans which were carried out in parallel (Zupo *et al.* 2007). Aldehydes are highly reactive compounds towards biomolecules bearing sulphydryl groups, as well as glutathione, coenzyme A, *etc*., and amino acids. Through Michael addition, in fact, aldehydes react with such nucleophylic groups, negatively influencing many cellular functions, *e.g.* inhibition of both DNA and protein synthesis, arrest of cell cycle, and depletion of glutathione *inter alia* (Adolph *et al.* 2004). In *C. scutellum*, however, the participation of other kinds of oxylipins cannot be excluded yet and further analyses should be performed on this topic.

	Compounds	*RI*	R_t	Key ions (*m*/*z*)*	EE	BE
1	L-Alanine[a,b]	1117	4.00	116, 147, 180		0.14
2	L-Valine[a,b]	1235	5.16	144, 218, 246		0.23
3	Urea[a,b]	1252	5.33	147, 189		2.34
4	UC	1290	5.71		0.12	
5	L-Leucine[a,b]	1292	5.72	158, 232, 260		0.33
6	Glycerol[a,b]	1295	5.75	205, 147, 218	0.07	8.62
7	Phosphoric acid[a,b]	1298	5.79	299, 314	0.01	
8	L-Isoleucine[a,b]	1314	5.95	158, 218		0.26
9	Succinic acid[a,b]	1330	6.09	147, 247		0.20
10	UC	1335	6.14			0.96
11	UC	1358	6.38			0.40
12	L-Serine[a,b]	1380	6.59	204, 218, 278		0.07
13	L-Threonine[a,b]	1407	6.86	218, 219, 291		0.03
14	Glutaric acid[a,b]	1416	6.94	147, 216, 158		0.07
15	Decanoic acid (10:0)[a,b,c]	1461	7.40	117, 229, 244**	0.02	0.04
16	Aspartic acid[a,b]	1486	7.65	232, 334		0.01
17	Dodecanol[a,b,c]	1570	8.49	243***, 75, 103	0.02	
18	Hexadecane[a,b,c]	1603	8.82	57, 71, 226**	0.01	
19	Tridecanoic acid, methyl ester (13:0)[h]	1629	9.10	74, 87, 228**	tr	
20	Ornithine[a,b]	1630	9.11	142, 204, 348**		0.08
21	1-Tetradecanol[a,b,c]	1637	9.20	271***, 75, 103	0.01	
22	L-Phenylalanine[a,b]	1644	9.30	218, 192, 294***		0.27
23	Pentonic acid-1,4-lactone[b]	1654	9.43	217, 147, 231		0.28
24	Dodecanoic acid (12:0)[a,b,c]	1655	9.44	117, 257***, 272**	0.04	
25	Arabinose 1[a,b,d]	1659	9.50	217, 230, 191		0.15
26	Arabinose 2[a,b,d]	1974	9.68	217, 230, 191		0.53
27	UM	1689	9.88			0.41
28	Heptadecane[a,b,c]	1700	10.01	57, 71, 240**	0.01	
29	1-Pentadecanol[a,b,c]	1728	10.34	285***, 103, 75	tr	
30	UM	1748	10.65			3.56
31	Glycerol-2-phosphate[a,b]	1750	10.67	243, 299, 445***	0.24	
32	Hydroxycinnamic acid[a,b]	1771	10.94	179, 192, 310**		0.06
33	Glycerol-3-phosphate[a,b]	1789	11.17	357, 299, 445***	0.02	0.09
34	UC	1793	11.23			0.07
35	Octadecane[a,b,c]	1802	11.33	57, 71, 254**	0.01	
36	UC	1810	11.44		0.39	
37	2-Ketogluconic acid[a,b]	1814	11.50	292, 217, 305		1.78
38	Hypoxanthin[a,b]	1823	11.63	265***, 280**		0.28
39	9-Tetradecenoic acid (14:1Δ^9)[a,b,c]	1833	11.78	117, 298***, 283**	0.02	6.94
40	UC	1844	11.93		0.40	
41	Tetradecanoic acid (14:0)[a,b,c]	1857	12.13	117, 285***, 300**	7.18	6.94
42	Galactofuranose[a,b,d]	1875	12.42	217, 191, 204		0.34
43	Adenine[a,b]	1883	12.54	264***, 279**		0.46

44	UM	1892	12.67		0.12	
45	9,12-Hexadecadienoic acid, methyl ester (16:2 $\Delta^{9,12}$)[h]	1914	12.70	81, 95, 266**	tr	
46	UM		13.00			0.59
47	UC	1916	13.01		0.45	
48	Talose[a,b,d]	1929	13.19	204, 191, 217		3.47
49	Pentadecanoic acid (15:0)[a,b,c]	1950	13.55	117, 299***, 314**	6.89	0.44
50	L-Tyrosine[a,b]	1959	13.68	218, 280, 382***		0.32
51	1-Hexadecanol[a,b,c]	1963	13.75	75, 103, 299***	0.10	
52	UC	1995	14.22			0.10
53	6,9,12,15-Hexadecatetraenoic acid (16:4$\Delta^{6,9,12,15}$)[c]	2015	14.53	79, 305***, 320**	4.16	
54	6,9,12-Hexadecatrienoic acid (16:3$\Delta^{6,9,12}$)[b,c]	2019	14.60	79, 307***, 322**	0.92	
55	Glucose[a,b,d]	2020	14.61	204, 191, 217		3.99
56	9-Hexadecenoic acid (16:1Δ^{9})[a,b,c]	2042	14.96	117, 311***, 326**	21.74	5.64
57	11-Hexadecenoic acid (16:1Δ^{11})[a,c]	2046	15.03	117, 311***, 326**	0.37	
58	Hexadecanoic acid (16:0)[a,b,c]	2059	15.23	117, 313***, 328**	12.29	16.59
59	UC	2065	15.34	79, 91, 108	0.28	
60	Heneicosane[a,b,c]	2101	15.92	57, 71, 296**	0.02	
61	Inositol[a,b,d]	2130	16.34	305, 217, 191		0.12
62	Heptadecanoic acid (17:0)[a,b,c]	2149	16.67	117, 327***, 342**	0.01	
63	Octadecanol[a,b,c]	2161	16.87	327***, 75, 103	0.08	0.19
64	Phytol[a,b]	2184	17.23	143, 123, 353***	0.74	0.34
65	Octadecanoic acid polyene (18:?5)	2189	17.31	79, 91, 117	0.06	
66	6,9,12-Octadecatrienoic acid (18:3$\Delta^{6,9,12}$)[a,b,c]	2199	17.47	79, 335***, 350**	0.34	
67	6,9,12,15-Octadecatetraenoic acid (18:4$\Delta^{6,9,12,15}$)[c]	2206	17.59	79, 333***, 348**	0.78	
68	9,12-Octadecadienoic acid (18:2$\Delta^{9,12}$)[a,b,c]	2217	17.76	79, 337***, 352**	0.31	
69	*cis*-11-Octadecenoic acid (18:1Δ^{11})[a,b,c]	2223	17.86	117, 339***, 354**	0.69	0.11
70	*trans*-11-Octadecenoic acid (18:1Δ^{11})[a,b,c]	2230	17.97	117, 339***, 354**	1.39	1.06
71	Octadecanoic acid (18:0)[a,b,c]	2248	18.26	117, 341***, 356**	0.70	0.76
72	UC	2254	18.36		0.15	
73	UM	2270	18.69			0.25
74	Tricosane[a,b,c]	2300	19.08	57, 71, 324**	0.13	
75	4,8,12,16-Tetramethyl-heptadecane-4-olide[a,b]	2358	19.99	99, 114, 324**	0.02	
76	2-*O*-Glycerol-D-Galactopyranoside (floridoside)[a,b,e]	2369	20.16	204, 337, 671***		11.22
77	5,8,11,14-Eicosatetraenoic acid (AA, 20:4$\Delta^{5,8,11,14}$)[a,c]	2376	20.28	117, 361***, 376**	2.68	0.20

78	5,8,11,14,17-Eicosapentaenoic acid (EPA, 20:5$\Delta^{5,8,11,14,17}$)[c]	2391	20.51	117, 359***, 374**	12.44	1.33
79	Eicosatrienoic acid (20:3$\Delta^{5,8,11}$)[c]	2397	20.61	129, 363***, 378**	0.05	
80	Tetracosane[a,b,c]	2401	20.66	57, 71, 338**	0.10	
81	1-Monotetradecanoylglycerol (14:0)[a,c]	2413	20.86	343, 147, 431**	0.36	0.22
82	11-Eicosenoic acid (20:1Δ^{11})[a,b,c]	2425	21.07	117, 367***, 382**	0.04	
83	Eicosanoic acid (20:0)[a,b,c]	2446	21.36	117, 369***, 384**	1.51	2.88
84	Uridine[a,b]	2473	21.78	217, 259, 445***		0.44
85	Pentacosane[a,b,c]	2500	22.17	57, 71, 352**	0.11	
86	2-Monohexadecenoylglycerol (16:1)[c]	2556	23.03	129, 457***, 472**	1.05	0.06
87	UC	2572	23.29			0.57
88	2-Monohexadecanoylglycerol (16:0)[a,c]	2573	23.30	129, 218, 459***	1.30	0.12
89	1-Monohexadecenoylglycerol (16:1)[c]	2590	23.54	369, 457***, 472**	2.05	0.40
90	Hexacosane[a,b,c]	2600	23.67	57, 71, 366**	0.05	
91	1-Monohexadecanoylglycerol (16:0)[a,b,c]	2606	23.80	371, 459***, 474**	2.94	1.12
92	Docosanoic acid (22:0)[a,b,c]	2641	24.30	117, 397***, 412**	0.11	0.25
93	Adenosine[a,b]	2670	24.70	230, 445***, 460**		4.27
94	Sucrose[a,b,d]	2709	25.26	361, 217, 437		0.87
95	2-Monooctadecenoylglycerol (18:1)[c]	2748	25.81	103, 339, 485***	0.10	
96	1-Monooctadecenoylglycerol (18:1)[a,c]	2782	26.28	397, 485***, 500**	0.08	
97	1-Monooctadecanoylglycerol (18:0)[a,b,c]	2797	26.51	399, 487***	0.03	
98	Tetracosenoic acid (24:1)[c]	2815	26.76	117, 423***, 438**	0.07	
99	Squalene[a,b]	2829	26.95	69, 81, 410**	0.15	
100	Tetracosanoic acid (24:0)[a,b,c]	2840	27.08	117, 425***, 440**	0.70	1.33
101	UC	2876	27.58			0.61
102	UC	2922	28.19		0.33	
103	Ergosta-5,22-dien-3-ol acetate[a,c]	2945	28.50	380**, 255	0.27	0.56
104	1-Monoeicosanoylglycerol (20:0)[a,c]	2991	29.12	427, 515***	0.03	
105	Triacontane[a,b,c]	2999	29.18	57, 71, 422**	0.02	
106	Hexacosanoic acid (26:0)[a,b,c]	3037	29.71	117, 453***, 468**	0.01	0.06
107	β-Tocopherol[a]		29.94	151, 416**	tr	
108	α-Tocopherol[a,b]	3157	31.22	502**, 237	2.63	0.82
109	Cholesterol[a,b,c]	3163	31.29	329, 368, 458**	0.07	0.08
110	Brassicasterol[a,c]	3208	31.86	255, 380, 470**	0.10	0.49
111	UC	3217	31.96			0.77
112	24-Methylenecholesterol[f]	3265	32.57	314, 271, 398**	3.33	1.26
113	Campesterol[a,b,c]	3373	32.63	342, 382, 472**	0.07	0.04

114	UC	3270	33.93		0.08
115	1-Tetradecanoyl-2-hexadecenoylglycerol (14:0; 16:1)[c]	3851	39.91	129, 357, 595***	0.23
116	1-Tetradecanoyl-2-hexadecanoylglycerol (14:0; 16:0)[c]	3871	40.16	145, 129, 597***	0.28
117	1-Tetradecanoyl-3-hexadecenoylglycerol (14:0; 16:1)[c]	3922	40.80	343, 369, 595***	0.09
118	1-Tetradecanoyl-3-hexadecanoylglycerol (14:0; 16:0)[c]	3871	41.07	343, 371, 597***	0.09
119	1,2-Dihexadecenoylglycerol (16:1; 16:1)[c]	4273	45.21	129, 383, 621***	0.22
120	1-Hexadecanoyl-2-hexadecenoylglycerol (16:0; 16:1)[c]	4307	45.62	129, 385, 623***	1.00
121	1,2-Dihexadecanoylglycerol (16:0; 16:0)[a,b]	4333	45.96	129, 385, 625***	0.43
122	1,3-Dihexadecenoylglycerol (16:1; 16:1)[c]	4380	46.55	369, 385, 621***	0.07
123	1-Hexadecanoyl-3-hexadecenoylglycerol (16:0; 16:1)[c]	4411	46.94	371, 369, 623***	0.39
124	1,3-Dihexadecanoylglycerol (16:0; 16:0)[a,b,c]	4439	47.27	371, 385, 625***	0.06

Table 4.1. Metabolites of *Cocconeis scutellum* contained in the diethyl ether extract (EE) and *n*-butanol extract (BE) and presented as % of TIC (total ion current). First key ion (*m*/*z*) is the base peak, **Molecular ion $[M]^+$, ***$[M - 15]^+$ ion, UC: unidentified compound, UM: unidentified monosaccharide. Identification: [a]NIST 2005 mass spectral library, [b]The Golm Metabolome Database, [c]Metabolite assignment by comparison with similar compounds reported in the literature, [d]Medeiros & Simoneit 2007, [e]Nagashima & Fukuda 1981, [f]Souchet & Laplante 2007 (as TMSi derivatives) and Gladu *et al.* 1991 (as non-derivatized compounds), [h]The Lipid Library (Christie 2003).

Compounds	EE	BE
Amino acids and *N*-containing metabolites		9.51
Organic acids		2.51
Phosphates	0.27	0.10
Fatty acids	75.82	44.59
Saturated	29.47	29.30
Monoenes	24.32	13.76
Dienes	0.31	
Polyenes	21.72	1.53
Alcohols	0.28	8.81
Alkanes	0.47	
Carbohydrates		24.54
Monosaccharides		23.67
Disaccharides		0.87
Glycerides	10.80	4.35
Monoglycerides	7.95	1.93
Diglycerides	2.85	2.42
Sterols	4.74	
Isoprenoids	3.55	1.17
Identified compounds (% of TIC)	95.93	95.58

Table 4.2. Metabolite groups in the EE and BE of *C. scutellum* presented as % of TIC. Partial values are indicated in red.

Compounds	R_t (min)	fr. 1	fr. 2	fr. 3
Glycerol	5.73			tr.
Tetradecanoic acid	12.06		8.33	7.70
11-Hexadecenoic acid	14.82	0.5	33.80	51.71
Hexadecanoic acid	15.12	1.86	17.15	6.70
9-Octadecenoic acid	16.70		1.20	
Octadecanol	16.89	tr.		
Phytol	17.24	3.64	0.51	
Octadecanoic acid	18.27	tr.		
5,8,11,14,17-Eicosapentaenoic acid	19.46		6.24	15.55
2-Monotetradecanoylglycerol TMSi	20.40	0.59		
1-Monotetradecanoylglycerol	20.89		0.32	
2-Monohexadecenoylglycerol	23.07	5.59	2.45	tr.
2-Monohexadecanoylglycerol	23.34	9.34	1.89	
1-Monohexadecenoylglycerol	23.56	4.65	3.80	
1-Monohexadecanoylglycerol	23.83	7.32	2.53	
1-Monooleylglycerol	26.33	tr.		
24-Methylenecholesterol	32.12		0.60	
24-Methylcholesterol	32.58		2.48	2.31
1,2-Dihexadecanoylglycerol	45.56	14.09		
1,2-Diglycerol of hexadecanoic and hexadecenoic acid	46.05	21.38		
1,2-Dihexadecanoylglycerol	46.28	6.17		
1,3-Dihexadecenoylglycerol	46.85	3.07		
1,3-Diglycerol of hexadecanoic and hexadecenoic acid	47.24	4.03		
1,3-Dihexadecanoylglycerol	47.53	1.01		

Table 4.3. Composition of the three fractions originated from the diethyl ether extract (presented as % of TIC).

5. Biological assays on *Cocconeis scutellum* diatoms

5.1. Introduction

An important phase of the PHARMAPOX Project was the evaluation of the biological activities of *Cocconeis scutellum*. In parallel to the chemical analysis, in fact, several assays were performed on *C. scutellum* diatoms in order to:

- test the influence of the diatoms on the sex reversal of *Hippolyte inermis* shrimps, quantifying the activity of the apoptotic compound(s) in terms of number of females/total individuals and, finally, carry out a bio-guided fractionation with the purpose to attribute the apoptotic activity to smaller and smaller fractions until isolating the active compound(s);
- test the diatoms and their extracts on human cancer cell lines in order to estimate their efficacy for medical purposes;
- evaluate possible biotechnological applications administrating the diatoms and their extracts on commercially relevant crustaceans.

5.2. *In vivo* assays with *H. inermis*

An essential step within the project was to individuate first the extract, then the fractions, provided with apoptotic activity on *H. inermis*' androgenic gland and to be subjected to further purification. For this purpose, both the diethyl ether and the butanol extracts were incorporated at three different concentrations (0.7, 7 and 70 µg of extract/mg of food) into the shrimp diet and administrated to *H. inermis* postlarvae. In this experiment apoptosis was evaluated in terms of F/tot, since in *H. inermis* the direct occurrence of females is due to the disruption of the AG by diatom-induced programmed cell death. In parallel, several diets were tested in order to find that one able to minimize the death and guarantee high survival in the shrimps.

As demonstrated by *in vivo* experiments (Fig. 5.1), the diethyl ether extract resulted to be more active than the butanol fraction in triggering apoptosis in *H. inermis*, producing a 51.3% ± 15.6% of F/tot at 70 µg of extract/mg of food, and 51.1% ± 23.2% at 7 µg of extract/mg of food. In turn, the butanol extract yielded a maximum of 36.7% ± 16.8% of F/tot when administrated at 7 µg of extract/mg of food, which was a lower value with respect to the control.

Subsequently, fractions **1-3** obtained from the diethyl ether extract were incorporated into the shrimp food (1 µg of each fraction/mg of food) and administrated to the postlarvae in order to evaluate the fraction producing the highest F/tot ratio. The experiment was carried out with five replicates for each treatment.

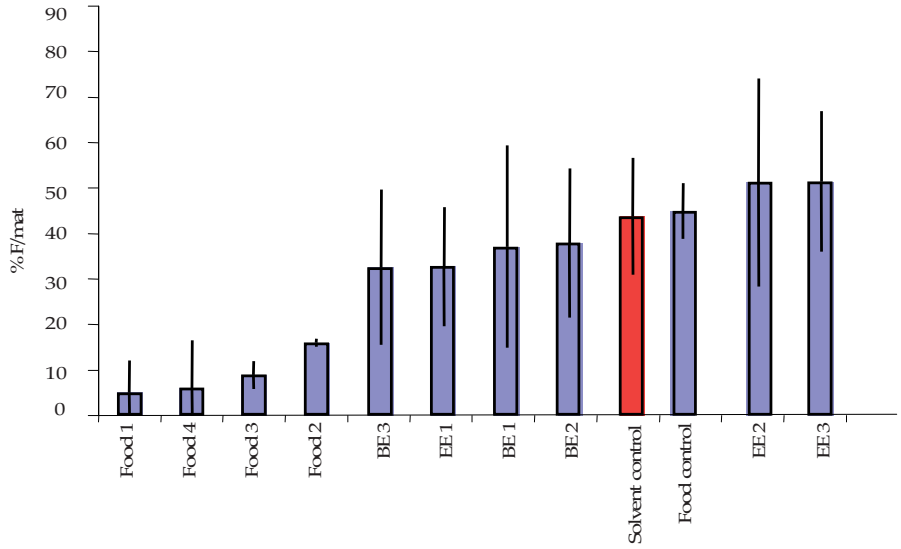

Fig. 5.1. *In vivo* assays on *H. inermis* postlarvae. Food 1: 200 mg freeze-dried *Artemia* + 200 mg pure *Spirulina* + 200 mg Algamac; Food 2: 200 mg freeze-dried *Artemia* + 200 mg pure *Spirulina* + 200 mg Tetra AZ; Food 3: 200 mg freeze-dried *Artemia* + 200 mg pure *Spirulina* + 200 mg granulated SHG; Food 4: 500 mg freeze-dried *Artemia* + 500 mg pure *Spirulina* + 250 mg Baby food; Food control: 15 g freeze-dried *Artemia* + 15 g *Spirulina* flakes + 1 g Baby food. Both the diethyl ether and the butanol extracts were incorporated into the basic shrimp food at three different concentrations: EE1 and BE1 (0.7 µg of extract/mg of food), EE2 and BE2 (7 µg of extract/mg of food), and EE3 and BE3 (70 µg of extract/mg of food).

As indicated in Fig. 5.2, the highest F/tot ratio was recorded for fraction **3** (F/tot 48.32% ± 17.65%) *vs*. fraction **1** (42.21% ± 11.79%) and fraction **2** (45.28% ± 17.72%). The control contained a low percentage of females (4%) in comparison with fractions **1**-**3**. One way Anova test was applied to check the significance of the observed differences along with Bonferroni's test to compare the replicates. The statistical analysis showed a significant difference between fractions **1**-**3** and the control ($p < 0.0001$), but no significant differences among the three fractions. It is noteworthy that

fraction **3** was the richest in fatty acids, among which eicosapentaenoic acid (EPA) was one of the most abundant.

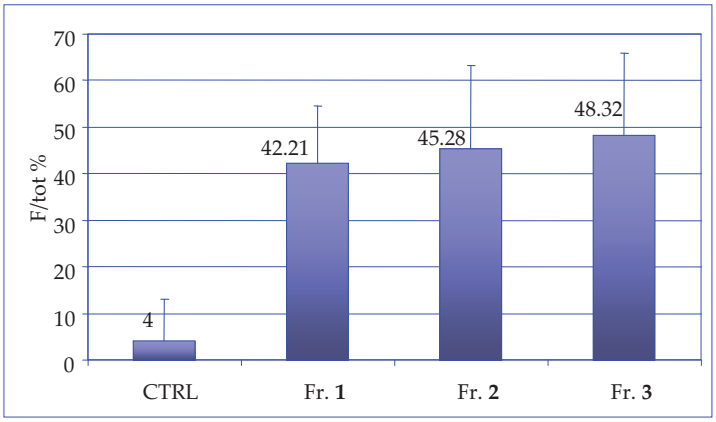

Fig. 5.2. Results of *in vivo* assays upon treatment of *H. inermis* postlarvae with fractions **1-3**. Fraction **3** demonstrated to produce the highest F/tot with respect to the control (CTRL), although no significant differences were observed among the fractions.

As previously demonstrated by analyzing the shrimp tissues by means of molecular tools (TUNEL test), the diatom-induced apoptosis occurring in the shaping AG determines the development of female sexual characters in *H. inermis* by-passing the male stage (Zupo & Messina 2007). These authors reported that the diatom-induced apoptosis was species specific, localized in both the male gonad and the AG, and limited to a very short period of time, from the 5th to the 12th day of the postlarval growth.

5.3. Experiments with crustaceans of commercial interest

The production of all male populations of some commercially relevant prawns and crayfishes represents a key strategy for increasing the yields and, thus, the incomes.

The procedure used so far, consisting in the surgical ablation of the crustacean's AG, is quite laborious and requires skilled personal. It is necessary to find, thus, novel technologies for inducing sex reversal. The employment of an apoptotic agent able to specifically act on the AG, along with molecular sex markers to identify candidates, could be an elegant and less difficult method for avoiding long progeny testing. Two kinds of experiments were carried out in collaboration with the group of the BGU (Israel): *in vivo* assays with the prawn *Macrobrachium rosenbergii*, and *in vitro* assays with the crayfish *Cherax quadricarinatus*' AG. Both species are characterized by a bimodal pattern of growth, in which males are bigger and grow faster than females.

5.3.1. *In vivo* experiments with *Macrobrachium rosenbergii*

In vivo experiments were carried out with *M. rosenbergii* juveniles including the diatom acetone extract into their diet at two different concentrations, 20 ng/larva and 2 ng/larva. In this assay, consisting in three treatments and three replicates, postlarval survival rate was relatively low, although it could not be correlated with the treatment, and high mortality was also observed in the control group (Fig. 5.3). In six tanks (2 controls, four treatments) survival rate was 44% or more (red dashed line). In those crustaceans which were treated with the two concentrations of acetone extract, the percentage of females was higher than males. Nevertheless, due to the high mortality and high fluctuations in male/female ratios in the control triplicates,

we could not correlate the reduced male/female ratio in the treatment groups to the administration of the extract itself. The lack of diatoms prevented us to carry out more experiments and these should be further performed in order to clarify this point.

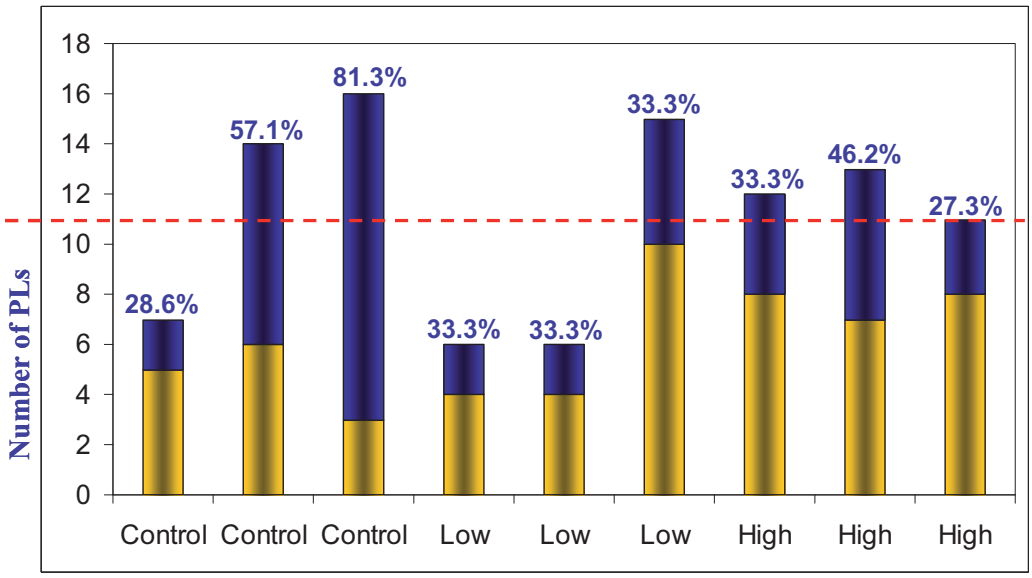

Fig. 5.3. Three groups (control, low dose and high dose) with male/female ratio. In each group the three bars represent the triplicates with number of postlarvae (PLs) which survived to sexing. Blue indicates number of male individuals, yellow indicates number of female individuals. On the top of each column the percentage of males is reported. Red dashed line indicates groups with 44% or more survival.

5.3.2. *In vitro* experiments with *Cherax quadricarinatus*

Prior to the experiments, *C. quadrinatus* crustaceans were eye stalk ablated in order to remove the endocrine control and cause hypertrophy of the AG (Khalaila *et al.* 2002). The AGs (Fig. 5.4) were dissected along with a small portion of the sperm duct by

means of surgical ablation of *C. quadricarinatus* males, endocrinologically induced 11 days before the dissection. After that, the AGs were incubated for 24 h in presence of fractions **1-3** derived from the diethyl ether extract at three different concentrations (100, 10 and 1 µg/ml) along with staurosporine, an antibiotic inducing apoptosis, which was used as positive control. EPA and arachidonic acid (AA) were tested as well, since EPA, which was very abundant in fraction **3**, could be involved in the diatom-induced apoptosis. After incubation, samples were fixed, sectioned in 5 µm slices, stained and examined by fluorescent microscope. The Apoptag kit was used to detect apoptotic nuclei. The microscope observation demonstrated that, within the concentration ranges we used, no specific apoptotic effect was detected on the AGs. Weak and not significant apoptotic activity was observed to be induced by fraction **1** and the ethanol control at the maximum tested concentration.

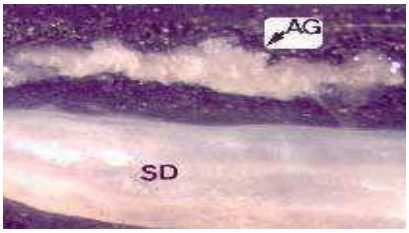

Fig. 5.4. AG = androgenic gland and SD = sperm duct.

5.4. Cytotoxicity tests

Cytotoxicity tests were carried out in order to establish whether *C. scutellum* diatoms were able to affect the cell survival also in human tissues.

Three typologies of experiments were performed during the investigation:

- evaluation of both the cell apoptosis and vitality by annexin V-FITC along with isotonic propidium iodide (PI) labelling and flow cytometry analysis;
- analysis of the cell cycle by hypotonic PI staining and flow cytometry analysis (Yi *et al.* 2003);
- analysis of the caspase activation (caspases 8, 9 and 3) by Western blotting.

5.4.1. Annexin V-FITC isotonic PI labelling

The annexin V-FITC method relies on the principle that a certain group of phospholipids, called phosphatidylserine (PS), located inside the plasmatic cell membrane in normal living cells, are translocated to the external surface of the membrane during the early apoptotic phase (Bossy-Wetzel & Green 2000). Presence of PS outside the membrane is diagnostic for cells entering the apoptotic phase. Annexin V is a protein belonging to a family of phospholipid-binding proteins able to specifically link negatively charged phospholipids, like PS, in presence of Ca^{2+} (van Heerde *et al.* 1995). In turn, annexin V is labelled with fluoresceine isothiocyanate (FITC). Translocation of PS outside the cell membrane, a clear signal of beginning apoptosis, occurs before DNA condensation, fragmentation, membrane blebbing and permeabilisation, and marks the apoptotic cells to be recognized by neighboring macrophages, facilitating the non-inflammatory removal of dying cells by phagocytosis. Once on the external layer, PS can be detected by binding of FITC-

labelled annexin V. Combining this method with isotonic PI labelling, it is possible to detect simultaneously the morphological changes occurring in cell membranes in the first phases of the apoptosis (with annexin V-FITC: green light emission) and also necrotic cells (with PI: red light emission) (Vermes *et al.* 1995). PI is a DNA inserting agent and, when it is isotonic, it can link DNA only after membrane break and, thus, release of cell components and presence of DNA outside the cell. Early apoptotic cells are positive to annexin V-FITC conjugate, but do not stain with PI, because their membranes are still intact. Late-stage apoptotic cells or dead cells, which have damaged permeable plasma membranes, stain concurrently with annexin V-FITC conjugate and PI.

5.4.2. Hypotonic PI staining

The DNA fragmentation and the belated phases of apoptosis can be detected by hypotonic PI staining along with flow cytometry. This method enables to determine DNA fragmentation in apoptotic cells, whereas it does not allow marking still intact DNA. Hypotonic PI, in fact, enters the cells and binds DNA, originating fluorescence of different intensities which are recorded by the optic and electric system of the flow cytometer. A low fluorescence corresponds to fragmented DNA, whereas a peak (high fluorescence) represents the intact DNA.

5.4.3. Western blotting

Western blotting is a method to analyze the cell-expressed proteins by using specific antibodies. The protein homogenate is charged onto a polyacrylamide-SDS gel where, since all the proteins have a negative charge because of SDS (sodium dodecylsulphate), they migrate towards the positive pole according to their molecular weight. After transferring the proteins from the gel to a nitrocellulose paper, the protein that we are looking for is linked by the specific antibody, and the protein-antibody complex is revealed by autoradiography (Watson *et al.* 2002).

5.5. Results of the apoptosis assays

Within the cytotoxicity assays, a preliminary screening was performed incubating several human cell populations, both normal and cancer cells, in presence of freeze-dried *C. scutellum* diatoms at different concentrations (in the range 0.1-10 ng/ml) for 24 h in order to find which lines were more responsive to the treatment (Fig. 5.5). The cancer cell lines were originated by different kinds of human tumors: BT20 and MB-MDA468 (breast carcinoma and breast adenocarcinoma, respectively), LNCaP (prostate adenocarcinoma), BRG-M [Burkitt's lymphoma originated by the chromosomic translocation t(8;14) and involving the c-*myc* oncogene], and JVM2 [Burkitt's lymphoma originated by the chromosomic translocation t(11;14) and involving the *BCL11* oncogene]. The normal cell line, in turn, was represented by

COR, *i.e.* EBV (Epstein-Barr virus) transformed B cells which were extracted from human tonsils. T lymphocytes, represented by BRG-M and JVM2, were extracted from peripheral blood. The percentage of apoptotic cells was detected by annexin V-FITC isotonic PI double staining and flow cytometry analysis. The most responsive cell line resulted to be BT20, with 26.1% of apoptotic cells in presence of 2.5 ng/ml of *C. scutellum* diatoms, 24.6% at 10 ng/ml, and 24.3% of apoptotic cells when the concentrations of *C. scutellum* were 0.1 and 1 ng/ml. In absence of diatoms, 8.3% of apoptotic cells was observed in BT20 populations.

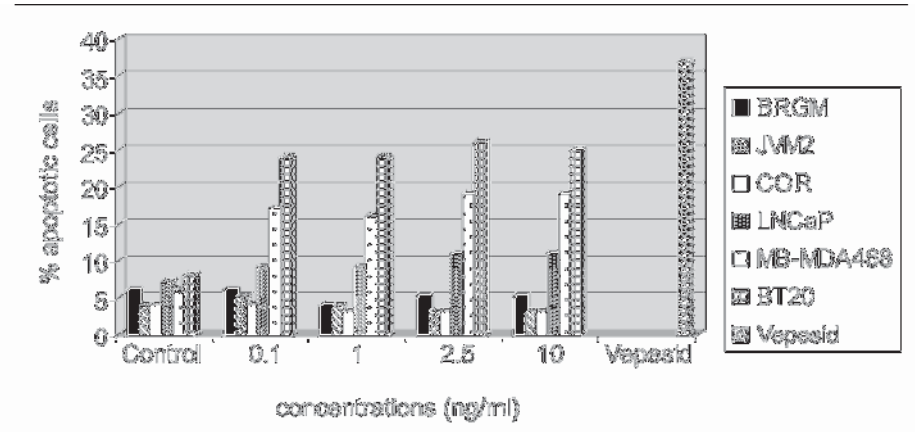

Fig. 5.5. Apoptotic activity of *C. scutellum* on different human cell lines cultured for 24 hours in presence of the diatoms.

MB-MDA468 followed a similar trend, with 19.2% of apoptotic cells at diatom concentrations of 2.5 and 10 ng/ml, 16.4% of apoptotic cells in presence of 1 ng/ml of diatoms, and 17.5% of apoptotic cells at 0.1 ng/ml of *C. scutellum*, whereas the

percentage of apoptotic cells in MB-MDA 468 control was 5.4%. LNCaP was less responsive to *C. scutellum* than BT20 and MB-MDA468, with 11.3% of apoptotic cells in presence of 2.5 and 10 ng/ml of diatoms, and 9.2% of apoptotic cells at diatom concentrations of 0.1 and 1 ng/ml, against the 7.7% in LNCaP control. The difference with respect to the negative control (only medium used) resulted to be statistically significant for BT20 and MB-MDA468 (exact Fisher's test, $p < 0.05$), and a certain apoptotic activity was observed on LNCaP. In turn, diatoms did not exhibit a significant apoptotic activity on haematological tumors (BRG-M, JVM2) and COR cell lines in comparison with the negative control. Etoposide (Vepesid), a drug inducing apoptosis, was used as positive control. This preliminary assay indicated, thus, that solid tumours (BT20, MB-MDA 468, and LNCaP) were more responsive to the diatoms than normal cells and lymphomas. Once established that BT20 was the most diatom-receptive cancer cell line, both the diethyl ether and the butanol extracts were tested on this selected population in order to define the more active extract able to trigger apoptosis. In particular, BT20 cells were incubated for 18 h in presence of both the extracts at different concentrations (0-1,700 ng/well). In dose/response experiments on BT20 cells (Fig. 5.6) apoptosis was evaluated by hypotonic PI staining of permeabilized cells, along with flow cytometry analysis. As shown, at 17 ng/well of the diethyl ether extract 50% of BT20 apoptotic cells was recorded, while apoptosis reached 40% in those populations treated with the same concentration of butanol extract.

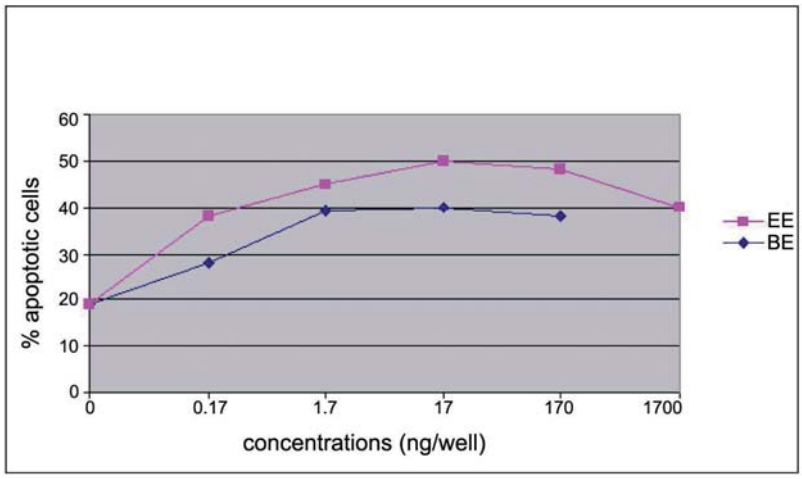

Fig. 5.6. Dose/response curve indicating the percentage of apoptosis in BT20 cells treated with the diethyl ether extract (EE) and the butanol extract (BE) for 18 h.

Both the extracts produced increasing apoptosis at increasing concentrations up to 17 ng/well, after which apoptosis underwent a gradual reduction. The graph resulting from the annexin V-FITC isotonic PI labelling (Fig. 5.7, on the left) consists of four quadrants, each one representing a particular state in which cells can find: LL (lower-left) indicating live cells; UL (upper-left) representing necrotic, dead cells; UR (upper-right) corresponding to the late phase of apoptosis and LR (lower-right) indicating the early phase of apoptosis. In this experiment, we compared BT20 cells treated with 1.7 ng/well of EE with those incubated with the medium only. As reported in Fig. 5.7, a remarkable presence of apoptosis (31.9% of the total cells, LR) and a reduction of live cells (49.9%, LL) were observed in BT20 cells treated with 1.7 ng/well of EE, whereas in the control apoptotic and live cells were 14.9% and 72.9%, respectively. On the right of Fig. 5.7, the results of hypotonic PI staining experiments

are reported, along with the quantification of the fragmented DNA. It was shown that fragmented DNA was 40% on total DNA in presence of 1.7 ng/well of diethyl ether extract, while fragmented DNA was 5% in the control.

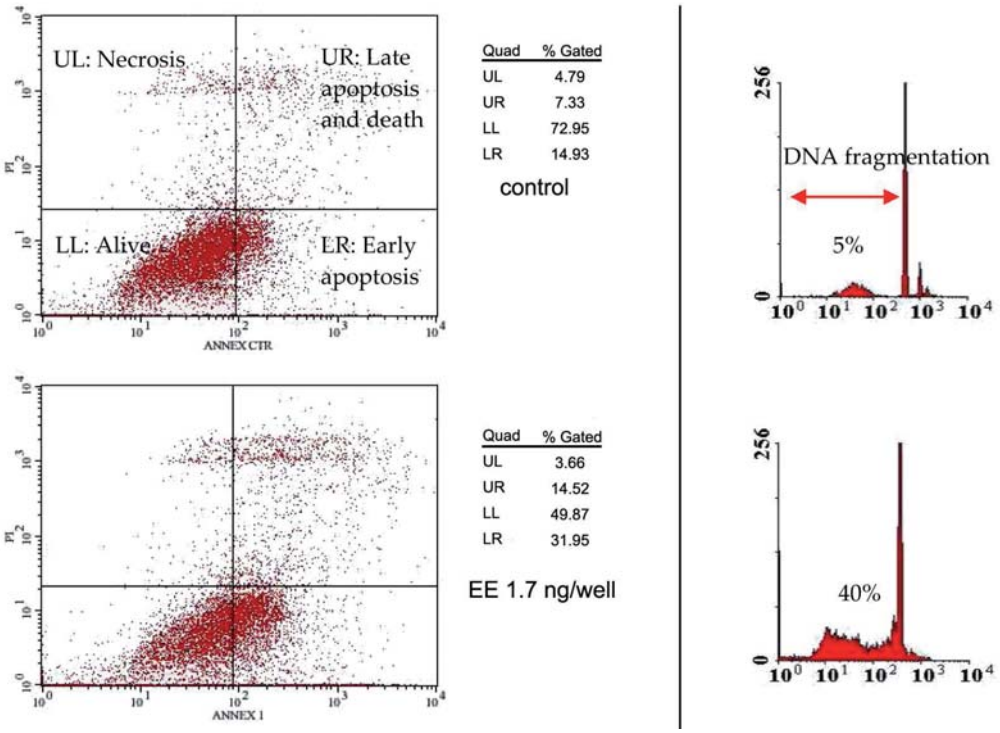

Fig. 5.7. Detection of apoptosis in diethyl ether extract-treated BT20 cells by annexin V-FITC isotonic PI labelling (on the left) and hypotonic PI staining (on the right). Control: only medium used.

Subsequently, BT20 cell lines were incubated for 24 h in presence of fractions **1-3**. In Table 5.1 the percentages of apoptotic cells produced by different concentrations of fractions **1-3** are reported. The average apoptosis and the standard deviations were calculated on 10 replicates. Apoptosis was measured as percentage of fragmented

DNA on total DNA by hypotonic PI staining in permeabilized cells and flow cytometry analysis. As observed in Table 5.1, the maximum of apoptosis produced by fraction **1** (at 1.5 μg/well) was 40.3%, whereas it was 39.3% (at 0.1 μg/well) in fraction **2**-treated cells. The maximum of apoptosis induced by fraction **3** in BT20 cells was significantly higher than that produced by fractions **1** and **2**, *i.e.* 81.4% of apoptotic cells at 2.0 mg/well of fraction **3** (Pearson x^2 test; $p \leq 0.001$).

	Concentrations (μg/well)	**Average apoptosis (%)**	**Standard Deviation (±)**
fr. 1			
	4.0	29.7	11.0
	1.5	40.3	9.0
	0.1	36.0	5.0
fr. 2			
	2.5	31.1	11.0
	1.0	36.6	8.0
	0,1	39.3	5.6
fr. 3			
	4.0	80.0	13.0
	2.0	81.4	14.0
	1.0	58.0	0.0
	0.5	56.2	33.0
	0.25	25.0	0.0

Table 5.1. Average apoptosis and corresponding standard deviations in BT20 cells treated with fractions **1**-**3**.

A clear idea can be given by building a dose/response curve in which we evaluated parameters as well as cell vitality and apoptosis of BT20 cell lines, incubated for 24 h at different concentrations of fractions **1**-**3**. In Fig. 5.8 a high vitality was observed in

those populations cultivated in presence of fraction **1** and fraction **2.** The highest vitalities of both fractions **1** (82.0% of live cells) and **2** (64.0% of live cells) were recorded at 0.1 μg/well, and continued constantly high even at higher concentrations of fraction **1** and fraction **2**. In presence of fraction **3**, BT20 cell vitality was 72.0% at 0.25 μg/well and it reached 13.5% at 0.5 μg/well. After that, a reduction of live cells was recorded in the range 0.5-4 μg/well of fraction **3**.

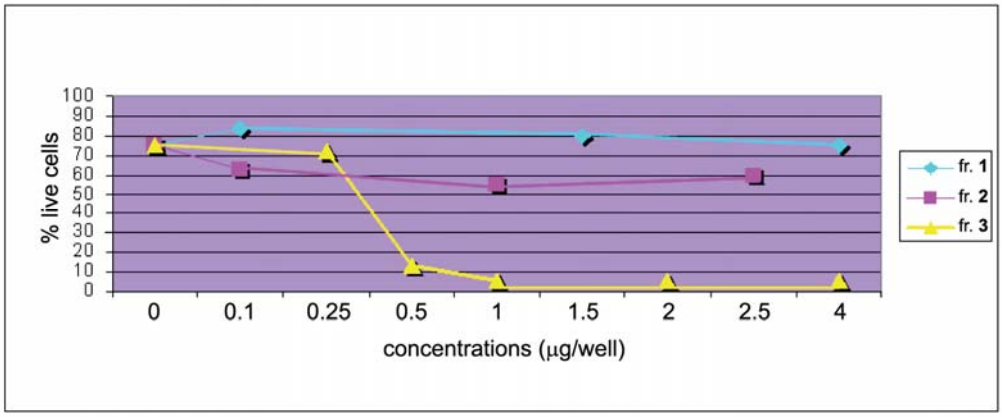

Fig. 5.8. Dose/response curve indicating the percentages of live cells in BT20 populations incubated with fractions **1-3** at different concentrations.

Analogously, in Fig. 5.9 the dose/response curve was drawn considering apoptosis in BT20 cells induced by different concentrations of fractions **1-3**. Also these dose/response experiments confirmed the highest apoptotic activity of fraction **3** among all the tested fractions and demonstrated, furthermore, an increase of apoptosis at increasing concentrations of fraction **3**.

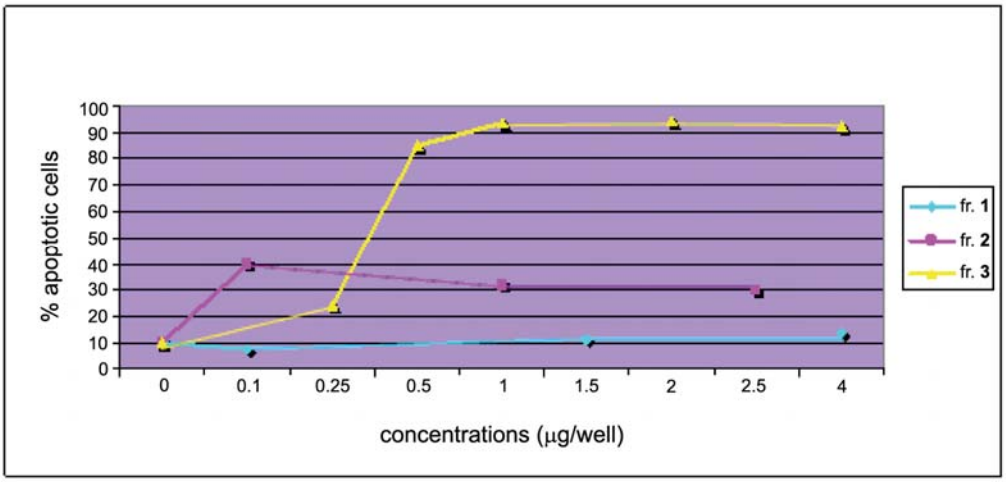

Fig. 5.9. Dose/response experiment indicating the percentages of apoptotic cells, after incubation of BT20 population with fractions **1-3** at different concentrations.

In Fig. 5.10 we have reported the results of the annexin V-FITC isotonic PI labelling experiments on BT20 lines incubated for 24 h with fractions **1-3**. The control population (BT20 cells in presence of the medium only) exhibited a high vitality (LL 90.9%). After the treatment, the BT20 vitality demonstrated not to be significantly affected by fraction **1** and fraction **2**, since the vitality values were very close to the BT20 control (LL 93.5% and 92.1%, respectively), whereas the vitality was lower in BT20 samples treated with fraction **3** (LL 56.2%). Physical parameters as well as dimension and granulation were evaluated in the dot-plot graph in annexin V-FITC isotonic PI experiments (first panel on the left, Fig. 5.10). The different concentrations of fractions **1-3** were determined by previous titration experiments (fraction **1**: 0.1-4 μg/well; fraction **2**: 0.1-2.5 μg/well; fraction **3**: 0.25-4 μg/well).

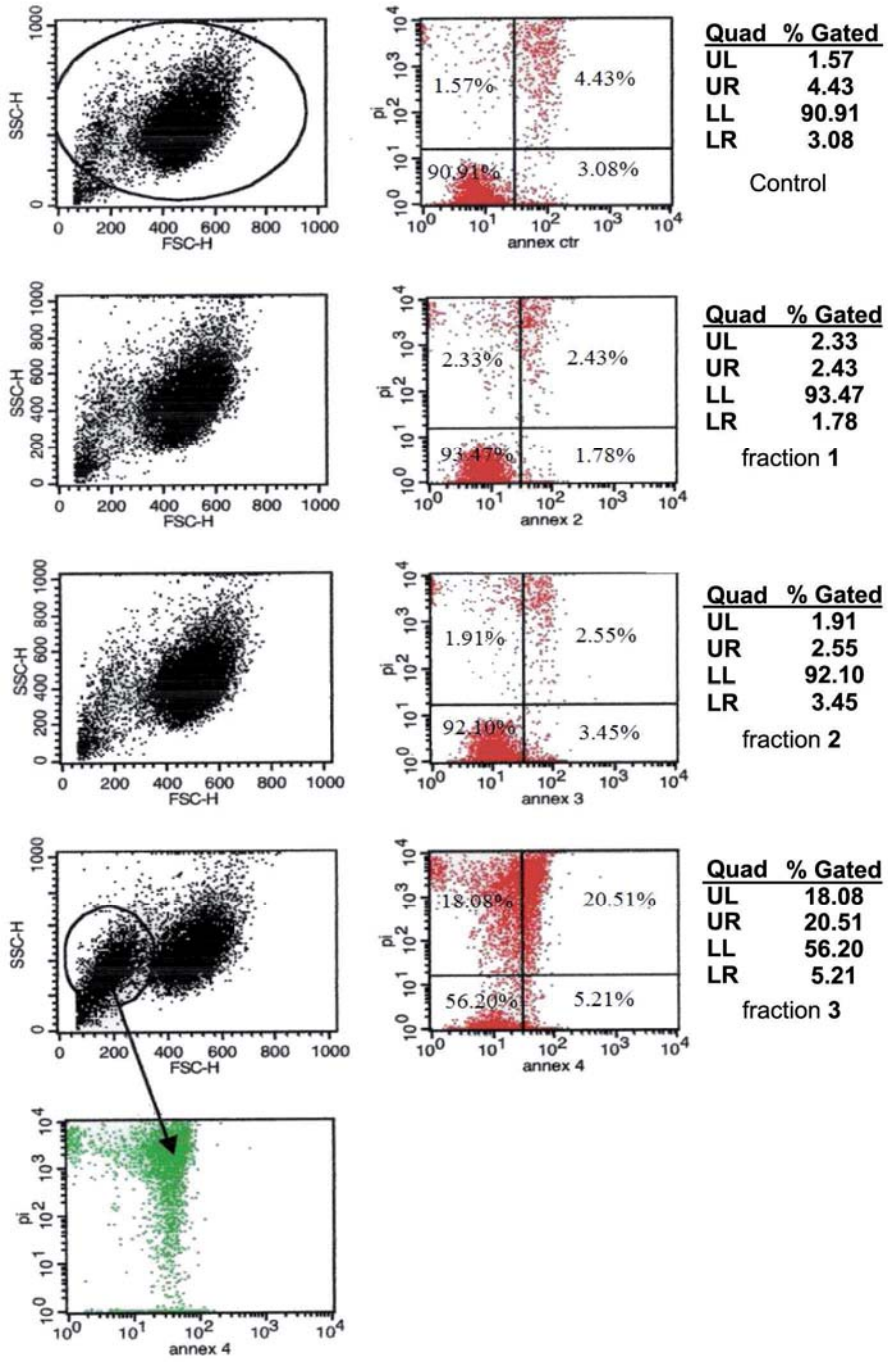

Fig. 5.10. Detection of apoptosis by annexin V-FITC isotonic PI labelling in BT20 cells treated with fractions **1-3**.

The presence of a new cell population, absent in the control and in both the populations treated with fraction **1** and fraction **2**, was observed in BT20 cells (indicated in green on the lower-left quadrant, Fig. 5.10) incubated with fraction **3**. This new population consisted in necrotic and late apoptotic cells which resulted to be positive to the annexin V-FITC isotonic PI treatment.

The occurrence of apoptosis in fraction **3**-stimulated BT20 cells was also confirmed by morphological studies. Analysis of Giemsa-stained BT20 cells, upon exposure to the medium only, fraction **1**, fraction **2** and fraction **3** at different concentrations (0.5, 1 μg/well), showed condensed and fragmented nuclei in fraction **3** treated-BT20 cells, but not in cells cultured in presence of fractions **1**-**2** or the control.

Since the chemical analysis indicated **3** to be the richest fraction in eicosapentaenoic acid (15.6 % of the total ion current *vs.* 6.2% in fraction **2**), EPA was supposed to have an important role in the effects displayed by this fraction. For this purpose, both EPA and AA, another PUFA present in the diethyl ether extract (2.7% of TIC) but not detected in the fractions, were tested on BT20 cell lines at 7 μg/well for 24 h. In this experiment the percentage of apoptotic cells was determined by annexin V-FITC isotonic PI labelling. The analysis of the data showed a high vitality either in BT20 control (78.0% of live cells), and in presence of 0.9% NaCl solution (76.1% of live cells) and AA (70.4% of live cells). On the contrary, the vitality level reduced when BT20 populations were incubated with EPA, reaching 34.1% at 7 μg/well of EPA. Analogously, apoptotic BT20 cells were 45.3% at 7 μg/well of EPA.

Dose/response curves were built considering both vitality and apoptosis in BT20 cells incubated at increasing concentrations of EPA and AA for 18 h (Fig. 5.11 and 5.12).

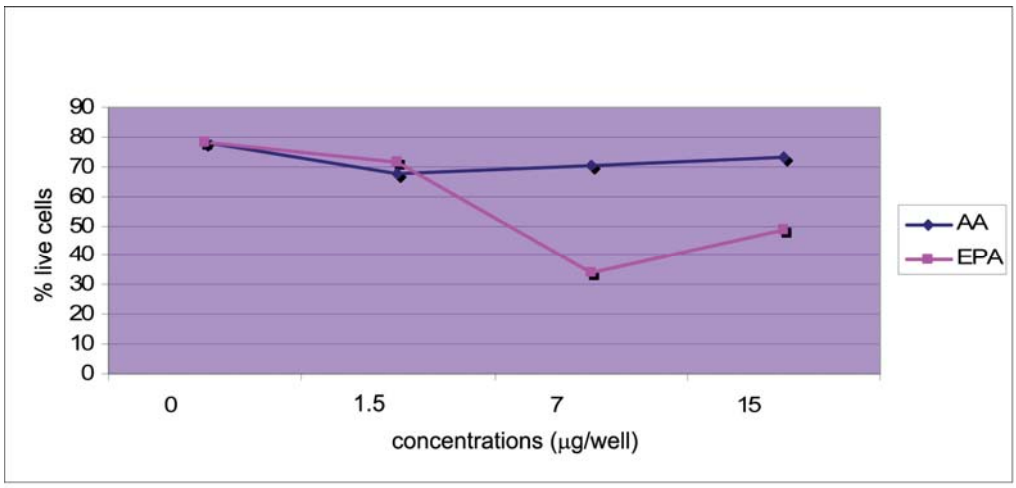

Fig. 5.11. Dose/response curves indicating the percentages of BT20 live cells incubated for 18 h in presence of EPA and AA at different concentrations.

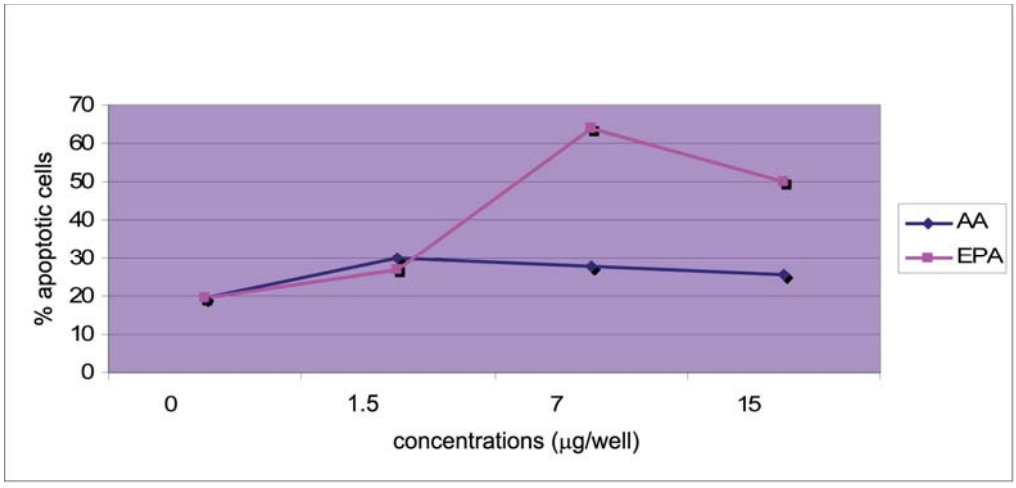

Fig. 5.12. Dose/response curves indicating the percentages of apoptotic cells in BT20 populations treated for 18 h with AA and EPA at different concentrations.

The percentage of live cells was calculated by isotonic PI exclusion test with flow cytometry analysis, whereas the apoptosis was evaluated as fragmented DNA on total DNA by hypotonic PI staining with flow cytometry analysis. In presence of AA, both apoptosis and vitality did not suffer remarkable modifications, whereas BT20 samples incubated with EPA showed a significant variation in both values. The most noteworthy increase of apoptosis and reduction of cell vitality were observed at concentrations of EPA higher than 7 μg/well.

Annexin V-FITC PI labelling experiments were also realized on LNCaP cell lines treated with fractions **1**-**3** (0-4 μg/well) for 24 hours. The results demonstrated the highest apoptotic activity of fraction **3** also on this cell population. In presence of the medium only, the vitality in LNCaP cells was 46.2%. In presence of fraction **3** (0.005 μg/well), cell vitality of LNCaP reduced to 23.5%, just increasing to 31.3% when fraction **3** was 0.015 μg/well. Within the range 0.015-0.05 μg/well of fraction **3**, cell vitality underwent a drastic reduction, reaching almost 0% over 0.05 μg/well of fraction **3**. Analogously, the percentage of apoptotic cells increased at higher concentrations of fraction **3**. On the other hand, LNCaP vitality did not undergo a significant reduction in presence of fraction **1** and fraction **2**.

The solvents used during the diatom extraction and fractionation were also tested in the cytotoxicity tests, with the purpose to exclude that the apoptotic activity observed in fraction **3** was due to toxicity of one of the solvents rather than the

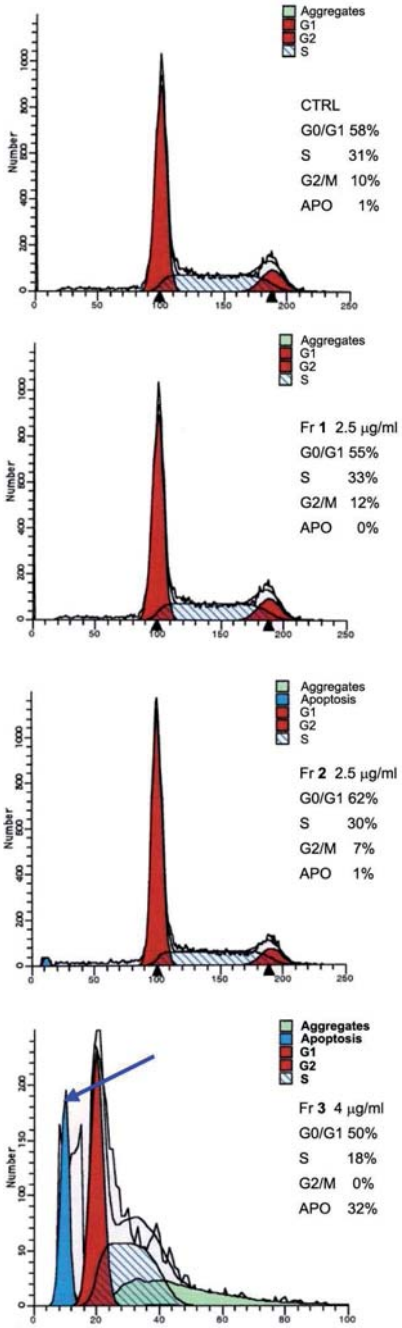

Fig. 5.13. Analysis of the cell cycle. The peaks indicate the number of BT20 cells in each phase of the cell cycle.

fraction itself. The results demonstrated that the solvents did not exhibit any effect on both cell vitality and apoptosis in cultivated cells.

The flow cytometry analysis along with hypotonic PI staining enabled to evaluate the influence of fractions **1**-**3** on the cell cycle (Fig. 5.13). The cell cycle consists of several phases. After the latent period G0, the cell enters G1 phase, in which proteins and cell components are synthesized without duplicating DNA. At S phase DNA is duplicated and, afterwards, cell undergoes the normally brief G2 phase. Upon G2, mitosis (M) produces the division of each cell into two cells, which start again the cycle from G1 phase (Wolfe 2000).

BT20 cells were incubated for 48 h with fractions **1**-**2** (2.5 µg/well each) and fraction **3** (4 µg/well). The analysis of the cell cycle of treated BT20 populations confirmed the results furnished by the annexin V-FITC isotonic PI labelling

experiments, demonstrating the highest apoptotic activity of fraction **3**. As shown in Fig. 5.13, the four graphs represent the distribution of BT20 cells in the different phases of the cell cycle: G1, S, G2/M and apoptosis, respectively. The percentage of cells at G0/G1 phase remained almost unchanged in presence of fraction **1** (55%), fraction **2** (62%), and fraction **3** (50%) in comparison with the control (58%). At S phase we recorded 31% of cells in presence of the control, 33% in fraction **1**-treated cells, 30% in fraction **2**-treated cells, and 18% in fraction **3**-treated cells. The significant difference was observed at G2/M phase, with 10% of cells in presence of the control, 12% in fraction **1**-treated cells, 7% in fraction **2**-treated cells, and 0% in fraction **3**-treated cells. A consistent presence of apoptotic cells (32%) was observed in those populations incubated with fraction **3**, whereas the presence of apoptosis was 1% in both the control and BT20 cells treated with fraction **2**, and 0% in those populations incubated with fraction **1**. The apoptotic population in fraction **3**-treated BT20 cells was represented by the blue peak, indicated by the arrow (Fig. 5.13, last graph).

Western blotting analysis was performed in order to define the diatom-induced apoptotic pathway. Apoptosis can be initiated by the two different pathways, extrinsic and intrinsic, by cleavage of the two different initiator caspases, caspase 8 and 9, respectively. Both inactive and active form of each caspase can be distinguished by their molecular weight (caspase 8: inactive form 55-50 kDa, active form 40-36 kDa; caspase 9: inactive form 47 kDa, active form 37 kDa). Fig. 5.14 and

5.15 show the results of Western blotting experiments in which the activation of caspase 9 and 8 was searched for, respectively, in BT20 populations incubated for 5, 6 and 18 h in presence of the medium (-), fractions **1**-**3** and Vepesid (V). Fraction **1** was tested at 4.11 μg/well, fraction **2** at 2.67 μg/well, and fraction **3** was administrated at both 4 μg/well (indicated as **3***) and 2 μg/well (indicated as **3**). As shown in Fig. 5.14, the activation of caspase 9 (37 kDa) was low in BT20 samples treated with Vepesid for 5 hours, while it was absent in cells cultivated in presence of fractions **1**-**3**.

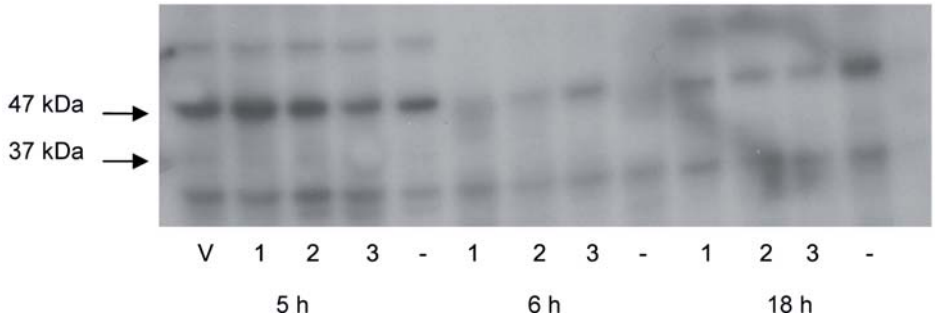

Fig. 5.14. Western blotting experiment for detecting caspase 9 (47 kDa: inactive form; 37 kDa: active form).

On the contrary, as shown in Fig. 5.15, the not cleaved/procaspase 8 (55-50 kDa) was found in all the treated populations, whereas the presence of active caspase 8 (40-36 kDa) was evident in BT20 samples incubated with fraction **3** at the two tested concentrations. In addition, the cleaved/activated caspase 8 (40-36 kDa) was detected, although in less evident manner, also in those samples treated with fraction **2** and

Vepesid. The Western blotting analysis demonstrated, therefore, that caspase 8 (extrinsic pathway) was involved in the diatom-induced apoptosis.

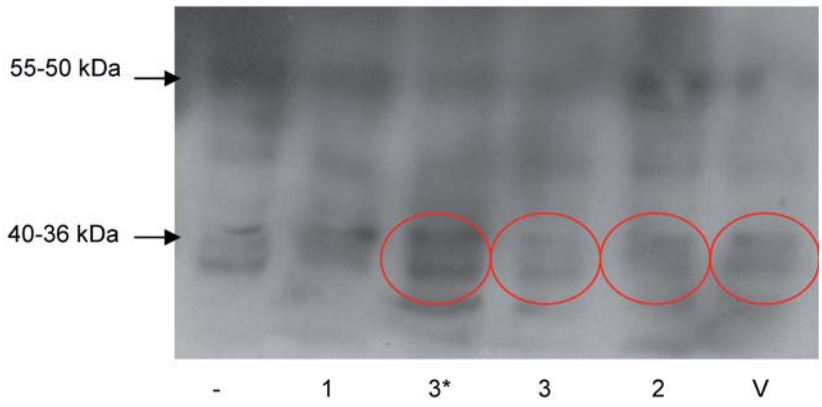

Fig. 5.15. Western blotting experiment for detecting caspase 8 (55-50 kDa: inactive form; 40-36 kDa: active form). Time of incubation: 5 hours.

The activation of caspase 3, apoptosis effector enzyme which acts on protein targets by proteolysis, was studied as well by Western blotting (Fig. 5.16). Caspase 3 is characterized by 34 kDa molecular weight in its inactive/uncleaved form, and 20 kDa in the activated/cleaved state. In this experiment BT20 cells were incubated for 3, 6 and 18 hours in presence of fraction **1** (4.11 μg/well), fraction **2** (2.67 μg/well), fraction **3** (4 μg/well) and, in addition, EPA (7 μg/well). The medium (CTRL) and Vepesid (V) were used as negative and positive controls, respectively. The experiment highlighted that the inactive/not cleaved form (34 kDa) was detected in all the samples at every time of incubation. The activated/cleaved form (20 kDa) of caspase 3

was found only when BT20 cells were incubated for 6 hours in presence of fraction **3** and EPA.

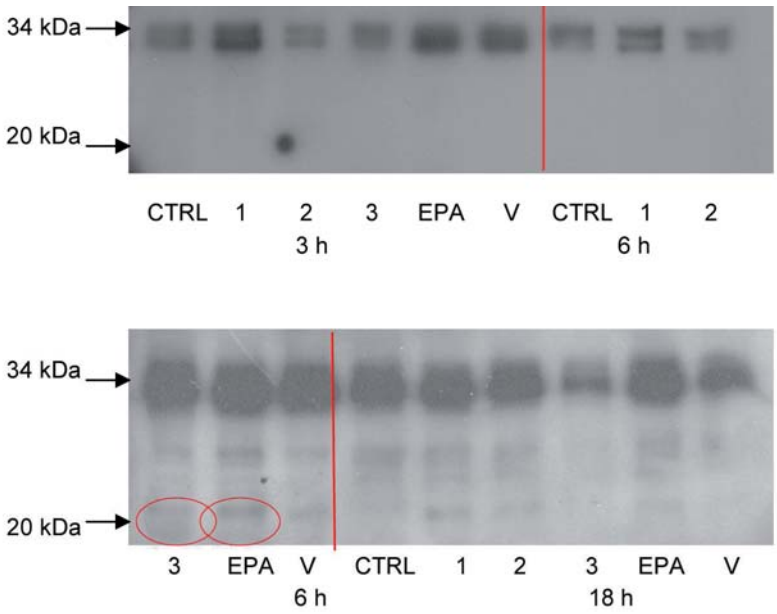

Fig. 5.16. Western blotting experiment for detecting caspase 3 in BT20 cells treated with fractions **1-3** and EPA (34 kDa: uncleaved caspase 3; 20 kDa: active caspase 3). Times of incubation: 3, 6 and 18 h. CTRL (control, only medium used).

5.6. Results and Discussion

The evaluation of the potential applications of *C. scutellum* diatoms represented a crucial aim of the PHARMAPOX Project. The biological assays, carried out in collaboration with SZN, BGU and INRC, allowed the individuation of the most active extract/fraction able to trigger apoptosis, and the evaluation of the effect of the microalgae also on human cells and crustaceans of commercial interest. The

experiments on *H. inermis* postlarvae highlighted the higher apoptotic activity of the diethyl ether extract with respect to the butanol extract, suggesting the apolar nature of the compound(s) involved in the diatom-induced apoptosis. Among the fractions of the diethyl ether extract, fraction **3** demonstrated to be the most active to induce apoptosis of *H. inermis*' androgenic gland. The chemical analysis revealed that this fraction was rich in polyunsaturated fatty acids, mainly EPA. The apoptotic activity of some PUFAs, in particular EPA, is known in the literature (Hawkins *et al.* 1998; Gillis *et al.* 2002; Shirota *et al.* 2005). It was demonstrated that some PUFAs trigger apoptosis in pancreatic and leukaemia cell lines, with a level of cytotoxicity proportional to the number of double bonds (Hawkins *et al.* 1998). Similarly, orally administrated PUFAs have proven to suppress the growth of human mammary carcinomas in mouse models, by forming lipid peroxidation products (González *et al.* 1993). EPA, besides preventing arrhythmia, atherosclerosis and cardiovascular diseases (Pulz & Gross 2004), has shown to inhibit proliferation of some tumors, as well as pancreatic cell lines, both inducing apoptosis and suppressing the cyclooxygenase-2 expression (Shirota *et al.* 2005). The employment of EPA, in addition, has been patented to reduce the proliferation of prostate cells (US 2003054053) and conjugate anticancer drugs as well as camptothecin (WO 2004012661). It has been demonstrated that ω-3 fatty acids have an inhibitory effect on tumour growth and proliferation contrastingly to ω-6 fatty acids, which would be involved in some kinds of cancer, as well in breast carcinoma (Karmali *et al.* 1984;

Cave & Jurkowski 1987), although it is not completely known the exact mechanism by which PUFAs affect mammary carcinogenesis. Some studies have reported that EPA would be able to inhibit estrogen-receptor positive human breast cancer cell growth (Chamras *et al*. 2002).

The experiments realized in collaboration with the BGU group demonstrated not significant effects of *C. scutellum* diatoms neither on the prawn *Macrobrachium rosenbergii* nor in the crawfish *Cherax quadricarinatus*. In fact, *in vivo* bioassays on *M. rosenbergii* juveniles were biassed by high mortality and high variation of male/female ratio in both controls and treatments. However, considering the replicates in which survival rate was more than 44%, an increase in percentage of females with respect to the males was observed in those crustaceans treated with the diatom acetone extract. *In vitro* assays carried out on androgenic glands and sperm ducts from *C. quadricarinatus* showed weak and not significant apoptosis in those samples incubated with fractions **1**-**3**. Further experiments are requested in order to clarify these points, although the obtained results seem to indicate that *C. scutellum* diatoms did not have a remarkable influence on the tested crustaceans of commercial interest. This could mean that such diatoms act on specific targets, which are present in *H. inermis* shrimps, but not in other crustaceans.

In turn, noteworthy results were obtained on cancer cell lines. First, it was demonstrated that solid tumours were more responsive to *C. scutellum* than lymphomas and normal cells, suggesting that the observed apoptosis was not a

general toxic effect, but a targeted action. Among solid tumours, breast cancer (BT20) showed to be the most responsive to the treatment and it was used as model in all the cytotoxicity tests. The assays performed on BT20 cell lines demonstrated a higher apoptotic activity of the diethyl ether extract in comparison with the butanol extract. According to the biological assays with *H. inermis*, fraction **3** showed to be the most active fraction to induce programmed cell death also on BT20 cells. In addition, a drastic cell reduction at G2/M phase was observed in those samples treated with fraction **3**, contrastingly to the populations incubated with fraction **1** and **2**, suggesting a possible arrest of the cell growth at G2/M phase induced by fraction **3**. In parallel, the presence of a significant amount of apoptotic cells (32%) was observed only in BT20 cells treated with fraction **3**, as shown in hypotonic PI staining experiments. It was demonstrated, in addition, that *C. scutellum* diatoms triggered apoptosis by the extrinsic pathway, requiring the activation of caspase 8, and caspase 3 was involved in the proteolytic cascade as well. The effects induced by fraction **3** were compared with those produced by EPA and they resulted to be similar in terms of both induction of apoptosis and reduction of cell vitality. These results could confirm the hypothesis that EPA is involved in the diatom-induced programmed cell death. However, it is not still clear whether EPA is the only factor triggering apoptosis both in *H. inermis* and cancer cell lines or the effect is due to synergistic interaction among more compounds. The knowledge that some diatom species are able to trigger apoptosis not only in their predators' offspring (Miralto *et al.* 1999;

Fontana *et al.* 2007), but also in human cancer cells (Caldwell *et al.* 2002; Romano *et al.* 2003; Tosti *et al.* 2003), positively supports our study.

6. New compounds from the Mediterranean mollusc *Aplysia fasciata* (Mollusca, Anaspidea)

6.1. Marine molluscs and terpene compounds

Among marine organisms, opisthobranch molluscs have been recognized as a rich source of new bioactive molecules with interesting ecological implications. Many of these secondary metabolites, in fact, act like chemical weapons, and this could explain the scarce predation on such molluscs in spite of their lack of physical protection (Karuso 1987; Avila 1995, 2006; Cimino *et al.* 1999, 2001). The order of opisthobranchs we studied, anaspideans or sea hares, has been widely studied from the chemical point of view and has demonstrated to produce mainly terpenes and polyketides (Yamada & Kigoshi 1997).

Terpenes are a family of compounds based on C_5 (isoprene) scaffolds and originate by the mevalonate pathway. Isoprene units, in form of isopentenyl pyrophosphate (IPP) and dimethylallyl pyrophosphate (DMAPP), derive from three acetyl-CoA molecules, of which two combine each other by Claisen reaction, and the third acetyl-CoA molecule is added by stereospecific aldolic condensation, affording

hydroxymethylglutaryl-CoA (HMG-CoA). NADPH reduces the thioester to aldehyde *via* thiohemiacetal yielding the mevaldic acid, which is reduced by NADPH to the corresponding alcohol, the mevalonic acid. The intermediancy of three molecules of ATP favours the decarboxylation of the mevalonic acid to afford IPP, which undergoes stereospecific allylic isomerization whose equilibrium favours DMAPP (Fig. 6.1).

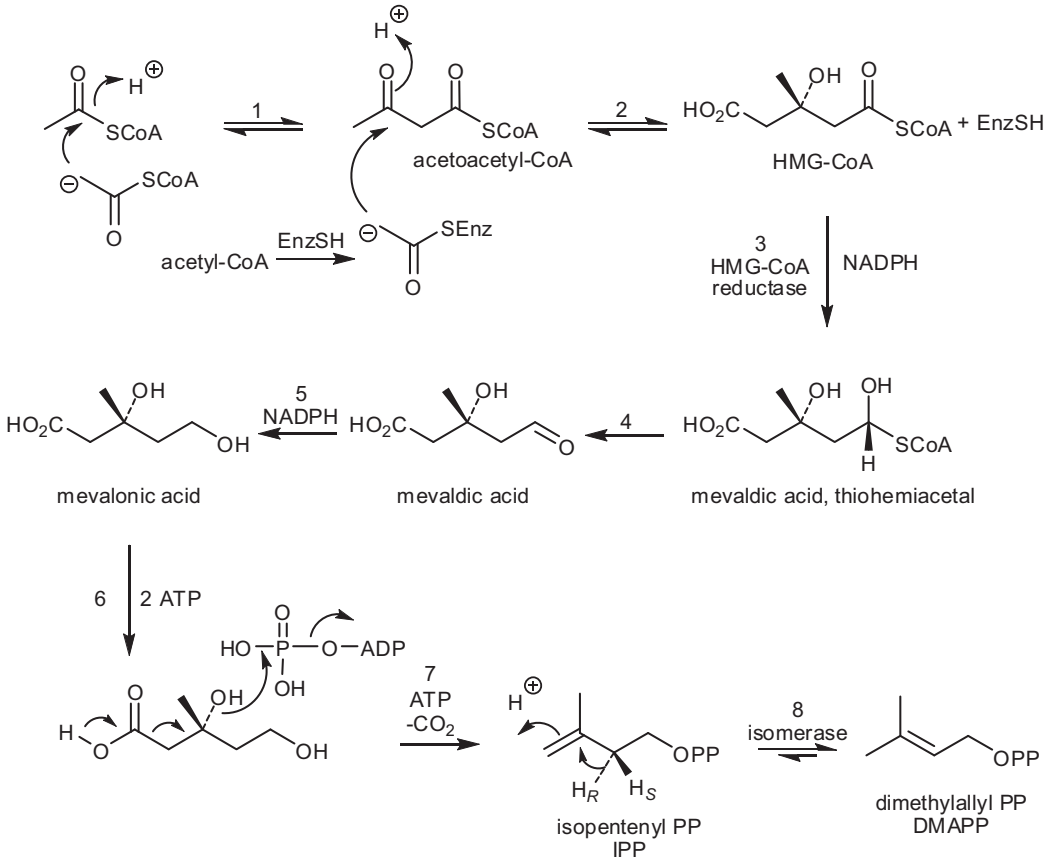

Fig. 6.1. Formation of IPP and DMAPP. 1: Claisen reaction; 2: stereospecific aldolic condensation; 3: reduction to thiohemiacetal; 4: reduction to mevaldic acid; 5: reduction to mevalonic acid; 6: phosphorylation of the primary alcohol to diphosphate; 7: decarboxylation-elimination; 8: stereospecific allylic isomerization.

In turn, DMAPP reacts with IPP affording geranyl pyrophosphate (GPP), which can be the precursor of monoterpenes, *i.e.* C_{10} compounds consisting of two isoprene units and usual constituents of essential oils, or can evolve to pharnesyl PP (PPP) in both *E,E* and *E,Z* isomers, the precursors of sesquiterpenes (Fig. 6.2).

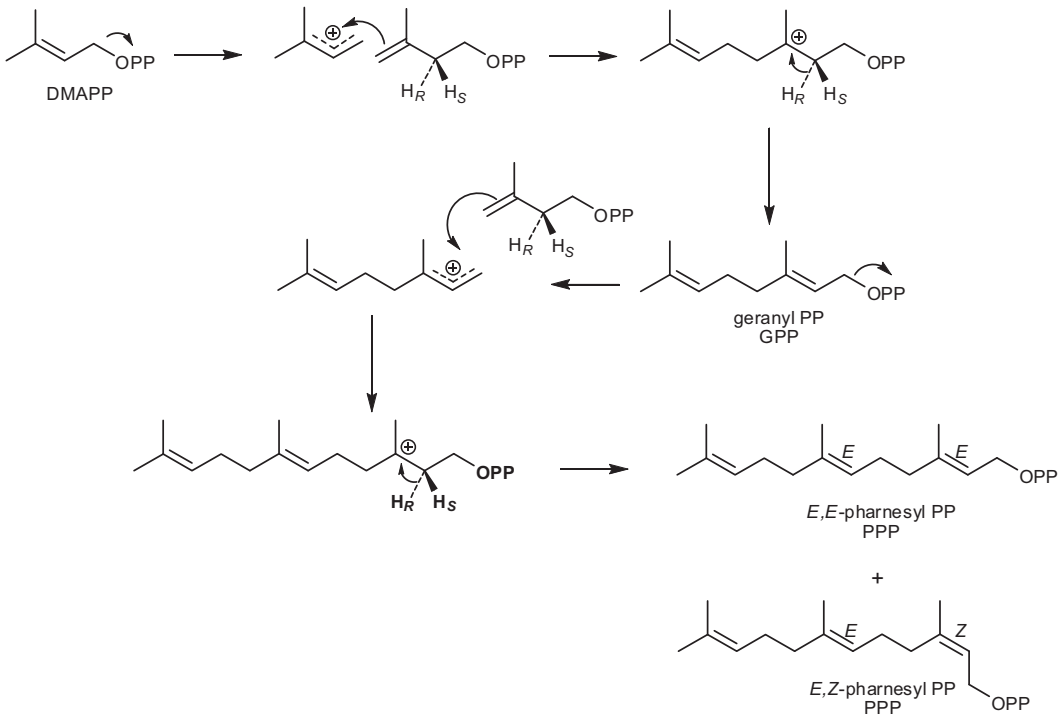

Fig. 6.2. Formation of both *E,E* and *E,Z*-pharnesyl PP, precursors of sesquiterpenes.

The different cyclization of both *E,E* and *E,Z* pharnesyl PP originates the huge diversity of sesquiterpene skeletons, thus characterized by combination of three isoprene units (Dewick 2001). Some sesquiterpene skeletons are reported in Fig. 6.3.

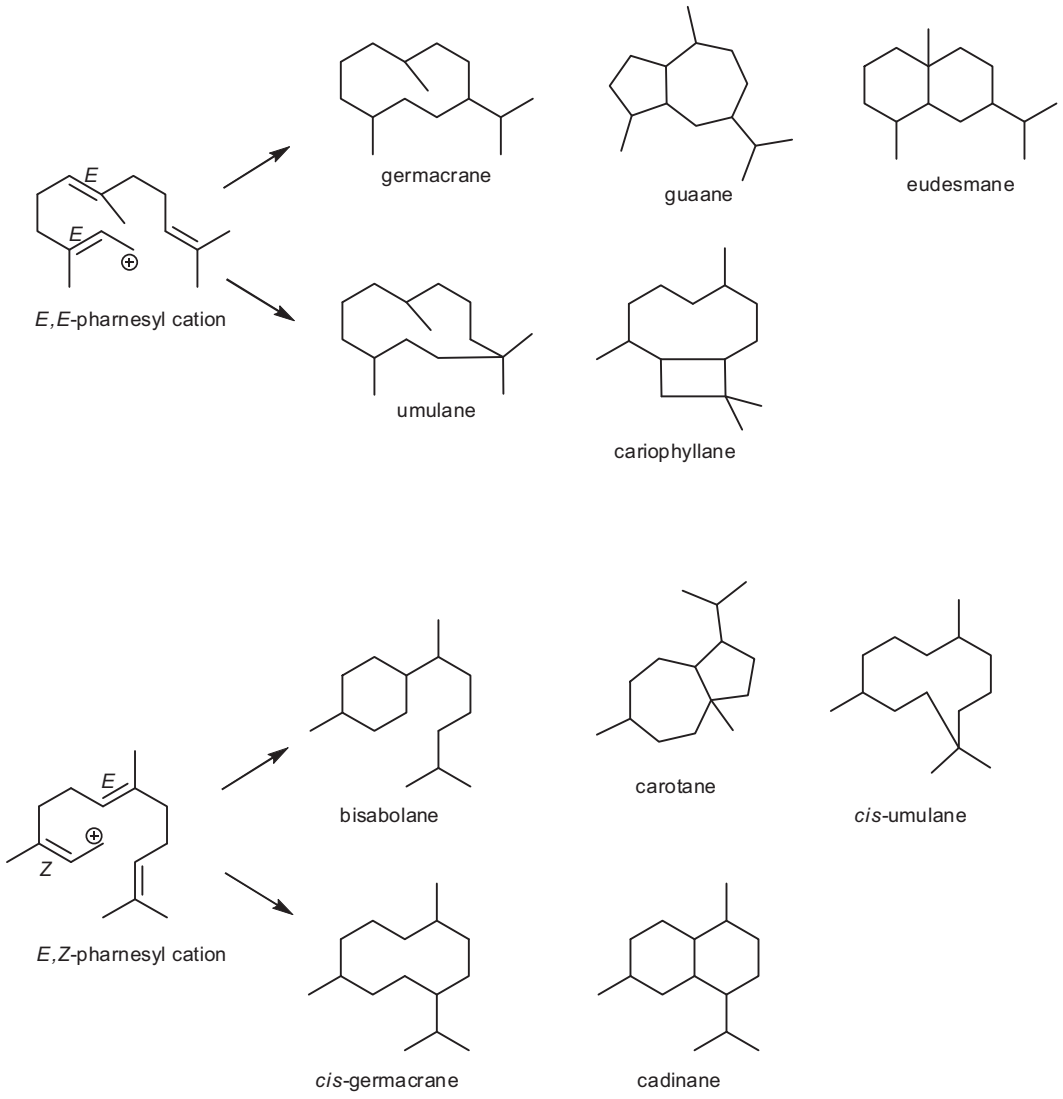

Fig. 6.3. Sesquiterpene skeletons.

On the other hand, PPP reacts with another IPP molecule affording geranylgeranyl PP (GGPP), the precursor of diterpenes (C_{20} compounds). Among them, phytol,

which forms the lipophilic side chain of chlorophylls, and vitamin K are very common in the nature (Fig. 6.4).

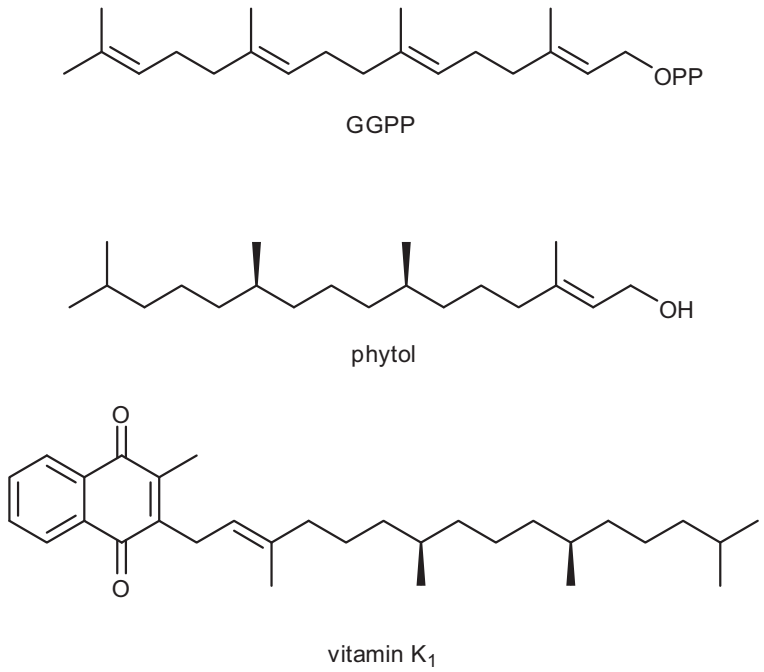

Fig. 6.4. Diterpenes derived from GGPP.

Sesterterpenes (C_{25} compounds) consist of 5 isoprene units and derive by cyclization of geranylpharnesyl PP. The most common type of marine sesterterpene is scalarine, obtained by a sequence of chain cyclization (Fig. 6.5).

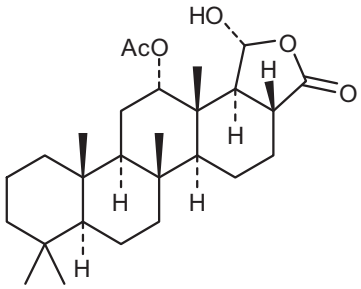

Fig. 6.5. Structure of scalarine.

Triterpenes are C_{30} compounds obtained by head-to-tail addition of two pharnesyl PP molecules to give squalene, the precursor of this class of terpenes. Squalene undergoes a series of transformations resulting in two molecules, lanosterol (in animals and fungi) and cycloartenol (in plants). Steroids are modified triterpenes containing the tetracyclic system of lanosterol (Fig. 6.6).

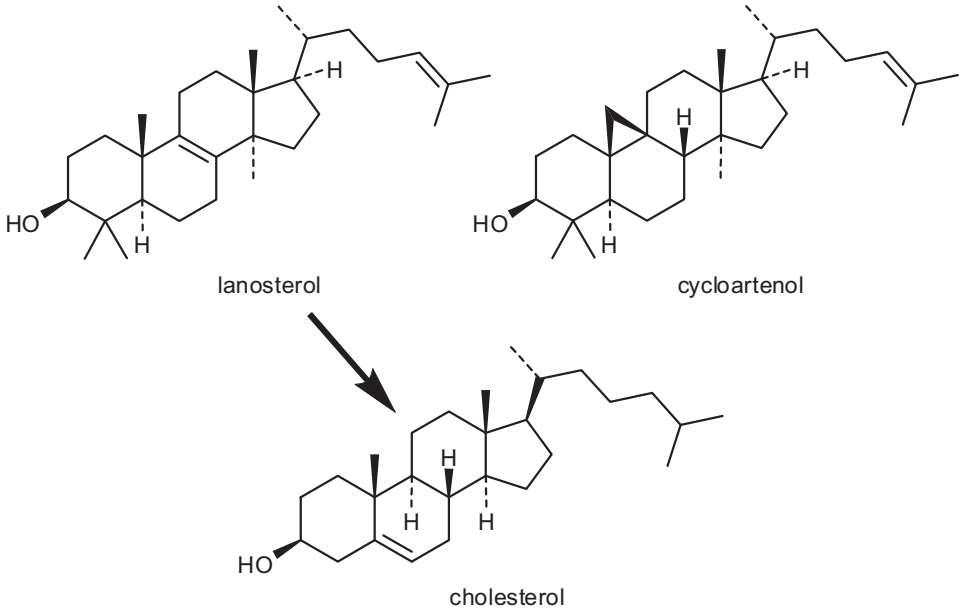

Fig. 6.6. The tetracyclic triterpenes lanosterol and cycloartenol, and cholesterol, obtained by lanosterol.

Pentacyclic triterpene skeletons, as well as lupeol, α-amirine and β-amirine, are usual constituents of triterpenoid saponins, *i.e.* glycosides with tensioactive properties able to form lathery aqueous solutions (Fig. 6.7).

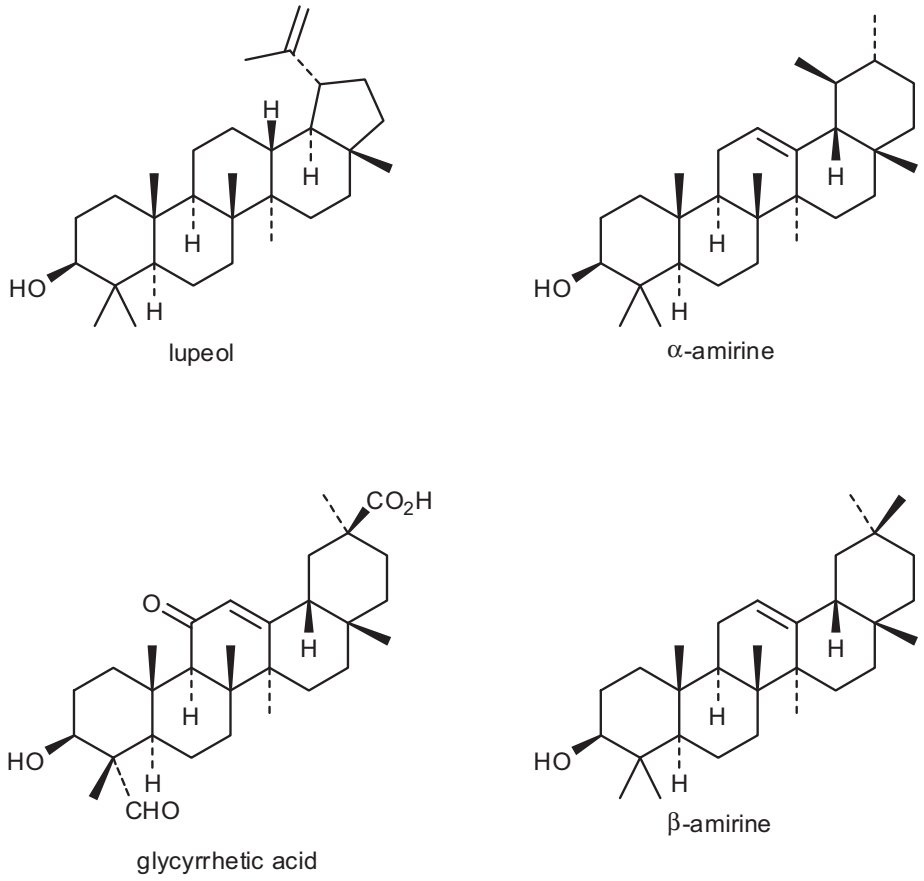

Fig. 6.7. Pentacyclic triterpenes: lupeol, α-amirine, glycyrrhetic acid and β-amirine.

One molecule of glycyrrhetic acid and two units of glucuronic acid form the glycyrrhizic acid, and the mixture of both potassium and calcium salts of glycyrrhizic acid constitutes the glycyrrhizine, contained in liquorice roots (*Glycyrrhiza glabra*, Leguminosae).

The tetraterpene skeleton (C_{40}) derives from phytoene, obtained by tail-to-tail coupling of two GGPP molecules. Carotenoids are the main members of this class of terpenes and play an important role not only in photosynthesis, but also in non-photosynthetic organisms, as well as bacteria and fungi. Lycopene and carotenes are the main representatives of this class (Fig. 6.8).

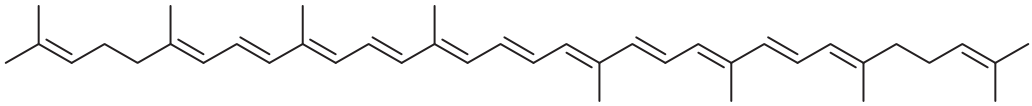

lycopene

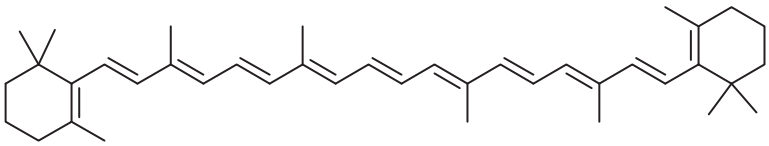

β-carotene

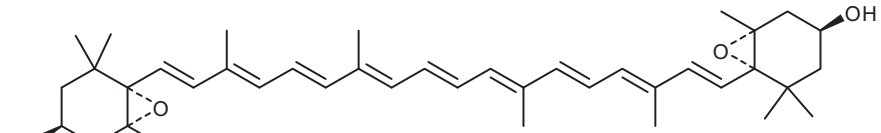

violaxanthin

Fig. 6.8. Some tetraterpene compounds: lycopene, β-carotene and violaxanthin.

Polyketides, which are often isolated from anaspideans along with terpenes, constitute a wide class of compounds with a common biogenesis, the acetate pathway. In fact, all these compounds derive from Claisen condensation of n acetyl-

CoA molecules and consist in fatty acids, polyacetilene compounds and prostaglandins (Dewick 2001). Since sea hares are herbivorous, many isolated allelochemicals have revealed to be typical algal metabolites (in particular from *Laurencia* and *Plocamium* species) which are stored in the animal and used against the predator in case of aggression (Cimino *et al*. 2001).

Our chemical study focused on the anaspidean mollusc *Aplysia fasciata* Poiret, 1789 (Fig. 6.9), which is widely distributed in shallow waters of the Mediterranean Sea and along the Atlantic coast of France and West Africa. It is a large species, reaching up to 40 cm in length, with a thin, internal, and a little bit convex shell. *A. fasciata* lives on coastal vegetal communities, in particular *Ulva*, *Cystoseira*, *Cymodocea* and *Zostera* upon which the mollusc feeds. When disturbed, the mollusc produces a repellent whitish substance, which becomes purple in combination with another secretion (Rudman 2001).

Fig. 6.9. The anaspidean mollusc *Aplysia fasciata.*

6.2. Isolation and purification

6.2.1. Biological material

A sample of three specimens of *Aplysia fasciata* was collected by snorkeling along the Delta de l'Ebre, Tarragona (Spain) during January 2008. The molluscs were transferred to the Facultat de Biologia (Universitat de Barcelona) and dissected into several parts, including mantle and internal organs, in order to differentiate the compounds involved in the chemical defence (which are usually localized in the external parts of the animal) from those acquired by the food (usually present in the digestive gland). The different anatomical sections were stored at -20°C, freeze-dried and, afterwards, shipped to the School of Pharmacy (University of Athens) where the chemical investigation was carried out.

6.2.2. Extraction

The different anatomical sections of *A. fasciata* [mucous secretion (A1), stomach walls (A2), opaline gland (A3), buccal bulb (A4), stomach contents (A5), reproductive system (A6), mantle and foot (A7), and both hermaphroditic and digestive glands (A8)] were separately extracted overnight with a mixture of dichlomethane/methanol 2:1 v/v, sonicating in an ultrasound bath and crumbling in a mortar the coarsest parts. The suspensions were filtrated and, afterwards, *in vacuo* evaporated until

dryness affording eight crude extracts which were subjected to a preliminary TLC screening using various mixtures of solvents as eluants (Fig. 6.10).

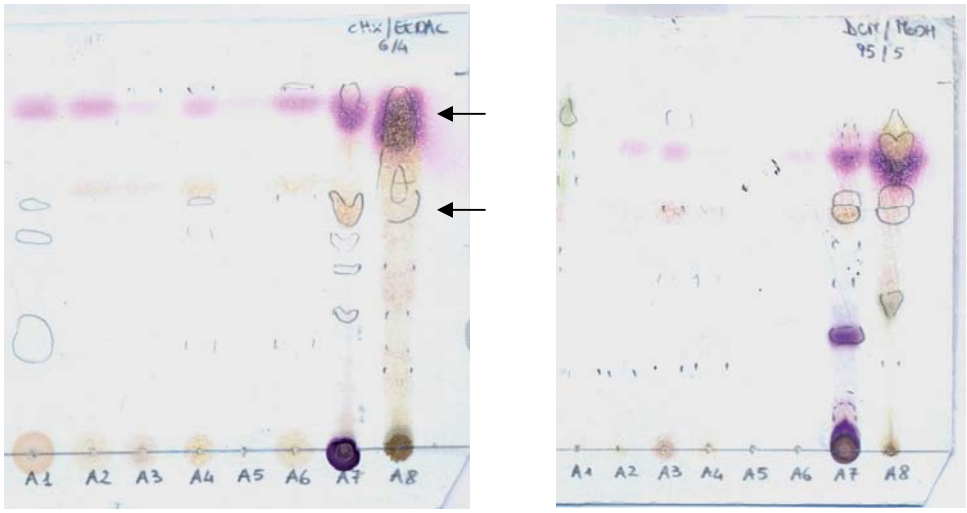

Fig. 6.10. TLC analysis of the different anatomical parts of *A. fasciata* using several eluant systems (cHx/EtOAc 6:4 v/v and DCM/MeOH 95:5 v/v).

6.2.3. Purification

The TLC analysis of the crude extracts highlighted that the fraction consisting in both the digestive and hermaphroditic glands of *A. fasciata* (indicated as A8 in Fig. 6.10.) appeared to be interesting because, besides the usual lipidic components (fatty acids and sterols), it was characterized by two UV-visible bands at R_f 0.9 and R_f 0.7 (cyclohexane/ethylacetate 6:4 v/v). The extract A8 (3.0 g) was, herein, subjected to a preliminary ^{1}H NMR analysis, which showed the presence of remarkable and interesting signals within the range δ 3.0-5.5.

Consequently, the organic extract A8 was purified by means of different chromatographic methods: vacuum liquid chromatography (VLC), solid phase extraction (SPE) and high performance liquid chromatography (HPLC).

The extract was *a priori* fractionated by means of VLC. The column, consisting in a glass funnel provided with a silica septum, was packed with silica gel and connected to the vacuum. The funnel was filled with silica gel which was pressed in order to avoid the presence of air inside the column. The extract, previously dissolved in a flask with DCM/MeOH 2:1 v/v, was mixed with silica gel. The mixture was completely dried by vacuum until obtaining a powder, which was hence put into the column, trying to form a thin layer. Afterwards, the column was eluted with cHx and increasing amounts of EtOAc. The recovered fractions were combined into nine groups (A-I). Fraction C (54.7 mg) was further fractionated by normal phase SPE, which consists in a separation by pre-packed cartridges. In particular, an aliquot of fraction C was dissolved in cHx, loaded onto a normal phase cartridge and forced, by means of a syringe, to be eluted by an increasing polarity gradient of cHx/EtOAc. The separation was analogously repeated on the remaining part of the extract, and afforded three fractions (C1-C3). Fraction C1 (24.1 mg) was subjected to normal phase HPLC, using *n*-Hx/EtOAc 98:2 v/v as eluant and at 2 ml min^{-1} flow rate, to yield compounds **1** (2.2 mg), **3** (0.6 mg), **4** (1.1 mg), **12** (8.0 mg), **13** (1.3 mg) (Fig. 6.11). By means of repetitive normal phase HPLC purifications of fraction C1 (*n*-Hx/EtOAc

98:2 v/v as mobile phase at 1.5 ml min^{-1} flow rate), compounds **5** (0.6 mg), **6** (0.7 mg), **7** (0.6 mg), **8** (1.0 mg), **11** (0.8 mg) and **14** (0.6 mg) were obtained as well.

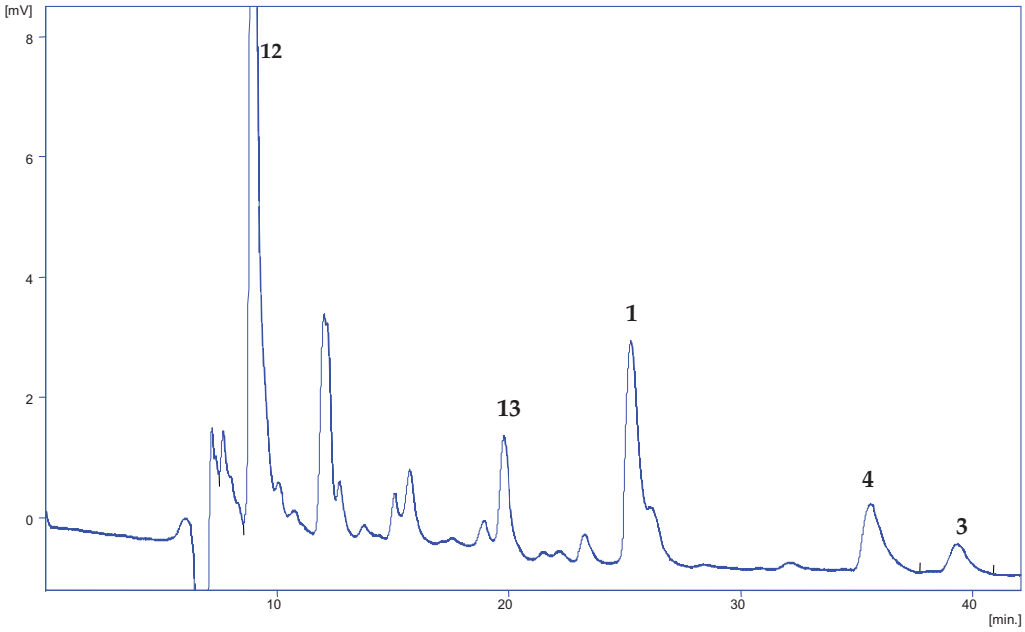

Fig. 6.11. HPLC purification of fraction C1 (*n*-Hx/EtOAc 98:2 v/v mobile phase, 2 ml min^{-1} flow rate). The numbers correspond to the purified compounds.

Fraction C2 (29.0 mg) was purified by normal phase HPLC (cHx/EtOAc 95:5 v/v at 1.5 ml min^{-1}) to yield compounds **2** (0.8 mg) and **8** (1.0 mg) (Fig. 6.12).

Fraction F was further fractionated by normal phase SPE using cHx with increasing amounts of EtOAc as mobile phase, to yield eight fractions (F1-F8). Fractions F3 (30.6 mg), F4 (36.9 mg), and F5 (20.5 mg) were purified by normal phase HPLC, using cHx/EtOAc 75:25 v/v as eluant, to yield compounds **10** (3.3 mg), **15** (8.4 mg), and **16** (11.3 mg). The HPLC purification of fraction F3 is reported in Fig. 6.13.

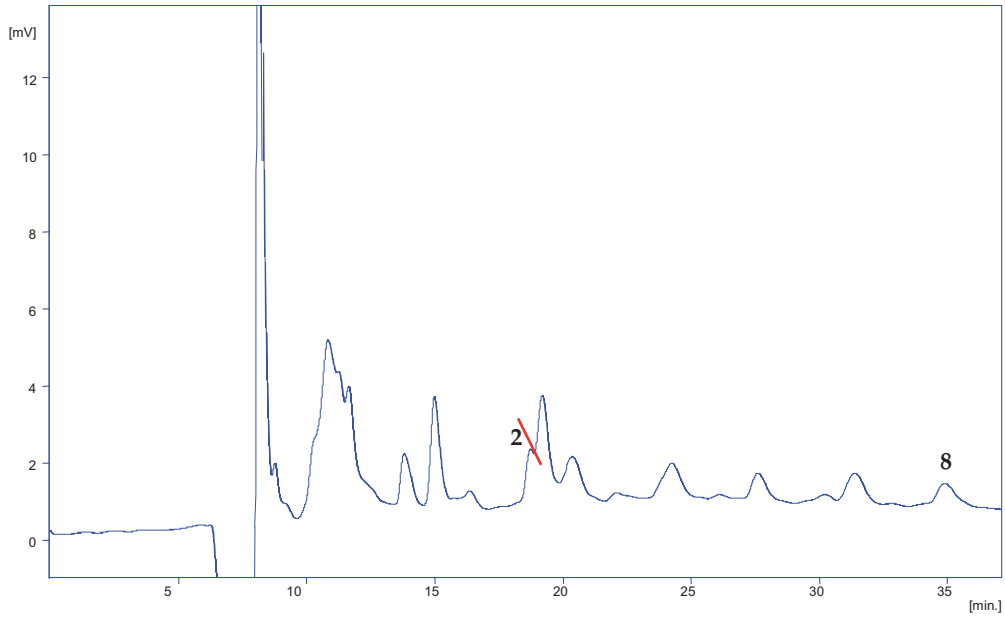

Fig. 6.12. HPLC purification of fraction C2 (cHx/EtOAc 95:5 v/v eluant, 1.5 ml min^{-1} flow rate).

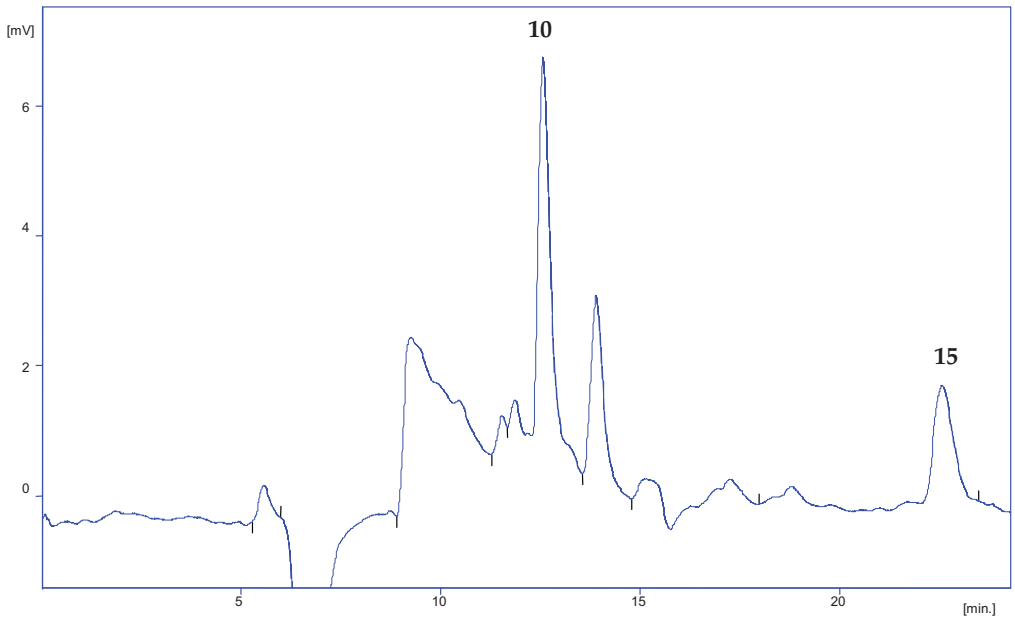

Fig. 6.13. HPLC purification of fraction F3 (cHx/EtOAc 75:25 v/v eluant, 1.5 ml min^{-1} flow rate).

The HPLC purification of fraction F5 is shown in Fig. 6.14.

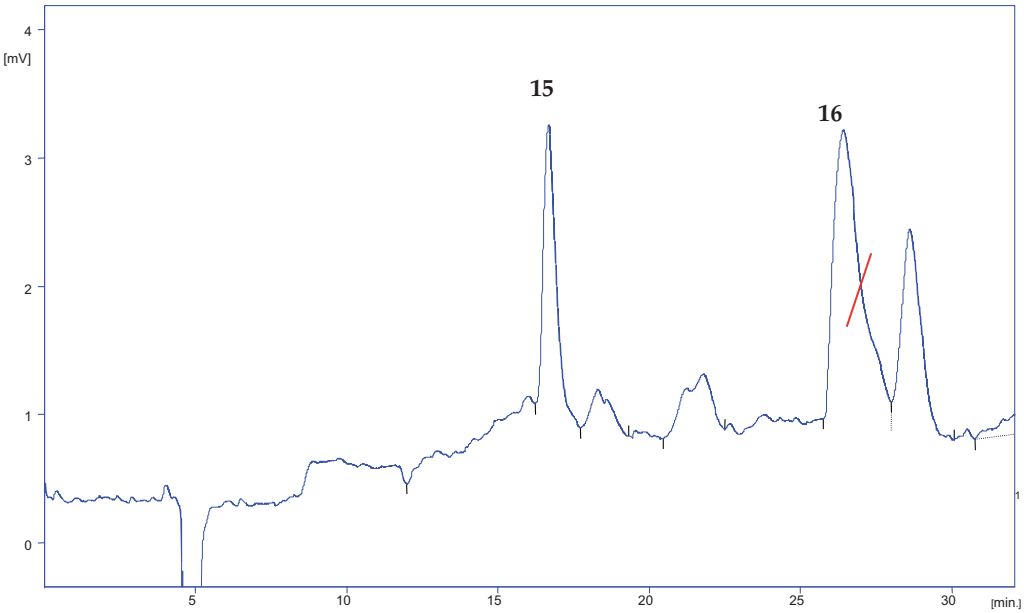

Fig. 6.14. HPLC purification of fraction F5 (cHx/EtOAc 75:25 v/v eluant, 2 ml min^{-1} flow rate).

Fraction G (102.3 mg) was fractionated by SPE on normal phase pre-coated cartridges, employing cHx with increasing amounts of EtOAc as movil phase to yield seven fractions (G1-G7). Fractions G3 (23.9 mg), G4 (37.9 mg), and G5 (15.4 mg) were purified by normal phase HPLC in isocratic conditions, using cHx/EtOAc 75:25 v/v as eluant, to yield compounds **9** (6.8 mg), **15** (2.0 mg), and **16** (10.4 mg).

6.3. Chemical characterization

The structural elucidation of the purified metabolites was carried out by combining the results of mono- and bidimensional NMR spectra (^{1}H NMR, ^{13}C NMR, ^{1}H-^{1}H COSY, NOESY, HSQC, HMBC) and comparing the recovered data with those reported in the literature for similar compounds.

The chemical analysis carried out on the organic extract of both the digestive and hermaphroditic glands of the anaspidean mollusc *Aplysia fasciata* led to the isolation of 16 metabolites, six of which (compounds **4**, **6**, **7**, **8**, **10**, **15**) were isolated for the first time from natural sources.

Brasilenol (**1**) and its epimer at C-2, epibrasilenol (**2**), along with brasilenol acetate (**5**) (Stallard *et al.* 1978), 4-hydroxy-5-brasilene (**3**), and 4-acetoxy-5-brasilene (**7**) (Amico *et al.* 1991; Wright *et al.* 1991) are nonisoprenoid sesquiterpene alcohols characterized by the rare brasilane skeleton (Fig. 6.15).

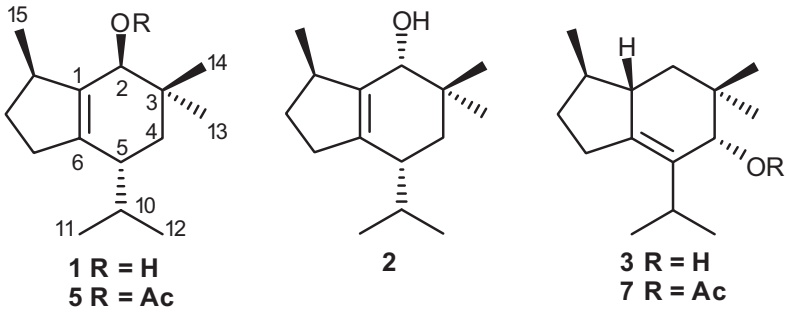

Fig. 6.15. Structures of compounds **1**-**3**, **5**, and **7**.

Brasilenol (**1**) is a secondary alcohol with molecular formula $C_{15}H_{26}O$. The three degrees of unsaturation were satisfied by the bicyclic carbon skeleton and a double bond. Absorption at 3650 cm^{-1} in the IR spectrum was diagnostic for the presence of the hydroxy group. Two low field singlets at δ 142.1 and 138.7 ppm in the off-resonance ^{13}C NMR spectrum were indicative of the tetrasubstituted olefinic carbons. The ^{1}H NMR spectrum, on the other hand, was characterized by five high field methyl signals, composed by two singlets at δ 1.02 and 0.82, corresponding to the *gem*-dimethyl system at C-3, and three doublets ($J \approx 7$ Hz each), of which two at δ 0.87, 0.67, corresponding to the *gem*-dimethyl at C-10, and one at δ 1.10, attributed to the methyl protons at C-15. The acetylation of **1** to afford **5** determined the downfield shift of H-2α from δ 4.01 (in **1**, *dddd*, J = 1, 3, 3, 3) to δ 5.36 (in **5**, *dddd*, J = 1, 3, 3, 3), which also confirmed that OH was allylic.

Epibrasilenol (**2**) was highly spectrally comparable with brasilenol. In the ^{1}H NMR spectrum the presence of a singlet at δ 3.47, corresponding to H-2β, was noteworthy. The relative stereochemistry of **1** and **2** was determined by semiquantitative analysis of the lanthanide-induced ^{1}H shift NMR data (Stallard *et al.* 1978).

Analogously to compounds **1**-**2**, the ^{1}H NMR spectrum of 4-hydroxy-5-brasilene (**3**, Fig. 6.16) showed the presence of two tertiary methyls and three secondary methyl functions, of which two composing an isopropyl moiety. The singlet at δ 3.51 was attributed to the allylic alcohol.

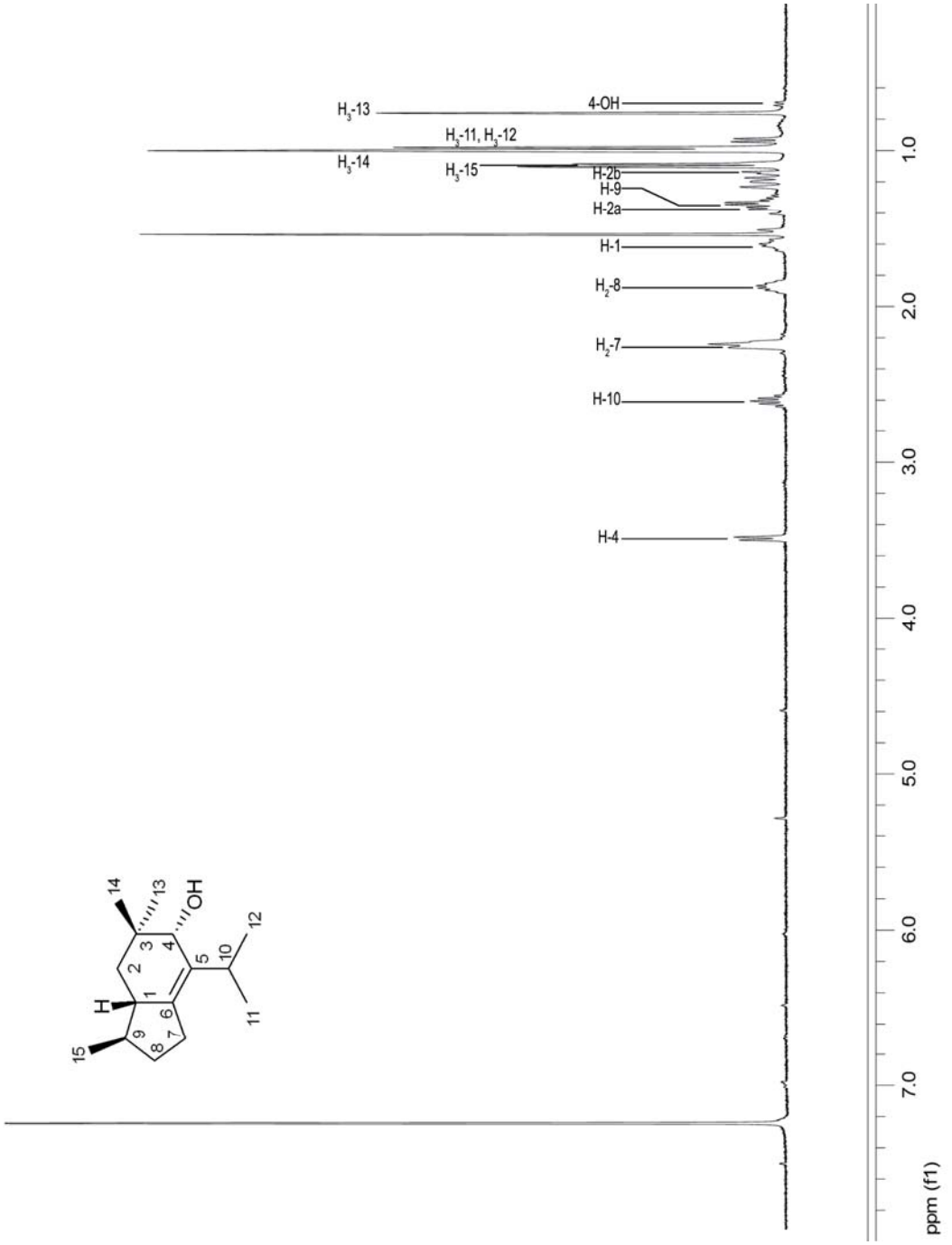

Fig. 6.16. ^{1}H NMR spectrum of compound **3**.

In the ^{13}C NMR spectrum of **3** the presence of two sp^2 hybridized carbons at δ 133.6 (*s*) and 140.7 (*s*) was remarkable. The IR band at 3470 cm^{-1} as well as the peak at δ 72.9 (*d*) in the ^{13}C NMR spectrum indicated the presence of a secondary alcohol group. The IR spectrum, in addition, showed the presence of an isopropyl substituent (1375 and 1360 cm^{-1}) and the absence of a carbonyl functionality. ^{1}H-^{1}H COSY data, along with both one-bond and long-range ^{13}C-^{1}H correlation experiments, allowed assigning a brasilane skeleton to **3**. The stereochemistry of the three chiral centers was deduced from the results of 2D NOE measurements (Amico *et al.* 1991).

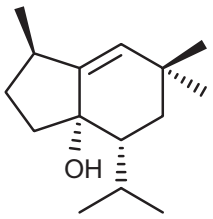

Fig. 6.17. Structure of **4**.

Compound **4** (Fig. 6.17), isolated as a colorless oil, displayed an ion peak at *m/z* 221.1909 (FAB-HRMS), corresponding to $C_{15}H_{25}O$ and consistent with $[M - H]^+$. The fragment ion at *m/z* 204 $[M - H_2O]^+$ in the mass spectrum, as well as the absorption band at 3485 cm^{-1} in the IR spectrum, indicated the presence of a hydroxy group. The ^{13}C NMR spectrum (Fig. 6.18), along with DEPT experiments, revealed 15 carbon signals, in particular three quaternary carbon atoms, four methines, three methylenes, and five methyls. Among them, two olefinic carbons (one methine and one quaternary resonating at δ 129.2 and 148.3, respectively), one oxygenated quaternary carbon (δ 79.9), and a shielded tetrasubstituted carbon (δ 33.0) were evident. Since the carbon-carbon double bond accounted for one of the three degrees of unsaturation, the molecular structure of **4** was determined as bicyclic.

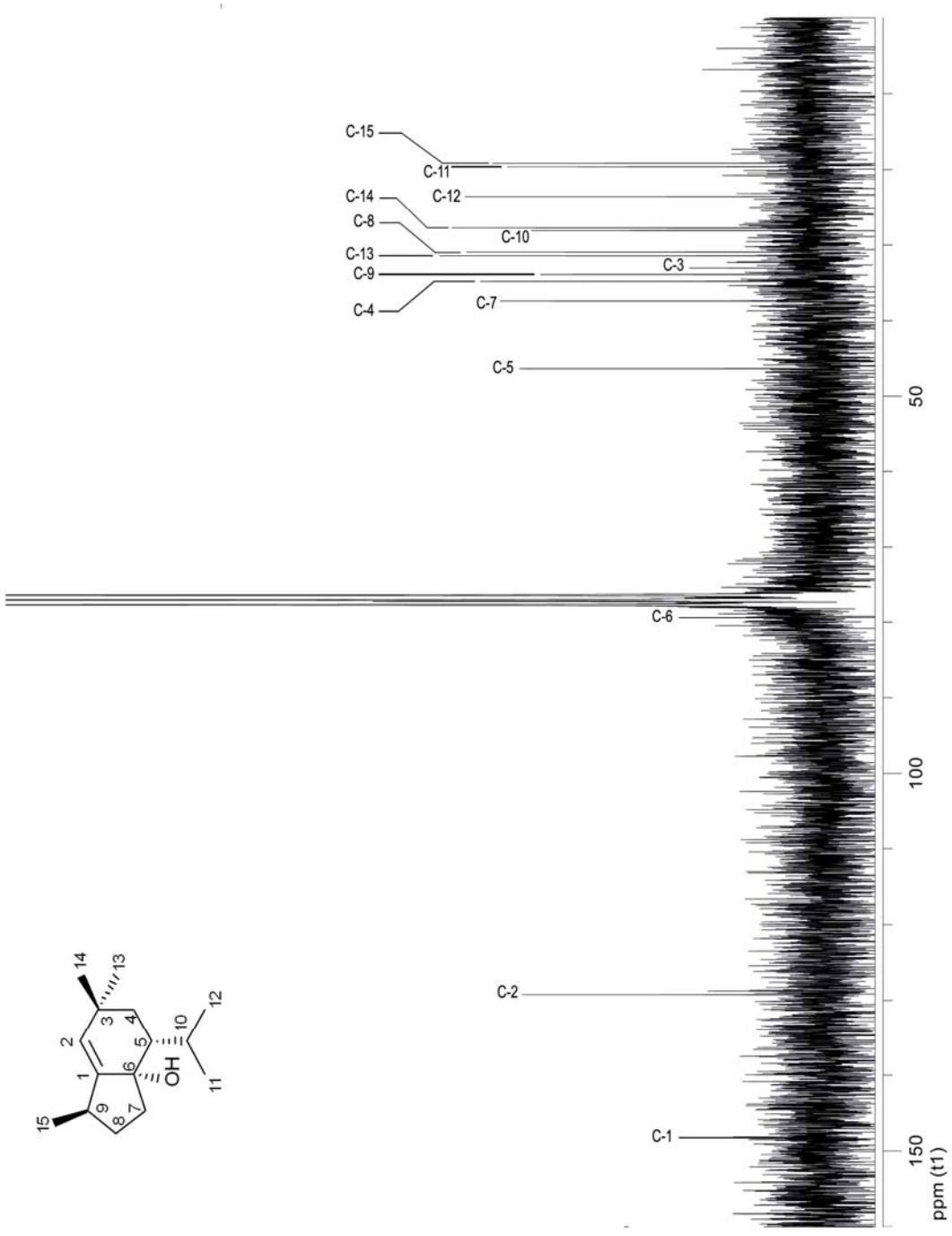

Fig. 6.18. ^{13}C NMR spectrum of **4**.

The structural elements displayed in the ^{1}H NMR spectrum of **4** (Fig. 6.19) included five methyl groups, two on quaternary (δ 1.02 and 0.89) and three on methine (δ 0.99, 0.97, and 0.96) carbon atoms, and an olefinic methine of a trisubstituted double bond (δ 5.05). Two of the five methyls (singlets) were assigned to a *gem*-dimethyl group, as indicated by the HMBC correlations of C-3 with H_3-13 and H_3-14, while two of the remaining (doublets) were part of an isopropyl moiety, as revealed from the cross-peaks of H-10/H_3-11 and H-10/H_3-12 in the ^{1}H-^{1}H COSY spectrum, as well as the correlations of C-5 and C-10 with both H_3-11 and H_3-12 in the HMBC spectrum. ^{13}C NMR and ^{1}H NMR resonance values are reported in Table 6.1. This information, in conjunction with further correlations provided by ^{1}H-^{1}H COSY, HSQC-DEPT, and HMBC experiments (Fig. 6.20-6.22), suggested a brasilane skeleton with a trisubstituted double bond and one oxygenated site, according to reference compounds reported in the literature (Stallard *et al.* 1978; Amico *et al.* 1991; Wright *et al.* 1991). The correlations of C-2 with H-9, H_3-13, and H_3-14 positioned the trisubstituted double bond between C-1 and C-2, whereas the correlations of C-6 with H-2, H_2-4, and H-10 placed the hydroxy group at C-6. The relative configuration of **4** was assigned on the basis of interactions observed in the NOESY spectrum. In particular, the n.O.e. enhancement of H-5/H_3-14 suggested an equatorial orientation for the isopropyl group and a pseudoaxial orientation for H_3-14 on the cyclohexene ring.

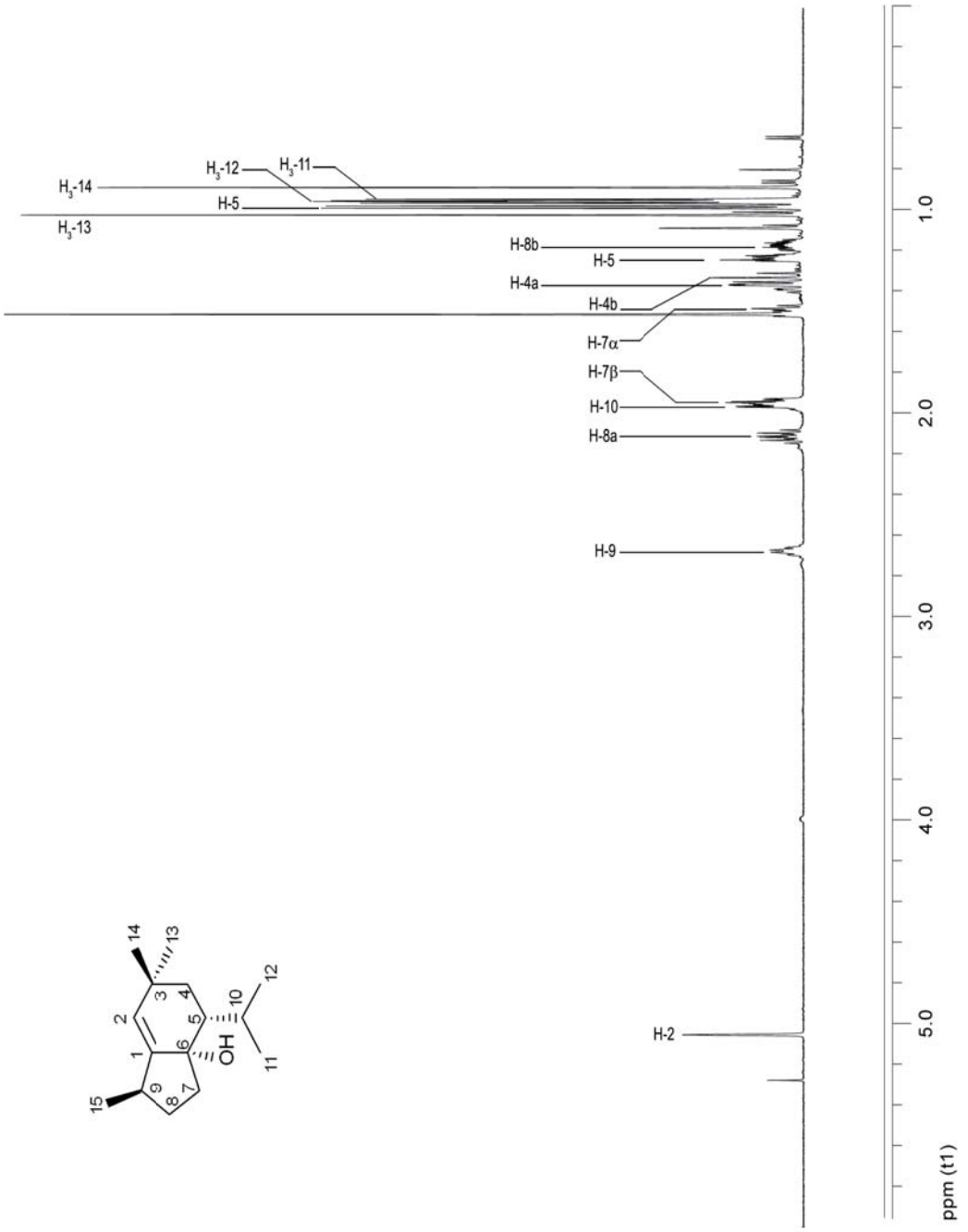

Fig. 6.19. ^{1}H NMR spectrum of **4**.

As a consequence, the only possible stereostructure that could justify the critical NOE correlation observed between H-7β and H_3-15 in the cyclopentane ring required a pseudoaxial orientation for both H_3-15 and the hydroxy group at C-6. The n.O.e enhancement of H-5/H-7β, even though partially overlapping with the H-5/H-10 cross-peak, further supported the proposed relative configuration of **4**.

C	δ ^{13}C	mult.	δ ^{1}H	mult., J_{H-H} (Hz)	Significant long-range correlations (HMBC)
1	148.3	*s*	-	-	H-8a, H-9, H_3-15
2	129.2	*d*	5.05	br *s*	H-9, H_3-13, H_3-14
3	33.0	*s*	-	-	H-2, H_3-13, H_3-14
4	34.8	*t*	a 1.38	*m*	
			b 1.33	*m*	
5	46.3	*d*	1.24	*m*	H_3-10, H_3-11, H_3-12
6	79.9	*s*	-	-	H-2, H-4a, H-4b, H-8b, H-10
7	37.4	*t*	α 1.50	*m*	
			β 1.95	*m*	
8	30.9	*t*	a 2.12	*m*	
			b 1.18	*m*	
9	33.9	*d*	2.68	*m*	H_3-15
10	28.1	*d*	1.97	*m*	H-4a, H4b, H_3-11, H_3-12
11	19.6	*q*	0.96	*d*, 6.9	H_3-12
12	23.6	*q*	0.97	*d*, 6.8	H_3-11
13	31.4	*q*	1.02	*s*	
14	27.7	*q*	0.89	*s*	
15	19.2	*q*	0.99	*d*, 6.8	

Table 6.1. ^{13}C and ^{1}H NMR resonance values of compound **4**.

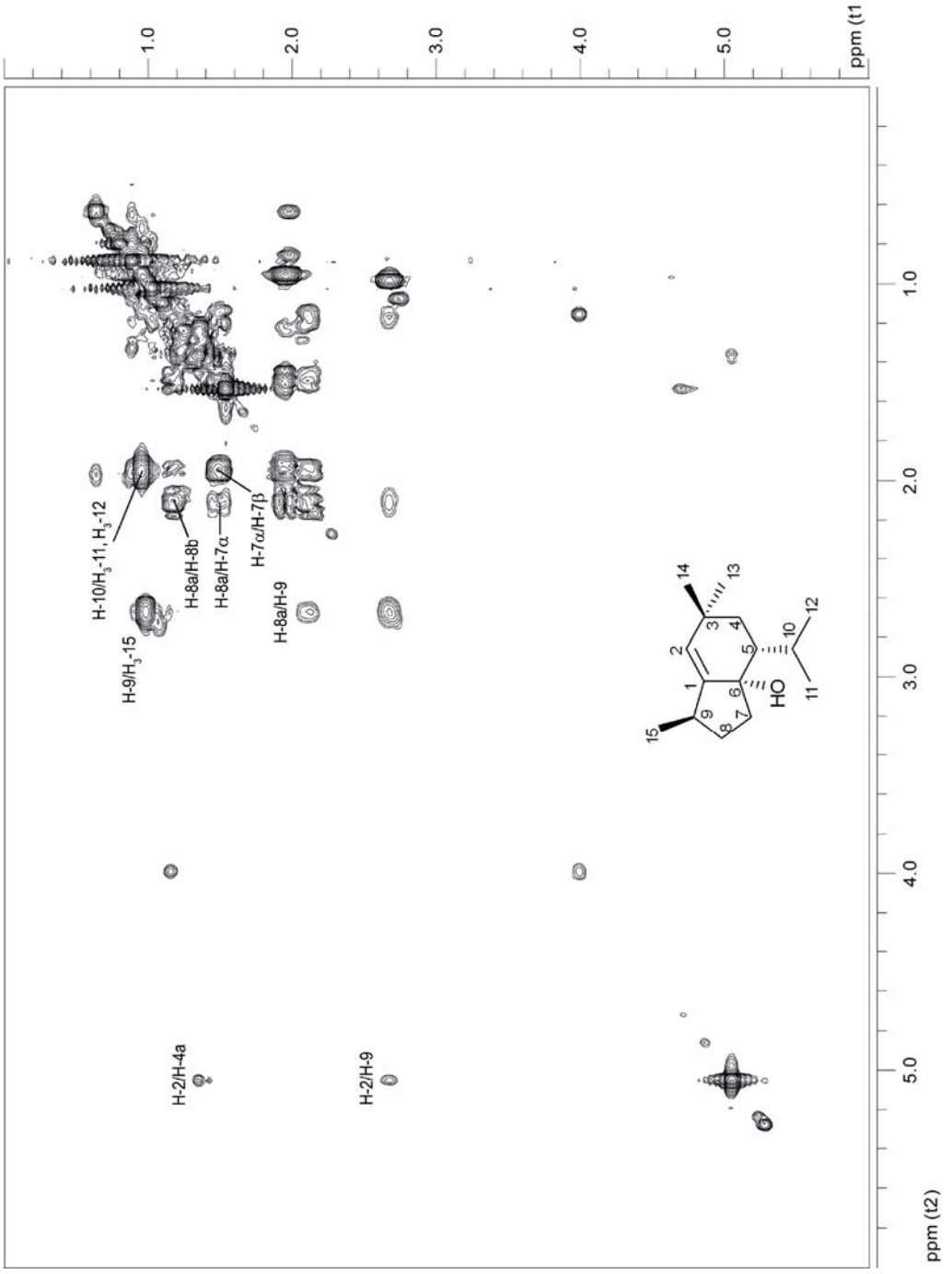

Fig. 6.20. Significant ^{1}H-^{1}H correlations in the COSY spectrum of compound **4**.

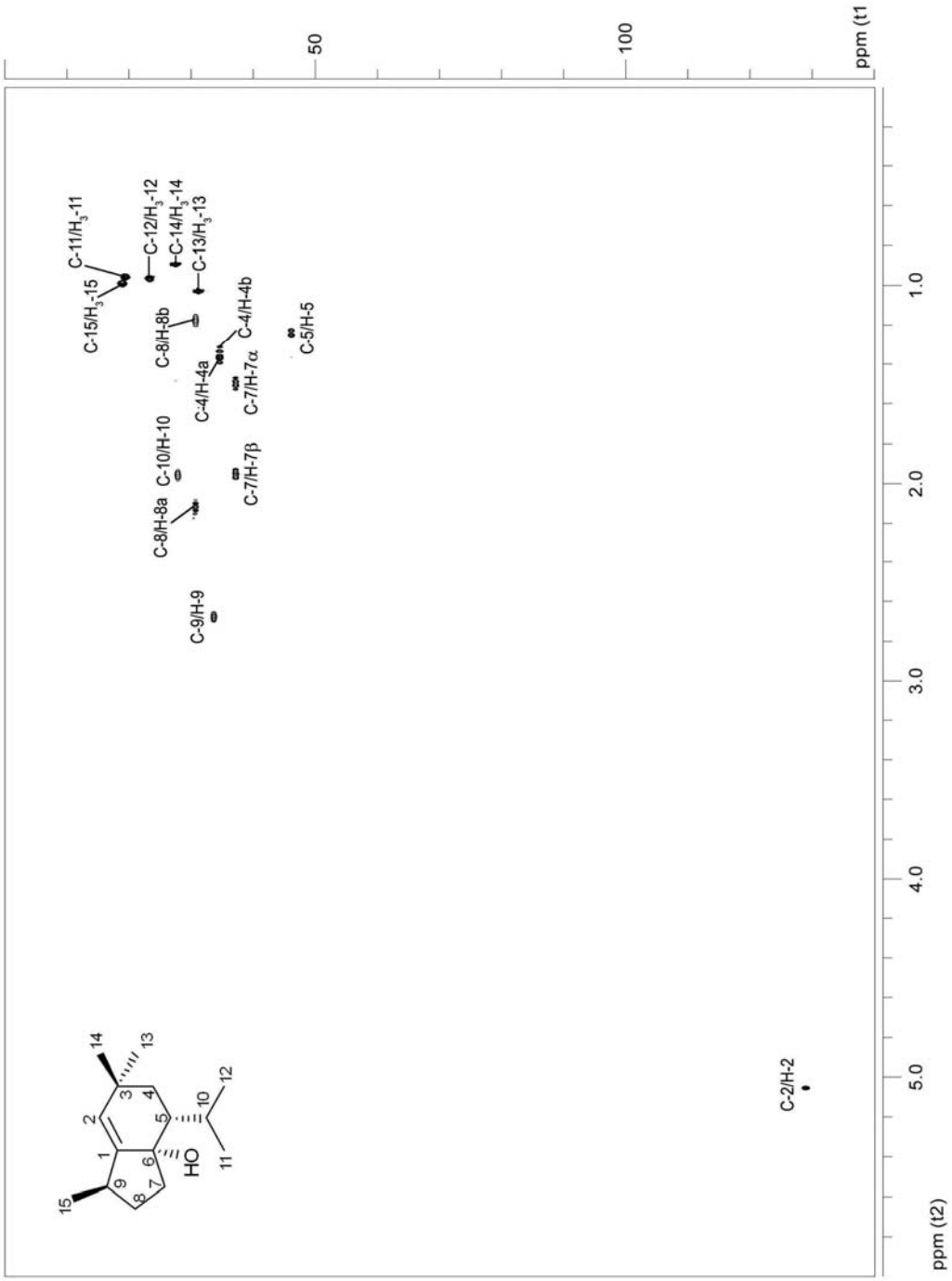

Fig. 6.21. HSQC-DEPT spectrum of compound **4**.

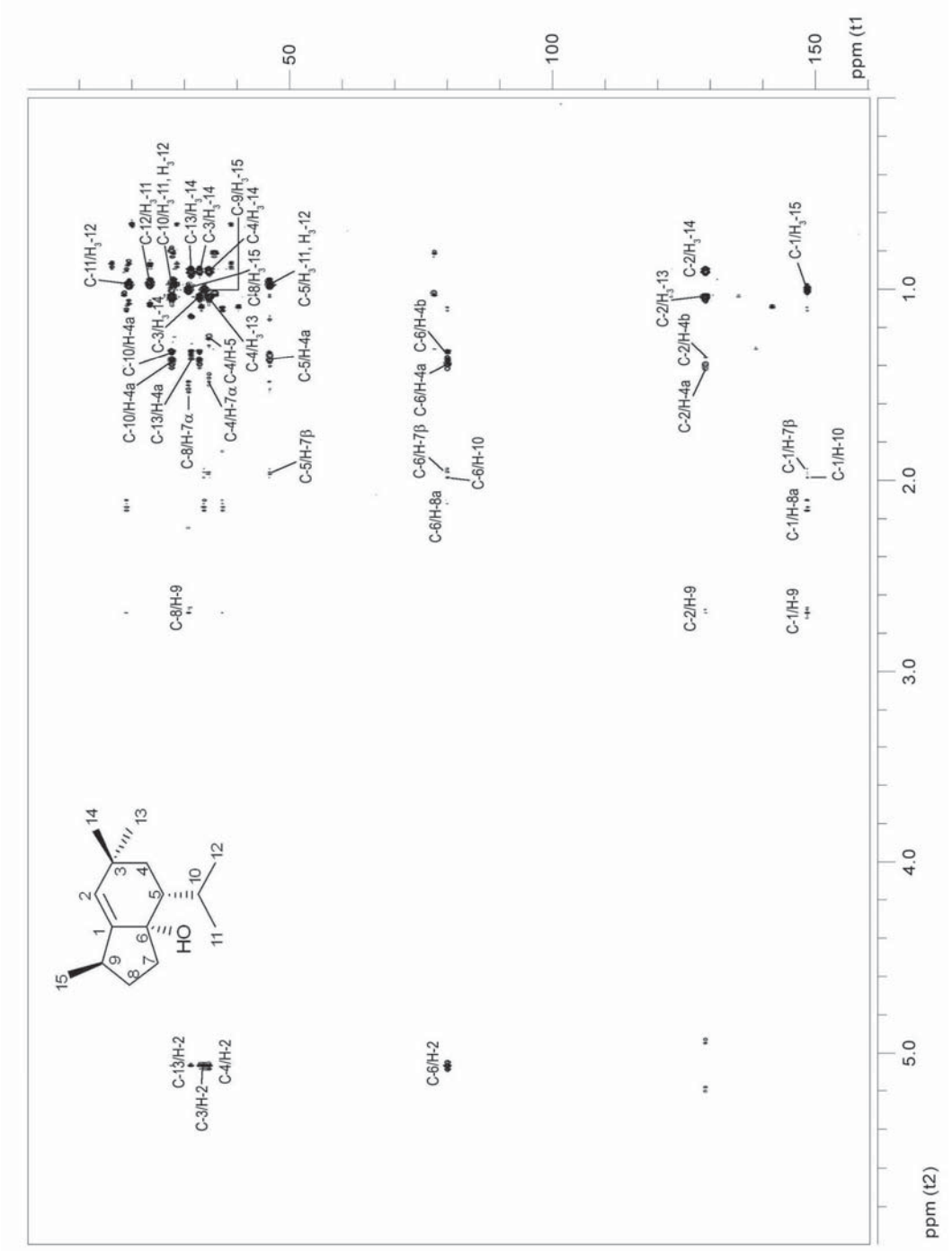

Fig. 6.22. Significant long-range correlations in the HMBC spectrum of compound **4**.

Compound **6** (Fig. 6.23), isolated as a colorless oil, displayed an ion peak at *m*/*z* 265.2195 (FAB-HRMS), corresponding to $C_{17}H_{29}O_2$ and consistent with $[M + H]^+$. The fragment ion at *m*/*z* 204 $[M - AcOH]^+$ in the mass spectrum, in conjunction with the absorption band at 1733 cm^{-1} in the IR spectrum, indicated the presence of an acetoxy group. The ^1H NMR spectrum of **6** (Fig. 6.24), which included signals for five methyl groups (two on quaternary carbons resonating at δ 0.90 and 0.82, and three on methine carbons at δ 0.97, 0.91, and 0.70), an acetate methyl group (δ 2.01), and a deshielded oxygenated methine (δ 4.96), closely resembled that of brasilenol acetate (**5**). ^{13}C NMR and ^1H NMR assignments of compound **6** are reported in Table 6.2. Analysis of the 2D NMR spectra (^1H-^1H COSY, HSQC-DEPT, and HMBC, Fig. 6.25-6.27) of **6** suggested the same planar structure, thus indicating that **5** and **6** were stereoisomers. Proof of the latter hypothesis and identification of **6** were provided by acetylation of epibrasilenol (**2**) with Ac_2O in pyridine for 16 hours at 70°C, which yielded epibrasilenol acetate, identical in all with respect to the natural product **6**.

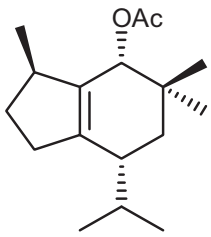

Fig. 6.23. Structure of **6**.

4-Acetoxy-5-brasilene (**7**) has been described in the literature as semisynthetic compound obtained by acetylation of **3** (Amico *et al.* 1991), but in our investigation it was isolated for the first time as natural product.

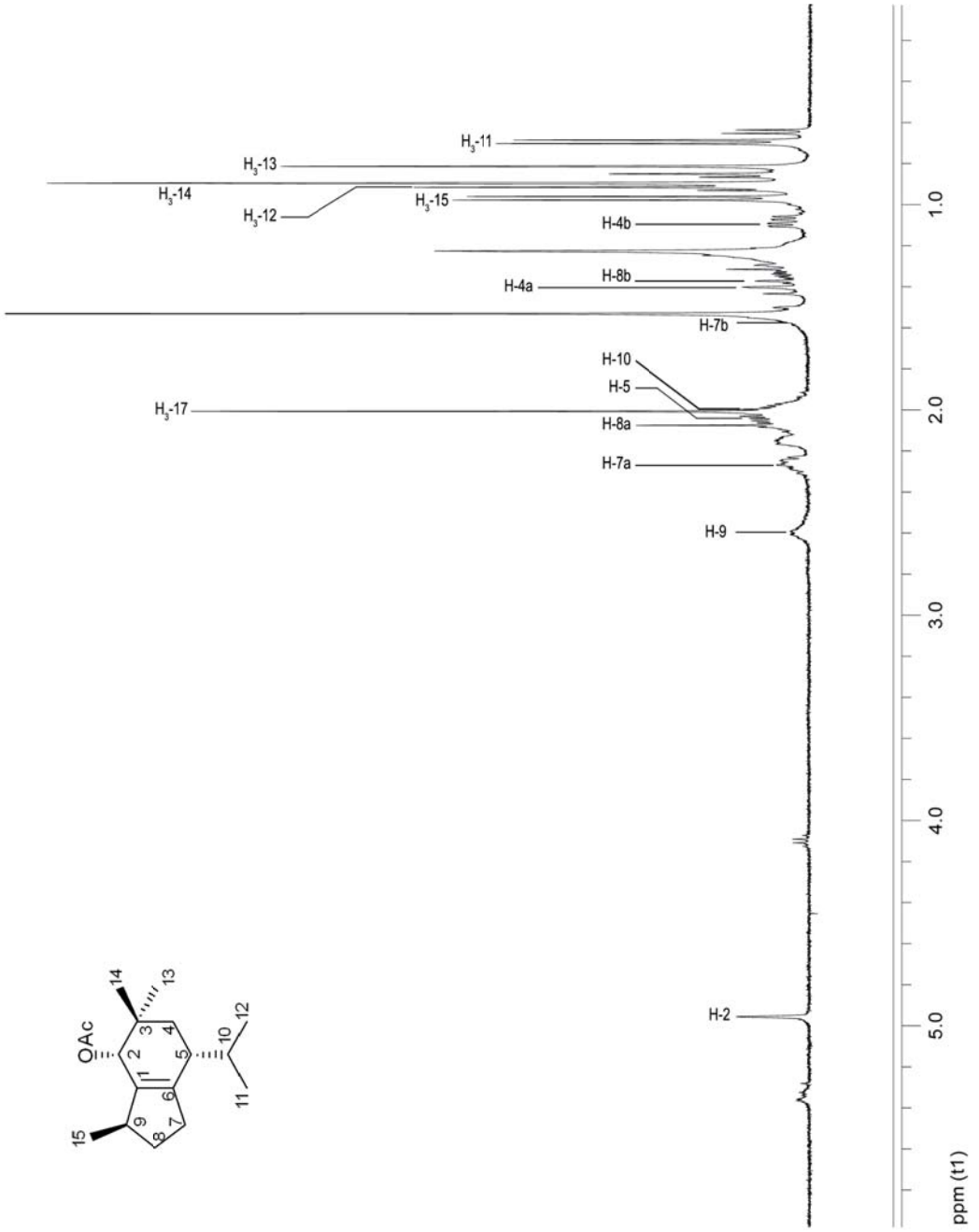

Fig. 6.24. ^{1}H NMR spectrum of compound **6**.

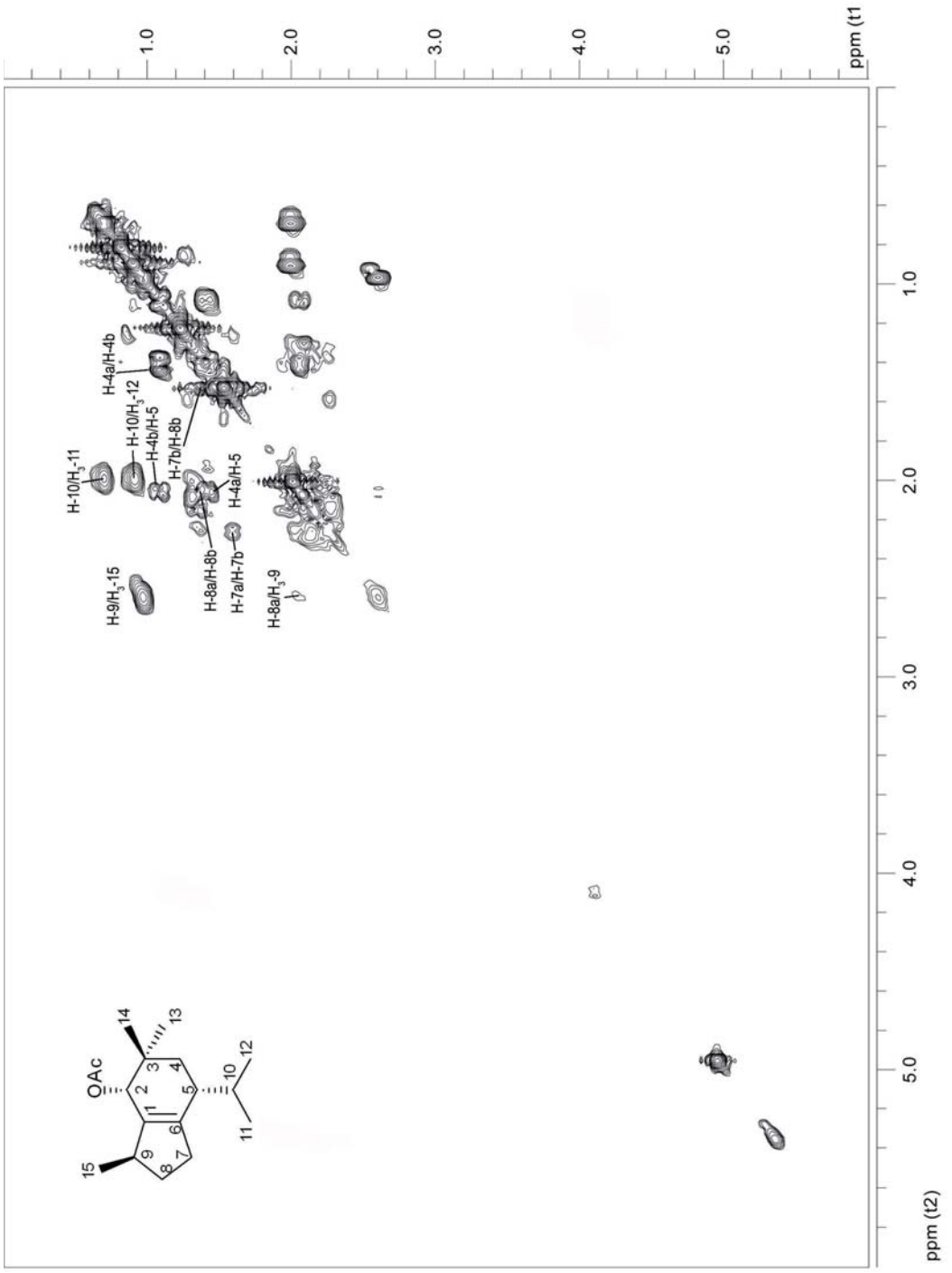

Fig. 6.25. Significant ^{1}H-^{1}H correlations in the COSY spectrum of compound **6**.

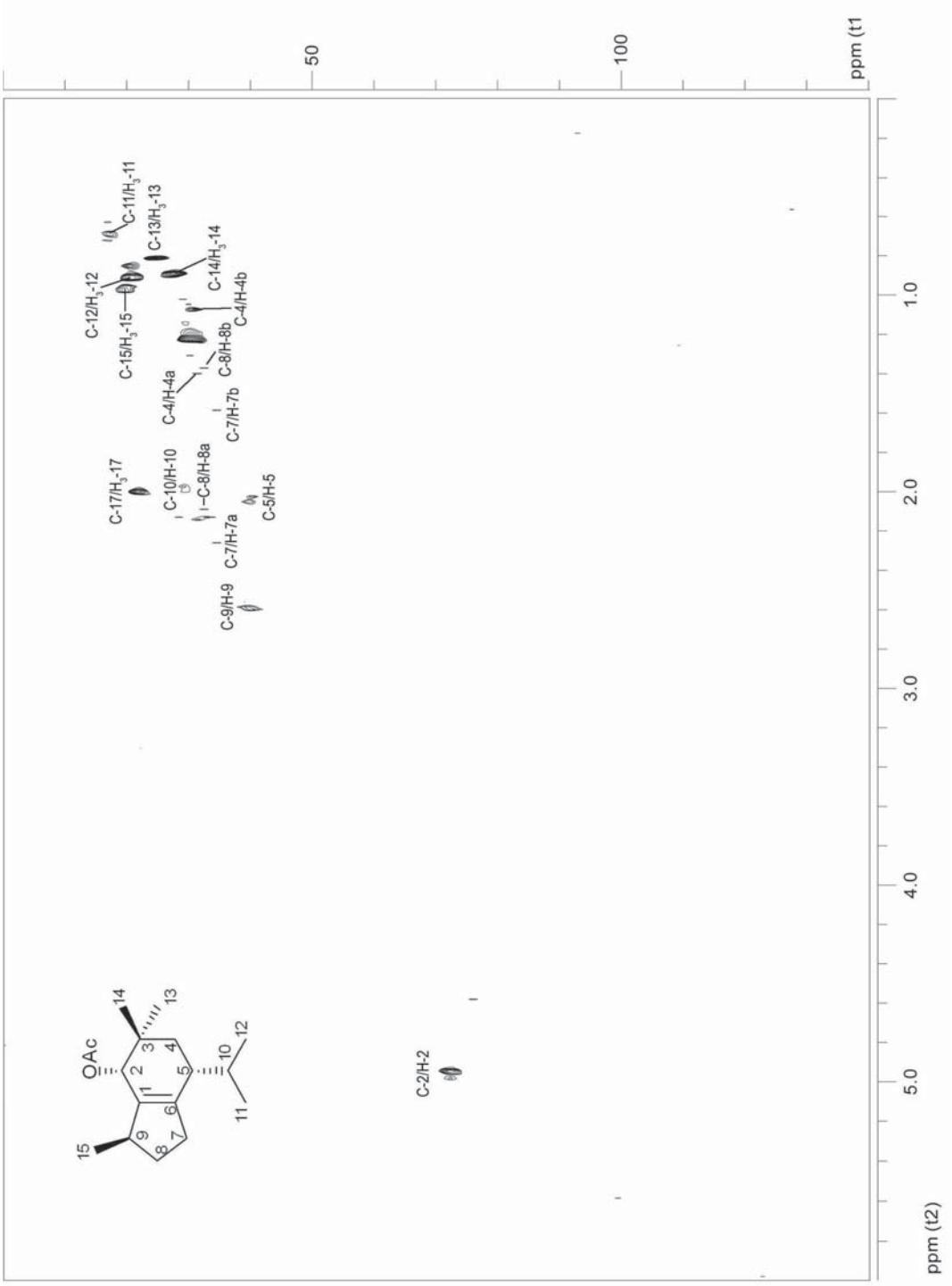

Fig. 6.26. HSQC-DEPT spectrum of compound **6**.

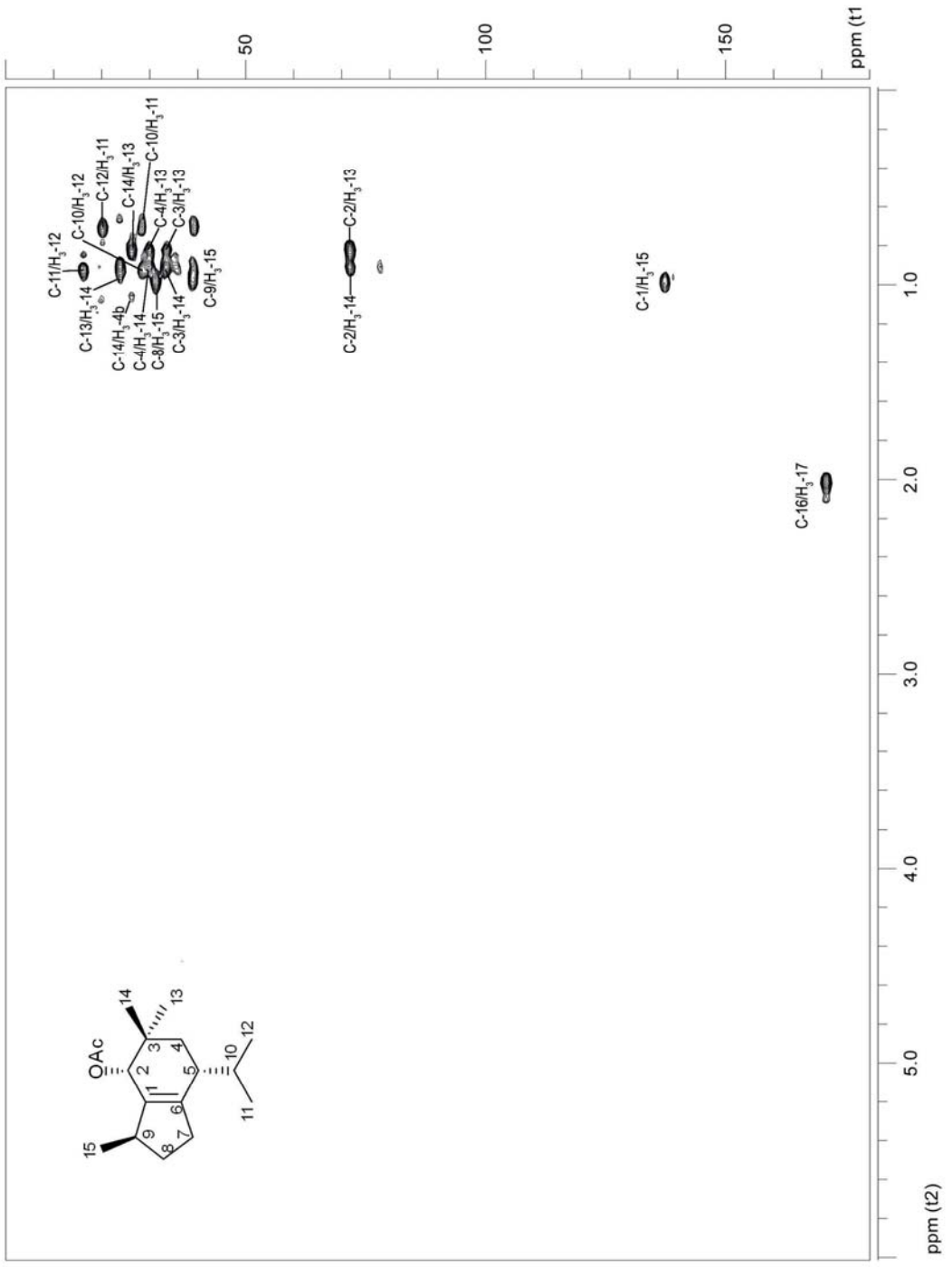

Fig. 6.27. Significant long-range correlations in the HMBC spectrum of compound **6**.

C	δ ^{13}C	mult.	δ ^{1}H	mult., J_{H-H} (Hz)	Significant long-range correlations (HMBC)
1	138.0	*s*	-	-	H-8a, H$_3$-15
2	72.3	*d*	4.96	br *s*	H$_3$-13, H$_3$-14
3	33.9	*s*	-	-	H$_3$-13, H$_3$-14
4	30.6	*t*	a 1.41	*m*	H$_3$-13, H$_3$-14
			b 1.09	*m*	
5	40.2	*d*	2.05	*m*	H$_3$-11, H$_3$-12
6	141.8	*s*	-	-	
7	34.4	*t*	a 2.27	*m*	
			b 1.59	*m*	
8	32.0	*t*	a 2.08	*m*	H$_3$-15
			b 1.38	*m*	
9	39.6	*d*	2.60	*m*	H$_3$-15
10	29.6	*d*	1.98	*m*	H$_3$-11, H$_3$-12
11	17.3	*q*	0.70	*d*, 6.8	H$_3$-12
12	20.8	*q*	0.91	*d*, 6.8	H$_3$-11
13	24.7	*q*	0.82	*s*	H$_3$-14
14	27.6	*q*	0.90	*s*	H-4b, H$_3$-13
15	19.7	*q*	0.97	*d*, 6.9	
16	171.7	*s*	-	-	H$_3$-17
17	21.8	*q*	2.01	*s*	

Table 6.2. ^{13}C and ^{1}H NMR resonance values of compound **6**.

In the ^{1}H NMR spectrum of **7** (Fig. 6.28) the presence of a singlet at δ 2.00 was indicative for the methyl of an acetoxy group. The presence of the acetyl substituent modifies the resonances of the olefinic carbons of **7** with respect to compound **3**. In fact, the ^{13}C NMR signal of C-5, resonating at δ 133.6 in **3**, moves upfield to δ 131.0 in **7**, whereas C-6, resonating at δ 140.5 in **3**, moves downfield to δ 141.5 in **7**. The comparison of the recovered data with those reported in the literature for the semisynthetic 4-acetoxy-5-brasilene enabled to assign the same structure to **7**.

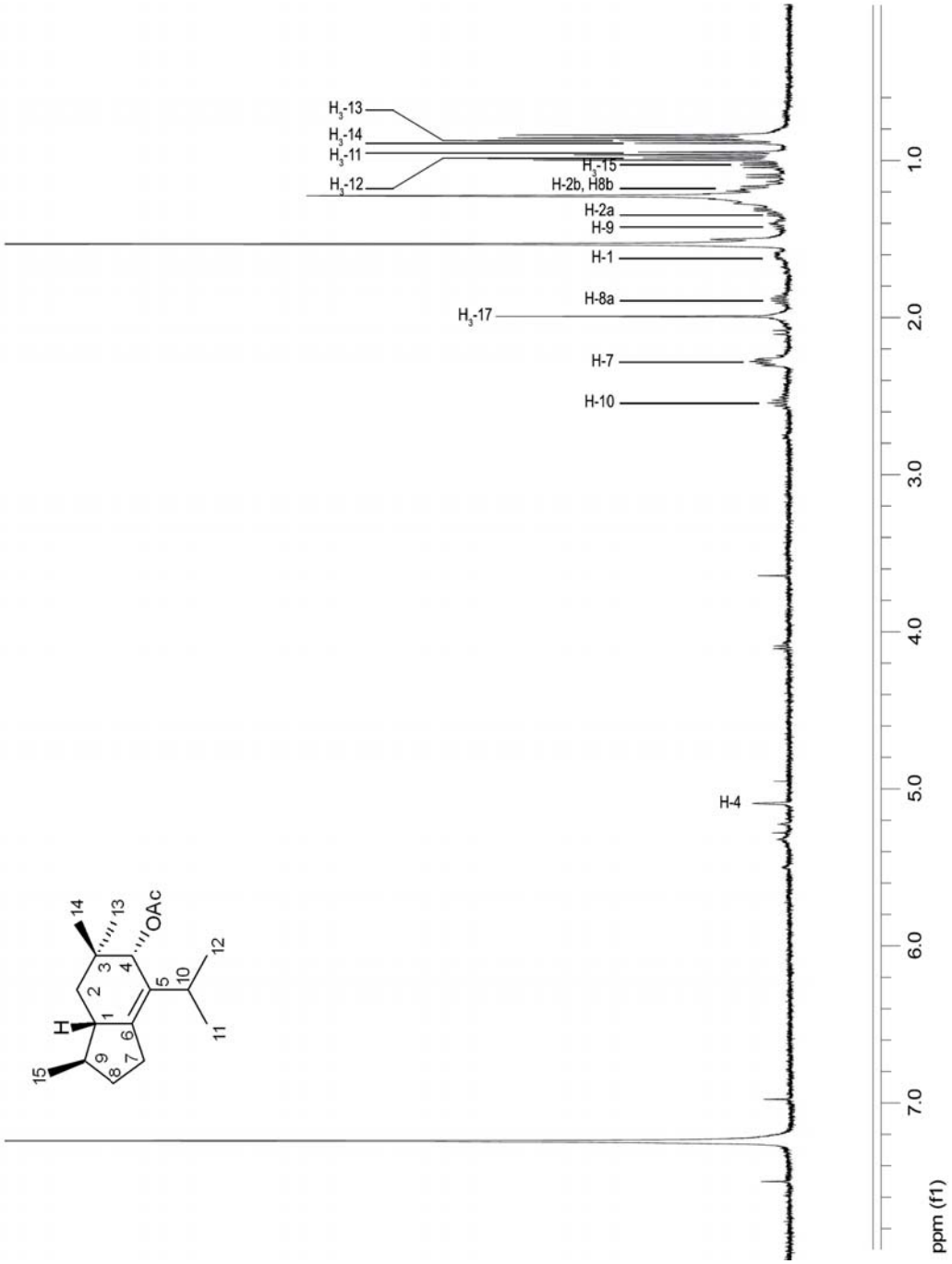

Fig. 6.28. ^{1}H NMR spectrum of compound **7**.

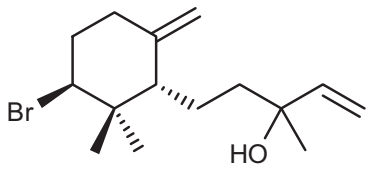

Fig. 6.29. Structure of **8**.

Compound **8** (Fig. 6.29) was isolated as a colorless oil. The ^{13}C NMR spectrum exhibited 15 signals, corresponding to three methyl, six methylene, three methine, and three quaternary carbon atoms (Fig. 6.30). One quaternary, one methine, and two methylene carbons resonated in the sp^2 region of the ^{13}C NMR spectrum at δ 146.1, 144.9, 111.8, and 111.7, indicating the presence of both a monosubstituted and a 1,1-disubstituted double bonds in the molecule. An oxygenated quaternary carbon (δ 73.2) and one halogenated methine carbon (δ 63.3) were also evident. In the ^1H NMR spectrum (Fig. 6.31) three methyl groups on quaternary carbons (δ 1.25, 1.04, and 1.01), five olefinic protons of the monosubstituted (δ 5.84, 5.17, and 5.04) and the 1,1-disubstituted (δ 4.78 and 4.59) double bonds, and a halogenated methine (δ 4.31) were identifiable. The structural features observed in both the ^1H NMR and ^{13}C NMR spectra of **8** were very similar to those of β-snyderol, a brominated monocyclic sesquiterpene (Howard & Fenical 1976; Topcu *et al.* 2003). ^{13}C NMR and ^1H NMR resonance values of compound **8** are reported in Table 6.3. Careful examination of the homonuclear and heteronuclear correlations exhibited in the ^1H-^1H COSY, HSQC-DEPT, and HMBC spectra (Fig. 6.32-6.34), as well as of the fragment ions in the mass spectrum, suggested the same planar structure of β-snyderol. The relative configuration of metabolite **8** was assigned on the basis of n.O.e. enhancements and coupling constant values of certain proton signals.

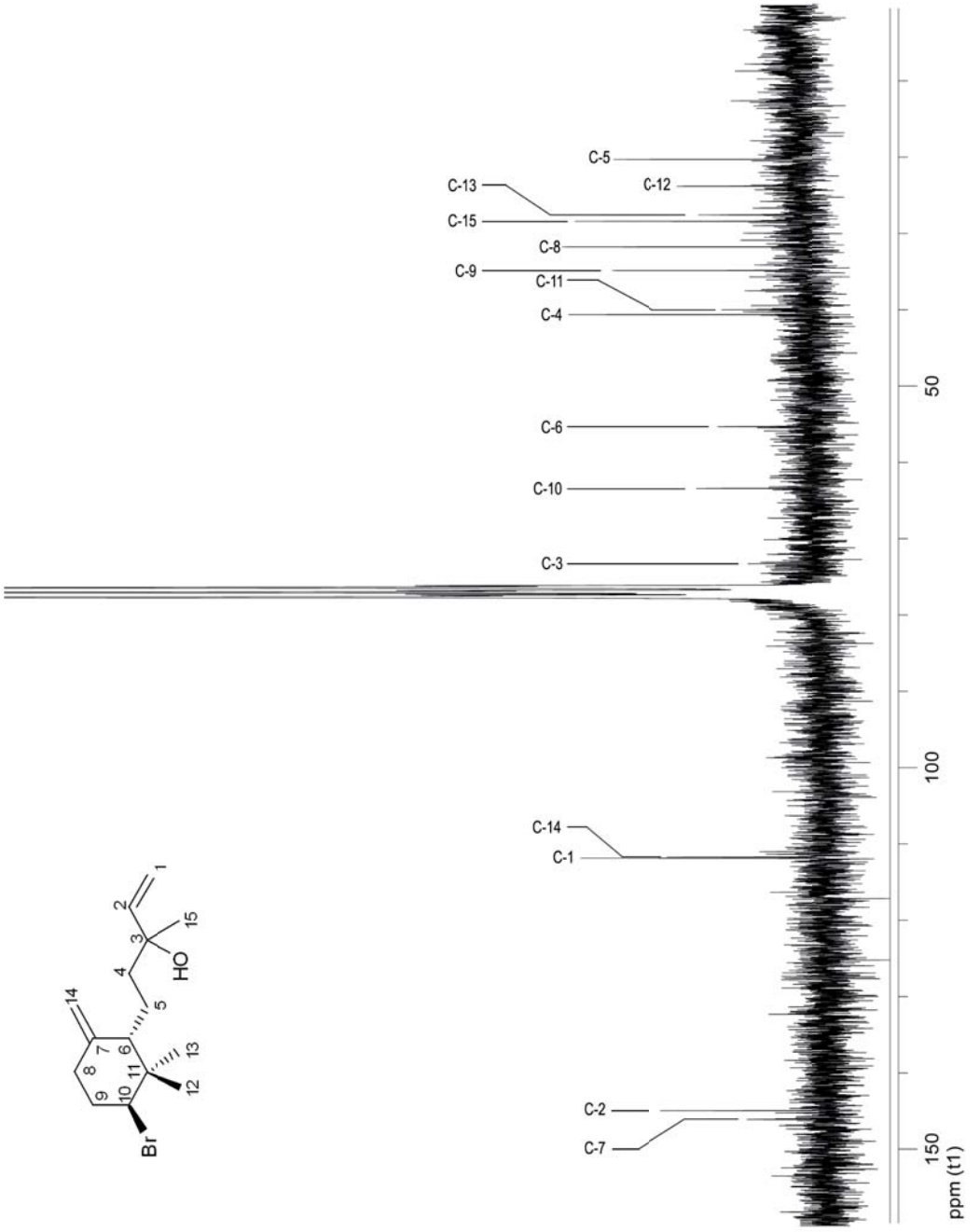

Fig. 6.30. ^{13}C NMR spectrum of compound **8**.

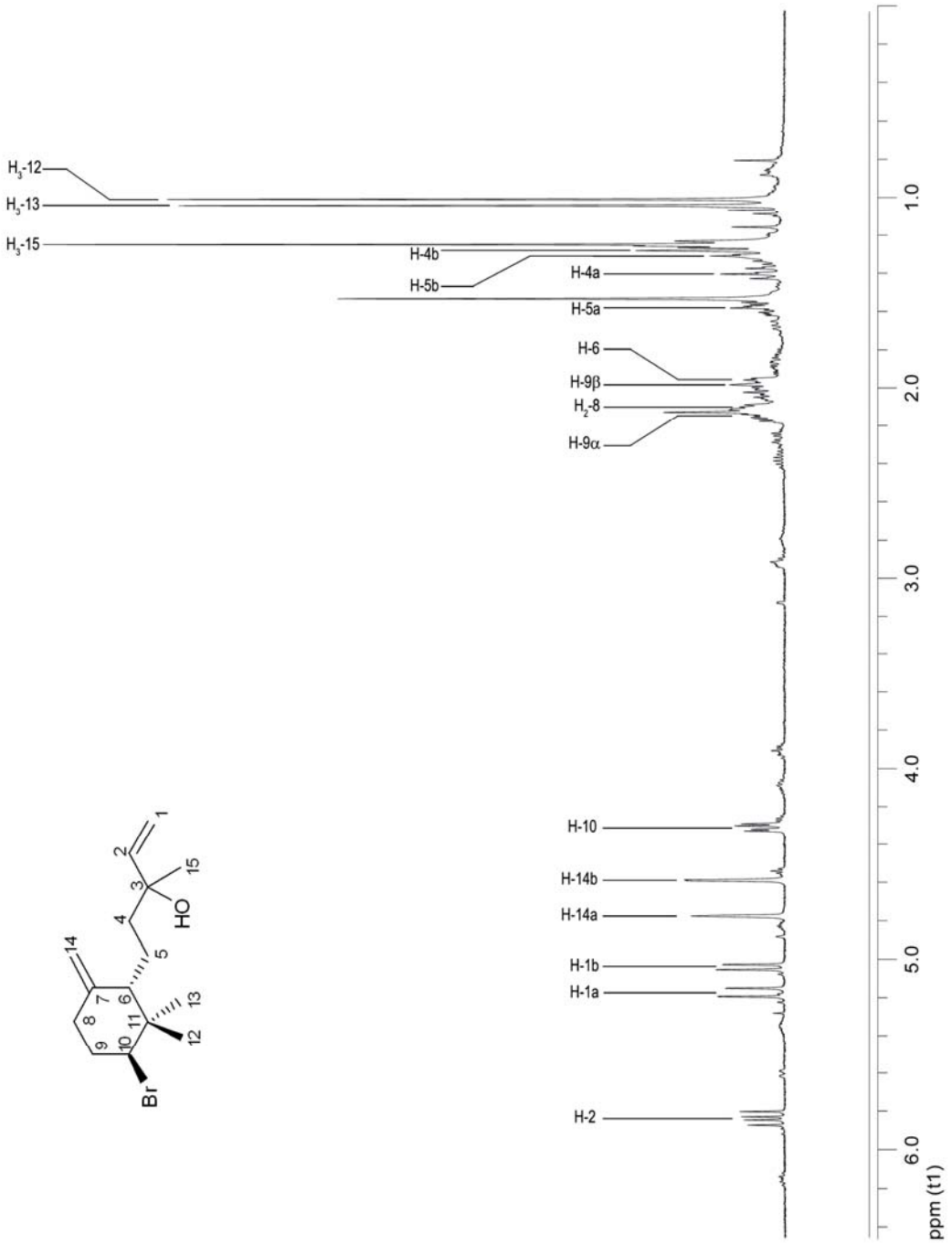

Fig. 6.31. ^{1}H NMR spectrum of compound **8**.

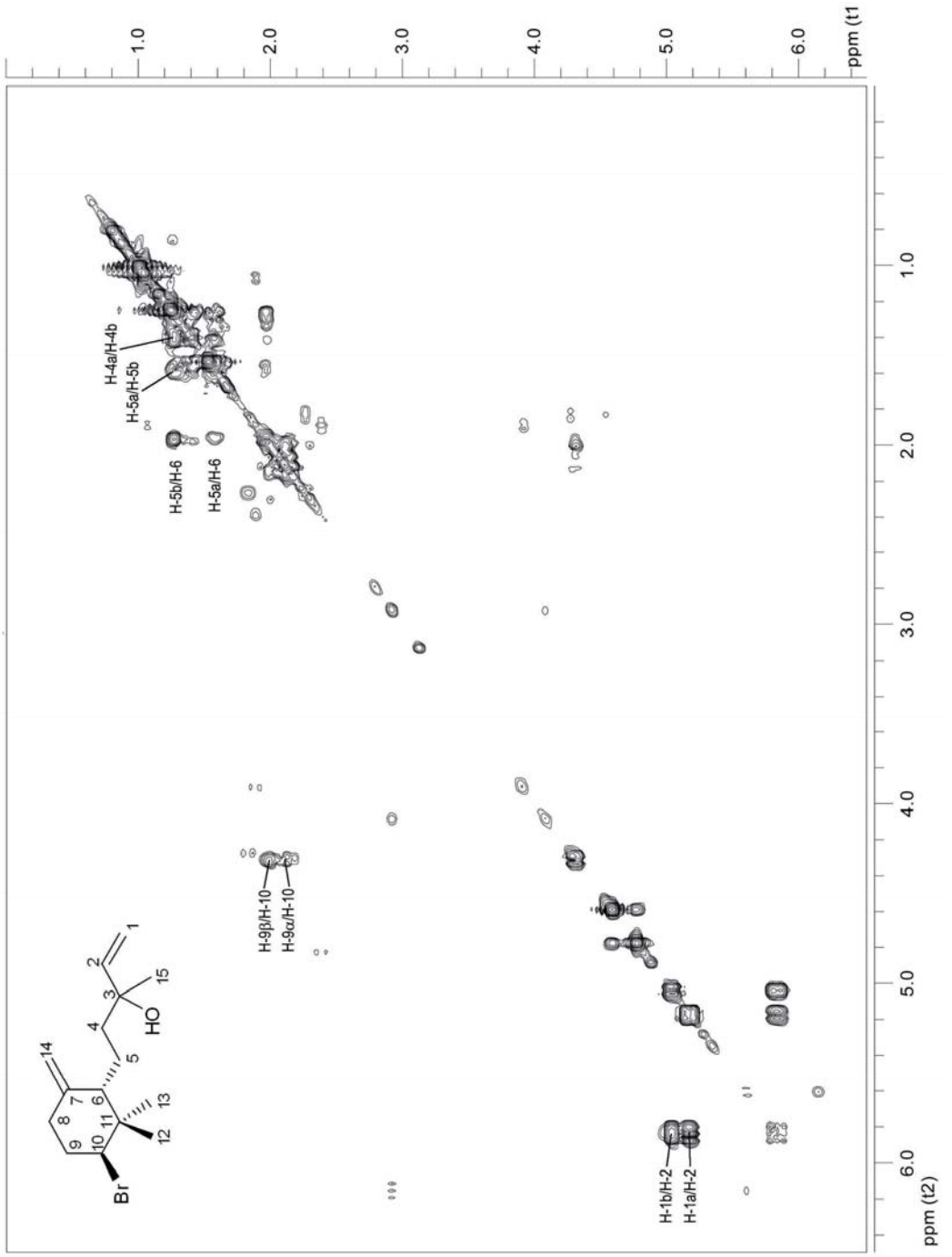

Fig. 6.32. Significant ^{1}H-^{1}H correlations in the COSY spectrum of compound **8**.

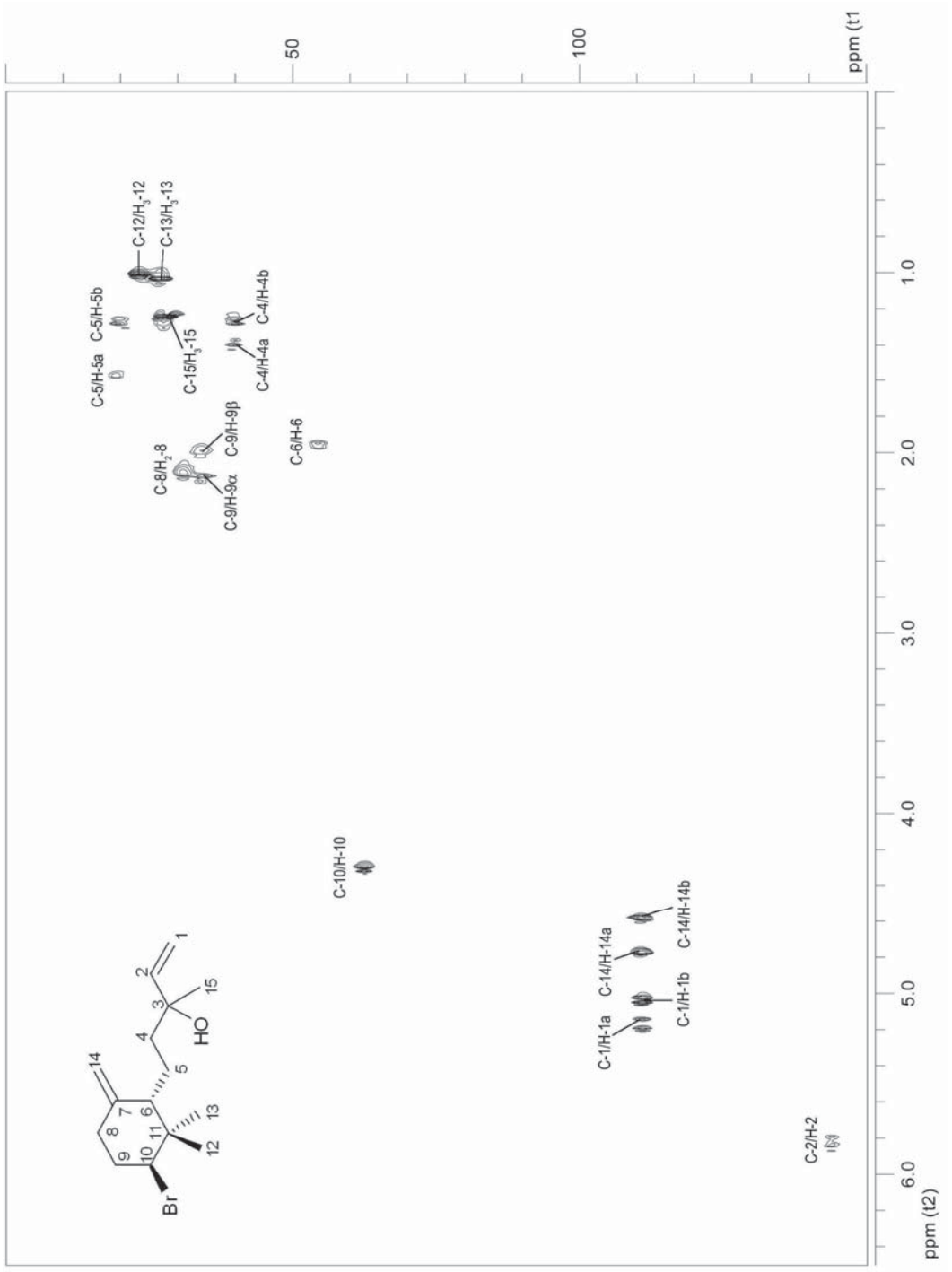

Fig. 6.33. HSQC-DEPT spectrum of compound **8**.

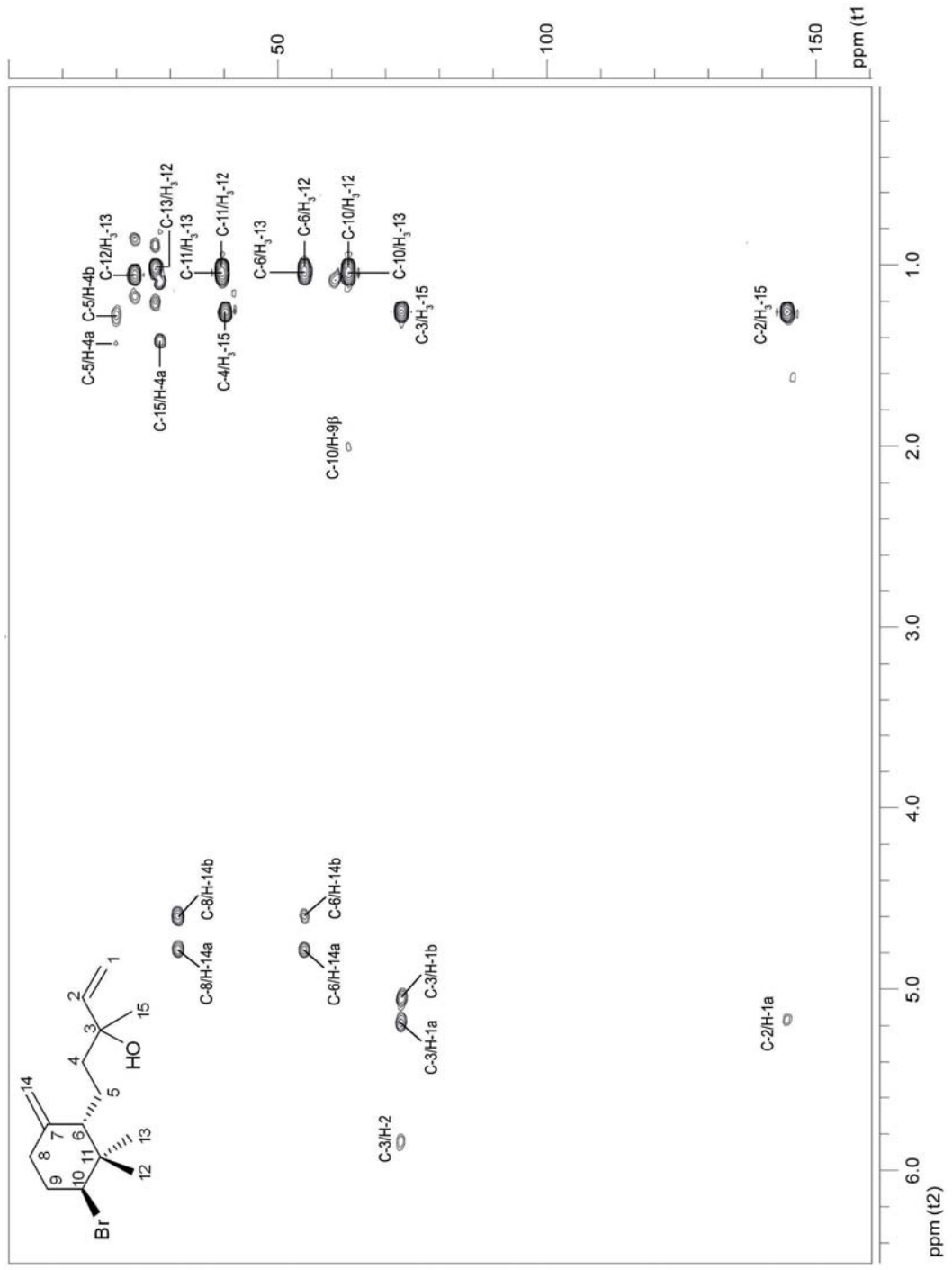

Fig. 6.34. Significant long-range correlations in the HMBC spectrum of **8**.

C	δ ^{13}C	mult.	δ ^{1}H	mult., J_{H-H} (Hz)	Significant long range correlations (HMBC)
1	111.8	*t*	a 5.17	br *d*, 17.4	
			b 5.04	br *d*, 10.7	
2	144.9	*d*	5.84	*dd*, 17.4, 10.7	H-1a, H_3-15
3	73.2	*s*	-	-	H-1a, H-1b, H-2, H_3-15
4	40.5	*t*	a 1.39	*m*	H_3-15
			b 1.27	*m*	
5	20.2	*t*	a 1.58	*m*	H-4a, H-4b
			b 1.28	*m*	
6	55.2	*d*	1.95	*m*	H_3-12, H_3-13, H-14a, H-14b
7	146.1	*s*	-	-	
8	31.7	*t*	2.11	*m*	H-14a, H-14b
9	34.7	*t*	α 2.14	*m*	
			β 1.98	*m*	
10	63.3	*d*	4.31	*dd*, 11.2, 4.0	H-9β, H_3-12, H_3-13
11	39.9	*s*	-	-	H_3-12, H_3-13
12	23.7	*q*	1.01	*s*	H_3-13
13	27.5	*q*	1.04	*s*	H_3-12
14	111.7	*t*	a 4.78	br *s*	
			b 4.59	br *s*	
15	28.3	*q*	1.25	*s*	H-4a

Table 6.3. ^{13}C and ^{1}H NMR resonance values of compound **8**.

In particular, the fact that the methine at C-10 exhibited one large (11.2 Hz) and one medium (4.0 Hz) coupling constant with H_2-9, implied an axial orientation for H-10 and, thus, an equatorial orientation for the bromine atom, as in the case of β-snyderol (Topcu *et al.* 2003). In turn, the n.O.e. correlations observed for H-6/H_3-12, H-9α/H-10, H-9β/H_3-12, and H-10/H_3-13 suggested that H-6 was equatorial. This was also supported by the lack of interaction between H-6 and H-10, which was oberved in β-snyderol (Topcu *et al.* 2003). Therefore, metabolite **8** was identified as the epimer of β-

snyderol at C-6, 6-*epi*-β-snyderol. The configuration at C-3 was not possible to determine through spectroscopic analyses.

Compound **9** (Fig. 6.35) is a diterpene with molecular formula $C_{20}H_{35}BrO_2$, which is characterized by a brominated cyclohexane ring in the middle of a geranylgeranyl skeleton. $[M - H_2O]^+$ peaks at *m*/*z* 368 and 370 ($C_{20}H_{33}BrO$) were indicative for the presence of a bromine atom, whereas an intense IR band at 3434 cm^{-1} along with ^{13}C NMR signals at δ 73.4 and 72.9 revealed that both oxygen atoms belonged to two hydroxy groups. The ^1H and ^{13}C NMR spectra (Fig. 6.36-6.37) showed the presence of five methyl, six methylene, two methine, three quaternary carbons, and four olefinic groups. Of the two double bonds, one was terminal [δ_H 5.92 (*dd*, *J* = 17.5, 10.5 Hz), 5.23 (*d*, *J* = 10.5 Hz), 5.11 (*d*, *J* = 17.5 Hz); δ_C 144.5 (CH), 112.2 (CH_2)], and another one was trisubstituted [δ_H 5.05 (*m*); δ_C 131.6 (C), 123.7 (CH)]. As observed in the ^1H NMR spectrum of **9,** of the five methyl groups, two (δ_H 1.70 *s*, 1.64 *s*) were linked to a sp^2 carbon, two (δ_H 1.30 *s*, 1.19 *s*) were attached to the oxygenated carbons, and one (δ_H 1.11 *s*) to a quaternary carbon. The mono- and bidimensional NMR data, in comparison with those reported in the literature, allowed attributing the structure of **9** to luzodiol (Kuniyoshi *et al.* 2005). The relative stereochemistry was assigned by the authors considering the n.O.e. effects of certain protons, whereas the configuration at C-3 has not been determined yet.

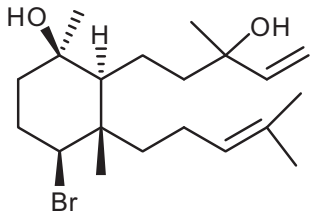

Fig. 6.35. Structure of **9**.

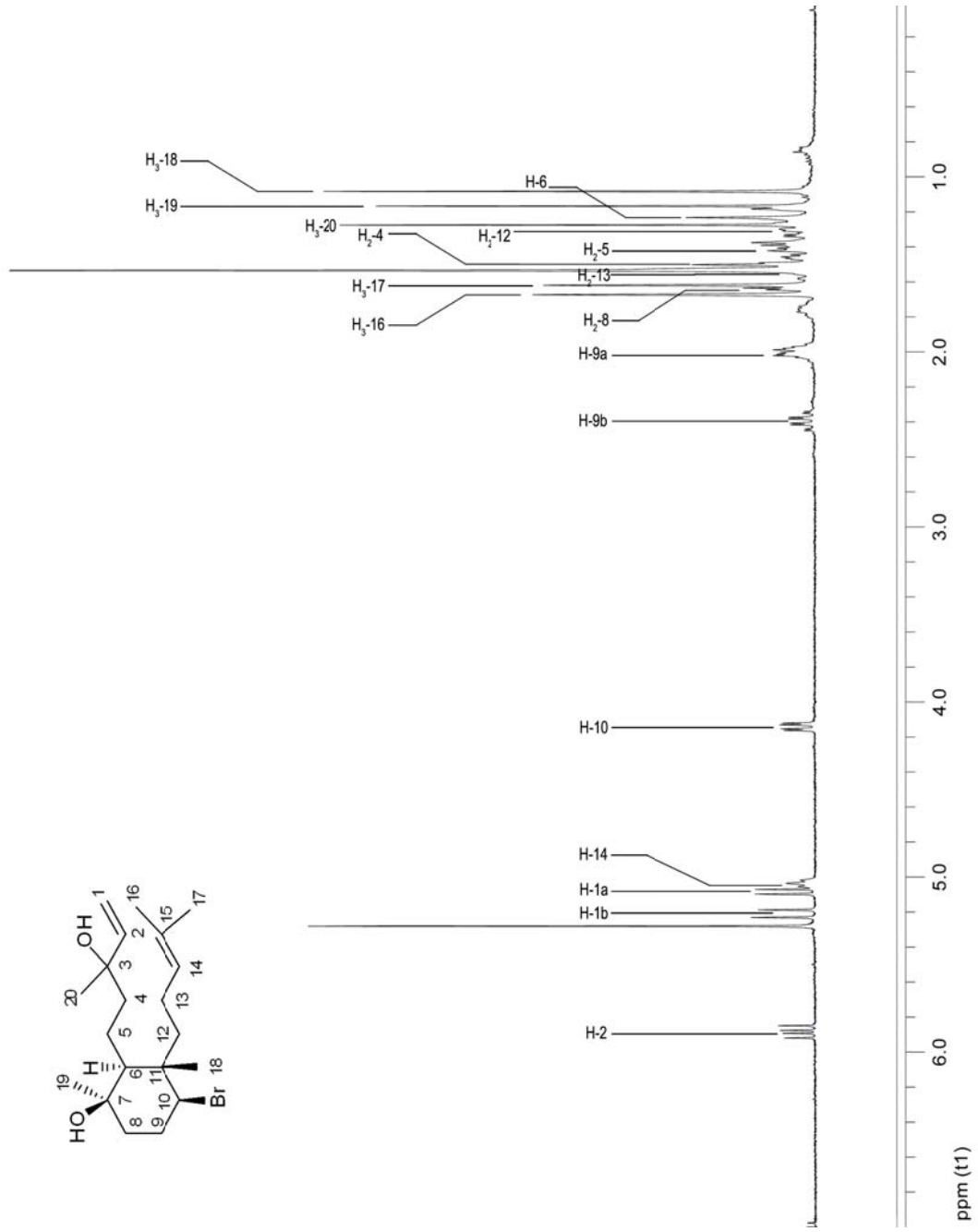

Fig. 6.36. ^{1}H NMR spectrum of compound **9**.

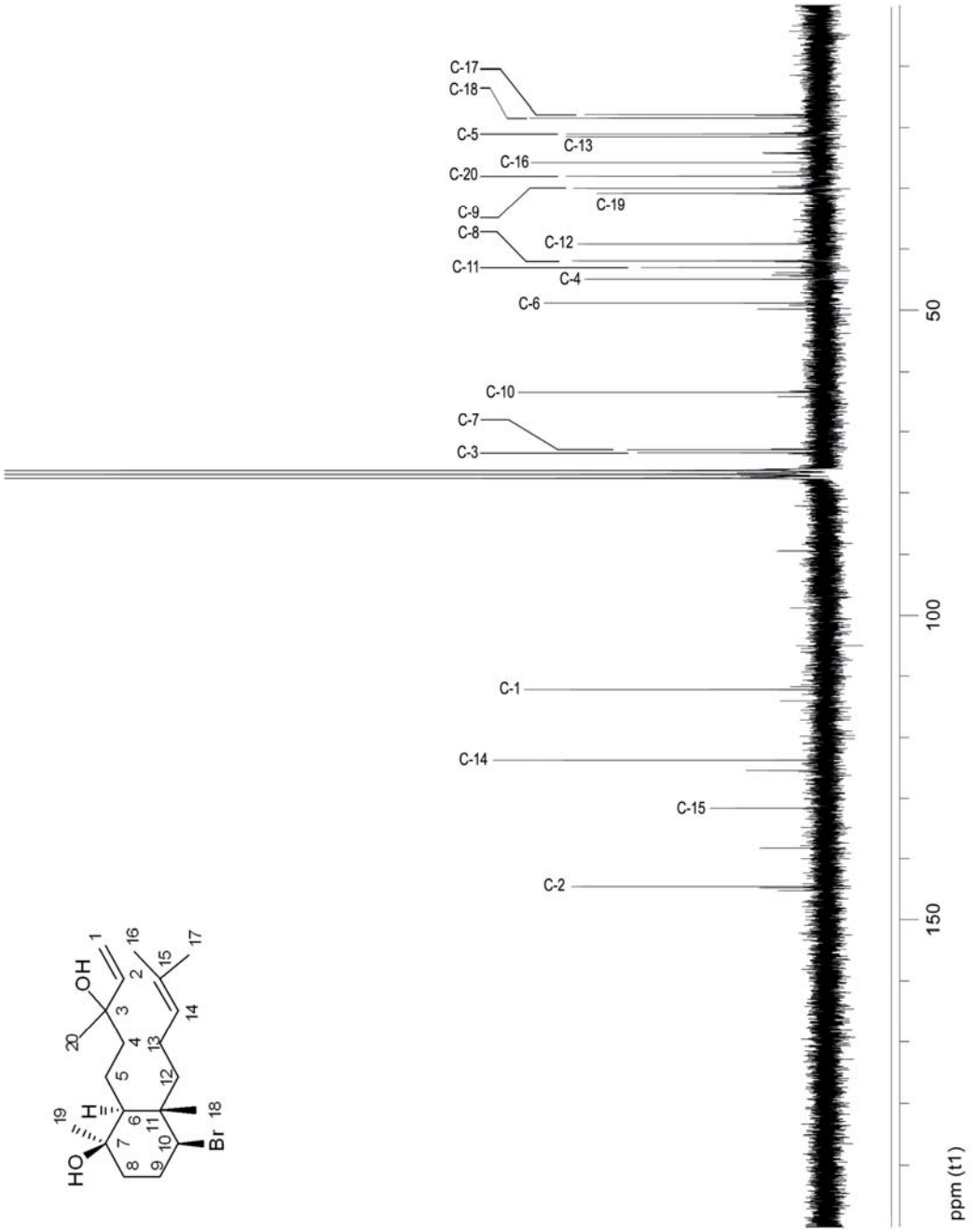

Fig. 6.37. ^{13}C NMR spectrum of compound **9**.

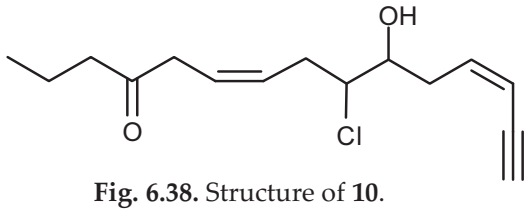

Fig. 6.38. Structure of **10**.

Compound **10** (Fig. 6.38), isolated as a colorless oil, displayed a pseudomolecular ion peak at *m/z* 291.1140 in the ESI-HRMS spectrum, corresponding to $C_{15}H_{21}ClNaO_2$, and consistent with $[M + Na]^+$. The mass spectrum exhibited pseudomolecular ions $[M + H]^+$ at *m/z* 269 and 271 (3:1), and fragment ions $[M - H_2O]^+$ and $[M - C_5H_6]^+$ at *m/z* 251 and 253 (2:0.7), and 203 and 205 (13:4), respectively, characteristic for the presence of one chlorine atom in the molecule (Fig. 6.39).

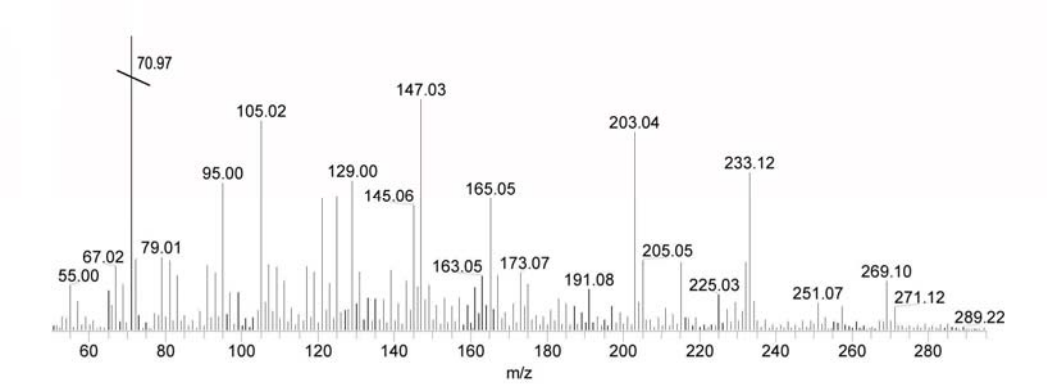

Fig. 6.39. Mass spectrum of compound **10**.

The IR band at 1716 cm^{-1} was indicative for a keto function. In addition, in the UV spectrum a band at 225.0 (3.18) nm was diagnostic for the conjugated *cis*-enyne system. The ^{13}C NMR spectrum (Fig. 6.40) revealed 15 signals, corresponding to one

methyl, five methylene, seven methine, and two quaternary carbon atoms. Among them, one carbonyl (δ 208.7), four methine sp^2 carbons (δ 140.3, 128.1, 124.7, and 111.1), two *sp* carbons of a triple bond (δ 82.4 and 77.2), one halogenated methine carbon (δ 66.5), and an oxygenated methine carbon (δ 71.9) were evident. The ^{1}H NMR spectrum (Fig. 6.41) included signals for one methyl group on a methylene carbon (δ 0.90), four olefinic methines (δ 6.08, 5.73, 5.61, and 5.59), two halogenated or oxygenated methines (δ 3.91 and 3.77), and one methine on a triple bond (δ 3.13). Since the carbonyl, the carbon–carbon triple bond, and the two carbon-carbon double bonds accounted for all five degrees of unsaturation, metabolite **10** was determined to be linear. The correlations C-H by their ^1J were established on the basis of the HSQC-DEPT experiment (Fig. 6.42). The correlations between all geminal and vicinal protons observed in the ^{1}H-^{1}H COSY spectrum (Fig. 6.43), as well as the HMBC correlations (Fig. 6.44) of C-12 with H_2-11, H_2-13, and H_2-14, assisted in establishing the structure of **10** unambiguously. The geometry of the Δ^3 and Δ^9 double bonds was assigned as *Z* on the basis of the measured coupling constants (using decoupling experiments) between H-3 and H-4 (J = 10.7 Hz) and H-9 and H-10 (J = 10.9 Hz). The relative configuration at C-6 and C-7 could not be determined through spectroscopic analysis. Therefore, compound **10** was identified as (3*Z*,9*Z*)-7-chloro-6-hydroxy-12-oxopentadeca-3,9-dien-1-yne. ^{13}C NMR and ^{1}H NMR assignments of compound **10** are reported in Table 6.4.

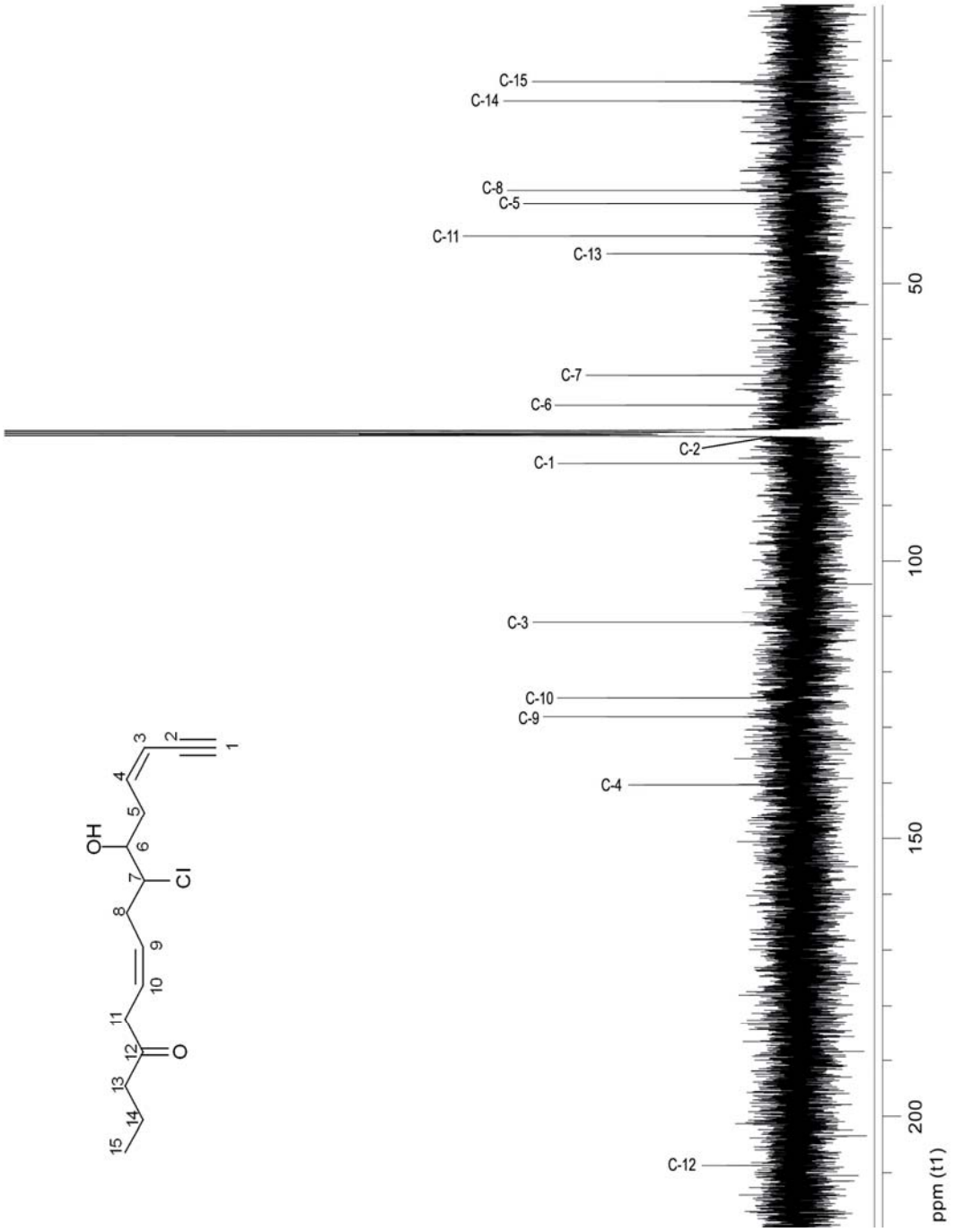

Fig. 6.40. ^{13}C NMR spectrum of compound **10**.

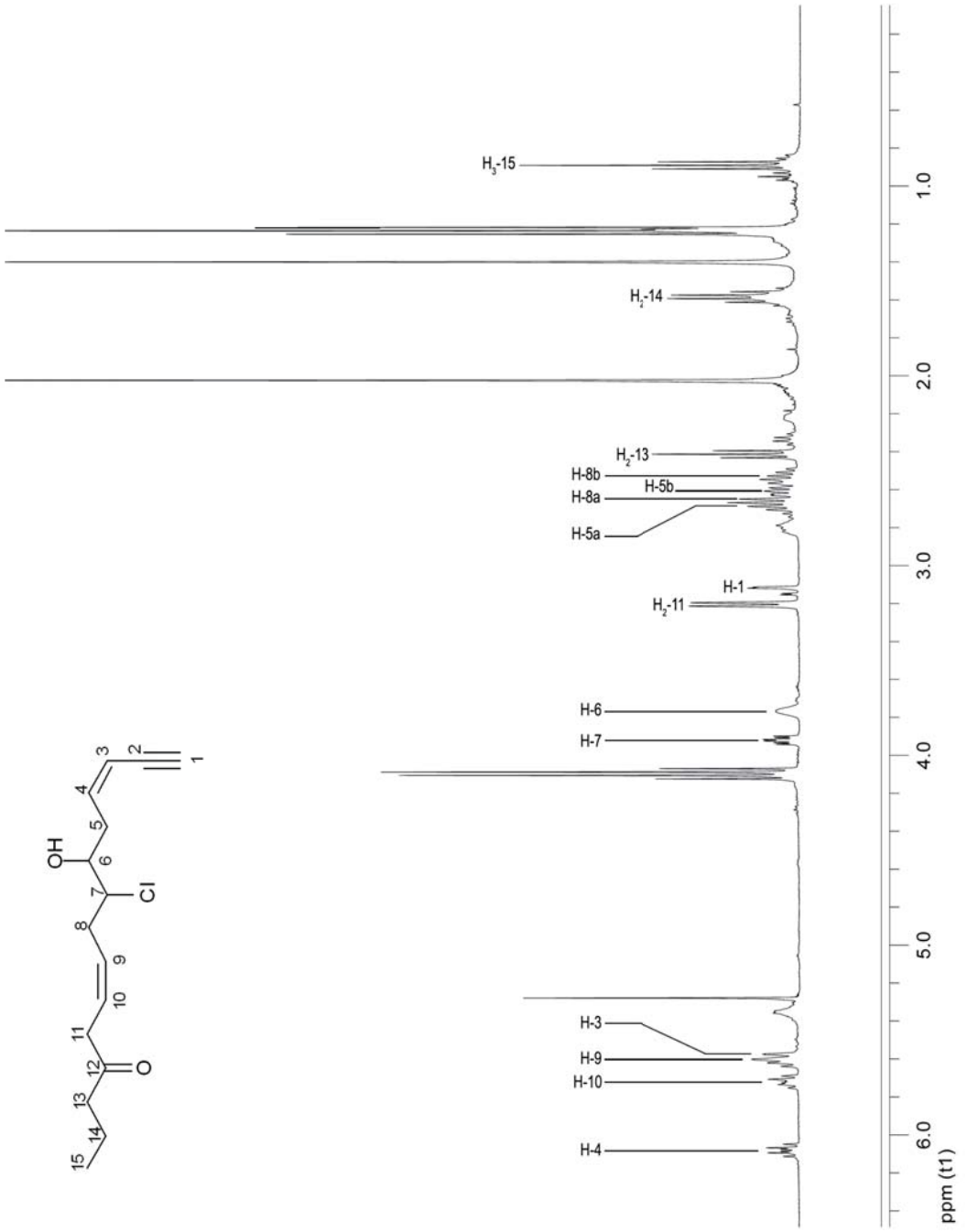

Fig. 6.41. ^{1}H NMR spectrum of compound **10**.

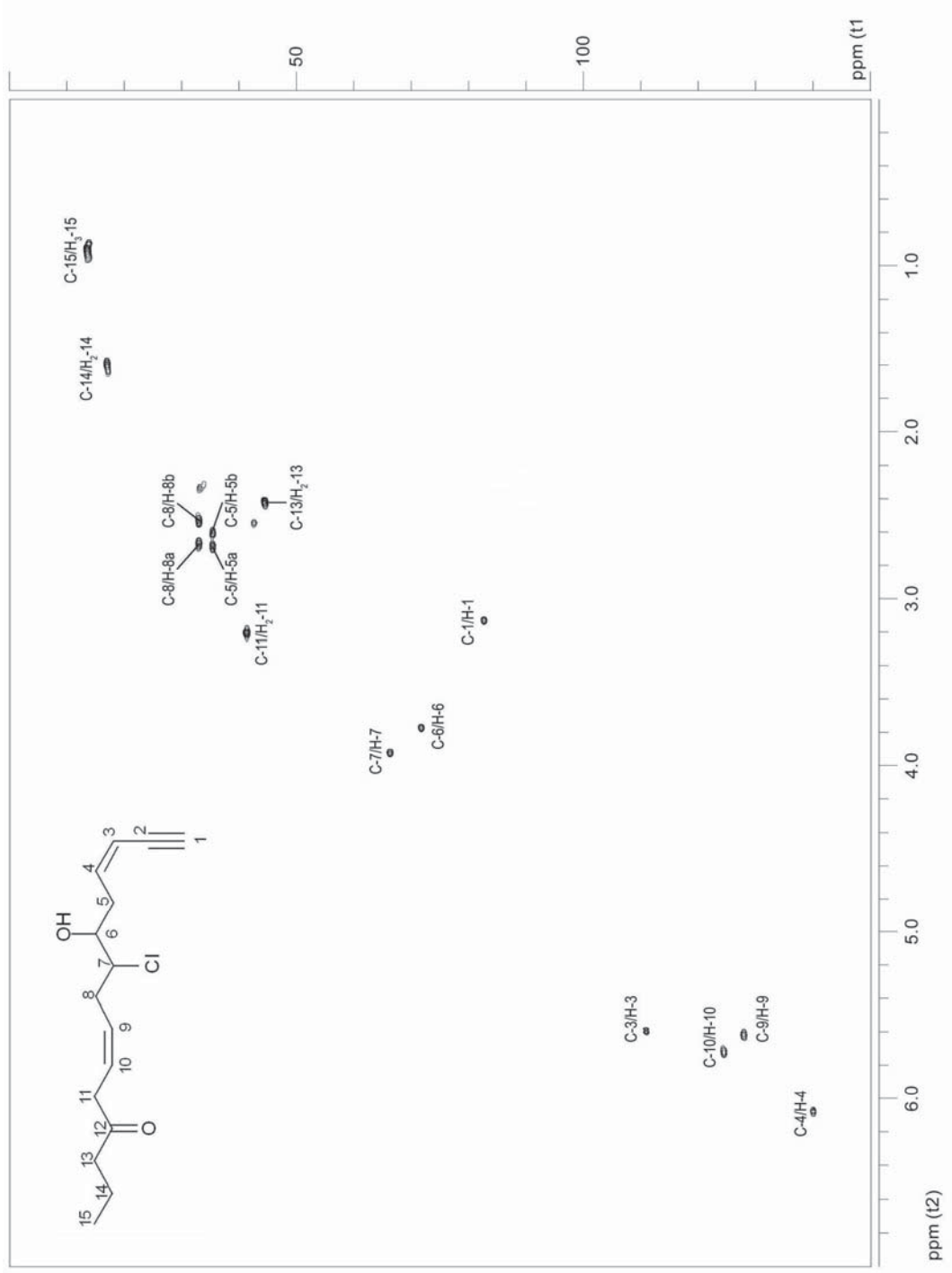

Fig. 6.42. HSQC-DEPT spectrum of compound **10**.

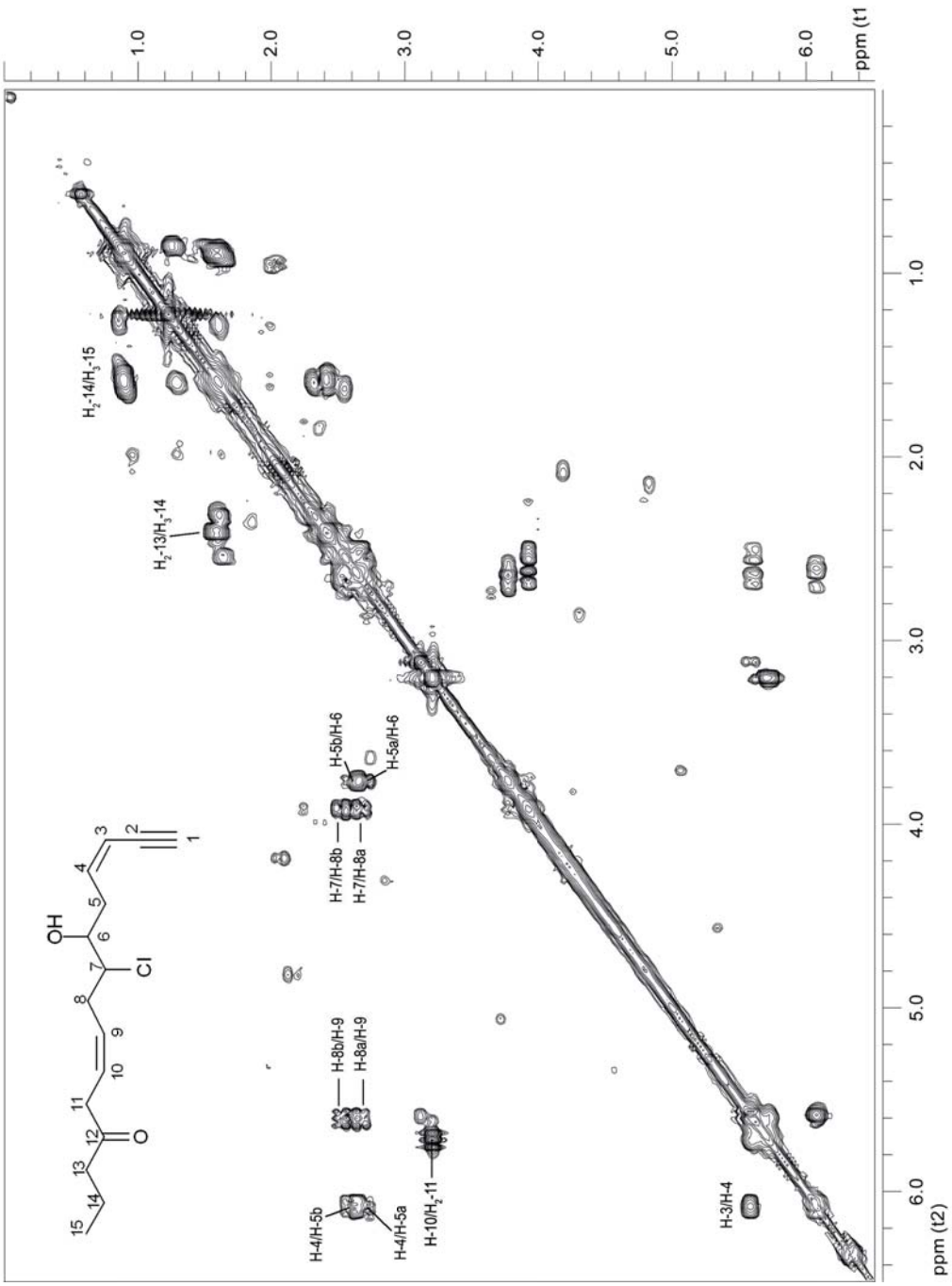

Fig. 6.43. Significant ^{1}H-^{1}H correlations in the COSY spectrum of compound **10**.

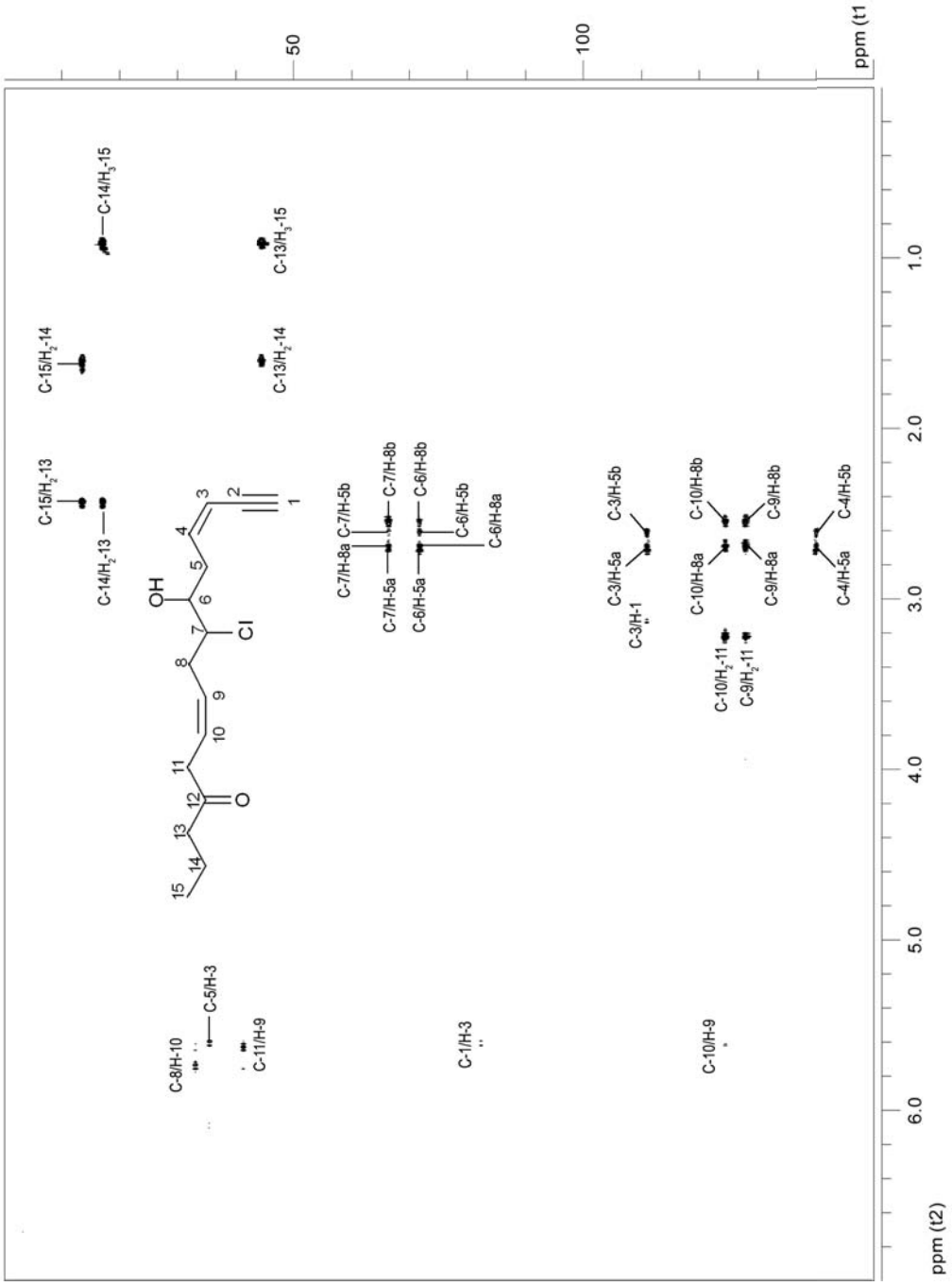

Fig. 6.44. Significant long-range correlations in the HMBC spectrum of compound **10**.

C	δ ^{13}C	mult.	δ ^{1}H	mult., J_{H-H} (Hz)	Significant long range correlations (HMBC)
1	82.4	*d*	3.13	*d*, 2.0	H-3
2	77.2	*s*	-	-	
3	111.1	*d*	5.59	*m*	H-1, H-5a, H-5b
4	140.3	*d*	6.08	*dt*, 10.7, 7.4	H-5a, H-5b
5	35.6	*t*	a 2.69	*m*	H-3
			b 2.60	*m*	
6	71.9	*d*	3.77	*m*	H-5a, H-5b, H-8a, H-8b
7	66.5	*d*	3.91	*ddd*, 7.7, 6.8, 3.2	H-5a, H-5b, H-8a, H-8b
8	33.2	*t*	a 2.66	*m*	H-10
			b 2.52	*m*	
9	128.1	*d*	5.61	*m*	H-8a, H-8b, H_2-11
10	124.7	*d*	5.73	*m*	H-8a, H-8b, H-9, H_2-11
11	41.5	*t*	3.21	*d*, 7.1	H-9
12	208.7	*s*	-	-	H_2-11, H_2-13, H_2-14
13	44.7	*t*	2.41	*t*, 7.3	H_2-14, H_3-15
14	17.2	*t*	1.58	*m*	H_2-13, H_3-15
15	13.7	*q*	0.90	*t*, 7.4	H_2-13, H_2-14

Table 6.4. ^{13}C and ^{1}H NMR resonance values of compound **10**.

Compound **11** (Fig. 6.45) is a vinyl acetylene metabolite with molecular formula $C_{17}H_{23}ClO_2$, which required six degrees of unsaturation. The IR spectrum showed the presence of an acetylene group at 3300 cm^{-1}, an ester group at 1720 cm^{-1}, and multiple double bonds at 3030 and 1640 cm^{-1}. The UV absorption λ_{max} (EtOH) 224 nm (ε 13,100) indicated the presence of a conjugated *cis*-enyne group. The ^{1}H NMR (Fig. 6.46) and ^{13}C NMR (Fig. 6.47) experiments also revealed the presence of three disubstituted double bonds [δ_H 5.93 (*dt*, *J* = 10.9, 7.5 Hz), 5.58 (*dd*, *J* = 10.9, 2.2

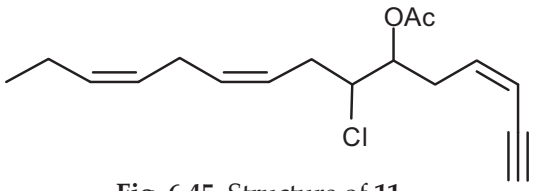

Fig. 6.45. Structure of **11**.

Hz), 5.52 (*m*), 5.42 (*m*), 5.39 (*m*), and 5.24 (*m*); δ_C 138.9 (CH), 132.4 (CH), 131.7 (CH), 126.4 (CH), 124.3 (CH), 111.7 (CH)], and one terminal acetylene group [δ_H 3.13 (*d*, *J* = 2.2 Hz); δ_C 82.7 (CH), 77.2 (C)]. Since the carbonyl, the three double bonds and the triple bond accounted for all the six degrees of unsaturation, compound **11** was established to be linear. The comparison of both ^{1}H NMR and ^{13}C NMR spectra with those reported in the literature, allowed identifying **11** as (3*Z*,9*Z*,12*Z*)-6-acetoxy-7-chloropentadeca-3,9,12-trien-1-yne (González *et al.* 1982; Norte *et al.* 1991). The absolute configuration at C-6 and C-7 was assigned as *R* for both carbons (González *et al.* 1982). A careful analysis of the spectroscopic data of **11** allowed re-assigning a number of ^{1}H NMR and ^{13}C NMR resonance values, which are shown in Table 6.5.

C	δ ^{13}C	mult.	δ ^{1}H	mult., J_{H-H} (Hz)
1	82.7	*d*	3.13	*d*, 2.2
2	77.2	*s*	-	-
3	111.7	*d*	5.58	*dd*, 10.9, 2.2
4	138.9	*d*	5.93	*dt*, 10.9, 7.5
5	32.4	*t*	2.74	*m*
6	73.4	*d*	5.15	*ddd*, 7.5, 5.4, 4.0
7	62.5	*d*	3.94	*ddd*, 8.2, 5.4, 4.0
8	32.2	*t*	2.53	*m*
9	124.3	*d*	5.42	*m*
10	132.4	*d*	5.52	*m*
11	25.7	*t*	2.77	*m*
12	126.4	*d*	5.24	*m*
13	131.7	*d*	5.39	*m*
14	20.9	*t*	2.04	*m*
15	14.2	*q*	0.95	*t*, 7.5
16	170.3	*s*	-	-
17	20.6	*q*	2.10	*s*

Table 6.5. ^{13}C NMR and ^{1}H NMR re-assignments of compound **11**.

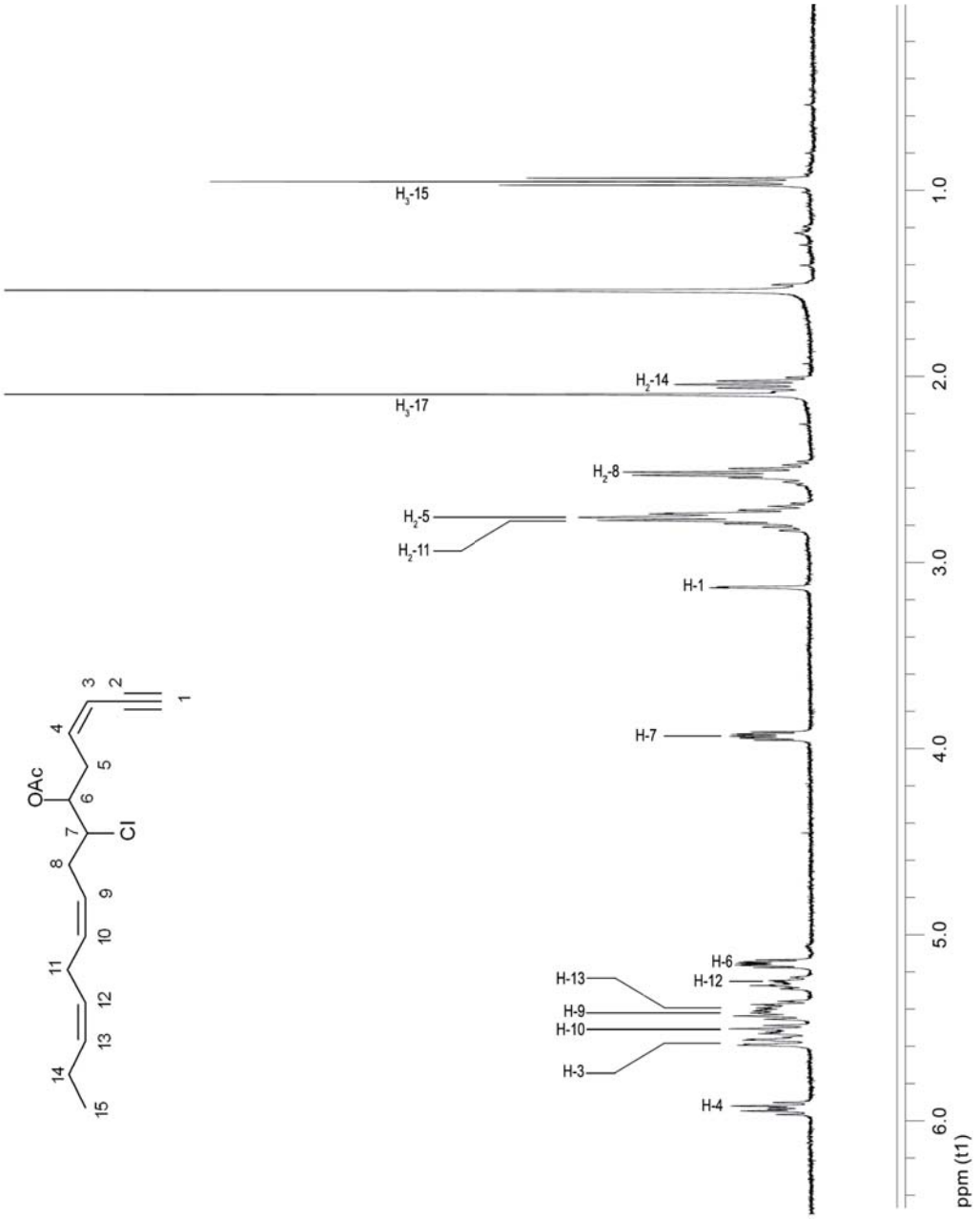

Fig. 6.46. ^{1}H NMR spectrum of compound **11**.

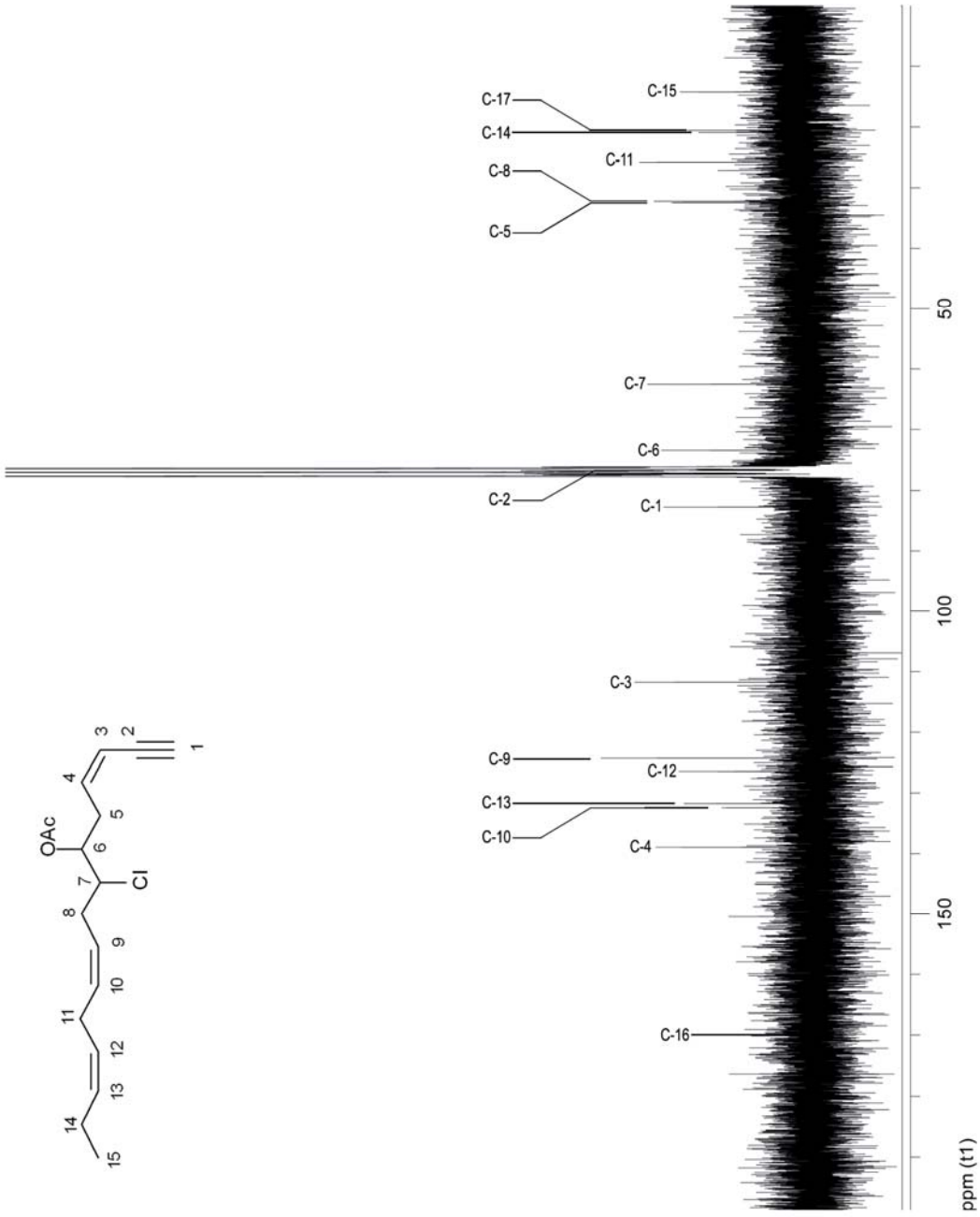

Fig. 6.47. ^{13}C NMR spectrum of compound **11**.

The molecular formula of compound **12** (Fig. 6.48) $C_{15}H_{19}OCl$ (MW 250) required six degrees of unsaturation. The UV spectrum showed absorption at $\lambda_{max\ (EtOH)}$ 267 nm (ε 4,900) due to a conjugated diene moiety, and λ_{inf} 231 nm (ε 8,000), λ_{max} 221 nm (ε 10,600), and λ_{inf} 214 nm (ε 9,800) due to a conjugated terminal enyne system. The absence in the IR spectrum of hydroxy and carbonyl functions indicated that the oxygen atom was involved in an ether link. Thus, only a cyclic system could justify the sixth degree of unsaturation.

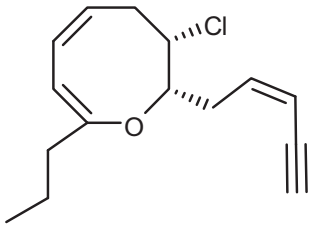

Fig. 6.48. Structure of **12**.

In the ^{1}H NMR spectrum, the chemical shift of the acetylenic proton (δ 3.13) and the coupling constant between the olefinic protons at C-3 and C-4 (J = 11 Hz) indicated the double bond at C-3 to be *Z*. The *cis* relationship between the chlorine atom at C-7 and the pentenyne side chain at C-6 was suggested by the coupling constant (J = 2 Hz) between the protons at C-7 and C-6. The comparison of both ^{1}H NMR and ^{13}C NMR data with those reported in the literature suggested that **12** was the halogenated C_{15} non-terpenoid (3Z)-venustinene (Suzuki *et al.* 1983), an acetogenin characterized by an oxocane ring with a propyl side chain. The ^{1}H NMR spectrum of **12** is reported in Fig. 6.49.

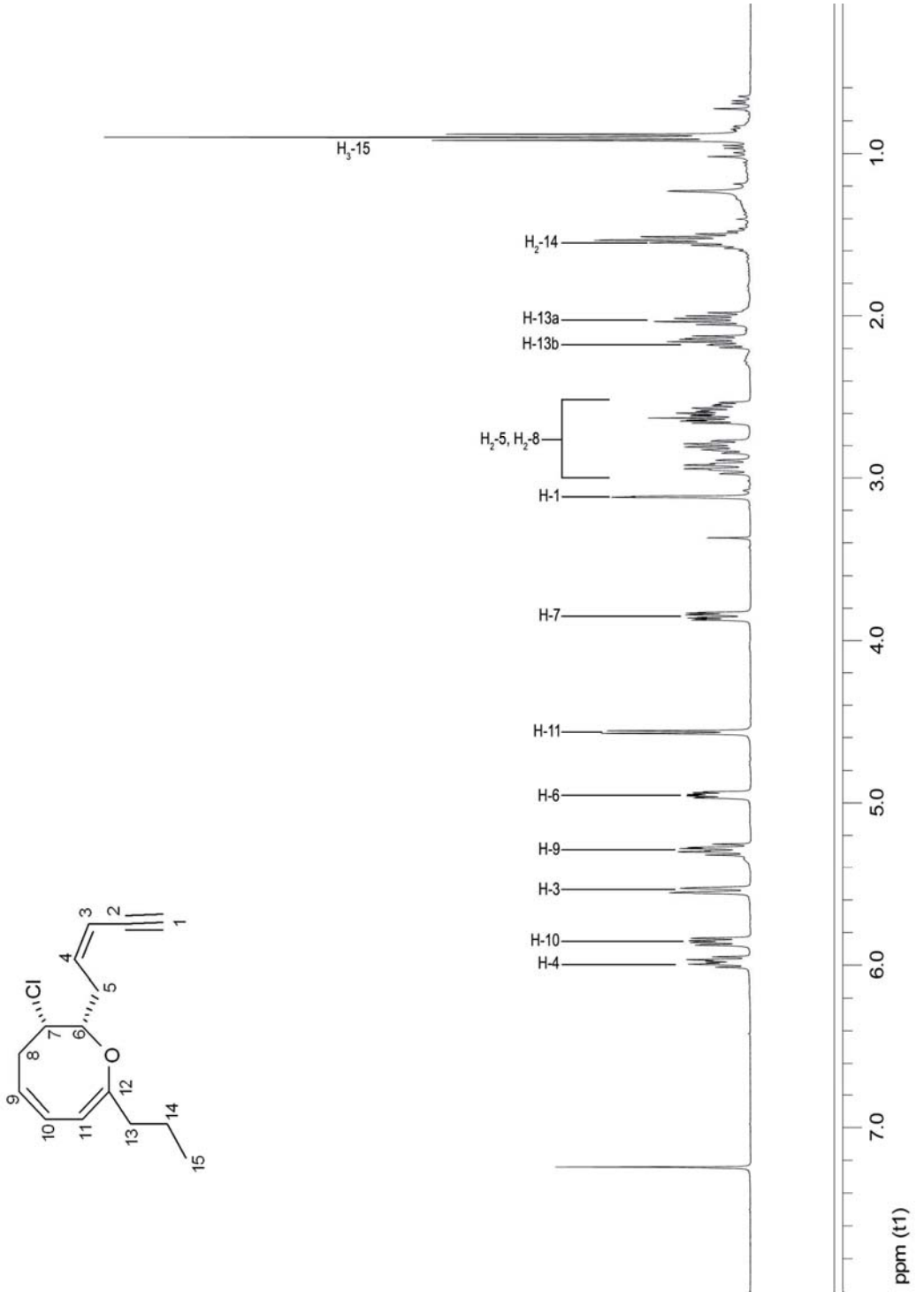

Fig. 6.49. ^{1}H NMR spectrum of compound **12**.

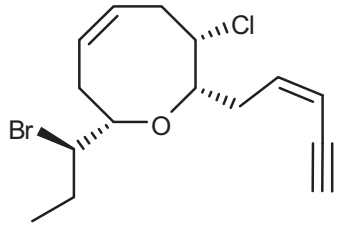

Fig. 6.50. Structure of **13**.

Compound **13** (Fig. 6.50) was structurally related to **12**, having an oxocane skeleton and a conjugated enyne moiety. The EI molecular ion peak at *m*/*z* 330 corresponded to the molecular formula $C_{15}H_{20}BrClO$, along with isotopic peaks at *m*/*z* 332 and 334. The IR spectrum showed the presence of two bands at 3300 and 2100 cm^{-1}, which were indicative for a conjugated enyne system, also confirmed by the UV absorption at λ_{max} 224 nm. The structure of **13** was assigned on the basis of its ^{1}H NMR and ^{13}C NMR data in comparison with the literature. The compound, in fact, resulted to be described as (3*Z*)-13-*epi*-pinnatifidenyne (San-Martín *et al.* 1997).

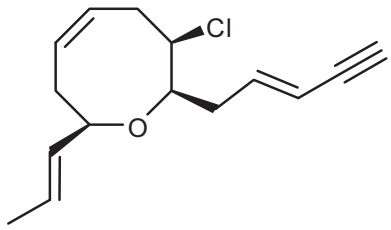

Fig. 6.51. Structure of **14**.

Compound **14** ($C_{15}H_{19}ClO$, Fig. 6.51) was characterized by the same carbon skeleton of **12** and **13**. The UV absorption at λ_{max} (MeOH) 226 nm along with the IR bands at 3310 and 2095 cm^{-1} were indicative for the conjugated enyne system. The ^{1}H NMR and ^{13}C NMR experiments allowed attributing the structure of (3*E*)-laurenyne to **14**, according to the literature (Falshaw *et al.* 1980; Overman & Thompson 1988). It consisted in a laurenane skeleton characterized by an 8-membered cyclic ether.

The ^{1}H NMR spectra of compound **13** is reported in Fig. 6.52.

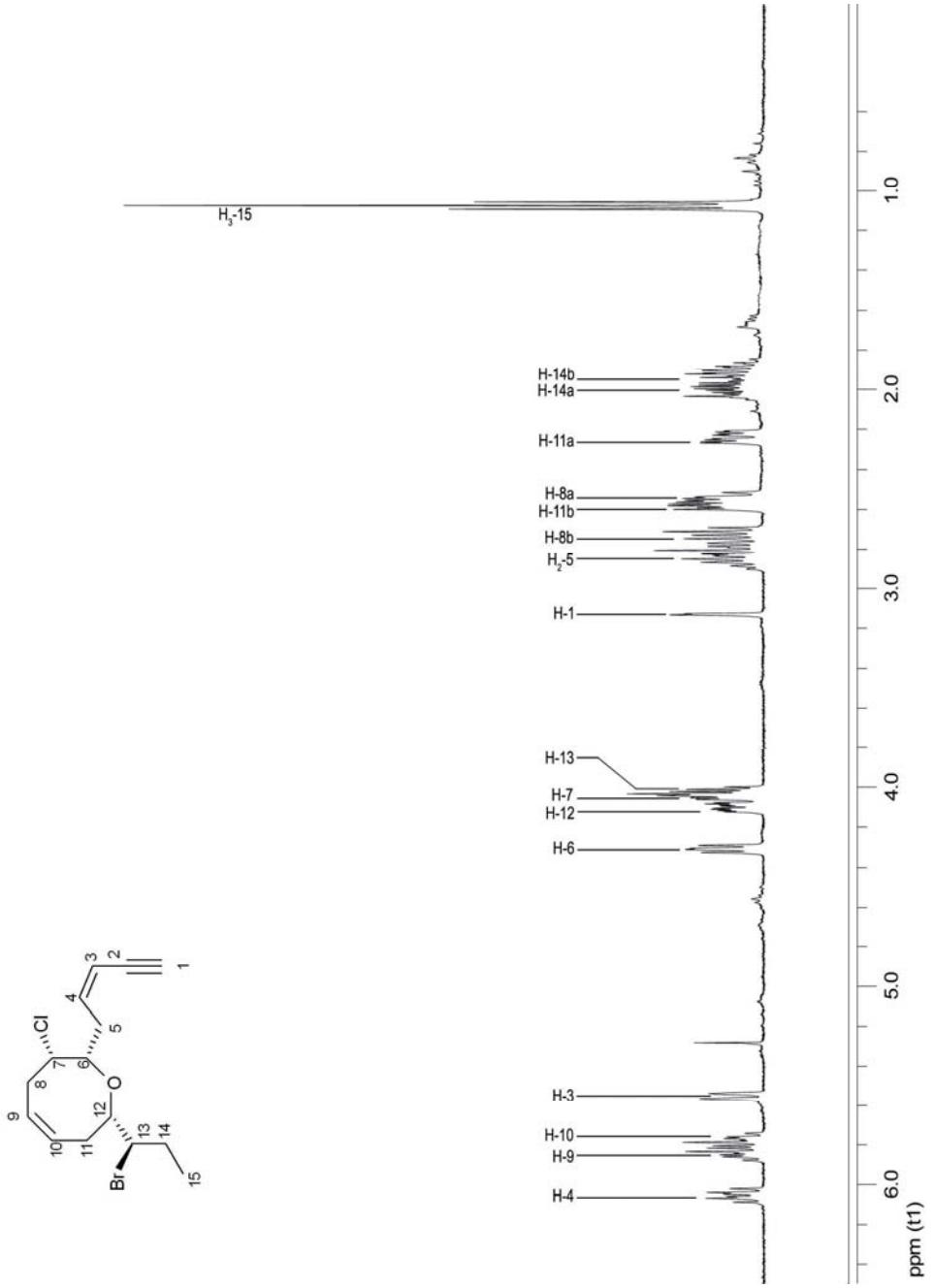

Fig. 6.52. ^{1}H NMR spectrum of compound **13**.

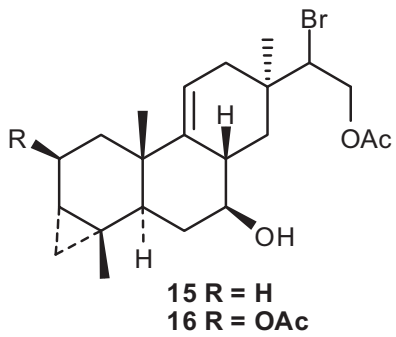

Fig. 6.53. Structures of **15** and **16**.

Compound **15** (Fig. 6.53) was isolated as a yellow oil. Combination of its ^{13}C NMR and FAB-HRMS data suggested the molecular formula of $C_{22}H_{33}BrO_3$. The strong absorption bands at 3417 and 1734 cm^{-1} observed in the IR spectrum indicated the presence of a hydroxy group and an ester carbonyl, respectively. The ^{13}C NMR spectrum (Fig. 6.54) revealed 22 carbon signals, corresponding to four methyl, seven methylene, six methine, and five quaternary carbon atoms. Among them, one ester carbonyl (δ 170.7), two olefinic carbons (one methine and one quaternary resonating at δ 116.8 and 144.1, respectively), one halogenated methine carbon (δ 59.8), and two oxygenated carbons (one methylene and one methine resonating at δ 66.1 and 77.4, respectively) were evident. Since the carbonyl and the carbon-carbon double bond accounted for two of the six degrees of unsaturation, the molecular structure of **15** was determined as tetracyclic. The ^{1}H NMR spectrum (Fig. 6.55) confirmed the presence of three aliphatic methyl groups on quaternary carbons (δ 1.05, 0.97, and 0.96), one acetate methyl group (δ 2.09), one olefinic proton of a trisubstituted double bond (δ 5.33), and one trisubstituted cyclopropane ring (δ 0.63, 0.40, and -0.05). The correlations observed in the ^{1}H-^{1}H COSY (Fig. 6.56), HSQC (Fig. 6.57), and HMBC spectra of **15** suggested a parguerane skeleton with a trisubstituted double bond, one halogenated and two oxygenated carbons (Schmitz *et al.* 1982).

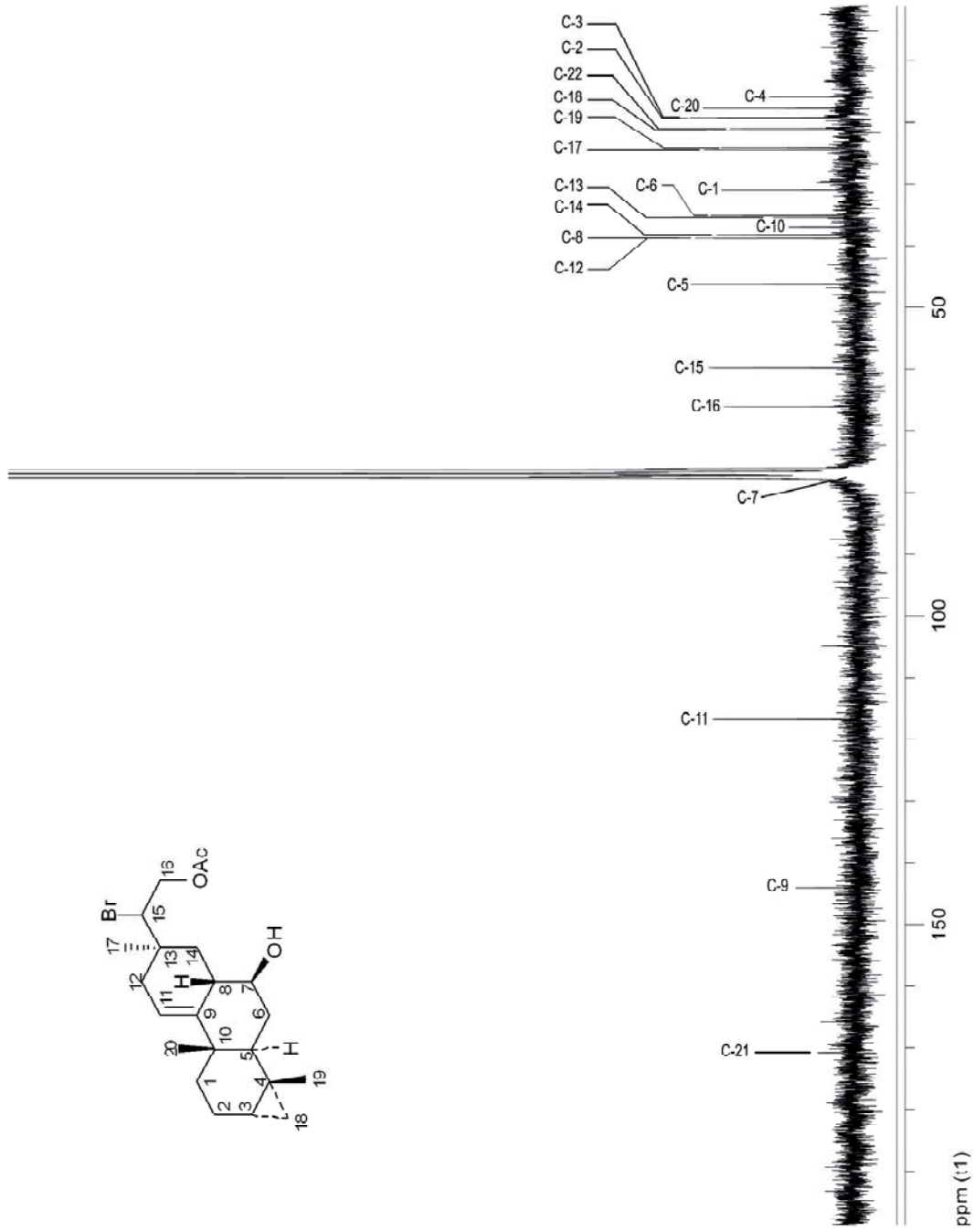

Fig. 6.54. ^{13}C NMR spectrum of compound **15**.

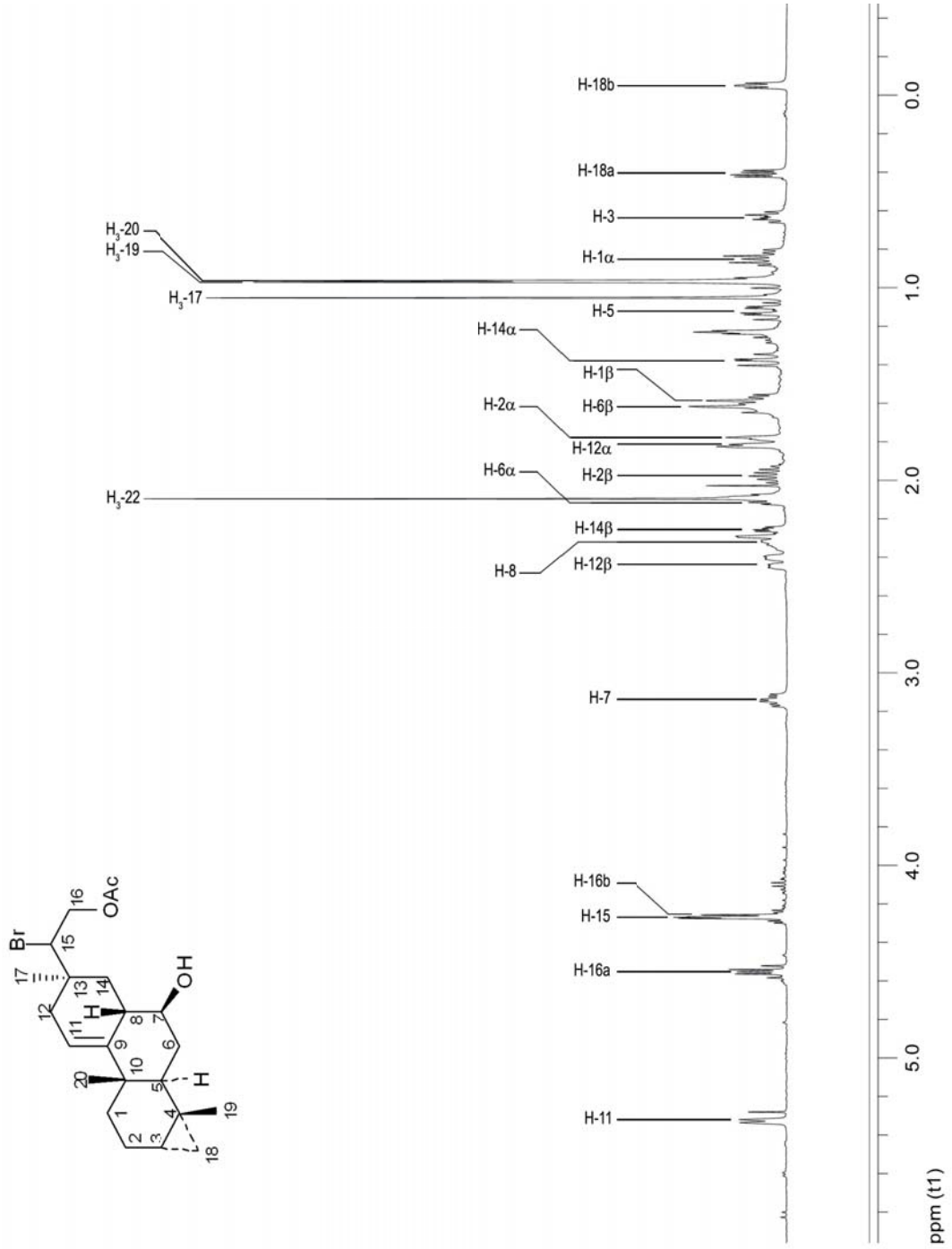

Fig. 6.55. ^{1}H NMR spectrum of compound **15**.

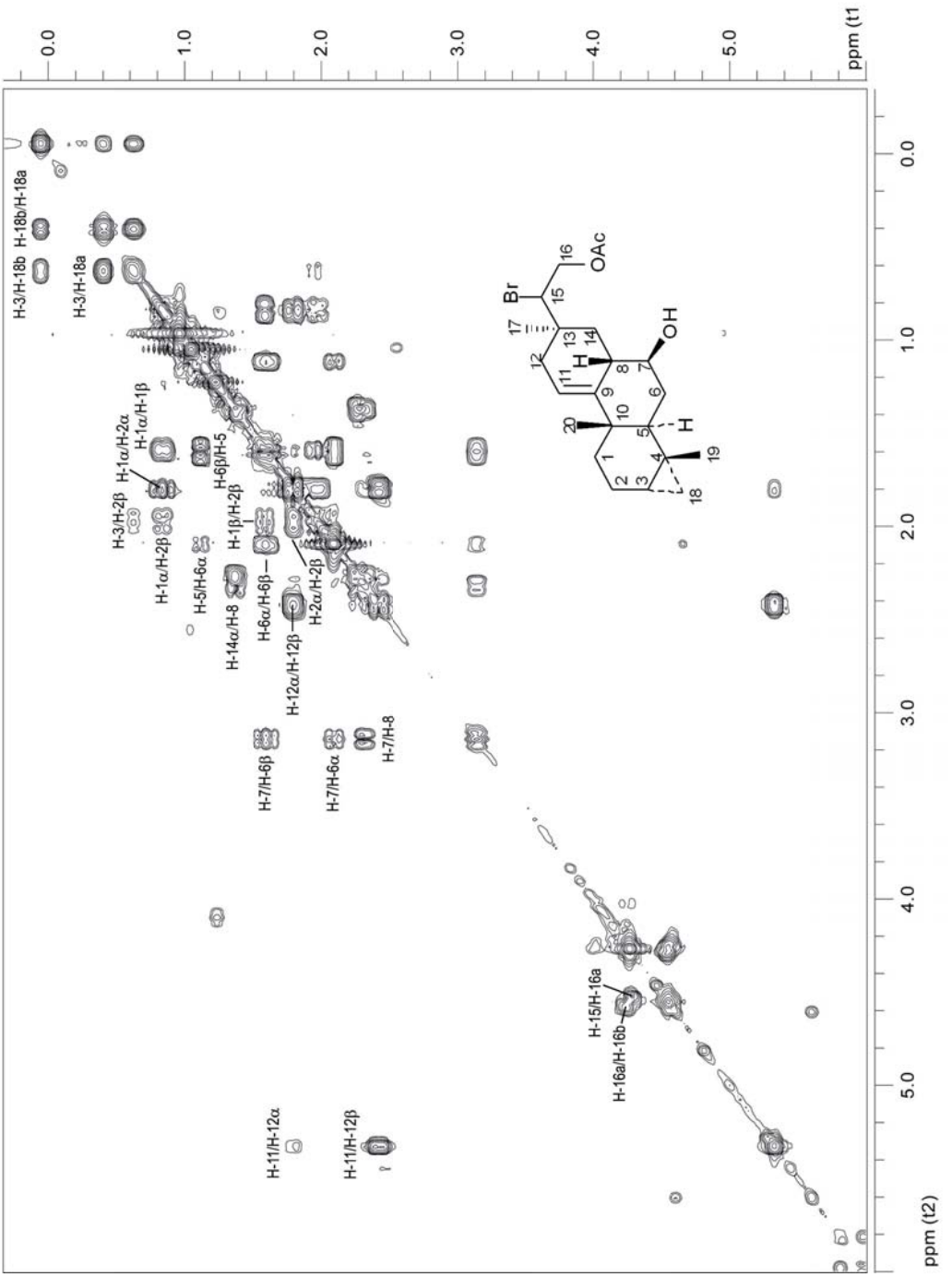

Fig. 6.56. Significant ^{1}H-^{1}H correlations in the COSY spectrum of **15**.

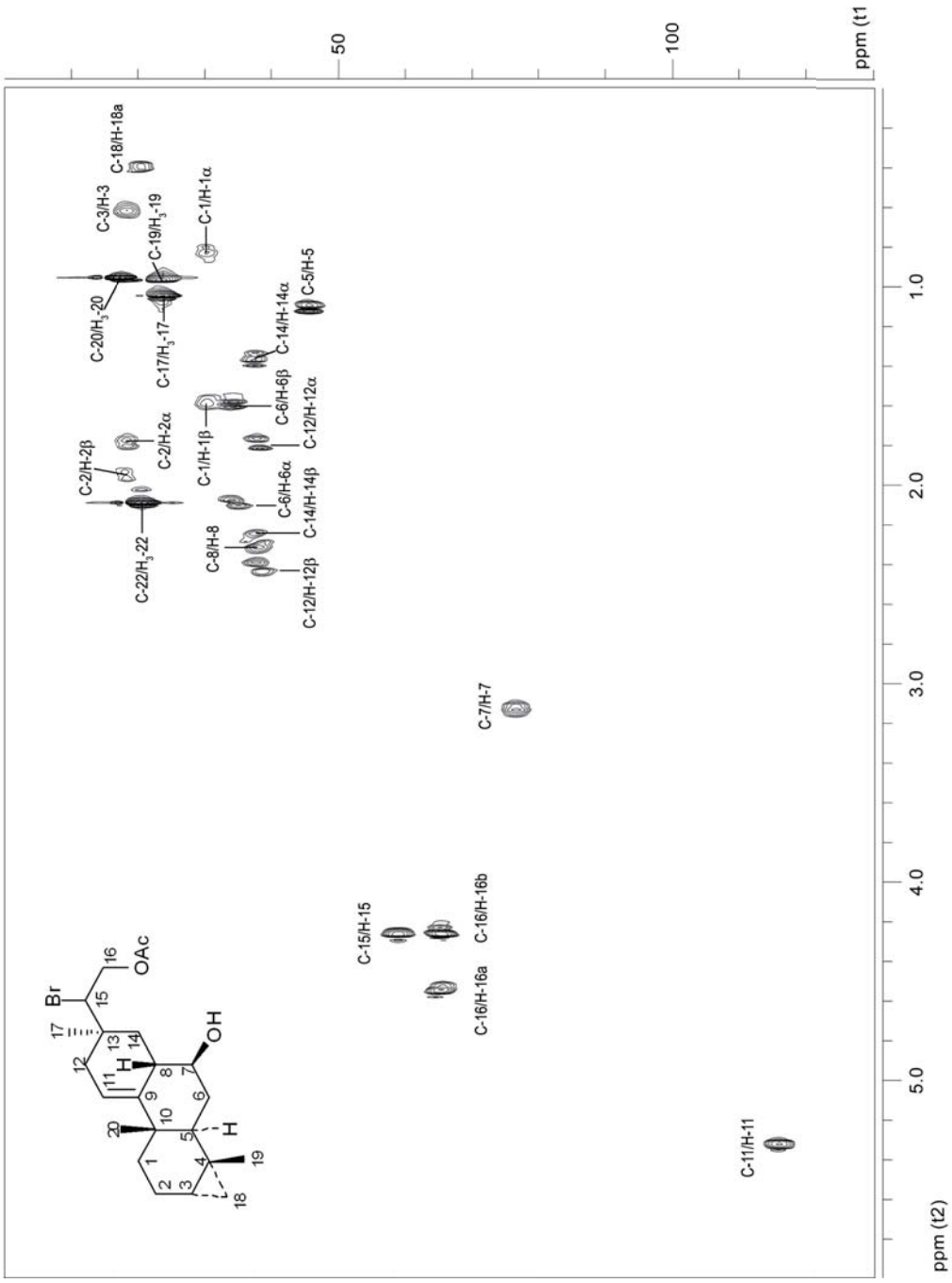

Fig. 6.57. HSQC-DEPT of compound **15**.

The heteronuclear correlations observed between H-11 and C-8, C-10, and C-13 positioned the trisubstituted double bond between C-9 and C-11. The acetoxy group was placed at C-16 on the basis of HMBC correlations of H_2-16 with C-13, C-17, and C-21. The hydroxy group was placed at C-7 due to the H_2-6 and H-8 interactions with C-7, whereas the correlations of H-15 with C-13, C-16, and C-17 positioned the bromine atom at C-15. The relative configuration of **15** was determined on the basis of n.O.e. enhancements and coupling constants of certain proton signals. In particular, the fact that the methine at C-7 appeared as a triplet of doublets with two large (10.4 Hz) and one medium (4.6 Hz) coupling constants with H_2-6 and H-8 suggested an axial orientation for H-7 and H-8, and an equatorial orientation for the hydroxy group. In addition, the n.O.e. correlations observed for H-3/H_3-19, H-3/H_3-20, H-5/H-7, H-5/H-18b, H-7/H-14α, H-8/H_3-20, and H-14α/H_3-17 provided evidence that H-3, H-8, H_3-19, and H_3-20 were on one side of the molecule, while H-5, H-7, and H_3-17 were on the opposite side. The configuration at C-15 was not possible to determine by spectroscopic analysis. ^{13}C NMR and ^{1}H NMR data of **15** are reported in Table 6.6. Therefore, the diterpene **15** resulted to be 16-acetoxy-15-bromo-7-hydroxy-9(11)-parguerene, a diterpene monoacetate with a modified pimarane skeleton, characterized by a cyclopropane ring fused with a tricyclic system. It has been proposed that the cyclopropyl moiety had resulted from cyclization of a methyl group to a ring carbon in the diterpene system (Higgs & Faulkner 1982).

C	δ ^{13}C	mult.	δ ^{1}H	mult., J_{H-H} (Hz)	Significant long range correlations (HMBC)
1	31.0	*t*	α 0.85	*dt*, 12.9, 6.0	H-2α, H-2β, H-3, H-5
			β 1.59	*m*	
2	19.3	*t*	α 1.79	*m*	H-1β, H-3, H-18α
			β 1.96	*m*	
3	19.2	*d*	0.63	*dt*, 9.2, 6.2	H-1β, H-2α, H-2β, H_3-19
4	15.9	*s*	-	-	H-2α, H-2β, H_3-19
5	46.4	*d*	1.12	*dd*, 13.5, 3.4	H-1β, H-18α, H_3-19, H_3-20
6	35.1	*t*	α 2.11	*m*	
			β 1.60	*m*	
7	77.4	*d*	3.14	*td*, 10.4, 4.6	H-6α, H-6β, H-8, H-14α, H-14β
8	38.8	*d*	2.33	*m*	H-11
9	144.1	*s*	-	-	H-5, H-12α, H-12β, H-14α
10	37.0	*s*	-	-	H-11
11	116.8	*d*	5.33	br *d*, 6.2	H-12α, H-12β
12	38.9	*t*	α 1.80	*m*	
			β 2.42	*m*	
13	35.5	*s*	-	-	H-11, H-15, H_2-16
14	38.2	*t*	α 1.38	*dd*, 13.1, 10.3	
			β 2.24	*m*	
15	59.8	*d*	4.27	*m*	H-12α, H-14β, H_2-16, H_3-17
16	66.1	*t*	a 4.55	*m*	H-15
			b 4.25	*m*	
17	24.3	*q*	1.05	*s*	H-15, H_2-16
18	21.3	*t*	a 0.40	*dd*, 9.3, 4.1	
			b -0.05	*dd*, 5.6, 4.4	
19	24.0	*q*	0.97	*s*	
20	17.8	*q*	0.96	*s*	
21	170.7	*s*	-	-	H_2-16
22	21.0	*q*	2.09	*s*	

Table 6.6. ^{13}C NMR and ^{1}H NMR resonance values of compound **15**.

Compound **16** had a molecular formula $C_{24}H_{35}BrO$, corresponding to seven degrees of unsaturation. The IR spectrum contained bands at 3360 and 1725 cm^{-1}, indicative for a hydroxy and a carbonyl, respectively. The ^{13}C NMR experiment showed the

presence of two acetate carbonyl signals at δ 170.4 and 169.7, and two olefinic carbon signals at δ 144.1 (*s*) and 117.1 (*d*). This meant that **16** was tetracyclic. In addition, the ^{13}C NMR spectrum contained the typical signals of a 1,1,2-trisubstituted cyclopropane ring [δ 24.1 (*d*), 21.8 (*t*), and 17.2 (*s*)]. The geminal protons of the cyclopropyl moiety, resonating at 0.67 and δ 0.03, were coupled to a signal at δ 0.80 (C-3), which was in turn coupled to an α-acetoxy proton signal at δ 5.31 (C-2). The ^{1}H NMR spectrum (Fig. 6.58) contained, in addition, one signal of an olefinic proton at δ 5.34 (*dt*, C-11), the two methyl singlets of the acetoxy groups at δ 2.12 and 2.08, and two downfield multiplets at δ 4.58 (C-15) and 4.29 (C-16), corresponding to the proton attached to the brominated carbon and the methylene linked to the acetyl group, respectively. The ^{13}C NMR spectrum showed signals at δ 66.2 (*t*) and 60.3 (*d*), indicative for a primary acetate and a secondary bromine, respectively. The comparison with the literature data (Higgs & Faulkner 1982) allowed us to assign **16** the structure of 15-bromo-2,16-diacetoxy-7-hydroxy-9(11)-parguerene, a brominated diterpene diacetate. The ^{1}H and ^{13}C NMR spectra of **16** were very similar to those of **15**. The only difference was the presence in **16** of an acetoxy group linked to C-2, responsible for determining the downfield shift of H-2α from δ 1.79 (*m*, in **15**) to δ 5.31 (br *d*, in **16**).

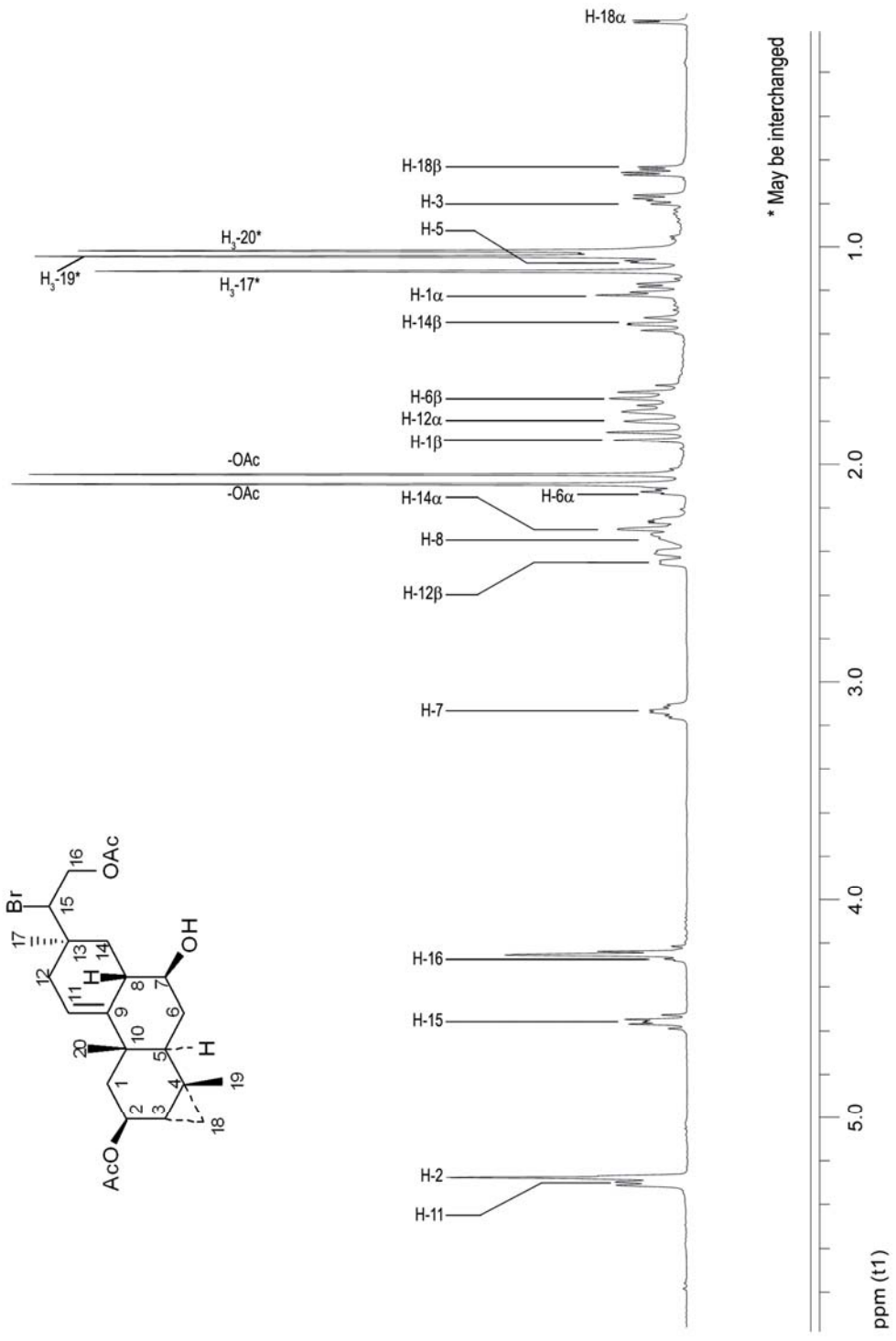

Fig. 6.58. ^{1}H NMR spectrum of compound **16**.

6.4. Discussion

The scarce predation on sea hares in spite of the lack of an adequate physical protection, has always attracted the scientific interest, suggesting the involvement of chemical weapons in the defence of the animals. Marine mollusc can *de novo* synthesize chemicals by using simple precursors (primary metabolites) or store antipredation metabolites of dietary origin. Sea hares, in particular, have revealed to accumulate in their digestive gland, more than in the external part, secondary metabolites contained in the diet, mainly seaweeds (Stallard & Faulkner 1974). Among algae, anaspideans have specific preferences for the species *Laurencia*, *Plocamium* and *Dictyota*, and for some cyanobacteria as well as *Lyngbya*, *inter alia* (Carefoot 1967), which are rich in terpenes, halogen-containing compounds and products derived from the acetate metabolism. These metabolites, which appear to act as feeding deterrent compounds towards the predators of the algae, are then acquired by the sea hares probably to furnish a similar protective function (Kittredge 1974), determining an important energetic saving for the animals themselves.

In the frame of our study on the anaspidean mollusc *Aplysia fasciata*, a particular interest was focused on the organic extract of both its digestive and hermaphroditic glands. Usually the digestive gland is not the optimal localization for containing defensive weapons which, in turn, are normally found in the mantle, which is more exposed to the predators. Nevertheless, it can be hypothesized that *A. fasciata*

sequesters food metabolites in its digestive gland to create its chemical arsenal to be used in case of aggression. In fact, most of the metabolites involved in the chemical defence of *Aplysia* molluscs have been identified to derive from the red alga *Laurencia* (Rhodophyta) (Stallard *et al*. 1978; Higgs & Faulkner 1982). At the beginning of the investigation, our first idea was that *A. fasciata* had a food relation with the sea grass *Cymodocea nodosa* since, at the moment of the sampling, the animals were found feeding on the leaves of this plant species, and some fragments of the plant were found in their digestive systems. For this reason, *C. nodosa* was chemically analyzed in parallel to the mollusc. Nevertheless, the ^{1}H NMR analysis of the sea grass extract and its fractions, and the comparison of these data with those of the mollusc extracts rejected the hypothesis of an ecological relationship between *A. fasciata* and *C. nodosa*. On the contrary, the chemical analysis of the metabolic pattern of *A. fasciata* did demonstrate that these compounds derived from algae of the genus *Laurencia*. The genus *Laurencia* has demonstrated to contain halogenated sesquiterpenes, diterpenes and, in addition, it is unique in producing bromoallenyl and bromoenyne C_{15} acetogenins (Faulkner 1995b). Anaspideans, on the other hand, have been described as rich producers of poliketides, halogenated compounds, including acetogenins and terpenes, and degraded sterols (Miyamoto 2006). The structure elucidation and the assignment of the relative configurations of the isolated compounds were established on the basis of a careful analysis of their spectroscopic and spectrometric data (mono- and bidimensional NMR, IR, MS). Our study on both the digestive and

hermaphroditic glands led to the isolation of sixteen metabolites, including eight sesquiterpenes (**1**-**8**), three diterpenes (**9**, **15**-**16**), and five C_{15} acetogenins (**10**-**14**). Four of the sesquiterpenes (**4**, **6**–**8**), one acetogenin (**10**), and one diterpene (**15**) were found for the first time from natural sources. Among the isolated sesquiterpenes, brasilenol (**1**), epibrasilenol (**2**), 4-hydroxy-5-brasilene (**3**), 6-hydroxy-1-brasilene (**4**), brasilenol acetate (**5**), epibrasilenol acetate (**6**), 4-acetoxy-5-brasilene (**7**) are non-isoprenoid sesquiterpene alcohols characterized by a brasilane skeleton and differing each other in the position of both the double bond and the hydroxy group. Compounds **1**, **2** and **5** were originally isolated from the digestive gland of the anaspidean *A. brasiliana* (Stallard *et al.* 1978). In addition, **1** and **2** were also isolated from the red alga *Laurencia obtusa*, which the animal thrives on. This could mean that the acetylation of **1** and **2** to give **5** and **6**, respectively, occurs after storing these food metabolites in the digestive gland. It would be interesting to clarify the function of the acetylation in terms of reduction/increase in the activity/toxicity of the stored metabolites. The new 6-hydroxy-1-brasilene (**4**) is characterized by an unusual 1-2 double bond and a hydroxy function linked to C-6. Laboratory experiments, furthermore, showed the repellent action of brasilane compounds against model animals (Stallard *et al.* 1978). Compound **3** was isolated for the first time from another red alga of the genus *Laurencia*, *L. implicata* (Wright *et al.* 1991). Compound **7**, the 4-acetoxy derivative of **3**, has been described in the literature as semisynthetic molecule obtained by acetylation of **3** (Wright *et al.* 1991), but in our investigation it was found as a natural

product. The finding of the acetoxy derivative **7** in the sea hare rather than in the diet would provide further evidence to the previous observation: the acetylation occurs in the mollusc's digestive gland in order to modify the toxicity/activity of the compound.

Sesquiterpene **8**, 6-*epi*-β-snyderol, is the epimer at C-6 of β-snyderol (Fig. 6.59a), a metabolite which was found in different species of *Laurencia* (Howard & Fenical 1976; Topcu *et al.* 2003). The structure, a snyderane skeleton, is characterized by a brominated cyclohexane with an exocyclic methylene group, and a side chain with a terminal double bond and a hydroxy substituent. A brominated derivative of **8** from *L. obtusa* (Fig. 6.59b) has shown a strong antimalarial activity against *Plasmodium falciparum* (Topcu *et al.* 2003).

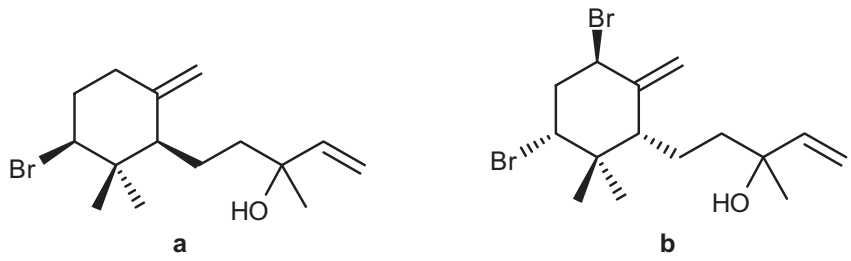

Fig. 6.59. Structure of a) β-snyderol, and b) the antimalarian 8-bromo-10-*epi*-6-*epi*-β-snyderol.

Luzodiol (**9**) is a diterpene which was isolated for the first time from the tropical *L. luzonensis* (Kuniyoshi *et al.* 2005). This compound has got a rare carbon skeleton, consisting in a brominated hydroxy cyclohexane ring in the middle of a

geranylgeranyl system. Compound **16**, 15-bromo-2,16-diacetoxy-7-hydroxy-9(11)-parguerene, is a diterpene with a modified pimarane skeleton. Parguerane diterpenes have been isolated from different red algae of the genus *Laurencia*, such as *L. obtusa* (Higgs & Faulkner 1982), *L. filiformis* (Rochfort & Capon 1996) and *L. nipponica* (Lyakhova *et al.* 2004). The related new compound (**15**) we isolated from *A. fasciata*, 16-acetoxy-15-bromo-7-hydroxy-9(11)-parguerene, lacks the 2-acetoxy group with respect to **16**. Other parguerane compounds, as well as 2-acetoxy-15-bromo-7,16-dihydroxy-9(11)-parguerene, the cytotoxic parguerol, along with deoxyparguerol and isoparguerol, were also isolated from the sea hare *A. dactylomela* (Schmitz *et al.* 1982). More recently, the parguerane diterpene 15-bromo-2,7,19-triacetoxyparguer-9(11)-en-16-ol (Fig. 6.60) was isolated from the red alga *L. saitoi*, and it showed to have an opposite stereochemistry at some chiral carbons with respect to **15-16** (Ji *et al.* 2008). These examples provide further evidence of the chemoecological relationship mollusc/alga.

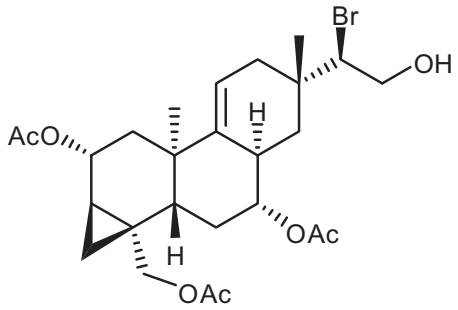

Fig. 6.60. The parguerane diterpene 15-bromo-2,7,19-triacetoxyparguer-9(11)-en-16-ol isolated from the red alga *Laurencia saitoi*.

The other class of compounds isolated from *A. fasciata* is represented by C_{15} acetogenins, both linear chains and cyclic ethers. Compound **10**, (3*Z*,9*Z*)-7-chloro-6-hydroxy-12-oxopentadeca-3,9-dien-1-yne, is a linear polyunsaturated chlorinated alcohol with a terminal conjugated enyne system which has been here described for the first time as a natural product. Compound **11**, 3*Z*,9*Z*,12*Z*)-6-acetoxy-7-chloro-pentadeca-3,9,12-trien-1-yne, is chemically related to **10** and it is a known compound (González *et al.* 1982; Norte *et al.* 1991), although its ^{1}H NMR and ^{13}C NMR resonance values have been re-assigned in our investigation. On the other hand, the cyclic ethers in *A. fasciata* were comprehensive of (3*Z*)-venustinene (**12**), (3*Z*)-13-*epi*-pinnatifidenyne (**13**) and (3*E*)-laurenyne (**14**). These compounds are characterized by a laurenane skeleton, which is composed by an oxocane ring, *i.e.* an eight-membered cyclic ether, one or more halogen atoms, a propyl side chain and a terminal enyne moiety. Compound **12** was originally isolated from *L. venusta* (Suzuki *et al.* 1983), **13** from *L. claviformis* (San-Martín *et al.* 1997), and **14** from *L. obtusa* (Falshaw *et al.* 1980). The absolute configuration of natural (+)-laurenyne (**14**), originally established as 2*S*, 7*S*, 8*S*, was reassigned by total synthesis as 2*R*, 7*R*, 8*R* (Overman & Thompson 1988). It is noteworthy that some linear compounds related to **10** and **11** are the biogenetic precursors of the laurenane skeleton (González *et al.* 1982). Acetogenins derive from straight chain fatty acids by condensation of acetyl-CoA (Erickson 1983), and differ from C_{15} sesquiterpenes for the biogenetic pathway. The co-occurrence in the same alga, and thus in the same mollusc, of both C_{15} acetogenins and terpenes is frequent

and provides a further example of secondary metabolite variation within a species (Wright *et al.* 1991). The presence of a propyl side chain at C-12, as displayed by compound **12**, is quite rare in acetogenins, whereas C_{15} non-terpenoids from *Laurencia* algae generally contain bromopropyl or ether side chain at C-12 or C-13, respectively (Suzuki *et al.* 1983). Acetogenins, which have shown to play an important paper in chemical defence (Kinnel *et al.* 1979), are common metabolites not only in sea red algae of the genus *Laurencia* (Moore 1978; Erickson 1983), but also in plants and in marine invertebrates (Faulkner 1999; Dembitski *et al.* 2003). The high diversity of variants of *O*-heterocyclization of acetogenins is responsible for a wide repertory of biological activities (Dembitsky *et al.* 2003). Some laurenane compounds as well as laurencin, *Z*- and *E*-laurentin, and isoprelaurefucin (Fig. 6.61), isolated from different species of *Laurencia*, have shown to inhibit the effect of pentobarbital in mice and exhibit a high insecticide activity on gnat and mosquito larvae (Watanabe *et al*. 1989).

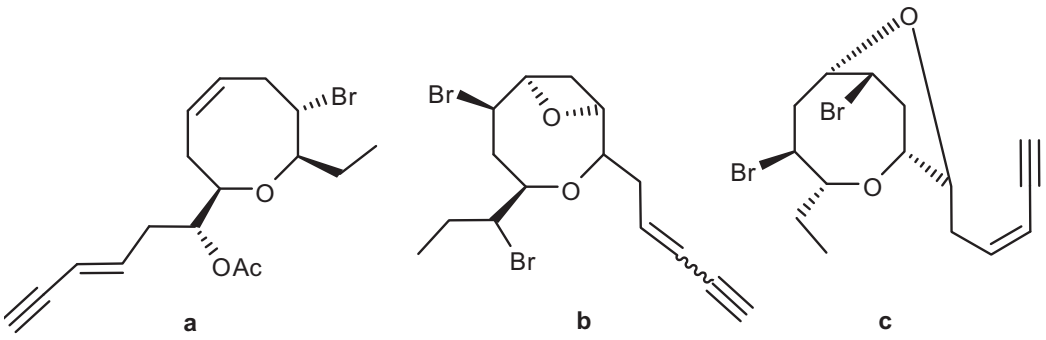

Fig. 6.61. Structures of a) laurencin, b) *Z*- and *E*-laurentin, and c) isoprelaurefucin, laurenane compounds able to inhibit the effect of pentobarbital in mice, and with insecticide activity.

Venustinene (**12**) and similar compounds, instead, exhibit antibacterial activity (Suzuki & Kurosawa 1980; Suzuki *et al.* 1983).

Anaspidean molluscs, and the genus *Aplysia* in particular, have been widely studied from the chemical point of view (Yamada & Kigoshi 1997; Yamada *et al.* 2000). In particular, many reports in the literature deal with the metabolites extracted from the molluscs' mantle, as well as degraded sterols, which have revealed to have a protective role in sea hares (Miyamoto *et al.* 1986; Spinella *et al.* 1992; Ortega *et al.* 1997). In Fig. 6.62 the structures of some aplykurodins belonging to the group of the degraded sterols and including aplykurodin A from *A. kurodai* (Miyamoto *et al.* 1986), 3-*epi*-aplykurodinone B from *A. fasciata* (Ortega *et al.* 1997), and aplykurodinone-1 from the anaspidean *Syphonota geographica* (Gavagnin *et al.* 2005), are reported.

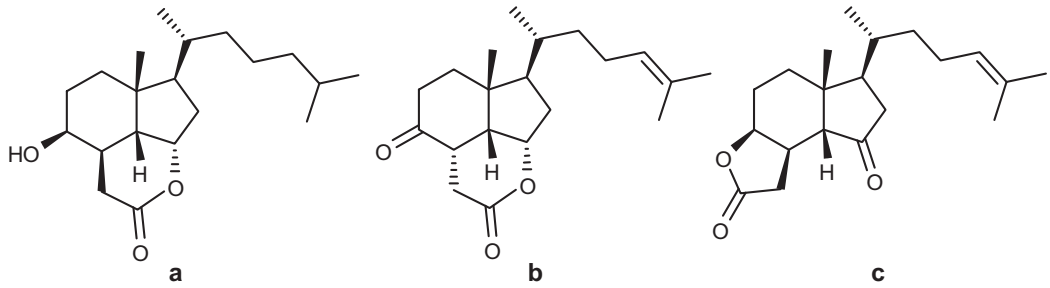

Fig. 6.62. Some degraded sterols involved in the chemical defence of anaspidean molluscs: a) aplykurodin A, b) 3-*epi*-aplykurodinone B, and c) aplykurodinone-1.

Aplykurodins probably derive biogenetically from a parent sterol by oxidative pathways involving the loss of A-ring carbon atoms (Gavagnin *et al.* 2005). Besides

the ichthyotoxic activity exhibited by some of these compounds, aplykurodin A and 3-*epi*-aplykurodinone B display cytotoxicity against several human cancer cell lines (Miyamoto *et al.* 1986; Ortega *et al.* 1997).

7. New casbane diterpenes from the Chinese soft coral *Sinularia* sp.: structures and biological activities

7.1. Introduction

The South China Sea, with a 3.5 million km^2 area, represents a "biodiversity hotspot", characterized by over 95% of the invertebrates found there and nowhere else in China (Zhang *et al.* 2006). For this reason, most of the Chinese biological material collected for chemical investigations derives from this region, especially from off Hainan, Taiwan, Hong Kong, Xisha, and Nansha Islands, as well as Guangdong province. Research on marine natural products in China developed at the beginning of the '80s, but only by the end of the twentieth century the number of publications about the isolation of marine natural products from this geographical area has significantly increased (MarinLit database). The main animals that have been studied are sponges, cnidarians, molluscs, echinoderms, bryozoans and tunicates. Among Chinese marine invertebrates, soft corals have been the first to be investigated, probably due to their abundance. In fact, corals of the class Anthozoa are the most dominant benthic invertebrates living in tropical seas, with more than 6,100 species

all over the world of which 496 are found in the China Seas (Zhang *et al.* 2006). The Chinese anthozoan fauna has been estimated to contain about 570 species, comprehensive of 53 families and ten orders, namely Zoanthidea, Actiniaria, Scleractinia, Antipatharia, Helioporacea, Stolonifera, Gorgonacea, Alcyonacea, Pennatulacea, and Telestacea. Among soft corals, more than 67 species have been chemically analyzed, and about 370 metabolites have been isolated (Zhang *et al.* 2005a). Despite the lack of a hard protective exoskeleton in a highly competitive and hostile habitat, marine invertebrates including soft corals (Alcyonacea) and gorgonians (Gorgonacea) can survive, mainly relying on their chemical defensive systems based on secondary metabolites accumulated in their bodies and released into the environment. Their compounds consist mainly in diterpenes with dolabellane, xenicane, prenylgermacrane, cembrane and meroterpene skeletons (Fig. 7.1), some of which have shown interesting pharmacological activities (cytotoxicity, neurotoxicity and/or activity on the cardiovascular system, *inter alia*).

In the frame of this doctoral project, a Chinese soft coral has been chemically analysed. Although taxonomic studies are still in progress in order to determine the species, the presence of characteristic fusiform sclerites in the internal section of the stem allowed us to place it into the genus *Sinularia*. This soft coral is widely distributed and it represents a dominant part of the reef biomass. It belongs to the phylum Cnidaria, class Anthozoa, subclass Octorallia, order Alcyonacea, and family Alcyoniidae. The genus *Sinularia* consists of almost 90 species, of which more than 50

have been chemically examined (Kamel & Slattery 2005). It produces a great variety of secondary metabolites including sesquiterpenes, diterpenes, polyhydroxylated steroids and polyamine compounds, some of which display strong antimicrobial, antiinflammatory and cytotoxic activities (Venkateswarlu *et al.* 2001).

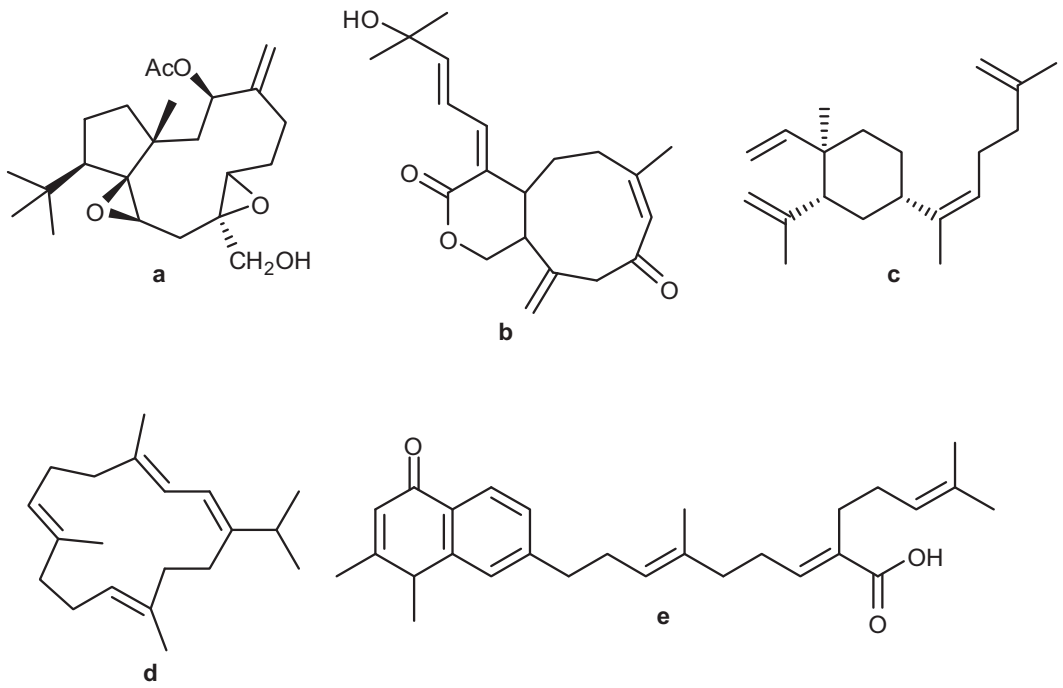

Fig. 7.1. Typical diterpene skeletons isolated from soft corals: dolabellane (**a**), xenicane (**b**), prenylgermacrane (**c**), cembrane (**d**) and meroterpene (**e**) compounds.

It is still questioned whether the origin of the terpenes can be ascribed to symbiotic associations between marine invertebrates and algae (Zooxanthellae), even if many authors agree with the fact that zooxanthellae do not produce terpenes and coral polyps are directly involved in terpene biosynthesis (Kobbe *et al.* 1984).

7.2. Isolation and purification

7.2.1. Biological material

A sample of *Sinularia* sp. (Fig. 7.2a) was collected off Lingshui Bay, Hainan Island, China (Fig. 7.3), by SCUBA diving at 20 m depth, during January 2004. It was immediately frozen, transferred to the laboratory of ICB (CNR, Naples, Italy) and stored at -20°C until extraction.

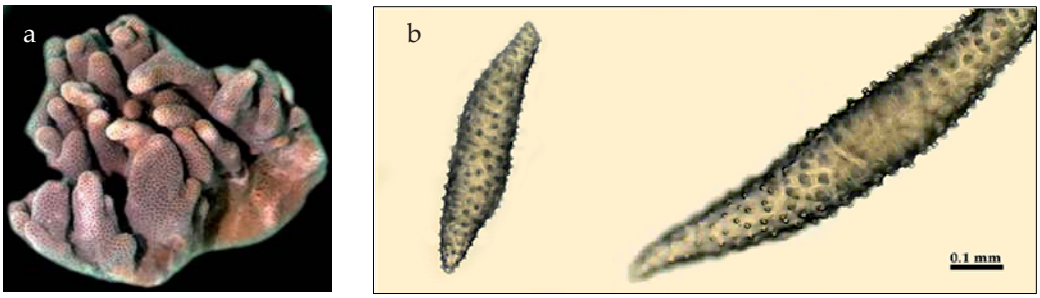

Fig. 7.2. a) *Sinularia* sp.; b) fusiform sclerites in the stem of the soft coral, characteristic of the genus *Sinularia.*

Fig. 7.3. Site of collection, Hainan Island, South Chinese Sea.

7.2.2. Extraction

The frozen biological material was cut and exhaustively extracted with acetone, improving the extractive process by sonicating in an ultrasound bath and crumbling the tissues in a mortar. After filtrating the suspension and removing the organic solvent under reduced pressure, the aqueous residue was diluted in distilled water and extracted with diethyl ether. The organic phases were combined and the solvent was *in vacuo* removed to afford a crude extract (2.2 g) which was preliminarily analyzed by TLC (Fig. 7.4) using different eluant systems.

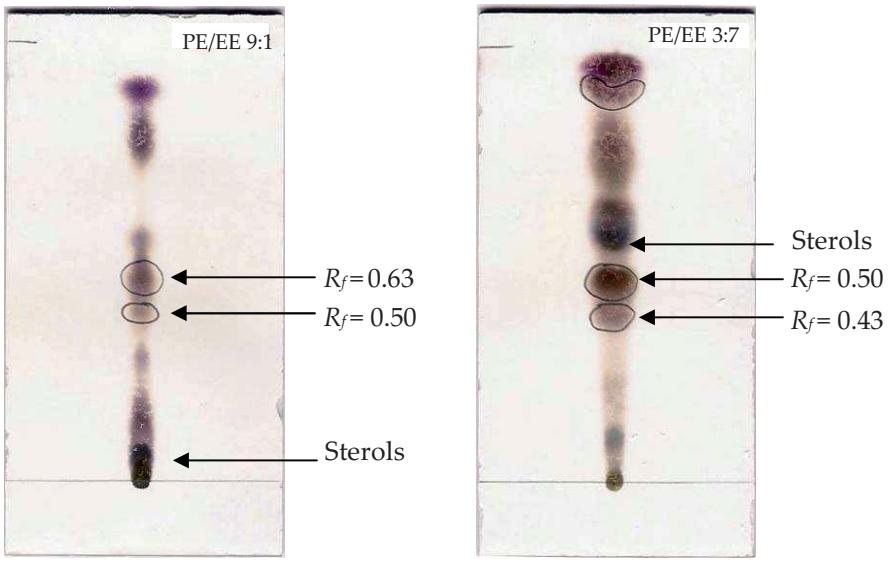

Fig. 7.4. TLC screening of the diethyl ether extract in light petroleum/diethyl ether 9:1 v/v and light petroleum/diethyl ether 3:7 v/v.

7.2.3. Purification

The chromatographic analysis of the diethyl ether extract of *Sinularia* sp. displayed an interesting metabolic composition, because of the presence of some UV-visible bands. In particular, two spots were observed at R_f 0.63 and 0.50 (light petroleum/diethyl ether 9:1 v/v), less polar than sterols, and two spots at R_f 0.50 and 0.43 (light petroleum/diethyl ether 3:7 v/v), more polar than sterols. Hence, an aliquot of the diethyl ether extract (389.0 mg) was fractionated by liquid chromatography. The mixture was charged onto a silica gel packed column and eluted with a gradient of light petroleum/diethyl ether. The recovered fractions were analyzed by TLC and then combined into 9 groups, as reported in Table 7.1.

Groups	
1	Containing compounds **1** and **2**
2	Containing compounds **1** and **2**
3	
4	Containing 4-cholesten-3-one
5	Containing 4-cholesten-3-one
6	Containing compounds **3** and **4**
7	Containing compounds **3** and **4**
8	
9	

Table 7.1. Groups afforded by fractionation of the diethyl ether extract.

The fractions containing the UV-visible bands were subjected to a preliminary ^{1}H NMR analysis, which showed the presence of a series of diterpene compounds

structurally related among them. Since these fractions were not so pure as to allow the immediate chemical characterization of these compounds, further purifications were required. In particular, compound **2** (5.5 mg) was obtained from fraction 1 by carrying out a semipreparative TLC purification with light petroleum/diethyl ether 9:1 v/v as eluant, whereas a two-step purification of the same fraction by semipreparative TLC (the first purification with light petroleum/diethyl ether 9:1 v/v as mobile phase, and the second one with benzene) led to the isolation of compound **1** (6.7 mg). Compounds **3** (40.6 mg) and **4** (5.1 mg) were isolated from fraction 6 by semipreparative TLC purification (light petroleum/diethyl ether 3:7 v/v as eluant) and structurally characterized. They resulted to be 14-hydroxy derivatives of **1** and **2**, respectively.

7.3. Structural characterization

The structural elucidation of compounds **1-4** was performed on the basis of the analysis of the mono- and bidimensional NMR experiments (^{1}H NMR, ^{13}C NMR, ^{1}H-^{1}H COSY, NOE, HSQC, HMBC) and by comparing the recorded data with those reported in the literature for related compounds (Burke *et al.* 1981; Ghisalberti *et al.* 1985; Choi *et al.* 1986; Moura *et al*. 1990; Xu *et al.* 1998). Because of the extreme instability in solution of compounds **1-4**, it was necessary to purify repeatedly aliquots from the crude extract.

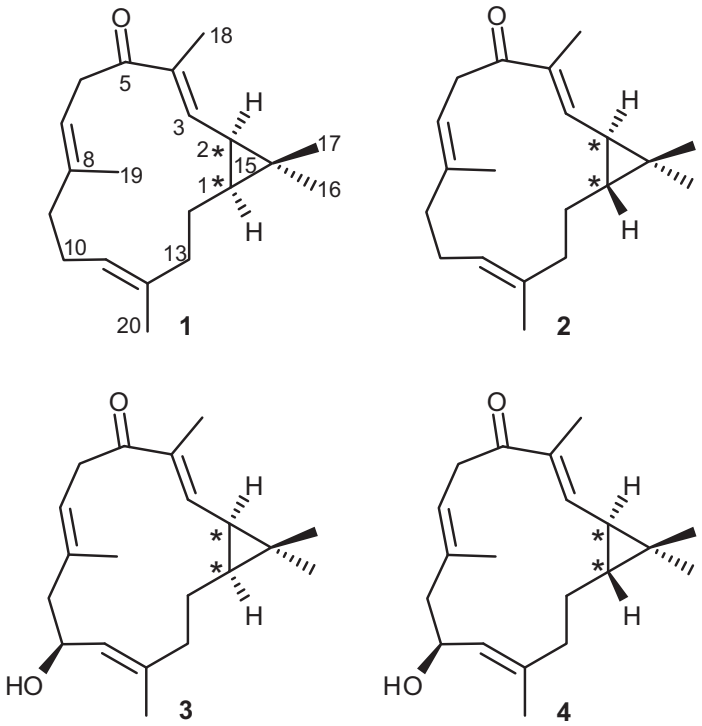

Fig. 7.5. Structures of compounds **1-4**.

From a structural point of view, compounds **1-4** belong to the casbane family, a group of diterpenes extremely rare in nature and characterized by a bicyclic structure composed by a cyclopropyl ring fused with a 14-membered macrocycle. In Fig. 7.6 the structure of casbene is reported. A preliminary ^{1}H NMR analysis showed that all the molecules shared the same carbon skeleton differing from each other in either the presence of a hydroxy group or the configuration of some chiral centers. The ^{1}H NMR experiments, therefore, highlighted the terpenoid

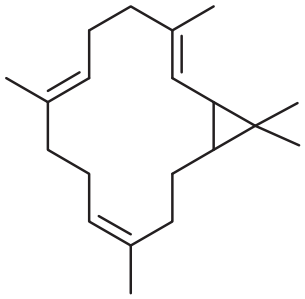

Fig. 7.6. Casbene.

nature of compounds **1**-**4** and the strong structural analogies among them. The ^{1}H NMR spectra were characterized by the presence of three olefinic protons and five methyls, of which three on double bonds, for all the four compounds. Compound **3** was the first to be analyzed because it resulted to be the most abundant component of the casbene fraction (40.6 mg). The molecular formula of **3** was deduced by both EI-HRMS and ^{13}C NMR analysis (Fig. 7.7). The molecular peak at *m*/*z* 302.2240 was attributed to $C_{20}H_{30}O_2$, which required 6 degrees of unsaturation. The ^{13}C NMR spectrum, along with the DEPT sequence, showed 20 carbon signals, including one carbonyl (δ 200.0) and six olefinic carbons, of which three methine and three quaternary groups (δ 142.9, 127.8, 120.5, and δ 140.8, 136.2, 134.5, respectively), one oxygenated methine (δ 67.5) and twelve aliphatic carbons (five methyl, four methylene, two methine and one quaternary). These data allowed assigning four of the six degrees of unsaturation, indicated by the molecular formula, to one keto function (confirmed in the IR spectrum by the presence of an intense absorption band at ν_{max} 1650 cm^{-1}, diagnostic for one α-β unsaturated ketone) and three double bonds. The absence of cross peaks between the vinylic protons in the homonuclear correlation ^{1}H-^{1}H COSY indicated that the three double bonds were trisubstituted. In particular, the ^{1}H NMR chemical shift of one of them at δ 6.30 (Fig. 7.8), along with the corresponding carbon at δ 142.9, confirmed the β-position of this olefinic proton with respect to the carbonyl function. The remaining two unsaturations were hypothesized to be satisfied by a bicyclic structure.

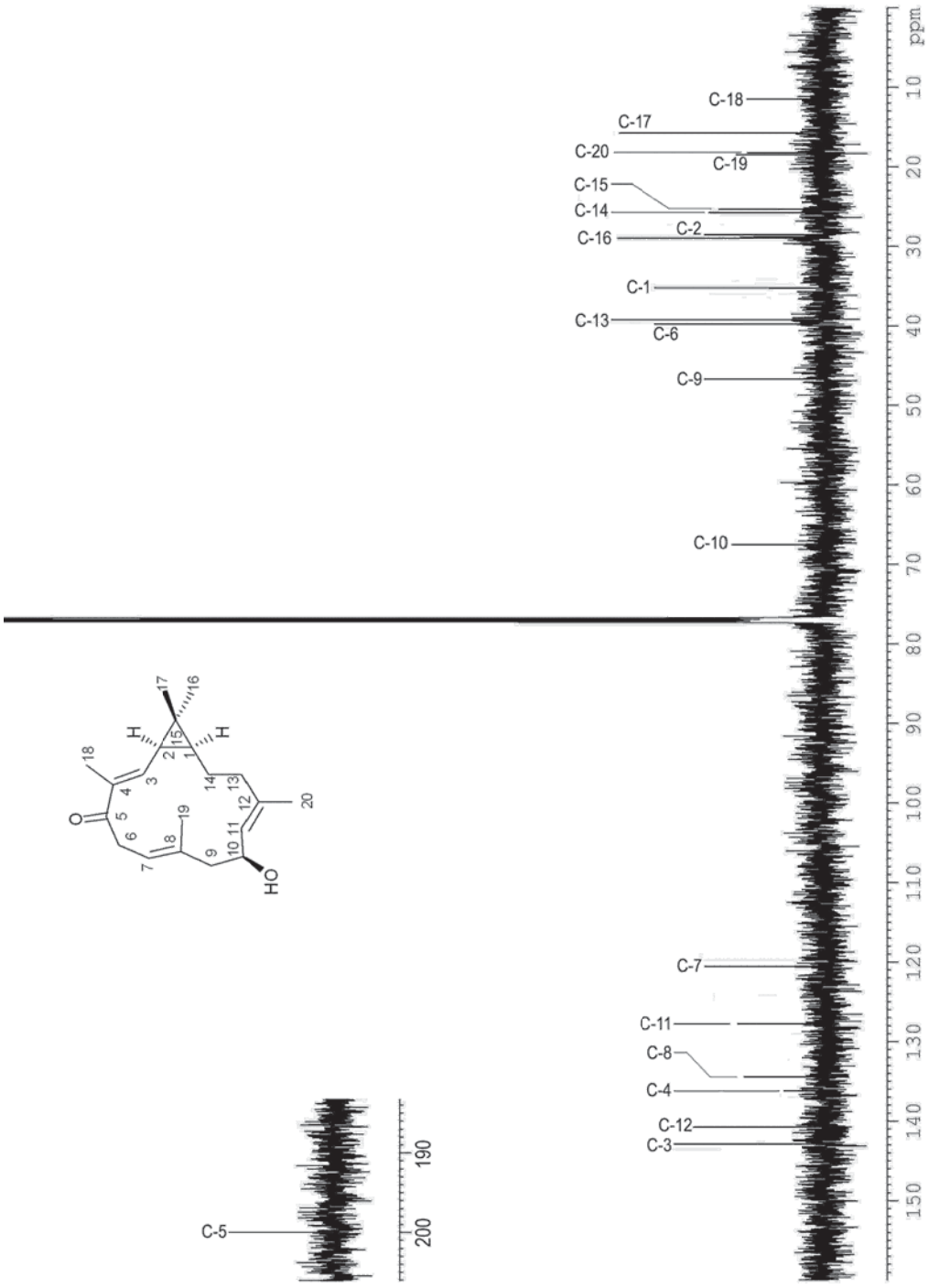

Fig. 7.7. ^{13}C NMR spectrum of compound **3**.

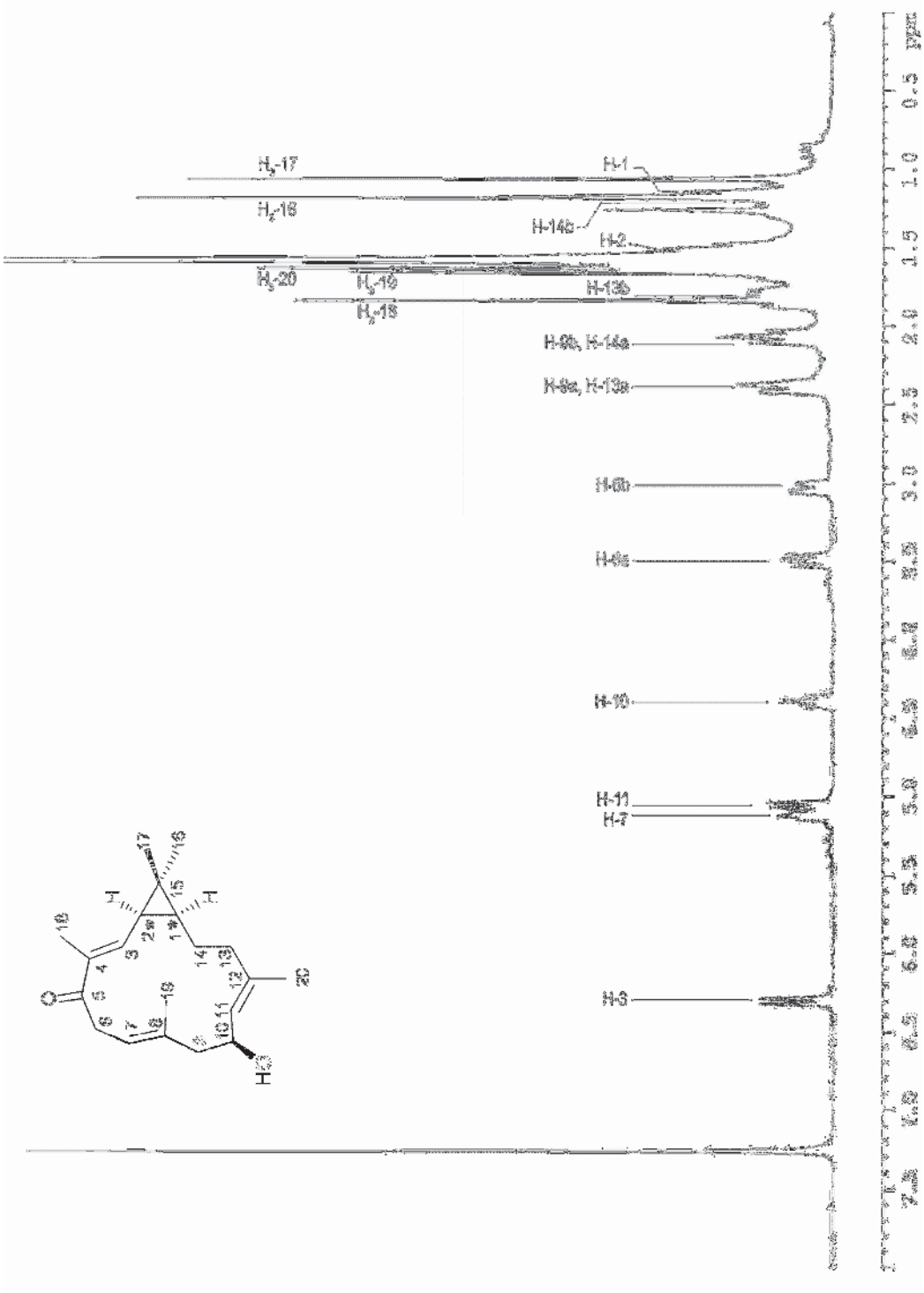

Fig. 7.8. ^{1}H NMR spectrum of compound **3**.

The direct ^{13}C-^{1}H correlations by their ^{1}J were established on the basis of the HSQC data (Fig. 7.9). The nature of the two cycles was, on the other hand, suggested by the presence in the ^{13}C NMR and ^{1}H NMR spectra of typical signals of a cyclopropyl ring (δ_C 35.2, 28.6, 25.3, and δ_H 1.50, 1.15) bearing two geminal methyls (δ_C 29.0, 15.7, and δ_H 1.18, 1.06), as indicated by HMBC analysis (Fig. 7.10). As a consequence, the remaining part of the structure was ascribed to a 14-membered macrocycle. These structural data resulted to be coherent with a casbane-type diterpenoid skeleton. In addition, the IR spectrum of **3** indicated the presence of a hydroxy group (ν_{max} 3388 cm^{-1}) which, along with the carbonyl group, accounted for the two oxygen atoms of the molecular formula. The analysis of the homonuclear correlation ^{1}H-^{1}H COSY (Fig. 7.11) allowed distinguishing three different *spin* systems corresponding to the partial structures **a-c** (Fig. 7.12). The partial structure **a** was described by the *spin* system characterized by the vinylic proton at δ 6.30 (1H, *d*, *J* = 10.5 Hz, H-3) which resulted to have an allylic correlation with the methyl at δ 1.83 (3H, *s*, H_3-18), and a correlation with the methine at δ 1.50 (1H, *dd*, *J* = 10.2, 8.4 Hz, H-2). This proton was coupled to another methine at δ 1.15 (1H, *m*, H-1), which was in turn correlated with the methylene at δ 2.07 (1H, *m*, H-14a) and δ 1.19 (1H, *m*, H-14b). Finally, the methylene H_2-14 was correlated with the methylene protons at δ 2.38 (1H, *m*, H-13a) and δ 1.80 (1H, *m*, H-13b).

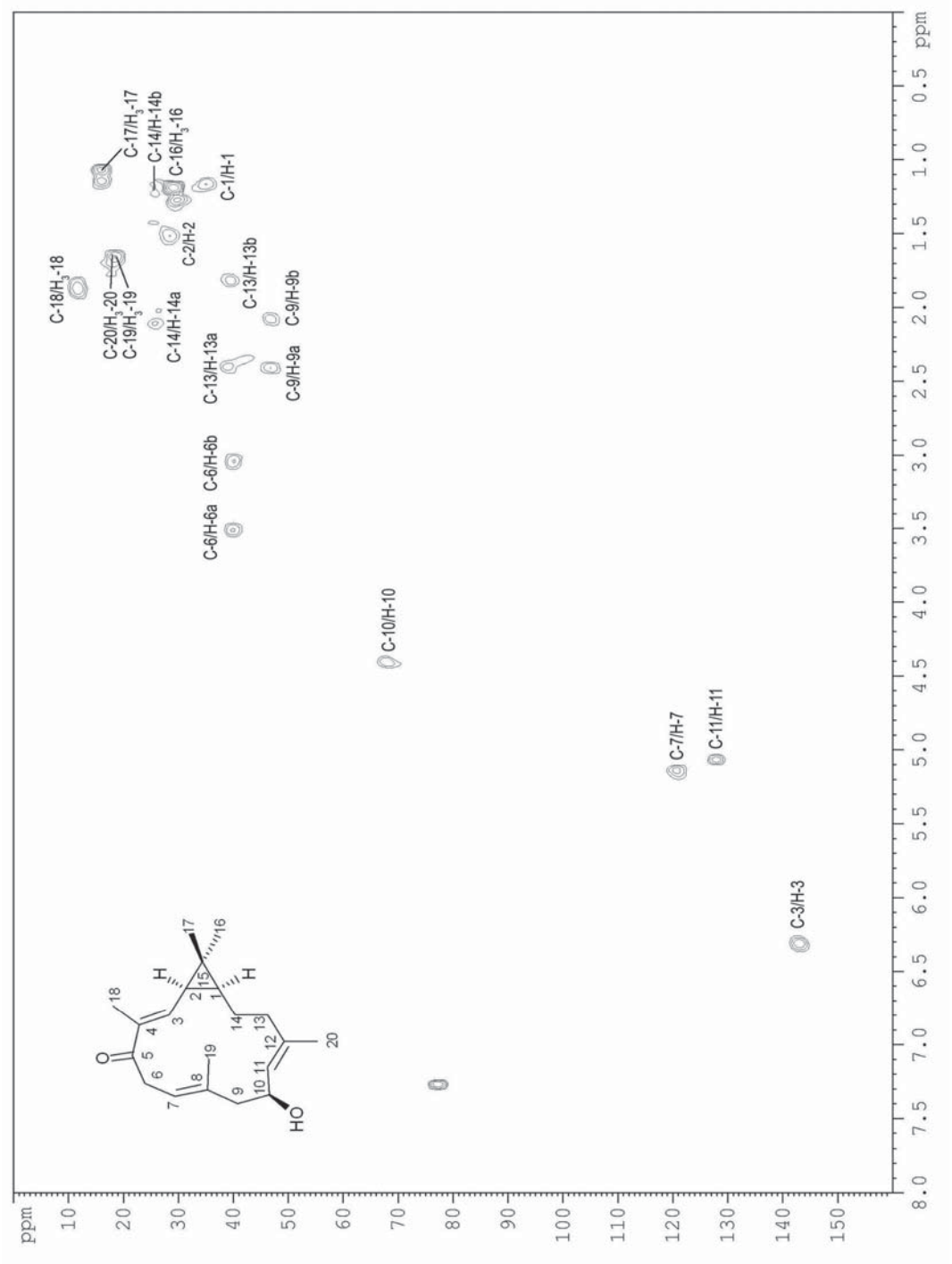

Fig. 7.9. HSQC spectrum of compound **3**.

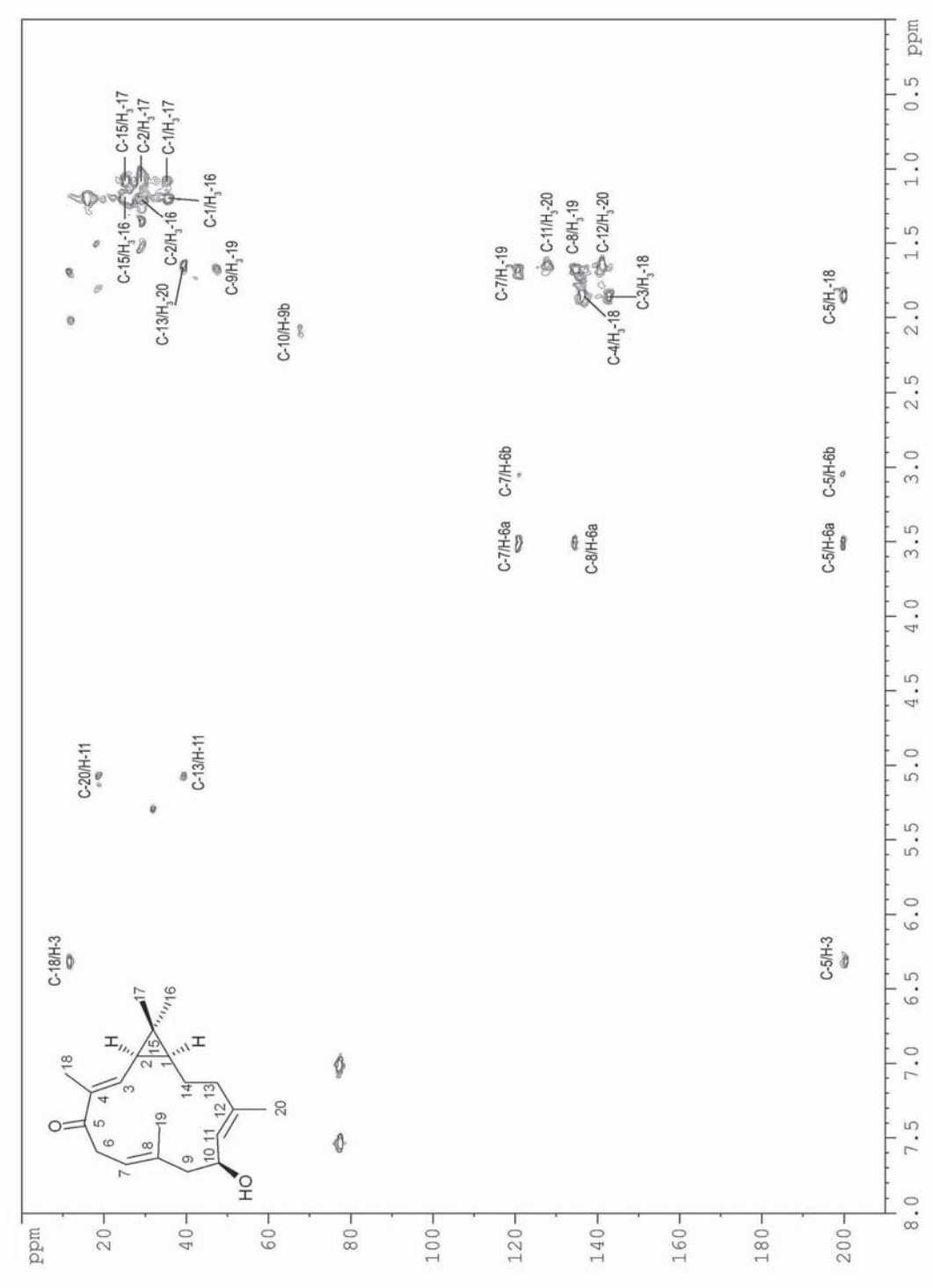

Fig. 7.10. Significant long-range correlations in the HMBC spectrum of compound **3**.

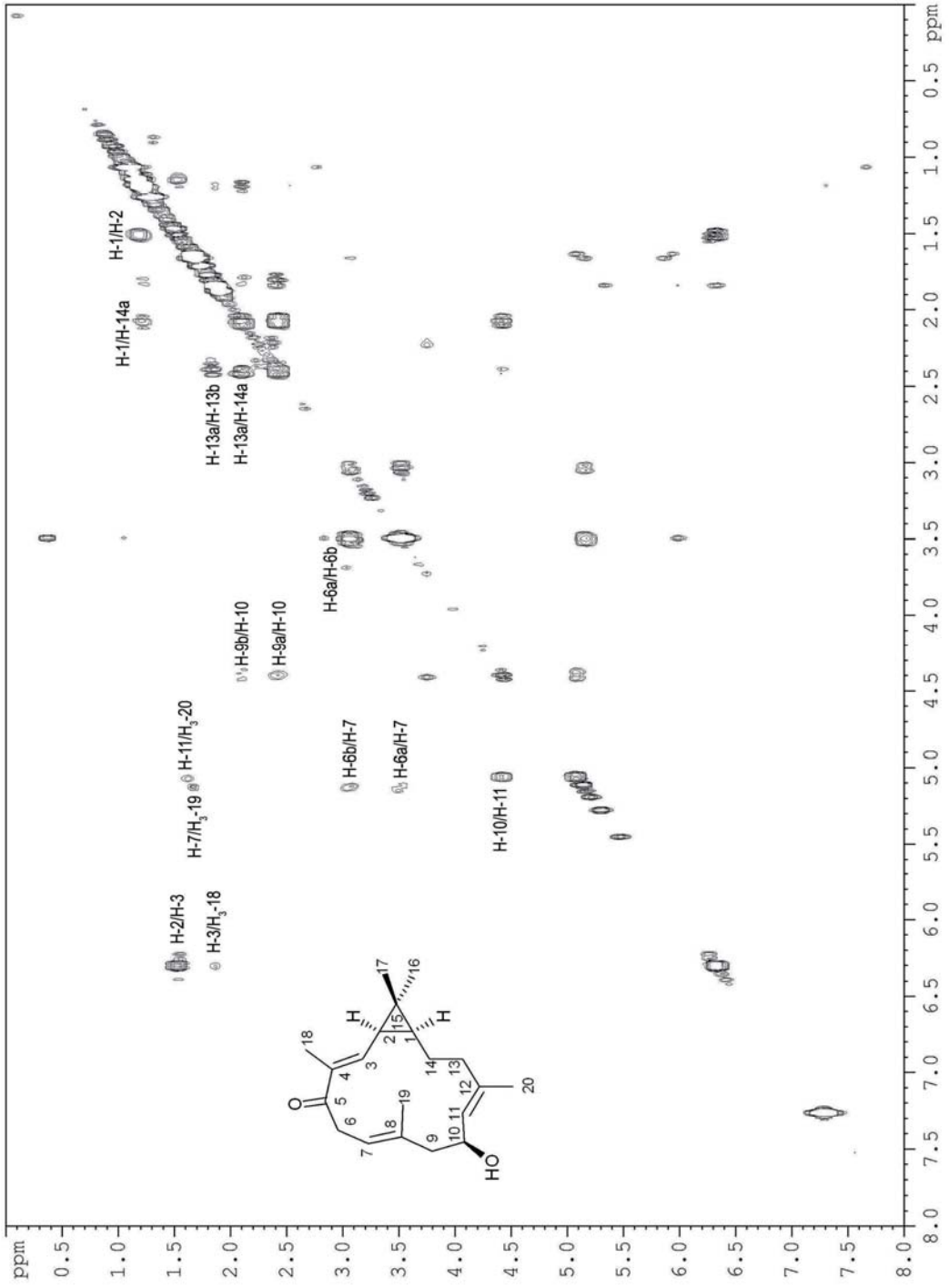

Fig. 7.11. Significant ^{1}H-^{1}H correlations in the COSY spectrum of compound **3**.

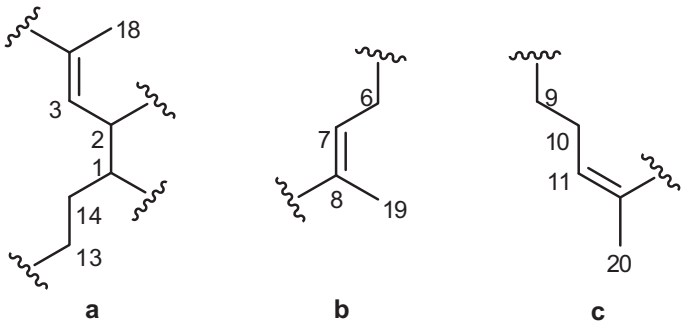

Fig. 7.12. Partial structures of the casbene skeleton of **3** deduced by ^{1}H-^{1}H COSY.

The *spin* system composed by the vinylic proton at δ 5.11 (1H, *t*, *J* = 6.6 Hz, H-7) and correlated with both the methyl at δ 1.66 (3H, *s*, H$_3$-19, allylic correlation) and the methylene at δ 3.50 (1H, *dd*, *J* = 13.8, 8.4 Hz, H-6a) and δ 3.02 (1H, *dd*, *J* = 13.8, 5.7 Hz, H-6b), which did not show further correlations, enabled to assign the partial structure **b**. Finally, the partial structure **c** was defined by the *spin* sequence observed in the ^{1}H-^{1}H COSY spectrum and characterized by the vinylic proton at δ 5.06 (1H, *d*, *J* = 9.3 Hz, H-11) correlated with both the methyl at δ 1.63 (3H, *s*, H$_3$-20, allylic correlation) and the carbinolic proton at δ 4.38 (1H, *td*, *J* = 9.3, 3.9 Hz, H-10). This latter proton was correlated with the methylene at δ 2.39 (1H, *m*, H-9a) and δ 2.07 (1H, *m*, H-9b). The analysis of the HMBC data of **3** enabled to place the quaternary carbons and connect the partial structures **a**-**c**, as resulted in the formula of **3**. Significant correlation peaks were observed between the carbonyl at δ 200.0 (C-5) and the protons H-3 (δ 6.30) and H$_2$-6 (δ 3.50 and 3.02), between the carbon at δ 39.2 (C-13) and the vinylic proton H-11 (δ 5.06), and finally between the quaternary carbon at

δ 134.5 (C-8) and one of the methylene protons H_2-9 at δ 2.07 (1H, *m*, H-9b), as reported in Table 7.2. The analysis of the mono- and bidimensional NMR spectra of **3** enabled the assignment of all the ^1H and ^{13}C resonances.

C	δ ^{13}C	mult.	δ ^1H	mult., $J_{H\text{-}H}$ (Hz)	Significant long range correlations (HMBC)
1	35.2	*d*	1.15	*m*	H_3-16, H_3-17
2	28.6	*d*	1.50	*dd*, 10.2, 8.4	H_3-16, H_3-17
3	142.9	*d*	6.30	*d*, 10.5	H_3-18
4	136.2	*s*	-	-	H_3-18
5	200.0	*s*	-	-	H-3, H_2-6, H_3-18
6	39.8	*t*	a 3.50	*dd*, 13.8, 8.4	
			b 3.02	*dd*, 13.8, 5.7	
7	120.5	*d*	5.11	*t*, 6.6	H_2-6, H-9b, H_3-19
8	134.5	*s*	-	-	H-6a, H_3-19
9	46.7	*t*	a 2.39	*m*	H_2-6, H_3-19
			b 2.07	*m*	
10	67.5	*d*	4.38	*td*, 9.3, 3.9	H-9b
11	127.8	*d*	5.06	*d*, 9.3	H_3-20
12	140.8	*s*	-	-	H_3-20
13	39.2	*t*	a 2.38	*m*	H-11, H_3-20
			b 1.80	*m*	
14	25.8	*t*	a 2.07	*m*	
			b 1.19	*m*	
15	25.3	*s*	-	-	H_3-16, H_3-17
16	29.0	*q*	1.18	*s*	
17	15.7	*q*	1.06	*s*	
18	11.5	*q*	1.83	*s*	H-3
19	18.5	*q*	1.66	*s*	
20	18.3	*q*	1.63	*s*	

Table 7.2. ^1H NMR and ^{13}C NMR data of **3**.

The *E* geometry of the three double bonds of the molecule was initially suggested by the δ_C values of the methyl carbons CH_3-18, CH_3-19 and CH_3-20 (< 20 ppm). Such a

structural hypothesis was confirmed later by the results of NOE experiments. Significant n.O.e. effects were, in fact, observed between the methylene H_2-6 and the methyl H_3-19, the methylene H_2-9 and the methyl H_3-20, and the proton H-2 and the methyl H_3-18. The junction of the two rings at carbons C-1/C-2 was suggested to be *cis* on the basis of the resonance values of the geminal methyl carbons CH_3-16 (δ 29.0) and CH_3-17 (δ 15.7), and by both comparison with similar *cis*-fused casbane diterpene structures reported in the literature (Ghisalberti *et al.* 1985; Choi *et al.* 1986, 1988; Xu *et al.* 1998) and a diagnostic n.O.e. interaction H-1/H-2. The absolute configuration at C-10 of compound **3** was assigned by applying the modified Mosher's method (Sullivan *et al.* 1973), a method for assigning the absolute stereochemistry of secondary amines and alcohols by employing a chiral derivatizing reagent (CDA), *e.g.* α-methoxy-α-trifluoromethylphenylacetic acid (MTPA). All the NMR-based methods for the determination of the absolute configuration require the conversion of the chiral substrate into two different species (diastereomers) showing slight differences of their chemical and physical properties, which can be differentiated by NMR spectroscopy. This is achieved by derivatization of the substrate with the CDA, followed by comparison of the ^{1}H NMR spectra of these two species to correlate the absolute stereochemistry of the chiral center of the reagent (known configuration) with that of the substrate (unknown configuration) (Seco *et al.* 2004). The Mosher's method is based on the anisotropic effect that the phenyl group of the CDA (MTPA) exerts on the substituents (L_1/L_2) of the alcohol. Such an effect allows making a

correlation, regarding the spatial position of L_1 and L_2, with respect to the phenyl group of the MTPA moiety on the basis of the signs of $\Delta\delta^{SR}$ of the substituents. Mosher assumed that the most representative conformation is that in which both the carbonyl group and CF_3 of MTPA are situated in the same plane. Accordingly, the protons of the substituent L_2 are shielded by the phenyl ring in the (*R*)-MTPA ester, whereas those on L_1 remain unaffected. On the other hand, in the (*S*)-MTPA ester L_1 and its protons are shielded, while L_2 is unaffected. Therefore, the substituent L_1 is more shielded in the (*S*)-MTPA ester than in the (*R*)-MTPA ester, and the substituent L_2 is more shielded in the (*R*)-MTPA ester than in the (*S*)-MTPA ester. These shieldings are expressed by $\Delta\delta^{SR}$, defined as the difference between the chemical shift of a certain proton in the (*S*)-MTPA ester and the chemical shift of the same proton in the (*R*)-MTPA ester. All the protons shielded in the (*R*)-MTPA show a positive $\Delta\delta^{SR}$ value, while those shielded in the (*S*)-MTPA derivative present a negative $\Delta\delta^{SR}$ value. In our study, pure compound **3** was derivatized with (*R*)- and (*S*)-MTPA chloride, affording the corresponding *S* and *R* diastereomers (Mosher's esters, Fig. 7.13) which, after work-up, were analyzed by NMR spectroscopy in order to assign all the protons and compare their chemical shifts. The evaluation of the $\Delta\delta^{SR}$ values showed the absolute stereochemistry *S* at C-10. Since the chiral centre C-10 could not be correlated with the other two chiral carbons, C-2 and C-1, the absolute configuration of the whole molecule was not defined. Actually, X-ray crystallographic analysis is in

progress in order to complete the stereochemical study and determine the absolute stereochemistry of all the chiral carbons.

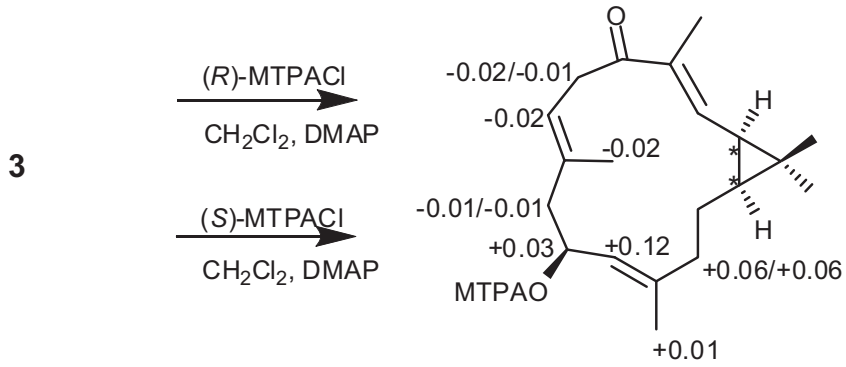

Fig. 7.13. Δδ (δ*S* – δ*R*) values (in ppm) for the MTPA esters of **3**.

Once compound **3** was characterized, the structures of metabolites **1**, **2** and **4** were easily deduced by comparison. In ESI-HRMS of **4**, the presence of a molecular peak $[M + Na]^+$ at *m*/*z* 325.2140 corresponding to $C_{20}H_{30}O_2Na$, the same molecular formula of **3**, and the close analogies observed between the ^1H NMR spectra of **3** and **4** suggested the stereochemical relationship between the two compounds. Initially, a different geometry of the double bonds was supposed, but such a hypothesis was rejected after the analysis of the ^{13}C NMR (Fig. 7.14) and DEPT spectra of **4**. In fact, the resonances of the carbons at α position with respect to the double bonds and, in particular, those of the methyls CH_3-20 (δ 14.8), CH_3-19 (δ 19.0) and CH_3-18 (δ 11.1), resulted to agree with the *E* geometry, analogously to those of the corresponding methyls in **3**.

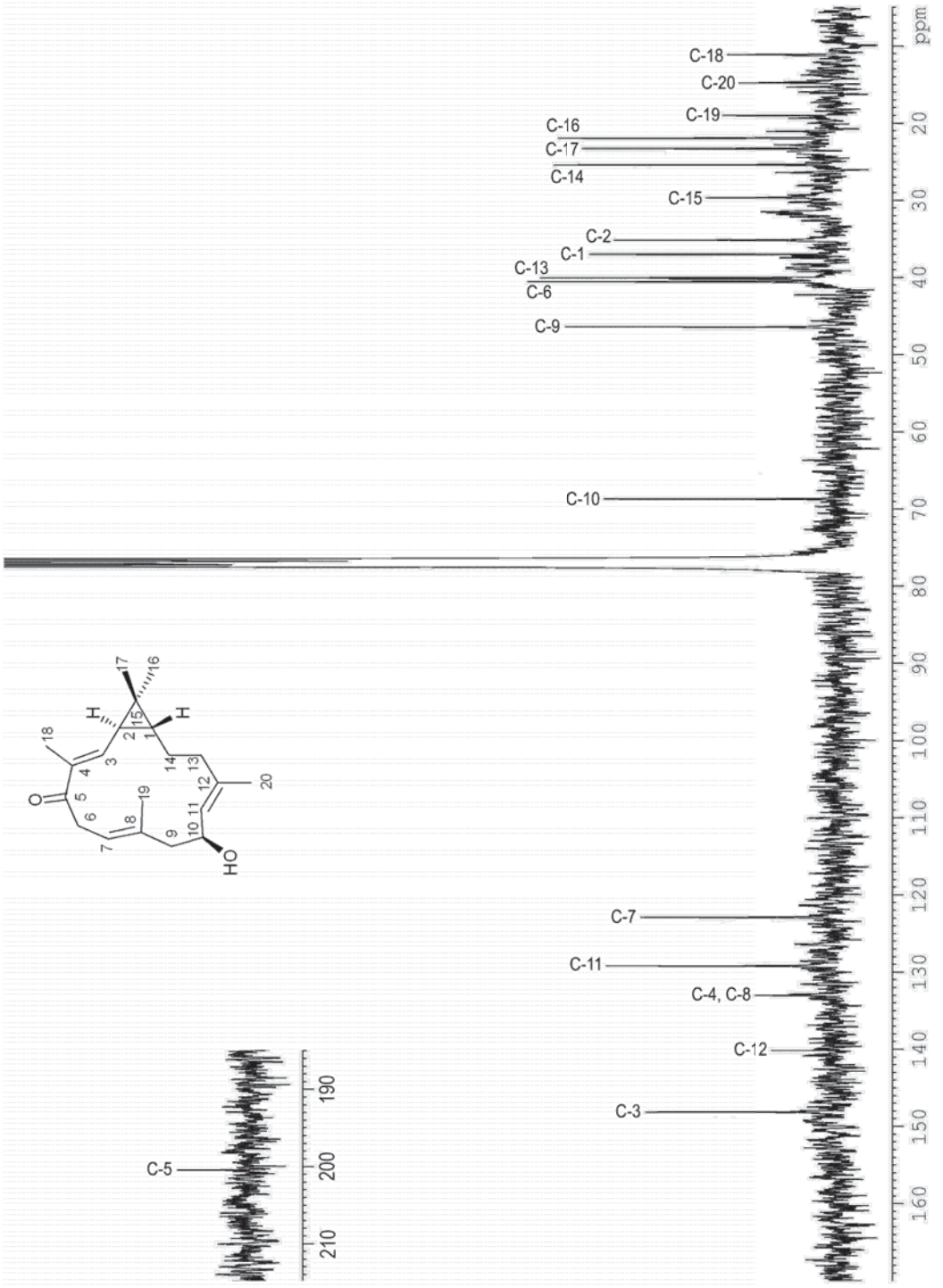

Fig. 7.14. ^{13}C NMR spectrum of compound **4**.

Thus, eliminating this possibility, the ring junction of the casbane skeleton was the only part of the molecule that could have a different stereochemistry. The results of the NOESY experiment and the comparison with some model structures reported in the literature (Ghisalberti *et al.* 1985; Xu *et al.* 1998) allowed us to establish that **4** exhibited the *trans* junction, as indicated by the diagnostic ^{13}C NMR values of the *gem*-methyls C-16 (δ_C 29.0 in **3** and 22.0 in **4**) and C-17 (δ_C 15.7 in **3** and 23.0 in **4**). This different spatial disposition of the two rings was responsible for some significant differences between **4** and **3** in the proton and carbon spectra. In the ^{1}H NMR spectrum of **4** (Fig. 7.15), in fact, the vinylic proton H-3 displayed a shift of 0.26 ppm with respect to the corresponding resonance value in the isomer **3** (δ 6.04 in **4** and δ 6.30 in **3**), as well as the differences observed about the protons H-2 (δ 1.03 in **4** and δ 1.50 in **3**) and H-1 (δ 0.57 in **4** and δ 1.15 in **3**). On the other hand, in the ^{13}C NMR spectrum the strongest differences were observed about the carbons C-3, C-2 and C-1, along with the resonances for the methyls CH_3-16 and CH_3-17, diagnostic for a *trans* junction and not so different between them as those of the isomer *cis* (**3**). All the carbon and proton resonances of **4** were assigned by analyzing the mono- and bidimensional NMR spectra (Table 7.3).

The configuration at C-10 of **4** was determined by the modified Mosher's method with the same procedure followed for **3** (Fig. 7.16). The $\Delta\delta^{SR}$ recorded for the Mosher's esters allowed us to assign the configuration *S* to C-10 of **4**, the same of the corresponding carbon in **3**.

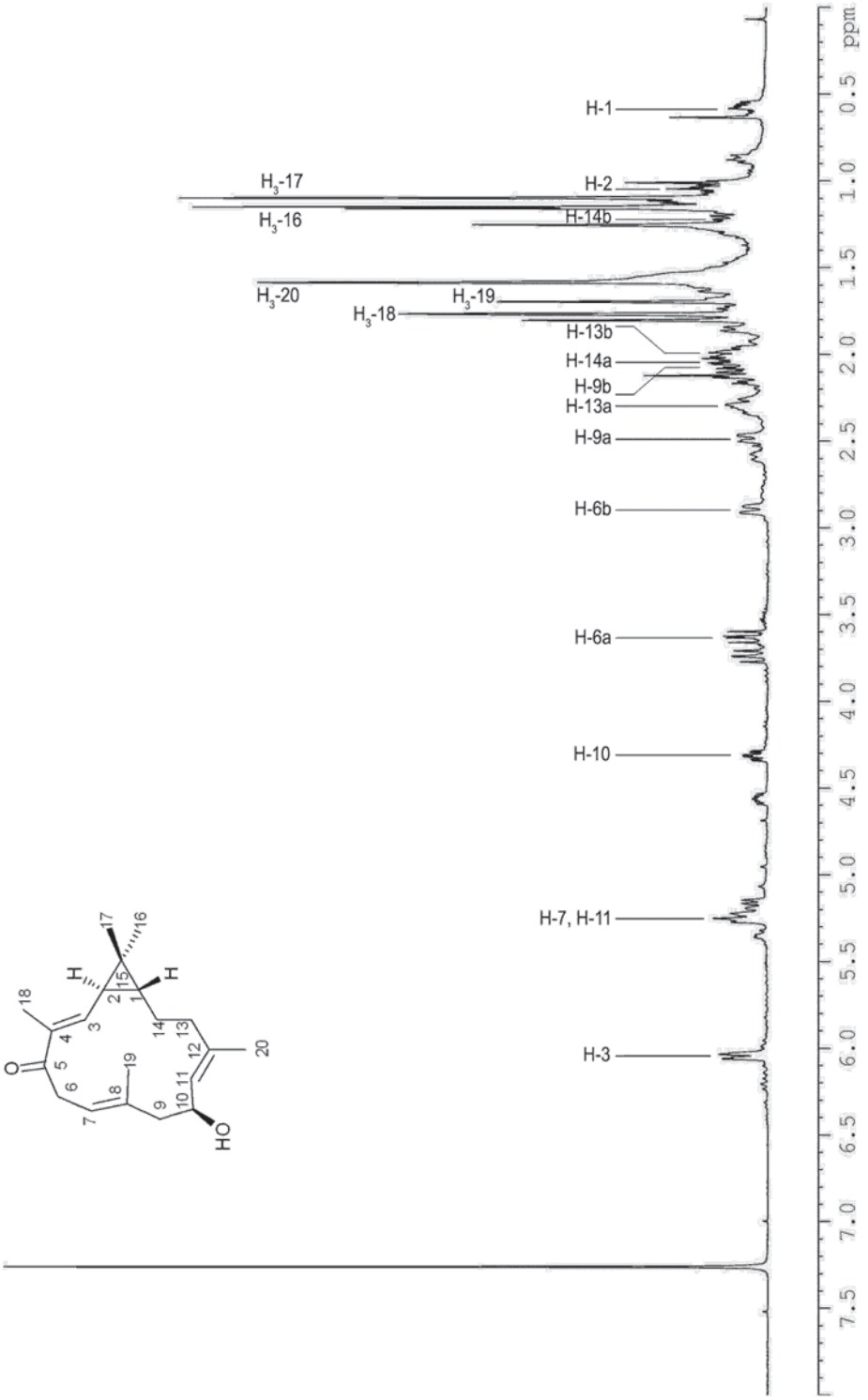

Fig. 7.15. ^{1}H NMR spectrum of compound **4**.

C	δ ^{13}C	mult.	δ ^{1}H	mult., J_{H-H} (Hz)	Significant long range correlations (HMBC)
1	37.0	*d*	0.57	*m*	H-3
2	35.2	*d*	1.03	*m*	
3	148.1	*d*	6.04	*d*, 10.2	
4	133.0	*s*	-	-	H_3-18
5	200.4	*s*	-	-	H-3, H-6a, H_3-18
6	40.6	*t*	a 3.63	*dd*, 14.3, 11.0	
			b 2.89	br *d*, 14.3	
7	122.9	*d*	5.27	overlapped	H-6a, H-9b, H_3-19
8	133.0	*s*	-	-	H-6a, H-9b, H_3-19
9	46.4	*t*	a 2.48	br *d*, 11.4	H-7, H_3-19
			b 2.06	*m*	
10	68.7	*d*	4.31	*td*, 9.6, 3.8	H-11, H_2-9
11	129.2	*d*	5.26	overlapped	H_3-20
12	140.1	*s*	-	-	H_3-20
13	40.1	*t*	a 2.33	*m*	H_3-20
			b 2.13	*m*	
14	25.4	*t*	a 1.99	*m*	
			b 1.27	*m*	
15	29.7	*s*	-	-	
16	22.0	*q*	1.15	*s*	
17	23.0	*q*	1.11	*s*	
18	11.1	*q*	1.77	*s*	H-3
19	19.0	*q*	1.71	*s*	
20	14.8	*q*	1.59	*s*	

Table 7.3 ^{1}H NMR and ^{13}C NMR data of **4**.

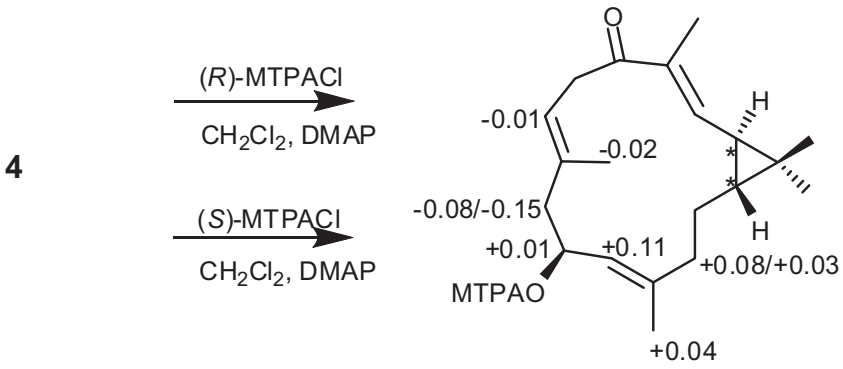

Fig. 7.16. Δδ (δ*S* – δ*R*) values (in ppm) for the MTPA esters of **4**.

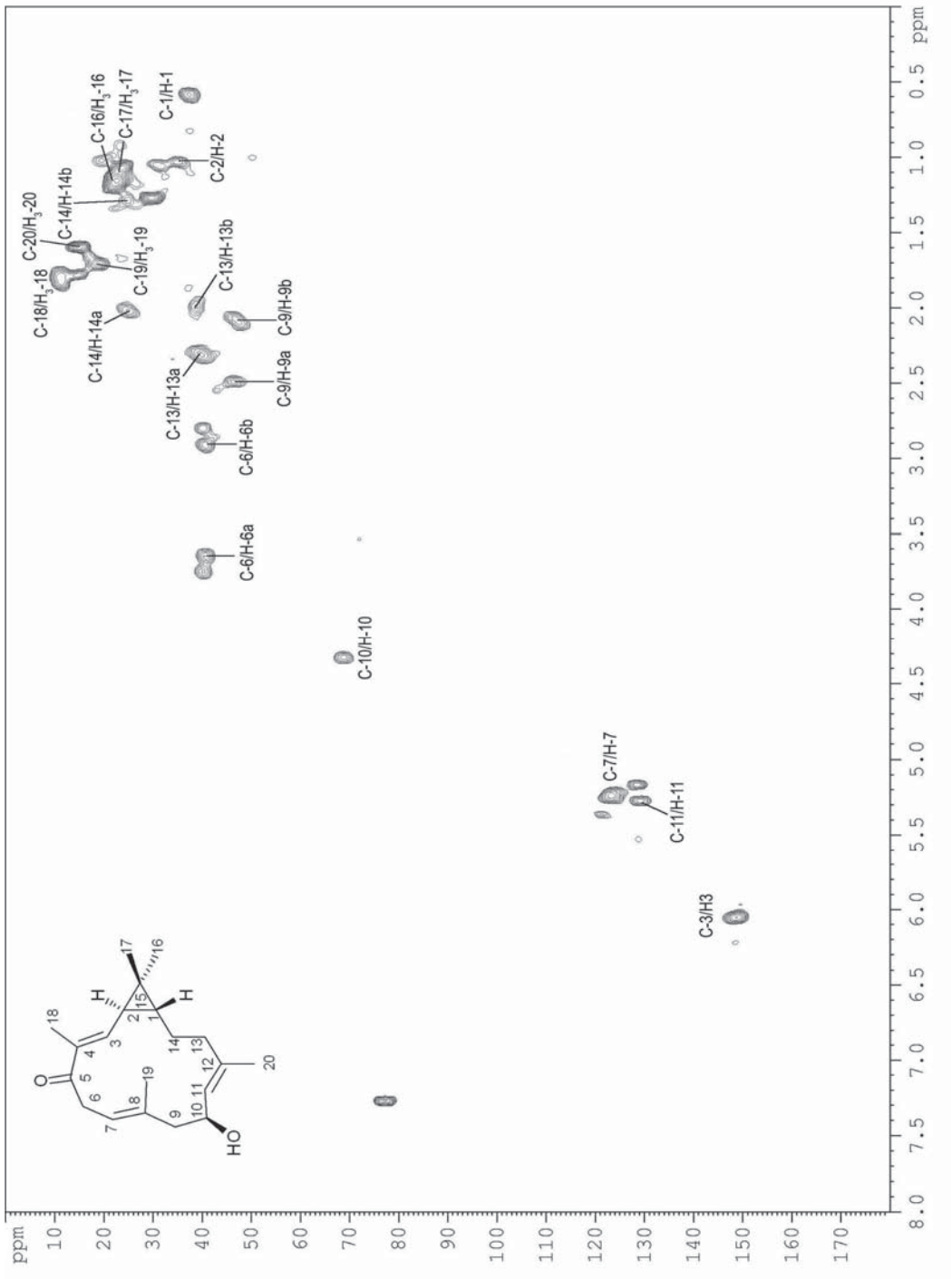

Fig. 7.17. HSQC spectrum of compound **4**.

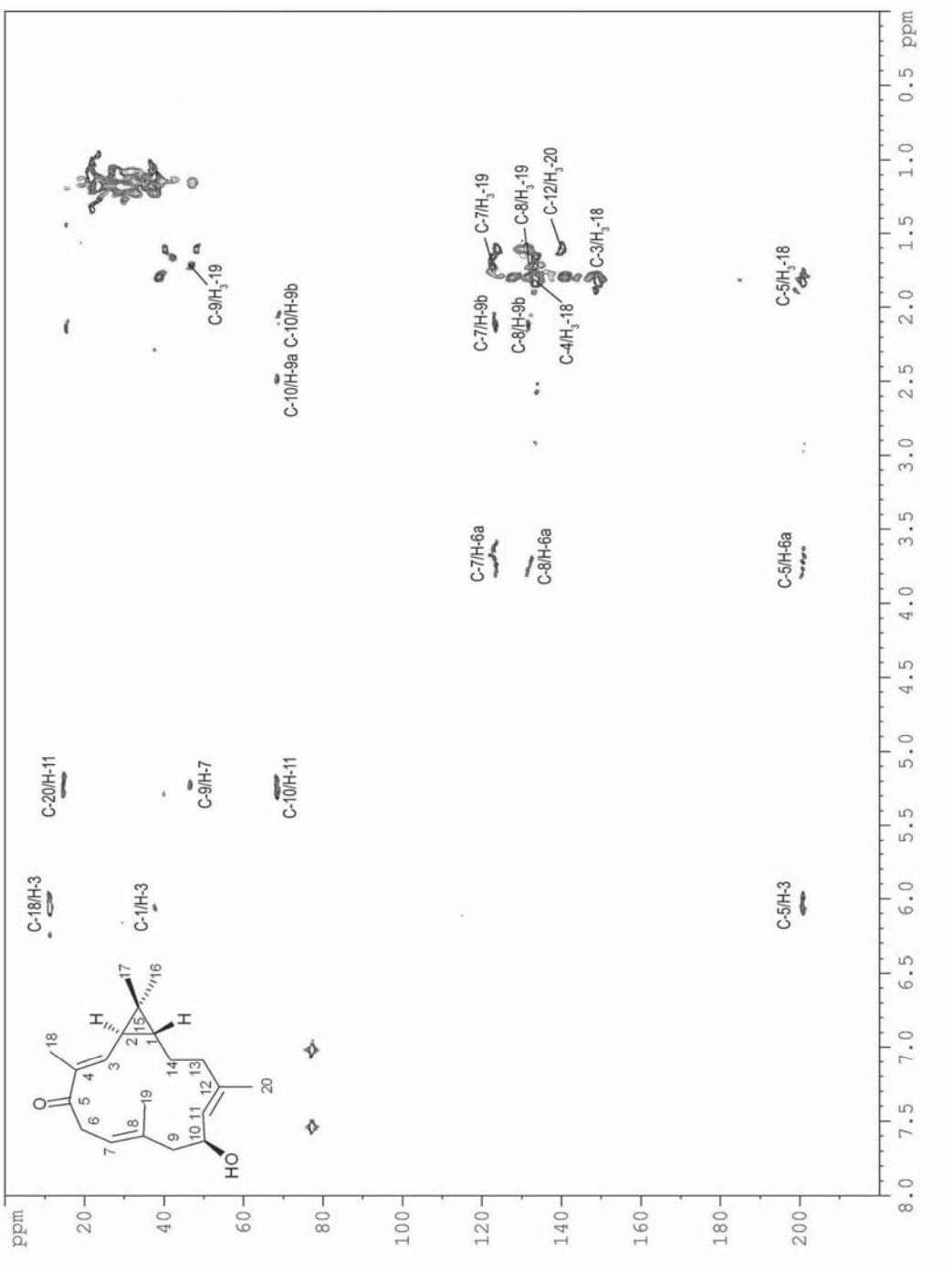

Fig. 7.18. Significant long-range correlations in the HMBC spectrum of compound **4**.

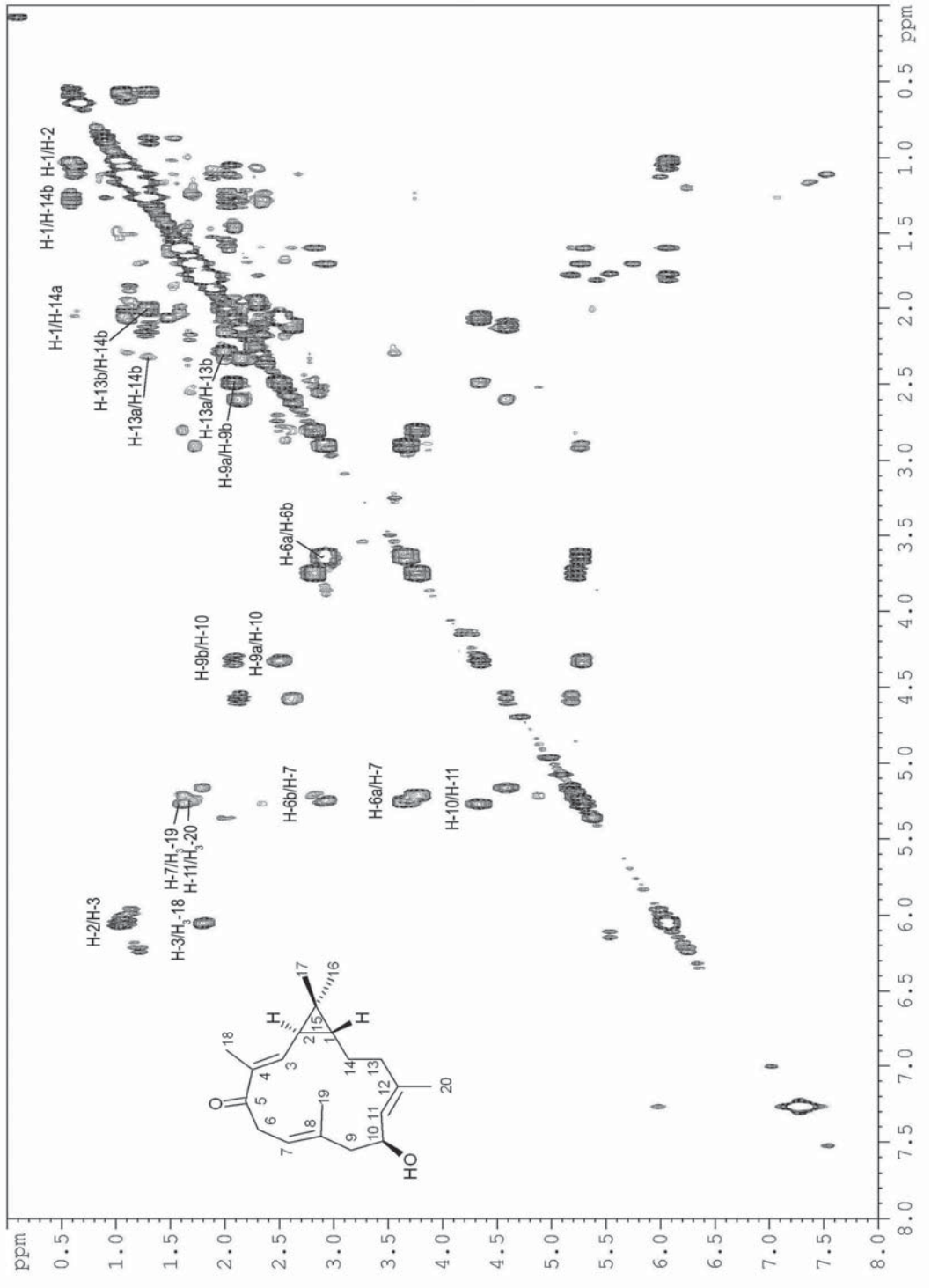

Fig. 7.19. Significant ^{1}H-^{1}H correlations in the COSY spectrum of compound **4**.

The analysis of the spectral data of **1** and **2** indicated that they were dehydroxylated derivatives of **3** and **4**, respectively. In fact, MS spectra of both **1** and **2** showed a molecular weight with 16 mass units less with respect to **3** and **4**. In particular, the molecular formula $C_{20}H_{30}O$ of **1** was deduced by the EI-HRMS molecular peak at *m*/*z* 286.2291. The main difference observed in the proton spectrum of **1** with respect to that of **3** was the absence of the signal of the carbinolic proton at δ 4.38, which was substituted by the multiplets at δ 2.17 and 1.96 of the allylic methylene protons at C-10 (Fig. 7.20). Analogously, in the ^{13}C NMR spectrum of **1** (Fig. 7.21) the signal at δ 67.5, corresponding to C-10 of **3**, was substituted by the signal at δ 23.9. The ^{13}C NMR spectrum of **1** and, in particular, the resonance values of the carbons of the three olefinic methyls, the methylenes CH_2-10, CH_2-13 and CH_2-9, as well as the two geminal methyls CH_3-16 and CH_3-17, indicated that **1** had the same *E* geometry of the double bonds of **3**, as well as the same *cis* ring junction. All the proton and carbon resonances were assigned for **1** by analyzing the mono- and bidimensional correlation spectra (Table 7.4).

Analogously, the ^{1}H NMR and ^{13}C NMR spectra of **2** revealed to be similar to those of compound **4**, indicating that the only structural difference between the two metabolites was the absence of the 10-hydroxy group in **2**. In the ^{1}H NMR spectrum, in fact, the signal at δ 4.31 of **4** was substituted by a methylene at δ 2.28 (*m*) and δ 2.07 (*m*), as well as in the ^{13}C NMR spectrum the most significant difference was observed for C-10 at δ 24.0 in **2** (CH_2) rather than at δ 68.7 in **4** (CH).

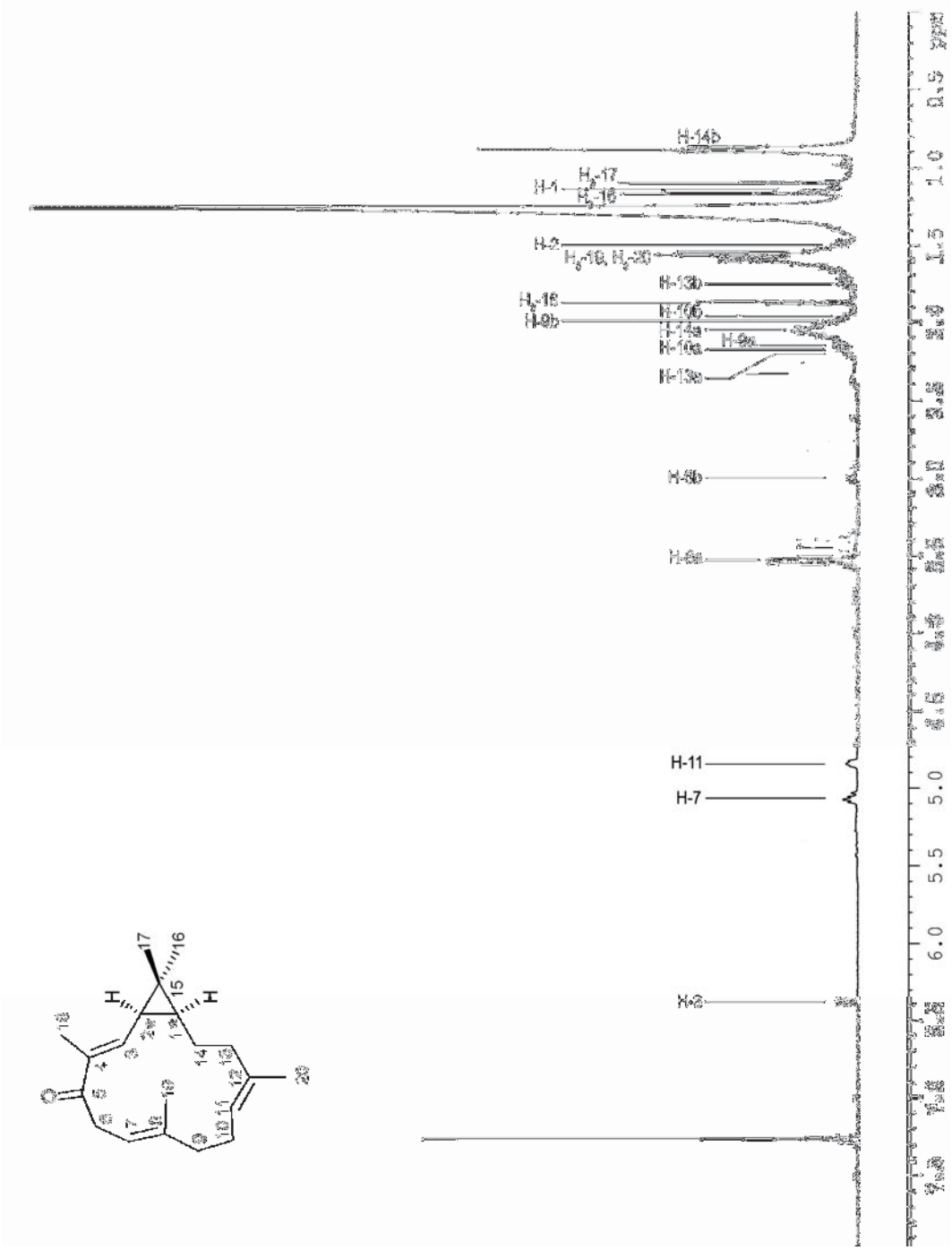

Fig. 7.20. ^{1}H NMR spectrum of compound **1**.

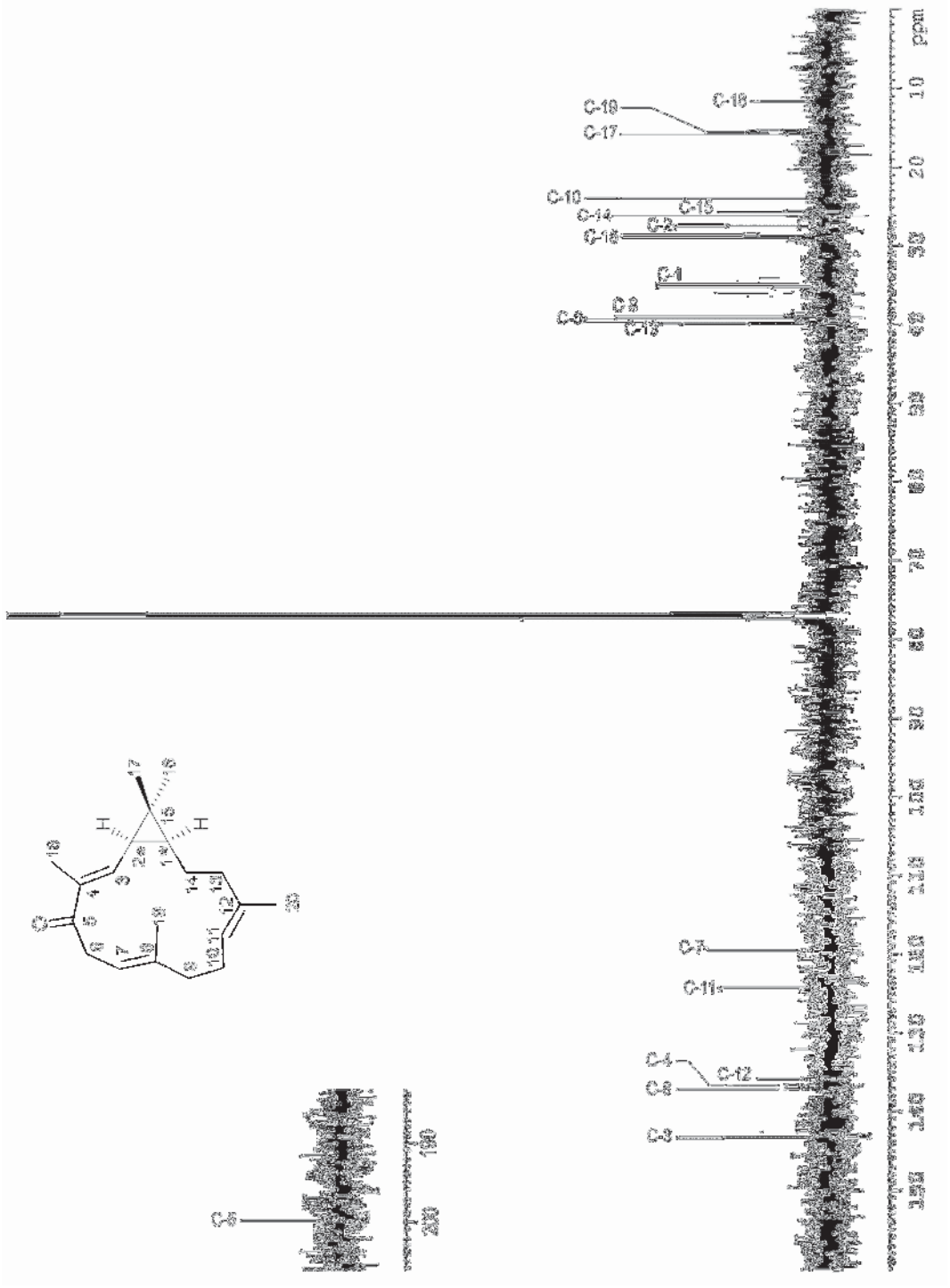

Fig. 7.21. ^{13}C NMR spectrum of compound **1**.

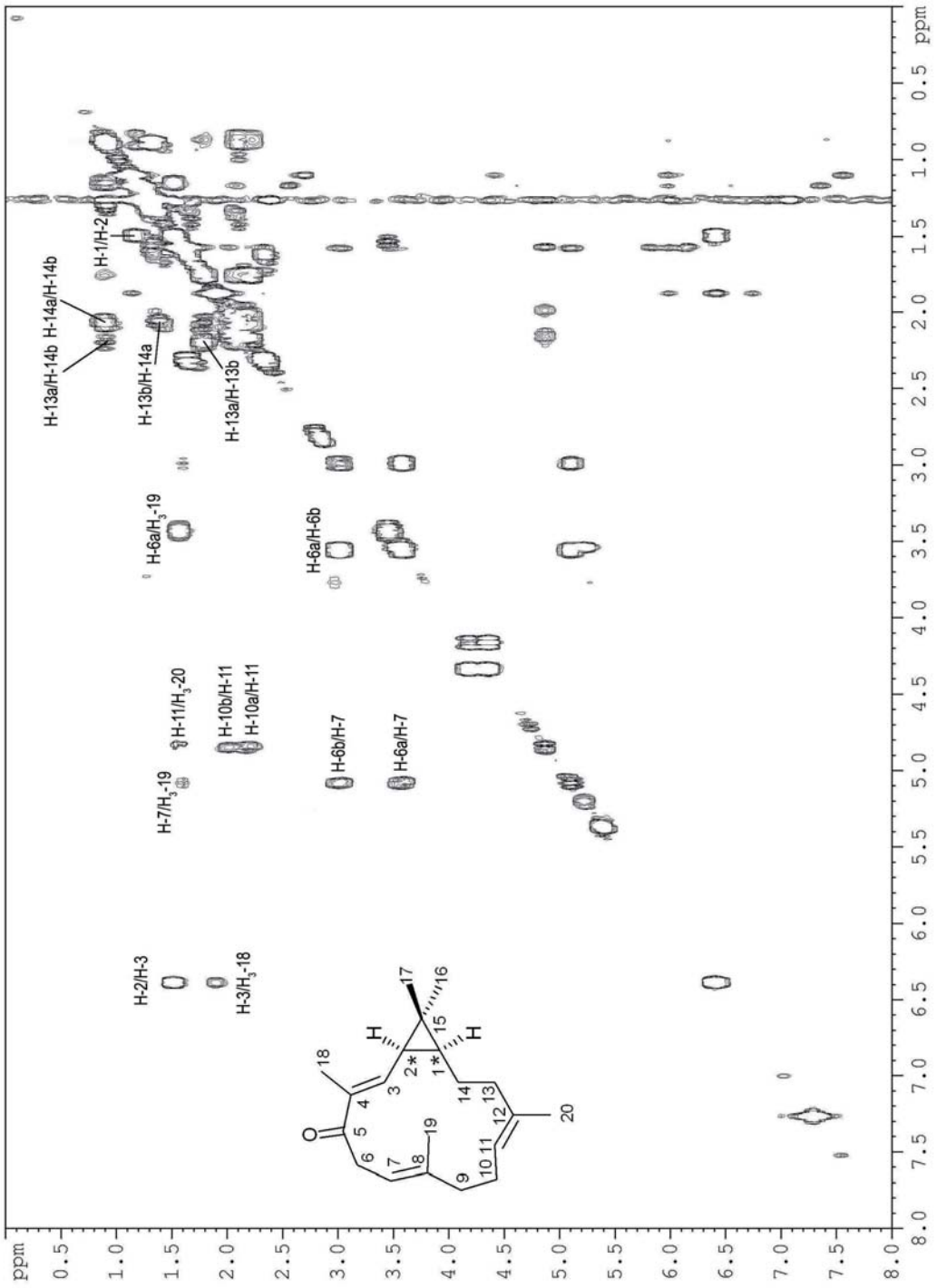

Fig. 7.22. Significant ^{1}H-^{1}H correlations in the COSY spectrum of compound **1**.

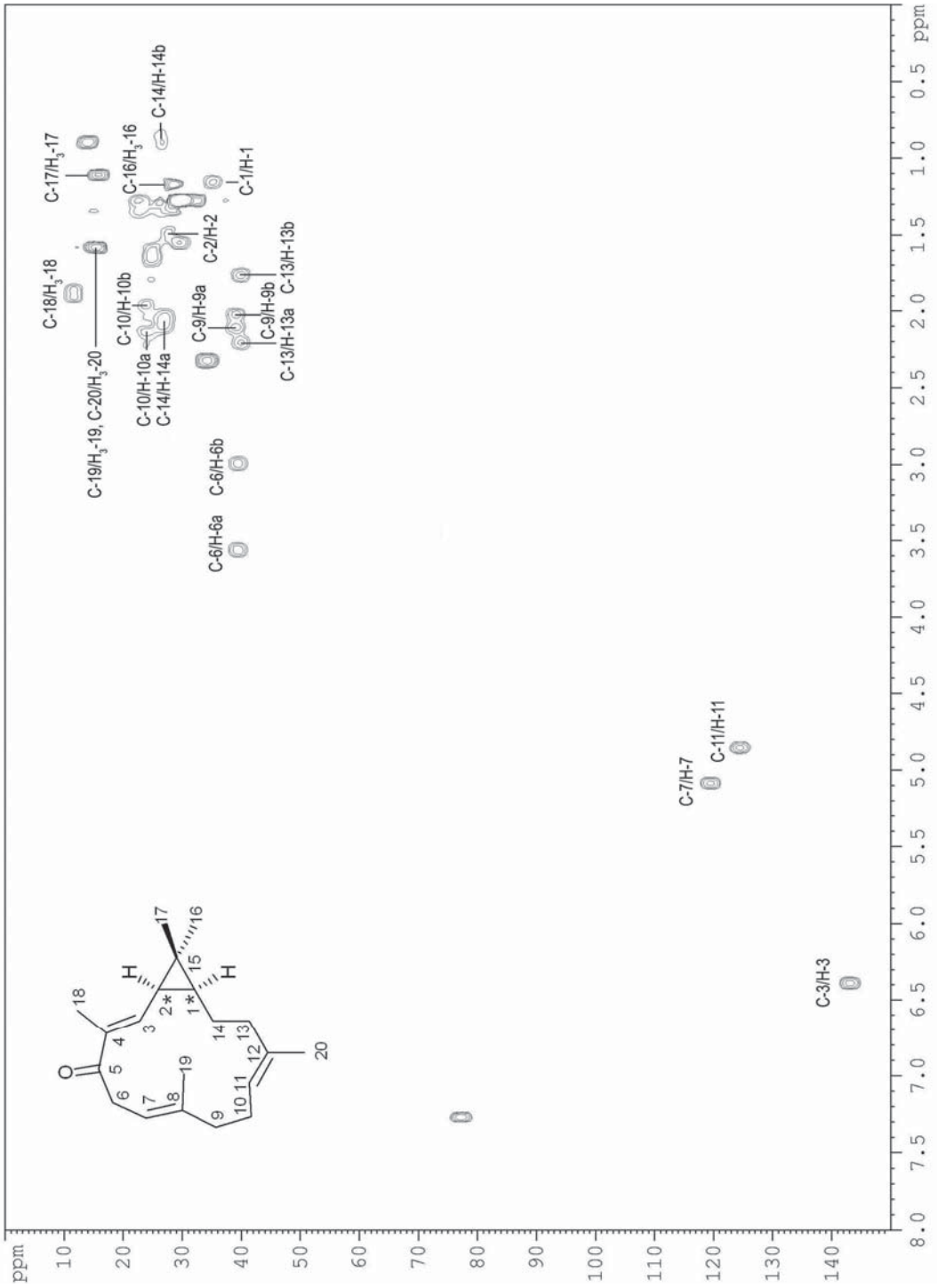

Fig. 7.23. HSQC spectrum of compound **1**.

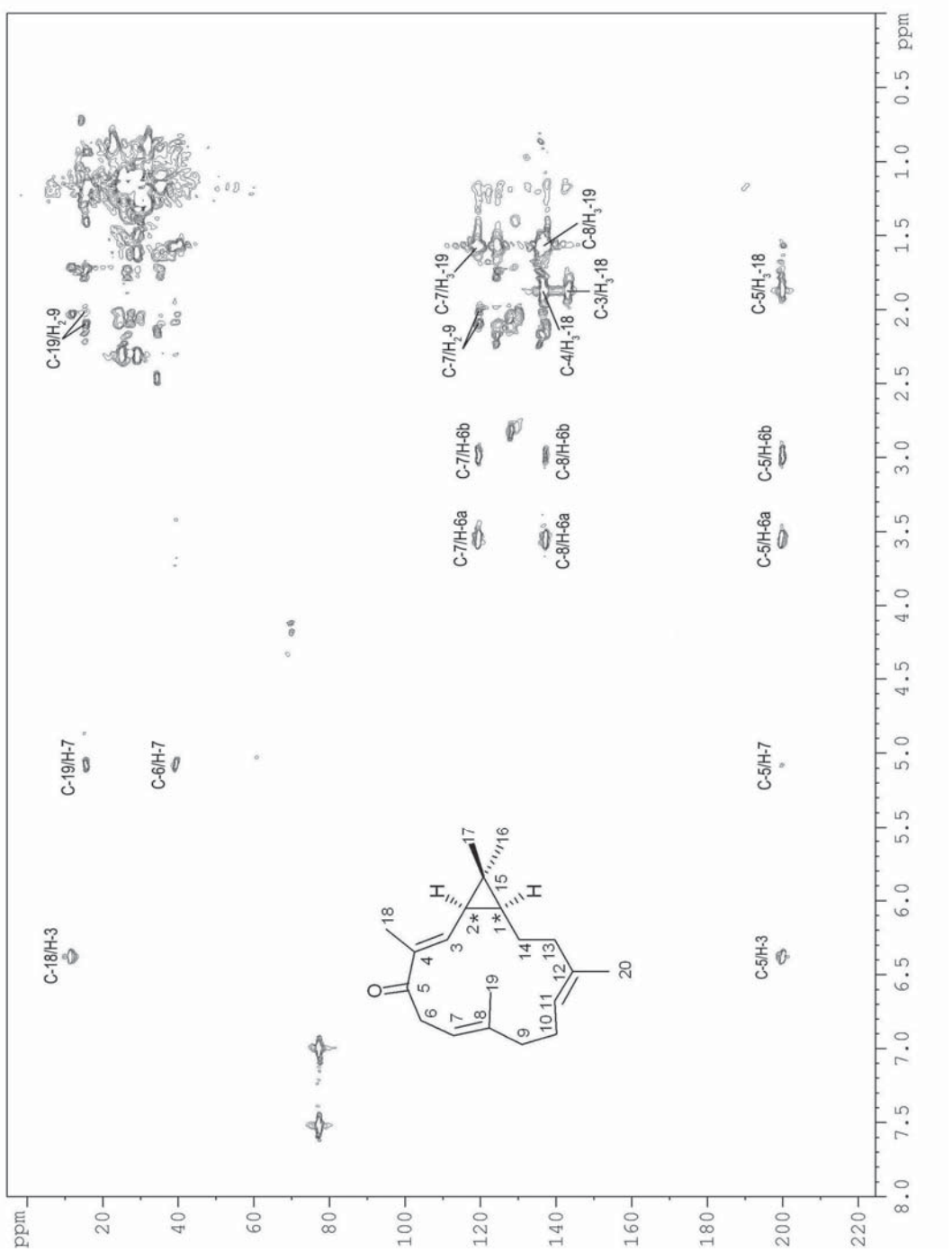

Fig. 7.24. Significant long-range correlations in the HMBC spectrum of compound **1**.

C	δ ^{13}C	mult.	δ ^{1}H	mult., J_{H-H} (Hz)	Significant long range correlations (HMBC)
1	35.2	*d*	1.15	*m*	H_3-16, H_3-17
2	27.6	*d*	1.50	*dd*, 10.2, 8.7	H_3-16, H_3-17
3	143.1	*d*	6.37	*d*, 10.2	H_3-18
4	136.6	*s*	-	-	H_3-18
5	199.9	*s*	-	-	H-3, H-7, H-6a, H-6b, H_3-18
6	39.4	*t*	a 3.55	*dd*, 13.8, 8.4	H-7
			b 2.97	*dd*, 13.8, 5.7	
7	119.4	*d*	5.08	*t*, 6.6	H_2-6, H_2-9, H_3-19
8	137.1	*s*	-	-	H_2-6, H_3-19
9	39.0	*t*	a 2.15	*m*	
			b 2.00	*m*	
10	23.9	*t*	a 2.17	*m*	
			b 1.96	*m*	
11	124.4	*d*	4.84	*t*, 5.4	H_3-20, H_2-13
12	135.9	*s*	-	-	H_3-20, H_2-13
13	39.9	*t*	a 2.20	*m*	
			b 1.75	*m*	
14	26.3	*t*	a 2.05	*m*	
			b 0.80	*m*	
15	25.4	*s*	-	-	
16	29.0	*q*	1.16	*s*	
17	15.8	*q*	1.09	*s*	
18	11.6	*q*	1.87	*s*	H-3
19	15.6	*q*	1.56	*s*	H-7
20	15.3	*q*	1.56	*s*	

Table 7.4 ^{1}H NMR and ^{13} C NMR data of **1**.

The chemical shifts of the *gem*-methyl protons (δ_H 1.16 and 1.11) and carbons (δ_C 22.0 and 23.7), as well as the methines at position C-2 and C-1, were diagnostic for a *trans* junction, as observed in **4**, which was confirmed by the NOE interactions H-1/H_3-17, and H-2/H_3-16, indicating that H-1 and H-2 were oriented in opposite directions. On the other hand, the values of the methyl carbons on the double bonds CH_3-18, CH_3-19

and CH_3-20, and the methylenes CH_2-10, CH_2-13 and CH_2-9 resulted to be according to the *E* geometry. All the proton and carbon resonances were assigned for **2** by analyzing the mono- and bidimensional correlation spectra (Table 7.5).

C	δ ^{13}C	mult.	δ ^{1}H	mult., J_{H-H} (Hz)	Significant long range correlations (HMBC)
1	37.5	*d*	0.71	*m*	H-3, H_3-16, H_3-17
2	31.9	*d*	1.08	*m*	H_3-16, H_3-17
3	149.4	*d*	6.11	*d*, 10.2	H_3-18
4	132.8	*s*	-	-	H-2, H_3-18
5	201.2	*s*	-	-	H_2-6, H-3, H_3-18
6	40.4	*t*	a 3.71	*dd*, 13.8, 11.1	
			b 2.83	br *d*, 13.8	
7	121.7	*d*	5.21	br *d*, 11.1	H_2-9, H_2-6, H_3-19
8	135.1	*s*	-	-	H_2-9, H_2-6, H_3-19
9	38.4	*t*	a 2.18	*m*	H_3-19
			b 2.10	*m*	
10	24.0	*t*	a 2.28	*m*	
			b 2.07	*m*	
11	125.4	*d*	4.88	br *d*, 8.4	H_3-20, H_2-10
12	133.5	*s*	-	-	H_3-20
13	38.8	*t*	a 2.17	*m*	
			b 1.93	*m*	
14	24.4	*t*	a 1.88	*m*	H_2-13
			b 1.03	*m*	
15	28.1	*s*	-	-	H_3-16, H_3-17
16	22.0	*q*	1.16	*s*	H-2, H_3-17
17	23.7	*q*	1.11	*s*	H_3-16
18	11.2	*q*	1.80	*s*	H-3
19	14.7	*q*	1.59	*s*	
20	14.8	*q*	1.59	*s*	H-11

Table 7.5. ^{1}H NMR and ^{13} C NMR data of **2**.

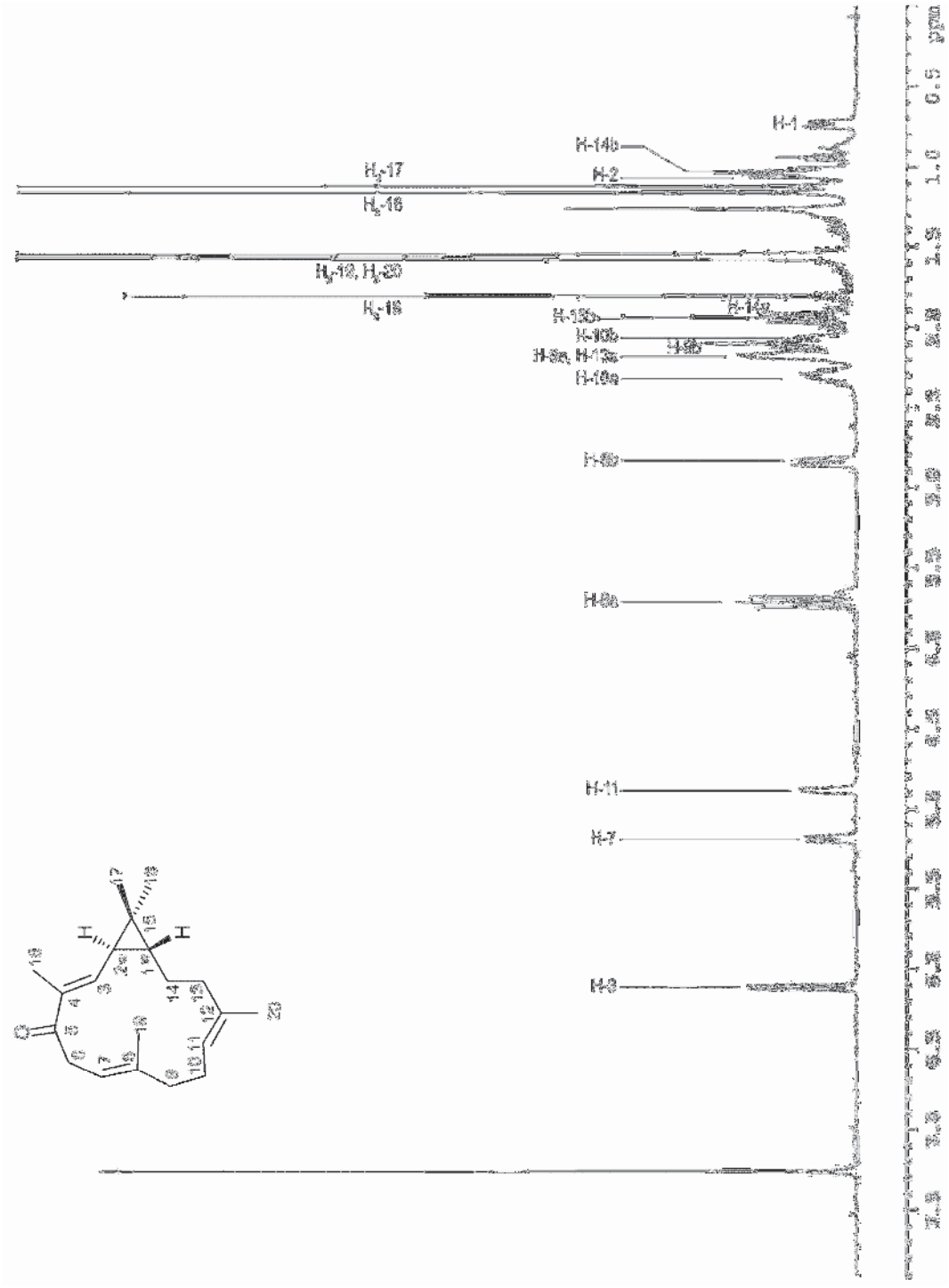

Fig. 7.25. ^{1}H NMR spectrum of compound **2**.

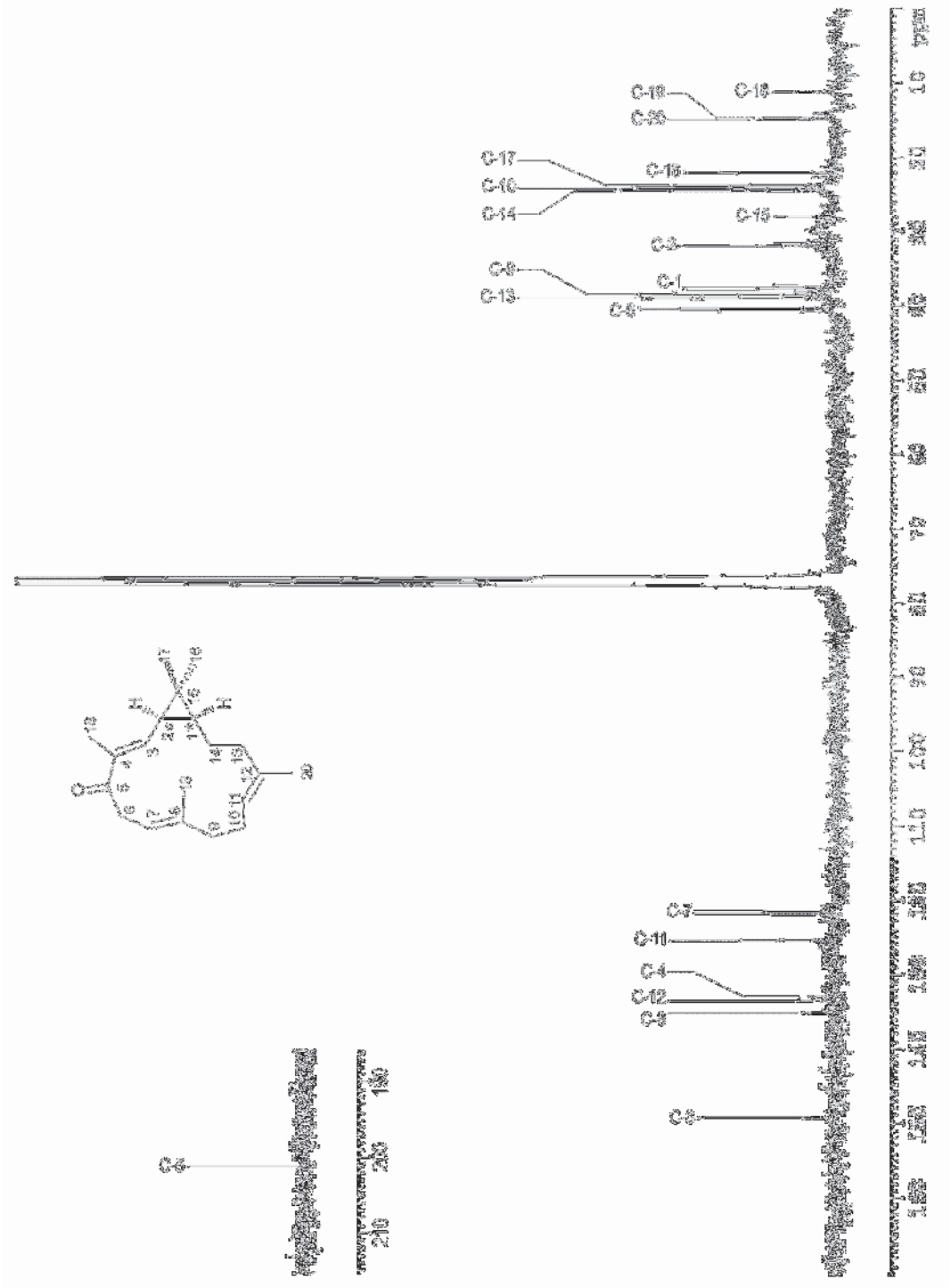

Fig. 7.26. ^{13}C NMR spectrum of compound **2**.

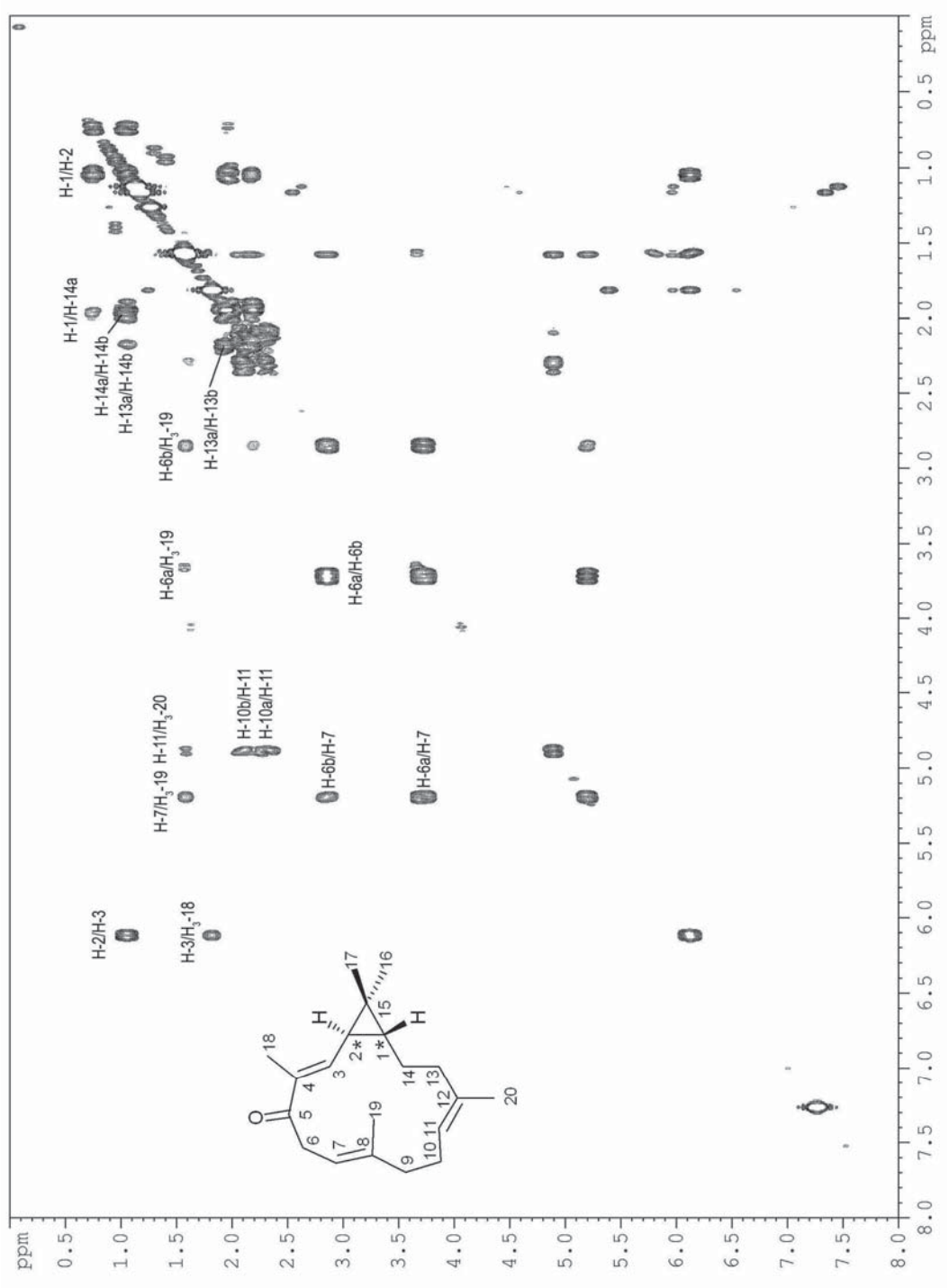

Fig. 7.27. Significant ^{1}H-^{1}H correlations in the COSY spectrum of compound **2**.

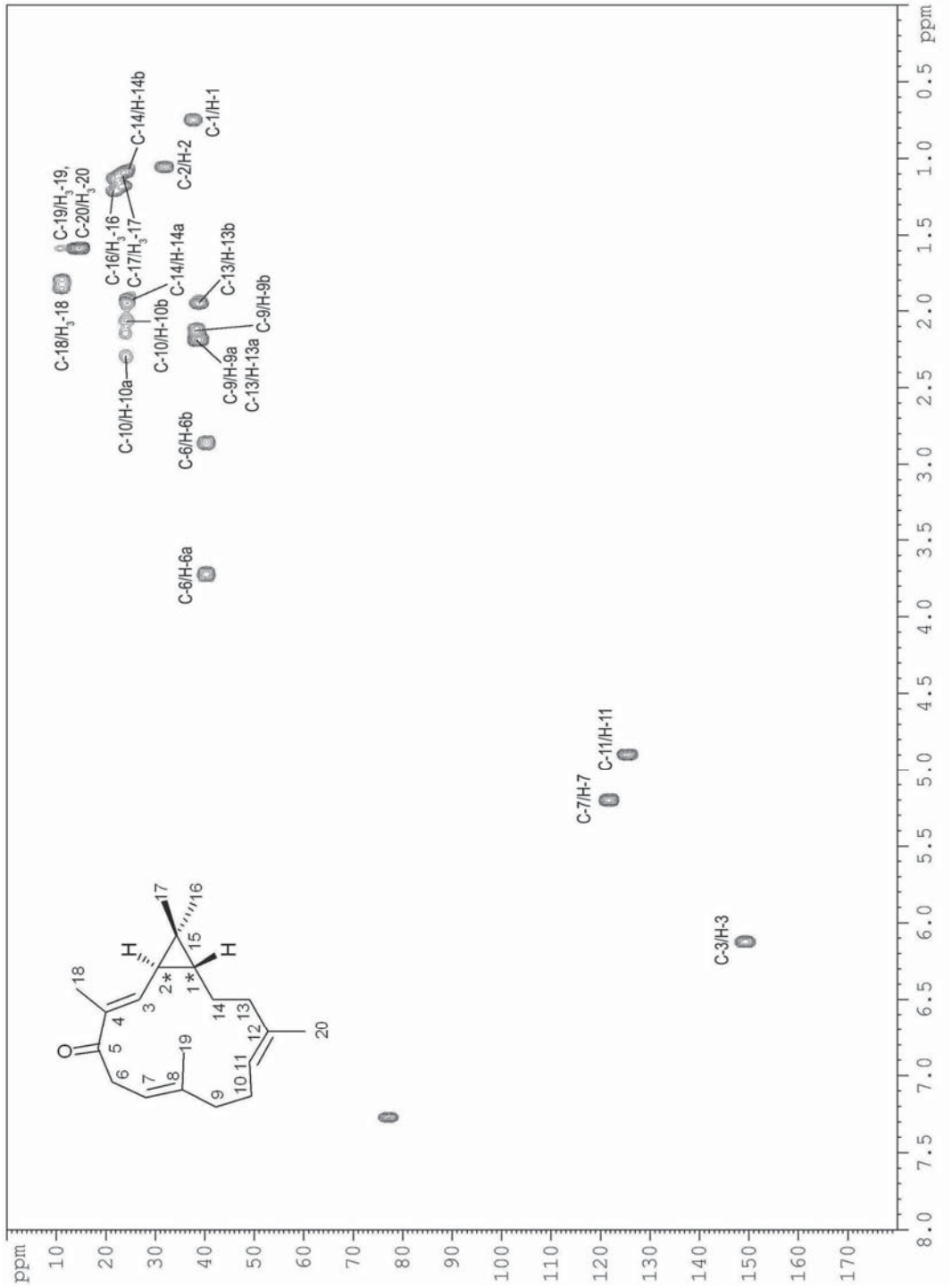

Fig. 7.28. HSQC spectrum of compound **2**.

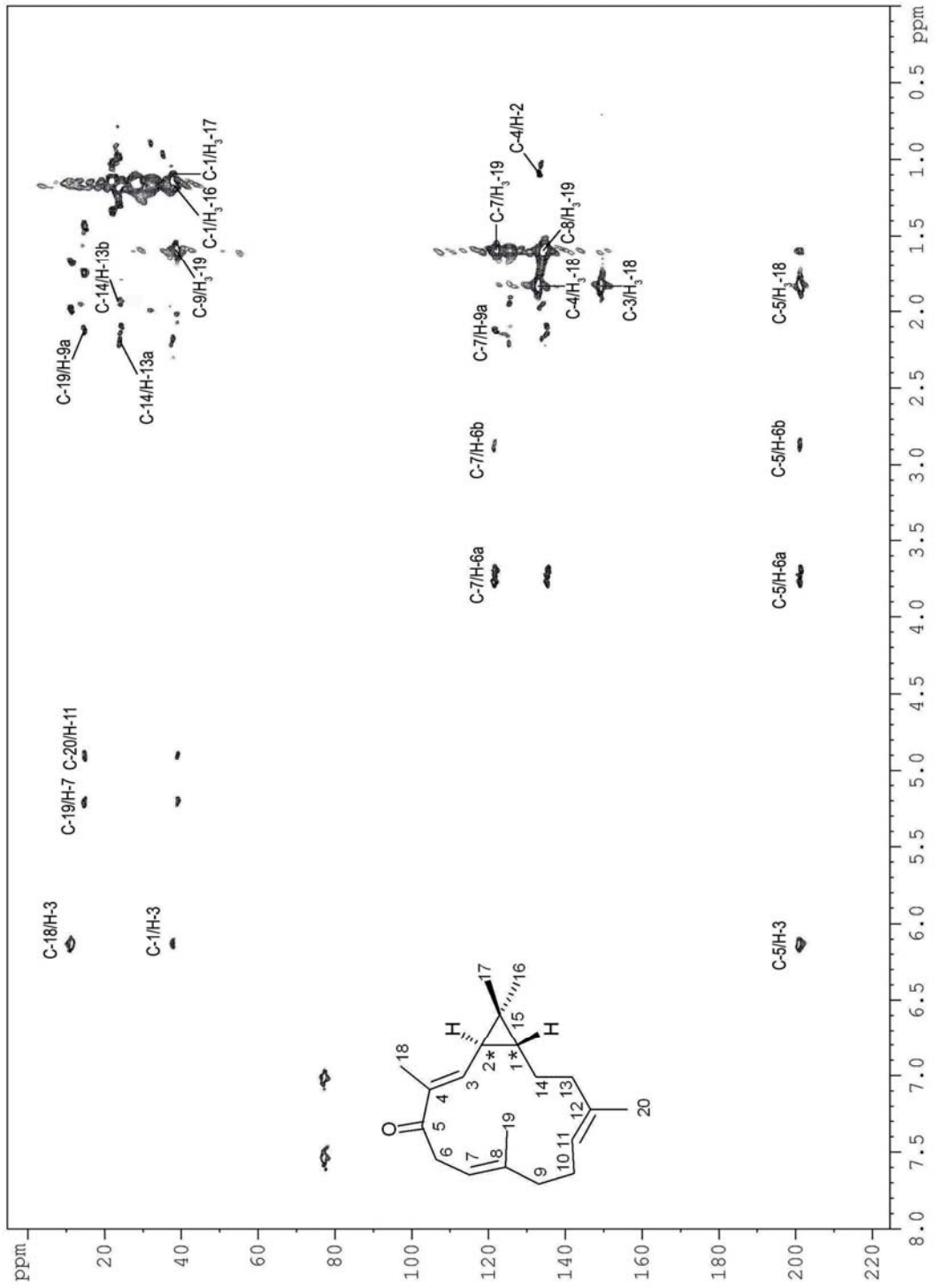

Fig. 7.29. Significant long-range correlations in the HMBC spectrum of compound **2**.

7.4. Biological activity

It is known that Octocorallia are a rich source of secondary metabolites with interesting biological activities and potential pharmacological applications, *e.g.* anticancer, antimicrobial, and HIV-inhibitory activity (Zhang *et al.* 2005b). The information reported in the literature about the pharmacological properties of casbene compounds induced us to do a preliminary evaluation of the biological activities of compounds **1**-**4**, in the attempt to propose new candidates for drug discovery. In particular feeding deterrence, antiproliferative and antimicrobial activity bioassays were performed as preliminary screening in order to evaluate the biological/ecological role of the isolated metabolites.

7.4.1. Feeding deterrence assays

Feeding deterrence assays enable to evaluate the ability of the isolated compounds to exhibit a deterrent action on the taste receptors of the tested predators. This kind of test has to account for the availability of the pure compounds, and be easy to perform in every laboratory, even with small quantities of product. A feeding deterrence test was carried out in the laboratory using the marine generalist shrimp *Palaemon elegans* (Mollo *et al.* 2008). This crustacean is very common in the Mediterranean Sea and it is characterized by a broad range of alimentary habits. The test, consisting in a slight variation of previous methods proposed in the literature (Pawlik *et al.* 1995), allows

evaluating the effects of the tested substances on food palatability. The compounds were incorporated into the shrimp diet at a concentration of 2.0 mg/ml and tested on 10-individual series. Since in this experiment the food is red-dyed, it is easy to distinguish, through the transparent shrimp's body, whether the animal eats or rejects the food (Fig. 7.30).

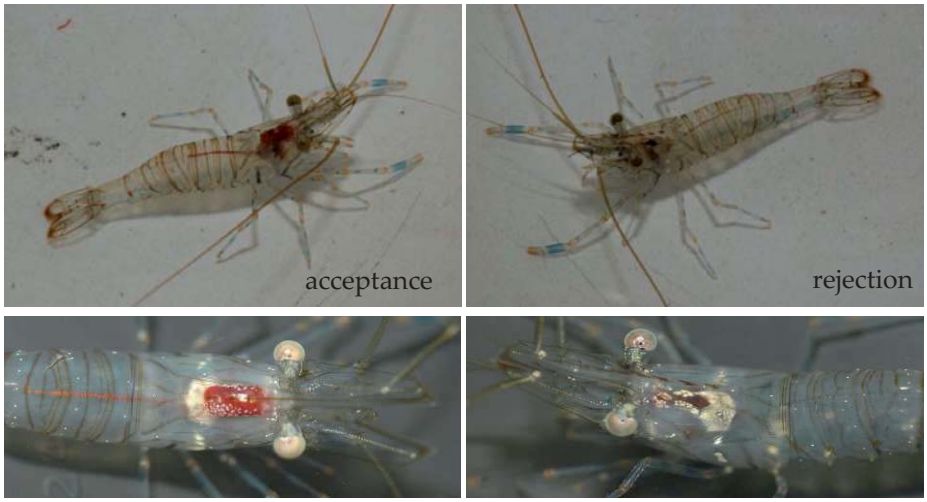

Fig. 7.30. *P. elegans* in case of acceptance (on the left) and rejection (on the right) of the administrated food.

Thirty minutes after the administration, each shrimp was checked in order to evaluate the presence/absence of the red food in the digestive tube. Among shrimps treated with compound **1**, only two animals rejected the food. Similar results were obtained with compound **2**-treatment, where just one animal rejected the food. In compound **3**-treatment, 6/10 of shrimps rejected the diet, while 7/10 did not eat

compound **4**-treated food. Although the available small quantities did not allow obtaining whole dose/effect curves for the pure compounds, the results suggested that compounds **3** and **4** displayed a deterrent role ($p < 0.05$), whereas the activity of compounds **1** and **2** was not significant (Fig. 7.31).

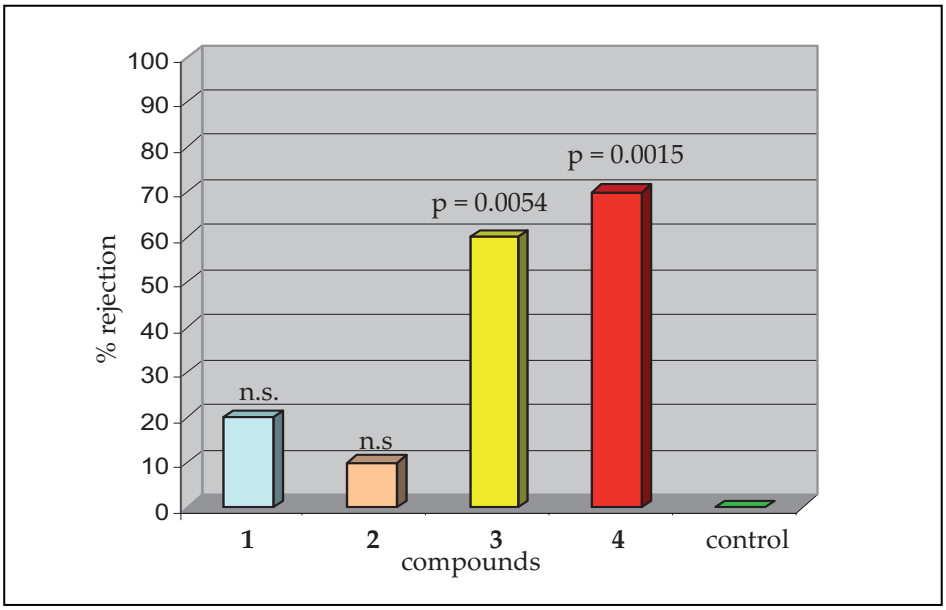

Fig. 7.31. Feeding deterrent assays. Results analyzed by Fisher's exact test, $p < 0.05$ *vs.* control, $n = 10$ per series, n.s. = not significant.

7.4.2. Antiproliferative activity assays

Preliminary antiproliferative activity assays on murine cells were performed in order to evaluate the anticancer properties of the isolated compounds. In particular, the antiproliferative effects of compounds **1-4** were tested on murine basophilic leukaemia cells (RBL-2H3). The compounds were tested at 5 µg/ml and 25 µg/ml. The

results suggested a low activity of compounds **1**-**4** on the considered cell line (IC_{50} > 25 μg/ml). The activity, thus, was not significant.

7.4.3. Antimicrobial activity assays

The octocoral polyps, like other cnidarians, have just one opening in their body acting both as mouth and anus. As a consequence, it can be easily infected by microbes present in food and wastes. In the natural environment, the polyp probably produces abundant antimicrobial substances against pathogenic microorganisms. Hence, compounds **1**-**4** were tested at a concentration of 5 μg/ml on isolated colonies of both *Staphylococcus aureus* ($Gram^+$) and *Escherichia coli* ($Gram^-$) bacteria, using chloramphenicol as positive control. The results of the experiments were evaluated considering the diameter of the inhibition halo generated by each metabolite. Chloramphenicol produced an inhibition halo larger than 25 mm on both *S. aureus* and *E. coli*, corresponding to response of both the tested $Gram^+$ and $Gram^-$ bacteria to this antibiotic. Both compounds **1** and **2** produced inhibition halos whose diameters were in the range of 15-25 mm in *S. aureus*, and less than 15 mm in *E. coli*, indicating a mean response of the $Gram^+$ bacterium, and a certain resistance of the $Gram^-$ bacterium, to the tested metabolites. Both *S. aureus* and *E. coli* were meanly responsive to compound **3**, which produced inhibition halos whose diameters were between 15 and 25 mm on both bacteria. Compound **4**, in turn, was more active

against *S. aureus* than *E. coli*, producing an inhibition halo which was larger than 25 mm diameter in the former, and smaller than 15 mm diameter in the latter. The results of the assay (Table 7.6), therefore, suggested that **1** and **2** displayed a moderate antimicrobial activity against *S. aureus*, whereas **3** showed a moderated activity both on *S. aureus* and *E. coli* bacteria. On the other hand, compound **4** exhibited a good antimicrobial activity on *S. aureus* bacteria, while *E. coli* is quite resistant to this metabolite.

Substances	***S. aureus***	***E. coli***
Chloramphenicol	++++	++++
Compound **1**	++	-
Compound **2**	++	-
Compound **3**	++	++
Compound **4**	+++	-

Table 7.6. Results of the antimicrobial assays adopting the conventional symbols.

7.5. Discussion

The chemical study of the Chinese soft coral *Sinularia* sp. led to the isolation of four new compounds, **1**-**4**, which were structurally determined on the basis of their spectroscopic data, mainly by NMR analysis, and by comparison with known correlated compounds reported in the literature. The collection of the spectroscopic

data was difficult because of the instability of the metabolites, which required repeated purifications of the compounds. From a structural point of view, metabolites **1-4** represent new members of the casbene-family, *i.e* diterpenes characterized by a 14-membered ring fused to a cyclopropane. The casbane structure is closely related to the cembrane ring (Fig. 7.32), differing from the latter for the presence of the cyclopropane moiety with two geminal methyls rather than the isopropyl residue of the cembrane skeleton.

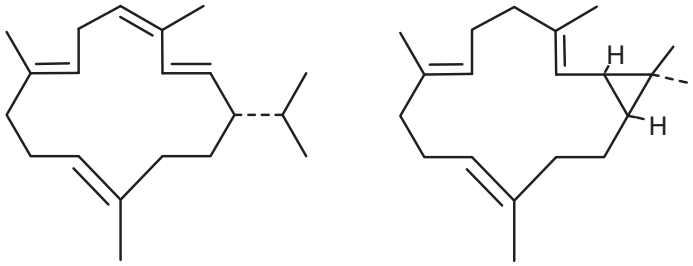

Fig. 7.32. Cembrene and casbene skeletons.

It is noteworthy that casbene diterpenoids are extremely rare in nature and have been extracted mainly from a few plant species belonging to the family Euphorbiaceae (Sitton & West 1975; Choi *et al.* 1986, 1988; Xu *et al.* 1998). Only rarely they have been found also in marine organisms, mainly soft corals as well as *Cespitularia hypotentaculata* (Duh *et al.* 2002) and in the genus *Sinularia* (Bowden *et al.* 1978), as well as microclavatin from *S. microclavata* (Fig. 7.33, Zhang *et al.* 2005b).

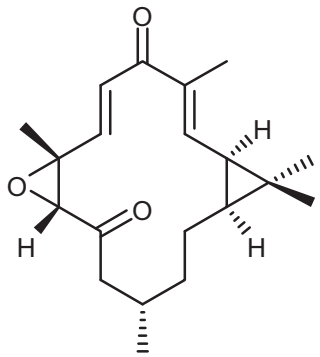

Fig. 7.33. Structure of microclavatin, isolated from *S. microclavata*.

Biosynthetic studies in plants with ^{13}C labelled precursors (Guilford & Coates 1982) showed that the casbene skeleton originates by the geranylgeranyl diphosphate (GGPP) after head-to-tail cyclization. Consequently, the cyclic cation generated by GGPP loses a proton, forming an intramolecular cyclopropane ring (Fig. 7.34).

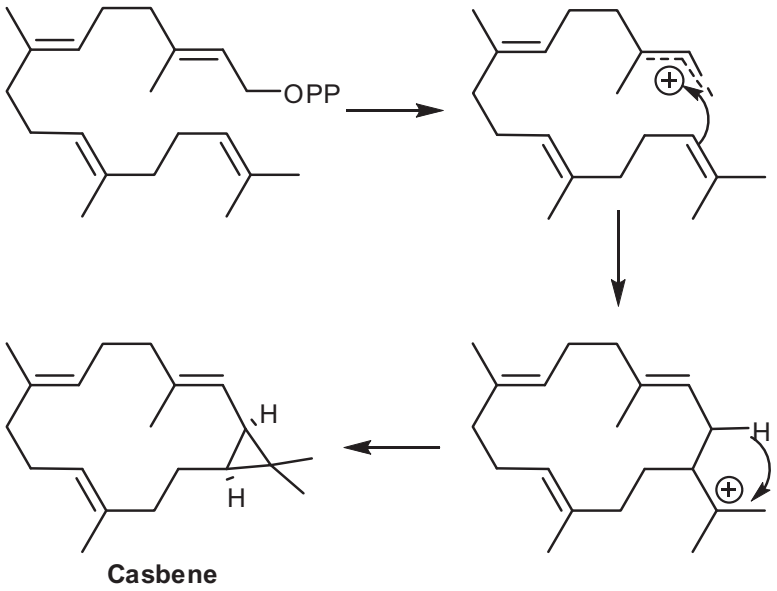

Fig. 7.34. Formation of the casbene skeleton as suggested by biosynthetic studies with ^{13}C labelled precursors.

It has been suggested that such a cyclization reaction occurs by stereospecific mechanism (Markovnikov/syn cyclopropanation) leading exclusively to the *cis* ring junction. This hypothesis seems to be confirmed by the high frequency of the *cis* fusion in nature. In fact, all the natural casbenes, excluding yuexiandajisu compounds (Fig. 7.35) from *Euphorbia ebracteolata* (Xu *et al.* 1998), are characterized by the *cis* junction. Finding both *cis*- and *trans*-fused casbenes in the same organism introduces a series of insights on the biosynthesis of these molecules in the soft coral *Sinularia* sp. The co-occurrence of both *cis* and *trans*-fused casbenes in the same animal suggests that the mechanism of formation is not stereospecific because the cyclization reaction happens from both sides of the carbocation moiety (Fig. 7.36).

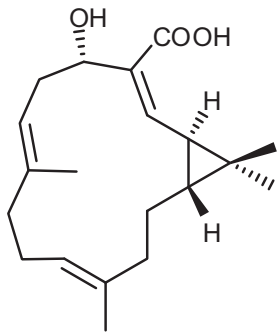

Fig. 7.35. Yuexiandajisu A, characterized by a *trans* fusion.

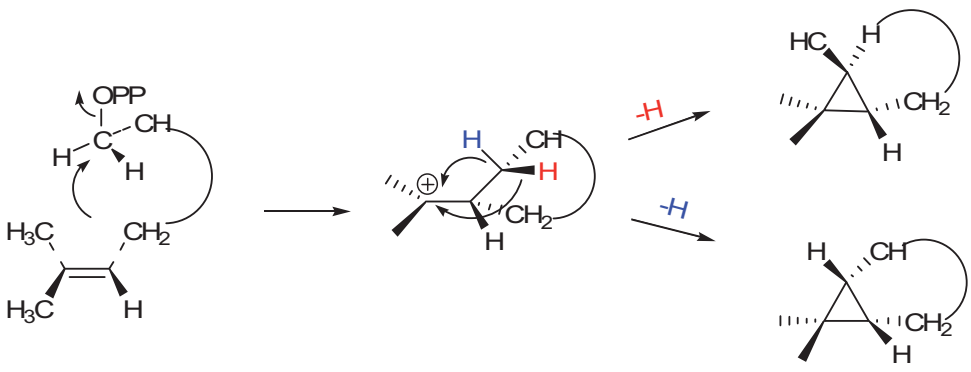

Fig. 7.36. Formation of the cyclopropane ring by H-elimination from both sides.

This could be due to the presence of a different enzymatic system in *Sinularia* sp. or, alternatively, casbenes could be originated by a chemical rearrangement of a definite cembrane precursor. It is known that most diterpenes found in soft corals of the genus *Sinularia* are characterized by a cembrane skeleton (Kamel & Slattery 2005; Zhang *et al.* 2005b). This seems to support the hypothesis of a possible derivation of the casbenes from cembrane precursors. This aspect could be highlighted by means of a specific biosynthetic study of the casbenes in *Sinularia* sp. Casbenes represent a group of extremely interesting natural compounds provided with important biological properties. The father of the family, the casbene, which was isolated from *Ricinus communis* seedlings, is a fungal growth antagonist (Robinson & West 1970; Crombie *et al.* 1980) proposed to display in the plant a role of phytoalexin, *i.e.* antifungal compounds which are produced and accumulated after biotic and abiotic aggressions (Sitton & West 1975). Considering the function of phytoalexin suggested for the casbene produced by superior plants, we wondered whether the diterpenes **1**-**4** detected in *Sinularia* sp. had an analogous defensive paper as well. The results of the feeding deterrence assays performed on the generalist predator *P. elegans* indicated a significant percentage of rejection only for casbenes **3** and **4**, suggesting that the presence of the 14-hydroxy function, which is absent in compounds **1** and **2**, represents a necessary structural element for the deterrence activity. As reported in the literature, besides the ecological properties, casbenes have significant pharmacological applications.

Agrostistachin (Fig. 7.37), isolated from *Agrostistachys hookeri* twigs, showed interesting antiproliferative and, in some cases, antimicrobial activities (Choi *et al.* 1986, 1988). Similar activities were observed in yuexiandajisu compounds as well (Xu *et al*. 1998). In addition, it is noteworthy that many compounds with interesting applications isolated from plants belonging to the family Euphorbiaceae seem to derive from the casbene skeleton after transanular cyclization. Some examples have been afforded by the phorbol esters (Seip & Hecker 1983) used in experiments of chemical carcinogenesis, and the antileukaemic jatrophone (Kupchan *et al.* 1976) (Fig. 7.38).

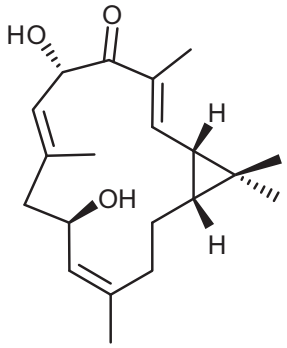

Fig. 7.37. Agrostistachin.

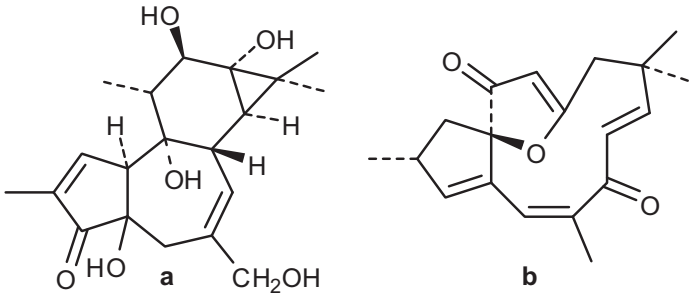

Fig. 7.38. Compounds with intriguing applications: a) a phorbol ester and b) jatrophone.

The strong structural similarities between compounds **1**-**4** and agrostistachin led us to suppose a possible antiproliferative activity also in the new molecules isolated

from *Sinularia* sp. Herein, antiproliferative and antimicrobial activity tests were performed on compounds **1**-**4**. Despite strong structural similarities with the agrostistachins, none of the tested compounds showed a significant antiproliferative activity on rat basophilic leukaemia (RBL-2H3) cell lines, whereas interesting results were observed in antimicrobial tests. All the tested compounds were active against *S. aureus* colonies at 5 μg/ml (and **4** more clearly than the others), whereas only compound **3** had antimicrobial activity on *E. coli* as well.

8. Experimental section

8.1. Increasing the diatom biomass production

8.1.1. Diatom cultures

Cocconeis neothumensis diatoms were collected during spring 2005 along the coasts of Ischia Island, using a special low-adhesion panel immersed on *Posidonia oceanica* meadows close to the Stazione Zoologica "A. Dohrn" (Ischia, Italy), at about 1.5 m depth for 1 month. Diatoms were sequentially transferred by means of a micromanipulator into sterile dishes containing Guillard f/2 medium (Guillard & Ryther 1962), until axenic (*i.e.* monospecific) cultures were obtained. Their taxonomical identification was carried out on the basis of the distinctive morphological characters identified by scanning electron microscopy (SEM), according to De Stefano & Marino (2001). Mother cultures, represented by single-species cultures of *C. neothumensis*, were grown in Petri dishes containing f/2 medium and incubated at 140 μmol photons m^{-2} sec^{-1}, at a 18:6 h photoperiod and at 17°C. Monospecific cultures of other active species (*C. scutellum*, *C. dirupta*, *C. posidoniae,*

Diploneis sp.) were also cultivated along with a strain of *Navicula incerta* (purchased from Bigelow Inc.) as negative control.

8.1.2. Influence of different light intensities and micronutrient concentrations on the diatom growth rate

A cell suspension of *C. neothumensis* was obtained by gently scraping off (with the aid of a sterile pipette) the diatoms from the bottom of the Petri dishes once reached the end of their exponential phase. Each replicate was generated inoculating aliquots (3 ml) of this suspension into cylindrical glass cups (5 cm diameter) provided with a grid on the bottom, which allowed the counts of the cells per unit of substrate area. After two days all the intact and metabolically active cells were strongly attached to the bottom of the glass cup. One series of treatments was incubated at 60, 100 and 140 µmol photons m^{-2} sec^{-1} in f/2 medium, at 17°C and at a 18:6 h photoperiod; the other series was incubated at 140 µmol photons m^{-2} sec^{-1}, at 17°C, at a 18:6 h photoperiod and in presence of f/2 medium enriched with 0.11 mM Na_2SiO_3 (control), 0.22 mM Na_2SiO_3, 10^{-8} M H_2SeO_3, and 0.22 mM Na_2SiO_3 and 10^{-8} M H_2SeO_3 contemporaneously. For each treatment five replicates were carried out. Cell counts were realized every two days until reaching the culture stationary phase.

8.1.3. Cultivation by Petri dishes

Mother populations of *C. neothumensis* diatom species were sowed into 2.5 cm diameter Petri dishes, containing 5 ml of f/2 medium. From three cultures grown in these conditions, a cell suspension was obtained to inoculate 14 cm diameter Petri dishes containing 90 ml of f/2 medium. The dishes were wrapped with synthetic film (Parafilm®), in order to prevent medium evaporation, and were incubated at 100 µmol photons m^{-2} sec^{-1}, at a 18:6 h photeriod and at 17°C until reaching the stationary phase. At the end of the experiment, cells still adherent to the dish bottom were washed with distilled water, frozen, freeze-dried and then scraped off with a metal blade. The amount of *C. neothumensis* dried powder was determined as mg of dry weight per cm^2 of substrate surface.

8.1.4. Bioreactor cultures

The small scale bioreactor (26 cm length, 4.7 cm diameter), filled with 2 mm diameter glass beads, was activated at a continuous f/2 medium flow of 7 l h^{-1} cm^{-2}. A cell suspension, obtained from three *C. neothumensis* species cultures grown in 2.5 cm diameter Petri dishes, was inoculated into the system. After 17 days of incubation, diatom-covered glass beads were drained with distilled water and lyophilized.

8.1.5. Preparation of the diethyl ether extract

Frieze dried diatoms, either obtained by Petri dishes or attached to the bioreactor glass beads (*ca.* 200 mg DW diatoms from Petri dishes, whereas the weight was not evaluated for the diatoms attached to the glass beads), were reconstituted with 5 ml of distilled water and extracted at room temperature with acetone for three times. In particular, diatoms originated by Petri dishes were treated with acetone (3 x 20 ml). Diatom-coated beads, instead, were first extracted with a larger amount of acetone (3 x 100 ml) and, after filtration, glass beads were separated from the diatom suspension. The extractions in both cases were improved by ultrasound vibration. The filtration was carried out on paper filter and the acetone was evaporated under reduced pressure. Both suspensions were further diluted in distilled water (20 ml) and, thus, extracted with diethyl ether (3 x 20 ml) by means of a separatory funnel. Upon separation of the two layers, the organic phases were combined and evaporated to dryness by vacuum, affording two greenish extracts. Three independent extractions were considered to calculate the average weight of diethyl ether extract for each culture system. Petri dishes afforded *ca.* 17 mg of diethyl ether extract, whereas the bioreactor yielded 24 mg. All the solvents were supplied by Sigma-Aldrich.

8.1.6. TLC comparison

The diethyl ether extracts obtained from diatoms originated by both cultivation systems were compared by TLC (Merck Kieselgel 60 F_{254} plates, 5 x 10 cm, 0.25 mm thickness) using different eluant systems (light petroleum, light petroleum/diethyl ether 8:2 v/v, light petroleum/diethyl ether 1:1 v/v, light petroleum/diethyl ether 2:8 v/v, diethyl ether, chloroform/methanol 9:1 v/v). The plates were observed under UV light (254 nm) and developed with 2 N cerium sulphate [$Ce(SO_4)_2$] in 10% H_2SO_4 solution.

8.1.7. Statistical analyses

Exponential growth rates and cell densities at saturation were statistically compared in order to identify significant differences among the different treatments (light intensities and nutrient concentrations). One-way ANOVA and *a posteriori* SNK test were utilized for both sets of data. The respective yields of the two culture systems were compared by t-test.

8.2. Chemical composition of the benthic diatom *C. scutellum*

8.2.1. Diatom cultures

C. scutellum benthic diatoms were isolated from mother cultures originated as reported in **8.1.1** and cultivated in the Stazione Zoologica "A. Dohrn" during all the

period of investigation (2005-2007). Axenic cultures were sowed into sterilized Petri dishes (14 cm diameter) containing 100 ml of f/2 medium (Sigma-Aldrich) and incubated in a thermostatic chamber (18°C, 12:12 h photoperiod) without sealing the plates. After 16 days, the Petri dishes were opened, the culture medium was drained and the dishes were washed twice with distilled water, then freeze-dried and scraped with a metal blade in order to collect the produced biomass (2.2 g DW).

8.2.2. Extraction

After reconstitution with distilled water (50 ml), the lyophilized diatoms were extracted at room temperature with acetone (3 x 100 ml), sonicating by means of ultrasound vibration for 2-3 min. The obtained suspension was filtered on a paper filter and, afterwards, concentrated under reduced pressure. The residual water was extracted with diethyl ether (3 x 150 ml) by means of a separatory funnel. After separation of the two layers, the organic phases were combined, treated with anhydrous Na_2SO_4 and *in vacuo* evaporated until dryness, affording 227.9 mg of oleous crude extract. The water residue was further extracted with *n*-butanol (100 ml). The *n*-butanol soluble part was recovered, evaporated until dryness yielding 102.9 mg of a yellow-greenish crude extract. The extractive procedure is summarized in Fig. 8.1.

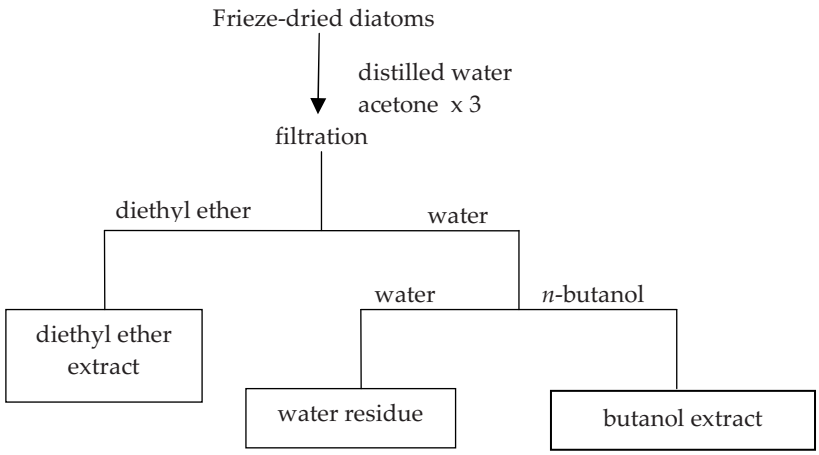

Fig. 8.1. Extractive procedure of *C. scutellum* diatoms.

8.2.3. TLC screening

Small amounts of both the diethyl ether and butanol extracts were deposed onto analytical silica plates (Merck Kieselgel 60 F_{254}, 5 x 10 cm, 0.25 mm thickness, aluminium support), eluted with different mixtures of solvents (light petroleum, light petroleum/diethyl ether 9:1 v/v, light petroleum/diethyl ether 8:2 v/v, light petroleum/diethyl ether 7:3 v/v, light petroleum/diethyl ether 1:1 v/v, diethyl ether, chloroform, chloroform/methanol 9:1 v/v) and, thus, observed under UV light at 254 and 356 nm. The plates were revealed with the following reagents: cerium sulphate [$Ce(SO_4)_2$] solution for detecting organic compounds; Ehrlich's reagent for nitrogenous and heterocyclic metabolites (*e.g.* furano compounds); diphenylboric acid and diazo/NaOH for phenolic compounds; ninhydrine for amino acids; modified Dragendorff's reagent for nitrogenous compounds and alkaloids.

8.2.4. Preparation of the reagent solutions

$Ce(SO_4)_2$ solution: 1 g of $Ce(SO_4)_2$ powder in 880 ml of distilled water and 120 ml of conc. H_2SO_4.

Ehrlich's reagent: 1 g of 4-dimethylaminobenzaldehyde ($C_9H_{11}NO$) in 30 ml of absolute EtOH and 9 ml of conc. HCl.

Diphenylboric acid solution: 1% p/v diphenylboric acid in MeOH.

Diazo: 1 g of "fast red b salt Echtrosalz" in 100 ml of distilled water; NaOH solution: 4 g of NaOH in 100 ml of distilled water. The silica plate is sprayed first with the diazo solution and, afterwards, heated and sprayed with the alkaline solution.

Ninhydrine: 1 g of ninhydrine powder in 100 ml of acetone and one drop of pyridine.

Dragendorff's reactive modified by Munier-Macheboeuf: it consists of two solutions, A and B. Solution A: 0.85 g basic bismuth nitrate in 10 ml of glacial acetic acid and 40 ml of distilled water. Solution B: 16.0 g potassium iodide in 40 ml of distilled water. Equal volumes of both solutions A and B are mixed affording the stock solution, to be stored in the fridge. To prepare the reagent mixture, X ml of the stock solution have to be diluted with 2X ml of glacial acetic acid and 10X ml of distilled water. All the reactives and solvents were supplied by Sigma-Aldrich.

8.2.5. Fractionation

The diethyl ether extract was fractionated by Sephadex™ LH-20 column (Amersham Pharmacia Biotech, Uppsala, Sweden). The sample was dissolved in chloroform/methanol 1:1 v/v, charged onto the column and eluted with chloroform/methanol 1:1 v/v. Fractions of *ca.* 10 ml were recovered in glass tubes and, after TLC analysis, combined into three main portions which were evaporated under reduced pressure: **1** (107.5 mg), **2** (94.6 mg) and **3** (20.0 mg). Each fraction was shared among the different Institutes to be subjected to the chemical analysis, the bioassays on *H. inermis*, the bioassays on crustaceans of commercial interest and the bioassays on human cancer cell lines.

8.2.6. Derivatization

Small amounts (*ca*. 2-3 mg) from both the diethyl ether extract and its fractions **1-3** were silylated with 50 μl of *N,O*-bis-(trimethylsilyl)trifluoroacetamide (BSTFA) in 50 μl of pyridine for 2 h at 50°C. Small amounts of the *n*-butanol extract (*ca*. 2-3 mg) were first methoxymated with 100 μl of methoxyamine hydrochloride (MOA, 20 mg ml^{-1} in pyridine) for 90 min at 50°C in order to stabilize the carbonyl moiety and prevent the ring formation in sugars, then silylated by addition of 100 μl of BSTFA and heated at 50°C for 1 h. The mixtures were evaporated under a stream of N_2 and re-dissolved in 100 μl of chloroform for GC-MS analysis. In parallel, FAME were

obtained from *ca*. 5 mg of both the diethyl ether extract and its fractions dissolved in 2 ml of 1.5% solution of HCl in absolute MeOH and heated overnight (12 h) at 60°C. After cooling, the work-up was carried out by adding 2 ml of water containing 5% of NaCl to the reaction mixture and extracting the acid solution with *n*-hexane (2 x 3 ml). The organic layer was separated, washed with 3 ml of distilled water containing 5% of Na_2CO_3 and dried over anhydrous Na_2SO_4. After evaporation of the *n*-hexane, the residue was dissolved in 100 μl of chloroform for GC-MS analysis.

8.2.7. Acquisition of GC-MS data

Data were recorded in the Serveis Científico-tècnics of the Universitat de Barcelona, on a Hewlett Packard 6890+MSD 5975 (Hewlett Packard Palo Alto, CA, USA) operating in both EI and CI modes with a HP-5 MS capillary column (30 m x 0.25 mm x 0.25 μm). The temperature program was: 100-180°C at 15°C min^{-1}, 1 min at 180°C, 180-300°C at 5°C min^{-1}, and 1 min at 300°C. The injector temperature was 280°C. The electric potential was 70 eV, and the flow rate of carrier gas (helium in EI mode, and methane in CI mode) was 0.8 ml min^{-1}.

8.2.8. Identification of metabolites

The metabolites of the diethyl ether extract and its fractions were identified as TMSi derivatives comparing their mass spectra and Kovats Indexes (*RI*) with those from

the on-line plant specific database (The Golm Metabolome Database, http://csbdb.mpimp-golm.mpg.de/csbdb/gmd/home/gmd_sm.html) and NIST 05 database. Additionally, the structure of FAs was confirmed after their conversion to FAMEs considering the characteristic mass spectral fragmentation of each subgroup, molecular ion, retention time and mass spectra from the on-line available lipid library (Christie 2003, http://www.lipidlibrary.co.uk/ms/ms01/index.htm), NIST 05 database and literature data. Peaks in the GC-MS of the *n*-butanol extract were identified as TMSi and/or MOA derivatives with the help of NIST 05 database and on-line available plant specific database (The Golm Metabolome Database), as well as literature data on the basis of the match of mass spectra and *RI*. The measured mass spectra were deconvoluted by the Automated Mass Spectral Deconvolution and Identification System (AMDIS), before comparison with the databases. Then, the spectra of individual components were transferred to the NIST Mass Spectral Search Program MS Search 2.0 where they were matched against reference compounds of the NIST Mass Spectral Library 2005 and the Golm Metabolome Database. *RI* of the compounds were calculated with a standard *n*-hydrocarbon calibration mixture (C_9-C_{36}) (Restek, Cat no. 31614, supplied by Teknokroma, Spain) using AMDIS 3.6 software.

8.2.9. Search for aldehydes

8.2.9.1. Diatom extraction

A sample of frozen *C. scutellum* diatoms (*ca.* 1 g), isolated and cultivated in the Stazione Zoologica "A. Dohrn", was defrosted, dissolved in 1 ml of distilled water and sonicated in an ultrasound bath for 1 min. The suspension was left on the bench for 30 min. Subsequently, it was treated with 1 ml of acetone and the resulting suspension was centrifuged three times at 4,000 rpm for 10 min. The centrifugation was carried out on a Sorvall RC28S. The supernatant was transferred into a separatory funnel and exhaustively extracted with chloroform (3 x 5 ml). The chloroform layers were combined, dried over anhydrous Na_2SO_4 and then evaporated under nitrogen flow to afford 91.0 mg of an oleous extract.

8.2.9.2. Derivatization

The chloroform extract (91.0 mg) was dissolved in 2 ml of chloroform and treated with one equivalent of carbethoxyethylidene-triphenylphosphorane (CET-TPP), corresponding to about 8 mg of derivatizing agent. The reaction was carried out at rt and under agitation for 18 h. After that, the reaction mixture was evaporated until dryness by means of N_2 flow and herein dissolved in 200 µl of $CHCl_3$ for GC-MS analysis. Standard CET-derivatives were prepared treating *ca*. 10 mg of each standard (2-*trans*-4-*trans*-heptadienal, 2-*trans*-4-*trans*-octadienal and 2-*trans*-4-*trans*-

decadienal, supplied by Sigma-Aldrich) with 1.1 equivalent of CET-TPP and 2 ml of chloroform. The reaction was carried out overnight, at room temperature and by magnetic stirring. The day after, the organic solvent was evaporated under nitrogen flow and the obtained derivatives were dissolved in 200 µl of chloroform for GC-MS analyses. The molecular ions of the CET-derivatives of heptadienal, octadienal and decadienal were at *m/z* 194, 208 and 236, respectively.

8.2.9.3. GC-MS analysis

GC-MS analysis was recorded on a Hewlett Packard 6890+MSD 5975 (Hewlett Packard Palo Alto, CA, USA) operating in EI mode with a HP-5 MS capillary column (30 m x 0.25 mm x 0.25 µm) and in the following conditions: T_i 130°C, T_f 220°C at a gradient of 3°C min^{-1}, $T_{injector}$ 240°C, $T_{detector}$ 260°C; He flow at 1 ml min^{-1}, 70 eV and split 1:50. The interpretation of the GC-MS spectra was realized by comparing the recorded data of the standard CET-derivatives with the spectrum of the CET-extract.

8.3. Biological assays on *C. scutellum* diatoms

8.3.1. Larval and postlarval growth of *H. inermis*

Adult *H. inermis* females were collected during spring 2006 and 2007 on *Posidonia oceanica* meadows in Lacco Ameno d'Ischia (Golfo di Napoli, Italy), and transferred to the SZN. Each sample was examined in the laboratory under a dissecting

microscope in order to confirm their identification and measure their total length (from the tip of the rostrum to the posterior medial notch). The specimens were individually reared in aerated 2 l bowls (containing filtered seawater and 1 individual of *Artemia*/ml in order to sustain the first development of larvae) until larvae were released (Le Roux 1963). Bowls were visually checked daily for the presence of larvae. When larvae were detected, the water was filtered through 60 μm plastic nets and larvae were collected by a Pasteur pipette and divided into different bowls, each one containing 80 larvae (a density of 1 larva per 10 ml of culture solution). The culture medium in each bowl was composed by 800 ml of filtered and UV sterilized seawater with the addition of 4 nauplii of *Artemia salina* (Select Microcysts) previously enriched for 18 hours with Algamac (Biomarine)/ml of culture medium, plus 4 individuals of *Brachionus plicatilis*/ml of culture medium. The culture medium was renewed at 2-day intervals, after filtering the larvae on a 60 μm net and counting survivors. All bowls were aerated by an air pump and maintained at 18°C in a thermostatic chamber, at an average irradiance of 200 μE, at a 12:12 h photoperiod. After 14 days the largest larvae of each bowl were combined, mixed in order to pool genetic differences due to maternal influences, and divided again into groups of 80 individuals. Each group was hosted in a 1 l bowl, containing 800 ml of filtered seawater. All the remaining larvae (the smallest individuals, slow growing, *etc*.) were discarded. Once individuals reached the postlarval phase, a 10 day-period of weaning followed, in which a pellet (5 mg) of dry food was added daily in each

bowl. *Brachionus* was not incorporated anymore into the diet, while *Artemia* was introduced into the pellets in decreasing abundance (during the first 4 days: 4 ind/ml; days 5-7: 3 ind/ml; days 8-9: 2 ind/ml; day 10: 1 ind/ml). On day 11, the postlarvae from each bowl were divided into groups of 20 individuals in 12 cm Petri dishes (filled with 400 ml of seawater).

8.3.2. *In vivo* assays on *H. inermis* postlarvae

In vivo assays on *H. inermis* postlarvae consisted in two phases, the first one in which both the diethyl ether and the butanol extracts were incorporated into the shrimp food, and the second one in which fractions **1-3** were enclosed into the pellets. In both steps, each treatment was composed by 20 *H. inermis* postlarvae and was repeated by three replicates. In the first part of the experiment each postlarva was treated with 5 mg-pellets containing the diatom extracts at three different concentrations (70, 7 and 0.7 μg of each extract/mg of food) for a total of 32 days. Every 2 days the 20 postlarvae were collected by a pipette and transferred into fresh filtered seawater. The different concentrations of extracts were prepared diluting both the diethyl ether and the butanol fractions in acetone and adding the basic shrimp food, which was represented by 15 g freeze-dried *Artemia* + 15 g flaked *Spirulina* + 1 g Baby food (SHG). The suspensions were evaporated to dryness. The dry material was weighed, divided into 5 mg portions and pressed to produce the

pellets. Pellets were stored at -20°C. In parallel, several diets were tested as well on the postlarvae (Food 1: 200 mg freeze-dried *Artemia* + 200 mg pure *Spirulina* + 200 mg Algamac; Food 2: 200 mg freeze-dried *Artemia* + 200 mg pure *Spirulina* + 200 mg Tetra AZ; Food 3: 200 mg freeze-dried *Artemia* + 200 mg pure *Spirulina* + 200 mg granulated SHG; Food 4: 500 mg freeze-dried *Artemia* + 500 mg pure *Spirulina* + 250 mg Baby food). Food control was represented by 15 g freeze-dried *Artemia* + 15 g flaked *Spirulina* + 1 g Baby food (SHG). In the second part of the experiment, the basic food was represented by Tetra AZ food (00, TetraWerke, 33% weight), pure *Spirulina* (Super High Group, 33% weight), and enriched lyophilized *Artemia* (SHG, 33% weight). This was the diet which proved to produce the highest survival in the bioassays.

Aliquots of fractions **1**-**3** (*ca.* 4 mg) were diluted in 9 ml of acetone. From each suspension 2 ml were taken and incorporated into *ca.* 1 g of shrimp food. The solvent was evaporated and the dry material was weighted and pressed in order to obtain 5 mg-pellets containing 1 µg of each fraction/mg of food. Every day one pellet was added to each treatment for a total of 32 days, according to the different treatments and controls. The controls received the basic food previously described, while the treatments received the basic food enriched with the diatom fractions. In both the experiments, at the 33rd day all postlarvae were collected and fixed in 3.7% buffered formaldehyde for 5 h and, afterwards, transferred into 70% alcohol. Each individual was photographed at a Leica APO 60 microscope and the presence/absence of the

appendix masculina was evaluated. The efficacy was expressed in terms of F/tot. One way Anova, Bartlett's test for equal variances and Bonferroni's Multiple Comparison Test, using Prism software (version 4.00 for Mac, GraphPad Software, San Diego, California, USA), were used to compare the data and establish their significance.

8.3.3. *In vivo* experiments with *M. rosenbergii*

An aliquot of the acetone extract (30.7 mg), prepared as reported above (see **8.2.2**), was added to a commercial algal extract (Algamac 2000, Biomarine, Inc., CA, USA) which was enriched with freshly hatched *Artemia* sp. nauplii (Salt Creek, Inc., UT, USA) prior to feeding. The experiment started with 5^{th}-6^{th} zoeae of the freshwater prawn *M. rosenbergii* which were placed in 500 ml tanks filled with distilled water and 12 parts per thousand of sea salt. Water was replaced daily. In each tank 25 larvae were incubated. Feeding included 2 concentrations of the acetone extract of *C. scutellum* (20 ng/larva and 2 ng/larva in high and low concentration, respectively) and carrier solution (2% methanol in distilled water) as control. Each treatment included three replicates. After transformation of larvae to postlarvae, individuals were kept in separate compartments and fed on fish pellets *ad libitum*. When individuals reached *ca.* 1 g body weight, they were sexed according to the appearance of the *appendix masculina* on the second pleopod.

8.3.4. *In vitro* experiments with *C. quadricarinatus*

Eye stalk ablated *C. quadricarinatus* crawfishes were subjected to surgical ablation of the AGs. AGs attached to a small portion of the sperm duct, were incubated for 24 h in culture medium adjusted to the osmolarity of the crustaceans and in presence of fractions **1**, **2** and **3**, control solvents (ethanol, acetone, diethyl ether, DMSO), standards (arachidonic acid and eicosapentaenoic acid, Sigma-Aldrich) and staurosporine (a general apoptotic agent). Fractions, control solvents and standards were tested at three different concentrations (100, 10 and 1 μg/ml), while staurosporine was administrated at a concentration of 10 μg/ml. Acetone was tested also at 150 μg/ml. Because of their solubility, the two standards were diluted in ethanol, whereas fractions **1**-**3** and control solvents were dissolved in DMSO. After incubation, samples were fixed, embedded in paraffin and 5 μm sections were loaded onto slides for examination by fluorescence microscopy.

8.3.5. Determination of apoptosis

Cell vitality was measured by hypotonic propidium iodide (PI) staining. The PI solution (10 ml 1% sodium citrate, 1 ml Triton 10X, 100 μl PI from a 50 μg/ml mother solution) was diluted to 100 ml final volume by adding distilled water. Permeabilized cells were suspended in 200 μl hypotonic PI solution and the amount of DNA fragmentation was calculated by flow cytometry analysis (Becton-Dickinson)

as described in the literature (Zupo *et al.* 2000). Results were expressed as percentage of fragmented DNA compared with total DNA. Alternatively, apoptosis was evaluated by double staining with annexin V-FITC conjugate and isotonic PI and, afterwards, by flow cytometry analysis. The cultured cells, which were separated from each well, were trypsinised, centrifuged, washed with physiological solution, and suspended in 200 µl binding buffer (ApoAlert Clontech, Palo Alto, CA) supplemented with 1 µl annexin V-FITC and 10 µl PI from a mother solution at 50 µg/ml. After 10 min incubation at rt, the suspension was analyzed by flow cytometry. The acquired data were elaborated by Cellquest software, and the percentages of live cells, apoptotic cells or dead cells were calculated as reported by De Totero *et al.* (2006). In selected experiments, cell viability was determined by PI exclusion tests and flow cytometry analysis, *i.e.* dead and late apoptotic cells were stained by PI, whereas live cells were unstained.

8.3.5.1. Apoptosis assays

The different cell lines (BT20, MB-MDA468, LNCaP, COR, JVM2, BRG-M) were cultured at a density of 1 x 10^6 cells/ml in RPMI-FCS medium (10%, GIBCO, Paisley, UK) supplemented with penicillin-streptomycin (1%), L-glutamine 200 mM (1%), sodium piruvate 100 mM (1%). COR line was obtained by treating B lymphocytes extracted from human tonsils with the Epstein-Barr virus (EBV) in order to transform

them into immortal cells. Both BRG-M and JVM2 cell lines, on the other hand, consisted in T lymphocytes extracted from peripheral blood.

Freeze-dried *C. scutellum* diatoms (3.5 mg) were dissolved in distilled water and administrated at different concentrations (0.1-10 ng/ml) to the cell lines, which were incubated for 24 h at a concentration of 80,000 cells/well at 37°C. Vepesid (VP-16 Bristol-Myers Squibb, Rome, Italy) was used as positive control at a concentration of 10 µl/ml. The results were statistically analyzed by exact Fisher's test. Aliquots of both the diethyl ether (12.5 mg) and the butanol (9.2 mg) extracts were dissolved in distilled water and DMSO to afford concentrations in the range 0-1,700 ng/well. BT20 cell lines, were incubated for 18 h with both the extracts at different concentrations, which were determined by preliminary titration experiments. Fractions **1**-**3** were diluted in DMSO to afford different concentrations (0.1-4 µg/well). BT20 and LNCaP cell lines were incubated for 24 h at various concentrations of fractions **1**-**3**, which were determined by previous titration assays. The experiments consisted in 10 replicates and the results were analyzed by Pearson x^2 test ($p \leq 0.001$). EPA and AA (Sigma-Aldrich) were tested at 7 µg/well on BT20 cells incubated for 18 and 24 hours.

8.3.5.2. Cell cycle analysis

Cell cycle analysis was carried out by staining BT20 lines with hypotonic PI. BT20 populations were incubated for 48 h with fractions **1**-**2** (2.5 µg/well each) and fraction **3** (4 µg/well). The PI stained samples were analysed by flow cytometry (Becton-

Dickinson) and the percentages of cells in each phase of the cell cycle were calculated by Mod-fit software.

8.3.5.3. Western blotting

After treatment with Vepesid, fractions **1**-**3** (fraction **1**: 4.11 μg/well; fraction **2**: 2.67 μg/well; fraction **3***: 4 μg/well; fraction **3**: 2 μg/well) and medium, 1 x 10^7 BT20 cells/ml were harvested, washed twice with cold phosphate-buffered saline solution, pelleted by centrifugation, and lysed in ice-cold buffer. Protein concentration of the cell lysates was measured using the Micro BCA protein assay reagent kit (Pierce, Milan, Italy). Equal amounts of proteins (10 μg/lane) from each sample were separated by SDS-PAGE (10% acrylamide) and were electrophoretically transferred to nitrocellulose (Hybond-C nitrocellulose membrane, Amersham). Both uncleaved and cleaved caspases were detected by probing the filters with anticaspase 8 and anticaspase 9 mAb (UBI, Lake Placid, NY) followed by horseradish peroxidase-conjugated goat antimouse immunoglobulin, used as developing reagent. The reaction was detected by enhanced chemiluminescence detection reagents (Amersham) and exposure to Hyperfilm-MP (De Totero *et al.* 2006).

8.4. New compounds from the Mediterranean mollusc *A. fasciata* (Mollusca, Anaspidea)

8.4.1. Collection of the biological material

Three specimens of *Aplysia fasciata* were collected by snorkeling in Bahía dels Alfacs, Delta de l'Ebre (Tarragona, Spain), during January 2008 at 1-1.5 m depth. The animals were transferred to the Departament de Biologia Animal (Invertebrats), Facultat de Biologia, Universitat de Barcelona, where they were dissected by means of a bistoury on a binocular microscope, and using glass Petri dishes in order to avoid possible contaminations from plastic material. Each individual was dissected into mantle and main internal organs, and the obtained sections were frozen and freeze-dried. The lyophilization was carried out in a Telstar CRYODOS freeze-drier and the specimens were stored at -20°C until shipment to the Department of Pharmacognosy and Chemistry of Natural Products (School of Pharmacy, University of Athens).

8.4.2. Extraction

The different anatomical parts of *A. fasciata* were separately and exhaustively extracted three times at room temperature with a mixture of CH_2Cl_2/MeOH 2:1 v/v (3 x 50 ml), and kept overnight. The samples with coarse texture were previously cut, crumbled in a mortar and subjected to ultrasound vibration in order to improve the

tissue fragmentation. The crude extracts of the several anatomical sections were filtrated on paper filter and the organic solvents were evaporated until dryness under reduced pressure. The afforded yields are reported in Table 8.1.

8.4.3. TLC screening

The TLC screening was performed on analytical silica TLC plates (Merck Kieselgel 60 F_{254}, 0.25 mm thickness, aluminium support) eluted with some mixtures of solvents (cHx/EtOAc 6:4 v/v, and CH_2Cl_2/MeOH 95:5 v/v). The plates were examined under UV light (254 and 365 nm) and revealed with 2 N cerium sulphate [$Ce(SO_4)_2$] in 15% H_2SO_4 in MeOH solution, by heating at 100°C for 1 min.

Anatomical sections	**Weight of the extracts**
Mucous secretion (A1)	527.4 mg
Stomach (A2)	58.6 mg
Opaline gland (A3)	8.8 mg
Buccal bulb (A4)	88.6 mg
Stomach content (A5)	32.8 mg
Reproductive system (A6)	126.1 mg
Mantle and foot (A7)	2.4 g
Digestive and hermaphroditic glands (A8)	3.0 g

Table 8.1. Anatomical sections of *A. fasciata* and corresponding yields of extraction.

8.4.4. Purification

The organic extract A8 (dark brown oil, 3.0 g) was fractionated by normal phase VLC. The separation was performed by VLC by means of a silica gel (Merck, 70-230 mesh) packed column. The extract, previously dissolved in a flask with CH_2Cl_2/MeOH 2:1 v/v (about 10 ml), was mixed with silica gel (5.0 g). The mixture, completely evaporated by vacuum until obtaining a dry powder, was distributed into the column in a thin layer. The column was eluted with cHx and increasing amounts of EtOAc (cHx 150 ml, cHx/EtOAc 9:1 v/v 150 ml, cHx/EtOAc 8:2 v/v 150 ml, cHx/EtOAc 7:3 v/v 150 ml, cHx/EtOAc 6:4 v/v 150 ml, cHx/EtOAc 1:1 v/v 150 ml, cHx/EtOAc 4:6 v/v 150 ml, cHx/EtOAc v/v 2:8 150 ml, EtOAc 150 ml). After TLC analysis, the recovered fractions were combined into 9 groups (A-I), as indicated in Table 8.2. Fraction C (20% EtOAc in cHx, 54.7 mg) was further fractionated by SPE. In particular, an aliquot of fraction C (about 20 mg) was dissolved in 1-2 ml of cHx, loaded onto a normal phase Sep-Pak pre-packed column (SiOH, Waters Associates) and eluted with a gradient of cHx/EtOAc: cHx 20 ml, cHx/EtOAc 95:5 v/v 20 ml, cHx/EtOAc 9:1 v/v 20 ml, cHx/EtOAc 85:15 v/v 20 ml, cHx/EtOAc 8:2 v/v 20 ml, cHx/EtOAc 1:1 v/v 20 ml, EtOAc 20 ml. The separation was repeated on *ca.* 20 mg-aliquots until exhausting fraction C. The recovered fractions, after analysis and comparison by TLC, were combined into three portions: C1 (24.1 mg), C2 (29.0 mg) and C3 (1.5 mg). Fraction C1 (24.1 mg) was previously subjected to normal phase

HPLC in isocratic conditions, using *n*-Hx/EtOAc (98:2 v/v) as eluant at 2 ml min^{-1} flow rate, to yield compounds **1** (2.2 mg), **3** (0.6 mg), **4** (1.1 mg), **12** (8.0 mg), and **13** (1.3 mg). Subsequently, fraction C1 was purified again by normal phase HPLC in isocratic conditions, using *n*-Hx/EtOAc (98:2 v/v) as mobile phase and at 1.5 ml min^{-1} flow rate, affording compounds **5** (0.6 mg), **6** (0.7 mg), **7** (0.6 mg), **8** (1.0 mg), **11** (0.8 mg), and **14** (0.6 mg). Fraction C2 (29.0 mg) was purified by normal phase HPLC, using cHx/EtOAc (95:5 v/v) in isocratic conditions as eluant and at 1.5 ml min^{-1} flow rate, to afford compounds **2** (0.8 mg) and **8** (1.0 mg).

Fraction	**Weight (mg)**	**Eluant system**
A	15.8	cHx
B	9.5	cHx/EtOAc 9:1 v/v
C	54.7	cHx/EtOAc 8:2 v/v
D	469.4	cHx/EtOAc 7:3 v/v
E	621.9	cHx/EtOAc 6:4 v/v
F	226.1	cHx/EtOAc 1:1 v/v
G	102.3	cHx/EtOAc 4:6 v/v
H	179.1	cHx/EtOAc 2:8 v/v
I	784.0	EtOAc

Table 8.2. VLC separation of A8.

Fraction F (50% EtOAc in cHx, 226.1 mg) was further fractionated by SPE on normal phase cartridges, eluting with a gradient of cHx/EtOAc (cHx 20 ml, cHx/EtOAc 98:2 v/v 20 ml, cHx/EtOAc 95:5 v/v 20 ml, cHx/EtOAc 9:1 v/v 20 ml, cHx/EtOAc 85:15 v/v 20 ml, cHx/EtOAc 8:2 v/v 20 ml, cHx/EtOAc 1:1 v/v 20 ml, EtOAc 20 ml) to yield eight fractions (F1-F8, Table 8.3). Fraction F3 (30.6 mg) was purified by normal phase HPLC by means of isocratic elution with cHx/EtOAc (75:25 v/v) and at 1.5 ml min^{-1} flow rate. Fractions F4 (36.9 mg) and F5 (20.5 mg) were repeatedly subjected to normal phase HPLC, using cHx/EtOAc (75:25 v/v) as eluant and at 2 ml min^{-1} flow rate. From these purifications we obtained pure compounds **10** (3.3 mg), **15** (8.4 mg), and **16** (11.3 mg).

Fraction	Weight (mg)	Eluant system
F1	11.7	cHx
F2	87.0	cHx/EtOAc 98:2 v/v
F3	30.6	cHx/EtOAc 95:5 v/v
F4	36.9	cHx/EtOAc 9:1 v/v
F5	20.5	cHx/EtOAc 85:15 v/v
F6	7.6	cHx/EtOAc 8:2 v/v
F7	8.3	cHx/EtOAc 1:1 v/v
F8	4.1	EtOAc v/v

Table 8.3. Yields of the SPE separation of fraction F.

Fraction G (60% EtOAc in cHx, 102.3 mg) was further fractionated by SPE on normal phase cartridges with a gradient of cHx/EtOAc (cHx 20 ml, cHx/EtOAc 95:5 v/v 20 ml, cHx/EtOAc 9:1 v/v 20 ml, cHx/EtOAc 85:15 v/v 20 ml, cHx/EtOAc 8:2 v/v 20 ml, cHx/EtOAc 1:1 v/v 20 ml, EtOAc 20 ml) to yield seven fractions (G1-G7, Table 8.4). Fractions G3 (23.9 mg), G4 (37.9 mg), and G5 (15.4 mg) were repeatedly purified by normal phase HPLC, using cHx/EtOAc (75:25 v/v) as eluant at 2 ml min^{-1} flow rate, to yield compounds **9** (6.8 mg), **15** (2.0 mg), and **16** (10.4 mg). All the normal phase HPLC purifications were performed using a CECIL 1100 Series liquid chromatography pump equipped with a GBC LC-1240 refractive index detector, and employing a Kromasil 100 SIL 5 µm column (MZ-Analysentechnik, 250 x 8 mm).

Fraction	**Weight (mg)**	**Eluant system**
G1	0.5	cHx
G2	13.2	cHx/EtOAc 95:5 v/v
G3	23.9	cHx/EtOAc 9:1 v/v
G4	37.9	cHx/EtOAc 85:15 v/v
G5	15.4	cHx/EtOAc 8:2 v/v
G6	10.7	cHx/EtOAc 1:1 v/v
G7	0.5	EtOAc

Table 8.4. Yields of the SPE separation of fraction G.

8.4.5. Acetilation of 2

An aliquot of epibrasilenol (**2**, 1 mg), previously isolated in the laboratory, was dissolved in 2 ml of pyridine in presence of an excess of Ac_2O. The mixture was stirred for 16 h at 70°C and, afterwards, the reaction was quenched by the addition of 5 ml of CH_2Cl_2 and 5 ml of distilled water. The mixture was separated in a funnel and the organic layer was evaporated to give a residue containing epibrasilenol acetate.

8.4.6. Acquisition of the spectroscopic data

Optical rotations were measured on a Perkin-Elmer model 341 polarimeter with a 10 cm cell. UV spectra were obtained on a Shimadzu UV-160A spectrophotometer, whereas IR spectra were recorded on a Paragon 500 Perkin-Elmer spectrometer. NMR spectra were recorded on Bruker AC 200, Bruker DRX 400, and Varian 600 spectrometers. Chemical shifts were expressed by the δ (ppm) scale using TMS as internal standard and referred to $CDCl_3$ like NMR solvent (δ_H 7.26 and δ_C 77.0). The 2D experiments (COSY, NOESY, HSQC, HMBC) were performed using standard Bruker or Varian pulse sequences. High resolution mass spectra were realized in the University of Notre Dame, Department of Chemistry and Biochemistry, Notre Dame, IN, USA. Low resolution EI mass spectra were recorded on either a Hewlett Packard 5973 mass spectrometer or a Thermo Electron Corporation DSQ mass spectrometer using a Direct-Exposure Probe. Low resolution CI mass spectra were recorded in the

positive mode on a Thermo Electron Corporation DSQ mass spectrometer, using a Direct-Exposure Probe and methane as CI reagent gas.

Brasilenol (1): Spectroscopic data according to those reported in the literature (Stallard *et al.* 1978).

Epibrasilenol (2): Spectroscopic data according to those reported in the literature (Stallard *et al.* 1978).

4-Hydroxy-5-brasilene (3): Spectroscopic data according to those reported in the literature (Amico *et al.* 1991; Wright *et al.* 1991).

6-Hydroxy-1-brasilene (4): colorless oil; $[\alpha]^{20}_{D}$ -70.0 (*c* 0.05, $CHCl_3$); UV ($CHCl_3$) λ_{max} (logε) 244.0 (2.32) nm; IR (thin film) ν_{max} 3485, 2956, 1383, 1264 cm^{-1}; ^1H NMR ($CDCl_3$, 400 MHz) δ 5.05 (1H, br *s*, H-2), 2.68 (1H, *m*, H-9), 2.12 (1H, *m*, H-8a), 1.97 (1H, *m*, H-10), 1.95 (1H, *m*, H-7β), 1.50 (1H, *m*, H-7α), 1.38 (1H, *m*, H-4a), 1.33 (1H, *m*, H-4b), 1.24 (1H, *m*, H-5), 1.18 (1H, *m*, H-8b), 1.02 (3H, *s*, H-13), 0.99 (3H, *d*, *J* = 6.8 Hz, H-15), 0.97 (3H, *d*, *J* = 6.8 Hz, H-12), 0.96 (3H, *d*, *J* = 6.9 Hz, H-11), 0.89 (3H, *s*, H-14); ^{13}C NMR ($CDCl_3$, 50.3 MHz) δ 148.3 (C, C-1), 129.2 (CH, C-2), 79.9 (C, C-6), 46.3 (CH, C-5), 37.4 (CH_2, C-7), 34.8 (CH_2, C-4), 33.9 (CH, C-9), 33.0 (C, C-3), 31.4 (CH_3, C-13), 30.9 (CH_2, C-8), 28.1 (CH, C-10), 27.7 (CH_3, C-14), 23.6 (CH_3, C-12), 19.6 (CH_3, C-11), 19.2 (CH_3, C-15); EIMS 70 eV *m*/*z* (rel. int. %) 222 (4), 204 (27), 189 (100), 179 (4), 161 (24), 147 (22), 131 (24), 119 (35), 105 (44), 91 (27), 77 (13), 55 (10); FAB-HRMS *m*/*z* 221.1909 $[M - H]^+$ (calcd. for $C_{15}H_{25}O$, 221.1905).

Brasilenol acetate (5): Spectroscopic data according to those reported in the literature (Stallard *et al.* 1978).

Epibrasilenol acetate (6): colorless oil; $[\alpha]^{20}_D$ +10.0 (*c* 0.05, $CHCl_3$); UV ($CHCl_3$) λ_{max} (logε) 243.0 (1.92) nm; IR (thin film) ν_{max} 2928, 1733, 1378, 1261 cm^{-1}; ^1H NMR ($CDCl_3$, 400 MHz) δ 4.96 (1H, br *s*, H-2), 2.60 (1H, *m*, H-9), 2.27 (1H, *m*, H-7a), 2.08 (1H, *m*, H-8a), 2.05 (1H, *m*, H-5), 2.01 (3H, *s*, H-17), 1.98 (1H, *m*, H-10), 1.59 (1H, *m*, H-7b), 1.41 (1H, *m*, H-4a), 1.38 (1H, *m*, H-8b), 1.09 (1H, *m*, H-4b), 0.97 (3H, *d*, *J* = 6.9 Hz, H-15), 0.91 (3H, *d*, *J* = 6.8 Hz, H-12), 0.90 (3H, *s*, H-14), 0.82 (3H, *s*, H-13), 0.70 (3H, *d*, *J* = 6.8 Hz, H-11); ^{13}C NMR ($CDCl_3$, 50.3 MHz) δ 171.7 (C, C-16), 141.8 (C, C-6), 138.0 (C, C-1), 72.3 (CH, C-2), 40.2 (CH, C-5), 39.6 (CH, C-9), 34.4 (CH_2, C-7), 33.9 (C, C-3), 32.0 (CH_2, C-8), 30.6 (CH_2, C-4), 29.6 (CH, C-10), 27.6 (CH_3, C-14), 24.7 (CH_3, C-13), 21.8 (CH_3, C-17), 20.8 (CH_3, C-12), 19.7 (CH_3, C-15), 17.3 (CH_3, C-11); EIMS 70 eV *m*/*z* (rel. int. %) 204 (37), 189 (100), 161 (38), 145 (19), 131 (16), 119 (34), 105 (34), 91 (18), 77 (9), 55 (6), 43 (17); FAB-HRMS *m*/*z* 265.2195 $[M + H]^+$ (calcd. for $C_{17}H_{29}O_2$, 265.2168).

4-Acetoxy-5-brasilene (7): Spectroscopic data according to those reported in the literature (Amico *et al.* 1991; Wright *et al.* 1991).

6-e*pi*-β-Snyderol (8): colorless oil; $[\alpha]^{20}_D$ -36.0 (*c* 0.05, $CHCl_3$); UV ($CHCl_3$) λ_{max} (logε) 242.5 (2.75) nm; IR (thin film) ν_{max} 3431, 2966, 1457, 1263, 897 cm^{-1}; ^1H NMR ($CDCl_3$, 400 MHz) δ 5.84 (1H, *dd*, *J* = 17.4, 10.7 Hz, H-2), 5.17 (1H, br *d*, *J* = 17.4 Hz, H-1a), 5.04 (1H, br *d*, *J* = 10.7 Hz, H-1b), 4.78 (1H, br *s*, H-14a), 4.59 (1H, br *s*, H-14b), 4.31 (1H, *dd*, *J* = 11.2, 4.0 Hz, H-10), 2.14 (1H, *m*, H-9α), 2.11 (2H, *m*, H-8), 1.98 (1H, *m*, H-9β), 1.95 (1H, *m*, H-6), 1.58 (1H, *m*, H-5a), 1.39 (1H, *m*, H-4a), 1.28 (1H, *m*, H-5b), 1.27 (1H, *m*, H-4b), 1.25 (3H, *s*, H-15), 1.04 (3H, *s*, H-13), 1.01 (3H, *s*, H-12); ^{13}C NMR ($CDCl_3$, 50.3 MHz) δ 146.1 (C, C-7), 144.9 (CH, C-2), 111.8 (CH_2, C-1), 111.7 (CH_2, C-14), 73.2 (C, C-3), 63.3 (CH, C-10), 55.2 (CH, C-6), 40.5 (CH_2, C-4), 39.9 (C, C-11), 34.7 (CH_2, C-9), 31.7 (CH_2, C-8), 28.3 (CH_3, C-15), 27.5 (CH_3, C-13), 23.7 (CH_3, C-12), 20.2 (CH_2, C-5); EIMS 70 eV *m*/*z* (rel. int. %) 282:284 (4:4), 267:269 (12:12), 254:256 (7:7),

240:242 (5:5), 225:227 (3:3), 203 (53), 187 (42), 173 (24), 159 (32), 145:147 (32:32), 131 (40), 119:121 (58:59), 105 (73), 91 (100), 79 (80), 71 (66), 55 (39), 41 (74); FAB-HRMS *m/z* 221.1882 $[M - Br]^+$ (calcd. for $C_{15}H_{25}O$, 221.1905).

Luzodiol (9): Spectroscopic data according to those reported in the literature (Kuniyoshi *et al.* 2005).

(3*Z*,9*Z*)-7-Chloro-6-hydroxy-12-oxopentadeca-3,9-dien-1-yne (10): colorless oil; $[\alpha]^{20}_D$ -9.5 (*c* 0.20, $CHCl_3$); UV ($CHCl_3$) λ_{max} (logε) 225.0 (3.18) nm; IR (thin film) ν_{max} 2932, 1716, 1265 cm^{-1}; ^1H NMR ($CDCl_3$, 600 MHz) δ 6.08 (1H, *dt*, *J* = 10.7, 7.4 Hz, H-4), 5.73 (1H, *m*, H-10), 5.61 (1H, *m*, H-9), 5.59 (1H, *m*, H-3), 3.91 (1H, *ddd*, *J* = 7.7, 6.8, 3.2 Hz, H-7), 3.77 (1H, *m*, H-6), 3.21 (2H, *d*, *J* = 7.1 Hz, H-11), 3.13 (1H, *d*, *J* = 2.0 Hz, H-1), 2.69 (1H, *m*, H-5a), 2.66 (1H, *m*, H-8a), 2.60 (1H, *m*, H-5b), 2.52 (1H, *m*, H-8b), 2.41 (2H, *t*, *J* = 7.3 Hz, H-13), 1.58 (2H, *m*, H-14), 0.90 (3H, *t*, *J* = 7.4 Hz, H-15); ^{13}C NMR ($CDCl_3$, 150 MHz) δ 208.7 (C, C-12), 140.3 (CH, C-4), 128.1 (CH, C-9), 124.7 (CH, C-10), 111.1 (CH, C-3), 82.4 (CH, C-1), 77.2 (C, C-2), 71.9 (CH, C-6), 66.5 (CH, C-7), 44.7 (CH_2, C-13), 41.5 (CH_2, C-11), 35.6 (CH_2, C-5), 33.2 (CH_2, C-8), 17.2 (CH_2, C-14), 13.7 (CH_3, C-15); PCIMS CH_4 *m/z* (rel. int. %) 269:271 (3:1), 251:253 (2:0.7), 233 (10), 203:205 (13:4), 191 (3), 165 (8), 147 (15), 129 (10), 121 (8), 105 (13), 95 (9), 71 (100), 55(3); ESI-HRMS *m/z* 291.1140 $[M + Na]^+$ (calcd. for $C_{15}H_{21}ClNaO_2$, 291.1128).

(3*Z*,9*Z*,12*Z*)-6-Acetoxy-7-chloropentadeca-3,9,12-trien-1-yne (11): ^1H NMR ($CDCl_3$, 400 MHz) δ 5.93 (1H, *dt*, *J* = 10.9, 7.5 Hz, H-4), 5.58 (1H, *dd*, *J* = 10.9, 2.2 Hz, H-3), 5.52 (1H, *m*, H-10), 5.42 (1H, *m*, H-9), 5.39 (1H, *m*, H-13), 5.24 (1H, *m*, H-12), 5.15 (1H, *ddd*, *J* = 7.5, 5.4, 4.0 Hz, H-6), 3.94 (1H, *ddd*, *J* = 8.2, 5.4, 4.0 Hz, H-7), 3.13 (1H, *d*, *J* = 2.2 Hz, H-1), 2.77 (2H, *m*, H-11), 2.74 (2H, *m*, H-5), 2.53 (2H, *m*, H-8), 2.10 (3H, *s*, H-17), 2.04 (2H, *m*, H-14), 0.95 (3H, *t*, *J* = 7.5 Hz, H-15); ^{13}C NMR ($CDCl_3$, 50.3 MHz) δ

170.3 (C, C-16), 138.9 (CH, C-4), 132.4 (CH, C-10), 131.7 (CH, C-13), 126.4 (CH, C-12), 124.3 (CH, C-9), 111.7 (CH, C-3), 82.7 (CH, C-1), 77.2 (C, C-2), 73.4 (CH, C-6), 62.5 (CH, C-7), 32.4 (CH_2, C-5), 32.2 (CH_2, C-8), 25.7 (CH_2, C-11), 20.9 (CH_2, C-14), 20.6 (CH_3, C-17), 14.2 (CH_3, C-15).

(3*Z*)-Venustinene (12): Spectroscopic data according to those reported in the literature (Suzuki *et al.* 1983).

(3*Z*)-13-*epi*-Pinnatifidenyne (13): Spectroscopic data according to those reported in the literature (San-Martín *et al.* 1997).

(3*E*)-Laurenyne (14): Spectroscopic data according to those reported in the literature (Falshaw *et al.* 1980; Overman & Thompson 1988).

16-Acetoxy-15-bromo-7-hydroxy-9(11)-parguerene (15): yellow oil; $[\alpha]^{20}_D$ -62.4 (*c* 0.50, $CHCl_3$); UV ($CHCl_3$) λ_{max} (logε) 248.5 (2.96) nm; IR (thin film) ν_{max} 3417, 2930, 1734, 1265, 1035 cm^{-1}; ^1H NMR ($CDCl_3$, 400 MHz) δ 5.33 (1H, br *d*, *J* = 6.2 Hz, H-11), 4.55 (1H, *m*, H-16a), 4.27 (1H, *m*, H-15), 4.25 (1H, *m*, H-16b), 3.14 (1H, *td*, *J* = 10.4, 4.6 Hz, H-7), 2.42 (1H, *m*, H-12β), 2.33 (1H, *m*, H-8), 2.24 (1H, *m*, H-14β), 2.11 (1H, *m*, H-6α), 2.09 (3H, *s*, H-22), 1.96 (1H, *m*, H-2β), 1.80 (1H, *m*, H-12α), 1.79 (1H, *m*, H-2α), 1.60 (1H, *m*, H-6β), 1.59 (1H, *m*, H-1β), 1.38 (1H, *dd*, *J* = 13.1, 10.3 Hz, H-14α), 1.12 (1H, *dd*, *J* = 13.5, 3.4 Hz, H-5), 1.05 (3H, *s*, H-17), 0.97 (3H, *s*, H-19), 0.96 (3H, *s*, H-20), 0.85 (1H, *dt*, *J* = 12.9, 6.0 Hz, H-1α), 0.63 (1H, *dt*, *J* = 9.2, 6.2 Hz, H-3), 0.40 (1H, *dd*, *J* = 9.3, 4.1 Hz, H-18a), -0.05 (1H, *dd*, *J* = 5.6, 4.4 Hz, H-18b); ^{13}C NMR ($CDCl_3$, 50.3 MHz) δ 170.7 (C, C-21), 144.1 (C, C-9), 116.8 (CH, C-11), 77.4 (CH, C-7), 66.1 (CH_2, C-16), 59.8 (CH, C-15), 46.4 (CH, C-5), 38.9 (CH_2, C-12), 38.8 (CH, C-8), 38.2 (CH_2, C-14), 37.0 (C, C-10), 35.5 (C, C-13), 35.1 (CH_2, C-6), 31.0 (CH_2, C-1), 24.3 (CH_3, C-17), 24.0

(CH_3, C-19), 21.3 (CH_2, C-18), 21.0 (CH_3, C-22), 19.3 (CH_2, C-2), 19.2 (CH, C-3), 17.8 (CH_3, C-20), 15.9 (C, C-4); PCIMS CH_4 *m/z* (rel. int. %) 407:409 (11:11), 347:349 (21:21), 326 (7), 313 (5), 285 (16), 267 (100), 251 (30), 241 (33), 225 (16), 211 (15), 197 (14), 185 (17), 171 (20), 145 (27), 131 (17), 109 (20), 95 (24), 81 (19), 61 (59); FAB-HRMS *m/z* 365.1505 $[M - OAc]^+$ (calcd. for $C_{20}H_{30}BrO$, 365.1480).

15-Bromo-2,16-diacetoxy-7-hydroxy-9(11)-parguerene (16): Spectroscopic data according to those reported in the literature (Higgs & Faulkner 1982).

8.5. New casbane diterpenes from the Chinese soft coral *Sinularia* sp.: structures and biological activities

8.5.1. Collection of the biological material

A grey-yellowish sample of *Sinularia* sp. was collected by SCUBA diving at 20 m depth, during January 2004 along the coast of Hainan Island, in Lingshui county, China. The biological material was frozen after collection, transferred to the laboratory of ICB, and stored at -20°C until extraction.

8.5.2. Extraction

The specimen was divided into small pieces and extracted three times with acetone (3 x 150 ml) at room temperature, improving the extractive process by crumbling in a mortar and sonicating in an ultrasound bath. The acetone extract was filtered on paper and, hence, evaporated under reduced pressure until removing the organic solvent. The remaining aqueous residue was diluted in distilled water, transferred

into a separatory funnel and extracted three times with diethyl ether (3 x 150 ml). The organic phase was dried *in vacuo* affording the crude diethyl ether extract (2.2 g).

8.5.3. TLC screening

The TLC screening was realized on silica plates (Merck Kieselgel 60 F_{254}, 5 x 10 cm, 0.25 mm thickness). Small amounts of the diethyl ether extract were deposed onto the silica plates, which were eluted with different mixtures of solvents at increasing polarity: light petroleum, light petroleum/diethyl ether 8:2 v/v, light petroleum/diethyl ether 1:1 v/v, light petroleum/diethyl ether 2:8 v/v, diethyl ether, chloroform/methanol 9:1 v/v, chloroform/methanol 95:5 v/v, chloroform/methanol 8:2 v/v, chloroform/methanol 7:3 v/v, chloroform/methanol 6:4 v/v. The TLC plates were observed under UV light (254 nm), and revealed with 2 N cerium sulphate [$Ce(SO_4)_2$] in 10% H_2SO_4 aqueous solution, by heating at 100°C for 1 min.

8.5.4. Fractionation of the diethyl ether extract

An aliquot of the diethyl ether extract (389.0 mg) was separated by liquid chromatography. The column was packed with silica gel Merck Kieselgel 60 (0.063-0.200 nm), equilibrated with light petroleum and eluted with an increasing polarity gradient of light petroleum/diethyl ether (light petroleum, light petroleum/diethyl ether 9:1 v/v, light petroleum/diethyl ether 8:2 v/v, light petroleum/diethyl ether 7:3

v/v, light petroleum/diethyl ether 6:4 v/v, light petroleum/diethyl ether 1:1 v/v, light petroleum/diethyl ether 4:6 v/v, diethyl ether and chloroform/methanol 1:1 v/v). After TLC analysis, the recovered fractions were combined into 9 groups, as reported in Table 8.5.

Fraction	Weight (mg)
1	96.7
2	27.2
3	29.3
4	45.5
5	58.8
6	69.3
7	27.5
8	31.8
9	1.9

Table 8.5. Yields of separation of the diethyl ether extract from *Sinularia* sp.

Fraction 1 (96.7 mg) was purified by preparative TLC. The sample was charged onto a semipreparative silica plate (Merck Kieselgel 60 F_{254}, 0.5 mm thickness), using light petroleum/diethyl ether 9:1 v/v as mobile phase. The silica gel corresponding to both the UV-visible bands at R_f 0.63 and 0.50 (light petroleum/diethyl ether 9:1 v/v) was

scraped off, charged into a Pasteur pipette and eluted with chloroform. This procedure allowed isolating 13.0 mg of a mixture, composed mainly by compound **1**, and 5.5 mg of compound **2**. The mixture containing **1** was further purified by preparative TLC using benzene as eluant. The silica gel corresponding to the UV-visible spot at R_f 0.26 (benzene) was scraped off, put into a Pasteur pipette and eluted with chloroform. Pure compound **1** (6.7 mg) was, hence, obtained.

Fraction 6 (69.3 mg) was purified by preparative TLC. The sample was charged onto a semipreparative silica plate Merck Kieselgel 60 F_{254} (0.5 mm thickness) and eluted with light petroleum/diethyl ether 3:7 v/v. The silica gel corresponding to both the UV-visible bands at R_f 0.50 and 0.43 (light petroleum/diethyl ether 3:7 v/v) was scraped off, charged into a Pasteur pipette and eluted with chloroform. This procedure allowed isolating 40.6 mg of pure compound **3**, and 5.1 mg of **4**.

8.5.5. Acquisition of the spectroscopic data

Optic rotation measurements were realized on a Jasco DIP-370 polarimeter, equipped with a 10 cm long cell. IR and UV spectra were acquired by a Bio-Rad FTS 155 FTIR spectrophotometer and an Agilent 8453 spectrophotometer, respectively. Mono- and bidimensional NMR spectra were recorded on a Bruker Avance DRX-400 spectrometer, operating at 400 MHz, and on a Bruker DRX-600 spectrometer, operating at 600 MHz and provided with an inverse TCI CryoProbe. ^{13}C NMR

spectra were, instead, recorded on a Bruker DPX-300 spectrometer, operating at 300 MHz and equipped with a dual probe. The chemical shifts have been reported in ppm and referred to $CDCl_3$ as internal standard (δ_H 7.26 and δ_C 77.0). Low and high resolution ESIMS mass spectra were recorded on a Micromass Q-TOF Micro™ spectrometer coupled with a Waters Alliance 2695 HPLC.

Compound 1: colorless oil; $[\alpha]^{25}_D$ -80.0 (*c* 0.26, $CHCl_3$); TLC R_f 0.63 (light petroleum/diethyl ether 9:1 v/v); UV (EtOH) λ_{max} (log ε) 271 (3.56) nm; IR (KBr) ν_{max} 1655 cm^{-1}; ^1H NMR ($CDCl_3$, 400 MHz) δ 6.37 (1H, *d*, *J* = 10.2 Hz, H-3), 5.08 (1H, *t*, *J* = 6.6 Hz, H-7), 4.84 (1H, *t*, *J* = 5.4 Hz, H-11), 3.55 (1H, *dd*, *J* = 13.8, 8.4 Hz, H-6a), 2.97 (1H, *dd*, *J* = 13.8, 5.7 Hz, H-6b), 2. 20 (1H, *m*, H-13a), 2.17 (1H, *m*, H-10a), 2.15 (1H, *m*, H-9a), 2.05 (1H, *m*, H-14a), 2.00 (1H, *m*, H-9b), 1.96 (1H, *m*, H-10b), 1.87 (3H, *s*, H-18), 1.75 (1H, *m*, H-13b), 1.56 (3H, *s*, H-19), 1.56 (3H, *s*, H-20), 1.50 (1H, *dd*, *J* = 10.2, 8.7 Hz, H-2), 1.16 (3H, *s*, H-16), 1.15 (1H, *m*, H-1), 1.09 (3H, *s*, H-17), 0.80 (1H, *m*, H-14b); ^{13}C NMR ($CDCl_3$, 300 MHz) δ 199.9 (C, C-5), 143.1 (CH, C-3), 137.1 (C, C-8), 136.6 (C, C-4), 135.9 (C, C-12), 124.4 (CH, C-11), 119.4 (CH, C-7), 39.9 (CH_2, C-13), 39.4 (CH_2, C-6), 39.0 (CH_2, C-9), 35.2 (CH, C-1), 29.0 (CH_3, C-16), 27.6 (CH, C-2), 26.3 (CH_2, C-14), 25.4 (C, C-15), 23.9 (CH_2, C-10), 15.8 (CH_3, C-17), 15.6 (CH_3, C-19), 15.3 (CH_3, C-20), 11.6 (CH_3, C-18); EI-HRMS *m*/*z* 286.2291 (calcd. for $C_{20}H_{30}O$, 286.2297).

Compound 2: colorless oil; $[\alpha]^{25}_D$ +34.0 (*c* 0.25, $CHCl_3$); TLC R_f 0.50 (light petroleum/diethyl ether 9:1 v/v); UV (MeOH) λ_{max} (log ε) 274 (5.0) nm; IR (KBr) ν_{max} 1653 cm^{-1}; ^1H NMR ($CDCl_3$, 400 MHz) δ 6.11 (1H, *d*, *J* = 10.2 Hz, H-3), 5.21 (1H, br *d*, *J* = 11.1 Hz, H-7), 4.88 (1H, br *d*, *J* = 8.4 Hz, H-11), 3.71 (1H, *dd*, *J* = 13.8, 11.1 Hz, H-6a), 2.83 (1H, br *d*, *J* = 13.8 Hz, H-6b), 2.28 (1H, *m*, H-10a), 2.18 (1H, *m*, H-9a), 2.17 (1H, *m*, H-13a), 2.10 (1H, *m*, H-9b), 2.07 (1H, *m*, H-10b), 1.93 (1H, *m*, H-13b), 1.88 (1H, *m*, H-

14a), 1.80 (3H, *s*, H-18), 1.59 (3H, *s*, H-19), 1.59 (3H, *s*, H-20), 1.16 (3H, *s*, H-16), 1.11 (3H, *s*, H-17), 1.03 (1H, *m*, H-14b), 1.08 (1H, *m*, H-2), 0.71 (1H, *m*, H-1); ^{13}C NMR ($CDCl_3$, 300 MHz) δ 201.2 (C, C-5), 149.4 (CH, C-3), 135.1 (C, C-8), 133.5 (C, C-12), 132.8 (C, C-4), 125.4 (CH, C-11), 121.7 (CH, C-7), 40.4 (CH_2, C-6), 38.8 (CH_2, C-13), 38.4 (CH_2, C-9), 37.5 (CH, C-1), 31.9 (CH, C-2), 28.1 (C, C-15), 24.4 (CH_2, C-14), 24.0 (CH_2, C-10), 23.7 (CH_3, C-17), 22.0 (CH_3, C-16), 14.8 (CH_3, C-20), 14.7 (CH_3, C-19), 11.2 (CH_3, C-18); EI-HRMS *m*/*z* 286.2306 (calcd. for $C_{20}H_{30}O$, 286.2297).

Compound 3: colorless oil; $[\alpha]^{25}_D$ -218.0 (*c* 0.55, $CHCl_3$); TLC R_f 0.50 (light petroleum/diethyl ether 3:7 v/v); UV (EtOH) λ_{max} (log ε) 270 (4.76) nm; IR (KBr) ν_{max} 3388, 1650 cm^{-1}; ^{1}H NMR ($CDCl_3$, 400 MHz) δ 6.30 (1H, *d*, *J* = 10.5 Hz, H-3), 5.11 (1H, *t*, *J* = 6.6 Hz, H-7), 5.06 (1H, *d*, *J* = 9.3 Hz, H-11), 4.38 (1H, *td*, *J* = 9.3, 3.9 Hz, H-10), 3.50 (1H, *dd*, *J* = 13.8, 8.4 Hz, H-6a), 3.02 (1H, *dd*, *J* = 13.8, 5.7 Hz, H-6b), 2.39 (1H, *m*, H-9a), 2.38 (1H, *m*, H-13a), 2.07 (1H, *m*, H-9b), 2.07 (1H, *m*, H-14a), 1.83 (3H, *s*, H-18), 1.80 (1H, *m*, H-13b), 1.66 (3H, *s*, H-19), 1.63 (3H, *s*, H-20), 1.50 (1H, *dd*, *J* = 10.2, 8.4 Hz, H-2), 1.19 (1H, *m*, H-14b), 1.18 (3H, *s*, H-16), 1.15 (1H, *m*, H-1), 1.06 (3H, *s*, H-17); ^{13}C NMR ($CDCl_3$, 300 MHz) δ 200.0 (C, C-5), 142.9 (CH, C-3), 140.8 (C, C-12), 136.2 (C, C-4), 134.5 (C, C-8), 127.8 (CH, C-11), 120.5 (CH, C-7), 67.5 (CH, C-10), 46.7 (CH_2, C-9), 39.8 (CH_2, C-6), 39.2 (CH_2, C-13), 35.2 (CH, C-1), 29.0 (CH_3, C-16), 28.6 (CH, C-2), 25.8 (CH_2, C-14), 25.3 (C, C-15), 18.5 (CH_3, C-19), 18.3 (CH_3, C-20), 15.7 (CH_3, C-17), 11.5 (CH_3, C-18); EI-HRMS *m*/*z* 302.2240 (calcd. for $C_{20}H_{30}O_2$, 302.2246).

Compound 4: colorless oil; $[\alpha]^{25}_D$ +4.5 (*c* 0.54, $CHCl_3$); TLC R_f 0.43 (light petroleum/diethyl ether 3:7 v/v); UV (EtOH) λ_{max} (log ε) 270 (4.82) nm; IR (KBr) ν_{max} 3399, 1651 cm^{-1}; ^{1}H NMR ($CDCl_3$, 400 MHz) δ 6.04 (1H, *d*, *J* = 10.2 Hz, H-3), 5.27 (1H, overlapped, H-7), 5.26 (1H, overlapped, H-11), 4.31 (1H, *td*, *J* = 9.6, 3.8 Hz, H-10), 3.63 (1H, *dd*, *J* = 14.3, 11.0 Hz, H-6a), 2.89 (1H, br *d*, *J* = 14.3 Hz, H-6b), 2.48 (1H, br *d*, *J* =

11.4 Hz, H-9a), 2.33 (1H, *m*, H-13a), 2.13 (1H, *m*, H-13b), 2.06 (1H, *m*, H-9b), 1.99 (1H, *m*, H-14a), 1.77 (3H, *s*, H-18), 1.71 (3H, *s*, H-19), 1.59 (3H, *s*, H-20), 1.27 (1H, *m*, H-14b), 1.15 (3H, *s*, H-16), 1.11 (3H, *s*, H-17), 1.03 (1H, *m*, H-2), 0.57 (1H, *m*, H-1); ^{13}C NMR ($CDCl_3$, 300 MHz) δ 200.4 (C, C-5), 148.1 (CH, C-3), 140.1 (C, C-12), 133.0 (C, C-8), 129.2 (CH, C-11), 122.9 (CH, C-7), 68.7 (CH, C-10), 46.4 (CH_2, C-9), 40.6 (CH_2, C-6), 40.1 (CH_2, C-13), 37.0 (CH, C-1), 35.2 (CH, C-2), 29.7 (C, C-15), 25.4 (CH_2, C-14), 23.0 (CH_3, C-17), 22.0 (CH_3, C-16), 19.0 (CH_3, C-19), 14.8 (CH_3, C-20), 11.1 (CH_3, C-18); ESI-HRMS *m/z* 325.2140 (calcd. for $C_{20}H_{30}O_2Na$, 325.2144).

8.5.6. Preparation of the MTPA esters of compounds 3 and 4

Aliquots of **3** (2.7 mg) and **4** (2.5 mg) were dissolved in 1 ml of anhydrous CH_2Cl_2. Afterwards, each solution was divided into two parts: one was derivatized with 15 µl of (*R*)-MTPA chloride and 0.2 ml of DMAP, and the other one with 15 µl of (*S*)-MTPA and 0.2 ml of DMAP. All the mixtures of reaction were kept overnight at room temperature and stirred. After evaporating the solvent under reduced pressure, the mixtures were worked-up by TLC. Every sample was charged onto a different analytic TLC silica plate (10 x 20 cm) and eluted with light petroleum/diethyl ether 8:2 v/v. The silica gel corresponding to the UV-visible bands at R_f 0.30 (light petroleum/diethyl ether 8:2 v/v) for both the MTPA esters of **3**, and at R_f 0.25 (light petroleum/diethyl ether 8:2 v/v) for both the MTPA esters of **4**, was scraped off, put into a Pasteur pipette and eluted with $CHCl_3$. After evaporation of the solvent, 1.0 mg of pure (*S*)-MTPA ester and 1.2 mg of the pure (*R*)-MTPA ester of **3**, as well as 0.9

mg of (*S*)-MTPA ester and 0.7 mg of (*R*)-MTPA ester of **4**, were obtained and subjected to ^{1}H NMR analysis.

(*S*)-MTPA ester of 3: selected ^{1}H NMR values ($CDCl_3$, 400 MHz): δ 6.27 (1H, *d*, *J* = 10.5 Hz, H-3), 5.65 (1H, *ddd*, *J* = 14.0, 10.0, 4.0 Hz, H-10), 5.17 (1H, *t*, *J* = 6.6 Hz, H-7), 5.06 (1H, *d*, *J* = 9.3 Hz, H-11), 3.53 (3H, *s*, OMe), 3.50 (1H, *m*, H-6a), 3.02 (1H, *dd*, *J* = 13.8, 5.7 Hz, H-6b), 2.41 (1H, *m*, H-13a), 2.35 (1H, *m*, H-9a), 2.18 (1H, *m*, H-9b), 1.85 (1H, *m*, H-13b), 1.85 (3H, *s*, H_3-18), 1.72 (3H, *s*, H_3-20), 1.64 (3H, *s*, H_3-19), 1.18 (3H, *s*, H_3-16), 1.05 (3H, *s*, H_3-17).

(*R*)-MTPA ester of 3: selected ^{1}H NMR values ($CDCl_3$, 400 MHz): δ 6.26 (1H, *d*, *J* = 10.5 Hz, H-3), 5.62 (1H, *ddd*, *J* = 14.0, 10.0, 4.0 Hz, H-10), 5.19 (1H, *t*, *J* = 6.6 Hz, H-7), 4.94 (1H, *d*, *J* = 9.3 Hz, H-11), 3.54 (3H, *s*, OMe), 3.52 (1H, *m*, H-6a), 3.03 (1H, *dd*, *J* = 13.8, 5.7 Hz, H-6b), 2.45 (1H, *m*, H-9a), 2.35 (1H, *m*, H-13a), 2.28 (1H, *m*, H-9b), 1.85 (1H, *m*, H-13b), 1.85 (3H, *s*, H_3-18), 1.71 (3H, *s*, H_3-20), 1.66 (3H, *s*, H_3-19), 1.18 (3H, *s*, H_3-16), 1.05 (3H, *s*, H_3-17).

(*S*)-MTPA ester of 4: selected ^{1}H NMR values ($CDCl_3$, 400 MHz): δ 6.02 (1H, *d*, *J* = 10.2 Hz, H-3), 5.66 (1H, *ddd*, *J* = 13.4, 9.8, 3.8 Hz, H-10), 5.35 (1H, br *d*, *J* = 8.3 Hz, H-7), 5.28 (1H, *d*, *J* = 9.3 Hz, H-11), 3.61 (1H, *dd*, *J* = 14.3, 10.9 Hz, H-6a), 3.53 (3H, *s*, OMe), 2.92 (1H, br *d*, *J* = 14.3 Hz, H-6b), 2.44 (1H, br *d*, *J* = 11.4 Hz, H-9a), 2.32 (1H, *m*, H-13a), 2.20 (1H, *dd*, *J* = 11.4, 10.5 Hz, H-9b), 2.16 (1H, *m*, H-13b), 1.99 (1H, *m*, H-14b), 1.78 (3H, *s*, H_3-18), 1.66 (3H, *s*, H_3-19), 1.62 (3H, *s*, H_3-20), 1.26 (1H, *m*, H-14a), 1.17 (3H, *s*, H_3-16), 1.10 (3H, *s*, H_3-17), 1.04 (1H, *m*, H-2), 0.56 (1H, *m*, H-1).

(*R*)-MTPA ester of 4: selected ^{1}H NMR values ($CDCl_3$, 400 MHz): δ 6.01 (1H, *d*, *J* = 10.2 Hz, H-3), 5.65 (1H, *ddd*, *J* = 13.2, 9.7, 3.7 Hz, H-10), 5.36 (1H, br *d*, *J* = 8.3 Hz, H-7),

5.17 (1H, *d*, *J* = 9.3 Hz, H-11), 3.60 (1H, *dd*, J = 14.3, 11.0 Hz, H-6a), 3.53 (3H, *s*, OMe), 2.93 (1H, br *d*, *J* = 14.3 Hz, H-6b), 2.52 (1H, br *d*, *J* = 11.4 Hz, H-9a), 2.35 (1H, *dd*, *J* = 11.4, 10.4 Hz, H-9b), 2.24 (1H, *m*, H-13a), 2.13 (1H, *m*, H-13b), 2.01 (1H, *m*, H-14a), 1.78 (3H, *s*, H_3-18), 1.68 (3H, *s*, H_3-19), 1.58 (3H, *s*, H_3-20), 1.25 (1H, *m*, H-14b), 1.15 (3H, *s*, H_3-16), 1.09 (3H, *s*, H_3-17), 1.04 (1H, *m*, H-2), 0.55 (1H, *m*, H-1).

8.5.7. Feeding deterrence assays on *Palaemon elegans*

Compounds **1**-**4** were separately dissolved in 0.5 ml of acetone, and added to a mixture consisting of alginic acid (30 mg), ground freeze-dried squid mantle (50 mg) and purified sea sand (30 mg, AppliChem). Sand was included in the mixture in order to prevent the pellets floating on the water surface during the experiments. After evaporation of the solvent, the mixture was treated with one drop of food dye (E124 and E110) and, afterwards, diluted in distilled water until reaching 1 ml-volume. Food dye was added for an easy detection of the ingested food in the digestive tube of the shrimps. The mixture was stirred, loaded into a 5 ml-syringe and extruded into a 0.25 M $CaCl_2$ solution for 2 min to harden. The resulting spaghetti-like red strand was cut into 10 mm long pellets. Control foods were analogously prepared, with the addition of 0.5 ml of acetone but without the purified metabolites.

Palaemon elegans shrimps (average length 30 mm), collected by net along the coast of Pozzuoli (Naples, Italy) during July 2008, were kept in an aquarium for 1 week to get them used to the artificial food. After three days of total fasting, they were

individually placed in 500 ml beakers filled with 300 ml of seawater. Control and treated pellets were presented to shrimps in series of 10 independent replicates.

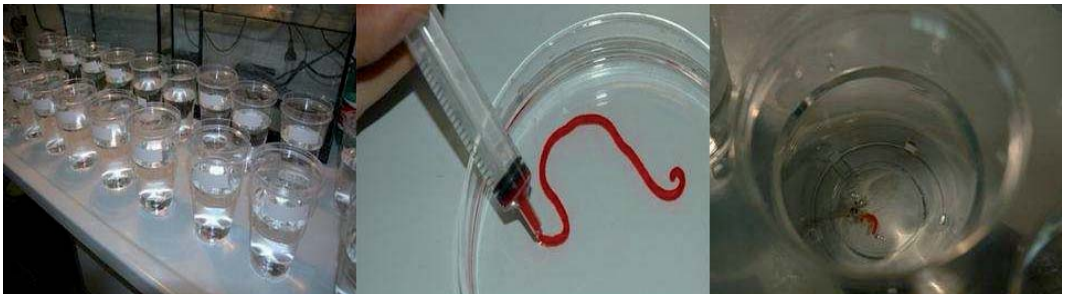

Fig. 8.2. Preparation of the feeding deterrence assay.

After 30 minutes, the presence of an evident red spot in the digestive tube of the shrimp was assumed as a proof of acceptance and, conversely, its absence was the sign of a rejection response. The differences between every treatment and the control were evaluated by exact Fisher's test. P values lower than 0.05 were considered statistically significant.

8.5.8. Antiproliferative activity assays

RBL-2H3 (rat basophilic leukaemia) cell line, kept in culture as indicated by the supplier (DSMZ, Germany), was seeded into a 6-well-multiwell (Falcon, Milan, Italy) at a density of about 5×10^4 cell/well. The cells were allowed to adhere for at least 4 h at 37°C at wet atmosphere (5% CO_2). Four hours after sowing, the compounds to be tested were added to the culture medium at the concentrations of 5 and 25 μg/ml.

The compounds were opportunely replaced at every change of the culture medium for the next 4 days. The cell vitality was evaluated by crystal violet coloration (Sigma, Milan, Italy).

8.5.9. Antibacterial activity assays

Isolated culture lines of both *Staphylococcus aureus* ($Gram^+$ bacterium) and *Escherichia coli* ($Gram^-$ bacterium) were cultured on LB medium (Luria Bertani broth: 10 g/l Bactotryptone, 5 g/l Bactoyeast and 10 g/l NaCl, pH 7.5) overnight under agitation at 37°C. The two *inocula* were diluted from 1 to 1,000 volumes on LB medium (= 10^8 CFU/ml). The bacterial suspensions (1 ml), hence, were homogeneously plated onto Petri dishes containing agar (LB solid medium). Aliquots of 20 µl (corresponding to 100 µg) of the compounds to be tested (**1**-**4**) were diluted in $CHCl_3$ to a concentration of 5 µg/ml. The obtained solutions were used to soak sterile absorbing paper dishes (5-6 mm diameter), whereas chloramphenicol (10 µg for both *S. aureus* and *E. coli*) was used to prepare the positive control dish. Each soaked dish was put into the middle of every Petri dish. Every compound was tested on both *S. aureus* and *E. coli*, for a total of 9 treatments. The dishes were incubated at 37°C turned downwards for 18-24 h. After that, the diameter of the bacterial growth inhibition (inhibition halo) was evaluated for each substance. Conventionally, the resistance or the susceptibility of the microorganism is expressed as: R (resistance): (-) or (+/-) if the inhibition halos

are less than 15 mm diameter; MS (mean susceptibility): (+) or (++) if the inhibition halos are included in the range 15-25 mm diameter; S (susceptibility): (+++) or (++++) if the inhibition halos are larger than 25 mm diameter.

9. Concluding remarks

The present report has dealt with the isolation, characterization and evaluation of possible applications of natural products from marine benthic organisms.

Within the PHARMAPOX project we have obtained some remarkable results. In the attempt to increase the diatom production in order to satisfy the amounts requested by the different partner Institutes, we have established better growth conditions for *Cocconeis neothumensis* diatoms, determining both the optimal light intensity and microelement concentration. In particular, diatom development was increased at 60 µmol photons m^{-2} sec^{-1} in presence of selenium or silicates in the medium, but not the two sources simultaneously. The bioreactor afforded a higher amount of diatom biomass compared with the traditional Petri dish system, but moving the system to the large scale production, new problems arose. In fact, the cultures in the large scale bioreactor were contaminated by cyanobacteria, which were not eliminated in spite of the applied sterilization measurements. Because of these problems, we went back to the Petri dishes, although this system was also improved with respect to the original growth conditions by not sealing the dishes and rendering better their scraping. Therefore, the target of achieving sufficient quantities of biological material was

satisfied. The change of the diatom species from *C. neothumensis* to *C. scutellum*, due to the loss of activity by the former, produced delays but *C. scutellum* demonstrated to keep a constant, although lower than *C. neothumensis*, apoptotic activity. A significant goal within the PHARMAPOX project was the determination of the metabolic pattern of *C. scutellum* diatoms, in particular the detection of 124 metabolites and the identification of more than 100 compounds. To our knowledge, this is the first time that this diatom species is chemically studied and the determination of its metabolic pattern has represented a first step to understand the apoptosis mechanisms on the basis of the sex reversal in *H. inermis*. The scarce available amounts of diatoms, the need to share the material with the other partner Institutes and all the other questions arisen during the investigation, did not allow us to individuate exactly the apoptotic factor(s). Nevertheless, the biological assays enabled us to establish that the apoptotic activity is mainly localized in that fraction containing the highest amount of eicosapentaenoic acid, a polyunsaturated fatty acid with known apoptotic activity. Considering both the huge number of metabolites identified by GC-MS and the low quantities of initial biological material, it would have been very difficult to purify each compound in sufficient amounts for the biological assays. On the other hand, the determination of the metabolic pattern of *C. scutellum* can be considered an important result. Thus, the individuation of the most active fraction able to trigger apoptosis on the AG of *H. inermis* could open the way to future investigations in this field. In addition, GC-MS analysis demonstrated the absence in *C. scutellum* diatoms of

aldehyde compounds, which could be supposed to be involved in the apoptotic effect/sex reversal of *H. inermis*. The *in vivo* bioassays on *H. inermis* postlarvae showed a higher activity of the diatom diethyl ether extract with respect to the butanol extract in inducing sex reversal, and the highest apoptotic activity of fraction **3**. A similar trend regarding the activity of both the diethyl ether extract and fraction **3** was observed also in *in vitro* bioassays on BT20 cell lines (breast carcinoma) and LNCaP (prostate adenocarcinoma) populations. *In vitro* experiments also demonstrated the apoptotic effect of EPA on BT20 cells, results that were comparable with those produced by fraction **3**.

Trying to answer the first question arisen during this study, it is not clear so far whether the diatom-induced apoptosis is provoked exclusively by EPA or more compounds are involved in the process by means of a synergistic mechanism. In addition, at the moment, we cannot say whether the compounds inducing apoptosis in human cell lines are the same affecting the sex reversal in *H. inermis* shrimps. Further studies are necessary in order to clarify this item. Western blotting experiments have shown that caspase 8 is involved in the activation of apoptosis, meaning that diatom-induced apoptotic process is triggered by the extrinsic pathway. The effector caspase 3, in addition, demonstrated to be one of the intermediaries of the proteolytic cascade. Since one of the main objectives of the current research has been discovering new proapoptotic agents from natural sources, diatoms can be considered as good candidates in providing compounds with a selective toxicity towards solid

tumours rather than haematological and normal cells. On the other hand, *in vitro* bioassays on commercially important crustaceans, the crayfish *Cherax quadricarinatus*, demonstrated that *C. scutellum* did not induce apoptosis in their androgenic glands, suggesting a very specific action of the diatoms on particular cell targets.

The chemical study of the anaspidean mollusc *Aplysia fasciata* led to the isolation of 16 metabolites, six of which were not identified so far, namely four sesquiterpenes (**4**, **6**–**8**), one C_{15} acetogenin (**10**), and one diterpene (**15**). Compounds **4** and **6**-**7** are structurally related to the brasilenols. In particular, compound **4** is characterized by the double bond at 1-2 instead of 1-6 in brasilenol (**1**), and a hydroxy group bonded to C-6. Compound **6** corresponds to 2-acetoxyepibrasilenol. Compound **7**, 4-acetoxy-5-brasilene, reported in the literature as obtained by acetylation of 5-brasilene, was isolated as a natural product from *A. fasciata*. Compound **8**, 6-*epi*-β-snyderol, resulted to be the epimer at C-6 of the known β-snyderol. Compound **10**, (3*Z*,9*Z*)-7-chloro-6-hydroxy-12-oxopentadeca-3,9-dien-1-yne, is characterized by a linear chain with one triple bond, two double bonds (of which one conjugated with the triple bond) and a carbonyl group. The diterpene **15**, 16-acetoxy-15-bromo-7-hydroxy-9(11)-parguerene, is the 2-deacetoxyderivative of the known compound **16**.

The chemical investigation of the Chinese soft coral *Sinularia* sp. led to the isolation of four new casbenes, *i.e.* diterpenes with a bicyclic structure consisting in a 14-membered cycle fused with a cyclopropane, which were all structurally related among them. Casbenes are extremely rare in nature and they are usually found in

plants belonging to the family Euphorbiaceae, as well as very occasionally in marine organisms. Most of the natural casbenes present *cis* fusion. Therefore, the co-occurrence of *cis* and *trans* fusions in *Sinularia* sp. is quite unusual and suggests a not stereospecific mechanism of synthesis. The fact that only casbenes **3** and **4** displayed a significant feeding repellence activity, means that the 14-hydroxy group, absent in compounds **1-2**, is an indispensable functional element for this biological property. Despite their structural similarities with agrostistachins, metabolites from *Agrostistachys hookeri* (Euphorbiaceae) with known antiproliferative activity, compounds **1-4** resulted to be inactive on the tested RBL-2H3 (rat basophilic leukaemia) cell line. On the contrary, compounds **1-4** demonstrated to be active against *S. aureus* ($Gram^+$ bacterium), whereas compound **3** displayed antimicrobial activity on both *S. aureus* and *E. coli* ($Gram^+$ and $Gram^-$ bacteria).

The results obtained during this PhD Thesis are a further proof, therefore, of the importance of marine natural products as new candidates in drug discovery, and underline the need to increase the research on this item. Answering the final question of our prefixed objectives, we can conclude that the examined benthic organisms, *Cocconeis scutellum* diatoms, *Aplysia fasciata* molluscs and *Sinularia* octocorals, represent sources of interesting compounds, some of which provided with biological/ecological activities, and others to be investigated in the future.

10. Resumen

10.1. Presentación de la memoria

El objeto de esta Tesis es el estudio de los productos naturales marinos y su posible relevancia en el desarrollo de nuevos medicamentos. El trabajo experimental se llevó a cabo en diferentes Institutos: el Centre d'Estudis Avançats de Blanes (CEAB-CSIC); la Universitat de Barcelona, Facultat de Farmàcia, Departament de Productes Naturals, Biologia Vegetal i Edafologia; la Universidad de Atenas "Panepistimiopolis Zografou", Facultad de Farmacia, Departamento de Farmacognosia y Química de Productos Naturales, Grecia; el Istituto di Chimica Biomolecolare (ICB), Consiglio Nazionale delle Ricerche (CNR), Pozzuoli, Napoli, Italia. En el CEAB y en la UB se realizó el trabajo químico del proyecto PHARMAPOX: Química, Farmacología, y Bioactividad de un nuevo compuesto apoptótico - un regulador sexual en crustáceos decápodos con aplicaciones ambientales y médicas. En colaboración con la Universidad de Atenas se efectuó el estudio químico del molusco *Aplysia fasciata*, y en el ICB se realizaron los análisis químicos y biológicos del coral blando chino *Sinularia* sp.

La memoria está dividida en nueve capítulos. En el primero se presenta una introducción general sobre los productos naturales marinos, evidenciando las implicaciones significativas de algunos compuestos marinos en la terapia farmacológica. El proyecto PHARMAPOX, por su complejidad, ha sido repartido en cuatro capítulos. El capítulo 2 trata de los antecedentes del proyecto y sus objetivos, y contiene también una explicación general de la apoptosis, el mecanismo de muerte celular programada. El capítulo 3 expone los experimentos realizados para incrementar la producción de biomasa de diatomeas, y el cambio de especies. El capítulo 4 describe la determinación del patrón metabólico de *Cocconeis scutellum*, y el 5 los ensayos biológicos efectuados con las postlarvas de *Hippolyte inermis*, los crustáceos de interés comercial y las líneas celulares tumorales. El estudio químico sobre el molusco *A. fasciata* se trata en el capítulo 6; mientras que en el capítulo 7 se aborda la investigación química y biológica del coral blando chino *Sinularia* sp. La parte experimental se describe en el capítulo 8, mientras que en el 9 están descritas las conclusiones del estudio.

10.2. Objetivos

Los objetivos a los que esta Tesis ha intentado dar una respuesta son:

6) ¿Cuáles son los compuestos de las diatomeas *C. scutellum* que afectan a la reversión sexual de *H. inermis*?

7) ¿Estos compuestos actúan específicamente sobre la glándula masculina de *H. inermis* o también sobre otros tejidos y otros organismos? Y además, ¿estos compuestos pueden actuar también en crustáceos de interés comercial? En caso afirmativo, ¿se podrían usar las diatomeas para manipular el sexo de los crustáceos? ¿Diatomeas del género *Cocconeis* pueden inducir apoptosis en tejidos humanos?
8) Teniendo en cuenta el efecto proapoptótico de las diatomeas *C. scutellum*, ¿se pueden explotar como fuente de compuestos antitumorales?
9) ¿Pueden *A. fasciata* y *Sinularia* sp. proporcionar nuevos compuestos interesantes? ¿Sus metabolitos exhiben actividades biológicas?
10) ¿Podemos concluir que los organismos marinos estudiados en esta Tesis son una buena fuente de potenciales nuevos medicamentos?

Estos objetivos se persiguieron extrayendo el material biológico con diferentes disolventes orgánicos, separando los extractos obtenidos y purificando los compuestos interesantes mediante varios métodos cromatográficos. La elucidación estructural se llevó a cabo mediante técnicas espectrométricas y espectroscópicas (GC-MS, RMN mono- y bidimensional) y se evaluaron las actividades biológicas de los compuestos aislados mediante ensayos *in vitro* e *in vivo*.

10.3. Introducción a los productos naturales marinos

10.3.1. Productos naturales y metabolismo secundario

La Química de Productos Naturales es una rama de la Química Orgánica que inicialmente se ocupaba casi exclusivamente de los compuestos obtenidos a partir de plantas y que, ahora, incluye también productos derivados de animales. El uso de plantas en el tratamiento de las enfermedades se origina en la noche de los tiempos, como se describe en papiros datados en los años 1500-1600 a.C. Sin embargo, sólo en el siglo XVIII, con la clasificación taxonómica de los seres vivos, se estandariza el empleo de las plantas medicinales. Hoy en día muchos medicamentos derivan de recursos naturales. Se calcula, de hecho, que la mayoría de los fármacos antitumorales y antiinfecciosos es de origen natural. Los productos naturales son básicamente metabolitos secundarios. A diferencia del metabolismo primario, cuyas rutas sintéticas y catabólicas son comunes a todos los organismos, el metabolismo secundario origina productos con una distribución limitada en la naturaleza. Además, tales moléculas son producidas en ocasiones particulares y son expresión de la individualidad de cada especie. A menudo no se conoce la función de los metabolitos secundarios, pero se asume que los gastos de su producción y transporte deben ser compensados mediante algún provecho para el organismo productor. Los metabolitos secundarios proporcionan la mayoría de las moléculas farmacológicamente activas. La naturaleza ha elaborado su propia versión de

química combinatorial reteniendo los genes involucrados en la síntesis de moléculas útiles para la supervivencia del organismo, o bien mediante modificaciones genéticas que han proporcionado mejoras en la especie. Los productos naturales presentan muchas ventajas en comparación con los productos sintéticos: tienen muchos más centros quirales y una mayor complejidad arquitectónica, más átomos de carbono, hidrógeno y oxígeno, y menos nitrógeno que los compuestos de síntesis. Además, son moléculas bastante grandes y polares, a pesar de que normalmente la parte que interacciona con la diana biológica es pequeña. Por otro lado, una desventaja es que los recursos naturales contienen generalmente metabolitos secundarios en cantidades escasas, por lo cual se requiere el apoyo de la síntesis orgánica para obtener cantidades mayores. Otro problema relacionado con los productos naturales es que es posible que sustancias que presentan una actividad farmacológica *in vitro*, no resulten efectivas *in vivo* debido a los procesos de metabolización en el organismo o por una incorrecta administración del medicamento. Estudios de relación estructura/actividad permiten mejorar el perfil farmacocinético y farmacodinámico del principio activo. Entre los productos naturales, los de origen marino han despertado gran interés en las últimas décadas por su complejidad estructural y por el amplio abanico de propiedades biológicas y farmacológicas exhibidas. Se calcula que sólo en 2008 se aislaron 1,065 sustancias nuevas a partir de recursos marinos, un incremento del 11% comparado con el número de compuestos identificados en 2007. Los organismos marinos que más frecuentemente contienen sustancias activas son

todos aquellos que presentan texturas blandas, son poco móviles o fijos al fondo (*bentos*), y carecen de mecanismos de defensa física y mecánica. En particular, destacan las esponjas, los moluscos sin concha, los corales blandos, *etc*., que, para sobrevivir en un ambiente muy competitivo, han desarrollado sistemas de defensa alternativos, sobre todo la producción de armas químicas.

Para estudiar los productos naturales se emplean varios métodos. El método tradicional se basa en purificar todos los metabolitos secundarios para luego evaluar su actividad biológica. Sus principales inconvenientes son el gran número de ensayos a los que se someten los compuestos aislados a fin de obtener la máxima información posible, y el trabajo necesario para aislar todos los componentes. Otro método es el fraccionamiento bio-dirigido, basado en efectuar los ensayos biológicos previamente a cada separación, para llegar a purificar sólo los compuestos activos. La limitación de este método es que se seleccionan sólo las fracciones que resultan activas en un determinado ensayo, excluyendo compuestos que podrían tener otras propiedades interesantes. En esta Tesis hemos aplicado el método ecológico, es decir el que se basa en seleccionar una especie tras la observación de una propiedad biológica particular. La ecología química es el estudio de las relaciones inter e intra-específicas entre los organismos que comparten el mismo ambiente. Las especies a estudiar fueron seleccionadas, de hecho, tras evaluar sus relaciones ecológicas. Las diatomeas del género *Cocconeis* tienen la particularidad de modificar el sexo de la gamba *H. inermis* mediante la producción de compuestos proapoptóticos. Se evaluó la actividad

de estas microalgas en otras especies también, en crustáceos de interés comercial, y en células tumorales, para evaluar posibles aplicaciones en acuicultura y en medicina. Por otro lado, la falta de protección física y mecánica junto a una movilidad escasa o nula, sugerían que el molusco *A. fasciata* y el coral blando *Sinularia* sp. podrían producir armas químicas para su defensa.

10.3.2. Diatomeas

Fig. 10.1. Diatomeas (http://chsweb.lr.k12.nj.us/mstanley/outlines/protista/protis3).

Las diatomeas son algas eucarióticas con una pared de sílice. El grupo de las Bacillariophyceae comprende dos subclases, Centricae y Pennatae, y cinco órdenes. Se conocen unas 10^5 especies que se encuentran en casi todos los ambientes acuáticos, tanto de agua dulce como salada, y también en suelos húmedos y musgo. Normalmente miden entre 2 µm y 1.5 mm, pero pueden llegar a ser más largas. El exterior de las diatomeas está compuesto por dos partes que se encajan entre ellas, la *epiteca* y la *hipoteca*, cada una recubierta por una capa (*valva*) y un cinturón (*pleura*). El citoplasma es incoloro y contiene cromatóforos cuyos pigmentos son clorofila, carotenoides y xantofilas. La identificación de las diatomeas se realiza mediante observación *in vivo*

al microscopio o tras tinción. Las diatomeas planctónicas flotan y se muestrean mediante redes; las diatomeas bentónicas se recolectan arrastrando el fondo o recogiendo el substrato donde viven. Se reproducen de manera vegetativa. Ya que en cada división la *hipoteca* se reconstruye *de novo* y progresivamente va disminuyendo su tamaño, esta reducción es compensada de vez en cuando por la generación de auxosporas.

10.3.3. Opistobranquios

Los opistobranquios son moluscos mayoritariamente bentónicos caracterizados por la pérdida parcial o total de la concha, lo cual, por un lado, es ventajoso porque permite al animal ahorrar los gastos de producción y de transporte de la concha, si bien por otro lo expone más al ataque de los depredadores. Están divididos en nueve órdenes (Cephalaspidea, Anaspidea, Notaspidea, Sacoglossa, Nudibranchia, Acochlidea, Rhodopemorpha, Thecosomata y Gymnosomata) y establecen relaciones tróficas con organismos que pertenecen a otros phyla, como poríferos, tunicados, briozoos y cnidarios, entre otros. Los opistobranquios han compensado la pérdida de la protección exterior mediante la adquisición de estrategias defensivas alternativas

Fig. 10.2. El anaspídeo *Syphonota geographica*.

que han garantizado su supervivencia. Tales estrategias se dividen en comportamentales, morfológicas y químicas. Unas especies son activas de noche o viven debajo de las rocas; otras presentan coloraciones, texturas o formas muy parecidas al substrato donde viven; otras presentan en el manto espículas calcáreas o nematocistos que adquieren a través de los cnidarios de los que se alimentan. Algunas especies pueden desprenderse de partes del cuerpo para distraer a los depredadores (autotomía). Sin embargo, el mecanismo de defensa más interesante y complejo es la producción de sustancias tóxicas y repelentes para los depredadores. Según la teoría pre-adaptativa, el desarrollo de armas químicas ha precedido a la pérdida de la concha. Las armas químicas pueden ser sintetizadas *de novo*, asimiladas a través de la comida y almacenadas en estructuras específicas, o transformadas a partir de compuestos de la dieta para convertirlos en menos tóxicos para el propio molusco o más activos contra los depredadores. De los nueve órdenes, los anaspídeos se encuentran entre los más estudiados. Su nombre significa "sin escudo cefálico" y, de hecho, algunos presentan una capa conchífera muy fina, parecida a una hoja. Los anaspídeos comprenden dos familias: Akeridae, muy poco estudiada desde el punto de vista químico, y Aplysiidae. Los moluscos que pertenecen a la familia Aplysiidae se denominan también liebres de mar por su aspecto, y comprenden nueve géneros. Pueden medir desde los 2 hasta los 70 cm de longitud. En el manto presentan dos glándulas, la glándula opalina (que produce sustancias

tóxicas blanquecinas) y la glándula de la tinta (que secreta una tinta violeta cuyos pigmentos derivan de algas rojas de la dieta).

10.3.4. Corales blandos

Los corales blandos son invertebrados bentónicos que pertenecen al phylum de los cnidarios, caracterizados por dos capas (ecto- y endodermo) y células urticantes (nematocistos). Además presentan una única cavidad que funciona como boca y ano, y una anatomía muy sencilla. Los cnidarios están divididos en tres clases: Scyphozoa, Hydrozoa y Anthozoa. La clase Scyphozoa comprende las medusas, mientras que la clase Hydrozoa incluye los hidroides y las hidromedusas. Los antozoos son polipoides y comprenden las anémonas de mar, los corales, *etc*. A su vez, los antozoos se dividen en dos subclases: Hexacorallia y Octocorallia, que se diferencian por la estructura morfológica de los tentáculos, entre otras características. Los hexacorales tienen mesenterios múltiplos de seis, mientras que los octocorales se caracterizan por la presencia de pólipos coloniales con ocho mesenterios y tentáculos. Tanto los octocorales como los hexacorales pueden presentar una textura blanda y estar fijados al fondo del mar. En cambio, otros

Fig. 10.3. *Thouarella* sp. (Anthozoa, Octocorallia).

están caracterizados por tener un esqueleto muy duro que sirve de protección física contra los depredadores.

10.4. El proyecto PHARMAPOX: antecedentes y objectivos

10.4.1. Introducción

El proyecto europeo PHARMAPOX "Química, Farmacología y Bioactividad de un nuevo compuesto apoptótico: un regulador sexual en crustáceos decápodos con aplicaciones ambientales y médicas (FP6-2003-NEST-A/STREP)", fruto de la colaboración entre varios países (España, Italia e Israel), se ha dedicado a aislar e identificar a partir de diatomeas bentónicas del género *Cocconeis* un(os) compuesto(s) que actúa(n) como regulador(es) sexual(es) en la gamba *H. inermis*. En el proyecto participaron: 1) el Departament de Productes Naturals, Biologia Vegetal i Edafologia, Facultat de Farmàcia, Universitat de Barcelona, Espanya (UB); 2) el Centre d'Estudis Avançats de Blanes (CEAB-CSIC), Girona, Espanya; 3) el Laboratorio di Ecologia del Benthos, Stazione Zoologica "A. Dohrn", Ischia, Nápoles, Italia (SZN); 4) el Dipartimento Diagnostica delle Malattie Linfoproliferative, Istituto Nazionale Ricerca sul Cancro, Génova, Italia (INRC); 5) el Departamento de Ciencias de la Vida y el Instituto Nacional para la Biotecnología en el Negev, Universidad de Ben-Gurion, Beer Sheva, Israel (BGU). Cada Instituto estuvo involucrado en una determinada tarea en el marco del proyecto. En la UB y el CEAB nos ocupamos del

estudio químico de *Cocconeis*, es decir extracción, aislamiento y determinación del patrón metabólico de las diatomeas. Las diatomeas se cultivaron en la SZN, donde se realizaron también los experimentos de bioactividad con los decápodos *H. inermis*. La administración de las diatomeas y sus fracciones a varias líneas celulares tumorales se llevó a cabo en el INRC, mientras que en la BGU se efectuaron los experimentos con crustáceos de interés comercial para evaluar el impacto de las diatomeas en acuicultura.

10.4.2. Decápodos y diatomeas

La idea del proyecto PHARMAPOX nació en 2004 a partir de experimentos previos sobre la influencia de las diatomeas bentónicas *Cocconeis* en la reversión sexual de los crustáceos *H. inermis*.

Fig. 10.4. El decápodo *Hippolyte inermis*.

H. inermis es un decápodo que vive en el Mediterráneo y a lo largo de las costas atlánticas de España formando poblaciones estables en las praderas de *Posidonia oceanica*. Ya que son proterándricos, los individuos experimentan una fase masculina antes de volverse hembras. El ciclo vital de *H. inermis* se caracteriza por dos temporadas reproductivas anuales, otoño y primavera, sincronizadas con el crecimiento estacional de *P. oceanica*. En otoño las gambas nacen machos y al cabo de

casi un año se transforman en hembras (hembras α). En cambio, en primavera, temporada de máximo desarrollo de *Cocconeis*, la nueva población está formada por machos y hembras (hembras β). Estas últimas se forman por diferenciación directa de las postlarvas, sin pasar a través del estadio masculino, son más pequeñas y crecen más rápidamente que las hembras α. Experimentos de laboratorio demostraron que las diatomeas afectaban al cambio sexual en *H. inermis* induciendo apoptosis, es decir muerte celular programada, en la glándula androgénica de los crustáceos durante el crecimiento postlarval, determinando así el desarrollo directo de los caracteres sexuales femeninos. La nueva glándula femenina es producida a partir de células indiferenciadas tras la completa destrucción de la glándula androgénica. La presencia de *Cocconeis* en la dieta primaveral de *H. inermis*, pues, acelera el proceso de apoptosis de la glándula androgénica que normalmente, en ausencia de diatomeas, tendría lugar 7-12 meses tras la eclosión. El efecto de las diatomeas es específico (dirigido exclusivamente a la glándula androgénica de *H. inermis*) y, además, su papel ecológico parece ser mantener una constante relación machos/hembras, garantizando un numero de hembras suficiente para la reproducción otoñal. El género *Cocconeis* comprende especies que se adhieren fuertemente al substrato mediante la producción de sustancias mucilaginosas. Las diatomeas bentónicas, en particular las Pennatae, han sido todavía poco estudiadas ya que son difíciles de muestrear y cuantificar respecto a las diatomeas planctónicas

que, en cambio, son muy conocidas en la literatura desde el punto de vista ecológico y biológico.

A pesar de la opinión tradicional según la cual las diatomeas juegan un papel clave en la cadena alimentaria marina, recientemente se ha destacado la capacidad de estas microalgas de producir compuestos tóxicos contra sus depredadores, en particular repelentes alimentarios y toxinas. Podemos destacar por ejemplo el ácido domoico, un aminoácido neuroexcitatorio producido por las diatomeas *Nitzschia pungens*, y capaz de contaminar moluscos bivalvos. Las diatomeas planctónicas *Thalassiosira rotula* y *Skeletonema costatum*, en cambio, producen compuestos deletéreos no hacia sus copépodos depredadores, sino hacia los embriones de éstos, induciendo abortos, defectos morfológicos y mortalidad. Las principales moléculas involucradas en estos mecanismos defensivos son aldéhidos de cadena corta (heptadienal, octadienal y decadienal) que pertenecen a la familia de las oxilipinas y que derivan de ácidos grasos poliinsaturados por acción de la fosfolipasa A2, una lipooxigenasa y una hidroperóxido liasa. Estas moléculas no son producidas en todas las condiciones, sino sólo cuando las diatomeas sufren un daño. Además de ejercer efectos tóxicos sobre las futuras generaciones de crustáceos, los aldéhidos han demostrado afectar negativamente también a embriones de erizos, poliquetos y ascidias, e inhibir la replicación de líneas celulares humanas tumorales. Otras clases de moléculas (hidroxi- y cetoácidos) también son responsables del fracaso reproductivo de los copépodos.

10.4.3. Apoptosis

La apoptosis es un proceso de muerte celular programada, regulada genéticamente en respuesta a estímulos específicos y tras varias formas de estrés o daño celular. Este proceso es responsable de la eliminación de aquellas células (*e.g.* los linfocitos autoinmunes) y tejidos (*e.g.* el tejido interdigital durante el desarrollo fetal) que resultarían inútiles en los individuos adultos. Durante la apoptosis ocurren cambios morfológicos en las células: contracción celular, formación de vesículas, condensación de la cromatina nuclear, fragmentación del ADN internucleosomal y empaquetamiento de las células en los cuerpos apoptóticos, de manera que no se generen procesos inflamatorios por la liberación de los componentes intracelulares. Proteasas cisteína-dependientes, las caspasas, participan en el desarrollo del proceso apoptótico efectuando cortes proteolíticos en varios polipéptidos intracelulares. Las caspasas activan proteínas proapoptóticas que se encuentran en forma de zimógenos, cortando los enlaces correspondientes al lado carboxílico de residuos de aspartato. Se conocen once o doce caspasas, dependiendo de un cierto polimorfismo hereditario, clasificadas en caspasas efectoras (como las caspasas 3, 6 y 7, que provocan la mayoría de los cortes de las proteínas) y caspasas iniciadoras (como las caspasas 8 y 9, que empiezan el proceso apoptótico). La apoptosis se puede inducir mediante dos vías: la intrínseca, mediada por las mitocondrias, y la extrínseca, regulada a través de

receptores activados por moléculas específicas. La vía intrínseca se inicia mediante la caspasa 9, mientras que la vía extrínseca se activa mediante la caspasa 8.

La apoptosis juega un papel importante en el desarrollo y la homeostasis de los organismos pluricelulares. De hecho, fallos en el mecanismo de control de la muerte celular programada pueden inducir varias patologías, como las enfermedades neurodegenerativas y el cáncer. Entre los avances de la investigación antitumoral, la comprensión de la función de la apoptosis en el desarrollo de la neoplasia es uno de los más notables. Además se ha demostrado que el mecanismo de acción de muchos medicamentos empleados en la quimioterapia tradicional consiste en la inducción de apoptosis en las células tumorales. Por ello, la apoptosis es una diana prometedora para el descubrimiento de nuevos medicamentos y, de hecho, las empresas farmacéuticas están cada vez más comprometidas en encontrar nuevas sustancias proapoptóticas, sobre todo a partir de recursos naturales. En particular, el mar ha demostrado ser una riquísima fuente de metabolitos secundarios de interés, así como precursores para la semisíntesis. La actividad antitumoral de estos compuestos puede estar relacionada con su papel ecológico en organismos como esponjas, tunicados, moluscos, *etc*., que producen un abigarrado arsenal químico contra sus depredadores. En este ámbito, el proyecto PHARMAPOX ha dado su contribución valorando el efecto apoptótico de las diatomeas *Cocconeis* sobre células tumorales.

10.4.4. Aplicaciones en acuicultura

Se valoró también la posibilidad de aprovechar las diatomeas en acuicultura para controlar el sexo de los crustáceos. Algunos crustáceos de interés comercial presentan patrones bimodales de desarrollo por los cuales los machos crecen más rápidamente o son más grandes que las hembras. Este es el caso de *Cherax quadricarinatus* y *Macrobrachium rosenbergii*, cuyos beneficios comerciales se han visto incrementados notablemente tras la producción de poblaciones únicamente de machos. Tradicionalmente, es posible manipular la diferenciación sexual de los crustáceos a través de la ablación quirúrgica de la glándula androgénica, que determina la ocurrencia de caracteres sexuales femeninos. Las nuevas hembras, genéticamente machos, se cruzan con los machos, produciendo poblaciones únicamente masculinas. Este protocolo es bastante laborioso, por lo cual se están buscando métodos más rápidos y elegantes, como el empleo de sustancias proapoptóticas, para modificar el sexo de los crustáceos. El empleo de compuestos obtenidos de las diatomeas del género *Cocconeis*, capaces de provocar apoptosis en la glándula androgénica de *H. inermis*, podría ayudar a obtener poblaciones de gambas monosexuales de otras especies también. En colaboración con el grupo de la BGU se valoraron las potencialidades de las diatomeas *C. scutellum* en acuicultura, administrándolas a crustáceos de interés comercial.

10.5. Incremento de la producción de biomasa de diatomeas

El primer objectivo en el marco del proyecto PHARMAPOX fue obtener cantidades suficientes de biomasa para los estudios químicos y los ensayos biológicos. Los primeros intentos de incrementar la producción se efectuaron con la diatomea *C. neothumensis*, que había demostrado ser la más activa en inducir apoptosis en *H. inermis* entre las especies valoradas en los estudios previos. En nuestros experimentos se tomaron en consideración diferentes intensidades de luz y concentraciones de micronutrientes, en particular silicatos y selenio. Se compararon dos diferentes sistemas de cultivos, las tradicionales placas de Petri, y un prototipo de bioreactor. El rendimiento de los dos sistemas se comparó utilizando el peso seco de los extractos etéreos obtenidos de cada uno por unitad de área.

10.5.1. Influencia de diferentes intensidades de luz y concentraciones de micronutrientes sobre la tasa de crecimiento de las diatomeas

Se probaron tres diferentes intensidades de luz (60, 100 y 140 µmol de fotones m^{-2} $segundo^{-1}$), que son las intensidades más frecuentes registradas en Abril, cuando ocurre el cambio sexual de *H. inermis*. Estos experimentos se realizaron a 17°C, con cinco réplicas para cada irradiación, en medio de cultivo f/2 y a un fotoperíodo de 18:6 horas. En paralelo se evaluaron también los efectos de diferentes concentraciones de micronutrientes sobre el desarrollo de las diatomeas. Estos

experimentos se llevaron a cabo con cinco réplicas para cada concentración, a 140 µmol de fotones m^{-2} $segundo^{-1}$, 17°C y a un fotoperíodo de 18:6 horas. Las diferentes concentraciones ensayadas fueron: 1) medio de cultivo f/2 sin selenio y con 0.11 mM de Na_2SiO_3; 2) medio de cultivo f/2 con doble concentración de silicatos (0.22 mM de Na_2SiO_3); 3) medio de cultivo f/2 con 10^{-8} M de H_2SeO_3; 4) medio de cultivo f/2 enriquecido con silicatos y selenio (0.22 mM de Na_2SiO_3 y 10^{-8} M de H_2SeO_3). Las cinco réplicas para cada una de las condiciones de crecimiento probadas se obtuvieron inoculando 3 ml de una suspensión de *C. neothumensis* en envases de vidrio con una rejilla en el fondo para facilitar el cómputo de las células por unidad de área durante los 17 días de incubación. La suspensión se obtuvo rascando las diatomeas del fondo de las placas de Petri una vez alcanzada la fase exponencial de desarrollo. La densidad celular inicial (número de células por mm^2) se calculó para cada réplica dos días después del inóculo, contando las células vivas mediante microscopía óptica, y resultó ser 3 células mm^{-2}. El contaje de las células se efectuó cada dos días hasta alcanzar la fase estacionaria de cultivo. De esta manera se construyeron las curvas de crecimiento para las diferentes variables ensayadas.

En cuanto a las diferentes intensidades de luz (Fig. 10.5), no se detectaron diferencias significativas en lo que se refiere a la máxima densidad celular, que fue casi 2,000 células mm^{-2} para cada intensidad valorada. Diferencias significativas entre las tres irradiaciones ($p \leq 0.05$) se observaron en lo que se refiere a la tasa de crecimiento, ya que la fase exponencial fue alcanzada primero por las diatomeas incubadas a 60 µmol

de fotones m^{-2} segundo^{-1}, luego por las incubadas a 100 µmol de fotones m^{-2} por segundo y, finalmente, por las incubadas a 140 µmol de fotones m^{-2} segundo^{-1}.

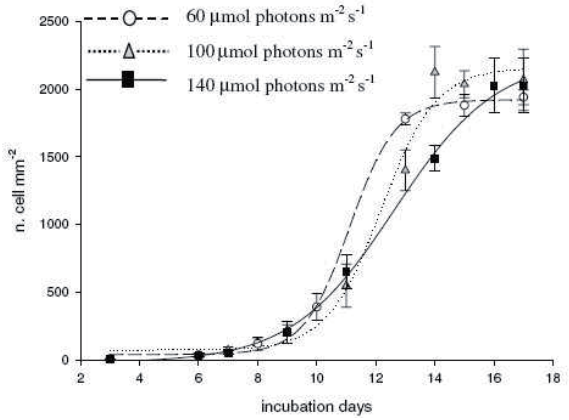

Fig. 10.5. Evaluación de las diferentes intensidades de luz sobre la tasa de crecimiento de *C. neothumensis*.

En el experimento en el que se probaron las diferentes concentraciones de micronutrientes (Fig. 10.6), las mayores tasas de crecimiento exponencial y las densidades celulares de saturación más altas se observaron en los cultivos enriquecidos con selenio y en los que contenían concentración doble de silicatos sin diferencias significativas entre los dos tratamientos. Las densidades celulares de saturación más bajas

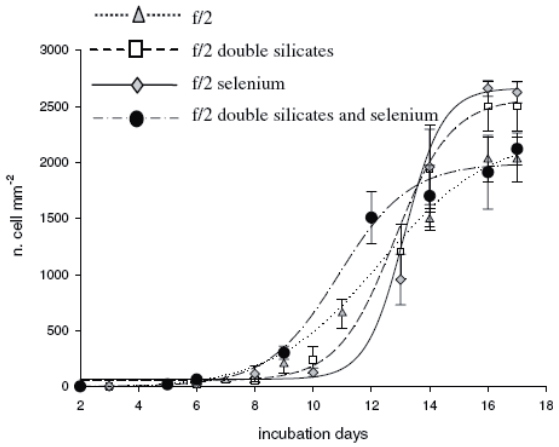

Fig. 10.6. Evaluación de las diferentes concentraciones de micronutrientes sobre la tasa de crecimiento de *C. neothumensis*.

y las menores tasas de crecimiento exponencial se registraron en los cultivos que contenían medio f/2 con 0.11 mM de Na_2SiO_3 (control), y en los que contenían contemporáneamente selenio y concentración doble de silicatos, sin diferencias significativas entre los dos tratamientos. La presencia de selenio en el medio de cultivo incrementaba la tasa de crecimiento exponencial y la máxima densidad celular probablemente por su acción antioxidante y, además, por su función de coenzima. En cambio, los silicatos son componentes de la pared celular de las diatomeas y son reguladores metabólicos. Sin embargo, la pérdida de efecto observada en medios enriquecidos contemporáneamente con selenio y silicatos sugirió un posible antagonismo entre los dos nutrientes.

10.5.2. Cultivos clásicos en placas de Petri

Las diatomeas *C. neothumensis* se cultivaron en placas de Petri a 100 µmol de fotones m^{-2} $segundo^{-1}$, a 17°C, y a un fotoperíodo de 18:6 horas, según las condiciones descritas en la literatura. Una vez alcanzada la fase estacionaria, las células todavía adheridas al fondo de las placas se lavaron con agua destilada, se liofilizaron y se rascaron, obteniendo un polvo seco de diatomeas. El rendimiento fue 4 mg de polvo de diatomeas (peso seco) por placa, es decir 200 mg de polvo seco de diatomeas a partir de 50 placas de Petri, correspondiente a un rendimiento medio de 17.3 mg de extracto etéreo.

10.5.3. Cultivos en bioreactor

El bioreactor a pequeña escala consistía en un tubo de plexiglas (26 cm de largo y 4.7 cm de diámetro) lleno de bolas de vidrio de 2 mm de diámetro, empleadas para aumentar la superficie de crecimiento de las diatomeas. Una de las ventajas de este sistema era el flujo continuo de medio de cultivo que, además, se cambiaba cada dos días para limitar la disminución de nutrientes. Una suspensión celular, obtenida a partir de tres cultivos de *C. neothumensis* en placas de Petri de 2.5 cm de diámetro, se inoculó en el bioreactor. Cuando el cultivo alcanzó la saturación, las bolas recubiertas de diatomeas se lavaron, se liofilizaron y se extrajeron. El rendimiento medio fue de 24 mg de extracto etéreo.

10.5.4. Hacia la producción a gran escala

Una vez demostrado el mejor rendimiento del bioreactor respecto a las placas de Petri, se intentó pasar de la producción a escala reducida a la gran escala empleando un bioreactor que consistía en dos tubos de plexiglas (150 cm de largo y 9 cm de diámetro) llenos de bolas de vidrio de 2 mm de diámetro. El cultivo resultó estar contaminado por cianobacterias. Se tomaron varias medidas de esterilización, se estabilizó el pH mediante un difusor de CO_2 y se redujo el flujo de medio de cultivo. Sin embargo, el sistema ya no proporcionaba más diatomeas, sino bacterias quitinolíticas. Se intentó poner a punto un sistema generador de olas pero los

resultados, en términos de actividad de los extractos, fueron negativos. Para no interrumpir la producción, se volvió al cultivo tradicional en placas de Petri aunque se mejoró la manera de rascar las diatomeas del fondo de las placas. Además, se observó que las placas no selladas con Parafilm proporcionaban cantidades mayores de diatomeas, probablemente por una mayor disponibilidad de CO_2 atmosférico.

10.5.5. Selección de una nueva especie de diatomeas

Los estudios previos al proyecto PHARMAPOX habían indicado que *C. neothumensis* era la especie más activa en la inducción de apoptosis en la glándula androgénica de *H. inermis*. Sin embargo, a lo largo de nuestra investigación se observó pérdida de la actividad apoptótica en *C. neothumensis*, demostrada por la ocurrencia de un número elevado de machos de *H. inermis* en los experimentos *in vivo* realizados incorporando las diatomeas y sus extractos en las dietas de las postlarvas. Por esa pérdida, probablemente causada por el empleo de una cepa de diatomeas diferente de la que se usó en los experimentos precedentes, se decidió cambiar de diatomeas. Entre las especies probadas se escogió *C. scutellum* porque producía un elevado numero de hembras, y porque sus efectos eran comparables con los de los estudios anteriores.

10.5.6. Mortalidad y estrés en el decápodo *Hippolyte inermis*

Los resultados de los experimentos *in vivo* con *H. inermis* se vieron afectados negativamente por la elevada mortalidad y por el estrés de larvas y postlarvas. Se probaron varias dietas para averiguar si el alimento era una fuente de estrés para las gambas. Al final se determinó que la mejor comida para las larvas era la constituida por 4 nauplii de *Artemia salina* (enriquecida durante 18 horas con Algamac antes de la administración) más 4 individuos de *Brachionus plicatilis* por ml de medio de cultivo. Por otro lado, la mejor dieta para las postlarvas era la que consistía en comida Tetra AZ, *Spirulina* pura y *Artemia* enriquecida.

10.6. Composición química de la diatomea bentónica *Cocconeis scutellum*

La determinación del patrón metabólico de *C. scutellum* se llevó a cabo mediante GC-MS (cromatografía de gases acoplada a espectrometría de masas), una de las técnicas más empleadas hoy en día para separar e identificar mezclas de compuestos volátiles y termoresistentes. Los compuestos polares deben ser derivatizados antes del análisis GC-MS: los ácidos grasos se convierten generalmente en sus metilésteres, mientras que los alcoholes se derivatizan con TMSi. Lípidos y glicéridos se hidrolizan para que se conviertan en compuestos de bajo peso molecular. El estudio químico de *C. scutellum* mediante GC-MS permitió determinar la composición metabólica de las

diatomeas y tener una idea de las clases de compuestos contenidos en ellas. La MS permite diagnosticar determinadas clases de compuestos gracias a sus fragmentaciones características, y mediante comparación con sustancias de referencia y bases de datos. Como parámetros se tomaron en consideración los R_t (tiempos de retención) y, principalmente, los *RI* (índices de Kovats).

10.6.1. Estudio químico

Las diatomeas, cultivadas en la SZN a lo largo de todo el período de investigación, se analizaron en el CEAB y en la UB. La extracción se realizó con acetona, sonicando y filtrando sobre papel de filtro. La suspensión se evaporó bajo presión reducida y, tras dilución con agua destilada, se repartió entre agua y éter etílico. La fase orgánica se evaporó, proporcionando 227.9 mg de extracto etéreo. La fase acuosa se extrajo sucesivamente con *n*-butanol. El disolvente orgánico se evaporó, proporcionando 102.9 mg de extracto butanólico. Los dos extractos se analizaron mediante cromatografía en capa fina (TLC) y, tras la oportuna derivatización, se sometieron a análisis GC-MS. El extracto etéreo se fraccionó mediante Sephadex LH-20 (cromatografía de exclusión molecular) y se obtuvieron las tres fracciones **1-3**, sucesivamente derivatizadas y analizadas mediante GC-MS con fuentes EI y CI. En paralelo, se evaluó también la presencia de compuestos aldehídicos en *C. scutellum*, siguiendo el protocolo descrito en la literatura para la búsqueda de aldéhidos de

cadena corta en las diatomeas planctónicas. El análisis GC-MS de los extractos etéreo y butanólico de *C. scutellum* proporcionó la detección de 124 metabolitos, de los que unos 100 fueron identificados. El patrón metabólico de la fracción etérea consistía en ácidos grasos (75.8% del TIC), glicéridos (10.8%), esteroles (4.7%), compuestos isoprenoides (3.6%), así como alcanos, alcoholes grasos y fosfatos en cantidades menores. Entre los ácidos grasos (de C_{10} a C_{26}) dominaban los de cadena C_{16} y C_{20}, y los saturados (38.9% del total de ácidos grasos), seguidos por los monoinsaturados (32.1%) y los poliinsaturados (28.6%). En la EIMS de los ácidos grasos, los picos $[M]^+$ y $[M - 15]^+$ de los derivados TMSi, y los picos $[M]^+$ y $[M - 31]^+$ de los derivados metilésteres, eran fácilmente reconocibles y permitieron, junto a otros iones característicos, su identificación. Para los ácidos grasos poliinsaturados se recurrió a la CIMS para poder identificar los iones moleculares. Entre los glicéridos, los monoglicéridos fueron los más abundantes. No se detectaron triglicéridos porque su temperatura de ebullición se sitúa más allá de las temperaturas empleadas en el programa de GC-MS. Se encontraron cinco esteroles, de los cuales el 24-metilencolesterol (con el pico característico a *m*/*z* 314) fue el más significativo (51.9% de los esteroles totales), seguido por el esterol A (23.0%), el brasicasterol (20.0%), el colesterol (3.4%) y el campesterol (1.6%). El extracto butanólico contenía ácidos grasos (44.6%), carbohidratos de bajo peso molecular (9.5%), alcoholes (8.8%), glicéridos (4.4%), ácidos orgánicos (2.5%), compuestos isoprenoides (1.2%) y fosfatos (0.1%). De los carbohidratos, el 96.5% eran monosacáridos, y el 3.5% era el disacárido

sacarosa. El azúcar de bajo peso molecular más abundante era el floridósido (45.7% de todos los carbohidratos), hallado previamente en otras microalgas. Se identificaron diez aminoácidos, que representaban el 18.1% de todos los compuestos nitrogenados, de los que los nucleósidos adenosina y uridina, y la uréa correspondían al 44.9%, 4.7%, y 24.6%, respectivamente. Entre los alcoholes destacaba sobre todo el glicerol (8.6% del extracto butanólico). Además, se encontraron trazas de ácidos orgánicos, como el ácido hidroxicinámico, monoglicéridos, compuestos isoprenoides (tocoferol y fitol) y glicerol-3-fosfato.

Por lo que se refiere a las tres fracciones del extracto etéreo, la fracción **1** contenía ácidos grasos (2.4% del TIC), compuestos isoprenoides (3.7%) y glicéridos (77.2%, *i.e.* un 27.5% de monoglicéridos y un 49.7% de diglicéridos). La fracción **2** estaba constituida por ácidos grasos (66.7% de TIC), *i.e.* por el 25.5% de ácidos grasos saturados, el 35.0% de monoinsaturados y el 6.2% de polienos. También se encontraron fitol (0.51%), esteroles (3.1%) y monoglicéridos (11.0%). En la fracción **3** se hallaron ácidos grasos (81.7% de TIC), de los que el 14.4% eran ácidos grasos saturados, el 51.7% monoinsaturados y el 15.6% poliinsaturados. Se encontró también el 24-metilcolesterol (2.31 %). Además, la fracción **3** contenía más EPA, el ácido eicosapentaenoico, que la fracción **2** (15.6% de la fracción **3** *vs.* el 6.2% de la fracción **2**), cuya actividad apoptótica y antitumoral es conocida en la literatura. Muchos compuestos presentes en el extracto etéreo crudo, como el ácido araquidónico, no se detectaron en las fracciones probablemente porque fueron

retenidos en la columna o porque se encontraban demasiado diluidos para poder ser identificados. El análisis GC-MS demostró la ausencia de los compuestos aldehídicos heptadienal, octadienal y decadienal en *C. scutellum*. Sin embargo, no se puede excluir la participación de otros tipos de oxilipinas en el mecanismo de apoptosis inducido por las diatomeas.

10.7. Ensayos biológicos con *Cocconeis scutellum*

Se llevaron a cabo diferentes ensayos biológicos con las diatomeas *C. scutellum* a fin de 1) cuantificar su efecto sobre la relación hembras/individuos totales (F/tot) de *H. inermis* y realizar un fraccionamiento bio-dirigido para localizar la actividad apoptótica en fracciones cada vez más pequeñas; 2) evaluar la actividad de las diatomeas en crustáceos de interés comercial y 3) en células tumorales.

10.7.1. Fraccionamiento bio-dirigido

Los extractos etéreo y butanólico de *C. scutellum* se administraron a las postlarvas de *H. inermis* para evaluar cuál de los dos producía la máxima relación F/tot. Los ensayos demostraron una mayor actividad del extracto etéreo a las dos máximas concentraciones probadas (51.3% ± 15.6% de F/tot inducida por 70 µg de extracto/mg de comida, y 51.1% ± 23.2% inducida por 7 µg de extracto/mg de comida) en comparación con el extracto butanólico (36.7% ± 16.8% de F/tot producida por 7 µg

de extracto/mg de comida). Sucesivamente, la administración a las postlarvas de las fracciones del extracto etéreo puso de manifiesto una mayor actividad de la fracción **3** (48.32% ± 17.65% de F/tot) en comparación con la fracción **1** (42.21% ± 11.79%) y la fracción **2** (45.28% ± 17.72%).

10.7.2. Ensayos con crustáceos de interés comercial

Los camarones *Macrobrachium rosenbergii* y los langostinos *Cherax quadricarinatus* fueron usados por el grupo de la BGU como modelo para evaluar las aplicaciones de las diatomeas *C. scutellum* en acuicultura. Los experimentos *in vivo* se llevaron a cabo incorporando el extracto acetónico de las microalgas en la dieta de los juveniles de *M. rosenbergii* a dos diferentes concentraciones (20 ng/larva y 2 ng/larva). Debido a la mortalidad elevada de las postlarvas y a las fluctuaciones en la relación machos/hembras en las tres réplicas del control, no se pudo correlacionar la reducción de la proporción machos/hembras con la administración del extracto.

En los experimentos *in vitro* las glándulas androgénicas de *C. quadricarinatus* se incubaron en presencia de las fracciones **1**-**3**, EPA, ácido araquidónico, y estaurosporina como control positivo, a diferentes concentraciones (100, 10 y 1 µg/ml). Posteriormente, las muestras se fijaron, se seccionaron, se tiñeron y se examinaron mediante microscopía de fluorescencia. Los resultados demostraron que, a las concentraciones ensayadas, no había ningún efecto apoptótico significativo en

las glándulas androgénicas. Se pudo observar una débil actividad apoptótica únicamente en las secciones tratadas con la fracción **1** (a la máxima concentración probada) y con etanol.

10.7.3. Ensayos de citotoxicidad

Se realizó un rastreo inicial administrando las diatomeas *C. scutellum* a diferentes líneas celulares tumorales y normales. Las líneas tumorales eran: BT20 y MB-MDA 468 (cáncer de mama), LNCaP (adenocarcinoma de próstata), y BRG-M y JVM-2 (linfomas de Burkitt de diferentes translocaciones cromosómicas). La línea normal (COR) estaba representada por linfocitos B extraídos a partir de amígdalas faríngeas humanas y transformados en línea continua mediante el virus de Epstein-Barr. Por otra parte, los linfocitos T de las líneas BRG-M y JVM-2 se obtuvieron a partir de sangre periférica. A lo largo del estudio se efectuaron tres tipos de experimentos: 1) valoración de la apoptosis y vitalidad celular mediante marcaje con anexina V-FITC y PI isotónico, y análisis con citometría de flujo; 2) análisis del ciclo celular mediante PI hipotónico, y análisis con citometría de flujo; 3) estudio de la activación de las caspasas 8, 9 y 3 mediante Western blotting. Los experimentos preliminares demostraron que los tumores sólidos eran mucho más sensibles a las diatomeas que los tumores hematológicos y las células normales, sugiriendo una actividad apoptótica específica hacia una determinada diana celular. Además, la línea celular

BT20 demostró ser la más sensible con un porcentaje de células apoptóticas del 26.1% en presencia de 2.5 ng/ml of *C. scutellum*, frente al 19.2% de MB-MDA468 y al 11.3% de LNCaP a la misma concentración de diatomeas. En los linfomas y en COR la presencia de apoptosis no fue significativa respecto al control. Una vez demostrada la mayor sensibilidad de la línea BT20, se escogió esta población celular para los ensayos de citotoxicidad. Primero se evaluó cuál de los dos extractos, el etéreo o el butanólico, era el más activo en la inducción de la apoptosis. Se incubaron las líneas BT20 durante 18 horas a diferentes concentraciones de los dos extractos (0-1,700 ng/ml) y se construyeron curvas dosis/respuesta. El experimento demostró que a 17 ng/ml el extracto etéreo producía el 50% de apoptosis, frente al 40% del extracto butanólico a la misma concentración. Las fracciones **1**-**3** se administraron a las células BT20 a diferentes concentraciones (0.1-4 μg/pocillo) durante 24 horas. La fracción **3** produjo la máxima apoptosis (81.4% de células apoptóticas) a una concentración de 2 μg/pocillo, frente al 40.3% de apoptosis inducido por la fracción **1** y al 39.3% inducido por la fracción **2**. Estos resultados fueron confirmados también mediante estudios de morfología de las células BT20 teñidas con Giemsa, que revelaron la presencia de núcleos condensados y fragmentados, indicativos de apoptosis, únicamente en las células incubadas con la fracción **3**. Dado que el EPA era el componente mayoritario de la fracción **3**, éste se administró a las células BT20 además del ácido araquidónico (AA), otro ácido graso poliinsaturado detectado en el extracto etéreo de *C. scutellum*, los dos a una concentración de 7 μg/pocillo. Se

observó una elevada vitalidad celular en las células BT20 tratadas con el medio, solución fisiológica y AA (78.0%, 76.1% y 70.4%, respectivamente). En cambio, la vitalidad celular bajaba al 34.1% en las células incubadas con EPA. Se probaron también los disolventes empleados durante las fases de extracción y purificación para cerciorarnos de que la apoptosis no estuviera provocada por la toxicidad de los mismos, sino por los compuestos contenidos en las diatomeas. Los experimentos demostraron la no toxicidad de los disolventes sobre las células valoradas. La línea celular LNCaP también se incubó con las fracciones **1**-**3** confirmando, incluso aquí, la mayor actividad de la fracción **3**. El análisis del ciclo celular permitió establecer cuál era la etapa afectada por la fracción **3**. Se incubaron las células BT20 durante 48 h con las fracciones **1**-**2** a una concentración de 2.5 μg/pocillo, y con la fracción **3** a una concentración de 4 μg/pocillo. Estos experimentos no sólo confirmaron el mayor efecto de la fracción **3** en la muerte celular programada (32% de apoptosis), sino que demostraron que esta fracción bloqueaba el desarrollo celular en fase G2, la que precede a la mitosis. Finalmente, se llevaron a cabo experimentos de Western blotting para evaluar cuáles eran las caspasas involucradas en la activación del proceso apoptótico. Primero se investigaron las caspasas 8 y 9. Se pueden distinguir las formas activas de las inactivas de cada caspasa por su peso molecular (caspasa 8: forma inactiva 55-50 kDa, forma activa 40-36 kDa; caspasa 9: forma inactiva 47 kDa, forma activa 37 kDa). Las células BT20 se incubaron durante 5, 6 y 18 horas en presencia del medio (control negativo), Vepesid (control positivo) y las fracciones **1**-**3**

a diferentes concentraciones. Los experimentos demostraron una baja activación de la caspasa 9 en las células BT20 tratadas con Vepesid durante 5 h de incubación, mientras que en las células cultivadas con las fracciones **1**-**3** no había activación de tal proteína. En cambio, la procaspasa 8 (forma inactiva) se encontraba en todos los tratamientos, y la caspasa 8 activa lo estaba en las células tratadas con la fracción **3** a las dos concentraciones probadas. La activación de la caspasa 8 se encontró también, aunque de manera no remarcable, en las células tratadas con la fracción **2** y el Vepesid. Estos resultados demostraron que la apoptosis producida por las diatomeas se activaba mediante la vía extrínseca, es decir por la caspasa 8. Sucesivamente, se estudió la implicación de la caspasa 3, una enzima efectora capaz de activar más caspasas por proteolisis. En este experimento, además de las fracciones **1**-**3**, Vepesid y control negativo, se administró también EPA, a una concentración de 7 μg/pocillo. Por lo que se refiere a la caspasa 3 (forma inactiva 34 kDa, forma activa 20 kDa), la forma inactiva se hallaba en todos los tratamientos para cada tiempo de incubación, en cambio la forma activa se detectó en las células incubadas con la fracción **3** y con EPA durante 6 horas.

10.8. Nuevos compuestos del molusco mediterráneo *Aplysia fasciata* (Mollusca, Anaspidea)

Entre los organismos marinos, los moluscos opistobranquios representan una rica fuente de nuevas moléculas bioactivas. De entre los nueve órdenes en los que los

opistobranquios están divididos, los anaspídeos son los más estudiados. La mayoría de ellos son herbívoros, por lo cual muchos metabolitos aislados han resultado derivar de algas. Los compuestos involucrados en la defensa del animal se hallan normalmente en el manto, la parte más externa del molusco y, por ende, más expuesta a los depredadores, mientras que en la glándula digestiva se encuentran las sustancias adquiridas por la dieta.

10.8.1. Aislamiento, purificación y caracterización

La investigación química se llevó a cabo con el anaspídeo *Aplysia fasciata*, un molusco común en el Mediterráneo entre las comunidades algales de *Ulva* y *Laurencia*, que constituyen su dieta preferente y, a veces, presente también entre las fanerógamas marinas *Cystoseira* y *Zostera*. Tres ejemplares de *A. fasciata* se recolectaron en el Delta de l'Ebre (Tarragona, España) y se diseccionaron en manto y principales órganos internos para diferenciar a los compuestos involucrados en la defensa química de los derivados de la comida. Se extrajeron separadamente las diferentes secciones anatómicas con diclorometano/metanol 2:1 v/v y se analizaron mediante cromatografía en capa fina. El extracto de las glándulas digestiva y hermafrodita resultó ser el más interesante y se purificó mediante diferentes técnicas cromatográficas (cromatografía líquida bajo vacío, extracción en fase sólida y HPLC). La glándula digestiva no es el órgano preferencial para la acumulación de sustancias

de defensa ya que éstas se hallan generalmente en el manto. Sin embargo, se puede suponer, en base a la bibliografía existente, que el molusco acumula metabolitos de las algas para luego transformarlos en compuestos tóxicos contra los depredadores.

El análisis de los experimentos RMN mono- y bidimensionales proporcionó la identificación de 16 metabolitos (8 sesquiterpenos, 3 diterpenos y 5 acetogeninas C_{15}), 6 de los cuales resultaron ser compuestos nuevos (4 sesquiterpenos, un diterpeno y una acetogenina). Los 16 compuestos identificados son de origen alimenticio, ya que derivan de varias especies del alga *Laurencia*, o están relacionados con metabolitos de algas.

Los compuestos **1** y **2** se identificaron como el brasilenol y su epímero, el epibrasilenol, respectivamente, junto al 4-hidroxi-5-brasileno (**3**) y el brasilenol acetato (**5**), todos miembros de la familia de los brasilenoles, *i.e.* sesquiterpenos no isoprenoides. El 4-acetoxi-5-brasileno (**7**), previamente descrito en la literatura como compuesto de semisíntesis obtenido por acetilación de **3**, se halló en *A. fasciata* por primera vez como producto natural.

Los compuestos **4**, **6**, **8**, **10** y **15** se describieron como moléculas nuevas, mientras que los compuestos **9**, **11**-**14** y **16** se identificaron como los conocidos luzodiol, (3*Z*,9*Z*,12*Z*)-6-acetoxi-7-cloropentadeca-3,9,12-trien-1-ino, (3*Z*)-venustineno, (3*Z*)-13-*epi*-pinnatifidenino, (3*E*)-laurenino y 15-bromo-2,16-diacetoxi-7-hidroxi-9(11)-parguereno, respectivamente.

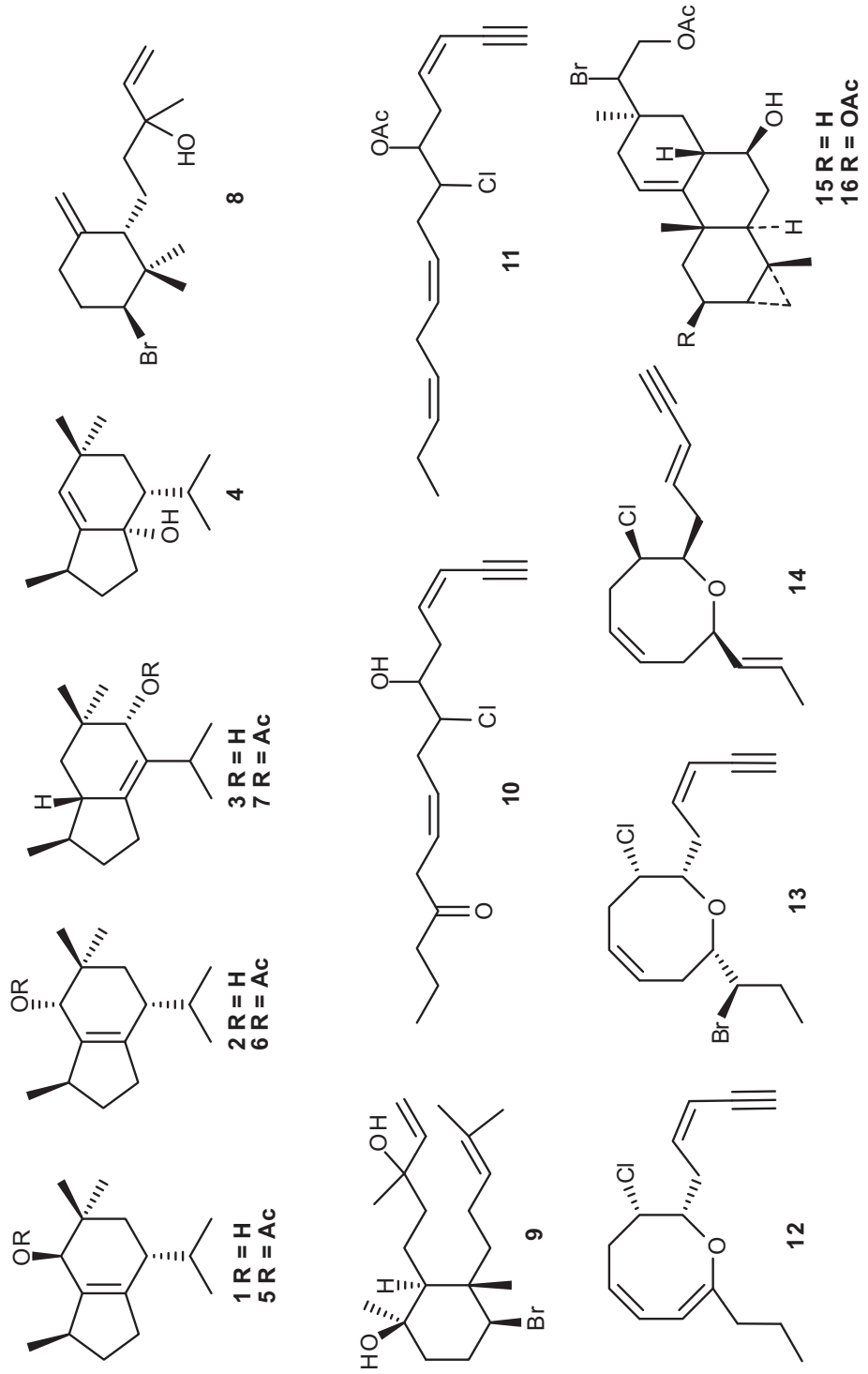

Fig. 10.7. Estructuras de los compuestos **1-16** de la glándula digestiva de *A. fasciata*.

El compuesto **4** presentaba un pico $[M - H]^+$ a *m/z* 221.1909 (FAB-HRMS), correspondiente a $C_{15}H_{25}O$. La presencia de un pico de fragmentación $[M - H_2O]^+$ a 204, así como la banda de absorción a 3485 cm^{-1} en el espectro IR, indicaron la presencia de un grupo hidroxilo. El espectro RMN ^{13}C reveló la presencia de 15 átomos de carbono, correspondientes a tres carbonos cuaternarios, cuatro metinos, tres metilenos y cinco metilos. Los tres grados de insaturación se debían a la presencia de un doble enlace y un sistema bicíclico. El análisis de los experimentos COSY ^1H-^1H, HSQC, y HMBC sugirieron que se trataba de un esqueleto de tipo brasilánico. La configuración relativa del compuesto **4** se asignó en base a las interacciones observadas en el espectro NOESY. En particular los incrementos n.O.e. de las señales H-7β/H_3-15, H-5/H_3-14, y H-5/H-7β sugerían una orientación cofacial para los protones H-5, H_3-14, y H_3-15 (todos β), y una orientación pseudoaxial del hidroxilo en posición 6. El compuesto **4** resultó ser, por ende, el 6-hidroxi-1-brasileno.

El compuesto **6** exhibía un pico $[M + H]^+$ a *m/z* 265.2195 en el espectro FAB-HRMS, correspondiente a la fórmula molecular $C_{17}H_{29}O_2$. El ión fragmento $[M - AcOH]^+$ en el espectro de masas a *m/z* 204 y la banda de absorción a 1733 cm^{-1} en el espectro IR indicaban la presencia de un grupo acetoxi. En el espectro RMN ^1H las 5 señales de grupos metilos (dos sobre carbonos cuaternarios y tres sobre carbonos metínicos), un grupo metilo de un acetato y un metino oxigenado desapantallado, sugirieron una estructura similar a la del brasilenol acetato (**5**). Un análisis detallado de los espectros RMN bidimensionales (COSY ^1H-^1H, HSQC, y HMBC) del compuesto **6** indicaron

que, en realidad, **5** y **6** eran estereoisómeros. La estructura de **6** se confirmó mediante acetilación del epibrasilenol (**2**) a epibrasilenol acetato, cuyos espectros RMN ^{1}H y ^{13}C eran idénticos a los del compuesto **6**.

Por lo que se refiere al compuesto **8**, el experimento RMN ^{13}C reveló la presencia de 15 señales, es decir tres metilos, seis metilenos, tres metinos y tres carbonos cuaternarios. Un carbono cuaternario, uno terciario y dos secundarios que resonaban en la región sp^2 del espectro RMN ^{13}C indicaron la presencia en la molécula de un doble enlace monosustituido y un doble enlace 1,1-disustituido. En el espectro RMN ^{13}C se observaron también un carbono cuaternario oxigenado y un carbono terciario halogenado. El análisis de los espectros RMN ^{1}H y ^{13}C, junto a los experimentos RMN bidimensionales (COSY ^{1}H-^{1}H, HSQC, y HMBC), atribuyeron a **8** la misma estructura planar del β-snyderol. La configuración relativa de **8** se asignó considerando los incrementos n.O.e. y los valores de las constantes de acoplamiento de determinadas señales protónicas. En particular, el hecho de que el metino en C-10 se acoplara con una *J* grande (11.2 Hz) y una *J* media (4.0 Hz) con el metileno H_2-9, implicaba una orientación axial del H-10 y, por tanto, una orientación ecuatorial del átomo de bromo, así como en el β-snyderol. Las correlaciones H-6/H_3-12, H-9α/H-10, H-9β/H_3-12, y H-10/H_3-13 indicaron que H-6 era ecuatorial (configuración opuesta a la del β-snyderol) lo cual, además, se veía reforzado por la falta de interacción n.O.e. entre H-6 y H-10. El compuesto **8** resultó ser, por ende, el 6-*epi*-β-snyderol. No se pudo determinar la configuración de C-3 mediante análisis espectroscópico.

El compuesto **10** presentaba un ión pseudomolecular $[M + Na]^+$ a *m*/*z* 291.1140 (ESI-HRMS) correspondiente a la fórmula molecular $C_{15}H_{21}ClO_2Na$. En el espectro de masas varios picos isotópicos + 2 de relación 3:1 respecto a los iones análogos indicaron la presencia en la molécula de un átomo de cloro. En el experimento RMN ^{13}C se observaron 15 señales: un metilo, cinco metilenos, siete metinos y dos carbonos cuaternarios. Particularmente evidentes fueron un carbonilo a δ 208.7, cuatro carbonos terciarios sp^2 a δ 140.3, 128.1, 124.7, y 111.1, dos carbonos *sp* de un triple enlace a δ 82.4 y 77.2, un carbono terciario halogenado a δ 66.5, y un carbono terciario oxigenado a δ 71.9. Ya que el carbonilo, el triple enlace carbono-carbono y los dos dobles enlaces carbono-carbono satisfacían los cinco grados de insaturación, el metabolito **10** debía ser linear. La geometría de tipo *Z* de los dos dobles enlaces Δ^3 y Δ^9 se asignó en base a las constantes de acoplamiento entre H-3 y H-4 (J = 10.7 Hz) y entre H-9 y H-10 (J = 10.9 Hz). No se pudo determinar mediante RMN la configuración relativa en C-6 y C-7.

Se reasignaron también los valores RMN ^1H y ^{13}C del compuesto conocido **11**, el (3*Z*,9*Z*,12*Z*)-6-acetoxi-7-cloropentadeca-3,9,12-trien-1-ino.

Mediante los experimentos RMN ^{13}C y FAB-HRMS, al compuesto **15** se atribuyó la fórmula molecular $C_{22}H_{33}BrO_3$. Las intensas bandas de absorción a 3417 y 1734 cm^{-1} observadas en el espectro IR indicaron la presencia de un grupo hidroxilo y de un éster carbonílico, respectivamente. El experimento RMN ^{13}C reveló la presencia de 22 señales: cuatro metilos, siete metilenos, seis metinos, y cinco carbonos cuaternarios.

Entre ellos fueron particularmente evidentes el éster carbonílico a δ 170.7, dos carbonos olefínicos (uno terciario y uno cuaternario a δ 116.8 y 144.1, respectivamente), un carbono terciario halogenado a δ 59.8, y dos carbonos oxigenados (uno secundario y uno terciario a δ 66.1 y 77.4, respectivamente). Como el carbonilo y el doble enlace C-C satisfacían dos de los seis grados de insaturación, **15** debía ser un tetraciclo. Las correlaciones evidenciadas en los experimentos COSY ^{1}H-^{1}H, HSQC, y HMBC sugirieron una estructura de tipo pargueránico, *i.e.* un diterpeno con un esqueleto pimaránico modificado, con un doble enlace trisustituido, un carbono halogenado y dos carbonos oxigenados. La configuración relativa se determinó en base a los incrementos n.O.e. y a las constantes de acoplamiento de ciertos protones. En particular, el hecho de que el metino C-7 resonara como triple doblete con dos *J* grandes (10.4 Hz) y una media (4.6 Hz) con H_2-6 y H-8, sugirió una orientación axial para H-7 y H-8, y una orientación ecuatorial para el grupo hidroxilo. Además, las correlaciones n.O.e. entre H-3/H_3-19, H-3/H_3-20, H-5/H-7, H-5/H-18b, H-7/H-14α, H-8/H_3-20, y H-14α/H_3-17 confirmaron que H-3, H-8, H_3-19 y H_3-20 se encontraban en el mismo lado de la molécula, mientras que H-5, H-7 y H_3-17 se hallaban en el lado opuesto. No se pudo determinar la configuración de C-15 mediante RMN.

10.9. Nuevos diterpenos casbánicos del coral blando chino *Sinularia* sp.: estructuras y actividades biológicas

10.9.1. Aislamiento, purificación y caracterización

Los corales blandos se hallan entre los invertebrados chinos más estudiados. El género *Sinularia* es muy rico en diterpenos, algunos de los cuales presentan actividades antimicrobianas, antiinflamatorias y citotóxicas. Una muestra de *Sinularia* sp. se recolectó en la costa de la isla de Hainan, y su identificación se llevó a cabo por la presencia de escleritos fusiformes característicos en la sección interior del tronco.

El material biológico se extrajo con acetona, sonicando y triturando los tejidos en un mortero. Tras filtración y evaporación del disolvente orgánico, el residuo acuoso se diluyó con agua destilada y se extrajo con éter etílico. Una vez evaporado el disolvente, se obtuvo el extracto crudo que se analizó mediante cromatografía en capa fina. En las placas TLC se observaron interesantes bandas UV-visibles, en particular dos a R_f 0.63 y 0.50 (éter de petroleo/éter etílico 9:1 v/v), menos polares que los esteroles, y dos a R_f 0.50 y 0.43 (éter de petroleo/éter etílico 3:7 v/v), más polares que los esteroles. El extracto etéreo se fraccionó mediante cromatografía líquida sobre columna de sílica gel y las fracciones que contenían las sustancias UV-visibles se purificaron mediante TLC semipreparativa. Los compuestos puros **1**-**4** se sometieron a análisis espectroscópico, que reveló que los cuatro pertenecían a la familia de los casbenos.

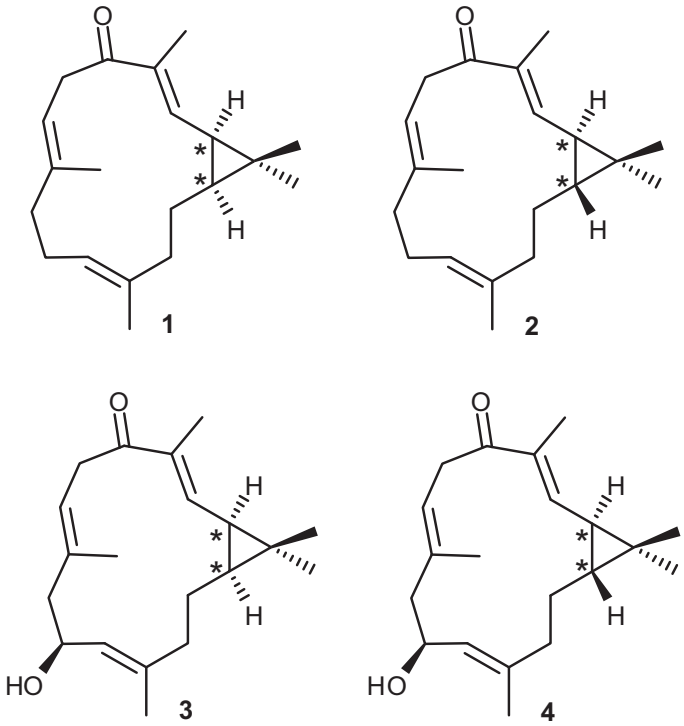

Fig. 10.8. Estructuras de los casbenos **1**-**4** de *Sinularia* sp.

Los casbenos son diterpenos poco frecuentes en la naturaleza, consisten en una estructura bicíclica formada por un anillo ciclopropánico fusionado a un macrociclo de 14 átomos, y están estructuralmente relacionados con los cembrenos.

El compuesto **3** se analizó primero ya que era el más abundante de la fracción casbénica. En EI-HRMS se observó un ión molecular a *m*/*z* 302.2240 que se asignó a $C_{20}H_{30}O_2$, y que requería seis grados de insaturación. Los experimentos RMN ^{13}C pusieron en evidencia 20 señales, correspondientes a un carbonilo a δ 200.0, seis carbonos olefínicos, de los cuales tres metínicos y tres cuaternarios, un metino oxigenado y doce carbonos alifáticos (cinco metílicos, cuatro metilénicos, dos

metínicos y uno cuaternario). Se asignaron de esta forma cuatro de los seis grados de insaturación a una función cetónica y tres dobles enlaces. Los tres dobles enlaces demostraron ser trisustituidos, como se observó por la ausencia de picos de correlación en el espectro COSY ^{1}H-^{1}H. Las restantes dos insaturaciones se atribuyeron a una estructura bicíclica. Ya que en los espectros RMN ^{13}C y ^{1}H se observaron señales típicas de un ciclopropilo, el otro ciclo debía ser un anillo de 14 átomos de carbono. El espectro IR del compuesto **3**, además, reveló la presencia de un grupo hidroxilo que, junto al carbonilo, satisfacían los dos átomos de oxígeno de la fórmula molecular. El experimento COSY ^{1}H-^{1}H permitió determinar tres estructuras parciales que fueron combinadas entre ellas mediante los datos del experimento HMBC. La geometría *E* de los tres dobles enlaces se dedujo por los valores de desplazamiento químico de los metilos enlazados a los C cuaternarios sp^2 (< 20 ppm) y de los metilenos en posición α respecto a los dobles enlaces, y por los resultados de los experimentos NOESY. La unión *cis* entre los dos ciclos se supuso en base a los valores de resonancia de los carbonos metílicos geminales, y por comparación con estructuras similares descritas en la literatura. La configuración absoluta en C-10 se asignó aplicando el método de Mosher modificado. En particular, dos alícuotas del compuesto **3** se trataron con los cloruros del ácido (*R*)- y (*S*)-α-metoxi-α-trifluorometilfenilacético. La evaluación de las diferencias de los valores de desplazamiento químico de los dos ésteres diastereómeros en el espectro RMN ^{1}H nos permitió atribuir la configuración absoluta *S* en C-10. Como el centro quiral C-10

no se correlacionaba con los otros dos carbonos quirales, el C-1 y el C-2, no se pudo definir la configuración absoluta de la molécula entera.

Una vez elucidada la estructura del compuesto **3**, los metabolitos **1**, **2** y **4** se caracterizaron por comparación.

Por lo que se refiere al compuesto **4**, la presencia en el espectro ESI-HRMS del pico $[M + Na]^+$ a *m*/*z* 325.2140 correspondiente a la misma fórmula molecular de **3** ($C_{20}H_{30}O_2Na$), y las analogías estrictas entre los espectros RMN ^1H de **3** y **4**, sugirieron una relación estereoquímica entre los dos compuestos. Los experimentos RMN ^{13}C y DEPT demostraron que todos los dobles enlaces del metabolito **4** tenían geometría *E*, análogamente a los de **3**. Los resultados de los experimentos NOESY y la comparación con los modelos estructurales descritos en la literatura permitieron atribuir la diferencia entre los dos compuestos a la unión entre los dos ciclos del núcleo casbánico, que resultó ser *trans* en **4** y *cis* en **3**. La diferente disposición espacial de las dos moléculas era responsable de diferencias significativas en los desplazamientos químicos de sus espectros RMN ^1H y ^{13}C. La configuración absoluta en C-10, valorada mediante el método de Mosher, demostró ser *S* en el compuesto **4** al igual que en el compuesto **3**.

El análisis espectroscópico de los compuestos **1** y **2** reveló que se trataba de los derivados dehidroxilados de **3** y **4**, respectivamente. Los espectros de masas de **1** y **2** mostraron un pico $[M + H]^+$ a *m*/*z* 287 con 16 unidades de masa menos que **3** y **4**, y correspondiente a la fórmula molecular $C_{20}H_{30}O$. El espectro RMN ^{13}C de **1** permitió

establecer que la geometría de todos sus dobles enlaces era también de tipo *E* y que la unión entre los dos ciclos del núcleo casbánico era *cis*.

Análogamente, los espectros RMN ^{1}H y ^{13}C de **2** resultaron ser similares a los del metabolito **4**, indicando que la única diferencia estructural entre los dos era la ausencia del 10-OH en **2**. Los desplazamientos químicos de los protones y carbonos de los metilos geminales, y de los metinos en posición 1 y 2, nos permitieron afirmar que la unión entre los dos ciclos del sistema casbánico **2** era *trans*, como ya se había observado en **4**. Además, los valores de resonancia de los carbonos metílicos sobre los dobles enlaces H_3-18, H_3-19 y H_3-20, y de los metilenos H_2-10, H_2-13 y H_2-9, permitieron asignar la geometría *E* a todos los dobles enlaces de la molécula.

Estudios de biosíntesis en plantas con precursores ^{13}C han demostrado que el esqueleto casbánico se origina de la ciclización cabeza-cola del geranilgeranildifosfato mediante un mecanismo estereospecífico que lleva exclusivamente a una unión de tipo *cis* entre los dos ciclos del núcleo casbánico. De hecho, no es muy frecuente en la naturaleza encontrar anillos casbánicos con unión *trans* entre los ciclos. De todas formas, la presencia en el mismo animal de ambas uniones *cis* y *trans* en los metabolitos casbénicos sugiere que el mecanismo de formación no es estereoespecífico y que, por tanto, la reacción de ciclización ocurre en ambos lados de la molécula. La explicación se podría atribuir a la presencia en *Sinularia* de sistemas enzimáticos diferentes o, tal vez, los casbenos podrían derivar de precursores cembrénicos.

10.9.2. Actividad biológica

Los octocorales son una rica fuente de productos naturales dotados de interesantes actividades biológicas y potenciales aplicaciones farmacológicas, como las propiedades antitumoral, antimicrobiana, antiviral, *etc.* Teniendo en cuenta la información existente en la literatura sobre la actividad biológica de los compuestos casbénicos, los metabolitos **1**-**4** se sometieron a ensayos de repelencia alimenticia, de actividad antiproliferativa y antimicrobiana.

Los ensayos de repelencia alimenticia permiten evaluar la capacidad de un compuesto de alejar a un depredador por acción sobre sus receptores del gusto. El experimento se llevó a cabo con la quisquilla *Palaemon elegans*. Cada compuesto puro se incluyó a una concentración de 2 mg/ml en la dieta de las gambas, que consistía en ácido algínico, manto de calamares liofilizados, arena y colorantes. Mediante una jeringa, se formaron tiritas de esta masa (similares a espaguetis) y se ofrecieron a las gambas. La presencia de fragmentos rojos en el tubo digestivo de los animales significaba que habían comido y que, por tanto, los compuestos no desempeñaban un papel repelente. A las concentraciones probadas, los compuestos **3** y **4** exhibieron actividad repelente, mientras que la actividad de los compuestos **1** y **2** no fue significativa.

Los ensayos de actividad antiproliferativa se realizaron con células murinas de leucemia basofílica (RBL-2H3) incubadas con los compuestos **1**-**4** a las

concentraciones de 5 μg/ml y 25 μg/ml, a 37°C durante 5 días. Los resultados revelaron una actividad antiproliferativa no significativa de ninguno de los cuatro compuestos en las células consideradas (IC_{50} > 25 μg/ml).

En los ensayos de actividad antimicrobiana, los compuestos **1**-**4** fueron probados a una concentración de 5 μg/ml en colonias aisladas de *Staphylococcus aureus* (bacteria $Gram^+$) y *Escherichia coli* (bacteria $Gram^-$), empleando cloramfenicol como control positivo. En particular, con cada compuesto diluido con cloroformo se empapó un disco de papel absorbente. Los discos se pusieron en los pocillos conteniendo las bacterias *S. aureus* y *E. coli*, y se incubaron a 37°C durante 18-24 horas. Sucesivamente, se evaluó el diámetro del halo de inhibición para cada sustancia. Los resultados del experimento demostraron que los compuestos **1** y **2** tenían una moderada actividad antimicrobiana frente a *S. aureus*, mientras que el compuesto **3** mostraba una moderada actividad frente a *S. aureus* y *E. coli*. Por otro lado, el metabolito **4** exhibía buena actividad antimicrobiana frente a *S. aureus*.

10.10. Parte experimental

10.10.1. Incremento de la producción de diatomeas

Las diatomeas *Cocconeis neothumensis* se recolectaron en la primavera de 2005 a lo largo de la isla de Ischia (Italia), empleando paneles adhesivos encima de las praderas de *Posidonia oceanica* hundidos a una profundidad de 1.5 m durante un mes.

Tras la identificación taxonómica, se obtuvieron cultivos madre sembrando diatomeas de *C. neothumensis* en placas de Petri que contenían medio f/2, incubadas a 140 μmol de fotones m^{-2} $segundo^{-1}$, a un fotoperíodo de 18:6 horas y a 17°C. Una vez alcanzada la fase exponencial, se rascaron las diatomeas del fondo de las placas de Petri para obtener una suspensión celular, de la que unas alícuotas se inocularon en recipientes dotados de una rejilla en el fondo para permitir el contaje de las diatomeas. En los experimentos los cultivos se sometieron tanto a diferentes intensidades de luz (60, 100 y 140 μmol de fotones m^{-2} $segundo^{-1}$) en medio f/2, 17°C y a un fotoperíodo de 18:6 horas, como a diferentes concentraciones de micronutrientes (0.11 mM de Na_2SiO_3, 0.22 mM de Na_2SiO_3, 10^{-8} M de H_2SeO_3, y 0.22 mM de Na_2SiO_3 y 10^{-8} M H_2SeO_3 simultáneamente) a 140 μmol de fotones m^{-2} $segundo^{-1}$, 17°C y a un fotoperíodo de 18:6 horas. Se efectuaron 5 réplicas para cada tratamiento, y las diatomeas se contaron cada dos días hasta conseguir la fase estacionaria de los cultivos.

Para evaluar el rendimiento de los cultivos en placas de Petri, cultivos madre de *C. neothumensis* se sembraron en placas de Petri de 2.5 cm de diámetro conteniendo 5 ml de medio f/2. A partir de tres de esos cultivos, se preparó una suspensión celular para inocular placas de Petri de 14 cm de diámetro conteniendo 90 ml de medio f/2, que se incubaron a 100 μmol de fotones m^{-2} $segundo^{-1}$, a un fotoperíodo de 18:6 horas y a 17°C hasta alcanzar la fase estacionaria. Las células aún adheridas al fondo de las placas se lavaron con agua destilada, se liofilizaron y se rascaron.

En el bioreactor (26 cm de largo, 4.7 cm de diámetro) lleno de bolitas de vidrio de 2 mm de diámetro, se inoculó una suspensión celular obtenida de tres cultivos de *C. neothumensis* en placas de Petri de 2.5 cm de diámetro. El sistema se puso en marcha a un flujo continuo de 7 l h^{-1} cm^{-2} de medio f/2. Tras 17 días de incubación, las bolitas recubiertas de diatomeas se lavaron y se liofilizaron. Las diatomeas obtenidas mediante los dos cultivos se extrajeron previamente con acetona y, luego, con éter etílico. Los extractos etéreos obtenidos a partir tanto de las placas de Petri como del bioreactor se compararon mediante cromatografía en capa fina (TLC) empleando diferentes mezclas de disolventes orgánicos como eluyentes. Las placas se revelaron con sulfato de cerio 2 N en solución acuosa al 10% de H_2SO_4. El rendimiento se expresó como peso medio de extracto etéreo producido por los dos sistemas.

10.10.2. Composición química de *C. scutellum*

Las diatomeas *C. scutellum*, cultivadas en la Stazione Zoologica (Ischia, Italia), se extrajeron previamente con acetona, y sucesivamente con éter etílico y butanol. El extracto etéreo se fraccionó mediante columna Sephadex LH-20 eluyendo con cloroformo/metanol 1:1 v/v, y se obtuvieron las fracciones **1-3**. Pequeñas cantidades de extracto etéreo y fracciones **1-3** se derivatizaron con BSTFA en piridina a 50°C durante 2 horas. Por otra parte, alícuotas del extracto butanólico se trataron previamente con MOA en piridina durante 90 minutos a 50°C, y luego con BSTFA.

Las mezclas se evaporaron con flujo de N_2 y se diluyeron con $CHCl_3$ para ser analizadas mediante GC-MS. Los ácidos grasos metilésteres se obtuvieron tratando alícuotas del extracto etéreo y fracciones **1-3** con HCl y metanol. El análisis GC-MS se realizó en los Serveis Científico-tècnics de la UB con un Hewlett Packard 6890+MSD 5975, en las modalidades EI y CI, y según el programa de temperatura: 100-180°C a 15°C min^{-1}, 1 min a 180°C, 180-300°C a 5°C min^{-1}, y 1 min a 300°C. La temperatura del inyector era 280°C, y el flujo de gas (helio en EI, y metano en CI) era 0.8 ml min^{-1}.

Los metabolitos del extracto etéreo y de las fracciones **1-3** se identificaron como derivados TMSi comparando sus espectros de masas e índices de Kovats con los de bases de datos on-line (The Golm Metabolome Database) y de la base de datos NIST 05. Los espectros de los FAMEs se compararon con librerías lipídicas on-line, con la base de datos NIST 05 y con los datos descritos en la literatura para compuestos similares. Los metabolitos del extracto butanólico se identificaron como derivados TMSi y/o MOA mediante comparación de sus espectros con los datos descritos en la literatura y en las diferentes bases de datos. Los *RI* se calcularon con una mezcla de calibración estándar de *n*-hidrocarburos (C_9-C_{36}) usando el software AMDIS 3.6.

Para evaluar la presencia de aldéhidos en *C. scutellum*, una muestra de diatomeas se diluyó con agua destilada y se sometió a sonicación con ultrasonidos. Tras 30 minutos, la suspensión se trató con acetona y se centrifugó a 4,000 rpm durante 10 minutos. El supernatante se extrajo con cloroformo y, tras deshidratación con Na_2SO_4 anhidro y evaporación del disolvente, se derivatizó con CET-TPP bajo agitación

durante 18 horas. La mezcla se evaporó mediante flujo de nitrógeno y se analizó mediante GC-MS. En paralelo, los estándares heptadienal, octadienal y decadienal se trataron con CET-TPP y cloroformo, removiendo magnéticamente durante toda la noche, y los CET-derivados así obtenidos se sometieron a análisis GC-MS. El análisis GC-MS se efectuó con un Hewlett Packard 6890+MSD 5975, en la modalidad EI y en las siguientes condiciones: temperatura inicial 130°C, temperatura final 220°C, con un gradiente de 3°C min^{-1}; temperatura del inyector 240°C, temperatura del detector 260°C; flujo de helio 1 ml min^{-1}, y split 1:50. Los espectros del extracto clorofórmico derivatizado con CET-TPP se compararon con los derivados de los estándares.

10.10.3. Ensayos biológicos con las diatomeas *C. scutellum*

Hembras adultas de *H. inermis* se recolectaron en primavera a lo largo de la investigación (2006-2007) entre las praderas de *P. oceanica* en Lacco Ameno d'Ischia (Italia), y se transferieron a la SZN donde se llevó a cabo su identificación y medida. Los individuos se cultivaron en vasos aireados de 2 l conteniendo agua de mar, y se alimentaron con *Artemia* sp. hasta liberación de las larvas. Las larvas se repartieron en grupos de 80 individuos, se pusieron en vasos llenos de 800 ml de agua filtrada y esterilizada con rayos UV, y se alimentaron con *Artemia salina* previamente enriquecida con Algamac durante 18 horas, más *Brachionus plicatilis*. El medio de cultivo se renovó cada dos días y los vasos se mantuvieron en una habitación a 18°C,

a un fotoperíodo de 12:12 horas y a una irradiación de 200 μE. Después de 14 días, las larvas más grandes se juntaron para luego ser divididas en grupos de 80 individuos. Alcanzada la fase postlarval, los individuos se alimentaron durante 10 días con pellets de comida carente de *Brachionus* y a una concentración decreciente de *Artemia* (primeros 4 días: 4 individuos/ml; días 5-7: 3 ind/ml; días 8-9: 2 ind/ml; día 10: 1 ind/ml). El día 11 las postlarvas de cada vaso se repartieron en grupos de 20 individuos en placas de Petri de 12 cm de diámetro llenas de 400 ml de agua de mar. Cada postlarva se alimentó con pellets de 5 mg enriquecidos con los extractos etéreo y butanólico de las diatomeas *C. scutellum* (70, 7 y 0.7 μg de cada extracto/mg de comida) durante 32 días. La dieta control estaba constituida por 15 g de *Artemia* liofilizada + 15 g de copos de *Spirulina* + 1 g de comida Baby (SHG). En paralelo, se evaluaron también diferentes comidas base (comida 1: 200 mg de *Artemia* liofilizada + 200 mg de *Spirulina* pura + 200 mg de Algamac; comida 2: 200 mg de *Artemia* liofilizada + 200 mg de *Spirulina* pura + 200 mg de Tetra AZ; comida 3: 200 mg de *Artemia* liofilizada + 200 mg de *Spirulina* pura + 200 mg de SHG granular; comida 4: 500 mg de *Artemia* liofilizada + 500 mg de *Spirulina* pura + 250 mg de comida Baby). Simultáneamente grupos de 20 postlarvas de *H. inermis* se trataron durante 32 días con pellets enriquecidos con las fracciones **1-3** (4 mg de cada fracción), y conteniendo comida Tetra AZ (33% en peso), *Spirulina* pura (33%), y *Artemia* enriquecida liofilizada (33%), *i.e.* la comida que demostró producir la mayor superviviencia en los experimentos anteriores. El día 33 todas las postlarvas se fijaron con formaldéhido

durante 5 horas, se trataron con alcohol al 70% y se examinaron al microscopio para evaluar la presencia/aunsencia de la *appendix masculina*.

En cuanto a los ensayos con los crustáceos de interés comercial, se realizaron experimentos *in vivo* con los camarones *M. rosenbergii*, y experimentos *in vitro* con los langostinos *C. quadricarinatus*. En el primer tipo de ensayo, grupos de 25 individuos de las larvas de *M. rosenbergii* se trataron con comida a base de algas representada por Algamac enriquecida con *Artemia* sp. más alícuotas de extracto acetónico a dos concentraciones (20 ng/larva y 2 ng/larva). Tras la transformación de las larvas a postlarvas, los individuos se separaron y se alimentaron con pescado hasta llegar a un peso medio de 1 g. Para evaluar su sexo, se examinó al microscopio el segundo pleópodo de cada postlarva, *i.e.* el que lleva la *appendix masculina*. En el segundo tipo de experimento, langostinos *C. quadricarinatus* sin base del ojo se sometieron a ablación quirúrgica de la glándula androgénica. Las glándulas androgénicas junto a los conductos espermáticos se incubaron durante 24 horas tanto con las fracciones **1**-**3** como con los estándares ácido araquidónico y ácido eicosapentaenoico, a las concentraciones de 100, 10 y 1 µg/ml. La estaurosporina, un antibiótico proaptoptótico, se empleó como control positivo a la concentración de 10 µg/ml. Tras la incubación, las muestras se fijaron y se empaparon con parafina, proporcionando secciones de 5 µm que se examinaron mediante microscopía de fluorescencia.

Por lo que se refiere a los ensayos de citotoxicidad, las líneas celulares BT20, MB-MDA468, LNCaP, COR, JVM2, y BRG-M se cultivaron a una densidad de 1 x 10^6

células/ml en medio RPMI-FCS enriquecido con penicilina-estreptomicina (1%), L-glutamina 200 mM (1%), y piruvato sódico 100 mM (1%). La línea COR consistía en linfocitos B extraídos de amígdalas faríngeas y tratados con el virus Epstein-Barr para volverlos inmortales. Por otro lado, las líneas BRG-M y JVM2 consistían en linfocitos T extraídos de sangre periférica. Las diferentes líneas se incubaron a una densidad de 80,000 células/pocillo durante 24 horas en presencia de concentraciones crecientes de una suspensión acuosa de *C. scutellum* (0.1-10 ng/ml) a 37°C. Se usó el Vepesid como control positivo a una concentración de 10 µl/ml. Las células BT20 se incubaron en presencia de concentraciones crecientes tanto de extracto etéreo como de extracto butanólico de *C. scutellum* (0-1,700 ng/pocillo) durante 18 horas. Además, tanto la línea BT20 como la LNCaP se incubaron con las fracciones **1-3** (0.1-4 µg/pocillo) durante 24 horas. A las células BT20 se administraron EPA y AA también a una concentración de 7 µg/pocillo durante 18 y 24 horas. La apoptosis se valoró bien mediante tinción con ioduro de propidio hipotónico y citometría de flujo (para determinar la cantidad de ADN fragmentado), o bien mediante tinción doble con anexina V-FITC y ioduro de propidio isotónico y citometría de flujo. Los datos obtenidos fueron analizados con el software Cellquest.

El análisis del ciclo celular se llevó a cabo tras tinción de las células BT20 con ioduro de propidio hipotónico. Las células BT20 se incubaron durante 48 horas con las fracciones **1-2** (2.5 µg/pocillo de cada una) y la fracción **3** (4 µg/pocillo). Las muestras

teñidas con PI se analizaron mediante citometría de flujo, y los porcentajes de células en cada fase del ciclo celular se calcularon mediante el software Mod-fit.

En cuanto a los experimentos de Western blotting, tras tratamiento con Vepesid, con las fracciones **1**-**3** (fracción **1**: 4.11 μg/pocillo; fracción **2**: 2.67 μg/pocillo; fracción **3***: 4 μg/pocillo; fracción **3**: 2 μg/pocillo), y con el medio como control negativo, 1×10^7 células BT20/ml se recogieron, se lavaron con una solución salina amortiguada con fosfato, se centrifugaron y se lisaron. La concentración proteica de los lisatos celulares se medió con el kit Micro BCA. Cantidades iguales de proteínas (10 μg/banda) de cada tratamiento se separaron mediante SDS-PAGE (10% acrilamida) y se transferieron electroforéticamente a una membrana de nitrocelulosa. Tanto las caspasas activas como las inactivas se detectaron sondeando los filtros con anticuerpos anticaspasas 8 y 9, marcados a su vez por la peroxidasa de rábano acoplada con inmunoglobulina de capra antiratón como revelador. La reacción se detectó mediante reactivos de fosforescencia química y exposición a Hyperfilm-MP.

10.10.4. Nuevos compuestos del molusco anaspídeo *A. fasciata*

Tres ejemplares de *Aplysia fasciata* se recolectaron mediante apnea en la Bahía dels Alfacs, Delta de l'Ebre (Tarragona), en enero de 2008 a una profundidad de 1-1.5 m. Los animales se diseccionaron en manto y principales órganos internos en el Departament de Biologia Animal (Invertebrats), Facultat de Biologia de la UB. Las

diferentes secciones se liofilizaron y se enviaron al Departamento de Farmacognosia y Química de Productos Naturales de la Facultad de Farmacia, Universidad de Atenas, donde se llevaron a cabo la extracción, la purificación y la elucidación estructural. Las varias porciones anatómicas se extrajeron con una mezcla de diclorometano/metanol 2:1 v/v y se dejaron macerar toda la noche. Los extractos se filtraron sobre papel de filtro y se evaporaron los disolventes orgánicos bajo presión reducida. El control cromatográfico se efectuó mediante placas TLC de sílica gel, eluidas con varias mezclas de disolventes (cHx/EtOAc 6:4 v/v, y CH_2Cl_2/MeOH 95:5 v/v). Las placas se observaron bajo luz UV (254 y 365 nm) y se revelaron con sulfato de cerio 2 N en solución metanólica al 15% en H_2SO_4, calentando a 100°C durante 1 minuto. El extracto de las glándulas hermafrodita y digestiva (3.0 g) se extrajo mediante VLC en fase normal. La columna, empaquetada con sílica gel, se eluyó con ciclohexano y concentraciones crecientes de acetato de etilo. Tras análisis TLC, las fracciones recogidas se combinaron en 9 grupos (A-I). La fracción C se separó ulteriormente mediante SPE en fase normal, eluyendo con ciclohexano y concentraciones crecientes de acetato de etilo. Se obtuvieron tres fracciones, de las cuales C1 (24.1 mg) se purificó mediante HPLC en fase normal en condiciones isocráticas, usando *n*-Hx/EtOAc 98:2 v/v como fase móvil a un flujo de 2 ml min^{-1}, proporcionando los compuestos **1** (2.2 mg), **3** (0.6 mg), **4** (1.1 mg), **12** (8.0 mg), y **13** (1.3 mg). Reduciendo el flujo a 1.5 ml min^{-1} y manteniendo inalteradas las demás condiciones de purificación de la fracción C1, se obtuvieron los compuestos **5** (0.6

mg), **6** (0.7 mg), **7** (0.6 mg), **8** (1.0 mg), **11** (0.8 mg), y **14** (0.6 mg). La purificación HPLC en fase normal de la fracción C2 (29.0 mg) mediante elución isocrática con cHx/EtOAc 95:5 v/v a un flujo de 1.5 ml min^{-1}, proporcionó los compuestos **2** (0.8 mg) y **8** (1.0 mg).

La fracción F (226.1 mg) se separó mediante SPE en fase normal, eluyendo con ciclohexano y concentraciones crecientes de acetato de etilo. Se obtuvieron 8 fracciones, de las cuales F3 (30.6 mg) se purificó mediante HPLC en fase normal, con cHx/EtOAc 75:25 v/v como fase móvil y a un flujo de 1.5 ml min^{-1}. Las fracciones F4 (36.9 mg) y F5 (20.5 mg) se purificaron mediante HPLC en fase normal, eluyendo con cHx/EtOAc 75:25 v/v a un flujo de 2 ml min^{-1} y se obtuvieron los compuestos **10** (3.3 mg), **15** (8.4 mg), y **16** (11.3 mg).

La fracción G (102.3 mg) se separó mediante SPE en fase normal, eluyendo con ciclohexano y concentraciones crecientes de acetato de etilo. Se obtuvieron 7 fracciones, de las cuales G3 (23.9 mg), G4 (37.9 mg), y G5 (15.4 mg) se purificaron mediante HPLC en fase normal, con cHx/EtOAc 75:25 v/v como fase móvil y a un flujo de 2 ml min^{-1}, proporcionando los compuestos **9** (6.8 mg), **15** (2.0 mg), y **16** (10.4 mg). Todas las purificaciones HPLC en fase normal se realizaron con una columna Kromasil 100 SIL 5 μm y con un equipo CECIL 1100 Series dotado de detector a índice de refracción GBC LC-1240.

Una alícuota del compuesto **2** (epibrasilenol, 1 mg), disuelta con 2 ml de piridina, se dejó reaccionar con un exceso de anhidrido acético. Tras agitación durante 16 horas a

70°C, la mezcla se trató con 5 ml de DCM y 5 ml de agua destilada. Sucesivamente se separó en un embudo, y la fase orgánica conteniendo el epibrasilenol se evaporó.

10.10.5. Nuevos compuestos casbánicos del coral blando chino *Sinularia* sp.

Un ejemplar de *Sinularia* sp. se muestreó mediante inmersión a una profundidad de 20 m, en enero de 2004, en la costa de la isla de Hainan, China. El material se trasladó al laboratorio del ICB, donde se llevaron a cabo el trabajo químico y los ensayos biológicos. La muestra se repartió en trozos más pequeños y se extrajo tres veces con acetona, machacándola en un mortero y sonicando en un baño de ultrasonidos. Se filtró el extracto acetónico sobre papel de filtro y la acetona se evaporó mediante presión reducida. El residuo acuoso se extrajo exhaustivamente con éter etílico y, tras evaporación del disolvente, se obtuvo el extracto etéreo crudo (2.2 g). El extracto etéreo se sometió a control cromatográfico con placas TLC, usando diferentes mezclas de disolventes orgánicos como eluyentes. Las placas se observaron bajo luz UV (254 nm) y se revelaron con sulfato de cerio 2 N en solución acuosa al 10% en H_2SO_4, calentando a 100°C durante 1 minuto. Una alícuota del extracto etéreo (389.0 mg) se separó mediante cromatografía líquida sobre columna de sílica gel (Merck Kieselgel 60, 0.063-0.200 nm). La columna se equilibró con éter de petróleo y la separación se efectuó eluyendo en gradiente de éter de petróleo/éter etílico. Se obtuvieron nueve grupos, de los cuales la fracción 1 (96.7 mg) se purificó mediante

TLC preparativa usando éter de petróleo/éter etílico 9:1 v/v como fase móvil. El gel de sílice correspondiente a las dos bandas UV-visibles a R_f 0.63 y 0.50 (éter de petróleo/éter etílico 9:1 v/v) se rascó y se eluyó con cloroformo en una pipeta Pasteur. Obtuvimos una mezcla de 13.0 mg, que contenía mayoritariamente el compuesto **1**, y 5.5 mg del compuesto **2**. La mezcla que contenía el compuesto **1** se purificó ulteriormente mediante TLC preparativa eluyendo con benceno. El gel de sílice correspondiente a la banda UV-visible a R_f 0.26 (benceno) se rascó y se eluyó con cloroformo en una pipeta Pasteur, obteniendo el compuesto **1** puro (6.7 mg). Por otro lado, la fracción 6 (69.3 mg) se purificó mediante TLC preparativa eluyendo con éter de petróleo/éter etílico 3:7 v/v. Se rascó la sílice correspondiente a las dos bandas UV-visibles a R_f 0.50 y 0.43 (éter de petróleo/éter etílico 3:7 v/v), que fueron cargadas en dos pipetas Pasteur y eluidas con cloroformo proporcionando 40.6 mg del compuesto **3**, y 5.1 mg del compuesto **4**.

Para obtener los ésteres de Mosher, una alícuota del compuesto **3** (2.7 mg) y otra del compuesto **4** (2.5 mg) se diluyeron con 1 ml de DCM anhidro. Cada solución se repartió en dos: una parte se derivatizó con 15 µl de *R*-MTPA cloruro y 0.2 ml de DMAP, y la otra con *S*-MTPA cloruro y 0.2 ml de DMAP. Las mezclas se dejaron bajo agitación toda la noche. Al día siguiente, tras evaporación del disolvente, las mezclas se purificaron mediante TLC preparativa, eluyendo con éter de petróleo/éter etílico 8:2 v/v. El gel de sílice correspondiente a las bandas UV-visibles a R_f 0.30 (éter de petróleo/éter etílico 8:2 v/v) para los dos ésteres del compuesto **3**, y a R_f 0.25 (éter de

petróleo/éter etílico 8:2 v/v) para los dos ésteres del compuesto **4**, se rascó y se eluyó con cloroformo en una pipeta Pasteur. Tras evaporación del disolvente, se obtuvieron 1.0 mg de (*S*)-MTPA éster y 1.2 mg de (*R*)-MTPA éster del compuesto **3**, así como 0.9 mg de (*S*)-MTPA éster y 0.7 mg of (*R*)-MTPA éster del compuesto **4**, para ser analizados mediante RMN ^{1}H.

En cuanto a los experimentos de repelencia alimenticia sobre la quisquilla *Palaemon elegans*, los compuestos **1**-**4** se diluyeron con acetona y se añadieron a una mezcla constituida por ácido algínico (30 mg), manto molido de calamar liofilizado (50 mg) y arena purificada (30 mg). Tras evaporación del disolvente orgánico, se añadió a la mezcla una gota de colorantes alimentarios (E124 y E110) y, sucesivamente, se diluyó con agua destilada hasta alcanzar el volumen de 1 ml. La mezcla se agitó y se cargó en una jeringa de 5 ml, con la cual se produjo una tirita roja que se dejó en una solución de $CaCl_2$ 0.25 M durante 2 minutos. El espagueti rojo así obtenido se cortó en trocitos de unos 10 mm de largo. La comida control se preparó análogamente, pero sin los metabolitos purificados. Las quisquillas *P. elegans* se recolectaron con una red a lo largo de la costa de Pozzuoli (Nápoles, Italia) en julio de 2008, y se dejaron en acuario una semana para que se acostumbraran a la comida artificial. Después de tres días de ayuno, las gambas se pusieron en vasos de precipitados de 500 ml llenos de 300 ml de agua de mar. A las gambas se les ofrecieron comida control y tratamientos en series de 10 réplicas independientes. Tras 30 minutos, la presencia de una mancha roja en el tubo digestivo del animal se consideró una prueba de la aceptación de la

comida, en cambio su ausencia manifestaba una respuesta negativa por parte de la gamba.

Los experimentos de citotoxicidad se llevaron a cabo con la línea celular RBL-2H3 (leucemia basofílica murina). Tras la siembra, se dejaron adherir las células durante 4 horas a 37°C en atmósfera húmeda (5% de CO_2) y, sucesivamente, los compuestos casbénicos **1-4** se añadieron al medio de cultivo a 5 y 25 µg/ml. Conforme se iba cambiando el medio de cultivo, se reemplazaban también los compuestos. Después de 4 días se evaluó la vitalidad celular mediante coloración con cristal violeta.

Los ensayos de actividad antibacteriana se efectuaron con líneas celulares de *Staphylococcus aureus* (bacteria $Gram^+$) y *Escherichia coli* (bacteria $Gram^-$), cultivadas en medio LB toda la noche y bajo agitación a 37°C. Los dos inóculos se diluyeron de 1 a 1,000 volúmenes en medio LB. Las suspensiones bacterianas (1 ml) así obtenidas se sembraron en placas de Petri conteniendo agar (medio LB sólido). Alícuotas de 20 µl de los compuestos casbénicos **1-4** se diluyeron con $CHCl_3$ a una concentración de 5 µg/ml y con esas soluciones se empaparon filtros de papel absorbente. El cloramfenicol a una concentración de 10 µg se usó como control positivo tanto frente a *S. aureus* como frente a *E. coli*. Los filtros empapados se pusieron en el centro de cada placa de Petri. Cada compuesto se administró tanto a *S. aureus* como a *E. coli*, con un total de 9 tratamientos. Las placas se incubaron giradas a 37°C durante 18-24 horas y, posteriormente, se evaluó el diámetro del halo de inhibición para cada sustancia. Según la metodología convencional, la resistencia o la sensibilidad de un

microorganismo se expresa como: R (resistencia): (-) o (+/-) si el halo de inhibición mide menos de 15 mm de diámetro; MS (susceptibilidad media): (+) o (++) si el diámetro del halo de inhición está incluido en un intervalo de 15-25 mm; S (susceptibilidad): (+++) o (++++) si el halo de inhición tiene un diámetro de más de 25 mm.

10.11. Conclusiones

La presente memoria de Tesis se ha dedicado al aislamiento, caracterización y evaluación de posibles aplicaciones de productos naturales del bentos marino.

Obtuvimos resultados muy relevantes en el ámbito del proyecto PHARMAPOX. A fin de incrementar la producción de diatomeas para satisfacer las cantidades requeridas por los diferentes Institutos participantes, conseguimos establecer las mejores condiciones de crecimiento para las diatomeas *Cocconeis neothumensis* en lo que se refiere tanto a la irradiación como a la concentración óptima de microelementos. En particular, el desarrollo y el crecimiento de las diatomeas se incrementaban a la intensidad de luz de 60 µmol de fotones m^{-2} $segundo^{-1}$ y en presencia de una fuente de selenio (10^{-8} M H_2SeO_3) o silicatos (0.22 mM de Na_2SiO_3) en el medio de cultivo, pero no los dos simultáneamente. El bioreactor proporcionó mayores cantidades de biomasa de diatomeas en comparación con el sistema de las placas de Petri (24 ± 5 mg *vs.* 17.3 ± 3 mg, respectivamente, expresado en mg de

extracto etéreo). Sin embargo, a la hora de pasar del cultivo a escala reducida a la producción masiva, surgieron varios problemas, en particular la contaminación por cianobacterias del bioreactor desarrollado para la producción a gran escala, a pesar de las medidas de esterilización adoptadas. Estos problemas nos obligaron a volver al sistema de cultivo mediante placas de Petri que, sin embargo, fue mejorado respecto a las condiciones iniciales de crecimiento, *e.g.* no cerrando las placas de Petri con Parafilm y optimizando el rendimiento de las mismas. Con ello, conseguimos obtener cantidades suficientes de material biológico. El cambio en la especie de diatomea de *C. neothumensis* a *C. scutellum*, debido a la pérdida de actividad de la primera, produjo varios retrasos pero *C. scutellum* demostró mantener una actividad apoptótica constante, aunque algo inferior a *C. neothumensis*.

Un importante resultado fue la determinación del patrón metabólico de las diatomeas *C. scutellum*. Mediante GC-MS, de hecho, se detectaron 124 metabolitos y se identificaron más de 100. En particular se observó la presencia en el extracto etéreo de fosfatos, ácidos grasos, alcoholes, alcanos, glicéridos, esteroles y compuestos isoprenoides, y en el extracto butanólico la presencia de aminoácidos y compuestos nitrogenados, ácidos orgánicos, fosfatos, ácidos grasos, alcoholes, carbohidratos, glicéridos y compuestos isoprenoides. Además, el ácido eicosapentaenoico (EPA), un ácido graso poliinsaturado con reconocida actividad apoptótica, fue uno de los componentes mayoritarios de la fracción **3**. El análisis GC-MS demostró también la ausencia en las diatomeas *C. scutellum* de compuestos aldehídicos, que *a priori* se

podrían considerar involucrados en el efecto apoptótico/reversión sexual en *H. inermis*. Cabe destacar que hasta ahora esta diatomea bentónica no había sido estudiada desde el punto de vista químico y la determinación de su patrón metabólico ha representado el primer paso para entender los mecanismos de apoptosis. Las escasas cantidades disponibles de diatomeas, la necesidad de compartir el material con los demás Institutos participantes y todos los problemas surgidos durante la investigación no nos permitieron identificar exactamente el/los factor(es) apoptótico(s). Y además, considerando el gran número de metabolitos identificados mediante GC-MS y las cantidades escasas de material biológico inicial, hubiera sido muy difícil purificar cada compuesto en cantidades suficientes para los bioensayos. Por otro lado, la determinación del patrón metabólico de *C. scutellum* se puede considerar un resultado importante, y la identificación de la fracción más activa en producir apoptosis en la glándula androgénica de *H. inermis* podría abrir el camino para investigaciones futuras en este ámbito.

Los ensayos *in vivo* con las postlarvas de *H. inermis* mostraron una mayor actividad del extracto etéreo de *C. scutellum* respecto al extracto butanólico en inducir reversión sexual, y la mayor actividad apoptótica de la fracción **3**, la que contenía la cantidad más significativa de ácido eicosapentaenoico. Una tendencia parecida en cuanto a la mayor actividad del extracto etéreo y de la fracción **3**, fue la que se observó en los experimentos *in vitro* sobre las líneas celulares BT20 (carcinoma de mama) y LNCaP (adenocarcinoma de próstata). Poblaciones BT20 cultivadas en presencia de 1.7

ng/pocillo de extracto etéreo manifestaron una reducción de la vitalidad celular (49.9%) y un incremento de la apoptosis (31.9%) respecto al control (72.9% de vitalidad celular, 14.9% de apoptosis). En presencia de 2 µg/pocillo de la fracción **3**, se observó la máxima apoptosis media en las células BT20 (81.4%), un resultado significativo en comparación con las fracciones **1**-**2**. Los experimentos *in vitro*, además, demostraron el efecto apoptótico del EPA sobre las células BT20, resultados que eran parecidos a los obtenidos con la fracción **3**. Se obtuvieron resultados similares con la poblaciones celulares LNCaP incubadas en presecia de la fracción **3**: la vitalidad celular sufrió una reducción drástica, alcanzando casi el 0% a concentraciones mayores de 0.05 µg/pocillo. También los experimentos *in vitro* demostraron el efecto apoptótico del EPA sobre la línea BT20. En presencia de 7 µg/pocillo de EPA en las poblaciones BT20, las células apoptóticas fueron el 45.3% de las células totales, mientras que con el medio de cultivo las células apoptóticas representaron el 14.3%.

Contestando a la primera pregunta surgida durante este estudio, podemos decir que no está todavía claro si la apoptosis inducida por las diatomeas es provocada exclusivamente por el EPA o si hay más compuestos involucrados en el proceso mediante un mecanismo de sinergia. Además, de momento no podemos decir si los compuestos responsables de la apoptosis en las líneas celulares humanas son los mismos que afectan a la reversión sexual en las gambas *H. inermis*. Son necesarios más estudios detallados basados en los resultados de esta Tesis para aclarar este

tema. Se demostró también, mediante experimentos de Western blotting, que la caspasa 8 es la enzima iniciadora de la apoptosis, lo que significa que el proceso apoptótico inducido por las diatomeas se produce mediante la vía extrínseca. La caspasa 3, además, demostró ser una de las enzimas efectoras intermediarias de la cascada proteolítica de la apoptosis.

Dado que uno de los principales objetivos de la investigación actual es descubrir nuevos agentes proapoptóticos a partir de recursos naturales, las diatomeas *Cocconeis* se pueden considerar buenos candidatos para proveer compuestos con una toxicidad selectiva hacia los tumores sólidos más que hacia los hematológicos y las células normales. Por otro lado, experimentos *in vitro* con los langostinos *Cherax quadricarinatus* demostraron que *C. scutellum* no provocaba apoptosis significativa en las glándulas androgénicas de los crustáceos de interés comercial evaluados, sugiriendo una acción muy específica de las diatomeas sobre dianas celulares específicas, que se encontraban en *H. inermis* y eran ausentes en otros crustáceos.

El estudio químico del molusco anaspídeo *Aplysia fasciata* llevó al aislamiento de 16 metabolitos, seis de los cuales son nuevos para la ciencia: cuatro sesquiterpenos (**4**, **6-8**), una acetogenina C_{15} (**10**), y un diterpeno (**15**). Todos estos compuestos derivaban de metabolitos de diferentes especies de *Laurencia*, ya que existe una relación alimenticia entre el molusco y las algas rojas. Los compuestos **4** y **6-7** están estructuralmente relacionados con los brasilenoles. De hecho, el compuesto **4** presenta el doble enlace en posición 1-2 en vez de 1-6 del brasilenol (**1**), y un grupo

OH enlazado al C-6. El compuesto **6** corresponde al 2-acetoxiepibrasilenol. El compuesto **7**, el 4-acetoxi-5-brasileno, ya descrito en la literatura como producto de la acetilación del 5-brasileno, se ha aislado aquí como sustancia natural de *A. fasciata*. El compuesto **10**, el (3*Z*,9*Z*)-7-cloro-6-hidroxi-12-oxopentadeca-3,9-dien-1-ino, está caracterizado por una cadena linear con un triple enlace, dos dobles enlaces (de los que uno conjugado con el triple enlace) y un grupo carbonilo. El compuesto **8**, el 6-*epi*-β-snyderol, es el epímero en C-6 del compuesto conocido β-snyderol. El diterpeno pimaránico **15**, el 16-acetoxi-15-bromo-7-hidroxi-9(11)-parguereno, es el 2-deacetoxiderivado del compuesto conocido **16**.

El estudio químico del coral blando chino *Sinularia* sp. llevó al aislamiento de cuatro nuevos compuestos casbénicos, que son diterpenos con una estructura bicíclica formada por un anillo de 14 términos unido con un ciclopropano, todos relacionados químicamente entre ellos. Los casbenos son muy raros en la naturaleza y se encuentran generalmente en plantas de la familia Euphorbiaceae y raramente en organismos marinos. Dado que la mayoría de los casbenos naturales presenta la fusión *cis*, la co-ocurrencia de fusiones *cis* y *trans* en *Sinularia* sp. es algo extraño y sugiere un mecanismo de síntesis no estereospecífico. El hecho de que sólo los casbenos **3** y **4** presentaran una significativa actividad de repelencia alimenticia quiere decir que la función 10-hidroxílica, ausente en los compuestos **1**-**2**, es un elemento imprescindible para esta propiedad biológica. A pesar de las similitudes estructurales con las agrostistaquinas, metabolitos de *Agrostistachys hookeri*

(Euphorbiaceae) con reconocida actividad antiproliferativa, los compuestos **1-4** resultaron no activos frente a la línea celular RBL-2H3 (leucemia basofílica en ratas). Por otro lado, los compuestos **1-4** demostraron ser activos frente a *S. aureus* (bacteria $Gram^+$) y sólo el compuesto **3** presentó actividad antimicrobiana frente a *S. aureus* y *E. coli* (bacteria $Gram^-$) también.

En conclusión, los resultados obtenidos en esta Tesis doctoral son una prueba más de la importancia de los productos naturales marinos como candidatos para el descubrimiento y el desarrollo de nuevos medicamentos, y evidencian la necesidad de incrementar la investigación sobre este tema. Contestando a la pregunta final de nuestros objetivos, podemos afirmar que los organismos bentónicos estudiados, es decir las diatomeas *Cocconeis scutellum*, el molusco *Aplysia fasciata* y el octocoral *Sinularia* sp., representan fuentes de compuestos interesantes, algunos de los cuales dotados de propriedades biológicas y ecológicas muy relevantes, y otros que se deberán estudiar con una mayor profundidad en trabajos futuros.

Bibliography

Abdel-Fattah, A.F.; Edrees, M. (1977). Carbohydrates of the brown seaweed *Padina pavonia*. Phytochemistry 16: 939-941.

Adolph, S.; Poulet, S.A.; Ponhert, G. (2003). Synthesis and biological activity of α,β,γ,δ-unsaturated aldehydes from diatoms. Tetrahedron 59: 3003-3008.

Adolph, S.; Bach, S.; Blondel, M.; Cueff, A.; Moreau, M.; Pohnert, G.; Poulet, S.A.; Wichard, T.; Zuccaro, A. (2004). Cytotoxicity of diatom-derived oxylipins in organisms belonging to different phyla. The Journal of Experimental Biology 207: 2935-2946.

Aflalo, E.D.; Hoang, T.T.T.; Nguyen, V.H.; Lam, Q.; Nguyen, D.M.; Trinh, Q.S.; Raviv, S.; Sagi, A. (2006). A novel two-step procedure for mass production of all-male populations of the giant freshwater prawn *Macrobrachium rosenbergii*. Aquaculture 256: 468-478.

Ahmed, A.F.; Hsieh, Y.T.; Wen, Z.H.; Wu, Y.C.; Sheu, J.H. (2006). Polyoxygenated sterols from the Formosan soft coral S*inularia gibberosa*. Journal of Natural Products 69: 1275-1279.

Amico, V.; Caccamese, S.; Neri, P.; Russo, G.; Foti, M. (1991). Brasilane-type sesquiterpenoids from the Mediterranean red alga *Laurencia obtusa*. Phytochemistry 30(6): 1921-1927.

Amsler, C.D.; Iken, K.B.; McClintock, J.B.; Baker, B.J. (2001). Marine chemical ecology. CRC Press, Boca Raton.

Andrianasolo, E.H.; Haramaty, L.; Vardi, A.; White, E.; Lutz, R.; Falkowski, P. (2008). Apoptosis-inducing galactolipids from a cultured marine diatom, *Phaeodactylum tricornutum*. Journal of Natural Products 71: 1197-1201.

Ashkenazi, A.; Dixit, V.M. (1998). Death receptors: signalling and modulation. Science 281: 1305-1308.

Avila, C. (1995). Natural products of opisthobranch molluscs: a biological review. Oceanography and Marine Biology: an Annual Review 33: 487-559.

Avila, C. (2006). Molluscan natural products as biological models. In Mollusc. From chemo-ecological study to biotechnological application. Cimino, G.; Gavagnin, M. (eds), Springer-Verlag Berlin Heidelberg New York, vol. 43, pp. 1-23.

Avila, C.; Taboada, S.; Núñez-Pons, L. (2008). Antarctic marine chemical ecology: what is next? Marine Ecology - an Evolutionary Perspective 29(1): 1-71.

Barclay, W.R.; Meager, K.M.; Abril, J.R. (1994). Heterotrophic production of long-chain omega-3 fatty acids utilizing algae and algae-like microorganisms. Journal of Applied Phycology 6(2): 123-129.

Bergsson, G.; Arnfinnsson, J.; Steingrimsson, O.; Thormar, H. (2001). *In vitro* killing of *Candida albicans* by fatty acids and monoglycerides. Antimicrobial Agents and Chemotherapy 45: 3209-3212.

Bhakuni, D.S.; Rawat, D.S. (2005a). Bioactive marine nucleosides. In Bioactive marine natural products. Anamaya Publisher, New Delhi/Springer, New York, pp. 208-234.

Bhakuni, D.S.; Rawat, D.S. (2005b). Bioactive marine peptides. In Bioactive marine natural products. Anamaya Publisher, New Delhi/Springer, New York, pp. 278-328.

Blée, E. (2002). Impact of phyto-oxylipins in plant defense. Trends in Plant Science 7: 315-321.

Blunt, J.W.; Copp, B.R.; Munro, M.H.G.; Northcote, P.T.; Prinsep, M.R. (2010). Marine natural products. Natural Product Reports 27: 165-237.

Bongiorni, L.; Pietra, F. (1996). Marine natural products for industrial applications. Chemical Industry 2: 54-58.

Borowitzka, M.A. (1997). Microalgae for aquaculture: opportunities and constraints. Journal of Applied Phycology 9(5): 393-401.

Bossy-Wetzel, E.; Green, D.R. (2000). Detection of apoptosis by annexin V labelling. In Methods in Enzymology. Reed, J.C. (ed), Academic Press, San Diego, vol. 322, pp. 15-18.

Boutry, J.L.; Saliot, A.; Barbier, M. (1979). The diversity of marine sterols and the role of algal biomasses: from facts to hypothesis. Experientia 35: 1541-1543.

Bowden, B.F.; Coll, J.J.; Mitchell, S.J.; Mulder, J.; Stokie, G.J. (1978). Studies of Australian soft corals. IX. A novel nor-diterpene from the soft coral *Sinularia leptoclados*. Australian Journal of Chemistry 31: 2049-2056.

Brown, M.R.; Mular, M.; Miller, I.; Farmer, C.; Trenerry, C. (1999). The vitamin content of microalgae used in aquaculture. Journal of Applied Phycology 11: 247-255.

Brusca, R.C.; Brusca, G. J. (2005). Invertebrados. McGraw-Hill, Interamericana, Madrid BFB.

Bryan, C.P. (1931). The Papyrus Ebers. New York, Appleton, D. & Co.

Buia, M.C.; Zupo, V.; Mazzella, L. (1992). Primary production and growth dynamics in *Posidonia oceanica*. PSZNI: Marine Ecology 13: 2-16.

Burke, B.A.; Chan, W.R.; Pascoe, K.O.; Blount, J.F.; Manchand, P.S. (1981). The structure of crotonitenone, a novel casbane diterpene from *Croton nitens* Sw. (Euphorbiaceae). Journal of the Chemical Society, Perkin Transactions 1 10: 1666-2669.

Buttke, T.M.; Sandstrom, P.A. (1994). Oxidative stress as a mediator of apoptosis. Immunology Today 15: 7-10.

Caldwell, G.S.; Olive, P.J.W.; Bentley, M.G. (2002). Inhibition of embryonic development and fertilization in broadcast spawning marine invertebrates by water soluble diatom extracts and the diatom toxin 2-*trans*-4-*trans*-decadienal. Aquatic Toxicology 60(1-2): 123-137.

Carefoot, T.H. (1967). Growth and nutrition of three species of opisthobranch molluscs. Comparative Biochemistry and Physiology 21(3): 627-652.

Carefoot, T.H. (1987). *Aplysia*: its biology and ecology. Oceanography and Marine Biology: an Annual Review 25: 167-284.

Cave, W.T.; Jurkowski, J.J. (1987). Comparative effects of ω-3 and ω-6 dietary lipids on rat mammary tumor development. In Proceedings of the American Oil Chemist' Society short course on polyunsaturated fatty acids and eicosanoids. Lands, W.E.M. (ed), Champaign, IL., pp. 261-266.

Chamras, H.; Ardashian, A.; Heber, D.; Glaspy, J.A. (2002). Fatty acid modulation of MCF-7 human breast cancer cell proliferation, apoptosis and differentiation. Journal of Nutritional Biochemistry 13: 711-716.

Changyun, W.; Haiyan, L.; Changlun, S.; Yanan, W.; Liang, L.; Huashi, G. (2008). Chemical defensive substances of soft corals and gorgonians. Acta Ecologica Sinica 28(5): 2320-2328.

Charniaux-Cotton, H. (1954). Découverte chez un Crustacé Amphipode (*Orchestia gammarella*) d'une glande endocrine responsable de la différenciation des caractères sexuels primaires et secondaires mâles. Comptes Rendus de l'Académie des Sciences Paris 239: 780-782.

Charniaux-Cotton, H. (1960). Sex determination. In Physiology of crustacean 1. Waterman T.H. (ed), Academic Press, New York, pp. 417-447.

Charniaux-Cotton, H.; Payen, G. (1988). Crustacean reproduction. In Endocrinology of Selected Invertebrates Types. Laufer, H.; Downer, R.G.H. (eds), Alan R. Liss, New York, vol. 2, pp. 279-303.

Chen, G.Q.; Jiang, Y.; Chen, F. (2007). Fatty acid and lipid class composition of the eicosapentaenoic acid-producing microalga, *Nitzschia laevis*. Food Chemistry 104: 1580-1585.

Choi, Y.H.; Kim, J.; Pezzuto, J.M.; Kinghorn, A.D.; Farnsworth, N.R.; Lotter, H.; Wagner, H. (1986). Agrostistachin, a novel cytotoxic macrocyclic diterpene from *Agrostistachys hookeri*. Tetrahedron Letters 27(48): 5795-5798.

Choi, Y.H.; Pezzuto, J.M.; Kinghorn, A.D.; Farnsworth, N.R. (1988). Plant anticancer agents, XLVI. Cytotoxic casbane-type constituents of *Agrostistachys hookeri*. Journal of Natural Products 51(1): 110-116.

Christie, W.W. (2003). Lipid analysis. The Oily Press, Bridgewater, England. http://www.lipidlibrary.co.uk/ms/ms01/index.htm.

Cimino, G.; Ghiselin, M.T. (1998). Chemical defense and evolution in the Sacoglossa (Mollusca: Gastropoda: Opisthobranchia). Chemoecology 8: 51-60.

Cimino, G.; Ghiselin, M.T. (1999). Chemical defense and evolutionary trends in biosynthetic capacity among dorid nudibranchs (Mollusca: Gastropoda: Opisthobranchia). Chemoecology 9: 187-207.

Cimino, G.; Fontana, A.; Gavagnin, M. (1999). Marine opisthobranch molluscs: chemistry and ecology in sacoglossans and dorids. Current Organic Chemistry 3: 327-372.

Cimino, G.; Ciavatta, M.L.; Fontana, A.; Gavagnin, M. (2001). Metabolites of marine opisthobranchs: chemistry and biological activity. In Bioactive compounds from natural sources. Isolation, characterisation and biological properties. Tringali, C. (ed), Taylor and Francis, London, pp. 578-637.

Clardy, J.; Walsh, C. (2004). Lessons from natural molecules. Nature 432: 829-837.

Cobos, V.; Díaz, V.; Raso, G.; Enrique, J.; Manjón-Cabeza, M.E. (2005). Insights on the female reproductive system in *Hyppolite inermis* (Decapoda, Caridea): is this species really hermaphroditic? Invertebrate Biology 124(4): 310-320.

Cory, S. (1995). Regulation of lymphocyte survival by the Bcl-2 gene family. Annual Review of Immunology 13: 513-543.

Cragg, G.M.; Newman, D.J.; Snader, K.M. (1997). Natural product in drug discovery and development. Journal of Natural Products 60: 52-60.

Cragg, G.M.; Newman, D.J. (2005). Biodiversity: a continuing source of novel drug leads. Pure and Applied Chemistry 77(1): 7-24.

Crombie, L.; Kneen, G.; Pattenden, G.; Whybrow, D. (1980). Total synthesis of the macrocyclic diterpene (-)-casbene, the putative biogenetic precursor of lathyrane, tigliane, ingenane, and related terpenoid structures. Journal of the Chemical Society, Perkin Transactions 1: 1711-1717.

Dayhuff, L.E.; Wells, M. (2005). Identification of fatty acids in fishes collected from the Ohio River using gas chromatography-mass spectrometry in chemical ionization and electron impact modes. Journal of Chromatography A 1098: 144-149.

Dembitsky, V.M.; Tolstikov, A.G.; Tolstikov, G.A. (2003). Natural halogenated non-terpenic C_{15} acetogenins of sea organisms. Chemistry for Sustainable Development 11: 329-339.

De Stefano, M.; Marino, D.; Mazzella, L. (2000). Marine taxa of *Cocconeis* on leaves of *Posidonia oceanica*, including a new species and two new varieties. European Journal of Phycology 35: 225-242.

De Stefano, M.; Marino, D. (2001). Comparison of *Cocconeis pseudonotata* sp. nov. with two closely related species, *C. notata* and *C. diruptoides*, from *Posidonia oceanica* leaves. European Journal of Phycology 36: 295-306.

De Totero, D.; Meazza, T.; Zupo, S.; Cutrona, G.; Matis, S.; Colombo, M.; Balleari, E.; Pierri, I.; Fabbi, M.; Capaia, M.; Azzarone, B.; Gobbi, M.; Ferrarini, M.; Ferrini, S. (2006). Interleukin-21 receptor (IL-21R) is up-regulated by CD40 triggering and mediates pro-apoptotic signals in chronic lymphocytic leukemia B cells. Blood 107: 3708-3715.

Dewick, P.M. (2001). Chimica, biosintesi e bioattività delle sostanze naturali. Piccin Nuova Libraria, Padova.

d'Ippolito, G.; Iadicicco, O.; Romano, G.; Fontana, A. (2002). Detection of short-chain aldehydes in marine organisms: the diatom *Thalassiosira rotula*. Tetrahedron Letters 43: 6137-6140.

Dixit, S.S.; Smol, J.P.; Kingston, J.C.; Charles, D.F. (1992). Diatoms: powerful indicators of environmental change. Environmental Science and Technology 26(1): 22-33.

Doucette, G.J.; Price, N.M.; Harrison, P.J. (1987). Effects of selenium deficiency on the morphology and ultrastructure of the coastal marine diatom *Thalassiosira pseudonana* (Bacillariophyceae). Journal of Phycology 23: 9-17.

Douglas, D.J.; Ramsey, U.P.; Walter, J.A.; Wright, J.L.C. (1992). Biosynthesis of the neurotoxin domoic acid by the marine diatom *Nitzschia pungens* forma *multiseries*, determined with [^{13}C]-labelled precursors and nuclear magnetic resonance. Journal of the Chemical Society, Chemical Communications 714-716.

Duh, C.Y.; El-Gamal, A.A.H.; Wang, S.K.; Dai, C.F. (2002). Novel terpenoids from the Formosan soft coral *Cespitularia hypotentaculata*. Journal of Natural Products 65: 1429-1433.

Earnshaw, W.C.; Martins, L.M.; Kaufmann, S.H. (1999). Mammalian caspases: structure, activation, substrates, and functions during apoptosis. Annual Review of Biochemistry 68: 383-424.

Edlinger, K. (1982). Color adaptation in *Haminea navicula* (Da Costa 1778) (Mollusca-Opisthobranchia). Malacologia 22: 593-600.

Edmunds, M. (2009). Do nematocysts sequestered by aeolid nudibranchs deter predators? - a background to the debate. Journal of Molluscan Studies 75(2): 203-205.

El-Deiry, W.S. (2003). The role of p53 in chemosensitivity and radiosensitivity. Oncogene 22: 7486-7495.

Erickson, K.L. (1983). In Marine Natural Product. Scheuer, P.J. (ed), Academic Press, New York, vol. V, chapter 4, pp. 1-3.

Evan, G.; Littlewood, T. (1998). A matter of life and cell death. Science 281: 1317-1322.

Falshaw, C.P.; King, T.J.; Imre, S.; Islimyeli, S.; Thomson, R.H. (1980). Laurenyne, a new acetylene from *Laurencia obtusa*: crystal structure and absolute configuration. Tetrahedron Letters 21: 4951-4954.

Faulkner, D.J.; Ghiselin, M.T. (1983). Chemical defense and the evolutionary ecology of dorid nudibranchs and some other opisthobranch gastropods. Marine Ecology Progress Series 13: 295-301.

Faulkner, D. J. (1995a). Chemical riches from the ocean. Chemistry in Britain 31: 680-684.

Faulkner, D. J. (1995b). Marine natural products. Natural Product Reports 12: 223-269.

Faulkner, D.J. (1999). Marine natural products. Natural Product Reports 16: 155-198.

Faulkner, D.J. (2000). Marine natural products. Natural Product Reports 17: 7-55.

Fenical, W. (1982). Natural product chemistry in the marine environment. Science 215: 923-928.

Fontana, A.; d'Ippolito, G.; Cutignano, A.; Miralto, A.; Ianora, A.; Romano, G.; Cimino, G. (2007). Chemistry of the oxylipin pathways in marine diatoms. Pure and Applied Chemistry 79(4): 481-490.

Fukami, K.; Nishimura, S.; Ogusa, M.; Asada, M.; Nishijima, T. (1997). Continuous cultures with deep seawater of a benthic food diatom *Nitzschia* sp. Hydrobiologia 358: 245-249.

Gambi, M.C.; Lorenti, M.; Russo, G.F.; Scipione, M.B.; Zupo, V. (1992). Depth and seasonal distribution of some groups of vagile fauna of the *Posidonia oceanica* leaf stratum: structural and trophic analyses. PSZNI Marine Ecology 13: 17-39.

Garson, M.J. (1994). The biosynthesis of sponge secondary metabolites: why it is important. In Sponges in Time and Space. van Soest, R.W.M.; van Kempen, T.M.G.; Braekman, J.C. (eds), Balkema, Amsterdam.

Gavagnin, M.; Carbone, M.; Nappo, M.; Mollo, E.; Roussis, V.; Cimino, G. (2005). First chemical study of anaspidean *Syphonota geographica*: structure of degraded sterols aplykurodinone-1 and -2. Tetrahedron 61: 617-621.

Gerschenson, L.E.; Rotello, R.J. (1992). Apoptosis: a different type of cell death. The FASEB Journal 6: 2450-2455.

Ghisalberti, E.L.; Jefferies, P.R.; Mori, T.A.; Skelton, B.W.; White, A.H. (1985). A new class of macrocyclic diterpenes from *Bertya dimerostigma* (Euphorbiaceae). Tetrahedron 41(12): 2517-2526.

Gillis, R.C.; Daley, B.J.; Enderson, B.L.; Karlstad, M.D. (2002). Eicosapentaenoic acid and γ-linolenic acid induce apoptosis in HL-60 cells. Journal of Surgical Research 107: 145-153.

Ginsburger-Vogel, T.; Charniaux-Cotton, H. (1982). Sex determination. In The Biology of Crustacea. Abele, L.G. (ed), Academic Press, Orlando, pp. 257-281.

Gladu, P.K.; Patterson, G.W.; Wikfors, G.H.; Chitwood, D.J.; Lusby, W.R. (1991). Sterols of some diatoms. Phytochemistry 30: 2301-2303.

The Golm Metabolome Database: http://csbdb.mpimp-golm.mpg.de/csbdb/gmd/home/gmd_sm.html.

González, A.G.; Martín, J.D.; Martín, V.S.; Norte, M.; Pérez, R.; Ruano, J.Z.; Drexler, S.A.; Clardy, J. (1982). Non-terpenoid C_{15} metabolites from the red seaweed *Laurencia pinnatifida*. Tetrahedron 38: 1009-1014.

González, M.J.; Schemmel, R.A.; Dugan, L.; Gray, J.I.; Welsch, C.W. (1993). Dietary fish oil inhibits human breast carcinoma growth: a function of increased lipid peroxidation. Lipids 28: 827-832.

Goodbody, I. (1961). Inhibition of the development of a marine sessile community. Nature (London) 190: 282-283.

Gordon, N.; Neori, A.; Shpigel, M.; Lee, J.; Harpaz, S. (2006). Effect of diatom diets on growth and survival of the abalone *Haliotis discus hannai* postlarvae. Aquaculture 252: 225-233.

Guilford, W.J.; Coates, R.M. (1982). Stereochemistry of casbene biosynthesis. Journal of the American Chemical Society 104: 3506-3508.

Guillard, R.R.L.; Ryther, J.H. (1962). Studies on marine planktonic diatoms. I. *Cyclotella nana* Hustedt and *Detonula confervacea* (Cleve) Gran. Canadian Journal of Microbiology 8: 229-239.

Guillén, J.E. (1990). Guia ilustrada de los crustáceos decápodos del litoral alicantino. Instituto de Cultura "Juan Gil-Albert". Diputación de Alicante, pp. 316.

Gupta, P.; Yadav, D.K.; Siripurapu, K.B.; Palit, G.; Maurya, R. (2007). Constituents of *Ocimum sanctum* with antistress activity. Journal of Natural Products 70(9): 1410-1416.

Hannun, Y.A. (1997). Apoptosis and the dilemma of cancer chemotherapy. Blood 89(6): 1845-1853.

Harrison, P.J.; Yu, P.W.; Thompson, P.A.; Price, N.M.; Philips, D.J. (1988). Survey of selenium requirements in marine phytoplankton. Marine Ecology Progress Series 47: 89-96.

Hartnoll, R.G. (1982). Growth. In The Biology of Crustacea. Bliss, D.E. (ed), Academic Press, New York, pp. 111-197.

Haslam, E. (1986). Secondary metabolism - fact and fiction. Natural Product Reports 3: 217-249.

Hasle, G.R.; Syvertsen, E.E. (1997). Marine Diatoms. In Identifying marine diatoms and dinoflagellates. Tomas, C.R. (ed), Academic Press, New York, pp. 5-385.

Hawkins, R.A.; Sangster, K.; Arends, M.J. (1998). Apoptotic death of pancreatic cancer cells induced by polyunsaturated fatty acids varies with double bond number and involves an oxidative mechanism. Journal of Pathology 185: 61-70.

Hay, M.E. (1997). The ecology and evolution of seaweed-herbivore interactions on coral reefs. Coral Reefs 16: S67-S76.

Higgs, M.D.; Faulkner, D.J. (1982). A diterpene from *Laurencia obtusa*. Phytochemistry 21(3): 789-791.

Hood, K.A.; West, L.M.; Northcote, P.T.; Berridge, M.V.; Miller, J.H. (2001). Induction of apoptosis by the marine sponge (*Mycale*) metabolites, mycalamide A and pateamine. Apoptosis 6: 207-219.

Howard, B.M.; Fenical, W. (1976). α- and β-snyderol: new bromo-monocyclic sesquiterpenes from the seaweed *Laurencia*. Tetrahedron Letters 1: 41-44.

Howe, G.A.; Schilmiller, A.L. (2002). Oxylipin metabolism in response to stress. Current Opinion in Plant Biology 5(1): 230-236.

Hügel, M.F. (1962). Étude de quelque constituants du pollen. Annis Abeille 5: 97-133.

Huschtscha, L.I.; Bartier, W.A.; Ross, C.E.A.; Tattersall, M.H.N. (1996). Characteristics in cancer cell death after exposure to cytotoxic drugs *in vitro*. British Journal of Cancer 73: 54-60.

Ianora A.; Poulet S.A.; Miralto A.; Grottoli R. (1996). The diatom *Thalassiosira rotula* affects reproductive success in the copepod *Acartia clausi*. Marine Biology 125: 279-286.

Ianora, A.; Miralto, A.; Poulet, S.A.; Carotenuto, Y.; Buttino, I.; Romano, G.; Casotti, R.; Ponhert, G.; Wichard, T.; Colucci-D'Amato, L.; Terrazzano, G.; Smetacek, V. (2004). Aldehyde suppression of copepod recruitment in blooms of a ubiquitous planktonic diatom. Nature 429: 403-407.

Isnansetyo, A.; Kamei, Y. (2003). MC21-A, a bacterial antibiotic produced by a new marine bacterium, *Pseudoaltermononas phenolica* sp. nov. O-BC30T against methicillin-resistant *Staphylococcus aureus*. International Journal of Antimicrobial Agents 47: 480-488.

Jackson, J.B.C; Buss, L. (1975). Allelopathy and spatial competition among coral reef invertebrates. Proceedings of the National Academy of Sciences 72: 5160-5163.

Jacobs, R.S.; Bober, M.A.; Pinto, J.; Williams, A.B.; Jacobson, P.B.; De Carvalho, M.S. (1993). In Marine biotechnology. Attaway, D.H.; Zaborsky, O.R. (eds), Plenum Press, New York, vol. 1, pp. 77-99.

Ji, N.Y.; Li, X.M.; Wang, B.G. (2008). Halogenated terpenes and a C_{15} acetogenin from the marine red alga *Laurencia saitoi*. Molecules 13(11): 2894-2899.

Jimeno, J. (2007). Yondelis® (trabectedin): major clinical impact of a marine anticancer compound in the era of targeted therapies. Proceedings of the V European Conference on Marine Natural Products, Ischia, Italy.

Kamel, H.N.; Slattery, M. (2005). Terpenoids of *Sinularia*: chemistry and biomedical applications. Pharmaceutical Biology 433(3): 253-269.

Kamlangdee, N.; Fan, K.W. (2003). Polyunsaturated fatty acid production by *Schizochytrium* sp. isolated from mangrove. Songklanakarin Journal of Science and Technology 25: 643-650.

Karmali, R.A.; Marsh, J.; Fuchs, C. (1984). Effect of ω-3 fatty acids on growth of a rat mammary tumor. Journal of the National Cancer Institute 73: 457-461.

Karuso, P. (1987). Chemical ecology of the nudibranchs. In Bioorganic Marine Chemistry. Scheuer P. J. (ed), Springer-Verlag Berlin, vol. 1, pp. 31-60.

Kaufmann, S. H. (1989). Induction of endonucleolytic DNA cleavage in human acute myelogenous leukaemia cells by etoposide, camptothecin, and other cytotoxic anticancer drugs: a cautionary note. Cancer Research 49: 5870-5878.

Kaufmann, S.H.; Earnshaw, W. (2000). Induction of apoptosis by cancer therapy. Experimental Cell Research 256: 42-49.

Keifer, D.M. (1997). A century of pain relief. Todays chem at work 6(12): 38-42.

Kelekom, A. (2002). Secondary metabolites from marine microorganisms. Annals of the Brazilian Academy of Sciences 74: 151-170.

Keller, M.D.; Selvin, R.C. (1987). Media for the culture of oceanic ultraphytoplankton. Journal of Phycology 23: 633-638.

Khalaila, I.; Manor, R.; Weil, S.; Granot, Y.; Keller, R.; Sagi, A. (2002). The eyestalk-androgenic gland-testis endocrine axis in the crayfish *Cherax quadricarinatus*. General and Comparative Endocrinology 127: 145-156.

Kijjoa, A.; Sawangwong, P. (2004). Drugs and cosmetics from the sea. Marine Drugs 2: 73-82.

Kinnel, R.B.; Dieter, R.K.; Meinwald, J.; van Engen, D.; Clardy, J.; Eisner, T.; Stallard, M.O.; Fenical, W. (1979). Brasilenyne and *cis*-dihydrorhodophytin: antifeedant medium-ring haloethers from a sea hare (*Aplysia brasiliana*). Proceedings of the National Academy of Sciences 76(8): 3576-3579.

Kittredge, J.S. (1974). In Proceedings of Food and Drugs from the Sea Conference, Mayaguez, Puerto Rico, Marine Technology Soc. Washington D.C., pp. 467-475.

Kobbe, W.C.M.; Epstein, S.; Look, S.A.; Rau, G.H.; Fenical, W.; Djerassi, C. (1984). On the origin of terpenes in symbiotic associations between marine invertebrates and algae (Zooxanthellae). The Journal of Biological Chemistry 259: 8168-8173.

Kuniyoshi, M.; Wahome, P.G.; Miono, T.; Hashimoto, T.; Yokoyama, M.; Shrestha, K.L.; Higa, T. (2005). Terpenoids from *Laurencia luzonensis*. Journal of Natural Products 68: 1314-1317.

Kupchan, S.M.; Sigel, C.W.; Matz, C.J.; Gilmore, C.J.; Bryan, R.F. (1976). Structure and stereochemistry of jatrophone, a novel macrocyclic diterpenoid tumor inhibitor. Journal of the American Chemical Society 98: 2295-2300.

Laabir, M.; Poulet, S.A.; Ianora, A. (1995). Measuring production and viability of eggs in *Calanus helgolandicus*. Journal of Plankton Research 17: 1125-1142.

Landsberg, J.H. (2002). The effects of harmful algal blooms on aquatic organisms. Reviews in Fisheries Science 10: 113-390.

Larsen, E.; Kharazmi, A.; Christensen, L.P.; Christensen, S.B. (2003). An antiinflammatory galactolipid from rose hip (*Rosa canina*) that inhibits chemotaxis of human peripheral blood neutrophils *in vitro*. Journal of Natural Products 66: 994-995.

Lebeau, T.; Robert, J.M. (2003a). Diatom cultivation and biotechnologically relevant products. Part I: Cultivation at various scales. Applied Microbiology and Biotechnology 60: 612-623.

Lebeau, T.; Robert, J.M. (2003b). Diatom cultivation and biotechnologically relevant products. Part II: Current and putative products. Applied Microbiology and Biotechnology 60: 624-632.

Legrand, C.; Rengefors, K.; Fistarol, G.O.; Graneli, E. (2003). Allelopathy in phytoplankton - biochemical, ecological and evolutionary aspects. Phycologia 42: 406-419.

Leist, M.; Jaattela, M. (2001). Four deaths and funeral: from caspases to alternative mechanisms. Nature Reviews Molecular Cell Biology 2: 589-598.

Lenoci, L.; Camp, P.J. (2008). Diatom structures templated by phase-separated fluids. Langmuir 24(1): 217-223.

Le Roux, A. (1963). Contribution à l'étude du développement larvaire d'*Hippolyte inermis* Leach (Crustacé Décapode Macroure). Comptes rendus de l'Académie des Sciences Paris 256: 3499-3501.

Lin, J.; Yan, X.J.; Zheng, L.; Ma, H.H.; Chen, H.M. (2005). Cytotoxicity and apoptosis induction of some selected marine bacteria metabolites. Journal of Applied Microbiology 99: 1373-1382.

Lowe, S.W.; Lin, A.W. (2000). Apoptosis in cancer. Carcinogenesis 21(3): 485-495.

Lyakhova, E.G.; Kalinovsky, A.I.; Kolesnikova, S.A.; Vaskovsky, V.E.; Stonik, V.A. (2004). Halogenated diterpenoids from the red alga *Laurencia nipponica*. Phytochemistry 65: 2527-2532.

Mansour, M.P.; Frampton, D.M.F.; Nichols, P.D.; Volkmann, J.K.; Blackburn, S.I. (2005). Lipid and fatty acid yield of nine stationary-phase microalgae: Applications and unusual C_{24}-C_{28} polyunsaturated fatty acids. Journal of Applied Phycology 17: 287-300.

MarinLit database, Department of Chemistry, University of Canterbury. http://www.chem.canterbury.ac.nz/marinlit/marinlit.shtml.

Mazzella, L.; Russo, G. (1989). Grazing effect of two *Gibbula* species (Mollusca, Archaegastropoda) on the epiphytic community of *Posidonia oceanica* leaves. Aquatic Botany 53: 357-373.

Mazzella, L.; Buia, M.C.; Spinoccia, L. (1994). Biodiversity of epiphytic diatom community on leaves of *Posidonia oceanica*. Proceedings of the XIII International Diatom Symposium 241-251.

Medeiros, P.M.; Simoneit, B.R.T. (2007). Analysis of sugars in environmental samples by gas chromatography-mass spectrometry. Journal of Chromatography A 1141: 271-278.

Michaelson, J. (1991). The significance of cell death. In Apoptosis: the molecular basis of cell death. Tomei, L.D.; Cope F.O. (eds), Cold Spring Harbor, NY, Cold Spring Harbor Laboratory p. 31.

Miralto, A.; Barone, G.; Romano, G.; Poulet, S.A.; Ianora, A.; Russo, L.G.; Buttino, I.; Mazzarella, G.; Laabir, M.; Cabrini, M.; Giacobbe, M.G. (1999). The insidious effect of diatoms on copepod reproduction. Nature 402: 173-176.

Miyamoto, T.; Higuchi, R.; Komori, T.; Fujioka, T.; Mihashi, K. (1986). Isolation and structures of aplykurodins A and B, two new isoprenoids from the marine mollusc *Aplysia kurodai*. Tetrahedron Letters 27: 1153-1156.

Miyamoto, T. (2006). Selective bioactive compounds from Japanese anaspideans and nudibranchs. In Molluscs. From chemo-ecological study to biotechnological application. Cimino, G.; Gavagnin, M. (eds), Springer-Verlag Berlin Heidelberg, vol. 43, pp. 199-214.

Mjos, S.A.; Pettersen, J. (2003). Determination of *trans* double bonds in polyunsaturated fatty acid methyl esters from their electron impact mass spectra. European Journal of Lipid Science and Technology 105: 156-164.

Mollo, E.; Gavagnin, M.; Carbone, M.; Castelluccio, F.; Pozone, F.; Roussis, V.; Templado, J.; Ghiselin, M.T.; Cimino, G. (2008). Factors promoting marine invasions: a chemoecological approach. Proceedings of the National Academy of Sciences 15(12): 4582-4586.

Moore, R.E. (1978). In Marine Natural Products. Scheuer, P.J. (ed), Academic Press, New York, vol. I, chapter 2.

Morimoto, T.; Nagatsu, A.; Murakami, N.; Sakakibara, J.; Tokuda, H.; Nishimo, H.; Iwashima, A. (1995). Antitumor promoting glyceroglycolipids from the green alga *Chlorella vulgaris*. Phytochemistry 40: 1433-1437.

Moura, V.L.A.; Monte, F.J.O.; Filho, R.B. (1990). A new casbane-type diterpenoid from *Croton nepetaefolius*. Journal of Natural Products 53(6): 1566-1571.

Müller, W.E.G.; Borejko, A.; Brandt, D.; Osinga, R.; Ushijima, H.; Hamer, B.; Krasko, A.; Xupeng, C.; Müller, I.M.; Schröeder, H.C. (2005). Selenium affects biosilica formation in the demosponge *Suberites domuncula*. FEBS Journal 272: 3838-3852.

Nagamine, C.; Knight, A.W.; Maggenti, A.; Paxman, G. (1980). Effects of androgenic gland ablation on male primary and secondary characteristics in the Malaysian prawn *Macrobrachium rosenbergii* (de Man) with first evidence of induced feminization in a non-hermaphroditic decapod. General and Comparative Endocrinology 41: 423-441.

Naganuma, T.; Horikoshi, K. (1994). Cellular fatty acids of marine agarolytic gliding bacteria. Systematic and Applied Microbiology 17: 125-127.

Nagashima, H.; Fukuda, I. (1981). Low molecular weight carbohydrates in *Cyanidium caldarium* and some related algae. Phytochemistry 20: 439-442.

Nelson, D.M.; Treguer, P.; Brzezinski, M.A.; Leynaert, A.; Queguiner, B. (1995). Production and dissolution of biogenic silica in the ocean. Revised global estimates, comparison with regional data and relationship to biogenic sedimentation. Global Biogeochemistry Cycles 9: 359-372.

Newell, G.E.; Newell, R.C. (1963). Marine plankton: a practical guide. Hutchinson Educational Ltd, London, p. 244.

Newman, D.J.; Cragg, G.M. (2007). Natural products as sources of new drugs over the last 25 years. Journal of Natural Products 70: 461-477.

Norte, M.; González, A.G.; Cataldo, F.; Rodríguez, M.L.; Brito, I. (1991). New examples of acyclic and cyclic C_{15} acetogenins from *Laurencia pinnatifida*. Reassignment of the absolute configuration for *E* and *Z* pinnatifidienyne. Tetrahedron 47(45): 9411-9418.

Okamura, T.; Hara, M. (2004). Androgenic gland cell structure and spermatogenesis during the molt cycle and correlation to morphotypic differentiation in the giant freshwater prawn, *Macrobrachium rosenbergii*. Zoological Science 21: 621-628.

Okita, T.W.; Volcani, B.E. (1978). Role of silicon in diatoms. IX. Differential synthesis of DNA polymerases and DNA-binding proteins during silicate starvation and recovery in *Cylindrotheca fusiformis*. Biochimica et Biophysica Acta 519: 76-86.

Okita, T.W.; Volcani, B.E. (1980). Role of silica in diatom metabolism. X. Polypeptide labelling patterns during the cell cycle, silicate starvation and recovery in *Cylindrotheca fusiformis*. Experimental Cell Research 125: 471-481.

Ortega, M.J.; Zubía, E.; Salvá, J. (1997). 3-e*pi*-Aplykurodinone B, a new degraded sterol from *Aplysia fasciata*. Journal of Natural Products 60(5): 488-489.

Overman, L.E.; Thompson, A.S. (1988). Total synthesis of (-)-laurenyne. Use of acetal-initiated cyclizations to prepare functionalized eight-membered cyclic ethers. Journal of the American Chemical Society 110: 2248-2256.

Parrish, C.C.; de Freitas, A.S.; Bodennec, G.; Macpherson, E.; Ackman, R. (1991). Lipid composition of the marine diatom *Nitzschia pungens*. Phytochemistry 30: 113-116.

Patterson, G.W. (1992). Sterols in algae. In Physiology and Biochemistry of Sterols III. Patterson, G.W.; Nes, W.D. (eds), American Oil Chemists Society, Champaign, pp. 118-157.

Patterson, G.W.; Tsitsa-Tzardis, E.; Wikfors, G.H.; Gladu, P.K.; Chitwood, D.J.; Harrison, D. (1993). Sterols of *Tetraselmis* (Prasinophyceae). Comparative Biochemistry and Physiology B 105: 253-256.

Paul, V.J. (1992). Ecological roles of marine natural products. Cornell University Press, Ithaca, NY.

Pawlik, J.R. (1993). Marine invertebrate chemical defenses. Chemical Reviews 93: 1911-1922.

Pawlik, J.R.; Chanas, B.; Toonen, R.J.; Fenical, W. (1995). Defenses of Caribbean sponges against predatory reef fish. I. Chemical deterrency. Marine Ecology Progress Series 127: 183-194.

Perrone, A.S. (1989). Functional duplication in the destructive aposematism in *Peltodoris atromaculata* Bergh, 1880 (Opisthobranchia: Nudibranchia). Bollettino Malacologico 24(9-12): 187-188.

Pietra, F. (2002). Biodiversity and natural product diversity. Williams, R.M.; Baldwin, J.E. (eds), Pergamon.

Pistocchi, R.; Trigari, G.; Serrazanetti, G.P.; Taddei, P.; Monti, G.; Palamidesi, S.; Guerrini, F.; Bottura, G.; Serratore, P.; Fabbri, M.; Pirini, M.; Ventrella, V.; Pagliarani, A.; Boni, L.; Borgatti, A.R. (2005). Chemical and biochemical parameters of cultured diatoms and bacteria from the Adriatic Sea as possible biomarkers of mucilage production. Science of the Total Environment 353: 287-299.

Ponhert, G. (2000). Wound-activated chemical defense in unicellular planktonic algae. Angewandte Chemie, International Edition 39: 4352-4354.

Ponhert, G. (2002). Phospholipase A_2 activity triggers the wound-activated chemical defense in the diatom *Thalassiosira rotula*. Plant Physiology 129: 103-111.

Ponhert, G.; Boland, W. (2002). The oxylipin chemistry of attraction and defense in brown algae and diatoms. Natural Product Reports 19: 108-122.

Price, N.M.; Harrison, P.J. (1988). Specific selenium-containing macromolecules in the marine *Thalassiosira pseudonana*. Plant Physiology 86: 192-199.

Pulz, O.; Gross, W. (2004). Valuable products from biotechnology of microalgae. Applied Microbiology and Biotechnology 65(6): 635-648.

Ratkowsky, D.A. (1990). Handbook of nonlinear regression models. Marcel Dekker, Inc., New York.

Raymont, J.E.G. (1983). Plankton and Productivity in the Oceans. In Phytoplankton 1. Food Industry, Moscow.

Reed, J.C.; Doctor, K.S.; Godzik, A. (2004). The domains of apoptosis: a genomic perspective [Re 9]. Science's STKE 239: 1-29.

Reed, J.C.; Pellecchia, M. (2005). Apoptosis-based therapies for hematologic malignancies. Blood 106(2): 408-418.

Reverberi, G. (1950). La situazione sessuale di *Hippolyte viridis* e le condizioni che la reggono. Bollettino Zoologico Italiano 4-6: 91-94.

Robinson, D.R.; West, C.A. (1970). Biosynthesis of cyclic diterpenes in extracts from seedlings of *Ricinus communis*. I. Identification of diterpene hydrocarbons formed from mevalonate. Biochemistry 9: 70-79.

Rochfort, S.J.; Capon, R.J. (1996). Parguerenes revisited: new brominated diterpenes from the southern Australian marine red alga *Laurencia filiformis*. Australian Journal of Chemistry 49(1): 19-26.

Roessler, P.G. (1988). Effects of silicon deficiency on lipid composition and metabolism in the diatom *Cyclotella cryptica*. Journal of Phycology 24: 394-400.

Romano, G.; Russo, G.L.; Buttino, I.; Ianora, A.; Miralto, A. (2003). A marine diatom-derived aldehyde induces apoptosis in copepod and sea urchin embryos. The Journal of Experimental Biology 206: 3487-3494.

Rontani, J.F.; Volkman, J.K. (2005). Lipid characterization of coastal hypersaline cyanobacterial mats from the Camargue (France). Organic Geochemistry 36: 251-272.

Ros, J.D. (1976). Sistemas de defensa en los opistobranquios. Oecologia Aquatica 2: 41-77.

Round, F.E.; Crawford, R.M. (1990). The diatoms. Biology and morphology of the genera. Cambridge University Press, UK.

Rousch, J.M.; Bingham, S.E.; Sommerfeld, M.R. (2003). Changes in fatty acid profiles of thermo-intolerant and thermo-tolerant marine diatoms during temperature stress. Journal of Experimental Marine Biology and Ecology 295: 145-156.

Roy, S.; Nicholson, D.W. (2000). Cross-talk in cell death signalling. The Journal of Experimental Medicine 192: 21-26.

Rudman, W.B.; Willan, R.C. (1998). Opisthobranchia Introduction. In Mollusca: The Southern Synthesis. Beesley, P.I.; Ross, G.J.B.; Wells, A. (eds), Fauna of Australia, Melbourne, CSIRO Publishing, vol. 5, part B, pp. 915-1025.

Rudman, W.B. (2001). *Aplysia fasciata* Poiret, 1789. In Sea Slug Forum. Australian Museum, Sydney. http://www.seaslugforum.net/factsheet.cfm?base=aplyfasc.

Rudman, W.B. (2004). Anaspidea. In Sea Slug Forum. Australian Museum, Sydney. http://www.seaslugforum.net/factsheet.cfm?base=anaspide.

Ruxton, C.H.S.; Reed, S.C.; Simpson, M.J.A.; Millington, K.J. (2004). The health benefits of omega-3 polyunsaturated fatty acids: a review of the evidence. Journal of Human Nutrition and Dietetics 17(5): 449-459.

Sagi, A.; Ra'anan, Z.; Cohen, D.; Wax, Y. (1986). Production of *Macrobrachium rosenbergii* in monosex population: yield characteristics under intensive monoculture conditions in cages. Aquaculture 51: 265-275.

Sagi, A.; Cohen, D. (1990). Growth, maturation and progeny of sex-reversed *Macrobrachium rosenbergii* (de Man). Biological Bulletin 169: 529-601.

Sagi, A.; Snir, E.; Khalaila, I. (1997). Sexual differentiation in decapod crustaceans: role of the androgenic gland. Invertebrate Reproduction and Development 31: 55-61.

Sagi, A.; Aflalo, E.D. (2005). The androgenic gland and monosex culture of freshwater prawn reversed *Macrobrachium rosenbergii* (de Man): a biotechnological perspective. Aquaculture Research 36: 231-237.

Salvesen, G.S.; Renatus, M. (2002). Apoptosome: the seven-spoked death machine. Developmental Cell 2: 256-257.

San-Martín, A.; Darias, J.; Soto, H.; Contreras, C.; Herreras, J.S.; Rovirosa, J. (1997). A new C_{15} acetogenin from the marine alga *Laurencia claviformis*. Natural Product Letters 10: 303-311.

Schmitz, F.J.; Michaud, D.P.; Schmidt, P.G. (1982). Marine natural products: parguerol, deoxyparguerol and isoparguerol. New brominated diterpenes with modified pimarane skeletons from the sea hare *Aplysia dactylomela*. Journal of the American Chemical Society 104: 6415-6423.

Scipione, B.; Mazzella, L. (1992). Epiphytic diatoms in the diet of crustacean amphipods of *Posidonia oceanica* leaf stratum. Oebalia, suppl. 17: 409-412.

Seco, J.M.; Quiñoá, E.; Riguera, R. (2004). The assignment of absolute configuration by NMR. Chemical Reviews 104: 17-117.

Seip, E.H.; Hecker, E. (1983). Lathyrane type diterpenoid esters from *Euphorbia characias*. Phytochemistry 22(8): 1791-1795.

Shapiro, S. (2003). Unsung aspirin hero. Modern Drug Discovery 9.

Shaw, B.A.; Andersen, R.J.; Harrison, P.J. (1995). Feeding deterrence properties of apo-fucoxanthinoids from marine diatoms. I. Chemical structures of apo-fucoxanthinoids produced by *Phaeodactylum tricornutum*. Marine Biology 124: 467-472.

Shirota, T.; Haji, S.; Yamasaki, M.; Iwasaki, T.; Hidaka, T.; Takeyama, Y.; Shiozaki, H.; Ohyanagi, H. (2005). Apoptosis in human pancreatic cancer cells induced by eicosapentaenoic acid. Nutrition 21: 1010-1017.

Sicko-Goad, L.; Andresen, N.A. (1991). Effect of growth and light/dark cycles on diatom lipid content and composition. Journal of Phycology 27: 710-718.

Sitton, D.; West, C.A. (1975). Casbene: an antifungal diterpene produced in cell-free extracts of *Ricinus communis* seedlings. Phytochemistry 14: 1921-1925.

Souchet, N.; Laplante, S. (2007). Seasonal and geographical variations of sterol composition in snow crab hepatopancreas and pelagic fish viscera from Eastern Quebec. Comparative Biochemistry and Physiology B 147: 378-386.

Spinedi, A.; Piacentini, M. (1999). Ciclo cellulare e apoptosi. In Farmacologia generale e molecolare. Clemente, F.; Fumagalli, G. (eds), UTET Torino, pp. 317-329.

Spinella, A.; Gavagnin, M.; Crispino, A.; Cimino, G. (1992). 4-Acetylaplykurodin B and aplykurodinone B, two ichthyotoxic degraded sterols from the Mediterranean mollusc *Aplysia fasciata*. Journal of Natural Products 55(7): 989-993.

Stallard, M.O.; Faulkner, D.J. (1974). Chemical constituents of the digestive gland of the sea hare *Aplysia californica*. I. Importance of diet. Comparative Biochemistry and Physiology 49 B: 25-35.

Stallard, M.O.; Fenical, W.; Kittredge, J.S. (1978). The brasilenols, rearranged sesquiterpene alcohols isolated from the marine opisthobranch *Aplysia brasiliana*. Tetrahedron 34: 2077-2081.

Sullivan, G.R.; Dale, J.A.; Mosher, H.S. (1973). Correlation of configuration and fluorine-19 chemical shifts of a α-methoxy-α-trifluoromethylphenyl acetate derivatives. The Journal of Organic Chemistry 38: 2143-2147.

Suzuki, M.; Kurosawa, E. (1980). Venustin a and b, new halogenated C_{15} metabolites from the red alga *Laurencia venusta* Yamada. Chemistry Letters 9: 1177-1180.

Suzuki, M.; Kurosawa, E.; Furusaki, A.; Matsumoto, T. (1983). The structures of (3*Z*)-epoxyvenustin, (3*Z*)-venustin, and (3*Z*)-venustinene, new halogenated C_{15} nonterpenoids from the red alga *Laurencia venusta* Yamada. Chemistry Letters 779-782.

Taguchi, S.; Hirata, J.A.; Laws, E.A. (1987). Silicate deficiency and lipid synthesis of marine diatoms. Journal of Phycology 23: 260-267.

Takeuchi, M.; Rothe, M.; Goeddel, D.V. (1996). Anatomy of TRAF2. Distinct domains for nuclear factor-kappa B activation and association with tumour necrosis factor signalling proteins. The Journal of Biological Chemistry 271: 19935-19942.

Thompson, C.B. (1995). Apoptosis in the pathogenesis and treatment of disease. Science 267: 1456-1462.

Thompson, T.E. (1960). Defensive adaptation in opisthobranchs. Journal of Marine Biology Ass. U.K. 39: 123-124.

Thompson, T.E. (1976). In Biology of opisthobranch molluscs. Ray Society, London, vol. 1, p. 26.

Todd, C.D. (1981). The ecology of nudibranch molluscs. Oceanography and Marine Biology: an Annual Review 19: 141-234.

Topcu, G.; Aydogmus, Z.; Imre, S.; Gören, A.C.; Pezzuto, J.M.; Clement, J.A.; Kingston, D.G.I. (2003). Brominated sesquiterpenes from the red alga *Laurencia obtusa*. Journal of Natural Products 66: 1505-1508.

Tosti, E.; Romano, G.; Buttino, I.; Cuomo, A.; Ianora, A.; Miralto, A. (2003). Bioactive aldehydes from diatoms block the fertilization current in ascidian oocytes. Molecular Reproduction and Development 66(1): 72-80.

Tulp, M.; Bohlin, L. (2005). Rediscovery of known natural compounds: nuisance or goldmine? Bioorganic and Medicinal Chemistry 13: 5274-5282.

Turner, J.T.; Ianora, A.; Miralto, A.; Laabir, M.; Esposito, F. (2001). Decoupling of copepod grazing rates, fecundity and egg-hatching success on mixed and alternative diatom and dinoflagellate diets. Marine Ecology Progress Series 220: 187-199.

van Heerde, W.L.; de Groot, P.G.; Reutelingsperger, C.P.M. (1995). The complexity of the phospholipid binding protein annexin V. Thrombosis and haemostasis 73: 172-179.

Vaux, D.L.; Korsmeyer, S.J. (1999). Cell death in development. Cell 96: 245-254.

Veillet, A.; Dax, J.; Vouaux, A.M. (1963). Inversion sexuelle et parasitisme par *Bopyrina virbii* (Walz) chez la crevette *Hyppolite inermis* (Leach). Comptes rendus de l'Académie des Sciences Paris 256: 790-791.

Venkateswarlu, V.; Reddy, S.N.; Venkatesham, U. (2001). Novel bioactive compounds from the soft corals: chemistry and biomedical applications. In Recent advances in marine biotechnology. Fingerman, M.; Nagabhushanam, R. (eds), Bio-organic Compounds and Biomedical Applications, Science Publisher, Inc. NH, vol. 6, pp. 101-129.

Verdine, G.L. (1996). The combinatorial chemistry of nature. Nature 384, suppl. 11-13.

Vermes, I.; Haanen, C.; Steffens-Nakken, H.; Reutelingsperger, C. (1995). A novel assay for apoptosis. Flow cytometric detection of phosphatidylserine expression on early apoptotic cells using fluoresceine labelled annexin V. Journal of Immunological Methods 184: 39-51.

Véron, B.; Dauguet, J.C.; Billard, C. (1998). Sterolic biomarkers in marine phytoplankton. II. Free and conjugated sterols of seven species used in mariculture. Journal of Phycology 34: 273-279.

Vogelstein, B.; Lane, D.; Levine, A.J. (2000). Surfing the p53 network. Nature 408: 307-310.

Volkman, J.K. (1986). A review of sterol markers for marine and terrigenous organic matter. Organic Geochemistry 9: 83-99.

Wallace, R.W. (1997). Drugs from the sea: harvesting the results of aeons of chemical evolution. Molecular Medicine Today 291-295.

Walsh, C. (2003). Antibiotics: actions, origins, resistance. ASM, Washington.

Wang, W.X.; Dei, R.C.H. (2001). Influences of phosphate and silicate on Cr(VI) and Se(IV) accumulation in marine phytoplankton. Aquatic Toxicology 52: 39-47.

Watanabe, K.; Umeda, K.; Miyakado, M. (1989). Isolation and identification of three insecticidal principles from the red alga *Laurencia nipponica* Yamada. Agricultural Biology and Chemistry 53(9): 2513-2515.

Watson, J.D.; Gilman, M.; Witkowski, J.; Zoller, M. (2002). DNA ricombinante. Zanichelli Editore, Bologna.

Weber, H. (2002). Fatty acid-derived signals in plants. Trends in Plant Science 7: 217-224.

Werner, D. (1978). Regulation of metabolism by silicates in diatoms. In Biochemistry of silicon and related problems. Bendez, G.; Lindqvist, I. (eds), Plenum, New York, pp. 149-179.

Willan, R.C. (1998). Order Anaspidea. In Mollusca: The southern synthesis. Beesley, P.I; Ross, G.J.B.; Wells, A. (eds), Fauna of Australia, Melbourne, CSIRO Publishing, vol. 5, part B, pp. 915-1025.

Williams, D.E.; Sturgeon, C.M.; Roberge, M.; Andersen, R.J. (2007). Nigricanosides A and B, antimitotic glycolipids isolated from the green alga *Avrainvillea nigricans* collected in Dominica. Journal of the American Chemical Society 129(18): 5822-5823.

Wolfe, S.L. (2000). Introduzione alla Biologia Cellulare e Molecolare. EdiSES, Napoli.

Wood, A.M.; Everroad, R.C.; Wingard, L.M. (2005). Measuring growth rates in macroalgal cultures. In Algal culturing techniques. Andersen, R.A. (ed), Academic, Amsterdam, pp. 269-285.

Wright, A. D.; König, G.M.; Sticher, O. (1991). New sesquiterpenes and C_{15} acetogenins from the marine red alga *Laurencia implicata*. Journal of Natural Products 54(4): 1025-1033.

Xu, Z.H; Sun, J.; Xu, R.S.; Qin, G.W. (1998). Casbane diterpenoids from *Euphorbia ebracteolata*. Phytochemistry 49(1): 149-151.

Yamada, K.; Kigoshi, H. (1997). Bioactive compounds from the sea hares of two genera: *Aplysia* and *Dolabella*. Bulletin of the Chemical Society of Japan 70: 1479-1489.

Yamada, K.; Ojika, M.; Kigoshi, H.; Suenaga, K. (2000). Cytotoxic substances from opisthobranch molluscs. In Drugs from the sea. Fusetani, N. (ed), Karger, Basel, pp. 59-73.

Yi; J.M.; Kim, M.S.; Lee, E.H.; Wi, D.H.; Lee, J.K.; Cho, K.H.; Hong, S.H.; Kim, H.M. (2003). Induction of apoptosis by *Paljin-Hangahmadan* on human leukaemia cells. Journal of Ethnopharmacology 88: 79-83.

Zariquey, R. (1968). Crustáceos Decápodos Ibéricos. Investigación Pesquera 32: 1-510.

Zhang, W.; Guo, Y.W.; Mollo, E. (2005a). Chemical studies on sesquiterpenes in soft coral *Lobophytum* sp. from the South China Sea. Natural Product Research and Development 17(6): 740-742.

Zhang, C.X.; Yan, S.Y.; Zhang, G.W.; Lu, W.G.; Su, J.Y.; Zeng, L.M.; Gu, L.Q.; Yang, X.P.; Lian, Y.J. (2005b). Cytotoxic diterpenoids from the soft coral *Sinularia microclavata*. Journal of Natural Products 68: 1087-1089.

Zhang, W.; Guo, Y.W.; Gu, Y. (2006). Secondary metabolites from the South China Sea Invertebrates: chemistry and biological activity. Current Medical Chemistry 13(17): 2041-2090.

Zupo, S.; Massara, R.; Dono, M.; Rossi, E.; Malavasi, F.; Cosulich, M.E.; Ferrarini, M. (2000). Apoptosis or plasma cell differentiation of CD38-positive B-chronic lymphocytic leukemia cells induced by cross-linking of surface IgM or IgD. Blood 95(4): 1199-1206.

Zupo, V. (1994). Strategies of sexual inversion in *Hippolyte inermis* Leach (Crustacea, Decapoda) from a Mediterranean seagrass meadow. Journal of Experimental Marine Biology and Ecology 178: 131-145.

Zupo, V. (2000). Effect of microalgal food on the sex reversal of *Hyppolite inermis* (Crustacea: Decapoda). Marine Ecology Progress Series 201: 251-259.

Zupo, V. (2001). Influence of diet on the sex differentiation of *Hyppolite inermis* Leach (Decapoda: Natantia) in the field. Hydrobiologia 449: 131-140.

Zupo, V.; Messina, P. (2007). How do dietary diatoms cause the sex reversal of the shrimp *Hyppolite inermis* Leach (Crustacea, Decapoda). Marine Biology 151: 907-917.

Zupo, V.; Messina, P.; Buttino, I.; Sagi, A.; Avila, C.; Nappo, M.; Bastida, J.; Codina, C.; Zupo, S. (2007). Do benthic and planktonic diatoms produce equivalent effects in crustaceans? Marine and Freshwater Behaviour and Physiology 40: 169-181.

The pictures which appear along the text have been realized by:

Authors	**Pictures**
Aflalo, E.	5.4, 10.4
Avila, C.	10.3
Ballesteros, M.	6.9
Mollo, E.	7.2, 7.30, 8.2, 10.2
Riesgo, A.	1.7
Ventura, T.	2.12
Villani, G. ©	1.8
Zupo, V.	1.6, 2.2, 3.1, 3.3, 3.7, 3.8, 3.9, 4.1

. . . e ad Alfredo

"Solo nel giardino delle menti
siede il tempo che verrà"
(pfm)